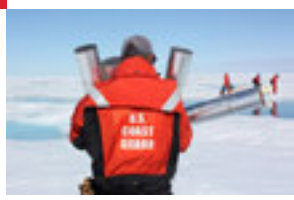

Abstract Volume
12th Swiss Geoscience Meeting

Fribourg, 21st – 22nd November 2014

Drilling the Earth

sc | nat

Swiss Academy of Sciences
Akademie der Naturwissenschaften
Accademia di scienze naturali
Académie des sciences naturelles

UNI FR

UNIVERSITÉ DE FRIBOURG
UNIVERSITÄT FREIBURG

Large picture: Drilling rig in Noville (VD), (Picture: Pierre Dèzes)
Small picture: Containers for ice cores collected from the final sea ice station of the 2011 ICESCAPE mission. The ICESCAPE mission, or «Impacts of Climate on Ecosystems and Chemistry of the Arctic Pacific Environment,» is NASA›s two-year shipborne investigation to study how changing conditions in the Arctic affect the ocean›s chemistry and ecosystems. (Picture: NASA/Kathryn Hansen)

12th Swiss Geoscience Meeting, Fribourg 2014

Table of contents

Organisation

Host Institution

Department of Geosciences of the University of Fribourg

Patronnage

Platform Geosciences, Swiss Academy of Sciences

Program Committee

Daniel Ariztegui
Reto Burkhalter
Pierre Dèzes
Hans-Ruedi Egli
Werner Eugster
Karl Föllmi
Leander Franz
Marcel Frehner
Alain Geiger
Christoph Graf
Bernard Grobéty
Irka Hajdas
Alain Morard
Thomas Nägler
Beat Oertli
Nils Oesterling
This Rütishauser
Elias Samankassou
Bruno Schädler
Guido Schreurs
Otto Smrekar
Peter Waldner

Local Organizing Committee

Christine Bichsel
Reynald Delaloye
Olivier Ejderyan
Anneleen Foubert
Olivier Graefe
Bernard Grobéty
Christian Hauck
Martin Hölzle
Matthias Huss
Walter Joyce
Ildiko Katona-Serneels
Jon Mosar
Nadine Salzmann
Vincent Serneels
Silvia Spezzaferri

Participating Societies and Organisations

Federal Office of Topography (swisstopo)
Forum for Climate and Global Change (ProClim–)
International Continental Scientific Drilling Program (ICDP)
International Geosphere-Biosphere Programme, Swiss Committee (IGBP)
International Ocean Discovery Program (IODP)
International Union of Geodesy and Geophysics, Swiss Committee (IUGG)
International Union of Geological Sciences, Swiss Committee (IUGS)
Kommission der Schweizerischen Paläontologischen Abhandlungen (KSPA)
National Research Programme «Sustainable Use of Soil as a Resource» (NRP 68)
Naturhistorisches Museum der Burgergemeinde Bern
Swiss Academic Society for Environmental Research and Ecology (SAGUF)
Swiss Association of Energy Geoscientists (SASEG)
Swiss Association of Geologists (CHGEOL)
Swiss Commission on Atmospheric Chemistry and Physics (ACP)
Swiss Commission for Phenology and Seasonality (CPS)
Swiss Commission for Remote Sensing (SCRS)
Swiss Committee on Polar and High Altitude Research
Swiss Committee for Stratigraphy (Platform Geosciences/SCNAT)
SwissDrilling
Swiss Geodetic Commission (SGC)
Swiss Geography Association (ASG)
Swiss Geological Society (SGG/SGS)
Swiss Geological Survey (swisstopo)
Swiss Geomorphological Society (SGGm/SSGm)
Swiss Geophysical Commission (SGPK)
Swiss Geotechnical Commission (SGTK)
Swiss Geothermal Society (GEOTHERMIE.CH)
Swiss Hydrogeological Society (SGH)
Swiss Hydrological Commission (CHy)
Swiss Paleontological Society (SPG/SPS)
Swiss Snow, Ice and Permafrost Society (SIP)
Swiss Society for Hydrology and Limnology (SGHL / SSHL)
Swiss Society for Quaternary Research (CH-QUAT)
Swiss Society of Mineralogy and Petrology (SMPG / SSMP)
Swiss Soil Science Society (SSSS)
Swiss Tectonics Studies Group (Swiss Geologiocal Society)

1. Structural Geology, Tectonics and Geodynamics

Guido Schreurs, Neil Mancktelow, Paul Tackley

Swiss Tectonics Studies Group of the Swiss Geological Society

TALKS:

1.1 Abednego M., Vouillamoz N., Wust-Bloch H.G., Mosar J.: New 3D microseismic tomography model interpretation and principal stress axes analysis in the Fribourg area (swiss western Molasse Basin)

1.2 Bauville A., Schmalholz S. M.: Thin- vs thick-skinned tectonics, nappe formation and shear localization: numerical simulations and applications to the Helvetic Alps and Jura mountains

1.3 Cioldi S., Moulas E., Burg J.-P.: Geospeedometry in inverted metamorphic gradients of the Nestos thrust zone in central Rhodope (Northern Greece)

1.4 Dielforder A., Berger A., Herwegh M., Vollstaedt H.: A chronology of internal wedge deformation constrained by strontium isotopes of carbonate veins

1.5 Giuntoli F., Engi M., Manzotti P., Ballèvre M.: Internal geometry in the Sesia Zone (Aosta Valley, Italy)

1.6 Liao J., Gerya T., Wang Q.: On craton destruction: Insight from 2D thermal-mechanical numerical modeling

1.7 Manzotti P., Ballèvre M., Zucali M., Robyr M., Engi M.: The tectonometamorphic evolution of the Sesia – Dent Blanche nappes (internal Western Alps)

1.8 Mohammadi A., Burg J-B., Ruh J., Von Quadt A., Peytcheva I.: New age constraints for the geodynamic evolution of the Sistan Suture Zone, eastern Iran

1.9 Mozafari Amiri N., Tikhomirov D., Sümer Ö., Özkaymak Ç., Uzel B., Ivy-Ochs S., Vockenhuber Ch., Sözbilir H., Akçar N.: Recurrence behavior of destructive earthquakes in Western Anatolia, Turkey: Insights from cosmogenic ^{36}Cl dating method

1.10 Peters, M., Veveakis, M., Poulet, T., Regenauer-Lieb, K., Herwegh, M.: Numerical bifurcation study of the initiation of folding and necking in elasto-visco-plastic rocks

1.11 Pfiffner, O.A., Deichmann, N.: Recent movements in the Alps: geodetic and GPS derived data

1.12 Steck A., Masson H., Robyr M.: Tectonics of the Monte Rosa nappe: Tertiary phases of subduction and thrusting in the Pennine Alps

1.13 Zwaan F., Schreurs G.: 4D Modeling of Transfer Zones in Continental Rifts

POSTERS:

P 1.1 Ballèvre M., Manzotti P., Poujol M.: Detrital zircon grains in blueschist-facies meta-conglomerates: implications for the early Permian geomorphology of the future northern margin of the Liguria-Piemonte ocean

P 1.2 Berger, A., Mercolli, I., Herwegh, M., Gnos, M., Wiederkehr, M., Wicki, A., Möri, A.: A new 1:100'000 scaled geological map of the Aar massif

P 1.3 Collignon M., Fernandez N., Kaus B.J.P.: Do surface processes and/or the presence of an initial surface topography affect(s) the fold linkage? And if yes, how?

P 1.4 Duretz T., Schmalholz S. M., Podladchikov Y. Y.: Thermo-mechanical shear localisation: length scale and thermal imprint

P 1.5 Egli D., Mosar J.: Kinematic analyses on multiply reactivated fault systems in the Black Forest – Hegau – Lake Constance region

P 1.6 Fabbri S. C., Anselmetti F. S., Herwegh M., Schlunegger F., Volken S., Möri A.: Neotectonic Activity at the Front of the Alps: Earthquake-induced Geomorphology in the Aare Valley & Lake Thun

P 1.7 Falco T., Mosar J.: Tectonics and Strain partitioning in the Mont Pèlerin Subalpine Molasse

P 1.8 Fischer R., Gerya T.: Early Earth tectonics: A high-resolution 3D numerical modelling approach

P 1.9 Golabek G., Jutzi M., Gerya T., Asphaug E.: Towards coupled giant impact and long term interior evolution models

P 1.10 Hawemann F., Mancktelow N., Wex S., Pennacchioni, G., Camacho, A: High-pressure pseudotachylytes as field evidence for lower crustal seismicity

P 1.11 Heerwagen E., Martini R.: The relationship between the Vizcaíno "composite" Terrane and the "Antimonio Terrane" during the Upper Triassic

P 1.12 Houlie N., Guilhem A.: Shear stress and seismic cycle length of SAF at Parkfield

P 1.13 Jaquet Y., Schmalholz S.: Impact of elasticity on lithospheric shear localization

P 1.14 Lechmann, A.K., Burg, J.-P., Faridi, M.: The Neo-Tethyan subduction zone(s,?) in Azerbaijan, NW Iran: preliminary results

P 1.15 Lohmann, H.: Salt dissolution in the underground of Switzerland, especially in the canton of Fribourg

P 1.16 Magni, S.: The water circulation In the fractured rock: The role of stylolites in the development of karst

P 1.17 Mancktelow N., Pennacchioni G., Hawemann F., Wex S., Camacho A.: Field constraints on the rheology of quartz in "wet" or "dry" middle to lower continental crust

P 1.18 Mosar J., Abednego M., Gruber M., Sommaruga A.: Tectonics between the Préalpes Klippen and the swiss western Molasse Basin in the Bulle region (Fribourg)

P 1.19 Moscariello A., Šegvić B.: Palaeosoils stacking patterns as a tool for unravelling the subsurface architecture of mud-rich fluvial reservoirs

P 1.20 Pleuger J., von Quadt A., Gallhofer D., Mancktelow N.: LA-ICP/MS U-Pb zircon ages of porphyritic dykes from the Sesia-derived Insubric mylonite belt (Piemonte/Ticino)

P 1.21 Schenker F. L., Fellin M. G., Burg J.-P.: Late Cretaceous-to-Pliocene thermo-tectonic history of Pelagonia (northern Greece) from zircon and apatite fission-track ages

P 1.22 Schneeberger R., Maeder U., Kober F., Spillmann Th., Waber N., Berger A., Herwegh M.: 3D visualization of the structures at the Grimsel Test Site GTS and their link with sampled groundwaters

P 1.23 Süssenberger A., Schmidt Th S: Dating low grade deformation of the Patagonian fold-and-thrust belt in the Torres del Paine area, Chile 51° 30'S: first results

P 1.24 Tackley P., Lourenco D., Fomin I., Nakagawa T.: Influence of melting on the long-term thermo-chemical evolution of Earth›s deep mantle

P 1.25 Valla P.G., Champagnac J.-D., Shuster D.L., Herman F., Fellin M.G., Enkelmann E.: Unravelling tectonics and surface processes in exhumation history of South Alaska: insights from the thermochronological record

P 1.26 von Tscharner, M., Schmalholz S.M.: 3D FEM modelling of fold nappe formation and the Rawil depression in western Switzerland

P 1.27 Wex S., Mancktelow N., Hawemann F., Camacho A., Pennacchioni G.: Interplay between seismic fracturing and aseismic creep during strain localization in the middle crust (Woodroffe Thrust, Central Australia)

1.1

New 3D microseismic tomography model interpretation and principal stress axes analysis in the Fribourg area (swiss western Molasse Basin)

Martinus Abednego[1], Naomi Vouillamoz[1], Hillel Gilles Wust-Bloch[2], Jon Mosar[1]

[1] *Department of Geosciences, Earth Sciences, University of Fribourg, Chemin du Musée 6 , CH-1700 Fribourg (martinussatiapurwadi.abednego@unifr.ch)*
[2] *Department of Geophysics and Planetary Sciences, Tel Aviv University, 69978 Tel Aviv*

An increased level of local microseismicity was recorded over the past decade within the Fribourg region (Kastrup et al., 2007). Since 2010, two portable sparse mini-arrays were deployed to enhance seismic monitoring capabilities in that area. The waveforms recorded by these arrays, together with those recorded by local stations of the Swiss Seismological Service (SED), were analyzed using supersonograms (Sick et al., 2012) in order to detect very weak (ML ≥ 0.5) events. By significantly lowering the detection threshold, 314 events were detected in the Fribourg area from the detection of continuous record since 2010 and discontinuous record back to 2001, of which 112 events were detected routinely by the SED until 2013. After filtering, the arrival time data and raypaths of 200 high-quality events and 16 identified quarry blasts were selected for a microseismic tomography analysis.

The first stage of the microseismic tomography analysis consisted in building up an initial 3D P-wave velocity model, which was designed on the basis of: a) interpretations of controlled-source seismology data by NAGRA (National Cooperative for the Disposal of Radioactive Waste), b) time-depth chart of boreholes in Swiss Molasse Basin (Sommaruga et al., 2012), and c) complex 3D velocity model of Switzerland used by the SED for earthquake location. The tomography analysis was carried out with SIMULPS2000 (Thurber & Eberhart-Phillips, 1999). The output model has a minimal horizontal grid spacing of 8 km and vertical grid spacing of 700 m. That model was interpreted with prior knowledge of the area, such as cross-sections from Seismic Atlas of the Swiss Molasse Basin (Sommaruga et al., 2012). A vertical increase of velocity was observed to be linked to the density change of different lithological units as a function of depth. The model also displays lateral velocity increases (NW to SE) from the Molasse Basin through the Subalpine Molasse and Prealps.

The 3D microseismic tomography model was also used to evaluate principal stress axes in the Fribourg region. Take-off angles of events were estimated from the tomographic model and then combined with the first motion polarity of P-wave to estimate the orientation of principal stress axes and the focal mechanism of each event. Focal mechanisms solutions were calculated using FPFIT, which is a software used by the U.S. Geological Survey. Focal mechanisms were sorted and grouped on the basis of their uncertainties and their 3D spatial distribution. Solution quality was assigned according to the World Stress Map Project Guidelines for quality ranking (Barth et al., 2008). Our analysis shows that the principal stress axes derived from local earthquakes have the characteristics of the regional tectonics system: P-axis toward NW and T-axis toward SW with mostly strike-slip faults.

REFERENCES

Barth, A., Reinecker, J. & Heidbach, O. 2008: Stress derivation from earthquake focal mechanisms. World Stress Map Project Guidelines.

Kastrup, U., Deichmann N., Fröhlich, A. & Giardini, D. 2007: Evidence for an active fault below the northwestern Alpine foreland of Switzerland. Geophys. J. Int., 169, 1273-1288.

Sick, B., Walter, M., & Joswig, M. 2012: Visual event screening of continuous seismic data by supersonograms. Pure and Applied Geophysics, 1-11.

Sommaruga, A., Eichenberger, U., & Marillier, F. 2012: Seismic Atlas of the Swiss Molasse Basin. Matériaux pour la géologie de la Suisse. Géophysique. Federal Office of Topography.

Thurber, C. & Eberhart-Phillips, D. 1999: Local earthquake tomography with flexible gridding. Computers & Geosciences, 25(7), 809-818.

1.2

Thin- vs thick-skinned tectonics, nappe formation and shear localization: numerical simulations and applications to the Helvetic Alps and Jura mountains

Arthur Bauville[1], Stefan M. Schmalholz[1]

[1] *Institute of Earth Sciences, University of Lausanne, Quartier UNIL-Mouline, Bât. Géopolis, 1015 Lausanne*

Fold-and-thrust belts can exhibit two tectonic styles. Thin-skinned tectonics is characterized by stacks of allochtonous sedimentary nappes which have been displaced far away from their original basement. Thick-skinned tectonics involves the deformation of basement rocks to which are often associated (para)-autochtonous sedimentary nappes. It is still unclear what controls the development of one or the other tectonic style, whether it is tectonic inheritance, rheology or thermal conditions. In this study we used two dimensional (2D) thermo-mechanical numerical simulations to simulate the deformation of an idealized passive margin in compression. We investigated the control of stratigraphy, rheology, thermal conditions and initial geometry on the development of thick- or thin-skinned dominated tectonics. Results suggest that the viscosity ratio between the base of the upper crust and the sediments at the basement-cover interface controls to first order the dominant deformation style. Weaker basal upper crust allows the closure of pre-existing half graben basins. The sediments expulsed from these basins then acquire the shape of a fold nappe. On the contrary a stronger basal upper crust inhibits basement deformation, which leads to the developments thrust-like horizontal weakly localized sheared zone, even in material with linear viscous rheology. This work has implication for the mechanics of emplacement of the Morcles fold nappe, Wildhorn and Glarüs thrust sheets and the Jura mountains.

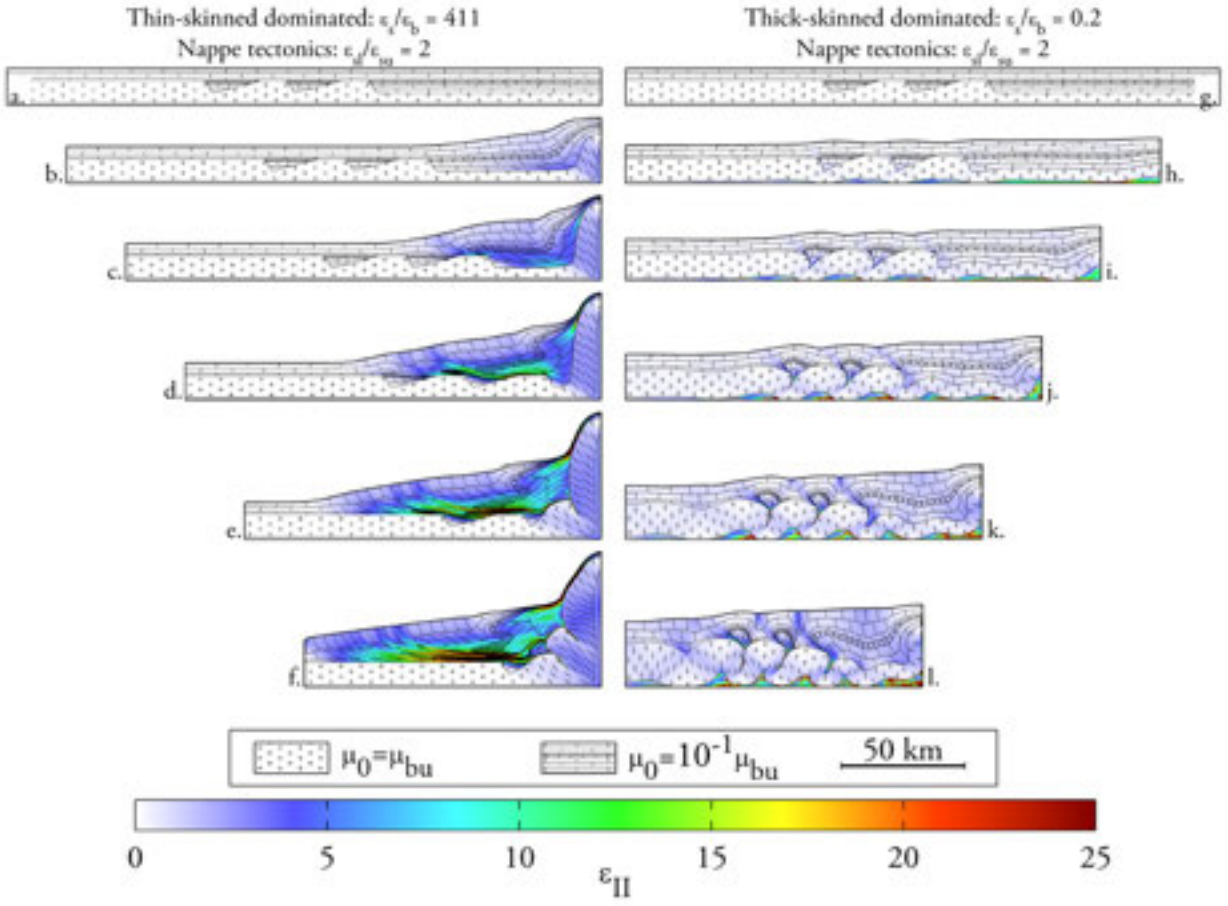

Figure 1. Evolution of two simulations with non-linear (n=4) rheology from 0% to 50% shortening. Patterns indicate initial viscosity, colors code for the second invariant of the finite strain tensor (a-f) The lower basement layer has the same viscosity as the upper basement (crosses pattern). Deformation is dominantly thin-skinned, horizontal weakly localized shear zones developped; (g-l) The lower basement is 1000 times weaker than the upper basement. Deformation is dominantly thick-skinned. Sediments expulsed during the closing of half-grabens form fold-nappe-like structures.

1.3

Geospeedometry in inverted metamorphic gradients of the Nestos thrust zone in central Rhodope (Northern Greece)

Stefania Cioldi[1], Evangelos Moulas[2] & Jean-Pierre Burg[1]

[1] *Geological Institute, ETH Zürich, Sonneggstrasse 5, 8092 Zürich (stefania.cioldi@erdw.ethz.ch, jean-pierre.burg@erdw.ethz.ch)*
[2] *Institute des sciences de la Terre, Bâtiment Géopolis, 1015 Lausanne (evangelos.moulas@unil.ch)*

Thrust tectonics and inverted metamorphic gradients are major consequences of large and likely fast movements in compressional environments. The purpose of this study is to investigate the tectonic setting and the timescale of inverted metamorphic zonations related to crustal-scale thrusting. The aim is to contribute understanding the link between mechanical and thermal evolution of major thrust zones and to clarify the nature and the origin of orogenic heat.
The Rhodope metamorphic complex (Northern Greece) is interpreted to be a deformed segment of the Alpine-Himalaya sutures and represents a collisional system with an association of both large-scale thrusting and pervasive exhumation tectonics. The Nestos Shear Zone overprints the suture boundary with a NEE-dipping pile of schists displaying inverted isograds. The inverted metamorphic zones start from chlorite-muscovite grade at the bottom and reach kyanite-sillimanite grades with migmatites in the upper structural levels.
In order to reconstruct the regional thermo-tectonic evolution of inverted metamorphic zonation, reliable geochronological data are essential.
U-Pb sensitive high resolution ion microprobe (SHRIMP) zircon geochronology on leucosomes from migmatitic orthogneisses were considered to estimate the age of peak metamorphic conditions, contemporaneous with anatexis. $^{40}Ar/^{39}Ar$ dating with step-heating technique on white mica from micaschists provided a temporal resolution with the potential to characterize shearing.
U-Pb ages of zircon rims extracted from migmatitic leucosomes specify regional partial melting during the Early Cretaceous (160-120 Ma). This is in disagreement with previous assertions, which argued that the formation of leucosomes in this region is Late Eocene (42-38 Ma) and implied multiple subductions and multiple metamorphic cycles during orogeny.
$^{40}Ar/^{39}Ar$ dating across the Nestos Shear Zone yields Late Eocene-Early Oligocene (40-30 Ma) cooling (~400-350 °C) ages, which correspond to local thermo-deformation episodes linked to late and post-orogenic intrusions. Garnet geospeedometry considers the kinetic response of minerals and allowed estimating the absolute time-dependent thermal evolution by diffusive element profiles in garnet. Preliminary results of Fe-Mg – Ca – Mn garnet diffusion modelling indicate very short timescale (~1 Ma) for peak metamorphic conditions in the Rhodope collisional system.

1.4

A chronology of internal wedge deformation constrained by strontium isotopes of carbonate veins

Armin Dielforder[1], Alfons Berger[1], Marco Herwegh[1], Hauke Vollstaedt[2,1]

[1] *Institute of Geological Sciences, University of Bern, Baltzerstrasse 1+3, CH-3012 Bern, Switzerland (armin.dielforder@geo.unibe.ch)*
[2] *Center for Space and Habitability, University of Bern, Sidlerstrasse 5, CH-3012 Bern, Switzerland*

Here we present a new approach to assess the conditions and relative timing of deformation within accretionary wedges by means of radiogenic strontium isotopes of vein carbonates. Our study area is located within the Paleogene accretionary complex of the central European Alps comprising a <5 km thick sequence of Upper Cretaceous to Eocene shelf sediments and syn-orogenic turbidites. We sampled different generations of carbonate veins that were formed during accretion related reverse faulting, nappe stacking, sediment compaction, folding, normal faulting, and extensional hydrofracturing. We show that the $^{87}Sr/^{86}Sr$ of these veins record the evolution from an initially seawater derived fluid toward a diagenetic-metamorphic fluid. Our approach enables us to resolve the conditions and relative timing of these different deformation events on a resolution that cannot be assessed by cross-cutting relationships solely.

1.5
Internal geometry in the Sesia Zone (Aosta Valley, Italy)

Francesco Giuntoli[1], Martin Engi[1], Paola Manzotti[2] & Michel Ballèvre [2]

[1] *Institut für Geologie, University of Bern, Baltzerstrasse 1+3, CH-3012 Bern, Switzerland (francesco.giuntoli@geo.unibe.ch)*
[2] *Université de Rennes, Géosciences Rennes, UMR-CNRS 6118, University of Rennes1, Rennes Cedex, France*

The Sesia Zone in the Western Alps is a HP terrain comprising fragments derived from the Adriatic continental margin. The classical subdivision of the Sesia Zone is based primarily on dominant lithotypes, as reflected in the names, from internal to external parts: *Eclogitic Micaschist Complex (EMC)*, *Seconda Zona Diorito-Kinzigitica (2DK)*, and *Gneiss Minuti Complex (GMC)*. Any effort to delineate the complex tectonic structure and understand its assembly must combine structural mapping of the polydeformed terrain with a sufficiently detailed analysis of its polymetamorphic record (e.g. Gosso, 1977).

Such attempts have been made (Babist et al., 2006) and have again recognized three (slightly different) main units / nappes. However, recent petrochronological and structural work in what was considered one internal unit has revealed that it comprises at least two tectonic slices that experienced substantially different PTdt-evolutions (Regis et al., 2014). While the boundaries between these slices have proven difficult to localize, Regis' study made it clear that further work is required to delineate contacts among such subunits and to quantify the PTdt-evolution for each of them. Understanding such a complex terrain demands an approach that is regional in scope, uses state-of-the-art techniques to analyze select samples, and integrates the results into a tectonic model.

Regional detailed petrographic and structural mapping (1:3k to 1:10k) was therefore undertaken with extensive sampling for petrochronological analysis. Based on this work, a first tectonic scheme is proposed here for the Sesia Zone between the Aosta Valley and Val d'Ayas, where all three classically recognized units are present in excellent outcrops. Some of this area already had been mapped by Passchier et al (1981), Vuichard (1989) and Stünitz (1989), but no consensus exists on the location and geometry of units. In view of the structural complexity and variable metamorphic overprint, a set of sober criteria was developed and applied, aiming to delimit the first order tectonic units. The approach rests on three criteria, and these have proven useful for the purpose: (1) Discontinuously visible metasedimentary trails, primarily of carbonates, (2) mappable high-strain zones; and (3) visible differences in the metamorphic imprint. Each of these, taken alone, may pose problems. For instance, certain metasediments are clearly polycyclic (containing HT relics of Paleozoic age), but others seem to be monometamorphic, as they resemble Mesozoic lithotypes and show no HT relics; some shear zones show evidence of reactivation and thus are difficult to correlate; retrograde effects occurring at cm- to km-scale variably affect the early HP-imprint. Therefore, none of the key features used are by themselves sufficient, but in combination they allow us to propose a new map that delimits ten sizeable units: some are lens-shaped, whereas others are laterally more uniform, but all of them comprise various lithotypes.

We propose an **Internal Complex with** three eclogitic sheets, each 0.5–3 km thick, from internal to external: *Croix Courma sheet*, *Loses Blanches sheet*, *Preal sheet.* Dominant lithotypes include micaschists associated with mafic rocks and minor orthogneiss. The main foliation is of HP, dipping moderately NW. Each of these sheets is bounded by (most likely monometamorphic) sediments, 10–50 m thick. HP-relics (of eclogite facies) are widespread, but a greenschist facies overprint locally is strong close to the tectonic contact to the neighboring sheet.
An **Intermediate Complex** lies external to the *Preal sheet* and comprises two thinner units called slices: the *Simonetta-Pian slice* is composed of siliceous dolomite marbles, meta-granites and -diorites with few mafic boudins. The main foliation dips SE and is of greenschist facies, but omphacite, glaucophane and garnet occur as relics. Towards the W (east of Mont Crabun), this slice makes way to a strongly dismembered package that is considered to be a *shear zone*: Glaucophane-garnet-phengite gneiss and minor orthogneiss bands are found repeatedly interleaved with impure dolomitic marbles. Gneiss fragments vary in thickness from centimeters to several meters, with phengite ± glaucophane- orthogneiss locally forming lenses within the marbles. The entire Intermediate Complex, some 500 meters wide on the ridge between Mont Crabun and Prial, is reduced to a few meters towards SW. The main greenschist foliation dips moderate SE but a previous HP foliation, marked by glaucophane and phengite, is still recognizable; it lies parallel to the younger one.

In the **External Complex**, several discontinuous lenses of 2DK-lithotypes occur, and these are aligned with greenschist facies shear zones mapped within the GMC. By combining these features, three main sheets can be delimited (from internal to external: *Crabun sheet*, *Dondeuil sheet* and *Chasten sheet)*. The main foliation in all of these is of greenschist facies; it dips moderately SE. Fragments of 2DK gneiss collectively outline two tectonic slices wedged in between the above three sheets: *Aquila-Lago slice* and *Nery-Torché slice*.

Petrological work and *in situ* U-Th-Pb dating of accessory phases is underway to reconstruct the PTDt-history of several of these subunits of the Sesia Zone.

REFERENCES
Babist, J., Handy, M.R., Hammerschmidt, K., Konrad-Schmolke, M., 2006. Precollisional, multistage exhumation of subducted continental crust: The Sesia Zone, western Alps. Tectonics 25.
Gosso, G., 1977. Metamorphic evolution and fold history in the Eclogitic Micaschists of the upper Gressoney valley (Sesia-Lanzo Zone, Western Alps). Rend. Soc. It. Min. Petr. 33, 389-407.
Passchier, C.W., Urai, J.L., van Loon, J., Williams, P.F., 1981. Structural geology of the central Sesia Lanzo Zone. Geologie en Mijnbouw 60, 497–507.
Regis, D., Rubatto, D., Darling, J., Cenki-Tok, B., Zucali, M., Engi, M., 2014. Multiple metamorphic stages within an eclogite-facies terrane (Sesia Zone, Western Alps) revealed by Th-U-Pb petrochronology. Journal of Petrology 55, 1429-1456.
Stünitz, H., 1989. Partitioning of metamorphism and deformation in the boundary region of the ''Seconda Zona Diorito-Kinzigitica'', Sesia Zone, Western Alps. Dissertation, ETH Zürich, 244 p.
Vuichard, J.P., 1989. La marge Austroalpine durant la collision Alpine: Evolution tectonométamorphique de la zone Sesia Lanzo. Doctoral thesis, Rennes, 307 p.

1.6

On craton destruction: Insight from 2D thermal-mechanical numerical modeling

Jie Liao[1], Taras Gerya[1], & Qin Wang[2]

[1] *Geophysical Fluid Dynamics, Institute of Geophysics, ETH Zurich, Sonneggstrasse 5, CH-8092, Zurich, Switzerland (jie.liao@erdw.ethz.ch)*
[2] *State Key Laboratory for Mineral Deposits Research, Department of Earth Sciences, Nanjing University, Nanjing, China.*

Although most cratons maintain stable, some exceptions are present, such as the North China craton, North Atlantic craton, and Wyoming craton, which have experienced dramatic lithospheric deformation/thinning. Mechanisms triggering cratonic thinning remains enigmatic [Lee et al., 2011]. Using a 2D thermo-mechanical coupled numerical model [Gerya and Yuen, 2007], we investigate two possible mechanisms: (1) stratification of cratonic lithospheric mantle [Liao et al., 2013; Liao and Gerya, 2014], and (2) rheological weakening due to hydration.

Lithospheric mantle stratification is a common feature in cratonic areas which has been demonstrated by geophysical and geochemical studies [Thybo and Perchuc, 1997; Griffin et al., 2004; Romanowicz, 2009; Rychert and Shearer, 2009; Yuan and Romanowicz, 2010]. The influence of lithospheric mantle stratification during craton evolution remains poorly understood. A rheologically weak layer representing hydrated and/or metasomatized composition is implemented in the lithospheric mantle. Our results show that the weak mantle layer changes the dynamics of lithospheric extension by enhancing the deformation of the overlying mantle and crust and inhibiting deformation of the underlying mantle [Liao et al., 2013; Liao and Gerya, 2014]. Modeling results are compared with North China and North Atlantic cratons. Our work indicates that although the presence of a weak layer may not be sufficient to initiate craton deformation, it enhances deformation by lowering the required extensional plate boundary force.

Rheological weakening due to hydration is a possible mechanism triggering/enhancing craton deformation, especially for cratons juxtaposing with subduction zones, since water can release from subducting slabs. We investigate the influence of wet mantle flow laws [Hirth and Kohlstedt, 2003], in which a water parameter (i.e. constant water content) is involved. Our results show that wet dislocation alone does not accelerate craton deformation significantly. However, if wet diffusion creep is incorporated, combined effect of wet dislocation and wet diffusion creeps enhance lithosphere deformation dramatically. Lithospheric material drips off rapidly from the lithosphere base to asthenosphere, and thins lithosphere by ~ 40 km.

REFERENCES
Fischer, K. M., H. A. Ford, D. L. Abt, and C. A. Rychert (2010), The lithosphere-asthenosphere boundary, Annu. Rev. Earth Planet. Sci., 38, 551–575, doi:10.1146/annurev-earth-040809-152438.
Gerya, T. V., and D. A. Yuen (2007), Robust characteristics method for modelling multiphase visco-elasto-plastic thermo-

mechanical prob- lems, Phys. Earth Planet. Inter., 163, 83–105, doi:10.1016/j.pepi.2007. 04.015.
Griffin, W. L., S. Y. O'Reilly, B. J. Doyle, N. J. Pearson, H. Coopersmith, K. Kivi, V. Malkovets, and N. Pokhilenko (2004), Litho- sphere mapping beneath the North American plate, Lithos, 77, 873–922, doi:10.1016/j.lithos.2004.03.034.
Hirth, G., and D. L. Kohlstedt (2003), Rheology of the upper mantle and the mantle wedge: a view from the experimentalists, in Inside the Subduction Factory, edited by J. E. Eiler, pp. 83–105, American Geophysical Union, Washington, DC.
Lee, C.-T. A., P. Luffi, and E. J. Chin (2011), Building and de- stroying continental mantle, Annu. Rev. Earth Planet. Sci., 39, 59–90, doi:10.1146/annurev-earth-040610-133505.
Liao, J., and T. Gerya (2014), Influence of lithospheric man- tle stratification on craton extension: Insight from two-dimensional thermo-mechanical modeling, Tectonophysics, In Press, doi:10.1016/j.tecto.2014.01.020.
Liao, J., T. Gerya, and Q. Wang (2013), Layered structure of the lithospheric mantle changes dynamics of craton extension, Geophys. Res. lett., 40, 1–6, doi:10.1002/2013GL058081.
Rychert, C. A., and P. M. Shearer (2009), A global view of the lithosphere-asthenosphere boundary, Science, 324(5926), 495–497, doi:10.1126/science.1169754.
Rychert, C. A., and P. M. Shearer (2009), A global view of the lithosphere-asthenosphere boundary, Science, 324(5926), 495–497, doi:10.1126/science.1169754.
Thybo, H., and E. Perchuc (1997), The seismic 8ı discontinuity and partial melting in continental mantle, Science, 275(5306), 1626–1629, doi:10.1126/science.275.5306.1626.
Yuan, H., and B. Romanowicz (2010), Lithospheric layering in the North American craton, Nature, 466, 1063–1068, doi:10.1038/nature09332.

1.7

The tectonometamorphic evolution of the Sesia – Dent Blanche nappes (internal Western Alps)

Paola Manzotti[1], Michel Ballèvre[1], Michele Zucali[2], Martin Robyr[3], Martin Engi[3]

[1] *Géosciences Rennes, UMR-CNRS 6118, Universitè de Rennes1, 35042 Rennes Cedex, France (paola.manzotti@univ-rennes1.fr)*
[2] *Dipartimento di Scienze della Terra «Ardito Desio», Università degli Studi di Milano, Via Mangiagalli 34, 20133 Milano, Italy*
[3] *Institute of Geological Sciences, University of Bern, Baltzerstrasse 1+3, 3012 CH Bern, Switzerland*

This study reviews and synthesizes the present knowledge on the Sesia – Dent Blanche nappes, the highest tectonic elements in the Western Alps, which comprise pieces of pre-Alpine basement and Mesozoic cover. All of the available data are integrated in a crustal-scale kinematic model with the aim to reconstruct the Alpine tectono-metamorphic evolution of the Sesia – Dent Blanche nappes. Although major uncertainties remain in the pre-Alpine geometry, the basement and cover sequences of the Sesia - Dent Blanche nappes are seen as part of a thinned continental crust derived from the Adriatic margin.

The earliest stages of the Alpine evolution are interpreted as recording late Cretaceous subduction of the Adria-derived Sesia - Dent Blanche nappes below the South-Alpine domain. During this subduction, several sheets of crustal material were stacked and separated by shear zones that rework remnants of their Mesozoic cover. The recently described Roisan-Cignana Shear Zone of the Dent Blanche Tectonic System (Manzotti et al 2014) represents such a shear zone, indicating that the Sesia – Dent Blanche nappes represent a stack of several individual nappes. During the subsequent subduction of the Piemonte-Liguria Ocean large-scale folding of the nappe stack (including the Roisan-Cignana Shear Zone) took place under greenschist facies conditions, which indicates partial exhumation of the Dent Blanche Tectonic System. Finally, the entrance of the Briançonnais micro-continent within the subduction zone led to a drastic change in the deformation pattern of the Alpine belt, with rapid exhumation of the eclogite-facies ophiolite-bearing units and thrust propagation towards the foreland. Slab breakoff probably was responsible for allowing partial melting in the mantle and Oligocene intrusions into the most internal parts of the Sesia - Dent Blanche nappes. Finally, indentation of the Adriatic plate into the orogenic wedge resulted in the formation of the Vanzone back-fold, terminating the pervasive ductile deformation within the Sesia - Dent Blanche nappes during the earliest Miocene.

REFERENCES

Manzotti, P., Zucali, M., Ballèvre, M., Robyr, M., Engi, M. 2014: Geometry and kinematics of the Roisan-Cignana Shear Zone, and the orogenic evolution of the Dent Blanche Tectonic System (Western Alps), Swiss Journal of Geosciences, 107, DOI 10.1007/s00015-014-0157-9

1.8

New age constraints for the geodynamic evolution of the Sistan Suture Zone, eastern Iran

Ali Mohammadi[1], Jean-Pierre Burg[1], Jonas Ruh[1], Albrecht von Quadt[2], Irena peytcheva[2]

[1] *Department of Earth sciences, Geological Institute, ETH Zurich, Sonneggstrasse 5, 8092, Zurich, Switzerland (ali.mohammadi@erdw.ethz.ch)*
[2] *Department of Earth sciences, Institute of Geochemistry and Petrology, ETH Zurich, Clausiusstrasse 25, 8092, Zurich, Switzerland*

The N–S trending Sistan Suture Zone (SSZ) in eastern Iran is attributed to eastward subduction beneath the Afghan continental block of an inlet of the Mesozoic Tethys Ocean. We present U-Pb zircon crystallization ages combined with petrography, major and trace element analyses, Hf isotopes, Rb-Sr and Sm-Nd isotopes of intermediate to granitic intrusions stretched along the southern segment of the SSZ. We obtained two clearly separated clusters of concordant ages, which are taken as the crystallization age of the host plutonic rocks. The first cluster, between ca 42.5 and ca 44.5 Ma from euhedral zircons of the main granodiorite to diorite and related dykes. The second age cluster span from ca 28.3 to ca 31 Ma. These ages were obtained for granites and dykes, the latter being consistently slightly younger than the country rock. The high SiO_2 content (62-75 wt %) of Eocene magmatic rocks points to melts with a high crustal contribution in consistency with their relatively high-K (3-4.4 wt %) calc-alkaline nature. The high SiO_2 and K contents in the Oligocene calk-alkaline rocks series shows adakite-like fractionation. Oligocene adakite-like rocks have relatively low to medium $^{87}Sr/^{86}Sr$ and $^{143}Nd/^{144}Nd$ ratios, which are similar to typical lower thick crust-derived adakites. The mix positive and negative $\varepsilon Hf_{(T)}$ values of all zircons from the 42.5-44.5 Ma shows mix nature of magma (the contamination of subduction related magma with partial melting of crust). The positive $\varepsilon Hf_{(T)}$ values of all zircons from the 28-31 Ma adakite-like rocks indicate that the magma was not produced from pure depleted mantle. Instead, they are consistent with a host magma source within a largely juvenile and subduction-related mafic lower crust. Eocene granitoids represent anatectic melts emplaced at higher crustal levels; in addition slab melts modified the mantle wedge and subsequent, contaminated mantle magmas fed intrusions such as the Zahedan diorite.

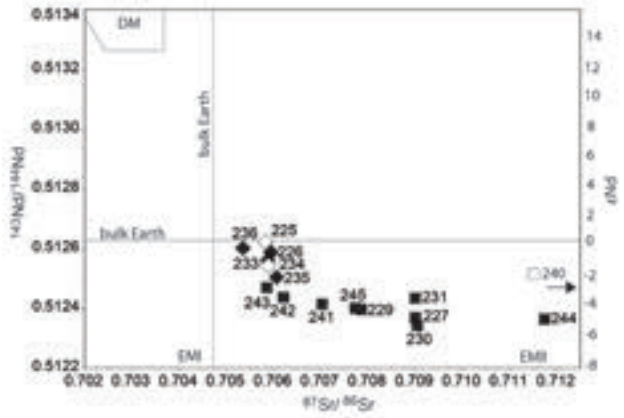

Figure 1. Plot of $^{143}Nd/^{144}Nd$ ratios versus $^{87}Sr/^{86}Sr$ ratios for comparison of Sr-Nd isotope compositions between Zahedan adakites and Zahedan and Shah Kuh magmatic rocks. DM: depleted mantel, EMI: enriched mantle type I has lower $^{87}Sr/^{86}Sr$; EMII: enriched mantle type II has higher $^{87}Sr/^{86}Sr$ (>0.720).

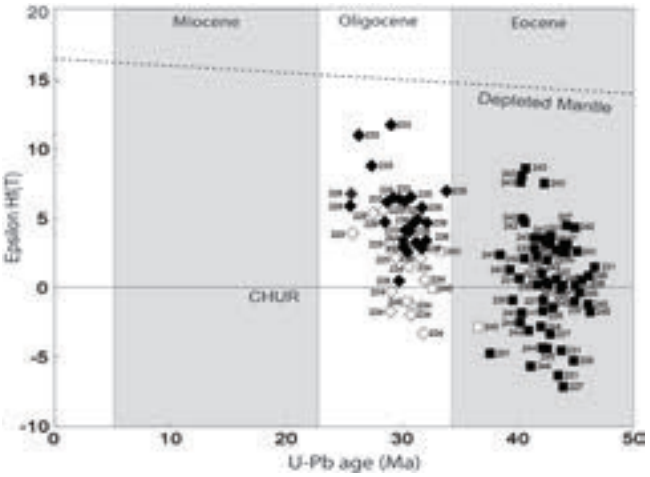

Figure 2. Plot of epsilon-$Hf_{(T)}$ versus $^{206}Pb/^{238}U$ age (Ma) for Zahedan and Shah Kuh granitoids and dykes. Corrections in function of age are based on chondritic values (CHUR), which become the reference value.

1.9

Recurrence behavior of destructive earthquakes in Western Anatolia, Turkey: Insights from cosmogenic ^{36}Cl dating method

Nasim Mozafari Amiri[1], Dmitry Tikhomirov[1], Ökmen Sümer[2], Çağlar Özkaymak[3], Bora Uzel[2], Susan Ivy-Ochs[4], Christof Vockenhuber[4], Hasan Sözbilir[2], Naki Akçar[1]

[1] *Institute of Geological Sciences, University of Bern, Baltzerstrasse 1-3, 3012 Bern, Switzerland (nasim.mozafari@geo.unibe.ch)*
[2] *Department of Geological Engineering, Dokuz Eylül University, 35160 İzmir, Turkey*
[3] *Department of Geological Engineering, Afyon Kocatepe University, Ahmet Necdet Sezer Kampusü, 03200 Afyonkarahisar, Turkey*
[4] *Swiss Federal Institute of Technology, Institute for Particle Physics, Otto-Stern-Weg 5, 8093 Zürich, Switzerland*

Instrumental records of destructive earthquakes in the Eastern Mediterranean and Middle East are only available for the last century and the historical ones date back only to 464 B.C. These are essential in order to assess how often significant earthquakes occur in a seismic-prone area and to forecast destructive events. However, since the major faults generally have return period of several hundreds of years, the time span of present seismic records is not long enough to precisely evaluate recurrence interval.

In this study, we focused on the normal faults within the graben systems of Western Anatolia in order to evaluate the earthquake recurrence time and reconstruct the paleoseismic history by employing fault scarp dating with cosmogenic ^{36}Cl. Deformation pattern in the Western Anatolia region is governed by E-W trending major grabens of Gediz, Küçük Menderes, Büyük Menderes and Gökava, as a result of roughly N-S extensional regime since early Miocene. There, large scale normal faults are built in limestone with evidence of ruptures during the Pleistocene-Holocene, which generally separate high-topographic pre-Neogene rock units from shallow Quaternary basins.

Our results from Priene-Sazlı Fault segment in the westernmost part of Büyük Menderes graben indicate destructive earthquakes in Holocene, in concordance with existing earthquake records. This yields a regular recurrence interval of approximately 2000 years. Further north, the combination of historical records and paleoseismological data with fault-scarp dating of Manisa and Mugirtepe faults in Gediz graben shows an irregular recurrence time, which is decreasing through the time.

To improve our understanding of seismic behaviour of Western Anatolia since the Late Pleistocene, Kalafat and Yavansu faults within Büyük Menderes graben in SE of *Kuşadası* residential area, Ören fault scarp within Gökava graben close to Kemerköy thermal power plant as well as Rahmiye fault in Akhisar urban area were sampled and their analysis is in progress.

1.10

Numerical bifurcation study of the initiation of folding and necking in elasto-visco-plastic rocks

Peters Max[1], Veveakis Manolis[2], Poulet Thomas[2], Regenauer-Lieb Klaus[2,3] & Herwegh Marco[1]

[1] *Institute of Geological Sciences, University of Bern, Switzerland*
[2] *CSIRO Earth Science and Resource Engineering, Kensington, Western Australia*
[3] *School of Earth and Environment, The University of Western Australia*

Folding and boudinage of a competent layer embedded in a mechanically weaker matrix are commonly thought to exclusively develop due to interactions arising from geometry. However, there exists an additional localization phenomenon, i.e. strain localization out of steady state in a homogeneous material for a critical material parameter (set) or deformation rate. This theory is closely associated with strain localization due to ductile shear heating of viscous materials, as is the case for creeping calcite at shallow to mid-crustal levels.

We present a numerical setup which accounts for grain size variations, using the paleowattmeter relationship of Austin and Evans (2007). This scaling theory has recently been numerically implemented into a thermo-mechanical framework (Herwegh et al., 2014). In a first step, we identify the parameter set for bifurcation, which is the critical amount of dissipation over the diffusive capacity of the system, defined by the *Gruntfest* number (Gruntfest, 1963). This number incorporates flow stress, the *Arrhenius* number (*Q*/*RT*) and the layer dimensions. We verify the robustness of the solution through an analysis of the system's sensitivity to material instabilities (Rudnicki and Rice, 1975). This second step aims at identifying the eigenfrequencies and natural mode shapes of the geometric structure and material parameters. In a third step, the eigenmodes are perturbed and superposed to the initial conditions. We then subject the composite structure to natural deformation conditions. Grain sizes within the layer relatively quickly equilibrate to a homogeneous state, which is in response to energy optimization following the paleowattmeter relationship. Upon continued loading, localization in terms of a necking or folding instabilities interestingly arise out of this steady state.

We obtain the criteria for the onset of localization from theory and numerical simulation, i.e. the critical *Gruntfest* number. Boudinage and folding instabilities occur when the mechanical work, which is translated into heat, overcomes the diffusive capacity of the system. Both instabilities develop for the exact same *Arrhenius* and *Gruntfest* numbers. We conclude that folding and boudinage instabilities can be placed at the same material behavior due to fundamental energy bifurcations triggered by dissipative work out of homogeneous state.

REFERENCES

Austin, N. and Evans, B. (2007). Paleowattmeters: A scaling relation for dynamically recrystallized grain size. Geology, 35.

Gruntfest, I.J. (1963). Thermal feedback in liquid flow; plane shear at constant stress. Transactions of the Society of Rheology, 7.

Herwegh, M., Poulet, T., Karrech, A. and Regenauer-Lieb, K. (in review). From transient to steady state deformation and grain size: A thermodynamic approach using elasto-visco-plastic numerical modeling. Journal of Geophysical Research.

Regenauer-Lieb, K. and Yuen, D. (2004). Positive feedback of interacting ductile faults from coupling of equation of state, rheology and thermal-mechanics. Physics of the Earth and Planetary Interiors, 142.

Rudnicki, J. W., Rice, J. R., 1975. Conditions for the localization of deformation in pressure-sensitive dilatant materials. Journal of Mechanics and Physics of Solids 23.

1.11

Recent movements in the Alps: geodetic and GPS derived data

O.Adrian Pfiffner & Nicolas Deichmann

The precise leveling data of swisstopo (e.g. Schlatter et al. 2005) show that the Alps are rising at a faster rate as compared to the Northalpine foreland. Relative to the fix point Aarburg the Central Alps are rising at around 1 mm/yr with two maxima in Graubünden and the Valais where rates of up to 1.5 mm/yr are reported. Whereas these uplift rates compare to the ones reported from the Austrian Alps, much higher rates have been published in the French Alps and the Southern Alps of Italy (Arca & Beretta, 1985). In a cross-section from Black Forest – Lucerne – Po Basin the rates as measured by the Swiss network drops across the Insubric Fault; at the junction with the Italian data a major discontinuity arises with rates being at least 1 mm/yr higher in the Southern Alps.

Considering the satellite derived uplift rates of the AGNES permanent network, the difference of uplift rates between the Northalpine Foreland to the Alps is also evident and more than 1 mm/yr. Interstingly the absolute rates of the GNNS data within the Alps are about 1.2 mm/yr higher as compared to the leveling data. Since the area of northern Switzerland (including Aarburg) is rising by about 1.2 mm/yr relative to the stable part of the European plate, the absolute uplift rate in the Alps must be even higher and might attain values of 3 mm/yr. The vertical uplift rates are in stark contrast to the horizontal velocities determined from the satellite derived data. The latter suggest a southward component of the Northalpine foreland of 0.2 mm/yr and a northward component of 0.35 mm/yr of the stations within the Alps if the above mentioned cross-section is considered. The resulting convergence rate of 0.5 mm/yr is much lower that the vertical uplift rate, indicating that the latter are likely to contain a component of large-scale buoyant rise. In map view the horizontal motions point to an extension parallel to the Alpine orogeny.

The uplift rates as determined from precise leveling show a high gradient across the Subalpine Molasse in the cross-section considered here. This corresponds to the latest thrust faulting within the Alpine orogen, the age of which is as young as 8 Ma. Interestingly, the apatite cooling ages are younger than 8 Ma in the areas of the two uplift maxima of Graubünden and Valais. It thus seems that the present day motions might reflect a continuation of the Neogene deformation.

The Subalpine Molasse also marks a transition from the foreland, where hypocenters of earth quakes are concentrated within the lower crust (Singer et al., 2014), and the Alpine orogen where hypocenters are restricted to the uppermost 10-15 km (Deichmann et al. 2000). Focal mechanisms sustain a component of NNW-SSE to NW-SE directed compression in the Alpine foreland in the Alps of central Switzerland, as opposed to an NE-SW extension within the Alps of Graubünden and N-S extension in the Valais.

REFERENCES:

Arca, S. & Beretta, G.P., 1985, Prima sintesi geodetico-geologica si movimenti verticali del suolo nell'Italia Settentrionale (1987-1957). – Bolletino di geodesia e scienze affini, N. 2, Anno XLIV, p. 125-156.

Brockmann, E., Ineichen, D., Marti, U., Schaer, S., Schlatter, A. & Villiger, A., 2012, Determination of Tectonic movements in the Swiss Alps using GNSS and fLevelling. In: Kenyon et al. (Eds.) Geodey for Planet Earth, International Association of Geodesy Symposia 136, DOI 10.1007/978-3-642-20338-1_85.

Deichmann, N., Ballarin Dolfin, D. & Kastrup, U. (2000): Seismizität der Nord- und Zentralschweiz. Nagra Technischer Bericht NTB 00-05. Nagra, Wettingen.

Schlatter, A., Schneider, D., Geiger, A. & Kahle, H.-G., 2005, Recent vertial movements from precise levelling in the vicinity of the city of Basel, Switzerland. – Int. J. Earth Sci (Geol Rundsch), 94, 507-514

1.12

Tectonics of the Monte Rosa nappe: Tertiary phases of subduction and thrusting in the Pennine Alps

Albrecht Steck[1], Henri Masson[1], Martin Robyr[2]

[1] *Institut des Sciences de la Terre, University of Lausanne, Geopolis, CH-1015 Lausanne*
[2] *Institut für Geologie, University of Bern, Baltzerstrasse 1-3. CH-3012 Bern*

The Monte Rosa basement fold nappe, surrounded by other continental units of the Briançonnais s.l. domain and ophiolites of the Piemont Ocean, represents a major structure of the Pennine Alps situated at the border of the Canton Valais (Switzerland) and Italy. The Central Alps were formed during the collision and SE-directed underthrusting of the European below the Adriatic plate by successive underthrusting, detachment and accretion of the Austroalpine Sesia continental crust, the Piemont oceanic crust and the continental Briançonnais-Europe plate border. The 90-60 Ma Sesia high-pressure metamorphism, followed by the 50-38 Ma Zermatt-Saas Fee and Monte Rosa high-pressure metamorphism and since 40 Ma by the Barrovian regional metamorphism reveal of a long-lasting Alpine evolution during convergence of both plates. The superposition of the ultra-high pressure Zermatt-Saas Fee ophiolites by the continental Cimes Blanche unit of the Briançonnais domain and the medium pressure ophiolitic Tsaté nappe is explained by delamination and tectonic flake detachment of the Cimes Blanches from the Briançonnais crust and its south directed thrust over the Zermatt-Saas Fee ophiolites. The main ductile deformational structures, related to the NW-directed nappe emplacement, were generated after 40 Ma under greenschist to amphibolite facies Barrovian orogenic metamorphism. Early extrusional structures have been transposed by the younger thrust structures. The NW-directed thrust of the Alps was accompanied since about 35 Ma by ductile dextral shear and back folding in the zone of dextral transpression between the converging European and Adriatic plates.

REFERENCES

Escher, A., 1988: Structure de la nappe du Grand Saint-Bernard entre le val de Bagnes et les Mischabel. Rappords géologiques du Service hydrogéologique et géologique national, 7, 26 pp.

Genier, F., Epard, J.L., Bussy, F., & Magna, T. 2008: Lithostrtatigraphy and U-Pb dating in the overturned limb of the Siviez-Mischabel nappe; a new key for the middle Penninic nappe geometry. Swiss Journal of Geosciences, 101, 431-452.

Pleuger, J., Froitzheim, N., & Jansen, E. 2005: Folded continental and oceanic nappes on the sothern side od Monte Rosa (Western Alps, Italy): Anatomy of double collision suture. Tectonics, 24, TC 4013, doi: 10.1029/2004TC001737.

Sartori, M. 1987: Structure de la zone du Combin entre les Diasblons et Zermatt (Valais). Eclogae geologicae Helvetiae, 80, 789-814.

Steck, A. & Hunziker, J. 1994: The Tertiary structural and thermal evolution of the Central Alps-compressional and extensional structures in an orogenic belt. Tectonophysics, 238, 229-254.

Steck, A., 2008: Tectonics of the Simplonmassif and the Lepntine gneiss dome: deformation structures due to collision between the underthrusting European plate and the Adriatic indenter. Swiss Journal of Geosciences, 101, 515-543.

Steck, A., Della Torre F., Keller, F., Pfeifer, H.R., Hunziker, J. & Mason H., 2013: Tectonics of the Lepontine Alps: ductile thrusting and folding in the deepest tectonic levels of the Central Alps.. Swiss Journal of Geosciences, 106, 427-450.

1.13

4D Modeling of Transfer Zones in Continental Rifts

Frank Zwaan[1], Guido Schreurs[1]

[1] *Institute of Geological Sciences, University of Bern, Baltzerstrasse 1, CH-3012 Bern (frank.zwaan@geo.unibe.ch)*

INTRODUCTION

Inherited structures in the Earth's crust represent weak zones along which deformation will focus during subsequent extension. To develop a full-scale rift system, such initial faults will connect trough transfer zones. Previous studies (eg. Acocella et al., 1999) have focused on the modeling of these transfer zones and their geometries, but our study improves upon them by: 1) Modeling the entire continental crust; 2) Applying a more distributed type of deformation.

MODEL SET-UP & METHODS OF ANALYSIS

The experimental machine consists of two rigid sidewalls with a base of alternating plexiglass and foam bars in between (Fig. 1). By moving the sidewalls apart, the foam expands and fills the extra space. This allows a uniform deformation at the base of the overlying material. In addition, one of the base plates can move laterally, allowing strike-slip and transtensional set-ups.

Sand and silicone are used to represent the Earth's crust. Lines of silicone on top of the basal silicone form pre-existing weak zones that localize deformation. Several models are analyzed with X-ray tomography (CT scanning, Fig. 1B and Fig. 3) to reveal the 3D evolution of internal structures with time (hence 4D).

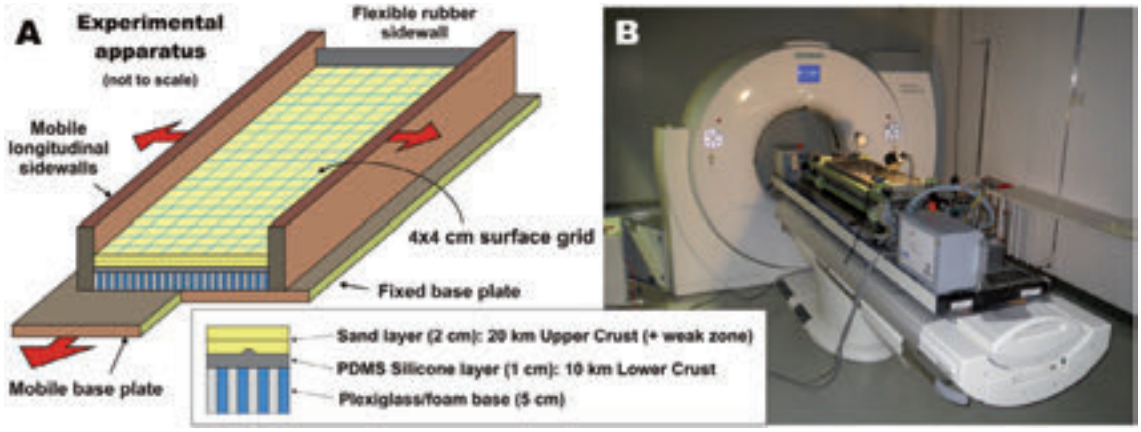

Figure 1. A: Model set-up for distributed deformation. B: CT-scanner installation.

RESULTS

Localizing deformation along weak zones works well, all models developed distinct rift structures (selection in Fig. 2). However, several models have no linkage between both rift zones. In this model set-up and contrary to previous studies, successful linkage is due to rift zone proximity instead of a connecting pre-existing weak zone. The strike-slip in the transtensional models created oblique features, perpendicular to the overall extensional direction, and a lateral displacement along the main rift. It is also clear that CT techniques offer promising potential for thorough model analysis (Fig. 3).

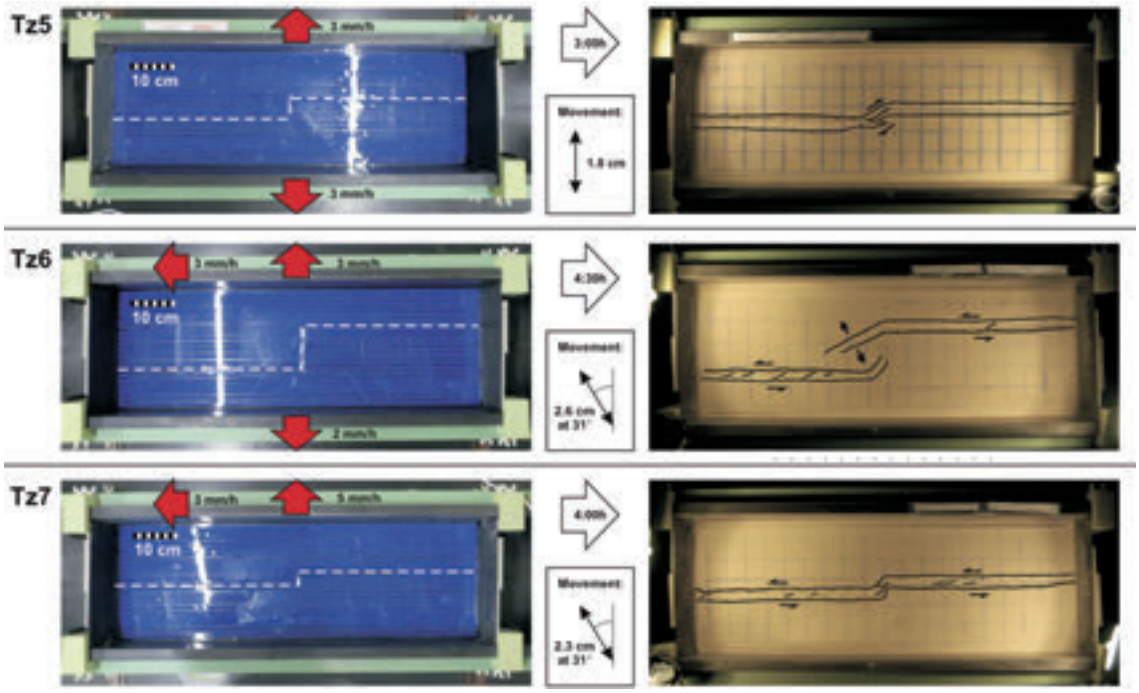

Figure 2. L: Model set-up (without sand cover) with weak zone geometry (white dotted lines) and deformation vectors (red arrows). R: resulting structures.

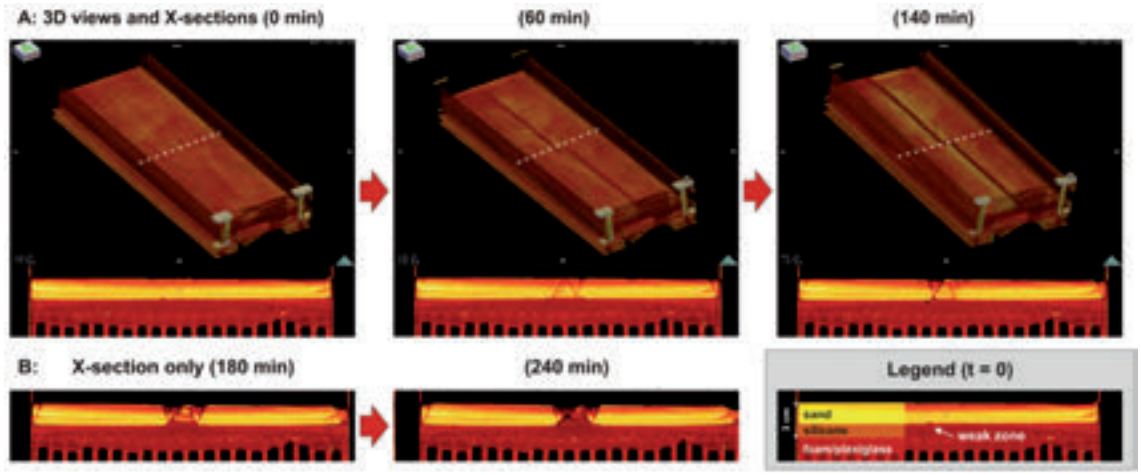

Figure 3. CT Imaging: A) 3D views of model Tz7, showing surface deformation with time; B) Sections of model Tz7 (location shown with dotted lines in A).

FUTURE MODELING

Future work within this project will focus on transtensional settings: testing different plate geometries and modeling of natural examples. Also collaboration with colleagues from the numerical domain will be arranged, to fully combine and exploit the possibilities of both sides of the modeling spectrum.

REFERENCES

Acocella, V., Faccenna, C., Funiciello, R., Rossetti, F. 1999: Sand-box modelling of basement-controlled transfer zones in extensional domains. Terra Nova 11, 149-156.

P 1.1

Detrital zircon grains in blueschist-facies meta-conglomerates: implications for the early Permian geomorphology of the future northern margin of the Liguria-Piemonte ocean

Michel Ballèvre[1], Paola Manzotti[1], Marc Poujol[1]

[1] *Géosciences Rennes, UMR-CNRS 6118, Universitè de Rennes1, 35042 Rennes Cedex, France (michel.ballevre@univ-rennes1.fr)*

In the Western Alps, the Money Complex of the Gran Paradiso Massif, metamorphosed under blueschist facies during the Alpine cycle, is considered to be Permo-Carboniferous in age, but no palaeontological or radiometric data constrain this interpretation.

A revision of the lithostratigraphy of the Money Unit allows recognizing a polygenic (graphite-rich) and a monogenic (graphite-poor) meta-sedimentary formation. Detrital zircon U-Pb geochronology in both meta-sedimentary formations shows that (i) the main population is Cambrian and Ordovician in age, (ii) the youngest grains are Silurian and Early Devonian and (iii) Carboniferous zircon grains are lacking.

A careful study of the age distributions in the Alps suggests that potential source for the detrital material in the Money Complex is the Briançonnais basement. Late Carboniferous magmatism is widespread in the Helvetic Zone of the Alps. Permian magmatism is dominant in the Briançonnais, the Austroalpine and the Southalpine unit. The lack of Carboniferous zircons in the Money Complex suggests that the detritus was not shed from the Helvetic zone, which was separated from the Money basin by the Zone Houillère basin, where the main drainage pattern was developed from south to north and where the depocenters migrated northwards from the Namurian to the Stephanian.

We suggest that the Money Complex may had been located to the east of the main river drainage inside the Zone Houillère basin or alternatively may represent a small basin, located on the east of the Zone Houillère.

P 1.2

A new 1:100’000 scaled geological map of the Aar massif

Alfons Berger[1], Ivan Mercolli[1], Marco Herwegh[1], Edwin Gnos[2], Michael Wiederkehr[3], Antonia Wicki[1], Andreas Möri[3]

[1] *Institut für Geologie, University of Bern, Baltzerstr. 1+3, CH-3012 Bern (alfons.berger@geo.unibe.ch)*
[2] *Natural History Museum of Geneva, Route de Malagnou 1, CH-1208 Geneva*
[3] *Landesgeologie, Seftigenstrasse 264, CH - 3084 Wabern*

Over the past century, a vast number of spatially restricted but very detailed maps of the Aar massif were mapped, some of them already published in the Geological Atlas of Switzerland. By using the vector data of these maps, complemented with compilations that were created in the frame of the GeoCover project at swisstopo, we correlated lithologies, outcrop geometries and tectono-geodynamic units and harmonized them in the entire Aar massif. Harmonisation was done according to the principles of HARMOS in Switzerland (for details see HARMOS project at swisstopo) In combination with already existing compilations (Heim 1922, Labhart 1977, Oberhänsli et al. 1988, Abrecht 1994, Steck et al. 1999), these maps served as a base to construct the new map. We present the result in form of a new geological map of the complete Aar massif ranging from the Lötschental in the W to the Tödi area in the E.

We summarized the lithologies in following groups:
(1) Mesozoic-Cenozoic cover, (2) Carboniferous-(Permian) sediments and volcanics (Maderaner Group), (3) Middle Paleozoic metasediments (Cavardiras Group), (4) Asselian plutonic rocks (Central Aar group), (5) Pennsylvanian plutonic rocks (Brunni group), (6) Visean plutonic rocks (Tödi group) and (7) polycyclic basement units («Altkristallin»). The latter are subdivided into seven major groups: (7a) Innertkirchen-Lauterbrunnen zone, (7b) Erstfeldergneiss zone, (7c) Guttannen zone, (7d) Ofenhorn-Stampfhorn zone, (7e) Grimsel zone, (7f) Lötschnetal zone and (7g) Ausserberg-Avat zone. Originially, these groups were defined for local rock assemblages. Based on the new compilation, we can extend the continuation of

these groups over the complete massif. This spatial continuity of old polycrystalline gneisses, Variscan to post-Variscan plutonites and volcanoclastic rocks, together with Mesozoic sediments, characterizes the large-scale structure of the Aar massif. Particularly deformation stages in the Maderaner group and Mesozoic sediments permit to differentiate the several tectonic movements and to understand the kinematics and geodynamics of the Aar massif. The overlapping strike of the different structures is only possible by the reactivation of pre-existing structures at different times. The map will serve as a base for further reconstructions of tectonic evolution during Mesozoic and Alpine times.

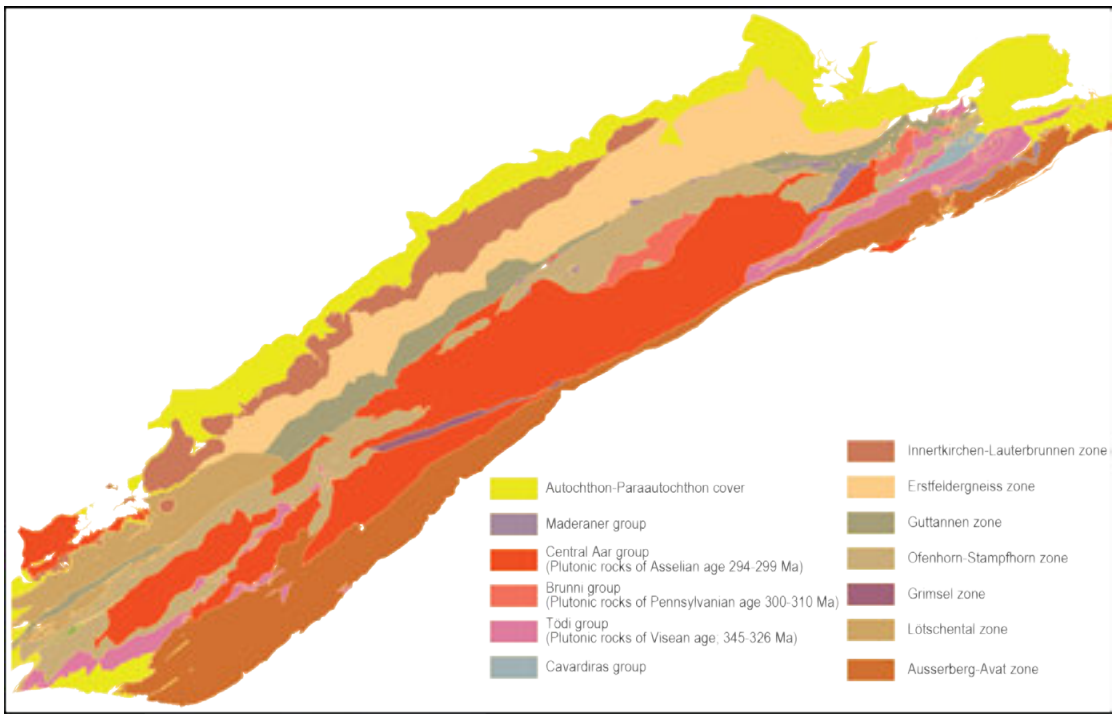

Figure 1. Sketch map of the Aar massif

REFERENCES

Abrecht, J. (1994) Geological units of the Aar massif and their pre-Alpine rock association: a critical review. Schweiz. Min. Petr. Mitt., 74, 5-27.

Heim, A. (1922): Geologie der Schweiz. 2 Bände. Leipzig, 1018 pp.

Labhart, T.P. (1977) Aarmassiv und Gotthardmassiv. 1-173 p. Gebrüder Borntraeger, Berlin.

Oberhänsli, R., Schenker, F. and Mercolli, I. (1988) : Indication of Variscan nappe tectonics in the Aar Massif. Schweiz. Min. Petr. Mitt., 68, 509-520.

Steck, A., Bigioggero, B., Dal Piaz, G.V., Escher, A., Martinotti, G. and Masson, H. (1999): Carte tectonique des Alpes de Suisse occidentale et des régions avoisinantes 1: 100'000, Carte géologique spéciale N. 123.

P 1.3

Do surface processes and/or the presence of an initial surface topography affect(s) the fold linkage? And if yes, how?

M. Collignon, N. Fernandez, B.J.P. Kaus.

Landscape geomorphology provides an indirect observation of the tectonic activity. Surface processes and tectonics interact one with another to create a wide variety of landscape. Geomorphic features such as wind gaps can record the amplification and lateral propagation of embryonic fold segments. Depending of their relative initial spacing, those growing fold segments can link and form long train folds. This mechanism has been suggested for the Zagros Folded Belt, where the axial lengths of folds can reach more than 100 km.

Previous studies have focused on fold linkage or on the response of the drainage network to tectonic forcing. Using seeds in their setup to prescribe the fold orientation, Grasemann and Schmalholz (2012) numerically investigated the distance between two isolated laterally propagating folds to explain the different modes of linkage. However, the effects of surface processes on the fold development have not been considered.

Our recent multilayer folding experiments, in which an initial random perturbation was prescribed, have shown that under efficient drainage network conditions, or when a non-zero initial topography was applied to the model, the type of fold linkage could be modified. In this study we systematically investigate the effects of surface processes on the mode of linkage and how the distance between two isolated growing perturbations, required for linkage, is affected.

In order to address this question, we use the 3D thermo-mechanical code LaMEM, which has been coupled to a finite-element based landscape evolution model (both erosion and sedimentation). The landscape evolution model uses a non-linear diffusion formulation (Simpson and Schlunegger, 2003) taking into account both hillslopes and channel processes.

REFERENCES

Graseman, B., and Schmalholz, S. M., 2012, Lateral fold growth and fold linkage: Geology, v. 40.

Simpson, G., and Schlunegger, F., 2003, Topographic evolution and morphology of surfaces evolving in repsonse to coupled fluvial and hillslope sediment transport: Journal of geophysical research, v. 108, p. 16p.

P 1.4

Thermo-mechanical shear localisation: length scale and thermal imprint

Thibault Duretz[1], Stefan M. Schmalholz[1], & Yuri Y. Podladchikov[1]

[1] *ISTE, University of Lausanne, rue de la Mouline, CH-1015 Lausanne (thibault.duretz@unil.ch)*

We present two-dimensional models of shear localization in geomaterials using laboratory derived flow laws. Under geologically relevant loading conditions, shear localisation is triggered by shear heating. The scale of such shear zones is physically controlled and hence does not depend on the numerical resolution. The width of such shear zones is the order of 1000 m, in agreement with some natural observations. A simple scaling law can be used to predict shear zone thicknesses and good agreement was obtained against systematic numerical models. We show the influence of non-linear and linear rheologies and investigate the impact of elasticity on the transient stages of shear localisation.

In a conservative system, shear localization takes place coevally with a temperature increase. We show that the thermal imprint is diffused across the shear zone whereas the strain remains localized inside the shear zone. Our results suggest that sharp temperature increases are not expected across shear zones, which is often observed in natural shear zones. This effect is amplified by taking into account a period of thermal relaxation after the deformation.

P 1.5

Kinematic analyses on multiply reactivated fault systems in the Black Forest – Hegau – Lake Constance region

Daniel Egli[1] & Jon Mosar[1]

[1] *Department of Geosciences, Université de Fribourg, Chemin du Musée 6, CH-1700 Fribourg, Switzerland (daniel.egli4@unifr.ch)*

The Black Forest – Hegau – Lake Constance region lies in a geodynamically particular position at the boundary zone of the Jura fold-and-thrust belt, the northern Alpine flexural Molasse basin and the uplifted Black Forest basement massif. The shallowly east-dipping flank of the Black Forest massif and its overlying sediments, comprise rocks ranging from pre-Mesozoic basement, Mesozoic cover units, Tertiary Molasse deposits to Quaternary cover, thus allowing insight into the sedimentary and tectonic evolution across a wide range of lithological levels. This zone can therefore serve as a natural laboratory for understanding the nature of the subsurface of the Swiss and German Molasse basin, which is a zone of high potential geo-economical interest. The tectonic framework of the study area is largely influenced by the combined effect of two major Cenozoic tectonic events, namely the uplift of the Black Forest Massif and the formation of the Molasse basin in the northern Alpine flexural foreland. In the southern Black Forest and its sedimentary cover, one can observe a dense network of differently oriented fault sets, with the dominating directions being NNE-SSW (Rhenic), WSW-ENE (Variscan) and WNW-ESE to NW-SE (Hercynian) (e.g. Geyer et al. 2011). Many of these faults are likely to have been initiated and to have a precursor from at least Late Variscan times and are thought to have been reactivated during the Cenozoic deformation events. Such pre-existing structures can have a strong influence on the local tectonic response to a regional stress field. Most deformation is localized along larger faults and fault zones, the Freiburg-Bonndorf-Bodensee fault zone (FBBFZ, e.g. Carlé 1955) being the most important one. This system of faults runs from the Upper Rhine Graben across the Black Forest massif into the region of Lake Constance, thereby connecting the volcanic fields of the Kaiserstuhl and the Hegau. Deformation is dominated by normal faulting, forming a series of graben structures. However, on a smaller scale, strike-slip movements very often reactivate former normal faults and transcurrent deformation appears to become more important with time. This study uses structural field data as well as map-view analysis of fault distribution in order to evaluate the timing and the differing kinematics of the region. Furthermore, the behaviour and effect of inherited structures, their surface expression and their potential for neotectonic activity is being investigated. Kinematic analysis of outcrop-scale features along the FBBFZ show a strong dependency of the fracture characteristics on the fault system and it is suggested that deformation in the area is strongly influenced by pre-existing structures and local stress perturbations in the vicinity of larger fault zones, which have to be considered carefully in the light of the larger geodynamic model.

REFERENCES

Geyer, M., Nitsch, E. & Simon, T. 2011: Geologie von Baden-Württemberg, Scheizerbart, Stuttgart, 627 pp.
Carlé, W. 1955: Bau und Entwicklung der südwestdeutschen Grossscholle, Geologisches Jahrbuch, Beihefte 16, 272 pp.

P 1.6

Neotectonic Activity at the Front of the Alps: Earthquake-induced Geomorphology in the Aare Valley & Lake Thun

Stefano C. Fabbri[1], Flavio S. Anselmetti[1], Marco Herwegh[1], Fritz Schlunegger[1], Stefan Volken[2], Andreas Möri[2]

[1] *Institute of Geological Sciences, University of Bern, Baltzerstrasse 1+3, CH-3012 Bern (stefano.fabbri@geo.unibe.ch)*
[2] *Bundesamt für Landestopografie swisstopo, Seftigenstrasse 264, CH-3084 Wabern*

Strong earthquakes (i.e. intensities >VI-VII) are considered as main triggers of subaquatic slope failures apart from collapsing shorelines and deltas due to their heavy sediment overload. Such earthquake-triggered mass movements occur frequently in Switzerland. Their triggers reflect recent tectonic activity in the Alpine region, and they have precisely been recorded by the Swiss Seismological Service (SED). The larger of these events (i.e. magnitudes >6) are expected to produce surface ruptures due to the size and displacement of the slipping surface. However, such ruptures can scarcely be found in the field as obvious imprinted geomorphologic features, such as offset moraine crests and fluvial terrace risers, deflected river courses and fault scarps, and are rare to absent. Likewise, only a few studies successfully showed the existence of an active fault cutting through Alpine nappe stacks (e.g. Sue et al. (2007), Ustaszewski et al. (2007)). Since erosional surface processes complicate the recognition of earthquake-caused topographic offsets, or often make it entirely impossible to trace them, the expected high preservation potential of a lake is the ideal environment to find such geomorphologic features.

This study uses a multi-disciplinary two step-approach to characterize potentially active faults in the Aare- valley between Interlaken and Bern. The perimeter crosses the North Alpine nappe front and hence lines up with the Lake Lucerne and Lake Zurich areas, which proved to show significant paleo-seismological activity along the Alpine arch and its foreland (Strasser et al., 2006). In addition to the earthquake catalogue of Switzerland ECOS-09 (Fäh et al., 2011), small-scale deformation structures (seismites), turbidite deposits and liquefaction structures ultimately prove the recent tectonic activity, and have all been observed in Lake Thun (Wirth et al., 2007).

In a first step, we will focus our investigation on Lake Thun starting with a review of high-resolution seismic data (3.5 kHz) of Lake Thun showing potential faults at the lake bottom (Wirth et al., 2011). This data will be complemented by a multibeam bathymetric survey, scheduled for September this year.

At a second stage, we will extend our investigation to terrestrial areas investigating LiDAR data and orthophotographs (courtesy of swisstopo), correlating lake findings with those on land. Promising identification of such features will be compared to the distribution of epicentres provided by ECOS-09 (Fäh et al., 2011).

The visual evaluation of the 3.5 kHz high-resolution seismic data revealed several structures, which deserve further analysis (see figure 1b). Earthquakes of moment magnitudes Mw 1.5 – 3.9 within and closely around Lake Thun were recorded, which though are too weak to trigger slope failures and hence were not imprinted in the sediment strata. However, the observed offset in figure 1b) might represent a potentially active area.

REFERENCES

Fäh, D., Giardini, D., Kästli, P., Deichmann, N., Gisler, M., Schwarz-Zanetti, G., Alvarez-Rubio, S., Sellami, S., Edwards, B., and Allmann, B., 2011, ECOS-09 earthquake catalogue of Switzerland release 2011 report and database. Public catalogue, 17. 4. 2011. Swiss Seismological Service ETH Zurich: Report SED/RISK.

Strasser, M., Anselmetti, F. S., Fah, D., Giardini, D., and Schnellmann, M., 2006, Magnitudes and source areas of large prehistoric northern Alpine earthquakes revealed by slope failures in lakes: Geology, v. 34, no. 12, p. 1005-1008.

Sue, C., Delacou, B., Champagnac, J. D., Allanic, C., Tricart, P., and Burkhard, M., 2007, Extensional neotectonics around the bend of the Western/Central Alps: an overview: International Journal of Earth Sciences, v. 96, no. 6, p. 1101-1129.

Ustaszewski, M., Herwegh, M., McClymont, A. F., Pfiffner, O. A., Pickering, R., and Preusser, F., 2007, Unravelling the evolution of an Alpine to post-glacially active fault in the Swiss Alps: Journal of Structural Geology, v. 29, no. 12, p. 1943-1959.

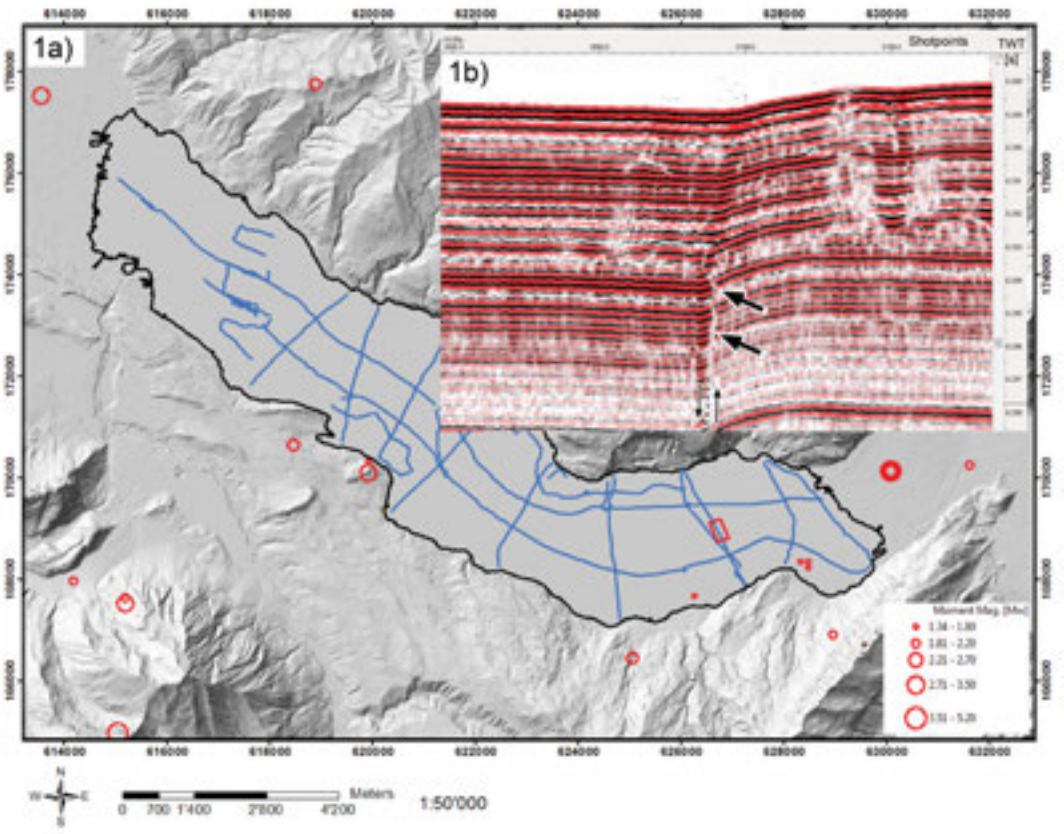

Fig. 1: a) Overview of seismic campaign (blue lines) on Lake Thun with superimposed paleo-seismic events. b) Seismic section revealing a potential fault with offset indicated by black arrows (shown section marked with square).

P 1.7

Tectonics and Strain partitioning in the Mont Pèlerin Subalpine Molasse

Thierry Falco & Jon Mosar

Département de Géosciences, Université de Fribourg, Chemin du Musée 6, CH-1700 Fribourg (thierry.falco@unifr.ch, jon.mosar@unifr.ch)

The Mont Pèlerin is situated between Vevey and Palézieux, in a vast NE to SW trending synclinal structure in the Subalpine molasse domain. The Mont Pèlerin is renowned for its important conglomeratic series produced by the erosion of the Prealpine Nappe de la Simme, during Chattian times (USM).

Overall the Mont Pèlerin area is structured by a serie of regional folds, as well as local small-scale folds, both determined from bedding dip data. It can be subdivided in three zones, depending of the orientation of the folds. In the southern part of Mont Pèlerin area, this folds orientation is E-W, whereas to the north the orientation shows the more typical alpine NE-SW trend. The western zone shows a more or less monoclonal east-dipping geometry. A gently SE dipping thrust surface cuts the whole upper part of the Mont Pèlerin and forms the flat portion of a regional ramp-flat thrust plane with a general transport top to the NNW. In addition, a series of important NW-SE to NNW-SSE trending strike-slip faults cut the whole structure. We view these faults as a possible extension of the conjugate fault system associated with the supra-regional Pontarlier fault to the NW in the Jura Mountains.
Deformations observed in the fields include: solution pits on pebbles, fractured pebbles, fractures, and veins. The study of the numerous solution pits on pebbles indicates two superposed deformations. A major pole density points to a subvertical compression that we tentatively attribute to the effect of loading due to burial in excess of four kilometers. A second maxima is oriented SSE with a gentle dip to the south. We attribute this latter to a regional compression associated with the general folding and thrusting.

P 1.8

Early Earth tectonics: A high-resolution 3D numerical modelling approach

Ria Fischer[1], Taras Gerya[1]

[1] *Department of Earth Sciences, Swiss Federal Institute of Technology (ETH Zurich), Sonneggstrasse 5, CH-8092 Zurich (ria.fischer@erdw.ethz.ch)*

Early Earth had a higher amount of remaining radiogenic elements as well as a higher amount of leftover primordial heat (Jaupart et al., 2007). Both contributed to the increased temperature in the Earth's interior and it is mainly this increased mantle potential temperature ΔTp that controls the dynamics of the crust and upper mantle and the style of Early Earth tectonics.

We conduct 3D petrological-thermomechanical numerical modelling experiments of the crust and upper mantle under Early Earth conditions and a plume tectonics model setup. For varying crustal structures and an increased mantle potential temperature ΔTp, a thermal anomaly in the bottom temperature boundary introduces a plume. The model is able to self-sufficiently form depleted mantle lithosphere after repeated melt removal. New crust can be produced in the form of volcanics or plutonics. To simulate differentiation the newly formed crust can have a range in composition from basaltic over dacitic to granitic depending on its source rock.

Compared to lower ΔTp where formation of a forearc can be observed, for ΔTp=200 K models show large amounts of subcrustal decompression melting and consequently large amounts of volcanics in the form of flood basalts. Mantle and crust are convecting separately. Dome-shaped plutons of mafic or felsic composition can be observed in the crust. Between these domes, circular to elongated belts of upper crust, volcanics and sediments of intermediate to felsic composition are formed and transported back into the mantle in a subduction like process. These structures look similar to, for example, the Kaapvaal craton in South Africa where the elongated shape of the Barberton Greenstone Belt is surrounded by multiple plutons (e.g. Van Kranendonk, 2011).

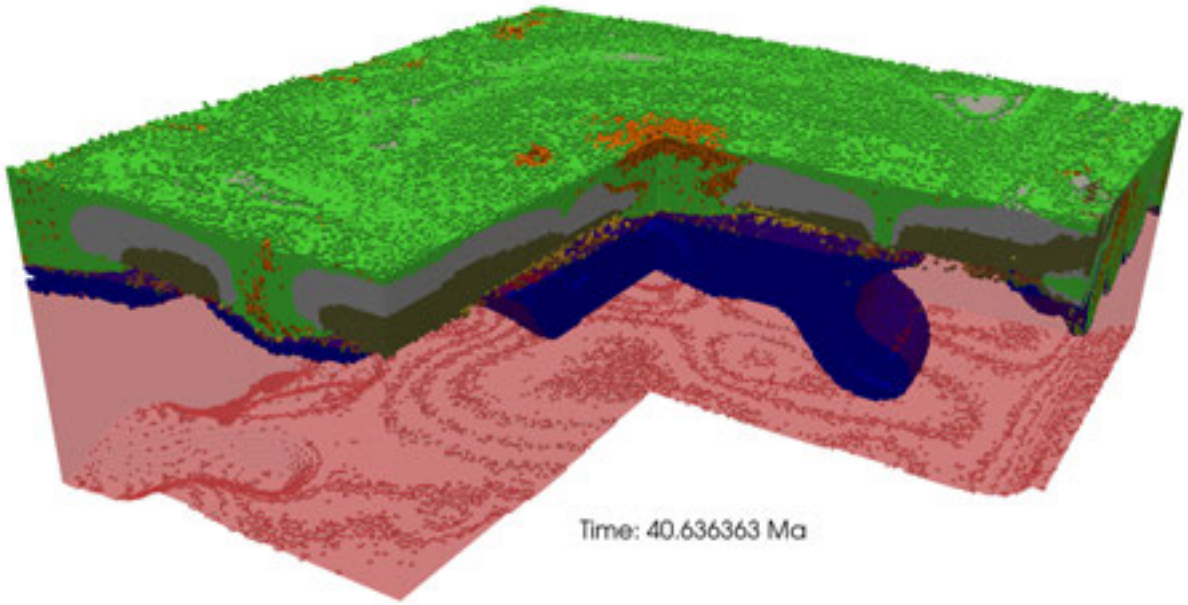

Figure 1. Snapshot of model ~40 Ma after model start with ΔTp=200K.

REFERENCES

Jaupart, C., Labrosse, S., and Mareschal, J. C., 2007, 7.06 - Temperatures, Heat and Energy in the Mantle of the Earth, in Schubert, G., ed., Treatise on Geophysics: Amsterdam, Elsevier, p. 253-303.

Van Kranendonk, M. J., 2011, Cool greenstone drips and the role of partial convective overturn in Barberton greenstone belt evolution: Journal of African Earth Sciences, v. 60, no. 5, p. 346-352.

P 1.9

Towards coupled giant impact and long term interior evolution models

Golabek Gregor[1], Jutzi Martin[2], Gerya Taras[1] & Asphaug Erik[3]

[1] *Institut für Geophysik, ETH Zürich, Sonneggstrasse 5, CH-8092 Zürich (gregor.golabek@erdw.ethz.ch)*
[2] *Physikalisches Institut, Universität Bern, Sidlerstrasse 5, CH-3012 Bern*
[3] *School of Earth and Space Exploration, Arizona State University, 550 East Tyler Mall, AZ 85287, Tempe, USA*

The crustal dichotomy (McCauley et al., 1972) is the dominant geological feature on planet Mars. The exogenic approach to the origin of the crustal dichotomy (Wilhelms and Squyres, 1984; Frey and Schultz, 1988; Andrews-Hanna et al., 2008; Marinova et al., 2008; Nimmo et al., 2008) assumes that the northern lowlands correspond to a giant impact basin formed after primordial crust formation. However these simulations only consider the impact phase without studying the long-term repercussions of such a collision.

The endogenic approach (e.g. Weinstein, 1995), suggesting a degree-1 mantle upwelling underneath the southern highlands (Zhong and Zuber, 2001; Roberts and Zhong, 2006; Zhong, 2009; Keller and Tackley, 2009), relies on a high Rayleigh number and a particular viscosity profile to form a low degree convective pattern within the geological constraints for the dichotomy formation. Such vigorous convection, however, results in continuous magmatic resurfacing, destroying the initially dichotomous crustal structure in the long-term.

A further option is a hybrid exogenic–endogenic approach (Reese and Solomatov, 2006, 2010; Reese et al., 2010; Golabek et al., 2011), which proposes an impact-induced magma ocean and subsequent superplume in the southern hemisphere. However these models rely on simple scaling laws to impose the thermal effects of the collision.

Here we present the first results of impact simulations performed with a SPH code (Benz and Asphaug 1995, Jutzi et al., 2013) serially coupled with geodynamical computations performed using the code I3VIS (Gerya and Yuen, 2007) to improve the latter approach and test it against observations. We are exploring collisions varying the impactor velocities, impact angles and target body properties, and are gauging the sensitivity to the handoff from SPH to I3VIS.

As expected, our first results indicate the formation of a transient hemispherical magma ocean in the impacted hemisphere, and the merging of the cores. We also find that impact angle and velocity have a strong effect on the post-impact temperature field (e.g. Marinova et al., 2008) and on the timescale and nature of core merger.

REFERENCES

Andrews-Hanna J.C., Zuber M.T. and Banerdt W.B. 2008: Nature 453, 1212-1215.
Benz W. and Asphaug E. 1995: Computer Physics Communications 87, 253–265.
Gerya T.V. and Yuen D. A. 2007: Phys. Earth Planet. Int. 163, 83-105.
Golabek G.J., Keller, T., Gerya, T.V., Zhu G., Tackley P.J. and Connolly J.A.D. 2011: Icarus 215, 346-357.
Frey H. and Schultz R.A. 1988: Geophys. Res. Lett. 15, 229-232.
Jutzi M., Asphaug E., Gillet P., Barrat J-A. and Benz W. 2013: Nature 494, 207–210.
Keller T. and Tackley P.J. 2009: Icarus 202, 429-443.
Marinova M.M., Aharonson O. and Asphaug E. 2008: Nature 453, 1216-1219.
McCauley J.F., Carr M.H., Cutts J. A., Hartmann W.K., Masursky H., Milton D.J., Sharp R.P. and Wilhelms D.E. 1972: Icarus 17, 289-327.
Nimmo F., Hart S.D., Korycansky D.G. and Agnor C.B. 2008: Nature 453, 1220-1223.
Reese C.C. and Solomatov V.S. 2006: Icarus 184, 102-120.
Reese C.C. and Solomatov V.S. 2010: Icarus 207, 82-97.
Reese C.C., Orth C. P. and Solomatov V.S. 2010: J. Geophys. Res. 115, E05004.
Roberts J.H. and Zhong S. 2006: J. Geophys. Res. 111, E06013.
Weinstein S.A. 1995: J. Geophys. Res. 100, 11719-11728.
Wilhelms D.E. and Squyres S. W. 1984: Nature 309, 138-140.
Zhong S. 2009: Nature Geosci. 2, 19–23.
Zhong S. and Zuber M.T. 2001: Earth Planet. Sci. Lett. 189, 75-84.

P 1.10

High-pressure pseudotachylytes as field evidence for lower crustal seismicity

Friedrich Hawemann[1], Neil Mancktelow[1], Sebastian Wex[1], Giorgio Pennacchioni[2], & Alfredo Camacho[3]

[1] *Department of Earth Sciences, ETH Zurich, Sonneggstrasse 5, CH-8092 Zurich*
[2] *Department of Geosciences, University of Padua, Via Gradenigo 6, 35131 Padua*
[3] *Department of Geological Sciences, University of Manitoba, 125 Dysart Rd, Winnipeg, Manitoba, R3T 2N2 Canada*

Seismic records show earthquakes in lower crustal levels in almost all collisional orogens, even though rocks are generally predicted to flow rather than fracture under these conditions. The experimentally determined creep flow law of quartz is used for most rheological models of the continental crust, since it is one of the most abundant mineral. In the typical "Christmas-tree" representation of lithospheric strength, the intersection between the line representing Mohr-Coulomb fracture and the experimental curve for power-law viscous flow of wet quartz occurs around 250-280°C, consistent with field observation that the transition to crystal-plastic flow in quartz starts around such temperatures.

The Musgrave Ranges in Central Australia expose sub-eclogitic facies shear zones of Petermann age (~ 550 Ma), overprinting granulites of Musgravian age (1.2 Ga). The distribution of deformation is very heterogeneous and all large-scale shear zones are associated with pseudotachylyte (pst). Since pst is thought to form by seismic-slip induced frictional melting, it can be used as an indicator of fossil seismogenic fault zones. Pst is identified in the field by the presence of injection veins, breccias, crosscutting relationships and their fine grain size. Observed pst is often not black and glassy as reported from many classic low-grade examples, but shows a caramel color and a well-developed foliation and a lineation, often parallel to the mylonitic fabric. Neocrystallized garnet and clinopyroxene with grain sizes of less than 5 µm have grown inside the pseudotachylyte veins. Geothermobarometric calculations based on microprobe analyses give temperatures around 650 °C and pressure around 1.2 GPa, identical to the conditions of deformation in the associated ductile shear zones. Evidence for cyclic development of both brittle and ductile structures is provided by sheared pst-breccias, which incorporate clasts of an older generation of sheared pseudotachylytes and by sheared pst crosscut by undeformed pst veins. Pst-veins also often act as a precursor structure for localized shear zones, as seen in low strain domains. Here, pst-veins are sheared and form mm-wide but 10's of meters-long localized shear zones in little deformed host-rock. In contrast, quartz veins with the same orientation did not localize shearing and are folded or boudinaged. This presumably reflects the "dry" deformation conditions, with generally no new growth of hydrous minerals or evidence for introduction of hydrous fluids. Shearing has preferentially localized on precursor fractures and fine grained pst rather than on compositional inhomogeneities.

P 1.11

The relationship between the Vizcaíno 'composite' Terrane and the 'Antimonio Terrane' during the Upper Triassic

Eric Heerwagen[1] & Rossana Martini[1]

[1] *Department of Earth Sciences, University of Geneva, Rue des Maraîchers 13, CH-1205 Geneva (eric.heerwagen@unige.ch)*

The North American Cordillera, from Alaska in the north to Mexico in the south, consists of several terranes that have a doubtful paleogeography (e.g. Coney et al. 1980). The major reason for this circumstance is, that the outcrop-situation for the time interval of the Upper Triassic is difficult. On the base of todays reconstructions for paleogeography, and tectonic history of the Cordillera, two potential terranes with shallow-water carbonates of Norian age were selected. These terranes are the "Antimonio Terrane" (Sonora, Mexico), and the Vizcaíno 'composite' Terrane (Baja California Sur , Mexico) (fig. 1). During field trips in 2012, and 2014, samples for the comparison of litho-, and microfacies of the two localities were collected.

With this study we try to prove a proximal relationship between the Antimonio, and Vizcaíno areas, allowing us to reconstruct these two potential terranes as a single "joint terrane" environment. Furthermore we want to compare these two localities with the previously-investigated Wallowa terrane in the Blue Mountain Province (Oregon, USA), also containing Upper Triassic shallow water carbonates.

The Upper Triassic succession of the Antimonio Terrane consists of shallow-marine sediments (González-León, 1997), whereas the deposits of the Vizcaíno 'composite' Terrane near the village of San Hipólito represent slope to deeper marine environments (Orchard et al. 2007). In Sonora, we found limestones, calcareous siltstones, and fine grained sandstones. The first two lithologies contain shallow-water fossil assemblages that include chambered sponges, and scleractinain corals. Near San Hipólito deepwater limestone, chert, a limestone breccia, and sandstone crop out. The Norian-dated clasts of the breccia contain shallow-water fossils. In particular the sponges, and corals show strong affinities to the fossils observed in the Antimonio area.

Acknowledgements: This project has been funded by the Swiss National Science Foundation No. RM 200020-13766.

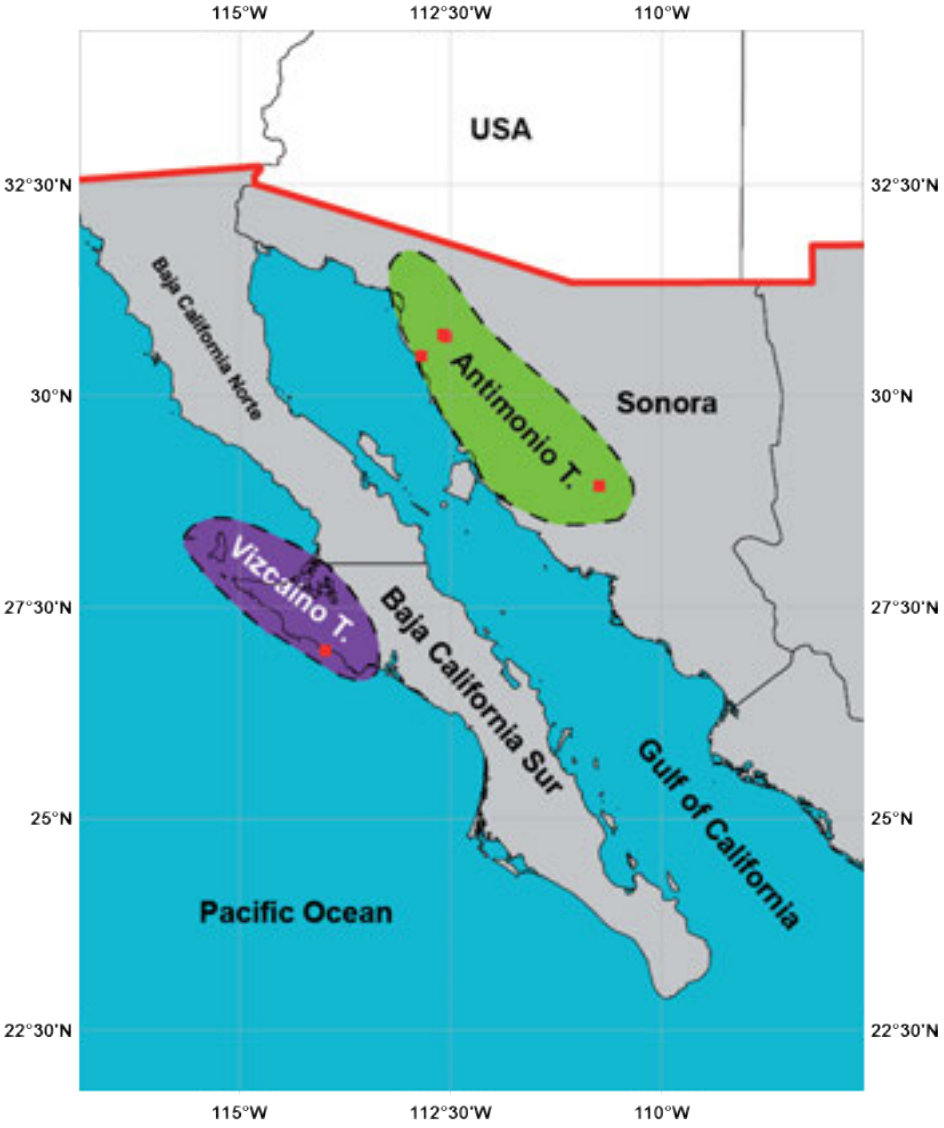

Figure 1. Map of Northwest Mexico with the terranes under investigation.

REFERENCES

Coney, P. J., Jones, D. L. & Monger, J. W. H. 1980: Cordilleran suspect terranes, Nature, 288, 329–333.

González-León, C. M. 1997: Sequence stratigraphy and paleogeographic setting of the Antimonio Formation (Late Permian-Early Jurassic), Sonora, Mexico, In Stanley, J., George D. and Gonzalez-Leon, C. M. (Editors), Special issue dedicated to the International workshop on the geology of northwestern Sonora, volume 14 of Revista Mexicana de Ciencias Geologicas, 136–148.

Orchard, M. J., Whalen, P. A., Carter, E. S. & Taylor, H. J. 2007: Latest

Triassic conodonts and radiolarian-bearing successions in Baja California Sur, New Mexico Museum of Natural History and Science Bulletin, 41, 355–365.

P 1.12

Shear stress and seismic cycle length of SAF at Parkfield

Nicolas Houlié[1,2] and Aurelie Guilhem[3]

[1] *ETH, Institute of Seismology and Geodynamics, NO F63, Sonneggstrasse 5, CH-8092 Zurich, Switzerland; Phone: +41 44 633 71 26, Fax: +41 44 633 10 66; Email: nhoulie@ethz.ch*
[2] *ETH, Institute of Geodesy and Photogrammetry, Wolfgang-Pauli-Str. 15, CH-8093 Zurich, Switzerland*
[3] *Swiss Seismological Service, ETH Zürich, Sonneggstrasse 5, Zürich, Switzerland*

With regular ruptures identified since more than 2000 years on a same fault segment the Parkfield mainshock sequence is probably one of the best earthquake sequence ever documented. The magnitude Mw6 earthquake in 1966 and the subsequent prediction of a following mainshock in 1988 +/- 5 years triggered the deployment of a dense geophysical network to monitor the central San Andreas Fault (SAF) near Parkfield, California. However, no mainshock occurred until September 2004, i.e. years after its prediction date. In addition to the incorrect forecast, the 2004 earthquake differed from the previous M6 mainshocks that occurred in 1922, 1934, and 1966, by the location of its hypocenter near the southern end of the fault segment, and its rupture propagation from south to north. Here, we show that both time delay and location of the 2004 hypocenter can be explained by static stress changes imposed by regional (i.e., within 100km) and local seismic activity (M>4) on the SAF in the vicinity of Parkfield. Our results suggest that the critical stress level leading to a mainshock is sensitive to shear stress disturbances, and has been constant since 1901. At last, we quantify that the interseismic slip rate along the SAF at Parkfield is ~ 14.3+/- 4.6 mm/yr.

P 1.13

Impact of elasticity on lithospheric shear localization

Yoann Jaquet[1], Stefan M. Schmalholz[1]

[1] *Institut de Géologie, Université de Lausanne, Unil Mouline, CH-1015 Lausanne (contact : yoann.jaquet@unil.ch)*

Lithospheric shear localization plays a fundamental role during the initiation of subduction zones, during the formation of extensional detachment zones and during the evolution of convergent orogens. However, the physical processes responsible for shear localization, such as shear heating or grain size reduction, and their relative importance for shear localization are until now incompletely understood. To better understand shear localization due to shear heating, we perform two dimensional (2-D) numerical simulations of lithospheric shortening. The numerical simulations are based on the finite element method using the mesh generator Triangle and the solver Milamin. Our model configuration consists of a lithosphere composed of an upper crust, a lower crust and a mantle. The rheology for each unit is a combination of experimentally derived flows for diffusion and dislocation creep. Two systematic series of simulations quantify the impact of the basal temperature and the shortening strain rate on the shear localization: in one series a visco-elasto-plastic rheology is applied and in the other series a visco-plastic rheology is applied to quantify the impact of elasticity on the shear localization.

The results show three general types of deformation for both series depending mainly on the shortening strain rate: 1) thickening (pure shear) dominated deformation, 2) folding dominated deformation and 3) shear localization dominated deformation. The visco-elasto-plastic models show a much stronger localization than the visco-plastic model. The impact of the elasticity will be quantified and implications for lithospheric deformation will be discussed.

P 1.14

The Neo-Tethyan subduction zone(s,?) in Azerbaijan, NW Iran: preliminary results

Anna Katharina Lechmann[1], Jean-Pierre Burg[1], Mohammad Faridi[2]

[1] *Geological Institute, ETH Zurich, Sonneggstrasse 5, CH-8092 Zurich (anna.lechmann@erdw.ethz.ch, jean-pierre.burg@erdw.ethz.ch)*
[2] *Geological Survey of Iran, Northwestern Regional Office, IR-5133-4359 Tabriz (mfaridi@gsi.ir)*

Azerbaijan in NW Iran, and in particular the Khoy ophiolitic complex, are relatively ill documented elements of the Alpine-Himalayan orogenic belt. They are attributed to multiple accretion and continental collision after subduction and closure of the Tethys Ocean and related seaways. We are interested in the pre- to syn-collisional relationships between the ophiolitic, arc and other magmatic units. This work investigates to what extent single or multiple collisions and orogeny have shaped the NW Iranian Plateau. In particular, we want to understand the changes in deformation style within the collision zone and the effects of several possibly coeval events such as closure of two suture zones separated by an arc and possibly followed by slab break-off(s). Aster satellite images and published geological maps provide fundamental background knowledge. New fieldwork focused on sampling the different magmatic rock units to specify the structural record and the structural relationships between the various lithological units. Cretaceous to Quaternary, regionally distributed magmatic rocks were collected to have good resolution of their changes in space and time. Petrological, geochemical and isotope studies characterize magmatic rocks and their sources. Fossil-bearing sediments provide stratigraphic ages of important contacts. Major and trace element geochemistry of mantle and crustal suites of the Khoy ophiolitic complex constrain their tectonic setting. Two complexes were defined on the basis of K-Ar dating (Khalatbari-Jafari et al., 2004). An older, probably subducted ophiolite of Triassic-Jurassic age and a younger non-metamorphic ophiolite of Late Cretaceous age. Previous work suggested that the basaltic lavas of the Khoy ophiolitic complex were created at an oceanic spreading centre. Structural data document a dominant top to the SW thrusting of an imbricate zone with stacked thrust sheets in a duplex system. Active faults, dominantly normal and strike-slip faults document current SSW-NNE compression, consistent with GPS and seismotectonic information.

This work is supported by SNF Research Grant (project 200021_153124/1).

REFERENCES

Khalatbari-Jafari, M., Juteau, T., Bellon, H., Whitechurch, H., Cotton, J. & Emami, H. 2004: New geological, geochronological and geochemical investigations on the Khoy ophiolites and related formations, NW Iran. Journal of Asian Earth Sciences, 23, 507-535.

P 1.15

Salt dissolution in the underground of Switzerland, especially in the canton of Fribourg

Hinrich Lohmann

Dorfstrasse 37, CH-4452 Itingen BL (h.lohmann@eblcom.ch)

Within the Triassic system of the non-Alpine part of Switzerland there are two salt formations, the Muschelkalk and the Gipskeuper. The geographical extent of the two formations is shown by Jordan (2008). The Muschelkalk salt is widespread from the North Sea to northwestern Switzerland where it is exploited by solution mining. Hauber (1993) describes three separate Swiss salt basins, Schweizerhall-Ergolz, Rheinfelden, and Zurzach. The discussion is still open if these three basins were originally discontinuous or secondarily separated by salt dissolution (also called subrosion). Detailed investigations reveal several zones of „breccia“ which may in fact be dissolution residues (the salt becoming raw material for the younger Gipskeuper formation ?).The Gipskeuper, the second salt formation of non-Alpine Switzerland, has a similar extent as the Muschelkalk salt. The thickness of both salt formations is difficult to establish because they were transformed into decollement planes of the Jura foldbelt.

Shapes of salt dissolution: If and when water undersaturated in NaCl reaches a salt formation it will start to dissolve it. This may occur from above, laterally, or from below (volcanism). Once started it will usually lead to increasing permeability and to an expansion of the leached volume. The void will be filled by residual sediments and collapse material and then expand laterally, perhaps forming a pear-shaped collapse zone. Eventually, the stalk of the pear will reach the surface and form a small diameter sinkhole. With more salt leached away more surface sediments will be collected. In the long run extensive subrosion basins may develop, having slopes several kilometer wide, the socalled salt slopes.

Canton of Fribourg: On the website www.bfe.admin.ch/dokumentation/publikationen/index.html you can find the report „Sicherheitsbericht Rahmenbewilligungsgesuch Ersatz Kernkraftwerk Mühleberg“. This report contains several reflection seismogrammes, for ex. FR.S750010. Its interpreted southwestern portion shows a more or less flat lying sequence of 4 horizons, from base Mesozoic to base Tertiary. Interpreting an additional horizon, Near top Triassic, we find a travel time for the Triassic interval of about 150 msec, possibly 250 m thickness. Proceeding northeastward, at geophone point 620, the whole series bends down, even the Quaternary surface beds (max. at GP 760). Between GP 760 and 860 the interval in question has a TWT of 30 msec, perhaps 50 m. From this minute seismogramme we arrive at a rough guess that 200 m salt have been dissolved in its central part. Combining this interpretation with the tectonic map included in the above report one may say “The Fribourg structure is a N-S trending salt dissolution basin promoted by several N-S trending faults“. The alignment of seismic epicentres on its western flank is the presently active dissolution front. The Swiss Seismological Serivice calculates the epicentre depth at about 2 km which is in full agreement with the reflection seismic interpretation. There are further small sinkholes on FR.S750010.

The Creux du Van, canton of Neuchâtel, is the most surprising morphological feature of the Jura foldbelt. In a way it is similar to an amphitheatre. To my knowledge until now its erosion has been explained by river and/or glacial forces. As an alternative a salt sinkhole explanation is proposed, affecting Triassic salt at approximately 3 to 4 km depth. Seismic section 11 (Sommaruga 1997) close by shows a complex structure. Further seismic investigation is almost impossible due to the abrupt morphology.

REFERENCES

Hauber, L. 1993 : Der Mittlere Muschelkalk am Hochrhein. N.Jb.Geol.Paläont.Abh.,189, 147-170

Jordan, P. 2008: Triassic basin evolution Switzerland. In: McCann, T.(ed.), The geology of central Europe, 2,785-788 Geol. Soc. London

Sommaruga, A. 1997: Geology of the central Jura and the Molasse basin. Mem.Soc.Neuchâteloise Sci.Nat.,12, 1-176

P 1.16

The Water Circulation In The Fractured Rock: The Role Of Stylolites In The Development Of Karst

Silvana Magni[1]

[1] *Geology-Phd student- Via Nino Bixio, 22-70024 Gravina in Puglia(Bari-Italy (magnisilvana@libero.it)*

Karst development is strongly influenced by the tectonic deformation of the area where they occur.This is because, the structure of the rock mass in which it occurs (eg. lithology, primary porosisty, environmental conditions, etc) affects the water circulation, thereby affecting permeability and porosity.Traditionally, in the field of karstology, it is maintained that water circulation is essentially related to extensional structures which, it is assumed, are more favorable to water circulation. In fact, the permeability of the fault zone is sufficiently high only in the early stages of the movement , because after a short period the deposition of minerals (e.g., calcite) coming from these same fluids reduces its porosity/permeability. Fault zones and fractures play an important role in fluid circulation, acting as permeability barriers or conductors, depending on the specific conditions (lithological and structural in particular), and on the distribution of other structures associated with them. Therefore, structural analysis can provide both qualitative and quantitative assessments of the relationship between structure and fluid circulation and allow us to determine whether a fault zone acts as a barrier or as a hydraulic conductor (Caine 1996).The stylolites (Rawling 2001), structure associated with the faults play an important role in the fluid circulation and in particular in the development of the karst.In this study, conducted in the karst area of Fasano it was verified that the karst tends to develop along tectonic stylolites formed by compression.

In the study area tectonic stylolites(fig.1) are shown to be the favoured structures for initiating the development of both, underground and epigean karsts.

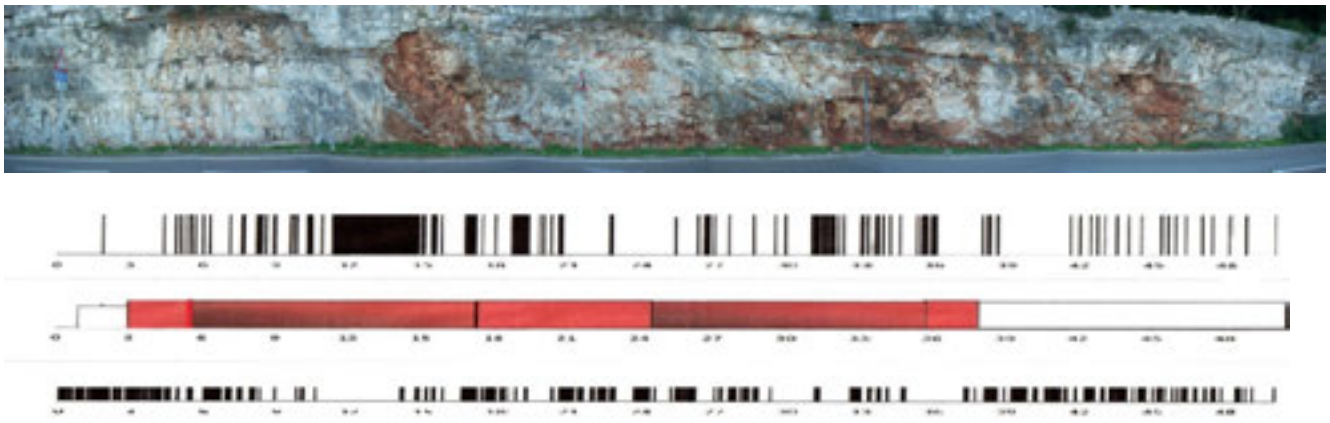

Figure.1. Starting from the top:-scanline; distribution of fracturing (joints and stylolites); distribution of karst; distribution of stylolites

The analysis performed(structural, XRD, on permeability) are allowing us to take the first considerations on the importance of stylolites in the development of karst (fig.2)

The aquifers represent about 40% of sources of drinking water and their Importance will increase in coming years due to the progressive deterioration of the quantity and quality of groundwater as a result of phenomena exploitation and pollution. Therefore, the future water supply will be increasingly dependent on these sources,so the importance of these studies

REFERENCES

Caine, J.S., Evans, J.P., Forster, C.B., 1996. Fault zone architecture and permeability structure. Geology 24, 1025–1028.

Rawling,G.C., Goodwin, L.B., Wilson, J.L., 2001.Internal architecture,permeability structure, and hydrologic significance of contrasting fault-zone types. Geology 29, 43–46.

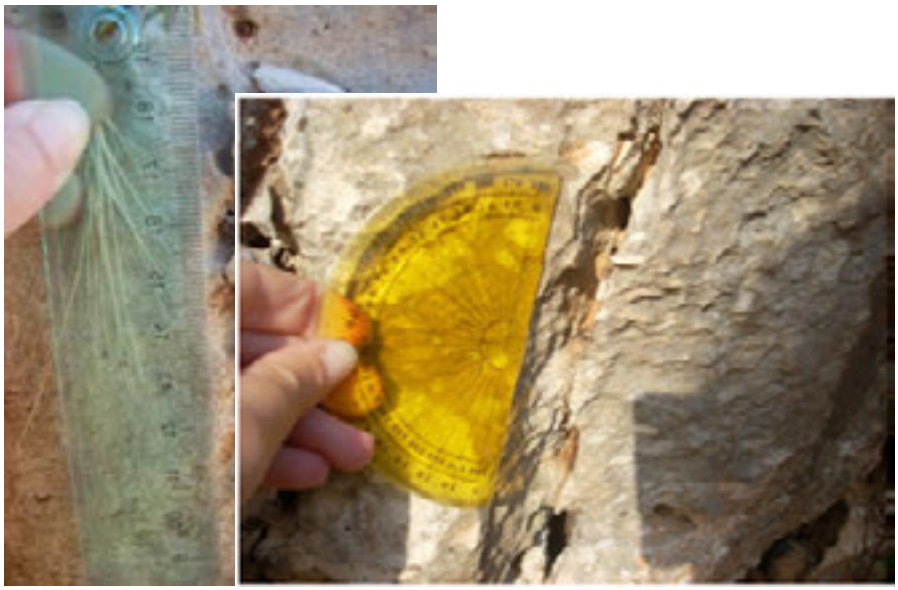

Figure 2. The karst is mainly present along the surfaces of tectonic stylolites. It is possible to observe the evolution of a stylolites.

P 1.17

Field Constraints on the Rheology of Quartz in "Wet" or "Dry" Middle to Lower Continental Crust

Neil Mancktelow[1], Giorgio Pennacchioni[2], Friedrich Hawemann[1], Sebastian Wex[1] & Alfredo Camacho[3]

[1] *Department of Earth Sciences, ETH Zurich, Sonneggstrasse 5, CH-8092 Zurich*
[2] *Department of Geosciences, University of Padua, Via Gradenigo 6, 35131 Padua*
[3] *Department of Geological Sciences, University of Manitoba, 125 Dysart Rd, Winnipeg, Manitoba, R3T 2N2 Canada*

Quartz is an abundant mineral in most rocks of the continental crust and is generally considered to be the main load-bearing component determining the viscous rheology of the middle to lower crust. However, it has long been known from laboratory experiments that quartz rheology is strongly influenced by the amount of water– and "dry" quartz is very difficult to deform crystal-plastically. Here we present direct field evidence for the markedly different behaviour of quartz under "wet" and "dry" conditions, on the corresponding differences in response to deformation of the middle to lower crust, and implicitly on the markedly different overall strength of the crust. We compare and contrast the behaviour using examples from the Tauern Window (Eastern Alps), the Simplon Fault Zone (Central Alps), the Adamello (Southern Alps) and Sierra Nevada (western USA) batholiths (all "wet") and the Mont Mary (Central Alps), Ivrea Zone (Southern Alps) and Musgrave Ranges (Central Australia) (all "dry"). The temperature conditions for these areas largely overlap and correspond to those present at middle to lower crustal levels.

Typical of "wet" conditions is that new quartz veins develop during deformation, whereas under "dry" conditions only older precursor veins are present. Under "wet" conditions, quartz veins and quartz-rich layers are weaker than the surrounding more quartzo-feldspathic gneisses or biotite-bearing granitoids and strongly localize shearing, typically developing a mylonitic fabric. In examples from the Tauern Windows metagranitoids, quartz is even weaker than large calcite crystals, which form porphyroclasts within the quartz mylonites. The interpreted shear flow stress in these examples is only on the order of 10 MPa or less (Mancktelow & Pennacchioni, 2010). Under the ambient upper amphibolite facies conditions (ca. 550°C), quartz recrystallizes by Grain Boundary Migration (GBM) and exaggerated grain growth leads to average grain sizes on the scale of many 100's of µm up to mm size. The strong CPO developed at moderate to high shear strain shows a point maximum of c-axes parallel to the intermediate Y fabric axis, consistent with a dominant prism <a> slip system. Directly comparable microstructures and CPO are observed for quartz veins deformed under similar conditions in the Simplon Fault Zone and during cooling of granitoid batholiths of Adamello and the Sierra Nevada (e.g. Pennacchioni et al. 2010). Under the Scanning Electron Microscope (SEM), secondary electron (SE) images of broken sample surfaces of quartz mylonites show a significant porosity and in some locations open space and coherent crystal faces along grain boundaries. Although shearing localizes both on compositional layers (e.g. quartz veins) and precursor fractures, generally no pseudotachylyte is observed associated with this localized shearing under "wet" conditions.

In marked contrast, under similar P-T but "dry" conditions (e.g. Ivrea, Musgrave Ranges), quartz veins or layers do not localize strain and shear is only localized on precursor fractures that largely ignore compositional layering. In the Musgrave Ranges, the one exception is that older finer-grained dolerite dykes do heterogeneously localize both pseudotachylyte formation and ductile shearing, especially towards the finer grained ("chilled") dyke margins. Recrystallization of quartz within shear zones is by Subgrain Rotation (SGR) and grain sizes are on the scale of only a few 10's of microns or less. Despite the fine grain size, the quartz mylonites show a strong CPO that, similar to the "wet" examples, is still characterized by a Y-maximum of c-axes, indicative of dominant prism <a> slip. Under the SEM (SE mode), the grain boundaries appear largely devoid of any porosity suggesting that there was almost no free water on the boundaries during deformation and recrystallization (Mancktelow & Pennacchioni, 2004). The fine recrystallized grain size indicates flow stresses on the order of many 100's of MPa. Pseudotachylyte is common with locally thick veins and breccias on the order of several centimetres. Pseudotachylyte veins can be either sheared and transposed or crosscut the mylonitic foliation, suggesting intermittent pseudotachylyte formation during ductile shearing. Despite the high strength of these rocks, deformation is still extensive, if markedly heterogeneous. The interpreted high stress during deformation promotes both shear heating and tectonic pressure effects, so it can no longer be *a priori* assumed that P-T conditions determined in the dynamically recrystallized shear zones accurately represent ambient conditions (e.g., Camacho et al., 2001; Mancktelow, 2008).

REFERENCES

Camacho, A., McDougall, I., Armstrong, R., & Braun, J. 2001: Evidence for shear heating, Musgrave Block, central Australia. Journal of Structural Geology, 23, 1007-1013.

Mancktelow, N. S. 2008: Tectonic pressure: theoretical concepts and modelled examples. Lithos, 103, 149-177.

Mancktelow, N. S., & Pennacchioni, G. 2004: The influence of grain boundary fluids on the microstructure of quartz-feldspar mylonites. Journal of Structural Geology, 26, 47-69.

Mancktelow, N. S., & Pennacchioni, G. 2010: Why calcite can be stronger than quartz. Journal of Geophysical Research-Solid Earth, 115.

Pennacchioni, G., Menegon, L., Leiss, B., Nestola, F., & Bromiley, G. 2010: Development of crystallographic preferred orientation and microstructure during plastic deformation of natural coarse-grained quartz veins. Journal of Geophysical Research-Solid Earth, 115.

P 1.18

Tectonics between the Préalpes Klippen and the swiss western Molasse Basin in the Bulle region (Fribourg)

Jon Mosar, Martinus Abednego, Marius Gruber, Anna Sommaruga

Department of Geosciences, Earth Sciences, University of Fribourg, Chemin du Musée 6 , 1700 Fribourg, Switzerland

The area of Bulle is located in the frontal part of the allochtonous Préalpes Klippen belt of western Switzerland, between SE-dipping imbricates of the Subalpine Molasse to the North and the overriding Préalpes Médianes to the South. The Bulle area is structured by two major tectonic elements: [i] a NE-SW trending, SE-dipping thrust system affecting the Subalpine Molasse unit and the Préalpes Klippen belt, [ii] a N-S trending subvertical strike-slip fault system. The thrust system encompasses very large tectonic slivers of Ultrahelvetic origin (to the SE and to the E) considered to be part of a tectonic "mélange"(Mélange infrapréalpin) associated with the basal detachment of the Préalpes Klippen; a series of tectonic slivers made of Gurnigel nappe sediments belonging to the Préalpes klippen belt, and the Subalpine Molasse. These different structural elements have a general NE-SW trend but are also juxtaposed in an E-W direction. This latter situation is due to the topographic incision of the S-N flowing Sarine river and the former Sarine glacier and results in a situation where the Subalpine Molasse unit is apparently almost in direct contact with the base of the Préalpes Médianes. Some authors have interpreted this arrangement as structural high associated with N-S left-lateral strike-slip faults forming a regional flower structure.

Interestingly the Ultrahelvetic tectonic slice bordering the city of Bulle to south, which is part of the Mélange infrapréalpin and which is sitting in the center of the "structural high", is made of series of lower Jurassic age only, whereas the more important tectonic sliver east of Lake Gruyère is made of series mostly younger, suggesting the possibility of E-W decoupling.

On the recent geological atlas of Switzerland, the 1:25'000 scale map of Gruyères, the faults of the eastern border of the structural high extend into the Sarine river valley to the South. The Sarine valley is a broad syncline where the Cretaceous series of the Préalpes médianes are exposed. This implies that in this region the basal thrust of the Préalpes Klippen is locally deeper by around 1 km than elsewhere in the Préalpes Klippen.

We thus would have in a N-S direction a juxtaposition along the same fault system of a structural high and a depression. We use a combination of surface data, information from boreholes in the vicinity and seismic surveys to propose a new NW-SE trending cross-section from the Plateau Molasse unit of the western Molasse Basin across the Subalpine Molasse unit into the Préalpes Klippen. The section will extend down to top basement which in the vicinity is characterized by a structural high known from seismic surveys and also from seismic tomography (See Abstract Abednego et al.). Our alternative structural model of the area will rely on structural topography, including basement inversion, to explain the important changes in basal décollement depth and structural style and possibly related to strain partitioning between a NW-SE direction of shortening and a NE-SW extension-related to shearing.

P 1.19

Palaeosoils stacking patterns as a tool for unravelling the subsurface architecture of mud-rich fluvial reservoirs.

Andrea Moscariello and Branimir Šegvić

Earth and Evironmental Sciences, Université de Genève, Rue de Maraîchaire 13, CH-1205 Genève (andrea.moscariello@unige.ch)

In the subsurface, robust well correlation represents the starting point in order to understand the architectural framework of any reservoirs rock. Especially in mud-rich continental barren sequences, characterised by scarce occurrence of sandstone beds, correlation may result a difficult task. In this type of depositional environment correlation techniques based on bio- or chemo-stratigraphic analyses have been successfully applied to identify discrete chronostratigraphic units which generally may represent 3rd or 4th order stratigraphic changes in response to either tectonic (e.g. increased erosion and sediment supply, changes in provenance) or climatic changes (e.g. weathering processes in the catchment, changes in erosion and sediment supply) or, in most cases, both.

Yet, when sand bodies in the subsurface are thought to be narrower than the actual well spacing, the correlation between them is becoming a challenge and more detailed information are then required to outline better the internal reservoir architecture and identify channel distribution.

Detailed insights on reservoir anatomy have been provided by the study of palaeosols. Their different types (pedofacies) and vertical trends can directly be related to different aggradation rates and in turn proximity to channel belt. Ultimately this can provide useful information on the overall stratigraphic pattern and sand connectivity within the fluvial reservoir.

Different pedofacies signatures, as a function of their maturity (e.g peds development, rootlets and nodules distribution, degree of preservation of primary sedimentary structures) can be identified both on core and logs and a different range of pedofacies types can be identified (usually 2 to 4).

Pedofacies composition highlighted by both standard petrographic microscopy and QEMSCAN automated mineralogy reflects the time of subaerial exposure and the pedologic processes (bioturbation and mineralisation) occurred during the soil formation. The presence of different stage of maturity in paleosoils can be also highlighted by shear sonic logs which may respond to the different degree of vertical discontinuities in the rock associated with paleosoils development (peds).

In general a highly mature paleosoils suggest very low aggradation rates of new sediments and hence a large distance from active channel belts or a temporary stop/decrease in sediment supply (e.g. no overbank deposition due to dry period or reduced water discharge). The staking pattern of these pedofacies can therefore unravel the avulsive and aggradational character of a river system. The study of several wells in a study area can unravel lateral changes in fluvial aggradational style within each chronostratigraphic zone (based on bio or chemo-stratigraphy) and therefore indicate large scale architectural changes at reservoir scale. The systematic mineralogical study of these pedofacies, with automated mineralogical techniques can help to unravel important changes in provenance or autogenic components throughout the stratigraphic record and thus help discriminating the tectonic vs. climatic signature recorded by the sedimentary succession.

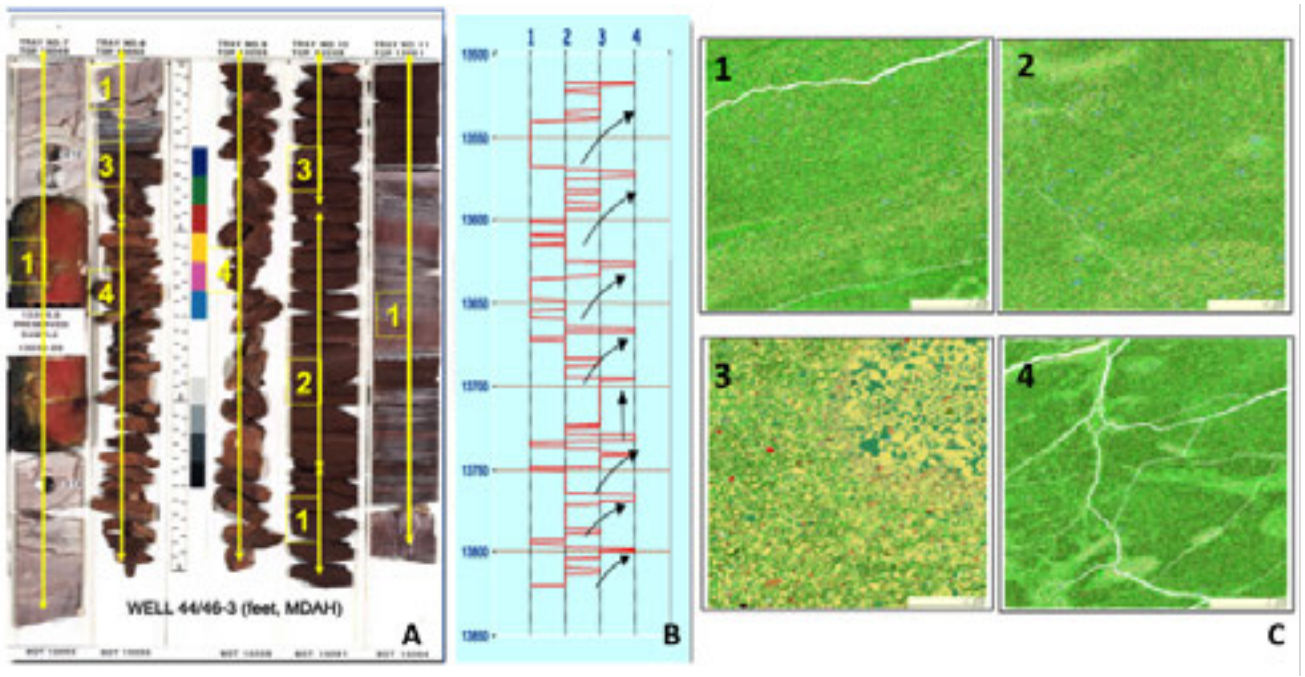

Fig. 1: A) Vertical sequences of pedofacies as recognised in core showing a vertical succession from 1 to 4 passing gradually form 2 and 3, the pedofacies 4 being the most mature and displaying clear peds structures. Top of core is in the top left of the picture. B) vertical succession of pedofacies in mud-rich fluvial reservoirs showing the sharp changes from pedofacies 4 to 1 suggesting a strong periodicity in the avulsive fluvial system which temporarily allowed the abandonment of flood plain and the development of mature paleosoils. C) QEMSCAN images of four types of pedofacies as indicated in each image.

P 1.20

LA-ICP/MS U-Pb zircon ages of porphyritic dykes from the Sesia-derived Insubric mylonite belt (Piemonte/Ticino)

Jan Pleuger[1,2] Albrecht von Quadt[3], Daniela Gallhofer[3] & Neil Mancktelow[2]

[1] *Institut für Geowissenschaften, FSU Jena, Burgweg 11, D-07749 Jena (jan.pleuger@uni-jena.de)*
[2] *Geologisches Institut, ETH Zürich, Sonneggstraße 5, CH-8092 Zürich*
[3] *Institut für Geochemie und Petrologie, ETH Zürich, Clausiusstraße 25, CH-8092 Zürich*

Along its central segment between Lago Maggiore and Valle d'Ossola, the Insubric fault is the southern boundary of the structural and metamorphic Lepontine dome which was uplifted with respect to the Southern Alps by about 20 km (Trümpy 1980). The horizontal displacement of the Insubric fault amounts to at least some tens of kilometres (e.g. Ahrendt 1980). The uplift amount decreases towards east and west as the eastern and western boundaries of the Lepontine dome turn away from the Insubric fault while the horizontal displacement amount increases eastward. These variations in horizontal and vertical displacement amounts are at least partly accommodated by fault branching off the Insubric fault (e.g. Handy et al. 2005) and the Insubric fault itself comprises several mylonite belts with different kinematics (e.g. Schmid et al. 1987, 1989). Between Lago Maggiore and Valle d'Ossola, the Insubric fault consists of two several hundred metres wide greenschist-facies mylonitic belts, a northern one (belt 1) with thrust kinematics in its present orientation, and a southern one (belt 2) with combined dextral and minor normal-fault kinematics (Schmid et al. 1987). Belt 1 affects the internal (southern) part of the Penninic Sesia zone and belt 2 the external (northern) part of the South Alpine Ivrea zone and/or sporadically intervening slivers of the Canavese zone.

Early Oligocene Alpine magmatism was spatially and temporally related to the Insubric fault (e.g. Rosenberg 2004). Greenschist-facies metamorphism in belt 1 was retrograde with respect to amphibolite-facies Lepontine regional metamorphism, dating of magmatic rocks with high-retentivity isotopic chronometers is the only possible way to constrain the onset of belt 1 shearing because dating of synkinematic minerals with low-retentivity isotopic chronometers generally yields cooling ages (e.g. Hurford 1986; Schmid et al. 1989; Steck and Hunziker 1994). LA-ICP-MS U-Pb zircon age dating of porphyritic dykes yielded concordant ages of 32.78±0.18 Ma and 32.75±0.16 Ma for oscillatory zoned rims. We therefore interpret these ages as magmatic emplacement ages. Ages of 287.7±1.0 Ma and 280.9±1.9 Ma (all errors are 95 % c.f) from inherited magmatic zircon cores additionally testify to an Early Permian magmatic stage.

The porphyritic veins are affected by belt 1 shearing to variable degree. Microtextural evidence shows that this shearing occurred exclusively under solid-state conditions and, therefore, the Early Oligocene ages provide a maximum time constraint for the onset of Insubric mylonitisation. While farther east the Insubric fault is immediately paralleled to the north by higher-grade amphibolite-facies, partly syn-magmatic Oligocene shearing in the Southern Steep Belt, this higher grade shear zone is clearly separated from Insubric mylonite belt 1 by the intervening Sesia zone in our study area.

REFERENCES

Ahrendt, H. 1980: Die Bedeutung der Insubrischen Linie für den tektonischen Bau der Alpen. Neues Jahrbuch für Geologie und Paläontologie Abhandlungen, 160, 336-362.

Handy, M.R., Babist, J., Wagner, R., Rosenberg, C.L. & Konrad, M. 2005: Decoupling and its relation to strain partitioning in continental lithosphere - insight from the Periadriatic Fault system (European Alps). In: Gapais, D., Brun, J. P. & Cobbold, P.R. (Eds.): Deformation mechanisms, rheology and tectonics: From minerals to the lithosphere. Geological Society, London, Special Publications, 243, 249-276.

Hurford, A.J. 1986: Cooling and uplift patterns in the Lepontine Alps South Central Switzerland and an age of vertical movement on the Insubric fault line. Contributions to Mineralogy and Petrology, 92, 413-427.

Rosenberg, C.L. 2004: Shear zones and magma ascent: A model based on a review of the Tertiary magmatism in the Alps. Tectonics, 23, TC3002, DOI: 10.1029/2003TC001526.

Schmid S.M., Zingg, A. & Handy, M. 1987: The kinematics of movements along the Insubric Line and the emplacement of the Ivrea Zone. Tectonophysics, 135, 47-66.

Schmid, S.M., Aebli, H.R., Heller, F. & Zingg, A. 1989: The role of the Periadriatic Line in the tectonic evolution of the Alps. In Coward, M. P., Dietrich, D. & Park, R.G. (Eds.): Alpine Tectonics. Geological Society, London, Special Publications, 45, 153-171.

Steck, A., & Hunziker, J. 1994: The Tertiary structural and thermal evolution of the Central Alps - compressional and extensional structures in an orogenic belt. Tectonophysics, 238, 229-254.

Trümpy, R. 1980: Geology of Switzerland, a guide book. Part A: An outline of the geology of Switzerland. Basel: Wepf & Co. (104 pp.)

P 1.21

Late Cretaceous-to-Pliocene thermo-tectonic history of Pelagonia (northern Greece) from zircon and apatite fission-track ages

Filippo Luca Schenker[1], Maria Giuditta Fellin[2], Jean-Pierre Burg[2]

[1] *ISTE, University of Lausanne, 1015 Lausanne, Switzerland (filippo.schenker@unil.ch)*
[2] *Department of Earth Sciences, ETH Zurich, Sonneggstrasse 5, 8092 Zurich, Switzerland*

The Pelagonian zone, between the External Hellenides/Cyclades to the west and the Axios/Vardar/Almopia (AVA) zone and Rhodope to the east, was involved in the late Early Cretaceous and in the Late Cretaceous-Eocene compressional events. Timing and spatial distribution of these events have remained so far partly unresolved. We will present new and published zircon (ZFT) and apatite (AFT) fission-track ages integrated with new field observations to constrain their thermal overprint.

The Early Cretaceous (130-110 Ma) thrust system of the Pelagonian basement and AVA zone was covered on a 99-to-80 Ma unconformity by marine sediments, whose deposition continued until ca. 66 Ma (documented by Globotruncanae). The metamorphic imbricates of the western AVA zone cooled below 240 °C between 102 and 93.5-90 Ma and the ones of northern Pelagonia, eastern AVA zone and western Rhodope between 80 and ca. 68 Ma. This regional ca. 30 Ma long cooling and subsidence was followed by the reactivation of thrusting that caused abrupt and rapid cooling and erosion of the Pelagonian basement at ca. 68 Ma, as documented by clasts in ca. 66 Ma old marine sediments with detrital ZFT ages clustering at ca. 68 Ma. In the Paleocene-Eocene thrusting migrated in the External Hellenides and cooled western Pelagonia below ca. 120 °C in the hanging wall of its sole thrust. Subsequently in central-eastern Pelagonia, ZFT and AFT ages attested rapid and uniform cooling between 24 and 16 Ma in the footwall of a major extensional fault. Extension started even earlier at 32.7 Ma in the western AVA zone according to reset AFT ages within normal faults. A final post-7 Ma rapid cooling is inferred by inverse modeling of AFT lengths along a E-W normal fault zone cutting Pliocene-to-recent sediments.

P 1.22

3D visualization of the structures at Grimsel Test Site GTS and their link with sampled groundwaters

Raphael Schneeberger[1], Urs Mäder[1], Florian Kober[2], Thomas Spillmann[2], Niklaus Waber[1], Alfons Berger[1] & Marco Herwegh[1]

[1] *Institut für Geologie, University of Bern, Baltzerstrasse 3, 3012 Bern (raphael.schubert@geo.unibe.ch)*
[2] *Nagra, Hardstrasse 73, 5430 Wettingen*

We present preliminary results from a research project aiming at the development of structural and hydrochemical models in the Grimsel region. For the last 30 years, numerous experiments and research investigations in the Grimsel Test Site (GTS) delivered a vast number of structural, physical and geochemical data (e.g. Keusen et al. 1989). In the context of the present study, the natural fluid flow pathes are investigated in 3D space by a combination of 3D structural modelling and geochemical approaches incorporating groundwater inflow rates and geochemistry. For this purpose, a 3D structural model will be developed in a first step, which links structures at the level of the GTS tunnels with the topographic surface. Information compiled from previous studies are combined with newly aquired tunnel and surface mappings. The subsequent structural 3D visualization of the geometry is performed with the Move™ software (from Midland Valley Exploration Ltd).
To investigate the groundwater pathways and their relation to the structural domains, samples have been taken at regular time intervals from different borehole locations in variably deformed granitoid rocks, shear zones, meta-basic dykes.
In-line measurements of pH, Eh and conductivity confirmed the previously observed low mineralisation of GTS groundwater (Frick et al 1992). The main cations and anions as well as the $\delta^{18}O$ and $\delta^{2}H$ are quantitiatively analysed.
A compilation of historic data (water chemistry, inflow rates, hydraulic heads, transmissivities, limited natural tracers) and a comparison with the present data is ongoing. First results of both 3D modelling and geochemical analyses will be presented in this presentation.

REFERENCES
Frick, U., Alexander, W.R., Baeyens, B., Bossart, P., Bradbury, M.H., Bühler, C., Eikenberg, J., Fierz, T., Heer, W., Hoehn, E., McKinley, I.G. & Smith, P.A. 1992: Grimsel Test Site: The radionuclide migration experiment – overview of investigations 1985-1990. Nagra Technical Report NTB 91-04
Keusen, H.R., Ganguin, J., Schuler, P. & Buletti, M. 1989: Felslabor Grimsel: Geologie. Nagra Technical Report NTB 87-14

P 1.23

Dating low grade deformation of the Patagonian fold-and-thrust belt in the Torres del Paine area, Chile 51° 30'S: first results

Annette Süssenberger[1], Susanne Th. Schmidt[1]

[1] *Departement des sciences de la Terre, Université de Genève, Rue de Maraîchaire 13, CH-1205 Genève (annette.suessenberger@unige.ch)*

K/Ar dating on syn-kinematicly formed illites has been used to date different deformation phases triggered by the subduction of the Antarctic plate beneath the South American plate, resulting in the formation of the Patagonian retro-arc fold-and-thrust belt.

The Cretaceous to Neogene Patagonian east-vergent fold-and-thrust belt in southern Chile consists of a >4000 m thick sequence of turbidites, sandstones and shales which were deposited in a basin structure formed throughout the Late Jurassic breakup of Gondwana. The kinematic evolution of the fold-and-thrust belt has been roughly defined by six different deformation stages of foreland shortening between the Late Cretaceous and the Neogene (Fosdick et al 2011).

Clay rich samples were selected within the Cretaceous Punta Barrosa and overlying Cerro Torro Formation south of the Torres del Paine Intrusion. Illite crystallinities of the <0.2 µm and <2µm clay mineral size fractions were determined and range from 0.23 to 0.58 °2Θ in the <0.2 µm and 0.28 to 0.46 °2Θ in the <2 µm fraction. Diagenetic values are observed in the East, where deformation was less intense. The alignment of illite crystallinity values seems to correlate best with the regional folding.

A carefully selected suite of <0.2 µm and <2 µm clay mineral size fractions has been subjected to K/Ar age dating to establish time constraints on the deformation stages of the fold-and-thrust belt. K-Ar ages vary between 46.2±0.7 and 62.1±0.1 Ma in the <0.2 µm fraction and between 55.3±0.9 and 80.8±1.2 Ma in the <2 µm fraction. Thus, the folding initiated at around 60 Ma and continued until 46 Ma in the westernmost part of the study area. In the East , ages of the <2 µm fraction indicate stratigraphic ages (80 Ma) and are therefore, not affected by deformation events. Furthermore, the age data indicate both, a continuous regression of deformation intensity and a regional low-grade metamorphic overprint from west to east related to deformational shortening. Based on this preliminary data any influence by the intrusive Torres del Paine Complex can be excluded.

REFERENCES
Fosdick, J.C., Romans, B., W., Fildani, A., Bernhardt, A., Calderon, M., Graham, S.,A. 2011: Kinematic evolution of the Patagonian retroarc fold-and-thrust belt and Magallanes foreland basin, Chile and Argentina, 51°30, Geol. Soc. Am. Bull., 123,no. 9-10, 1679-1698.

P 1.24

Influence of Melting on the Long-Term Thermo-Chemical Evolution of Earth's Deep Mantle

Paul J. Tackley[1], Diogo Lourenco[1], Ilya Fomin[1], Takashi Nakagawa[2]

[1] *Institut für Geophysik, Departement Erdwissenschaften, ETH Zürich, Sonneggstrasse 5, CH-8092, Zürich*
[2] *IFREE, JAMSTEC, Japan*

Melting has always played a key role in Earth evolution. Early solidification of a magma ocean may have left the mantle compositionally stratified and may have continued in the form of a long-lived basal magma ocean (BMO). Ongoing upper mantle/transition zone melting, perhaps associated with water and carbonate, may have caused 'internal differentiation', resulting in dense enriched products that sink. Throughout Earth's history melting in the shallow mantle has produced crust, most of which was recycled into the interior and some of which may have segregated above the core-mantle boundary, joining possible enriched products from early differentiation, internal differentiation and BMO solidification to produce a Basal Melange (BAM). Here we investigate the thermal and chemical evolution of Earth's interior from the ~molten state to billions of years later using global-scale numerical simulation. Our previously-published models that included only oceanic crustal production and recycling (e.g. Nakagawa & Tackley, 2014) indicated that (i) a layer of subducted crust can rapidly build up above the CMB, (ii) early-formed layering above the CMB may have been necessary to avoid rapid early core cooling and a too-large present-day inner core, (iii) magmatism is the dominant heat transport mechanism early on, (iv) melting acts as a thermostat, buffering mantle temperature. Here we improve the models to handle deep melting including melt fractions of up to 100%, fractional melting using a eutectic model, segregation of melt and solid, and a parameterized magma ocean treatment at high melt fractions (using an eddy diffusivity based on mixing length theory, similar to previous 1-D treatments). We investigate and characterize the evolution of deep mantle structure in the limits of negatively buoyant melt and positively buoyant melt. We focus on the interplay of deep melting and melt migration, primordial layering, recycled crust and harzburgite, and products of upper mantle internal differentiation, in producing a heterogeneous deep mantle.

REFERENCES

Nakagawa, T., and P. J. Tackley (2014), Influence of combined primordial layering and recycled MORB on the coupled thermal evolution of Earth's mantle and core, Geochem. Geophys. Geosyst., 15, 619-633, doi:10.1002/2013GC005128.

P 1.25

Unravelling tectonics and surface processes in exhumation history of South Alaska: insights from the thermochronological record

Pierre G. Valla[1], Jean-Daniel Champagnac[2], David L. Shuster[3,4], Frédéric Herman[1], Maria Giuditta Fellin[2] & Eva Enkelmann[5]

[1] *Institute of Earth Surface Dynamics, University of Lausanne, CH-1015 Lausanne (pierre.valla@unil.ch)*
[2] *Department of Earth Sciences, ETH Zurich, CH-8092 Zurich*
[4] *Department of Earth and Planetary Science, UC Berkeley, USA-94720 Berkeley*
[5] *Berkeley Geochronology Center, USA-94720 Berkeley*
[5] *Department of Geology, University of Cincinnati, USA-45221 Cincinnati*

The southern Alaska range presents an ideal setting to study complex interactions between tectonics, climate and surface processes in landscape evolution [e.g. Champagnac et al., 2012]. It exhibits active tectonics with the ongoing of subduction/collision between Pacific and North America, and major active seismogenic reverse and strike-slip faults [Meigs et al., 2008; Chapman et al., 2012]. The alpine landscape, rugged topography and the important present-day ice-coverage reveal a strong glacial imprint associated with high erosion and sediment transport rates [Berger et al., 2008]. Therefore, the relative importance of glacial erosion and tectonics for the observed late-exhumation history appears to be quite complex to decipher.

Here, we first perform a formal inversion [Herman et al., 2013; Fox et al., 2014] of an extensive bedrock thermochronological dataset collected in southern Alaska over the last decades to quantify the large-scale 20-Myr exhumation history. We show that almost half of the variability within the thermochronological record can be explained by modern annual precipitation spatial distribution, the residuals clearly evidencing localized exhumation along major tectonic structures of the frontal fold and thrust belt [Enkelmann et al., 2009; Spotila and Berger, 2010 ; Enkelmann et al., 2014]. Our results confirm high exhumation rates in the St Elias "syntaxis" and frontal fold and thrust belts for the last 0-2 Myr, where major ice fields and high precipitation rates likely promoted high erosion rates; the impact of late Cenozoic glaciations impact being less visible there than in less active mid-latitude mountain ranges such as the European Alps or British Columbia [e.g. Shuster et al., 2005; Valla et al., 2011]. On the contrary, our inversion outcomes highlight that north of the Bagley Icefield long-term exhumation has remained quite slow and continuous over the last ~20 Myr [e.g. Spotila and Berger, 2010 ; Enkelmann et al., 2010], with no late-stage signal of exhumation change since the onset of glaciations depiste clear glacial imprint in the landscape.

To overcome this potential bias in resolving the tectonic and glacial impact on exhumation history, we focus on the Granite Range (Wrangell-St Elias National Park, Alaska), an area presenting a strong glacial imprint but minor tectonic activity with only localized brittle deformation. We sampled four elevation profiles over an East-West transect for low-temperature thermochrometry. Apatite (U-Th-Sm)/He dating provides ages between ~10 and 30 Ma, in agreement with published data [Spotila and Berger, 2010 ; Enkelmann et al., 2010], and shows apparent low long-term exhumation rates (~0.1 km/Myr). 4He/3He thermochronometry on a subset of samples reveals a more complex exhumation history, with a significant increase in exhumation/erosion since ~6-4 Ma that we relate to the early onset of glaciations and glacial erosion processes. Our results, in agreement with offshore sediment records [Rea and Scnoeckx, 1995 ; Reece et al., 2011], thus confirm early glacial activity and associated erosion response in Alaska, well before the onset of Pliocene-Pleistocene Northern Hemisphere glaciations.

REFERENCES

Berger, A.L., Spotila, J.A., Chapman, J.B., Pavlis, T.L., Enkelmann, E., Ruppert, N.A. & Buscher, J.T. 2008: Architecture, kinematics, and exhumation of a convergent orogenic wedge: A thermochronological investigation of tectonic-climatic interactions within the central St. Elias orogen, Alaska. Earth and Planetary Science Letters, 270, 13-24.

Champagnac, J.□D., Molnar, P., Sue, C. & Herman, F. 2012: Tectonics, Climate, and Mountain Topography. Journal of Geophysical Research B: Solid Earth, 117, doi:doi:10.1029/2011JB008348.

Chapman, J.B., Pavlis, T.L., Bruhn, R.L., Worthington, L.L., Gulick, S.P.S. & Berger, A.L. 2012: Structural relationships in the eastern syntaxis of the St. Elias orogen, Alaska. Geosphere, 8, 105-126.

Enkelmann, E., Zeitler, P.K., Pavlis, T.L., Garver, J.I. & Ridgway, K.D. 2009: Intense localized rock uplift and erosion in the St Elias orogen of Alaska. Nature Geoscience, 2, 360-363.

Enkelmann, E., Zeitler, K., Garver, J.I. &Pavlis, T.L. 2010: The thermochronological record of tectonics and surface processes interaction at the Yakutat-North American collision zone in the southeast Alaska. American Journal of Science, 310, 231-260.

Enkelmann, E., Valla, P.G. & Champagnac, J.-D. 2014: Low-temperature thermochronology of the Yakutat Plate corner, St. Elias Range (Alaska): bridging short-term and long-term deformation. Quaternary Science Reviews, in press.

Fox, M., Herman, F., Willett, S.D. & May, D.A. 2014: A linear inversion method to infer exhumation rates in space and time from thermochronometric data. Earth Surface Dynamics, 2, 47-65.

Herman, F., Seward, D., Valla, P.G, Carter, A., Kohn, B., Willett, S.D. & Ehlers, T.A. 2013: Worldwide acceleration of mountain erosion under a cooling climate. Nature, 504, 423-426.

Meigs, A., Johnston, S., Garver, J. & Spotila, J. 2008: Crustal-scale structural architecture, shortening, and exhumation of an active, eroding orogenic wedge (Chugach/St Elias Range, southern Alaska). Tectonics, 27.

Rea, D.K. & Snoeckx, H. 1995: Sediment fluxes in the Gulf of Alaska: Paleoceanographic record from site 887 on the Patton-Murray seamount platform. In Rea, D.K., Basov, I.A., Scholl, D.W., and Allan, J.F., eds., Proceedings of the Ocean Drilling Program, Scientific results, Volume 145: College Station, Texas, Ocean Drilling Program, 247-256.

Reece, R.S., Gulick, S.P.S., Horton, B.K., Christeson, G.L. & Worthington, L.L. 2011: Tectonic and climatic infl uence on the evolution of the Surveyor Fan and

Channel system, Gulf of Alaska. Geosphere, 7, 830-844.

Shuster, D.L., Ehlers, T.A., Rusmore, M.E. & Farley, K.A. 2005: Rapid glacial erosion at 1.8 Ma revealed by 4He/ 3He thermochronometry. Science, 310, 1668-1670.

Spotila, J.A. & Berger, A.L. 2010: Exhumation at orogenic indentor corners under long-term glacial conditions: Example of the St. Elias orogen, Southern Alaska. Tectonophysics, 490, 241-256.

Valla, P.G., Shuster, D.L. & van Der Beek, P.A. 2011: Significant increase in relief of the European Alps during Mid□ Pleistocene glaciations. Nature Geoscience, 4, 688-692.

P 1.26

3D FEM modelling of fold nappe formation and the Rawil depression in western Switzerland

von Tscharner Marina & Schmalholz Stefan

Université de Lausanne, Institut des sciences de la Terre, Quartier UNIL-Mouline, Bâtiment Géopolis, CH-1015 Lausanne, (marina.vontscharner@unil.ch)

The Rawil depression is an axial depression located in Western Switzerland around the border between the cantons of Bern and Vallais. It is characterized by an opposite plunge of fold-axes in the Helvetic nappe system as well as the underlying basment. The fold axes of the Morcles fold nappe in the west of the Rawil depression plunges to the ENE whereas the fold axes in the more eastern Doldenhorn nappe plunges to the WSW. The Morcles nappe is mainly the result of layer parallel contraction and shearing (Ramsay, 1981). During the compression the massive limestones were more competent than the surrounding marls and shales, which led to the buckling characteristics of the Morcles nappe, especially in the north-dipping normal limb. The Doldenhorn nappe exhibits only a minor overturned fold limb and shows significantly more localized deformation at it's base (Steck et al., 1999). A possible explanation for this stronger localization at the base is that the weak basal sediments in the half graben deposits forming now the Doldenhorn nappe have been thinner than the sediments in the half graben sediments forming the Morcles nappe (Pfiffner, 2011). The Morcles nappe is tectonically separated from the more eastern Doldenhorn nappe due to the Rawil depression. The Helvetic nappe stack consists of the Morcles nappe in the west and Doldenhorn nappe in the East (both nappes are in the infrahelvetic domain) as well as the overlying Wildhorn and Diablerets nappes. In the Rawil depression the nappe stack is overprinted by a dexral transtension. In the deepest part of the depression, where the highest nappes are preserved, oblique normal faults with significant displacement are observed (Gasser and Mancktelow, 2010). The evolution during exhumation and cooling from ductile to brittle deformation is documented in this area where ductile folding led to the axial depression and brittle faulting led to the normal faults (grabens). The sediments of the Helvetic domain are a repetition of limestones, marls, shales and sandstones which were deposited from late Triassic to Early Oligocene at the European margin (Escher et al., 1993). After the last sedimentation the Helvetic nappes were progressively formed by folding and overthrusting. The lowermost nappes, the Morcles and Doldenhorn nappe are autochthonous and paraautochthonous, wheareas the overlying Wildhorn nappe, Diablerets nappe and Gellihorn nappe are detached from their basement. The future Helvetic nappes represented the distal margin of Europe north of the Valais domain. After the nappe stacking due to compression, the Helvetic nappe stack was folded and updomed due to continuous compression. This led to the exhumation of the external massifs.

The geometry and structures around the Rawil depression are relatrively well documented and described. However, the fundamental dynamics of the formation of the large-scale 3-D structure including the Morcles and Doldenhorn nappes and the related Rawil depression is still incompletely understood. Therefore, we perform simple 3-D numerical simulations to better understand the the dynamics of fold nappe formation with laterally varying initial geometry. Such simulations require a numerical algorithm that can accurately track material interfaces for large differences in material properties (e.g. between limestone and shale) and for large deformations.

We will present 2-D and 3-D numerical simulations using a finite element (FE) algorithm for large strain deformation of power-law viscous material. The simulations are applied to the formation of tectonic fold nappes as the Morcles and Doldenhorn nappes and to the later formation of the Rawil depression.

REFERENCES

Escher, A., Masson H., and Steck A. (1993), Nappe geometry in the Western Swiss Alps, Journal of Structural Geology, 15 (3-5), 501-509.

Gasser, D., and Mancktelow N. (2010), Brittle faulting in the Rawil depression: field observations from the Rezli fault zones, Helvetic nappes, Western Switzerland., Swiss Journal of Geoscience, 103, 15-32.

Pfiffner, A. (2011), Structural Map of the Helvetic Zone of the Swiss Alps, including Voralberg (Austria) and Haute Savoie (France),1:100000, Geological Special Map 128.Explanatory notes.

Ramsay, J. G. (1981), Tectonics of the Helvetic Nappes, Geological Society, London, Special Publications, 9, 293-309.

Steck, A., Bigioggero B., Piaz G. D., Escher A., Martinotti G., and Masson H. (1999), Carte tectonique des Alpes de Suisse occidentale et des regions avoisinantes,1:100000, Carte geologique speciale n 123, Swiss National Hydrological and Geological Survey.

P 1.27

Interplay between seismic fracturing and aseismic creep during strain localization in the middle crust (Woodroffe Thrust, Central Australia)

Sebastian Wex[1], Neil Mancktelow[1], Friedrich Hawemann[1], Alfredo Camacho[2] & Giorgio Pennacchioni[3]

[1] *Department of Earth Sciences, ETH Zurich, Sonneggstrasse 5, CH-8092 Zurich*
[2] *Department of Geosciences, University of Padua, Via Gradenigo 6, 35131 Padua*
[3] *Department of Geological Sciences, University of Manitoba, 125 Dysart Rd, Winnipeg, Manitoba, R3T 2N2 Canada*

The Musgrave Ranges in Central Australia provide an excellent exposure of the shallowly south-dipping Woodroffe Thrust, which placed ~1200 Ma granulites onto similarly-aged amphibolite and granulite facies gneisses. This ~ 400 km long E-W structure developed under mid-crustal conditions during the intracratonic Petermann Orogeny around 550 Ma (Maboko et al., 1992; Camacho and McDougall, 2000). From field observations, the shortening direction is constrained to vary between NNE-SSW and NNW-SSE and the sense of movement is consistently top-to-north thrusting. Ductile deformation along the Woodroffe Thrust almost entirely localized in the footwall rocks, developing a zone of protomylonites, mylonites, ultramylonites and sheared pseudotachylytes, several hundreds of metres wide, with pseudotachylyte abundance and the degree of mylonitization rapidly decreasing further into the footwall. In contrast, the immediate hanging wall largely behaved in a brittle manner, developing significant amounts of pseudotachylyte veins and breccias in a zone up to a few hundred metres wide. Only the lowermost few tens of metres of the pseudotachylyte breccia in the hanging wall were mylonitically overprinted, with subsequent pseudotachylyte veins cross-cutting the mylonitic foliation. Above this zone the pseudotachylyte veins in the hanging wall remain largely unsheared. This asymmetry might reflect lower ambient temperatures in the hanging wall (Camacho and McDougall, 2000) or result from a higher abundance of hydrous minerals in the footwall (Camacho et al., 1995).

Low-strain domains in the footwall reveal that localized shearing initiated along pseudotachylyte veins and that shear zones were in turn exploited by pseudotachylyte formation, establishing a cyclic interplay between fracture and flow in time and space (Figure 1). Neither phyllonitization nor synkinematic growth of new muscovite is observed on a regional scale. In contrast to models with a simple brittle-to-viscous transition, these observations show that continuous cycles of brittle fracturing (pseudotachylyte formation) and shearing (mylonitization) are active in “dry” mid-crustal environments. The product of multiple seismic slip events and ductile shear, repeatedly exploiting the same structural discontinuities, is the formation of composite layers of mylonite/ultramylonite and sheared pseudotachylyte, as frequently observed in the Woodroffe Thrust. In both the footwall and hanging wall, viscous shearing not only localizes on pseudotachylytes, but can also be concentrated along the (chilled) margins of fine-grained dolerite dykes, indicating a possible grain size dependence on the process of strain localization under dry mid-crustal conditions. However, most shear localization occurs on precursor fractures and associated pseudotachylyte and largely ignores any pre-existing compositional layering.

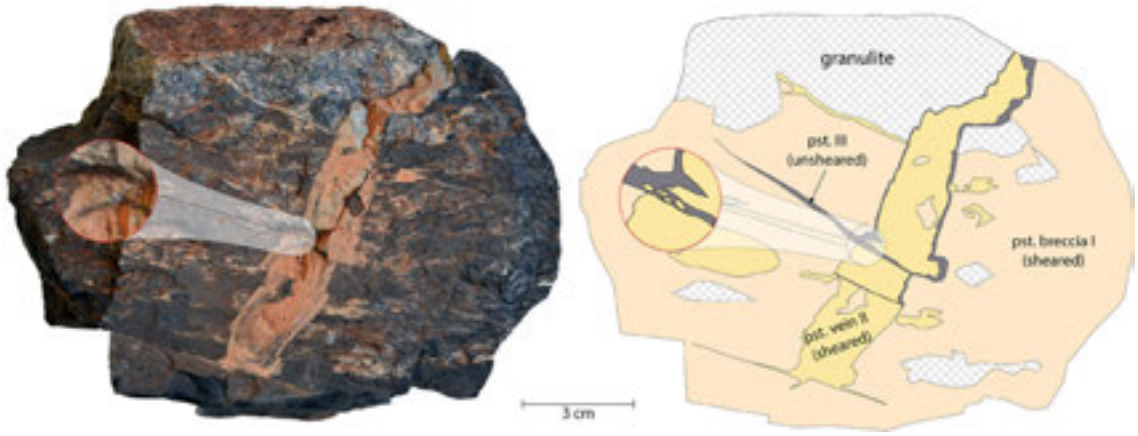

Figure 1. Sample from the Woodroffe Thrust revealing a detailed cyclicity between brittle fracturing (pseudotachylyte formation) and shearing. Three different generations of pseudotachylytes (I, II, III; in order: older to youngest) are observed cross-cutting each other. The two older generations (I, II) are both sheared and each incorporated as sheared fragments within the next younger pseudotachylyte. These observations are consistent with three phases of brittle fracturing separated by two intermediate episodes of shearing.

REFERENCES

Camacho, A., McDougall, I., 2000. Intracratonic, strike-slip partitioned transpression and the formation and exhumation of eclogite facies rocks: An example from the Musgrave Block, central Australia. Tectonics 19, 978–996.

Camacho, A., Vernon, R.H., Fitz Gerald, J.D., 1995. Large volumes of anhydrous pseudotachylyte in the Woodroffe Thrust, eastern Musgrave Ranges, Australia. Journal of Structural Geology 17, 371–383.

Maboko, M.A.H., McDougall, I., Zeitler, P.K., Williams, I.S., 1992. Geochronological evidence for ~ 530–550 Ma juxtaposition of two Proterozoic metamorphic terranes in the Musgrave Ranges, Central Australia. Australian Journal of Earth Sciences 39, 457–471.

2. Mineralogy, Petrology, Geochemistry

Eric Reusser, Sébastien Pilet

Swiss Society of Mineralogy and Petrology (SSMP)

TALKS:

2.1 Axelsson E., Mezger K., Villa I.M., Berndt J.: The Kuunga Orogeny in the Eastern Ghats Belt and the implications for the final assembly of Gondwanaland

2.2 Bergemann C., Gnos E., Berger A., Whitehouse M., Pettke T., Janots E.: Shear zone activity of the Grimsel are (Aar-massif): Th-Pb data in hydrothermal cleft monazite

2.3 Botter C., Meier M., Weber K., Kandler K., Weinzierl B., Grobéty B.: Mineralogical and morphological changes after long-range atmospheric transport: the Eyjafjallajökull volcanic plume

2.4 Burn, M., Lanari, P., Engi, M.: Subduction / exhumation dynamics: Petrochronology in Austroalpine outliers (Western Alps, Italy)

2.5 Bussien Grosjean D., Chazot G., Bollinger C., Vonlanthen P., Guillong M., Bachmann O., Langlade J., Rouget M.-L., Liorzou C.: The geochemical content of zircon as a potential tracer for geodynamic context of formation

2.6 Casanova V., Kouzmanov K., Audetat A., Ubrig N., Fontbote L.: First systematic study of synthetic fluid inclusions in opaque ore minerals: method development

2.7 Dolder, F., Mäder, U., Jenni, A.: Stability of bentonite under high-pH conditions

2.8 El Korh A., Luais B., Boiron M.C., Deloule E.: Ge and Ga mobility in high-pressure metabasites during subduction and exhumation processes

2.9 Ewing T., D›Abzac F., Chiaradia M., Müntener O., Schaltegger U.: Advances in fingerprinting crustal and mantle inputs to magmatic systems: in situ measurement of Hf isotopes in zircon at high precision and spatial resolution on the UNIGE Neptune Plus

2.10 Fekete Sz., Weis P., Driesner T., Heinrich C. A.: The physical hydrology of porphyry copper systems: Combining fluid flow modeling with oxygen isotope measurements of quartz by high-resolution SIMS microanalysis

2.11 Gilgen S. A., Diamond L. W., Mercolli I.: Exploring the significance of intense epidosite alteration of volcanic rocks from the Semail ophiolite (Oman) for ancient and modern oceanic hydrothermal systems

2.12 Lanari P., Riel N., Engi M.: Micro-mapping of chemical potential gradients: A new shovel to bury the concept of global equilibrium in metamorphic rocks

2.13 Robyr M., Goswami-Banerjee S.: Chemical and textural behaviour of REE accessory phases with increasing metamorphic grade in a well constrained prograde pelitic suite: implications for allanite and monazite petrochronology

2.14 Saintilan N.J., Spangenberg J.E., Stephens M.B., and Fontboté L.: Source and types of extrinsic organic compounds involved in thermochemical sulfate reduction at the Pb-Zn sandstone-hosted Laisvall deposit, Sweden

2.15 Schlöglová K., Wälle M., Heinrich C.A.: Chemical modification of fluid inclusions hosted by non-traditional minerals

2.16 Seitz S., Putlitz P., Baumgartner L., Escrig S., Meibom A.: Trace element diffusion in quartz-phenocrysts from a Jurassic meta-rhyolite: constrains from the contact-aureole of the Chaltén Plutonic Complex (Fitz Roy, Patagonia)

2.17 Siron G., Baumgartner L., Bouvier A-S., Putlitz B.: SIMS analysis of minerals with solid solution

2.18 Vrijmoed, J. C., Podladchikov, Y. Y., Moulas, E., Tajcmanova, L.: Heterogeneous phase equilibria in rocks under a pressure gradient

POSTERS:

P 2.1 Buchs N., Baumgartner L., Putlitz B., Vennemann,D.: Stable isotope ($\delta^{18}O$ and δD) record of fluid-rock interaction in the Zermatt-Saas Fee ophiolites (Pfulwe – Rimpfischorn): from sea floor to exhumation

P 2.2 Normand R., Schmidt S Th., Sartori M.: Pressure-temperature-time evolution in the high-grade metamorphic basement of the Siviez-Mischabel nappe (Val d'Hérens, Val d'Anniviers)

P 2.3 Picazo S., Müntener O., Manatschal G., Basch V.: Tectono-sedimentary breccias associated with mantle windows in hyper-extended domains (Eastern Swiss Alps): field observations, geochemistry, and consequences for the subduction interface

P 2.4 Xin Z., Vrijmoed J., Tajcmanova L.: Pressure-controlled formation of asymmetric chemical zoning in garnet

P 2.5 Burn, M., Lanari, P., Pettke, T., Engi, M.: Non-matrix-matched standardization in quadrupole LA-ICP-MS: New data reduction for allanite age-dating

P 2.6 Pape J., Mezger K., Grobéty B., Neururer C.: Pushing the spatial limits of electron backscatter diffraction (EBSD) analysis: orientation relationships of zircon exsolutions in UHT-rutile

P 2.7 Manzini M, Siron G., Bouvier A-S., Baumgartner L., Ulmer P., Putlitz B., Vennemann T.: $\partial^{18}O$ measurements of glasses using SIMS: a calibration of Instrumental Mass Fractionation

P 2.8 Naumenko M.O., Bouman C., Mezger K,, Nägler T.F., Villa I.M.: Simultaneous measurements of the whole range of Ca isotopes (^{40}Ca-^{48}Ca) by TIMS

P 2.9 Corthay, G. , Vennemann, T. Kalinaj, M. Vallance, J., Fontboté, L.: The Quenamari prospect, San Rafael tin district, southern Peru: geology, mineral assemblages, fluid inclusion microthermometry, and stable isotopes.

P 2.10 Harutyunyan M.: The hydrothermal sericites of copper- molybdenum porphyry ore-magmatic systems of the Zangezur ore district (Southern Armenia, Lesser Caucasus)

P 2.11 Mihoko Hoshino, Yasushi Watanabe, Robert Moritz, Maria Ovtcharova, Jorge Spangenberg, Benita Putlitz: Magmatic, hydrothermal and weathering REE mineralization of the Blockspruit fluorite prospect, Bushveld granitic complex, South Africa

P 2.12 Hovakimyan S., Tayan R., Moritz R., Harutyunyan M., Hovhannisyan A.: Structural features of the Kajaran ore field and world-class Mo-Cu-porphyry deposit, Southern Armenia, Lesser Caucasus

P 2.13 Schlatter D.M., Hughes J.W.: The gold potential of South East Greenland: new insights of the eastern extension of the > 150 km Nanortalik gold belt

P 2.14 Bejaoui J., Bouhlel S: Les minéralisations à Pb-Zn-F de la province fluorée tunisienne : cas du Jebel Mecella

P 2.15 Bejaoui J., Bouhlel S: Le district minier à Pb-Zn-Ba du Jebel Hamra-Jebel Ajered (Tunisie centrale) : Géologie, Minéralogie, Inclusions Fluides et Isotopes.

P 2.16 Rottier B., Kouzmanov K., Casanova V., Bendezú R., Cuéllar D., Fontboté L.: First evidence of multiple porphyry events in the Cerro de Pasco polymetallic district, central Peru

P 2.17 Tamagnone Cosmelli E.: Petrography and geochemistry of the Cusín and Cubilche volcanoes (Interandean Valley, Ecuador)

P 2.18 Šegvić B., Süssenberger A., Ugarkovic M., Moscariello A: Mineralogy and cultural heritage – introducing QEMSCAN® automated technology to the study of ancient artefacts

P 2.19 Hunger G., Ventra D., Veiga G., Moscariello A.: The Miocene Mariño Formation (Central Argentinian foreland, Mendoza region): a high-resolution integrated study of sedimentary and paleoenvironmental responses to tectonic and climatic forcing

P 2.20 Miron G.D., Kulik D.A., Dmytrieva S.V., Wagner T.: Gemsfits: A Code For Input Parameter Optimization Of Chemical Thermodynamic Models

P 2.21 Touzin M., Franz L., Wetzel A.: Petrographic and sedimentologic examinations of river gravel from the 'Kleine Wiese' river, Black Forest (D)

2.1

The Kuunga Orogeny in the Eastern Ghats Belt and the implications for the final assembly of Gondwanaland

Emelie Axelsson[1], Klaus Mezger[1], Igor M Villa[1] & Jasper Berndt[2]

[1] *Institut für Geologie, Bern Universität, Balzerstrasse 1+3, CH-3012, Bern (axelsson@geo.unibe.ch)*
[2] *Institut für Mineralogie, Westfälische Wilhelms-Universität, Corrensstrasse 24, D-48149, Münster*

The Eastern Ghats Belt extends along the north east coast of peninsular India. It exposes high to ultra-high temperature gneisses and migmatites. Mineral ages from these rocks show that the region was affected by at least two granulite facies events, at ca. 1600 Ma and at ca. 930 Ma (Mezger & Cosca 1999).

New U-Pb rutile- and Rb-Sr biotite ages (recording ages corresponding temperatures of ca 500°C or lower) span between 440 and 525 Ma. This reveals a large-scale overprint in almost all areas of the EGB in the Cambrian. Previously these younger ages have been found only locally and were thought to be restricted to shear zones crosscutting the terrane (Dobmeier & Raith 2003; Upadhyay & Raith 2006). Until now, the EGB had not been considered as being an active part of the East African Orogen and the amalgamation of Gondwanaland. However, the new mineral ages show that the younger ages are observed over the whole EGB, and are not restricted to shear zones but are representative for the orogenic belt in general.

Recent publications (Meert 2003) suggest that the East African Orogeny, extending S-N and assembling east and west Gondwana, was followed by an E-W oriented orogeny, named Kuunga Orogeny, assembling north and south Gondwana. This orogeny was described up to now in Mozambique, East Antarctica (Sør Rondane), Sri Lanka and southern India. On the basis of U-Pb and Pb-Pb ages in zircon and monazite the East African and Kuunga orogenies are estimated to have peaked around 750-620 and 570-530 Ma, respectively.

The new rutile and biotite mineral ages for the EGB impliy that the Kuunga Orogeny extended as far as to the northern most parts of the EGB, much further north than previously known. Furthermore, this is consistent with the model that the amalgamation of Gondwanaland happened in two steps, first a E-W motion in the East African Orogeny and after that an N-S motion in the Kuunga Orogeny.

REFERENCES

Dobmeier C.J., Raith, M.M. 2003: Crustal architecture and evolution of the Eastern Ghats Belt and adjacent regions of India, Geological Society, London, Special Publications, 206.1, 145-168.

Meert, J.G. 2003: A synopsis of events related to the assembly of eastern Gondwana, Techtonophysics, 362, 1-40.

Mezger, K., & Cosca, A. 1999: The thermal history of the Eastern Ghats Belt (India) as revealed by U-Pb and $^{40}Ar/^{39}Ar$ dating of metamorphic and magmatic minerals: implications for the SWEAT correlation, Precambrian Research, 94, 251-271.

Upadhyay, D., Raith, M.M. 2006: Intrusion age, geochemistry and metamorphic conditions of a quartz-monzosyenite intrusion at the craton-Eastern Ghats Belt contact near Jojuru, India, Gondwana Research, 10, 267-276.

2.2

Shear zone activity of the Grimsel area (Aar-massif) : Th-Pb data in hydrothermal cleft monazite

Christian Bergemann[1], Edwin Gnos[2], Alfons Berger[3], Martin Whitehouse[4],Thomas Pettke[3] & Emilie Janots[5]

[1] *Earth and Environmental Sciences, University of Geneva, Rue des Maraîchers 13, 1205 Geneva, Switzerland*
[2] *Natural History Museum of Geneva, route de Malagnou 1, 1208 Geneva, Switzerland*
[3] *Institut für Geologie, University of Bern, Baltzerstrasse 1+3, 3012 Bern, Switzerland*
[4] *Swedish Museum of Natural History, Box 50007, SE104-05 Stockholm, Sweden*
[5] *ISTerre, University of Grenoble, 1381 rue de la piscine, 38041, Grenoble, France*

Millimeter-sized hydrothermal monazites from open fissures (clefts) associated with different cleft generations in shear zones of the Grimsel area, Aar Massif, Switzerland, have been investigated by ion microprobe (SIMS). Interaction of cleft-filling hydrothermal fluids with wall-rock causes REE mineral dissolution and alteration of the wall-rock. Redistribution of elements via a fluid over short distances (cm) led to formation of cleft monazite, which started to grow towards the end of quartz crystallisation. Chemical zoning as revealed with BSE images indicates stepwise growth.

t The shear zones in the study area are SW-NE oriented including down dip as well as horizontal stretching lineations (Rolland et al. 2009, Wehrens et al. in prep.). One monazite is from a first generation of clefts oriented subhorizontally and related to vertical movements indicated by subvertical stretching-lineation in the rocks. The two other investigated monazites were found in clefts belonging to a second generation. These clefts are vertically oriented and associated with strike-slip movements.

High precision isotope dating yields monazite crystallization ages. Unlike ^{238}U-^{206}Pb ages, ^{232}Th-^{208}Pb hydrothermal monazite ages are not affected by excess Pb (Janots et al., 2012) and yield a higher precision than ages obtained through the U system. The analysed monazites yield growth domains between ~12 to ~10.5 Ma and one grain shows another growth step at ~7 Ma. Differing chemical domains within the crystals imply successive dissolution-reprecipitation steps, but individual crystallisation ages are not resolvable. Our monazite growth ages are interpreted as crystallisation following local brittle deformation associated with cleft formation during active shear zone evolution. Whereas the beginning of monazite crystallization in both types of shear zones is roughly coeval and starts around ~12 Ma. This implies that the transition from vertical movements to strike-slip faulting occurred around that time. One monazite clearly shows that the younger strike-slip movement lasted at least until 7 Ma.
Grimsel area monazite ages are in accordance with Rb-Sr in mica ages of 10-12 Ma (Challandes et al., 2008) thought to represent strong fluid circulation at that time. Slightly older ^{40}Ar-^{39}Ar ages of 13.9-12.0 Ma of white mica in mylonites (Rolland et al., 2009) interpreted to constrain ductile deformation further agree with this study. Mylonite and fault gouge K-Ar ages of Kralik et al. (1992) of 11.7 to 6.4 Ma, interpreted to date continuous recrystallization during fault activity in a shear zone slightly further north also agree well with our cleft monazite crystallization ages.

REFERENCES

Rolland, Y., Cox, S.F. and Corsini, M., 2009. Constraining deformation stages in brittle-ductile shear zones from combined field mapping and ^{40}Ar/^{39}Ar dating: The structural evolution of the Grimsel Pass area (Aar Massif, Swiss Alps). Journal of Structural Geology 31, 1377-1394.

Janots, E., Berger, A., Gnos, E., Whitehouse, M., Lewin, E. and Pettke, T., 2012. Constraints on fluid evolution during metamorphism from U-Th-Pb systematics in Alpine hydrothermal monazite. Chemical Geology326-327,61-71.

Kralik, M., Clauer, N., Holnsteiner, R., Huemer, H. and Kappel, F., 1992. Recurrent fault activity in the Grimsel Test Site (GTS, Switzerland): revealed by Rb-Sr, K-Ar and tritium isotope techniques. Journal of the Geological Society, London 149, 293-301.

Challandes, N., Marquer, D. and Villa, I.M., 2008. P-T-t modelling, fluid circulation, and ^{39}Ar-^{40}Ar and Rb-Sr mica ages in the Aar Massif shear zones (Swiss Alps). Swiss Journal of Geosciences 101, 269-288.

2.3

Mineralogical and morphological changes after long-range atmospheric transport: the Eyjafjallajökull volcanic plume

Cédric Botter[1], Mario Meier[1], Konradin Weber[2], Konrad Kandler[3], Bernadett Weinzierl[4] & Bernard Grobéty[1]

[1] *Départment des Géosciences et FRIMAT, University of Fribourg, Chemin du musée 6, CH-1700 Fribourg*
[2] *University of applied sciences Düsseldorf, Josef-Gockeln-Straße 9, DE-40474 Düsseldorf*
[3] *Institut für Angewandte Geowissenschaften, Technische Universität Darmstadt, Schnittspahnstraße 9, DE-64287 Darmstadt*
[4] *Deutsches Zentrum für Luft- und Raumfahrt (DLR), Institut für Physik der Atmosphäre, DE-Oberpfaffenhofen*

The dispersion of Eyjafjallajökull (EFJ) volcanic ash over Central Europe impacted severely the economy due to the closure of large parts of European airspace in 2010. During periods in May, the University of Applied Sciences Düsseldorf and the DLR performed airborne measurements and collected in-situ aerosol samples from plume patches encountered over northwestern Germany, the North Sea and the North Atlantic during the flights. In Iceland, re-suspended ash samples were collected on the southern slopes of EFJ using a PM10 filter-sampling device after the eruption at the end of August 2010. Automated single-particle analysis using SEM coupled with EDX was performed on the samples to investigate the mineralogy, chemistry and morphology of fine ash particles. The airborne samples were compared with the re-suspended ash samples and with pyroclastic deposits collected close to the EFJ vents. The bulk composition of the re-suspended material, which was rich in particle aggregates, matches that of the proximal EFJ pyroclastic deposits. The volcanic aerosol particles (ash) sampled over Germany, the North Sea and the North Atlantic however, differ distinctly in bulk composition from proximal material and both in mineralogy and morphology from the particles re-suspended in Iceland. The ash cloud sampled over Germany and the North Sea were lacking dense crystalline phases, which represent a major component of the re-suspended ash particles and of the aerosol cloud sampled over the North Atlantic. The glass-rich particles sampled in Iceland had larger aspect ratio and higher surface roughness (=higher surface to volume ratio) than the more glass-rich particles dominating the continental sample. Gravitational settling was most likely the main process responsible for the loss of denser components during the atmospheric transport of the ash cloud between Iceland and Europe. Morphological segregation was probably promoted by stronger aggregation and faster adsorption of water vapour by particles with high surface-to-volume ratio. The phase composition of fine ash clouds and, therefore, the particles' physical properties, which may affect airplane operation (hardness and melting point), depend clearly on the plume's atmospheric residence time.

2.4

Subduction / exhumation dynamics: Petrochronology in Austroalpine outliers (Western Alps, Italy)

Marco Burn[1], Pierre Lanari[1] & Martin Engi[1]

[1] *Universität Bern, Institut für Geologie, Baltzerstrasse 3, CH-3012 Bern, Switzerland (marco.burn@geo.unibe.ch)*

Petrochronology is the combination of in situ age-dating, geothermobarometry and structural geology and aims to unravel Pressure-Temperature-deformation-time (P-T-ε-t) paths. To link P-T conditions to deformation stages is daily business for metamorphic petrologists, but recent micro-mapping techniques (XMapTools program) provide an additional tool to achieve this goal. Absolute age is often difficult to assess in metamorphic rocks, as it is challenging to link specific P-T conditions to most of the mineral chronometers.

Allanite is a common accessory phase in high-P metamorphic rocks and is a potential target to determine Th(-U)/Pb ages. Allanite from a leucocratic gneiss of the Glacier-Rafray slice in the western Alps consists of several chemically different zones: one major zone can be linked to a first high-P phengite generation. To determine the age of this high-P growth zone we used LA-ICP-MS in situ techniques, which allowed us to date an appropriate growth rim per grain. Even so particular care was required when evaluating the isotope signals. Laser ablation leads to the excavation of a volume, which potentially can be chemically and/or age-zoned. We have developed a new method to track changes in the plasma during the

ablation. This method aims to identify discrete age zones. These results indicate that high-P allanite first grew in equilibrium with phengite at 44.4 ± 3.1 Ma, whereas a second growth event occurred at 38.1 ± 2.8 Ma. A final epidotic rim grew at greenschist facies conditions (~30 Ma), but this stage could not be dated. P-T estimates are based on bulk rock forward modelling, equilibration volume forward modelling and quartz-phengite-H2O equilibrium calculations. Peak metamorphic conditions were estimated to 13 kbar and 450°C and 12 kbar and 500°C for the second allanite growth stage. Preliminary data of allanite from an impure quartzite from the Tour Ponton basal contact to the Piemont Oceanic units indicate a prograde allanite growth at 52.2 ± 1.8 Ma and a high-P peak growth at 44.5 ± 4.4 Ma.

These findings are in agreement with the recent understanding of tectono-metamorphic evolution of the Western Alps: In the Sesia Zone (former Adriatic margin), the earliest high-P metamorphism occurred at 85 Ma (Regis et al., 2014), whereas high-P peak was estimated to 45 Ma in the Piedmont Oceanic units. Austroalpine outliers such as Glacier-Rafray and Tour Ponton are commonly seen as extensional allochthons, which entered the subduction zone together with the Piemonte Oceanic units. The data presented in this work indicates a high-P metamorphism of Austroalpine outliers together with the Oceanic units.

2.5

The geochemical content of zircon as a potential tracer for geodynamic context of formation

Denise Bussien Grosjean[1], Gilles Chazot[1], Claire Bollinger [2], Pierre Vonlanthen[3], Marcel Guillong[4], Olivier Bachmann[4], Jessica Langlade[2], Marie-Laure Rouget [2] & Céline Liorzou[1]

[1] *Université de Brest, CNRS UMR 6538 (Domaines Océaniques), Institut Universitaire Européen de la Mer, Place N. Copernic, 29280 Plouzané, France (denise.bussien.grosjean@gmail.com)*
[2] *CNRS UMS 3113, Institut Universitaire Européen de la Mer, Place N. Copernic, 29280 Plouzané, France*
[3] *Institut des sciences de la Terre, Université de Lausanne, Bâtiment Géopolis, 1015 Lausanne, Switzerland*
[4] *Institute of Geochemistry and Petrology, Department of Earth Sciences, ETH Zurich, Clausiusstrasse 25, 8092 Zurich, Switzerland*

The ability of zircon crystals to survive chemical and mechanical erosion has widened its use in geosciences. Classically sampled for decades with the purpose of dating magmatic rocks, it has been increasingly used in recent years to determine the maximum age of deposition and the provenance of sedimentary rocks. Indeed, the chemical content of zircon provides valuable information on the magmatic reservoir involved in its formation (crust and/or mantle), the crystallisation temperature and the continental or oceanic origin of the grains. However, those characteristics do not constrain the context of rock formation in terms of geodynamic settings, a key feature for paleotectonic evolution understanding.

Here we present preliminary results on the use of zircon chemistry as a potential tracer for geodynamic environments. Magmatic rocks of granitic and intermediate composition were sampled from various well-constrained geodynamic settings, including intraplate (Cameroon), active margin (Alps), ocean rift (Alps), pre-, syn- and post collision (Brittany, Alps) environments. Zircon grains were mounted in epoxy resin, imaged by cathodoluminescence, and dated when needed. In addition electron microprobe analyses were performed to provide internal standards for high-resolution LA-ICP-MS analyses. The major and trace element signatures of zircon were then investigated to highlight discriminant features for each geodynamic setting.

Y and Yb seem to behave similarly for all the magmatic zircon grains considered (criteria: LaN(ormalised) > 1, PrN > 10 and SmN/LaN < 10). Unlike the chondrite-normalised rare earth elements plots, which do not show any trends indicative of specific geodynamic settings, variations in the content of Th, Nb, Ta and Rb point towards a potential distinction between ocean rift and intraplate environments. This is particularly obvious in plots of Y/Th against Ce or Eu. Those preliminary results seem to confirm the geochemical control of the zircon crystallisation and the potential of zircon as a tracer for its geodynamic context of formation.

2.6

First systematic study of synthetic fluid inclusions in opaque ore minerals: method development

Vincent Casanova[1], Kalin Kouzmanov[1], Andreas Audétat [2], Nicolas Ubrig [3] & Lluis Fontboté[1]

[1] *Department of Earth Sciences, University of Geneva, (vincent.casanova@unige.ch)*
[2] *Bayerisches Geoinstitut, University of Bayreuth, Germany.*
[3] *Department of Condensed Matter Physics, University of Geneva.*

Near-infrared (NIR) microscopy of ore minerals can be used to study internal textures of minerals that are opaque to the visible light, such as pyrite, enargite, wolframite, hematite, stibnite. It has also been applyied in studies of fluid inclusions (FI) hosted in opaque ore minerals, thus providing direct insights into P-T-X of ore-forming fluids (Campbell 1991). An earlier study performed on enargite-hosted FIs (Moritz, 2006) pointed out an important overestimation of fluid salinities and underestimation of homogenization temperatures owing to shifts in recorded phase transition temperatures as a function of the used light intensity. Here we report results of the first systematic study of synthetic FIs in a variety of NIR-transparent ore minerals in an attempt to create standards for NIR-microthermometry experiments. For each mineral, we compare the span of recorded phase change temperatures to its intrinsic absorption.

Natural samples of enargite, pyrite, stibnite, hematite, Fe-rich, and Fe-poor sphalerite were selected upon their transparency to NIR and their paucity in fluid inclusions. For each batch, an opaque mineral was loaded together with powdered equivalent and synthetic quartz into a gold capsule to which a 10 wt% NaCl aqueous solution spiked with Cs was added. After several days of equilibration in an autoclave at fixed P-T conditions, the samples were cracked in-situ and held at the same P-T conditions for several more days in order for the cracks to seal. The recovered samples were prepared as doubly polished 120 mm-thick sections. Microthermometric measurements were performed using a Linkam stage FTIR-600 mounted on an Olympus BX51 microscope equipped with IR Olympus objectives. The microscope has been modified to accept a removable 1200 nm low-pass filter placed at the exit of the light source. NIR observations and image acquisition were done using an Olympus XM10 camera connected to the CellP® software. The 100 W lamp intensity is controlled by an Olympus TH4-200 controller and recorded by a voltmeter mounted in parallel. Reflection and transmission Fourrier transform infrared (FTIR) spectra were acquired in the 800 - 3500 nm interval, using a Bruker 70v spectrometer coupled to a microscope. The intrinsic absorption of each mineral was then calculated.

Synthetic FIs (up to 70 µm in size) were obtained in enargite, pyrite, stibnite, Fe-rich, and Fe-poor sphalerite as well as in all quartz samples. Microthermometry performed under low light intensity yields similar apparent salinities for FIs trapped in quartz and NIR-transparent minerals from the same batch. With increasing light intensity, important shifts are recorded. In contrast to results reported by Moritz (2006), the correlation between light intensity and recorded temperatures is not linear but rather exponential (Fig. 1). It is important to stress that it is the intensity of light effectively reaching the sample that locally overheats the sample. This overheating causes the recorded underestimated (the thermocouple being shielded). The obtained correlation trends are therefore dependent on the microscope settings (light source intensity, diaphragms aperture, filters; Fig. 1) and also on the intrinsic absorption of each mineral. Indeed, results obtained for FI hosted in minerals with different absorption spectra show that if the shape of the correlation trends are similar, the span of recorded phase change temperatures is a function of the intrinsic absorption (Fig. 1). For a given microscope setting, the more absorbent a mineral, the larger the shift is between true and recorded temperature.

This study shows that under the same conditions, cogenetic fluid inclusions in gangue and ore minerals trap the same fluid at least in terms of major elements. It also confirms that under poorly controlled light settings during NIR-microthermometry, important underestimation of phase change temperatures can be recorded leading to overestimation of salinities (up to more than 100%). This directly translates into important errors when interpreting fluid origins or assessing the internal standard for LA-ICP-MS analyses. The shift spread recorded is a function of the intrinsic absorption of the host. For each NIR-transparent ore mineral, there is a range of light and microscope settings for which no shift is noticeable (Fig. 1).

Aknowledgements: This study is supported by SNF grant 146353. Sponsoring and acces to the laboratory facilities was kindly provided by the Bayerisches Geoinstitut (Germany).

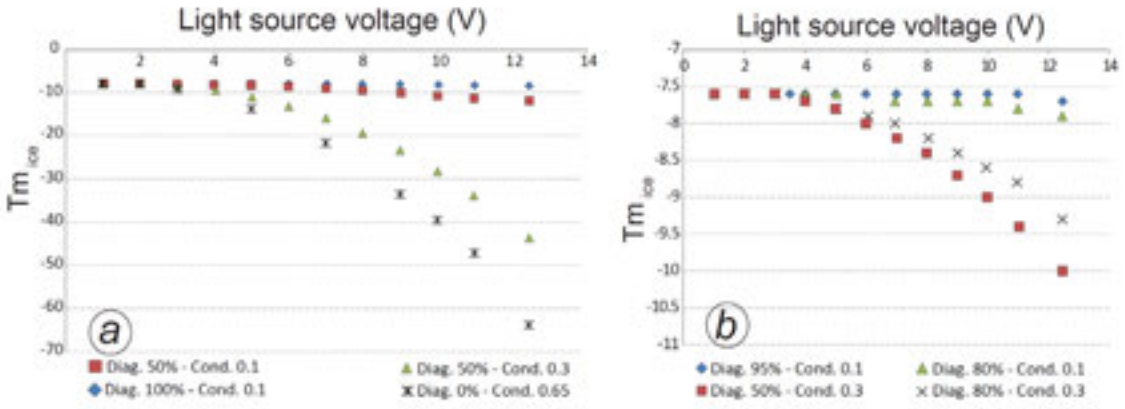

Figure 1: Correlation curves between recorded final ice melting temperature (Tm_{ice}) of FI hosted in minerals with different intrinsic absorption (**a**: enargite; **b**: Fe-poor sphalerite) as a function of light source intensity for different microscope settings. **Diag.**: Diaphragm controlling the incoming beam width (0%: fully open. 100% nearly closed). **Cond.**: Aperture iris diaphragm positioned before the condenser lens.

REFERENCES
Campbell, A. R. 1991: Geologic applications of infrared microscopy, SEPM short courses, 25, 161-171.
Moritz, R. 2006: Fluid salinities obtained by infrared microthermometry of opaque minerals: Implications for ore deposit modeling — A note of caution, Journal of Geochemical Exploration, 89, 284-287.

2.7

Stability of bentonite under high-pH conditions

Florian Dolder[1], Urs Mäder[1], Andreas Jenni[1]

[1] *RWI, University of Bern, Geological Sciences, Bern 3012, Switzerland*

Geological storage of radioactive waste foresees bentonite as buffer material enclosing spent fuel drums, as backfill and in tunnel seals. Concrete is proposed as building material for tunnel reinforcement. The emplacement of high-pH cementitious material next to clay generates a chemical gradient in pore-water chemistry that drives diffusive transport. Laboratory studies and reactive transport modeling predict significant mineral alteration near interfaces (Dauzeres et al., 2010; Fernández et al., 2009; Jenni et al., 2014).

We aim to characterize and quantify the cement/bentonite skin effects spatially and temporally, focusing on the advective-diffusive transport domain resolved at intermediate spacial scales. The core infiltration equipment is made of carbon fiber and plastics that hold a cylindrical bentonite sample under confining pressure and imposes a constant hydraulic gradient to drive a small advective flux (Dolder et al., 2014). Compacted and pre-saturated MX-80 bentonite is exposed to high-pH cementitious pore-fluids which alter the mineral assemblage over time. The related change in phase densities, porosity and local bulk density is tracked by computed tomography (CT) scans during ongoing infiltration.

In one experiment a potassium, sodium and hydroxide based infiltration fluid (0.28 molal), simulating an OPC pore-fluid (ordenary Portland cement) with a pH of 13.4, was used. The MX-80 bentonite sample had an initial saturated desity of 1.92 g/cm^3 and a water content of 25 wt.% and this shifted to 1.89 – 1.93 g/cm^3 and 31 – 33 wt.% over a time of 760 days. The hydraulic conductivity decreased after switching to a high-pH pore-fluid from ~$1.1^{*}10^{-13}$ m/s to ~$1.3^{*}10^{-14}$ m/s. A decrease in all ion concentrations with the exception of sulfate and potassium was observed, while pH just slightly increased from ~7.5 to ~8.

CT scans tracked a progressing reaction front from the filter into the first mm of the bentonite sample, revealing a bulk density increase (Figure 1, A). The reaction front was analyzed post-mortem in a longitudinal section as a zone of Mg and Ca enrichment. The Ca enrichment region consisted of two zones characterized by various amounts of precipitated calcite, confirmed by XRD measurements. The magnesium enriched zone showed an increased concentration in zone 1 but also extended into zone 2 in which the Mg enrichment appeared as spots in clay packages (Figure 1, B). The link beatween Mg enrichment and new mineral formation is in the XRD spectra not clear. In the same area a dissolution of cristobalithe (polymorph of silica) could be observed in the XRD spectra and in SEM morphology.

Further investigation are planned to resolve the newly formed Mg phase along with mor detailed investigations of the XRD spectra to detect possible newly formed minerals.

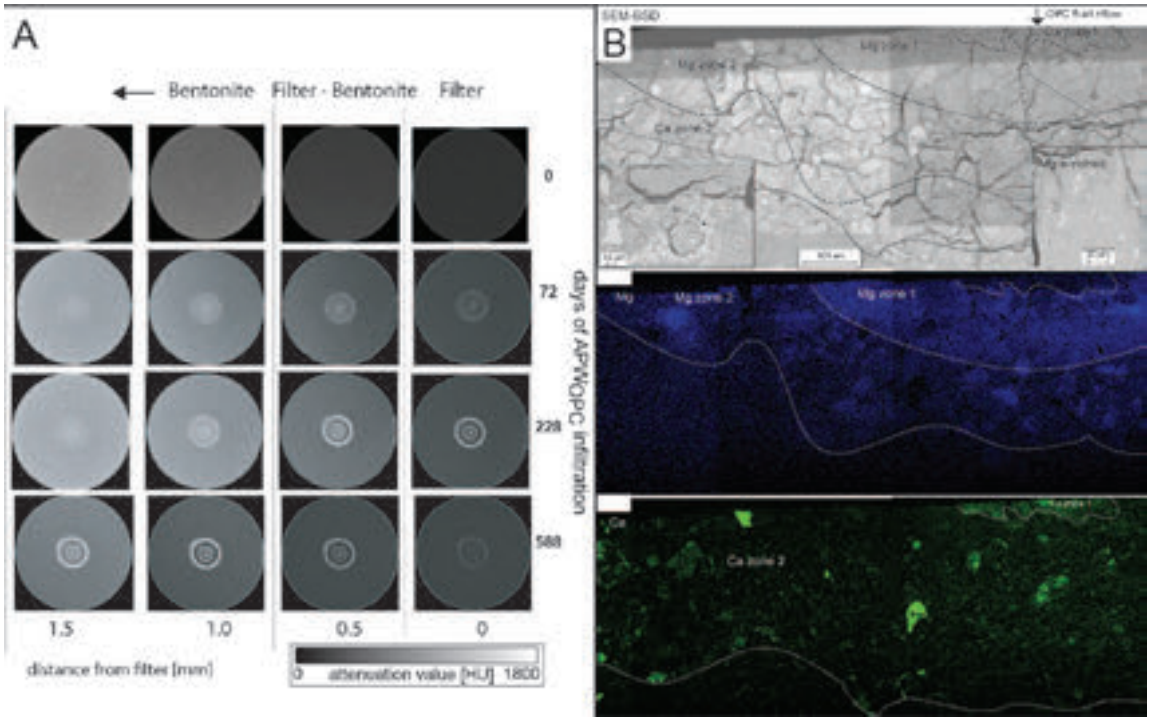

Figure 1: (A) Time series of CT scans showing the transition from inlet filter into the first mm of bentonite sample; (B) SEM-BSD image of a trans-section taken at the inlet of the bentonite sample along with the corresponding elemental mappings for magnesium and calcium.

REFERENCES

Dauzeres, A., Le Bescop, P., Sardini, P., Cau Dit Coumes, C., 2010. Physico-chemical investigation of clayey/cement-based materials interaction in the context of geological waste disposal: Experimental approach and results. Cement and Concrete Research 40, 1327-1340.

Dolder, F., Mäder, U., Jenni, A., Schwendener, N., 2014. Experimental characterization of cement–bentonite interaction using core infiltration techniques and 4D computed tomography. Physics and Chemistry of the Earth, Parts A/B/C 70–71, 104-113.

Fernández, R., Mäder, U., Rodríguez, M., de la Villa, R.V., Cuevas, J., 2009. Alteration of compacted bentonite by diffusion of highly alkaline solutions. European Journal of Mineralogy 21, 725-735.

Jenni, A., Mäder, U., Lerouge, C., Gaboreau, S., Schwyn, B., 2014. In situ interaction between different concretes and Opalinus Clay. Physics and Chemistry of the Earth, Parts A/B/C 70–71, 71-83.

2.8

Ge and Ga mobility in high-pressure metabasites during subduction and exhumation processes

Afifé El Korh[1], Béatrice Luais[1], Marie-Christine Boiron[2], and Etienne Deloule[1]

[1] *Centre de Recherches Pétrographiques et Géochimiques (CRPG), UMR7358 CNRS-Université de Lorraine, BP 20, 54501 Vandoeuvre-lès-Nancy Cedex, France (elkorh@crpg.cnrs-nancy.fr)*
[2] *GeoRessources, Université de Lorraine, CNRS, UMR7359, BP 70239, F-54506 Vandoeuvre-lès-Nancy, France*

Ge and Ga are trace elements that can be employed as fluid tracers in hydrothermal systems, as their solubility in fluid is temperature dependant (Pokrovski & Schott 1998). Due to similar chemical properties (oxidation state of 4+, ionic and covalent radii), Ge and Si share a strong affinity (Pokrovski & Schott 1998). Besides, Ga presents a strong affinity with Al (De Argollo & Schilling 1978). Physico-chemical conditions of hydrothermal processes would result either in Ge enrichment (Luais 2012), or Ge depletion of the basaltic crust in presence of hydrothermal sulphides (Malvin & Drake 1976). Variations in Ge and Ga concentrations were measured in a series of HP-LT rocks (peak P-T conditions: 1.7–2.3 GPa and 550–600°C) from the Ile de Groix (France), to investigate their behaviour during the subduction-zone metamorphism and associated fluid-rock interactions. The studied metabasites represent former MOR-type basalts, which underwent a pre-HP low-temperature hydrothermal alteration (El Korh et al. 2009).

Whole rock Ga and Ge concentrations were analysed by solution nebulisation ICPMS (± 8%; 1s). The Ga abundances in eclogites and blueschists (21.0–21.6 ppm) are similar to the values measured in tholeiitic basalts (18–22 ppm; De Argollo & Schilling 1978), while they decrease slightly in the greenschist facies metabasites (16.9–20.5 ppm). The Ge abundances measured in the metabasites (1.2–2.1 ppm) are generally higher than those of tholeiitic basalts (1.4–1.5 ppm; De Argollo & Schilling 1978), suggesting Ge enrichment during the low-T hydrothermal alteration. The Ge abundances decrease from blueschists and eclogites (1.6-2.0 ppm) to greenschists (1.2–1.9 ppm).

Ga and Ge abundances in minerals were obtained using LA-ICPMS (± 8-15%; 1s). Garnet and epidote are major phases in the metabasites. They are the main hosts for Ge (3.3–8.2 ppm in Grt; 2.4–12 ppm in Ep) and Ga (2.6–8.6 ppm in Grt; 33–112 ppm in Ep). Glaucophane and omphacite also contain significant amounts of Ga (3–15 ppm). The different generations of garnet and epidote formed during the prograde and retrograde metamorphic stages are distinguished based on the Ge/Si and Ga/Al ratios.

In garnet, the effect of prograde metamorphism from blueschists to eclogites, i.e. with increasing temperature from 500 to 550°C (El Korh et al. 2009), leads to an increase of the Ge/Si ratio, in line with a Ge/Si increase in rims. Ga/Al values remain relatively constant in garnet from blueschists, whereas in eclogites, the Ga/Al ratio weakly decreases in garnet rims, formed in equilibrium with Ga–rich omphacite. By contrast, the retrograde metamorphism from greenschist to blueschists does not modify the Ge/Si and Ga/Al ratios in garnet.

In epidote, the Ge/Si ratio also increases during the prograde path. At the peak metamorphic conditions (1.6–2.3 GPa, 500–600°C; El Korh et al. 2009) the Ge/Si ratio decrease in epidote formed in equilibrium with garnet rims and rutile (Ep III). Ge seems to be preferentially incorporated in garnet than in epidote. The Ga/Al ratio weakly increases in epidote with increasing P–T conditions. Epidote in eclogites has higher Ga/Al values, mirroring their higher whole rock Ga/Al values. During retrogression (< 1.6 GPa, < 500°C; El Korh et al. 2009), no variation of the Ge/Si and Ga/Al ratios is observed in the retrograde generation of epidote, while garnet is altered to chlorite.

These results allow the evaluation of the Ga and Ge exchange behaviour during the various P–T conditions. Ga is mainly exchanged between the various generations of epidote, Na–Ca amphiboles, omphacite and chlorite. However, the Ga abundances in the various HP minerals mirror the variation of Ga composition between the whole rocks. This suggests that the Ga composition of the metabasites reflects the protolith composition (MOR-type basalt). The Ga content decrease in greenschists compared to blueschists and eclogites, suggests a loss of Ga during retrogression. Ge is mainly exchanged between garnet and epidote during the prograde metamorphism. However, the decrease of the Ge abundances in greenschists compared to blueschists and eclogites indicates that a fraction of Ge left the metabasites during the fluid-rock interactions related to the retrograde metamorphism.

The study of the Ge and Ga partitioning between mineral phases and fluids in the subducted metabasites will allow the mobility of Ge and Ga into the fluid phase migrating to the mantle wedge to be characterised, with inferred consequences for the mantle composition and for the Ge cycle in the subduction zone.

REFERENCES

De Argollo, R. & Schilling, J. 1978: Ge–Si and Ga–Al fractionation in Hawaiian volcanic rocks. Geochimica et Cosmochimica Acta 42, 623-630.

El Korh, A., Schmidt S.Th., Ulianov, A. & Potel, S., 2009: Trace element partitioning in HP–LT metamorphic assemblages during subduction-related metamorphism, Ile de Groix, France: a detailed LA-ICP-MS study. Journal of Petrology 50, 1107-1148.

Luais, B. 2012: Germanium chemistry and MC-ICPMS isotopic measurements of Fe–Ni, Zn alloys and silicate matrices: Insights into deep Earth processes. Chemical Geology 334, 295-311.

Malvin, D.J. & Drake, M.J. 1976: Experimental determination of crystal/melt partitioning of Ga and Ge in the system forsterite-anorthite-diopside. Geochimica et Cosmochimica Acta 51, 2117–2128.

Pokrovski, G.S. & Schott, J. 1998: Thermodynamic properties of aqueous Ge(IV) hydroxide complexes from 25 to 350°C: implications for the behavior of germanium and the Ge/Si ratio in hydrothermal fluids. Geochimica et Cosmochimica Acta 62, 1631-1642.

2.9

Advances in fingerprinting crustal and mantle inputs to magmatic systems: in situ measurement of Hf isotopes in zircon at high precision and spatial resolution on the UNIGE Neptune Plus

Tanya Ewing[1], François–Xavier D'Abzac[2], Massimo Chiaradia[2], Othmar Müntener[1] & Urs Schaltegger[2]

[1] *Institute of Earth Sciences, University of Lausanne, UNIL-Mouline, CH-1015 Lausanne (tanya.ewing@unil.ch)*
[2] *Department of Earth Sciences, University of Geneva, Rue de Maraîchers 13, CH-1205 Genève*

The hafnium (Hf) isotope composition of zircon has long been recognised as an important tool for fingerprinting input from crustal and mantle reservoirs, for example in magmatic systems. Hf isotope measurements are performed by multi-collector (MC) ICP-MS, with sample introduction either by solution nebulisation or laser ablation (LA). The choice of sample introduction method represents a trade-off between precision and spatial resolution: solution MC-ICPMS is the higher precision technique, but requires dissolution of at least one entire zircon. LA-MC-ICPMS allows in situ analysis of subdomains within a single zircon, but at the cost of reduced precision. Individual zircons may contain multiple growth or replacement domains (e.g. Fig. 1) that can record a long and complex history, making in situ analysis essential in some cases.

The Thermo Scientific "Neptune Plus" at UNIGE is a state-of-the-art MC-ICPMS that is coupled to either a Photon Machines "Analyte G2" laser ablation system or an Aridus solution nebuliser. By careful tuning, regular monitoring of multiple zircon standards throughout analysis, and rigorous offline (post-analysis) data treatment, we are able to obtain excellent internal precision and external reproducibility for Hf isotopes measured by laser ablation. The Hf isotope composition of four international zircon standards (Mudtank, GJ-1, Plešovice and Temora) has been measured with internal precision of 0.3–0.4 ε-units and external reproducibility better than 1.0 ε-units (2SE), using a 50 µm spot. This represents an excellent compromise between precision and spatial resolution. In comparison, external reproducibility of ~0.3 ε-units (2σ) is typical for solution MC-ICPMS analysis of zircons. The very significant improvement in spatial resolution (often >10 times) obtained with laser ablation thus costs only a two- to three-fold decrease in precision with our system. The 2s errors of laser ablation analyses remain small with respect to the range of Hf isotope compositions of zircons in nature, allowing even subtle isotopic shifts to be resolved – including for different growth domains within the same zircon.

The full potential of our combined solution and laser ablation MC-ICPMS facility is exploited in a study of the Torres del Paine intrusive complex (Patagonia). This work employs both solution and laser ablation analyses of zircons that have previously been U–Pb dated, providing linked single-grain age and isotopic data. Hf isotopes are measured by solution for zircons that were dated by ID-TIMS, using the washes from U–Pb column chemistry. Other samples were dated in situ by LA-ICPMS, and the Hf isotope compositions of these zircons are determined using laser ablation. This combined approach allows us to obtain the highest precision possible in those samples analysed by solution, while exploring potential within-grain complexities in other samples with the high spatial resolution of laser ablation analyses. The results demonstrate that significant variability in source geochemistry is possible even for sheeted magmatic complexes built up on very short (<200 ka) timescales.

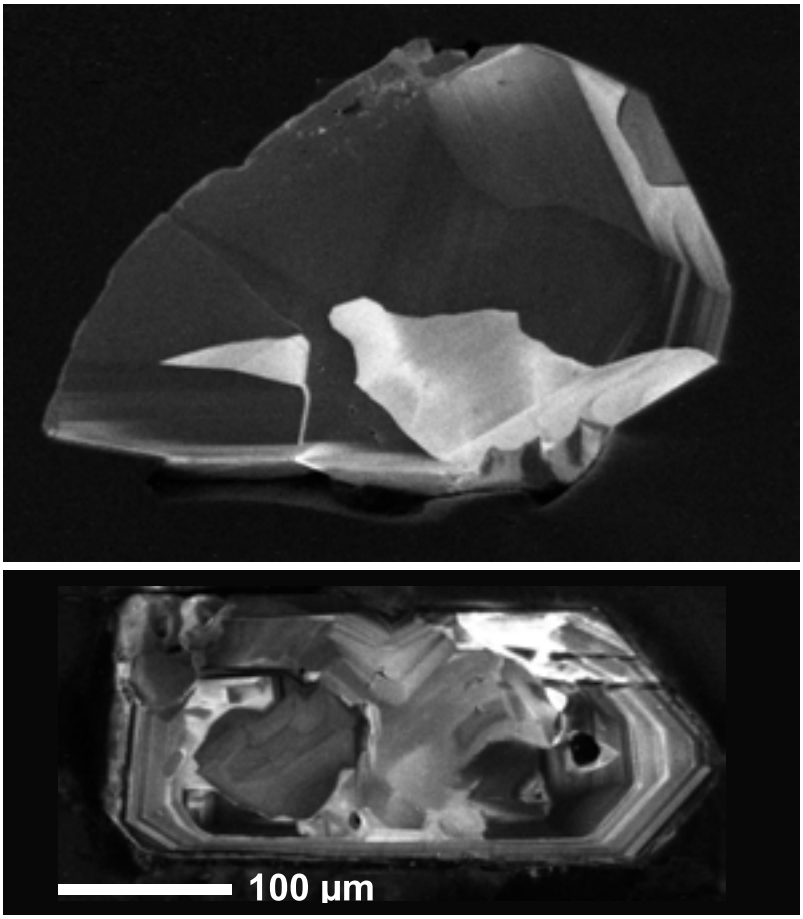

Figure 1. Cathodoluminescence images of complex zircons from (A) diorite, and (B) granite, both of the Torres del Paine intrusive complex, Patagonia. Typical LA-MC-ICPMS spot sizes for Hf isotopes (30–50 µm) are indicated by the dashed circles, and are small enough to allow analysis of multiple domains within individual zircons.

2.10

The physical hydrology of porphyry copper systems: Combining fluid flow modeling with oxygen isotope measurements of quartz by high-resolution SIMS microanalysis

Szandra Fekete[1], Philipp Weis[1], Thomas Driesner[1] & Christoph A. Heinrich[1]

[1] *Institut of Geochemistry and Petology, ETH Zürich, Clausiusstrasse 25, CH-8092 (szandra.fekete@erdw.ethz.ch)*

Porphyry copper systems are centered on intrusions above active and ancient subduction zones, located at depths of a few kilometers (Sillitoe 2010). They are important economic metal resources and provide nearly three-quarters of the world's copper, half of the molybdenum and a significant part of gold supply.

Recent numerical simulations of the physical hydrology of porphyry copper systems identify a significant role of meteoric fluids for the enrichment process, providing a cooling mechanism for metal-rich volatiles expelled from an upper crustal magma chamber (Weis et al. 2012). This model can calculate dynamic permeability changes in response to magmatic fluid expulsion, describing hydraulic fracturing and the transition from brittle to ductile rock behavior. The simulation results predict a stable front of copper precipitation between the hot lithostatically pressured magmatic fluid plume and the surrounding hydrostatically pressured meteoric flow regime.

The main aim of the present research is to quantify the degree of mixing of meteoric and magmatic water in porphyry copper systems. Due to their different isotopical characteristics, oxygen isotopes can be used to distinguish between magmatic and meteoric fluids.

The spatial and temporal evolution of oxygen isotope compositions are studied by numerical modeling of multiphase flow of H_2O-NaCl fluids in the subsurface. New modeling functionalities describing the equilibrium fractionation between quartz and water and advection of oxygen isotopes have been developed and coupled to our model for thermohaline convection (Weis et al. 2014), which is built within the Complex Systems Modeling Platform CSMP++ (Matthai et al. 2007).

The simulation results will be compared to analytical stable isotope studies. Oxygen isotope measurements are carried out with the high-resolution SIMS instrument located in the new SwissSIMS laboratory in Lausanne. Natural quartz samples from Bingham Canyon and Elatsite, Bulgaria are studied, which were used previously for microthermometry analysis and SEM cathodluminescence petrography (e.g. Stefanova et al. 2014). These samples show clear textural relationships between early and late quartz vein formation and ore precipitation with reliable temperature values derived from fluid inclusion analyses within both quartz generations.

Preliminary results from both numerical simulations and oxygen isotope measurements will be presented.

REFERENCES

Matthai, S.K., Geiger, S., Roberts, S.G., Paluszny, A., Belayneh, M., Burri, A., Mezentsev, A., Lu, H., Coumou, D., Driesner, T. & Heinrich, C. A. 2007: Numerical simulation of multi-phase fluid flow in structurally complex reservoirs: Structurally Complex Reservoirs, 292, 405-429.

Sillitoe, R. H., 2010: Porphyry copper systems: Economic Geology (Invited Special Paper), 105, 3-41.

Stefanova, E., Driesner, T., Zajacz, Z., Heinrich, C.A., Petrov, P. & Vasilev, Z. 2014: Melt and Fluid Inclusions in Hydrothermal Veins: The Magmatic to Hydrothermal Evolution of the Elatsite Porphyry Cu-Au Deposit, Bulgaria: Economic Geology, 109, 1359-1381.

Weis, P., Driesner, T., & Heinrich, C.A. 2012: Porphyry-Copper Ore Shells Form At Stable Pressure-Temperature Fronts Within Dynamic Fluid Plumes: Science, 338, 1613-1616.

Weis, P., Driesner, T., Coumou, D. & Geiger, S. 2014: Hydrothermal, multiphase convection of H2O-NaCl fluids from ambient to magmatic temperatures: a new numerical scheme and benchmarks for code comparison: Geofluids, 1-25.

2.11

Exploring the significance of intense epidosite alteration of volcanic rocks from the Semail ophiolite (Oman) for ancient and modern oceanic hydrothermal systems

Samuel A. Gilgen[1], Larryn W. Diamond[1] & Ivan Mercolli[1]

[1] *Institute of Geological Sciences, University of Bern, Baltzerstrasse 3, CH-3012 Bern (gilgen@geo.unibe.ch)*

Hydrothermally altered basalts that are entirely recrystallized to epidote + quartz + titanite ± hematite (i.e. epidosites) are surprisingly common in the volcanic sequence of the northern Semail ophiolite in Oman. Regional mapping of ten epidosites in the Fizh and Aswad blocks reveal manifold cross-cutting relations to previously known magmatic, plutonic and tectonic events. Linkage with whole-rock and mineral geochemical analyses allowed to pin down the stratigraphic position of these epidosites. Consequently, minima and maxima formation depths are calculated to range from 0.6 to 2.2 km below the paleo-seafloor. Since no subduction-related Alley or Boninitic-Alley lavas are epidotized – but early Alley dikes are – a formation during latest Alley volcanism is suggested for all epidosites. Therefore, epidosite formation within the volcanic sequence are not related to the main spreading volcanism, suggesting essential differences of mid-ocean-ridge and subduction-zone hydrothermal systems.

Additionally, we conducted detailed investigations on the largest (~1 km^2) epidosite, which is located in the distal footwall of a VMS deposit cluster. It is hosted by MOR-type pillow basalts of the lowermost (Geotimes) extrusive unit. The epidosite consists exclusively of epidote–quartz and laterally grades into and overprints lavas affected by regional chlorite–albite alteration. The dramatic mineralogical changes during epidotization are reflected by substantial changes in rock composition. Compared to the chlorite–albite altered pillows, the epidosites are enriched in Ca and Si and depleted in Na, Mg, Fe and notably Cu and Zn. Even the nominally immobile elements V and Ti are somewhat depleted. Whole-rock $^{87}Sr/^{86}Sr_{ini}$ values reveal that the hydrothermal fluid that caused epidotization was rock-buffered rather than seawater dominated, indicating a long history of fluid-rock interaction within the oceanic crust. Calculated water-to-rock ratios average at 4.6 $W/R_{effective}$. The average whole-rock $\delta^{18}O_{SMOW}$ value of +4.6 ‰ for epidosites indicates alteration temperatures above 300 °C. Calculated initial and final waters at these temperatures have $\delta^{18}O_{SMOW} \approx -0.3$ ‰ and +0.6 ‰, respectively. Accepting a $\delta^{18}O$ value of –1.0 ‰ for Cretaceous seawater, the calculated final waters are shifted towards heavier isotopes. Despite the potential difference to mid-ocean-ridge hydrothermal systems, this shift is remarkably similar to modern hydrothermal vents.

2.12

Micro-mapping of chemical potential gradients: A new shovel to bury the concept of global equilibrium in metamorphic rocks

Pierre Lanari[1], Nicolas Riel[2] & Martin Engi[2]

[1] *Institute of Geological Sciences, University of Bern, Baltzerstrasse 3, CH-3012 Bern, Switzerland (pierre.lanari@geo.unibe.ch)*
[2] *University of Grenoble Alpes, ISTerre, F-38041 Grenoble, France; present address: School of Geoscience, Monash University, Australia.*

Metamorphic rocks represent mosaics of local processes occurring mainly along reaction interfaces. It is generally uncertain to what extent and at what scale thermodynamic equilibria may be preserved in a sample. For instance, chemical zoning preserved in metamorphic minerals is evidence of disequilibrium and reflects changes in growth conditions. The grain interior became isolated from the matrix and was no longer in chemical equilibrium with the rim crystallizing. Complexity levels increase if we consider rocks with textural and chemical heterogeneities, both are often visible in domains of a sample. Any preconceived idea that such rocks reached global equilibrium is then untenable, and instead local domains (areas 20-1000 µm width) must be documented and understood.

In this study, X-ray maps were acquired using the electron microprobe to analyze metamorphic rocks showing local disequilibrium features. Examples such as migmatites (composite products of residuum and leucosome), eclogites (with porphyroblasts and matrix), and greenschist facies metapelites (with pro- and retrograde minerals) are used. The programs *XMapTools* for X-ray image processing, *Perple_X* for thermodynamic modelling were used to map the chemical potentials of components involved in the growth of local assemblages. Gradients in chemical potential can be established between adjacent domains, thus triggering chemical interaction. Diffusive transport between domains aims to reduce such chemical potential gradients. Along a modelled P-T path the chemical and mineralogical evolution of micro-domains can be reconstructed for (at least the reactive parts of) the crystallization history.

Standardized X-ray maps have proven to be powerful in calculating the local compositions of any select domain and in visualizing transects at the thin section scale. *XMapTools* package provides the numerical tools, which are essential for such studies to model local chemical potentials and to highlight diffusional interactions. Used for this purpose, the software is capable of delimiting how the reactive volume changes during the evolution of metamorphic rocks. Only within such domains does it make sense to apply tools that rely on equilibrium thermodynamics, such as most thermobarometers, or on isotopic equilibration, such as isochron methods (e.g. Rb-Sr or Sm-Nd).

2.13

Chemical and textural behaviour of REE accessory phases with increasing metamorphic grade in a well constrained prograde pelitic suite: implications for allanite and monazite petrochronology

Martin Robyr[1], Goswami-Barnerjee Sriparna[1]

[1] *Institut für Geologie, University of Bern, Baltzerstrasse 1+3, CH-3012 Bern (robyr@geo.unibe.ch)*

Because metamorphism comprises a complex sequence of structural changes and chemical reactions that can be extended over several millions of years, metamorphic rocks cannot in general be said to have “an age”. As a consequence, interpreting radiometric age data from metamorphic rocks requires first to establish the behaviour of the isotopic system used for dating relative to the P-T conditions that a metamorphic rock experienced. As the U-Th-Pb system in monazite and allanite is not easily reset during subsequent temperature increase, allanite and monazite ages are interpreted as reflecting crystallization ages. Consequently, to interpret allanite and monazite crystallization ages, it is crucial to determine the physical conditions of their crystallization.

A detailed account of the textural and chemical evolution of allanite and monazite along a well constrained prograde metamorphic suite of detrital sediments of the Greater Himalaya of Zanskar reveals that: (1) allanite is the stable REE accessory phase in the biotite and garnet zone and (2) at the staurolite-in isograd, allanite disappears abruptly from the

metamorphic assemblage, simultaneously with the occurrence of the first metamorphic monazite. The finding of both monazite and allanite as inclusion in staurolite indicates that the breakdown of allanite and the formation of monazite occurred during staurolite crystallization. The preservation of allanite and monazite inclusions in garnet core and rim respectively allows to accurately identify the P-T conditions of the formation of the first metamorphic monazite. Thermobarometry indicates that, in both cases, monazite crystallization occurred at 600 °C. The fact that the substitution of allanite by monazite occurs spatially close, i.e. at similar P-T conditions, in all types of rocks whether they are Al-rich metapelites or more psammitic metasediments indicates that major silicate phases like staurolite or garnet do not play a significant role in the monazite forming reaction. Our data shows that the occurrence of the first metamorphic monazites in the rocks is mainly dependent on the pressure-temperature conditions and not on the bulk chemistry of the rocks. Dating monazite in metapelites means thus constraining the timing when these rocks reached the 600 °C isotherm.

2.14

Source and types of extrinsic organic compounds involved in thermochemical sulfate reduction at the Pb-Zn sandstone-hosted Laisvall deposit, Sweden

Nicolas J. Saintilan[1], Jorge E. Spangenberg[2], Michael B. Stephens[3], & Lluís Fontboté[1]

[1] *Department of Earth and Environmental Sciences, University of Geneva, Rue des Maraîchers 13, CH-1205 Geneva (nicolas.saintilan@unige.ch)*
[2] *Institute of Earth Surface Dynamics, University of Lausanne, Building Geopolis, 1015 Lausanne, Switzerland*
[3] *Geological Survey of Sweden (SGU), Box 670 SE-751 28 Uppsala, Sweden*

The stratabound, non-stratiform, epigenetic galena-sphalerite Laisvall deposit hosted in late Ediacaran–Lower Cambrian autochthonous sandstone (64.3 Mt of ore at 0.6 % Zn, 4.0 % Pb and 9.0 g/t Ag) occurs at the eastern erosional front of the Caledonides in Northern Sweden.

The reactivation of basement structures triggered fault activity in the unconformable autochthonous cover rocks. Several feeders centered on these faults have been identified and are interpreted as conduits for metal-bearing fluids ascending from the crystalline basement (Saintilan et al., *in press*). Pb-Zn grade distribution depicts plume-like features with the highest grades centered on the feeder faults and towards the top of the two host paleoaquifers (i.e., Lower Sandstone and Upper Sandstone orebodies), at the contact with shale aquitards (incl. black shale with high Total Organic Carbon 1–22 % of the Alum Shale Formation; Thickpenny, 1984; Saintilan et al., *in press*). Such a spatial distribution is typical of sediment-hosted deposits (e.g., San Vicente deposit, Peru, Fontboté and Gorzawski; 1990; Spangenberg et al., 1999) where metal-bearing fluids from the basement mixed with H_2S-bearing fluids in sandstone or dolostone paleoaquifers (Saintilan et al., *in press*). An extensive and structurally-orientated sulfur isotope survey has identified three sources of reduced sulfur at Laisvall: i) mainly H_2S produced during Thermogenic Sulfate Reduction (TSR) by hydrocarbons and/or other organic compounds; ii) H_2S from diagenetic and biogenic pyrite replaced by galena ± sphalerite; iii) minor H_2S from sulfide leached in the crystalline basement rocks identified in sphalerite in feeder faults. TSR-derived reduced sulfur is identified as a key condition for Laisvall-type mineralization at economic level. Consumption of pyrite in Pb-Zn sulfides is indicative of a system starved in reduced sulfur once TSR-derived reduced sulfur is consumed.

The presence and involvement of organic compounds in TSR is illustrated by organic matter-ore relationships and evidence from sphalerite mineral chemistry: (i) pyrobitumen intimately intergrown with sphalerite and organic compounds included in barite, (ii) alkane-rich fluid inclusions in sphalerite (Rickard et al., 1975; this study), (iii) high Mn and Hg contents in sphalerite suggestive of marked reducing conditions and the possible transport of Hg as organic-metallic complexes sourced from black shale kerogen (Saintilan et al., submitted to Economic Geology).

An organic geochemistry study was carried out on a mineralized sample from each sandstone orebody, a barren sample from the Lower Sandstone, and a black shale sample with 1 % TOC. The similarity of the gas chromatographs (GC) and biomarker parameters of the saturate fraction (distribution of n-alkanes in the range C16–C27 with maximum in C22, Carbon Preference Index at 1.06, and pristane/phytane ratio in the range 0.38–0.44) of the mineralized samples suggest a common source of organic compounds whilst the difference with the biomarker parameters of the saturate fraction of the barren sample indicates that these organic compounds are extrinsic. Comparison of the GCs and biomarker parameters of the saturate fraction of the mineralized samples with those of the black shale sample suggests that these extrinsic organic compounds were derived from black shale from the overlying Alum Shale Formation.

It is consequently proposed that extrinsic-source organic compounds (probably organic acids or ketone), generated from algal-type kerogen (Bharati et al., 1995), migrated from the Alum Shale Formation, along with aqueous solutions with dissolved organo-metallic complexes, into sandstone paleoaquifers where they were involved in the production of H_2S and by-product pyrobitumen via TSR.

REFERENCES

Bharati, S., Patience, R.L., Larter, S.R., Standen, G., & Poplett, I.J.F. 1995: Elucidation of the Alum Shale kerogen structure using a multi-disciplinary approach. Organic Geochemistry, v. 23, p. 1043-1058.

Fontboté, L., & Gorzawski, H. 1990: Genesis of the Mississippi Valley-Type Zn-Pb deposit of San Vicente, Central Peru: Geologic and isotopic (Sr, O, C, S, Pb) evidence. Economic Geology, v. 85, p. 1401-1437.

Rickard, D.T., Willdén, M.Y., Mårde, Y., Ryhage, R.1975: Hydrocarbons associated with Pb-Zn ores at Laisvall, Sweden. Nature, v. 255, p. 131-133.

Saintilan, N.J., Stephens, M. B., Lundstam, E. & Fontboté, L. 2015: Control of reactivated basement structures on sandstone-hosted Pb-Zn deposits along the Caledonian Front, Sweden: Evidence from airborne magnetic data, Structural analysis, and ore-grade modeling. Economic Geology, in press.

Saintilan. N.J., Schneider, J., Kouzmanov, K., Stephens, M.B., Chiaradia, M., Wälle, M., & Fontboté, L., submitted to Economic Geology: Constraints on the age and origin of Laisvall-type Pb-Zn mineralization and basement-hosted vein deposits in Northern Sweden from sphalerite mineral chemistry and Rb-Sr systematics.

Spangenberg, J.E., Fontboté, L. & Macko, S.A. 1999: An evaluation of the inorganic and organic geochemistry of the San Vicente Mississippi Valley-Type Zn-Pb district, Central Peru: Implications for ore fluid composition, mixing processes, and sulfate reduction. Economic Geology, 94, 1067-1092.

Thickpenny, A., 1984, The sedimentology of the Swedish alum shales: London, Geological Society Special Publications 15, p. 511-525.

2.15

Chemical modification of fluid inclusions hosted by non-traditional minerals

Kateřina Schlöglová[1], Markus Wälle[1] & Christoph A. Heinrich[1]

[1] *Fluids and Mineral Resources Group, Institute of Geochemistry and Petrology, ETH Zürich, Clausiusstrasse 25, CH-8092 Zürich (katerina.schloglova@edrw.ethz.ch)*

Evolution of a hydrothermal fluid, the transport medium carrying metals and complexing agents from their source to the site of deposition, is important for the formation of economic metal accumulation, ore grade and spatial element distribution. Cooling and decompression of magmatic fluids during upward migration through the crust result in their separation into two coexisting phases: a low-salinity vapor-like and a high-salinity liquid-like fluid (Heinrich et al. 1999). Analysis of natural co-existing brine- and vapor-type inclusions and experimental work show that Zn, Pb, Fe, Sn, Ag, and K fractionate with NaCl into the liquid, whereas Au, As, Cu, Sb, and B is concentrated in various amounts in the vapor, enhanced by presence of the reduced sulfur. This specific geochemical behavior explains the distribution and variability of magmatic-hydrothermal ores such as porphyry-style, epithermal and greisen deposits.

Most information about fluid composition comes from analyses of fluid inclusions, however, there are certain issues concerning their preservation in natural samples. Fluid inclusions hosted in quartz may suffer from post-entrapment modification of their chemistry due to diffusion of some elements between the inclusion and the host. Diffusional re-equlibration experiments showed rapid diffusion of monovalent cations with small radius such as Na, Li, Ag, Cu and H between quartz crystal and entrapped inclusion (Zajacz et al. 2009). As samples of natural vapor-type fluid inclusions co-existing with brines commonly show high concentration of Cu, this may have been caused by a fluid acidity gradient driving H^+ from the inclusion while the charge balance is compensated by Cu^+ that combines with S to precipitate secondary sulfide crystal inside the inclusion (Lerchbaumer & Audétat 2012). By contrast, Au^+ cations are expected to migrate outwards as a result of gradient in concentration of Au-complexing bisulfide species being primarily higher inside the inclusion when compared to the rock-buffered environment outside (Seo & Heinrich 2013).

Widely used quantitative analysis of fluid inclusions hosted by widespread quartz does not necessarily yield the primary fluid composition at the time of entrapment. Our study attempts to compare the composition of fluids trapped simulta-

neously in different minerals typical for magmatic-hydrothermal systems such as topaz, garnet and pyroxene. Fluid inclusions in quartz co-existing with topaz or garnet trapping the same high-temperature fluid represent an excellent case to characterize the peculiar behavior of Cu, Au, and some other elements. The Sn-W deposits in the topaz-bearing Mole granite (Australia), the Sn-W-mineralized granites from the Erzgebirge Mts. (Czech Republic and Germany) and the skarn-hosted Cu deposit at Bingham Canyon (Utah, USA) are suitable systems to study the preservation of fluid composition as well as the vapor-brine separation. In addition, physical and chemical factors affecting the fluid evolution during cooling and their control on the ore grade in skarn ores at Bingham Canyon will be addressed. Distribution and size of fluid inclusions in non-traditional minerals bring about analytical challenges, which will be addressed by fast-scanning sector-field LA ICP MS at ETH Zürich.

REFERENCES

Heinrich, C.A., Günther, D., Audétat, A., Ulrich, T. & Frischknecht, R. 1999: Metal fractionation between magmatic brine and vapor, determined by microanalysis of fluid inclusions. Geology, 27, 755-758.

Lerchbaumer, L. & Audétat, A. 2012: High Cu concentrations in vapor-type fluid inclusions: an artifact? Geochimica et Cosmochimica Acta, 88, 255-274.

Seo, J.H. & Heinrich, C.A. 2013: Selective copper diffusion into quartz-hosted vapor inclusions: Evidence from other host minerals, driving forces, and consequences for Cu-Au ore formation. Geochimica et Cosmochimica Acta, 113, 60-69.

Zajacz, Z., Hanley, J.J., Heinrich, C.A., Halter, W.E. & Guillong, M. 2009: Diffusive reequlibration of quartz-hosted silicate melt and fluid inclusions: are the metal concentrations unmodified? Geochimica et Cosmochimica Acta, 73, 3013-3027.

2.16

Trace element diffusion in quartz-phenocrysts from a Jurassic meta-rhyolite: constrains from the contact-aureole of the Chaltén Plutonic Complex (Fitz Roy, Patagonia)

Susanne Seitz[1], Benita Putlitz[1], Lukas Baumgartner[1], Stephane Escrig[2], Anders Meibom[2]

[1] *Institut de Sciences de la Terre, Université de Lausanne, CH-1015 Lausanne*
[2] *2Laboratory for Biological Geochemistry, École Polytechnique Fédéral de Lausanne, CH-1015 Lausanne*

The Chaltén Plutonic Complex (CHPC) is located at the frontier between Chile and Argentina in southern Patagonia. It consists of a suite of calc-alkaline mafic and granitic rocks emplaced in successive batches between 16.90 to 16.37 Ma (Ramirez et al. 2012). The younger, main central granitic body is surrounded by an older, ~500 m thick gabbroic intrusion. The rhyolites and volcanoclastic rocks of the Jurassic El Quemado Complex are the most common host-rocks. Metamorphism increases from anchizone facies outside the contact aureole to produce partial melts at the contact with the mafic unit. Outside the aureole, rhyolites show typical magmatic textures like flow banding and vesicles. Here cathodoluminescence (CL) images reveal that quartz phenocrysts (several mm-size) preserved their magmatic zoning: light cores are surrounded by several darker and lighter zones towards the rim. Quartz-phenocrysts near the contact, in contrast, have complex textures (partly due to pre-and syn-intrusive deformation). The CL images show subgrain-formation with steep gradients in grey-scale intensity at the subgrain boundaries.

High-resolution trace element-profiles of this complex quartz grains were obtained by NanoSIMS with a beam size of ~200 nm and a minimum step size of ~120 nm. The profiles were measured perpendicular to the subgrain-boundaries and show sharp changes in the $^{48}Ti/^{29}Si$-ratio and $^{27}Al/^{29}Si$-ratio over a distance of 3µm respectively 7µm, which correlate with CL-intensity changes. Assuming that deformation pre-dates or occurred during the emplacement of the intrusion, we can use the steepness of the profiles to estimate the time span of the peak temperature. The observed distances agree for Ti and Al at 650°C, yielding a maximum diffusional relaxation time of 700 years. First melts in rhyolites formed at about 650°C which is in good agreement with the temperature estimation from diffusion calculations. Furthermore, the time span of 700 years is in the right order of magnitude we expect for the cooling of a 500 m thick intrusion like the gabbroic unit.

REFERENCES

Ramírez de Arellano, C., Putlitz, B., Müntener, O., & Ovtcharova, M. 2012: High precision U/Pb zircon dating of the Chaltén Plutonic Complex (Cerro Fitz Roy, Patagonia) and its relationship to arc migration in the southernmost Andes. Tectonics. 31, TC4009, doi:10.1029/2011TC003048.

2.17

SIMS analysis of minerals with solid solution

Guillaume Siron[1], Lukas Baumgartner[1], Anne-Sophie Bouvier[1] & Benita Putlitz[1]

[1] *Institut des Sciences de la Terre, University of Lausanne, CH-1015 Lausanne (guillaume.siron@unil.ch)*

Secondary Ion Mass Spectroscopy (SIMS) is a powerful and rapid method for stable isotope analysis. $\delta^{18}O$ measurements in minerals with high spatial resolution is possible, with ca. 5 minutes per analysis. This allows us to obtain a large amount of in-situ data with a spatial resolution of 5-15µm at low cost in one day. However, its is well established that SIMS instruments are plagued by large (1-10 ‰ $\delta^{18}O$) instrumental mass fractionation effects (IMF) due to variation in major element composition of minerals (e.g. Eiler et al. 1997; Valley and Kita 2009). Measured isotopic compositions can also depend on the orientation (Huberty et al. 2010) or mineral structure (Eiler et al. 1997). Here we present results on composition and orientation effects on IMF.

We have characterized 3 biotites for $\delta^{18}O$ (reproducibility 0.3‰- 0.5‰, 2σ), spanning a range in composition from 0.55 to 0.86 in XMg. Systematic studies were performed on the SIMS, orienting the biotite lattice of grains of the standards at different angles with respect to the primary and secondary ion beam. We did not find any effect on the IMF, despite the strong anisotropy of the sheet silicate lattice. This is in contrast to the cubic lattice of magnetite (Huberty et al. 2010).

In a second series of tests we demonstrate that the IMF associated with composition changes during a session. Analysing plagioclase feldspars (range X_{An}=0.0 to 0.92) results in a linear dependence of IMF on X_{An}, covering a range of ca. 4.5‰. Repeated sessions revealed that the actual dependence on composition was always similar, but varied slightly between sessions. We performed tests to see if the compositional dependence of IMF changes with time during a session. Over an 16 hour time span we measured a small drift in the compositional dependence of 1‰ for a change in X_{An} of 0.3.

We conclude that high precision analysis of oxygen isotopes require that standards bracketing the major element composition of the minerals are mounted directly on the sample mount, with 1-2 standards for every compositional variable. Re-measuring the standards systematically every 10-15 analysis is required to assure optimal standardization of the instrument.

REFERENCES

Eiler J. M., Graham C. & Valley J. W. 1997: SIMS analysis of oxygen isotopes: matrix effects in complex minerals and glasses. Chemical geology, 138, 221-244.

Huberty J. M., Kita N. T., Kozdon R., et al. 2010: Crystal orientation effects in $\delta^{18}O$ for magnetite and hematite by SIMS. Chemical geology, 276, 269–283.

Valley J. W. & Kita N. T. 2009 In situ oxygen isotope geochemistry by ion microprobe. MAC short course: secondary ion mass spectrometry in the earth sciences, 41, 19-63.

2.18

Heterogeneous phase equilibria in rocks under a pressure gradient.

Vrijmoed, J. C.[1], Podladchikov, Y. Y.[2], Moulas, E[1,2] & Tajčmanová, L.[1]

[1] *Institute of Geochemistry and Petrology, ETH Zürich, Clausiusstrasse 25, CH-8092 Zürich (johannes.vrijmoed@erdw.ethz.ch)*
[2] *Institute of Earth Sciences, University of Lausanne, Quartier UNIL-Mouline, Bâtiment Géopolis, CH-1015 Lausanne*

Mineral reactions and phase transformations greatly affect all properties of Earth's materials and impose first order controls on geodynamic processes.

Metamorphic petrologists as well as structural geologists bring direct observational constraints for geodynamic models. If properly quantified and interpreted, fabrics and microstructures in rocks provide fundamental constraints on lithospheric evolution. However, in the context of complex rock fabrics and microstructures, application of inappropriate quantification approaches may lead to flawed interpretations. The classical view of metamorphic microstructures assumes fast relaxation of stresses (therefore constant pressure) and constant temperature. In this case, mass transport is the only limiting factor in the thermodynamic equilibration of the microstructure. The presence of zoned porphyroblasts, coronal structures and spatially organized reaction zones thus points to the preservation of an apparent disequilibrium in the microstructures (e. g. Carlson, 2002 and references therein).

The classical petrology view is limited because it precludes the possibility that metamorphic microstructures involve mechanically maintained pressure variations. In fact, observations in natural rocks, as well as theoretical predictions indicate that pressure can be spatially heterogeneous on the grain-scale (e.g. see review of Moulas et al., 2013).

We investigate the effect of pressure gradients on phase equilibria in rocks. A newly developed tool based on constrained Gibbs minimization is used to show that apparent disequilibrium in microstructures such as plagioclase rims around kyanite in high temperature granulites can be explained with equilibrium, under contrained pressure variations. These microstructures thus need not be explained by disequilibrium and is consistent with current knowledge on diffusion kinetics. We systematically investigate the effect of mechanically feasible pressure gradients on phase distribution and stable mineral assemblage in a variety of rock compositions with the new thermodynamic software.

REFERENCES

Moulas, E., Podladchikov, Y.Y., Aranovich, L.Y., Kostopoulos, D., 2013. The problem of depth in geology: When pressure does not translate into depth. Petrology 21, 527–538. doi:10.1134/S0869591113060052

Carlson, W.D., 2002. Scales of disequilibrium and rates of equilibration during metamorphism. Am. Mineral. 87, 185–204.

P 2.1

Stable isotope ($\delta^{18}O$ and δD) record of fluid-rock interaction in the Zermatt-Saas Fee ophiolites (Pfulwe – Rimpfischorn): from sea floor to exhumation

Nicolas Buchs[1], Lukas Baumgartner[1], Benita Putlitz[1] & Torsten Vennemann[2]

[1] *Institut des sciences de la Terre, University of Lausanne, CH-1015 Lausanne,*
[2] *Institut des dynamiques de la surface terrestre , University of Lausanne, CH-1015 Lausanne*

The Zermatt-Saas Fee Zone (ZSZ) represents a dismembered part of the Piemontese ocean that underwent (ultra-) high pressure metamorphism at 40-42 Ma (Amato et al. 1999; Lapen et al. 2003, Skora et al. 2009). The study area is located to the East of Zermatt (CH), between the Fluehorn and the Strahlhorn. In this region, the ophiolites are composed of several kilometre-sized slices of metabasalts, metagabbros, and serpentinites. Specifically, the study focuses on the Pfulwe ophiolites, where the metabasalts are heterogeneous in their geochemical and mineralogical composition, mainly reflecting sea-floor hydrothermal water-rock interaction: abundant spilitisation, chloritisation and epidotisation can be documented (Widmer et al., 2000). This alteration is accompanied by large changes in $\delta^{18}O$ values (<2.5 to 8.0 ‰). The metagabbros have $\delta^{18}O$ values between 2.8 and 5.0 ‰, the serpentinites between 2.3 and 3.7 ‰. Variations can be attributed to differences in temperature of the water-rock interaction. Dehydration of the ZSZ rocks during subduction resulted in additional loss of fluid-mobile elements.

Individual slices were strongly retrogressed along the borders, which are associated with the formation of new hydrated phases. Blackwall (metasomatic zone) chlorite, prasinites and ovardites document fluid circulation between individual slices. The border zones have typically lower $\delta^{18}O$ values than the corresponding cores, where eclogites are better preserved. This slight decrease in $\delta^{18}O$ values is interpreted to be due to fluid-rock interaction during exhumation of Zermatt-Saas Fee Zone. Possible sources of fluids are the serpentinites since partial dehydration has occurred, with antigorite breaking down to form olivine after the eclogitic peak. Fluids with a $\delta^{18}O$ of about 6 ‰ and δD of about 45 ‰ interacted locally with the borders of the slices, being channelized mainly in the mylonitic serpentinite slices, which are often present between the mafic bodies. The serpentinite dehydration could explain the large amount of hydrated phases found in many of the retrogressed eclogites.

REFERENCES:

Amato, J. M., Johnson, C. M., Baumgartner, L. P., & Beard, B. L. 1999: Rapid exhumation of the Zermatt-Saas ophiolite deduced from high-precision Sm-Nd and Rb-Sr geochronology . Earth.Planet.Sci.Lett., 171 (3): 425-438.

Lapen, T. J., Johnson, C. M., Baumgartner, L. P., Mahlen, N. J., Beard, B. L. & Amato, J. M. 2003: Burial rates during prograde metamorphism of an ultra-high-pressure terrane: an example from Lago di Cignana, western Alps, Italy . Earth.Planet.Sci.Lett, 215 (1-2): 57-72.

Widmer, T., Ganguin, J., & Thompson, A., B. 2000: Ocean floor hydrothermal veins in eclogite facies rocks of the Zermatt-Saas Zone, Switzerland. Schweiz. Min.Pet.Mitt.,80 (1): 63-73.

Skora S., Lapen TJ. Baumgartner LP., Johnson CM, Mahlen NJ., Hellebrand E: 2009)The duration of prograde garnet crystallization in the UHP eclogites at Lago di Cignana, Italy. Earth.Planet.Sci.Lett. 287/3-4, 402-411

P 2.2

Pressure-temperature-time evolution in the high-grade metamorphic basement of the Siviez-Mischabel nappe (Val d'Hérens, Val d'Anniviers)

Raphaël Normand[1], Susanne Theodora Schmidt[1] & Mario Sartori[1]

[1] *Section des sciences de la Terre et de l'environnement, University of Geneva, Rue des Maraichers 13, CH-1205 Genève. (Raphael.Normand@etu.unige.ch)*

The Banded amphibolites, a mafic layer situated at the base of the Adlerflüe formation in the basement of the Sivez-Mischabel (SM) nappe (Valais, CH), contain local occurrences of eclogite; witnesses of a pre-Alpine high-grade metamorphic event. They have a composition of NMORB enriched in LILE, U, Th, Pb and LREE which are characteristic for a back-arc depositional environment. The pressure-temperature time path was modelled for these eclogite occurrences using the program DOMINO and the garnet-clinopyroxene Fe^{2+}-Mg geothermometer. Peak metamorphic conditions were estimated to be 15-17 kbar and 650-800°C. The retrograde event, responsible for the breakdown of omphacite and the growth of pargasite is estimated at approximatively 8 kbar and 500-600°C, which places it in the amphibolite facies. The age of the youngest zircon within the SOPA ("schistes oeillés à porphyroblastes d'albite"), a metasedimentary unit directly overlying the eclogites, was determined to be 520.9±7.1 Ma which, together with the age of the crosscutting Thyon metagranite (500+3-4 Ma), provides an age window for the deposition of the SOPA. Timing of the emplacement of the Banded amphibolites and related rocks can therefore be constrained to the mid to late Cambrian. The recrystallized domains in zircon of all studied rock types yield coherent ages, with a calculated mean value of 346.58±0.97 Ma. This lower Carboniferous age is consistent with the ultra-high pressure events linked to the Variscan orogeny and is proposed as the age of the eclogitic metamorphism in the Siviez-Mischabel nappe.

P 2.3

Tectono-sedimentary breccias associated with mantle windows in hyper-extended domains (Eastern Swiss Alps): field observations, geochemistry, and consequences for the subduction interface

Suzanne Picazo[1], Othmar Müntener[1], GIanreto Manatschal[2] & Valentin Basch[2]

[1] *Institut des Sciences de la Terre –ISTE Faculté des géosciences et de l'environnement Quartier UNIL-Mouline - Batiment Géopolis CH-1015 Lausanne Switzerland (suzanne.picazo@unil.ch)*
[2] *Université de Strasbourg. 1, Rue Blessig 67000 Strasbourg*

We describe new geological observations and geochemical data on tectono-sedimentary breccias that formed in hyper-extended domains of the Tethyan rift system. Such breccias are markers of detachment faults in the magma-poor Iberia-Newfoundland and Tethyan rifted margins and document the continuous exhumation of fault surfaces on the seafloor. We focus on a rift-related detachment fault in the most distal Adriatic rifted margin exposed at the interface between the Margna and Malenco nappes in the Eastern Central Alps of SE-Switzerland and N-Italy. These are the first syn-rift breccias along the Jurassic rift related detachment system in the Eastern Central Alps that document a mixture of both continental and mantle-derived clasts, indicating that hyperextension and the formation of mantle windows are intimately coupled.

3-D mapping of the breccia combined with a 73 m long drill core through the hanging and footwall of a detachment fault provide clear evidence that mantle exhumation and breccia formation was coeval. Downhole variations of major and trace elements, and $\delta^{18}O$ isotopes demonstrate m-scale extensive chemical exchange between crustal and mantle rocks.

The breccia-mantle contact is made of a meter wide fine-grained metasomatic chlorite ± amphibole-bearing zone. The breccias on top of the ultramafic rocks are made of mm- to cm-sized amphibole-bearing mantle-derived clasts, continental-derived rounded to elongated cm- to meter-sized blocks, and a fine- to coarse-grained foliated matrix, dominated by chlorite + mica + feldspar + quartz. Amphibole in amphibole-bearing clasts are Cr-Ni-rich, supporting the hypothesis of ultramafic clasts in the polymict breccia. Bulk rock major, minor and trace element data from the serpentinized peridotites to the continental-block bearing breccias show an increase in Al, Ca and elevated LREE. However, amphibole-rich clasts within the mica-rich matrix are very similar in composition to serpentinized peridotites with high Cr, Ni and low LREE, indicating that amphibole rich rocks are previous serpentinized peridotite clasts that are altered to form amphibole blackwalls, presumably related to recrystallization during Alpine metamorphism. We argue that recent findings of eclogite facies brecciation along the subduction interface might be the consequence of inherited brecciation of hyper-extended margins or oceanic core complexes.

P 2.4

Pressure-controlled formation of asymmetric chemical zoning in garnet

Xin Zhong [1], Johannes Vrijmoed [1], and Lucie Tajcmanova [1]

[1] *Institute of Geochemistry and Petrology. ETH Zurich.Sonneggstrasse 5. CH-8092. Zurich. Switzerland (xin.zhong@erdw.ethz.ch)*

Chemical zoning in garnet reflects variations in pressure (P) and temperature (T) along the path which the rock experienced. Such a zoning can be preserved in situations where diffusional homogenization and metasomatism is absent. Traditional inverse growth zoning models can only predict and explain symmetrical zoning. However, asymmetrical zoning is often observed in nature as well. In this contribution, we therefore focus on a prograde asymmetrical zoning in garnets that happens under fluid saturated conditions. In such examples, it is assumed that the surrounding fluid homogenizes its chemical composition rapidly and that it is in chemical equilibrium with rims of adjacent minerals. Therefore, a possibility of zoning caused by a local fluid chemical heterogeneity is ruled out. However, it has been proved that fluid pressure varies along the grain boundaries, in particular, during pressure solution processes. Hence, the asymmetrical zoning may be controlled by the variations in fluid pressure if the local equilibrium is satisfied. In this study, the influence of fluid pressure variation on chemical zoning is investigated using thermodynamic calculation with Perple_X implemented into a Matlab script to simulate the formation of asymmetrical chemical zoning caused by different pressure gradient along the grain boundaries. The possibility of comparing the thermodynamic calculation with numerical simulation is feasible, as the process of brute-force computational method using Perple_X can be segmented by taking into account the varying pressure. In contrast to the traditional point of view of the prograde growth zoning in garnet, it is proved that grain scale fluid pressure variation, even on the order of 0.1 GPa, can be a reason for the development of the asymmetric zoning. Future work will focus on the relation between grain scale chemistry and mechanics using numerical and analytical techniques. Diffusion is meanwhile possible to be incorporated into the model in case the inferred temperature is high enough.
This work was supported by ERC starting grant 335577 to Lucie Tajcmanova.

P 2.5

Non-matrix-matched standardization in quadrupole LA-ICP-MS: New data reduction for allanite age-dating

Marco Burn[1], Pierre Lanari[1], Thomas Pettke[1] & Martin Engi[1]

[1] *Universität Bern, Institut für Geologie, Baltzerstrasse 3, CH-3012 Bern, Switzerland (marco.burn@geo.unibe.ch)*

Allanite Th-U-Pb age-dating has recently been demonstrated to be powerful in unraveling the timing of geological processes such as the metamorphic dynamics in subduction zones and crystallization velocity of magmas. However, inconsistencies among analytical techniques have raised doubts about the accuracy of allanite age data. Spot analysis techniques such as LA-ICP-MS are claimed to be crucially dependent on matrix-matched standards, the quality of which is variable.

We present a new approach in LA-ICP-MS data reduction that allows non-matrix-matched standardization via well constrained zircon reference materials as primary standards. Our data were obtained using a GeoLas Pro 193 nm ArF excimer laser ablation system coupled to an ELAN DRC-e quadrupole ICP-MS. We use 32 µm and 24 µm spot sizes; laser operating conditions of 9 Hz repetition rate and 2.5 J/cm^2 fluence have proven advantageous. Matrix dependent downhole fractionation evolution is empirically determined by analyzing $^{208}Pb/^{232}Th$ and $^{206}Pb/^{238}U$ and applied prior to standardization. The new data reduction technique involvels the possibility for common Pb correction and was tested on three magmatic allanite reference materials (SISSb, CAPb, TARA); within error these show the same downhole fractionation evolution for all allanite types and in different analytical sessions, provided measurement conditions remain the same. Although the downhole evolution of allanite and zircon differs significantly, a link between zircon and allanite matrix is established by assuming CAPb and TARA to be fixed at the corresponding reference ages. Our weighted mean $^{208}Pb/^{232}Th$ ages are 30.06 ± 0.22 (2σ) for SISSb (N=44), 275.4 ± 1.3 (2σ) for CAPb (N=42), and 409.9 ± 1.8 (2σ) for TARA (N=41). Precision of single spot age data varies between 1.5 and 8 % (2σ), depending on spot size and common lead concentrations. Quadrupole LA-ICP-MS allanite age-dating has thus similar uncertainties as do other spot analysis techniques. The new data reduction technique is much less dependent on quality and homogeneity of allanite standard reference materials. This method of correcting for matrix-dependent downhole fractionation evolution opens new possibilities in the field of LA-ICP-MS data acquisition, e.g. the use of a NIST SRM glass to date all material types provided that a set of well constrained reference minerals is available to establish the analytical relationships between SRM glass and the mineral of interest.

P 2.6

Pushing the spatial limits of electron backscatter diffraction (EBSD) analysis: orientation relationships of zircon exsolutions in UHT-rutile

Jonas Pape[1], Klaus Mezger[1], Bernard Grobéty[2] & Christoph Neururer[2]

[1] *Institute of Geological Sciences, University of Bern, Baltzerstrasse 1+3, CH-3012 Bern (jonas.pape@geo.unibe.ch)*
[2] *Department of Geosciences, University of Fribourg, Chemin du Musée 6, CH-1700 Fribourg*

The recently calibrated Zr-in-rutile geothermometer (e.g. Watson et al., 2006; Zack et al., 2004) could be very suitable to identify and investigate UHT terranes (Ewing et al. 2013). It is based on the incorporation of Zr (as a trace element) into rutile, which is a common accessory mineral in a wide variety of metamorphic rocks including UHT rocks. However, the robustness of the thermometer is still under debate. A major question is: which stages of the metamorphic history are preserved by the Zr-in-rutile thermometer? It has been reported by different authors that rutile grains from HT and particularly UHT samples often contain regularly distributed µm-sized zircon or baddeleyite inclusions. It is assumed that these inclusions formed by the exsolution of a Zr-bearing phase from rutile during cooling from high grade metamorphic conditions. However, microstructural analyses of Zr-bearing exsolutions in UHT-rutile, which could provide valuable hints of their formation processes, have not been carried out yet. The small size of the exsolution needles/lamellae and the similar crystallographic structures of the rutile host grains and the zircon exsolutions present two major challenges for orientation measurements using electron backscatter diffraction (EBSD).

In this study we tried to determine orientation relationships of zircon exsolution needles and rutile host grains using EBSD. Rutile grains in pelitic xenoliths metamorphosed at temperatures up to 1200 °C by the surrounding gabbroic melt of the Mafic Complex in the Ivrea Zone were selected for the microstructural study. Orientation relationships between zircon needles and rutile host grains obtained by EBSD reveal crystallographically preferred orientations (CPO) of certain zircon needles. The measurements show that zircon needles with identical shape-preferred orientations (SPO) also show consistent crystallographically preferred orientations. The SPO of the zircon needles is a strong argument for their formation by solid-state precipitation, also referred to as exsolution. The EBSD measurements reveal that zircon exsolution needles with SPO also show crystallographic preferred orientations (CPO) which is another main criterion supporting their origin by exsolution (Proyer et al., 2013).
Using the information obtained with the EBSD analyses, the Zr contents of zircon needles were re-integrated to obtain the bulk Zr contents of rutile host grains prior to exsolution. This results in equilibration temperatures of 1,080 to 1,180 °C for some Ivrea Zone rutiles supporting their formation during UHT contact metamorphism.

REFERENCES

Ewing, T. A., Hermann, J., Rubatto, D. 2013: The robustness of the Zr-in-rutile and Ti-in-zircon thermometers during high-temperature metamorphism (Ivrea-Verbano Zone, northern Italy). Contrib Mineral Petrol, 165, 757-779.

Watson, E. B., Wark, D. A. & Thomas, J. B., 2006: Crystallization thermometers for zircon and rutile. Contrib Mineral Petrol, 151, 413-433.

Zack, T., Moraes, R. & Kronz A. 2004: Temperature dependence of Zr in rutile: empirical calibration of a rutile thermometer. Contrib Mineral Petrol, 148, 471-488.

Proyer, A., Habler, G., Abart, R., Wirth, R., Krenn, K. and Hoinkes, G. 2013: TiO2 exsolution from garnet by open-system precipitation: evidence from crystrallographic and shape preferred orientation of rutile inclusions. Contrib Mineral Petrol. 166, 211-234

P 2.7

$\delta^{18}O$ measurements of glasses using SIMS: a calibration of Instrumental Mass Fractionation

Mélina Manzini[1], Guillaume Siron[1], Anne-Sophie Bouvier[1], Lukas Baumgartner[1], Peter Ulmer[2], Benita Putlitz[1] & Torsten Vennemann[1]

[1] *Institut des Sciences de la Terre, University of Lausanne, CH-1015 Lausanne (melina.manzini@unil.ch)*
[1] *Institut f. Geochemie und Petrologie, ETH Zurich, Clausiusstrasse 25, CH-8092 Zürich*

Secondary ion mass spectrometry (SIMS) permits precise in situ analysis of $\delta^{18}O$, with a high spatial resolution of 5-15µm, and typically an analyses only takes about 5 minutes. This allows us to collect a large amount of data in a reasonable time period and at low costs. However a strong Instrumental Mass Fractionation (IMF), both due to structural (Eiler et al. 1997) and compositional changes (Valley and Kita 2009; Hartley et al. 2012), is observed and has to be carefully corrected for. This is particularly important for glasses because the compositional space is vast, since it is not constrained by the stoechiometry like in minerals.

A total of 10 international glass standards were complemented by a natural obsidian glass and 6 glasses synthetizised in a piston cylinder aparatus were analysed for oxygen isotope composition using the SwissSIMS IMS1280HR ion probe. Where available, data on oxygen isotope compositions were taken from the literature, and complemented by conventional laser-fluorination oxygen isotope analysis. The glass standards cover major elements compositions from olivine-normative basalts to rhyolites. As a function of composition we obtained a IMF covering ca. 7.5‰. Obviously, any successful analysis of $\delta^{18}O$ in glasses requires a rigorous correction for the IMF, as allready pointed out by Hartley et al. (2012).

To make the task feasable, we reduced the number of variables using a principle component analysis. Nevertheless, the result was not satisfactory. Alternatively, we reviewed the structure of glasses, which allows us to group elements. We choose to group (a) SiO_2 + TiO_2 (network forming cations), (b) FeO + MgO, and (c) K_2O + NaO_2. CaO was added as well, since has been shown in minerals to have a major effect on IMF. Hence we worked with: SiO_2+TiO_2, $AlO_{1.5}$, FeO+MgO, CaO, Na_2O+K_2O and the volatile content (calculated as H_2O). Systematic fitting of the IMF using all possible combination of variables resulted in a satisfactory fit using as variable for composition SiO_2+TiO_2 and CaO (χ^2 per point 2.0). Adding $AlO_{1.5}$ reduces the χ^2 per point marginally (by 0.05). Nevertheless, the gain in accuracy is not significant compared to the increase in complexity for routine analysis of glasses since this would require to have at least 5 standards on each sample mount, and repeating the standard analysis every 10-15 analysis of the unknown. The result is similar to that of Hartley et al. (2012), where they proposed to only use SiO_2 as a variable.

These results demonstrate that care is required in standardization of IMF at the beginning of each session, and the need of at least 3 standards in the sample mount, bracketing the composition in SiO_2+TiO_2 and CaO of the material to be analysed.

REFERENCES

Eiler, J. M., Graham, C., & Valley, J. W. 1997: SIMS analysis of oxygen isotopes: matrix effects in complex minerals and glasses. Chemical Geology, 138, 221-244.

Hartley, M. E., Thordarson T., Taylor C. & Fitton J. G. 2012: Evaluation oft he effects oft he composition on instrumental mass fractionation during SIMS oxygen isotope analyses of glasses. Chemical Geology, 334, 312-323.

Valley J. W., Kita N. T. 2009: In situ oxygen isotope geochemistry by ion microprobe. MAC short course: secondary ion mass spectrometry in the earth sciences, 41,19-63.

P 2.8

Simultaneous measurements of the whole range of Ca isotopes (^{40}Ca-^{48}Ca) by TIMS

Maria Naumenko[1], Claudia Bouman[2], Klaus Mezger[1], Thomas Nägler[1], Igor Villa[3]

[1] *Institut für Geologie, Universität Bern, Baltzerstrasse 1+3, CH-3012 Bern (naumenko@geo.unibe.ch)*
[2] *Thermo Fisher Scientific (Bremen) GmbH, Hanna-Kunath-Strasse 11, 28199 Bremen, Germany*
[3] *Università di Milano Bicocca, Italy*

Calcium is fifth most abundant element on Earth. It has five stable isotopes ^{40}Ca, ^{42}Ca, ^{43}Ca, ^{44}Ca, ^{46}Ca and the long lived ^{48}Ca with half-life of $4^{*}10^{19}$ a. The Ca isotopes are of significant importance for multiple disciplines like astrophysics, biology and geology, as they provide a proxy for paleoclimate, variations in biological cycles, fractionation in plants and animals, in minerals in the Early Solar System and present-day surface processes, as well as K-Ca geochronology [e.g. 1, 2, 5, 10].

The most commonly used methods for Ca isotope measurements are multicollector inductively coupled plasma mass spectrometry (MC-ICP-MS) and thermal ionization mass spectrometry (TIMS). Common issues with both measurements are isobaric interferences (^{40}K and in case of ICP-MS ^{40}Ar), high abundance range (^{40}Ca=96.9%, ^{46}Ca=0.004%) and wide mass range (8 amu difference between ^{40}Ca and ^{48}Ca).

So far there were two options to account for the wide mass range in multi collector set ups: either limit the amount of measured isotopes [e.g. 3, 8] or measure them in dynamic mode (e.g. first row masses 40, 42, 43, 44 and second row 44, 46, 48) [e.g. 4, 6]. The former is unfavorable if mass depended fractionation of Ca isotopes is the subject of interest; the later if the signal is weak, notably in case when small amounts of radiogenic ^{40}Ca are to be analyzed.

The Thermo Scientific Triton Plus multicollector TIMS with a newly developed unique large Faraday cup for ^{40}Ca allows to measure Ca isotopes from mass 40 to 48 simultaneously, i.e. in static mode. Application of different amplifiers (10^{11} and 10^{12} Ω) gives the opportunity to measure high (^{40}Ca) and low (^{43}Ca) intensity beams simultaneously with reduced uncertainty. This setup was used to measure NIST standards SRM 915a and SRM 915b. Several sets of measurements were performed over the period of five months to observe the external reproducibility, to check for possible drift and to monitor for cup surface degradation, such as was reported by [1].

In order to correct the ^{40}Ca/^{44}Ca ratio for mass spectrometric fractionation one can, in principle, apply three different isotope pairs: ^{48}Ca/^{44}Ca, ^{43}Ca/^{44}Ca, ^{42}Ca/^{44}Ca. Moreover, one can choose either the Russel et al (1978) [7] or the Shen et al (2008) [9] normalization values. The six possible outcomes are shown in Fig 1. The Russel normalization gives self-consistent ^{40}Ca/^{44}Ca corrected ratios, while the Shen normalization appears to be internally inconsistent, as it gives significantly discrepant ratios.

The reproducibility of results for low Ca concentration standards (100-200ng of Ca) was studied in particular detail as such concentrations are likely to be encountered in K-Ca dating of minerals. Low Ca concentrations and presence of Al in natural samples leads to short, unstable signals during data acquisition. The uncertainty of such measurements can be decreased with measurements of all six Ca isotopes as it gives the opportunity to use a ^{48}Ca-^{43}Ca double spike and perform a fractionation correction to four masses difference (correction to ^{48}Ca/^{44}Ca) instead of one (^{43}Ca/^{44}Ca) or two (^{42}Ca/^{44}Ca) mass differences. This leads to an improved uncertainty of 0.01% (2σ) on ^{40}Ca/^{44}Ca ratio.

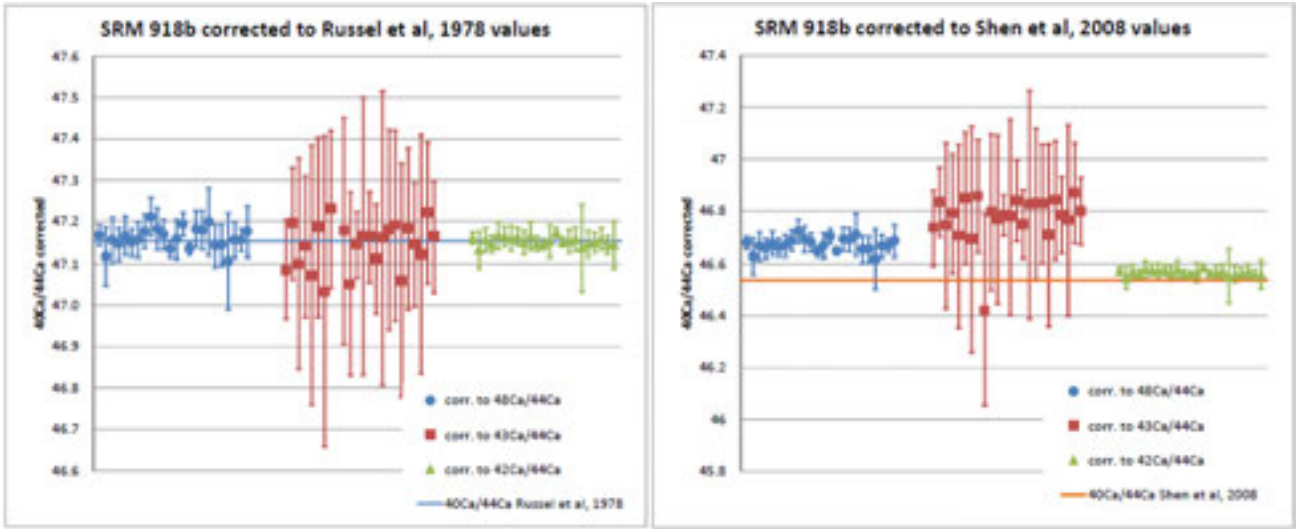

Figure 1. Comparison of the normalization protocols.

REFERENCES

1. Caro G., Papanastassiou D.A., Wasserburg G.J. 2010: ^{40}K-^{40}Ca isotopic constraints on the oceanic calcium cycle. Earth Planet. Sci. Lett. 29, 124-132.
2. Fantle M.S. 2010: Evaluating the Ca isotope proxy. Am. J. Sci. 310, 194-230.
3. Gopalan K., Macdougall D., Macisaac C. 2006: Evaluation of a ^{42}Ca-^{43}Ca double-spike for high precision Ca isotope analysis. Int.J.of Mass Spec. 248, 9-16.
4. Heuser A., Eisenhauer A., Gussone N., Bock B., Hansen B.T., Nägler T.F. 2002: Measurement of calcium isotopes (δ^{44}Ca) using a multicollector TIMS technique. Int.J. of Mass Spec. 220, 385-397.
5. Kreissig K., Elliot T. 2005: Ca isotope fingerprints of early crust-mantle evolution. Geochim. Cosmochim. Acta 69, 165-176.
6. Lehn G.O., Jacobson A.D., Holmden C. 2013: Precise analysis of Ca isotope ratios (δ$^{44/40}$Ca) using an optimized ^{43}Ca-^{42}Ca double-spike MC-TIMS method. Int.J. of Mass Spec. 351, 69-75.
7. Russel W.A., Papanastassiou D.A., Tombrello T.A. 1978: Ca isotope fractionation on the earth and other solar system materials. Geochim. Cosmochim. Acta 42, 1075-1090.
8. Schiller M., Paton Ch., Bizzarro M. 2012: Calcium isotope measurements by combined HR-MC-ICPMS and TIMS. J. Anal. At. Specrtom. 27, 38-49.
9. Shen J., Lee D-C., Liang W.-T. 2009: Absolute Ca isotopic measurement using an improved double spike technique. Terr Atmos. Ocean. Sci. 20, 3, 455-464.
10. Skulan J.S., DePaolo D.J., Owens T.L. 1997: Biological control of calcium isotopic abundances in the global calcium cycle. Geochim. Cosmochim. Acta 61, 12, 2505-2510.

P 2.9

The Quenamari prospect, San Rafael tin district, southern Peru: geology, mineral assemblages, fluid inclusion microthermometry, and stable isotope compositions.

Guillaume Corthay[1], Torsten Vennemann[2], Miroslav Kalinaj[3], Jean Vallance[4], Lluís Fontboté[1]

[1] *Department of Earth Sciences, University of Geneva, Rue des Maraîchers 13, CH-1205 Genève (guillaume.corthay@gmail.com)*
[2] *Institut des sciences de la Terre, University of Lausanne, Géopolis, CH-1015 Lausanne*
[3] *Minsur SA. Lima, Peru*
[4] *PUCP University, Lima , Peru*

The San Rafael tin district, comprising the underground San Rafael deposit, the Quenamari, and other prospects, is located in southern Peru, and represents the northernmost expression of the Andean tin belt. The ore mostly occurs as between 45° and 75°E dipping and NW-SE trending veins, mainly hosted by Late Oligocene cordierite-bearing granite (24.6 ± 0.2 Ma at San Rafael; Kontak and Clark, 2002) and Late Ordovician shale and quartzite.

Three of the four mineralization stages defined previously (e.g. Mlynarczyk et al., 2003) at San Rafael have been recognized at surface in the Quenamari prospect (2 km NE of San Rafael, >4700 m a.s.l.) during the present work (Corthay, 2014). Stage I is observable as small veins (< 3 cm wide) of fine-grained quartz and tourmaline in the Ordovician host rock. The main cassiterite stage II, also containing abundant quartz, muscovite, and chlorite at San Rafael, does not crop out at Quenamari (at San Rafael, cassiterite is mainly present below 4500 m whereas polymetallic veins are mostly found higher than 4500 m). The mineral association of polymetallic stage III consists of chalcopyrite, sphalerite, needle-tin cassiterite, galena, pyrite, marcasite, pyrrhotite, rhodonite, rhodochrosite and sulfosalts (including kobellite $(Cu,Fe)_2Pb_{11}(Bi,Sb)_{15}S_{35}$, tetrahedrite-freibergite $Cu_6[Cu_4(Fe, Zn)_2]Sb_4S_{13}$ - $Ag_6[Cu_4Fe_2]Sb_4S_{13-x}$, and canfieldite Ag_8SnS_6). The late stage IV is characterized by narrow (< 20 cm wide) barren quartz dominant veins.

Mapping at a scale 1:2000 at Quenamari has revealed generally NW-SE trending mineralized steeply dipping veins showing good continuity (> 1 km the Quenamari vein, > 3 km the parallel Nazareth vein) and considerable width emplaced in faults with normal and sinistral strike-slip displacement.

Tourmaline of stage I and within granite dykes shows a color and compositional evolution from orange-brown (intermediate composition between dravite and schorl) to blue tourmaline (schorl pole, 0.03 Mg apfu and 2.36 Fe apfu), similar to that described at San Rafael, and indicating a decrease of temperature. A colorless tourmaline vein (dravite pole, 1.9 Mg apfu and 0.19 Fe apfu), seems to be post orange-brown tourmaline which, if confirmed, would imply a hotter pulse. Microprobe analysis of sphalerite indicates a strong correlation between color and iron content. Opaque sphalerite has up to 11.4 wt. % Fe and orange-yellow sphalerite under microscope down to 3.3 wt. %.

At Quenamari, microthermometric analyses performed on liquid-vapor fluid inclusions occurring in quartz interpreted to be slightly later than sphalerite and in quartz intergrown with chalcopyrite of stage III, and in liquid-vapor fluid inclusions in quartz of stage IV, have salinity and homogenization temperatures for stage III ranging from 1.2 to 9.4 wt% NaCl eq. and 248 to 324 °C respectively (with values from 7.3 to 9.5 wt% NaCl eq. and 248 to 295 °C for sphalerite, 4.6 to 7.9 wt% NaCl eq. and 253 to 283 °C for quartz syn- to post sphalerite, and 1.3 and 5.8 wt% NaCl eq. and 283 to 324 °C for quartz intergrown with chalcopyrite). Salinities for stage IV quartz-hosted fluid inclusions are between 0.7 and 0.9 wt% NaCl eq. and homogenization temperatures between 170°C and 217°C. The minimum pressure of entrapment for stage III is 103 bar and for stage IV 16 bar.

At Quenamari, $d^{18}O_{V\text{-}SMOW}$ values have a range from 11.3 to 12.0 ‰ in tourmaline (stage I), 10.6 to 17.8 ‰ in stage III quartz, and 8.6 to 9.8 ‰ in stage IV quartz. For chlorite, the range is from 4.8 to 6.2‰ for stage III and 0.7‰ for stage IV. $\delta D_{V\text{-}SMOW}$ values range from -79.6 to -70.4 ‰ for tourmaline and from -76 to -59.2 ‰ and -90.1‰ for chlorite, from stage III and IV, respectively. Tourmaline (stage I) values are clearly magmatic; stage III but also stage IV chlorite values are close to the magmatic range and those of stage III suggest boiling and variable fluid $d^{18}O$ values. Quartz $d^{18}O_{V\text{-}SMOW}$ values decrease with time. Two quartz-chlorite pairs from Quenamari give temperatures for stage III of 270 °C and 290°C.

The results for Quenamari are comparable with previous findings at the San Rafael deposit (e.g. Wagner et al., 2009), suggesting that the Quenamari prospect is the upper part of a steep system similar to the one that formed the San Rafael tin deposit. Stable isotope data are indicative of magmatic fluids during stage I mineralization. Precipitation during stage III is accompanied by mixing between a, possibly magmatic, fluid (≥ 9.5 wt.% NaCl eq. and ≤ 250°C) and a low-salinity fluid of higher temperature (≤ 2 wt.% NaCl eq. and ≥340°C). Taking into account the stable isotope results, this second fluid could correspond to condensed magmatic vapor or, less likely, to isotopically exchanged, extraneous fluids. Stable isotope

and fluid inclusion data indicate that in stage IV ingression of meteoric fluids was important.

The fact that at comparable altitude above sea level, similar mineral paragenesis, fluid inclusion characteristics, and stable isotope ratios are found, suggests that the magmatic roots of the mineralizing system at Quenamari are located at a similar depth compared to San Rafael. This, together with the lateral extension and width of the mineralized veins revealed by the detailed surface mapping of the present work, points to an important potential at depth for Sn mineralization at the Quenamari prospect.

REFERENCES

Corthay, G. 2014. The Quenamari prospect, San Rafael tin district, southern Peru: geology, mineral assemblages, fluid inclusion microthermometry, and stable isotopes (with some mineralogical and stable isotope observations at Santo Domingo prospect). Master Thesis Univ. Geneva, Switzerland, 102 p. + map.

Kontak, J.K., & Clark, A.H. 2002: Genesis of the Giant, Bonanza San Rafael Lode Tin Deposit, Peru: Origin and Significance of Pervasive Alteration, Economic Geology, 97, 1741-1777.

Mlynarczyk, M.S.J., Sherlock, R.L. & Williams-Jones, A.E. 2003, San Rafael, Peru: geology and structure of the world's richest tin lode, Mineral. Deposita 38, 555-567.

Wagner, T., Mlynarczyk M.S.J, Williams-Jones A.E & Boyce A.J. 2009, Stable Isotope Constraints on Ore Formation at the San Rafael Tin-Copper Deposit, Southeast Peru, Economic Geology, 104, 223–248.

P 2.10

The hydrothermal sericites of copper- molybdenum porphyry ore-magmatic systems of the Zangezur ore district (Southern Armenia, Lesser Caucasus)

Harutyunyan Marianna

Institute of Geological Sciences, National Academy of Sciences of the Republic of Armenia, Yerevan (marah@geology.am)

The main mineral district is situated in the southern part of Tsaghkounk-Zanghezour metallogenic belt of the South-Armenian terrane and is represented by the giant Kajaran deposit, the smaller deposits of Agarak, Lichk, Dastakert and epithermal gold-ore deposits of Tey-Lichkvaz as well. Subduction and subsequent continental collision caused extensive calc-alkaline volcanic and plutonic igneous activity, including intrusion of Meghri pluton and small massives of Bargushat. The Meghri pluton is characterized by the abundant manifestation of polyphase collisional magmatism. According to Rb-Sr and U-Pb isotopic age determinations (Melkonyan et al., 2013) in the composition of the pluton Upper Eocene gabbro-monzonite syenogranite complex (41- 37Ma) and early Oligocene monzonite-syenite (31-28Ma) are distinguished, and in Lower Miocene (Tayan, 1998) the formation of pluton was completed by three-phase intrusive complex of porphyry granite-granodiorite (24 - 21Ma). Each stage was accompanied with the hydrothermal activity.

Early hydrothermal alteration produced propylitic assemblage (biotite and epidote-chlorite). Epidote-chlorite propylitic alteration was accomplished by the formation of secondary quartzites of mono-quartzite and quartz-sericite facies. The potassic alteration (orthoclase-biotite) occurred contemporaneously with the biotite propylitic alteration. Phyllic and argillic alterations occurred later, overprinting the earlier alteration. Phyllic alteration, consisting of quartz, sericite ± chlorite, accompanied the quartz-molybdenite, quartz-molybdenite-chalcopyrite, quartz-chalcopyrite mineralization stages. The sericite, kaolinite, quartz ± chlorite accompanied the quartz-pyrite, quartz-sphalerite-galena and other mineralization stages.

The crystal chemistry of the mica of quartz-sericite metasomatites in different formations of Agarak, Lichk, Kajaran and Dastakert ore fields in the Zangezur ore district was studied.

1. High- temperature (500-520^{0}C) polytype $2M_1$ (Karamyan et al., 1987) siliceous illites (Si –3,6-3,75pfu) with potassium deficit (interlayer K ≈0,4pfu), low content of Al^{IV} 0,19–0,37pfu (Al^{IV} – 1,50-1,70pfu), with hydration degrees ≈ 4,5 wt. %, are characteristic for hydrothermal secondary quartzites. The siliceous illites are characterized by low ferruginosity κ_{Fe3+} = 0,05-0,1 (κ_{Fe3+}= Fe^3+/ Fe^{3+} + Al^{IV}), they are low-charge, with 0,50-0,63; values for general-layered charge providing even distribution by tetrahedral and octahedral grids. The contents of phengite component varies from 0,13 to 0,30.

2. Medium -temperature (400-280^{0}C) 2M1 and 2M$_1$+1M polytype illites (Karamyan et al., 1987) with hydration of various degrees (≥ 4,5wt. %), Al^{IV} – 0,19–0,37pfu, Al^{IV} – 1,50-1,70pfu, are typical for phyllic alteration (quartz-molybdenum-chalcopyrite, quartz-molybdenum, quartz-chalcopyrite stages); κ_{Fe3+} = 0,02-0,07, the values of general-layered charge are in the range of 0,65-0,84, with tetrahedral charge prevailing octahedral. The content of phengite component is 0-0,30.

3. Low-temperature (210-140^{0}C) hydromicas of 1M and seldom illites 2M$_1$+1M polytype (Karamyan et al., 1987) are typical for argillic alteration (quartz-pyrite and polymetallic stages). There is a characteristic combination of maximal content of phengites from 0,34 to 0,65 with the wide interval of replacement of Si to Al in tetrahedral position Al^{IV} 0,55-0,99 pfu, Al^{IV} 1,21-1,52 pfu, values of general-layered charge from 0,89 to 1,0 with predominant localization of it in the tetrahedral grid. The number of octahedral cations is always more than 2, which is explained by the deviation from the dioctahedral type of structure.
All illites are characterized by the ratio $(^{87}Sr/^{86}Sr)_0$ = 0,70450±0,000129–0,70485±0,000314. Each stage of endogenous formation of sericites is characterized by predominance of certain volatile components: Cl and P are fixed in the illites of secondary quartzites; P, Cl, F – in the illites of phyllic alteration; and CO_2 and SO_3 are recorded in the sericites of argillic alteration.

REFERENCES

Karamyan, K., Tayan, R., Harutyunyan, M., Avagyan, A., Arevshatyan, T., Sarkisyan, S., Madanyan, H. & Vartanesov, V. 1987: The postmetasomatic formations of Zangezure ore district. Yerevan; Pyblishing House of the Academy of Seinces Armenian SSR. 199p. (in Russian).

Melkonyan, R., Ghukasyan, R., Tayan, R., Khorenyan, R. & Hovakimyan, S. 2010: The Stages of copper-molibdenum ore formation in southern Armenia (by the results of Rb-Sr isotope age estimations). The Izvestia of Academy of Sciences Armenian SSR, the series of geology and geography, v2, p 21-32. (in Russian).

Melkonyan, R., Moritz, R., Tayan, R., Selby, D. & Hovakimyan, S. 2013: Copper-molibdenum porphyry ore-magmatic sistems in the Lesser Caucasus. In Conference on Recent Research Activities and New Results about the Regional Geology, the Gejdynamics and the Metallogeny of the Lesser Caucasus. A SCOPES meeting. Tbilisi. 2013 April. 16-18p.

Tayan, R. 1998: On central magma-ore controlling zone of the Zangezour ore region. The Izvestia of Academy of Sciences Armenian SSR, the series of geology and geography, v3-4, p 65-88. (in Russian).

P 2.11

Magmatic, hydrothermal and weathering REE mineralization of the Blockspruit fluorite prospect, Bushveld granitic complex, South Africa

Mihoko Hoshino[1]&[3], Yasushi Watanabe[2], Robert Moritz[3], Maria Ovtcharova[3], Jorge Spangenberg[4] & Benita Putlitz[4]

[1] *Mineral Resources Research Group, National Institute of Advanced Industrial Science and Technology (AIST), Higashi 1-1-1, 305-8576 Tsukuba, Japan (hoshino-m@aist.go.jp)*
[2] *Faculty of International Resource Sciences, Akita University, Tegatagakuen 1-1, 010-8502 Akita, Japan*
[3] *Earth and Environmental Sciences, University of Geneva, Rue de Maraîchers 13, CH-1205 Genève, Switzerland*
[4] *Institute of Earth Sciences, University of Lausanne, Geopolis, Switzerland*

Fluorine is one of the liqands that form complexes with rare earth elments (REE) in melt and fluid, thus fluorite deposits may have elevated amounts of REE, by consquence. Many fluorite deposits and prospects occur in the Bushveld complex. The REE-bearing fluorite deposits and prospects in the complex are classified into two types, depending on the host rocks, which are either alkaline ultramafic rocks (Vergenoeg, Blockspruit, Ruigterpoort) or granite (Buffalo, Slipfontein). The former are enriched in heavy rare earth elements (HREE), and the latter in light rare earth elements (LREE). Ca-amphibole rocks that intrude into the Kenkelbos-type granites host REE mineralization in the Blockspruit prospect. The Ca-amphibole rocks are holocrystalline, variable in grain size (a milimeter to a few centimenter) are composed maninly of Ca-amphibole (>95% in volume) with a minor amount of phosphate minerals (up to a few percent in volume).

We examined REE mineralization and host rock mineralogy of the Blockspruit prospect on the samples collected by surface sampling and diamond drilling down to 200m from the surface. Mineralogical and geochemical analyses (portable XRF, ICP-MS, MLA, EPMA, XRD, TMIS and isotope analyses) were performed on samples collected from 9 drill holes. The results of the drilling project show that the HREE-rich Ca-amphibole rock intruding into the Kenkelbos-type granite extends over an area of at least 600m^2. The weighted mean $^{207}Pb/^{206}Pb$ age obtained by TIMS dating of zircons from the Kenkelbos-type granite is 2055.32 ± 0.34 Ma (MSWD=2, n=6), overlaps with the previously obtained U-Pb zircon age from

the Bushveld granite of 2054.2± 2.8 Ma (Harmer and Armstrong 2000). The intrusive rock is heavily weathered to form 30-50m thick surface iron-oxide rich zone, which has higher REE contents (5380 ppm; REO: 0.63 wt.%) than the non-weatherd part of the rock (3680 ppm; REO: 0.43 wt.%). The top of the non-weathered part of the intrusive rocks is partly hydrothermally altered. The result of EMPA studies shows that the hydrothermally altered Ca-amphibole rocks from shallow zone contain REE-free apatite grains replaced by REE phosphates such as xenotime-(Y) and monazite-(Nd). On the other hand, apatite grains in the fresh Ca-amphibole rock from the deeper zone consist of REE-rich cores (with up to 20.3 wt% ΣREE_2O_3) and REE-free rims including REE phosphates inclusions (Fig. 1).

The REE-free rims including the REE phosphates inclusions are similar in texture within the apatite in the hydrothermally altered Ca-amphibole rock of the shallow zone (Fig. 1). The completely weathered Ca-amphibole crust near the surface contains xenotime-(Y) and monazite-(Nd) as major REE minerals and do not contain apatite grains. EMPA data from drill holes show that Ca-amphibole grains in altered Ca-amphibole rocks from the shallow zone are edenitic ferro-actinolite to ferro-actinolite ($Ca_2Fe^{2+}{}_5Si_8O_{22}(F,Cl,OH)_2$), whereas those in fresh Ca-amphibole rocks from the deep zone are ferro-edenite ($NaCa_2Fe^{2+}{}_55Si_7AlO_{22}(F,Cl,OH_2)$) based on the classification of Leake et al. (2003). The former contains low fluorine, chlorine and alkaline (Na, K) elements compared to the latter. These data may suggest that fluorite mineralization in Blockspuit prospect results from fluorine leached from magmatic ferro-edenite. We conclude that primary REE-rich apatite grains in magmatic ferro-edenite rocks were decomposed by a fluorine-rich fluid, which formed REE-free apatite replaced by monazite-(Nd) and xenotime-(Y) in ferro-actinolite rocks. During the further progress of hydrothermal alteration and weathering, the REE-free apatite grains in the altered ferro-actinolite rocks were completely decomposed by F-rich hydrothermal fluid and only the xenotime-(Y) and monazite-(Nd) grains remain in the weathered ferro-actinolite crusts on near surface (down to a depth of about 30-50m).

Carbon isotope compositions of calcite minerals and veins in fresh ferro-edenite rocks range between -7.6 ‰ and +0.9 ‰ (V-PDB), and especially calcite minerals from ferro-edenite rocks with abundant REE-rich apatite are from -7.6 ‰ to -5.4 ‰ (V-PDB), which overlap with the carbon isotope value of the carbonatites of the region and the mantle (Hoefs 2004). δD values of fresh ferro-edenite minerals range from -113 ‰ to -80 ‰ (V-SMOW), and those of ferro-edenite associated with abundant REE-rich apatite fall between -101 ‰ and -85 ‰ (V-SMOW). These data are consistent with the δD values of pristine mantle (-70 ± 10 ‰ see Boettcher and O'Neil 1980; Kyser and O'Neil 1984). Therefore, two types of REE mineralization can be distinguished in the Blockspruit fluorite prospect as follows: (1) one related to magmatic ferro-edenite intrusive rocks accompanying REE-rich apatite, (2) a second one related to the decomposition of REE-rich apatite and re-precipitaion of monazite and xenotime by a fluorine-rich fluid, which was leached from ferro-edenite.

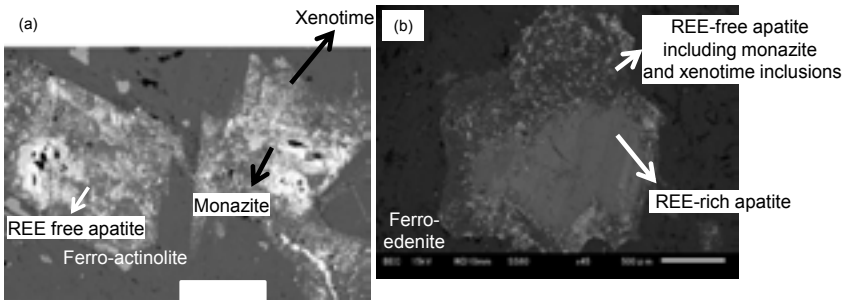

Figure 1. Back-scattered-electron (BSE) images of apatite grains from the Blockspruit fluorite prospect. (a) REE-free apatite grains replaced by monazite and xenotime in altered ferro-actinolite rock from shallow zones. (b) Apatite grains consisting of a REE-rich core and a REE-free rim including monazite and xenotime inclusions from the deep zone.

REFERENCES

Boettcher, A.L. & O'Neil, J.R. 1980: Stable isotope, chemical, and petrographic studies of high-pressure amphiboles and micas: evidence for metasomatism in the mantle source regions of alkaline basalts and kimberlites. American Journal of Science, 280A, 594–621.

Kyser, T.K. & O'Neil, J.R. 1984: Hydrogen isotope systematics of submarine basalts. Geochimica et Cosmochimica Acta, 48, 2123–2133.

Leake, B.E., Woolley, A.R., Birch, W.D., Burke, E.A.J., Ferraris, G., Grice, J.D., Hawthorne, F.C., Kisch, H.J., Krivovichev, V.G., Schumacher, J.C., Stephenson, N.C.N. & Whittaker, E.J.W. 2003: Nomenclature of amphiboles: additions and revisions to the International Mineralogical Association's amphibole nomenclature. Can Mineral, 41, 1355-1370.

Harmer, R.E. & Armstrong, R.A. 2000: Duration of Bushveld Complex (sensu lato) magmatism: Constraints from new SHRIMP zircon chronology. Abstracts, National Research Foundation, Bushveld Complex Workshop, Gethlane Lodge, South Africa, 11-12.

Hoefs, J. 2004: Stable Isotope Geochemistry, 5th ed. Springer-Verlag, Berlin, p. 201.

P 2.12

Structural features of the Kajaran ore field and world-class Mo-Cu-porphyry deposit, Southern Armenia, Lesser Caucasus

Hovakimyan Samvel[1,2], Tayan Rodrik[2], Moritz Robert[1], Harutyunyan Marianna[2], Hovhannisyan Arshavir[2]

[1] *Section des Sciences de la Terre, Université de Genève, Rue des Maraîchers 13, CH-1205 Genève, Switzerland (samvel.hovak@gmail.com)*
[2] *Institute of Geological Sciences, National Academy of Sciences of the Republic of Armenia, Yerevan*

The giant world-class Kadjaran Mo-Cu porphyry deposit (2244 Mt reserves, 0.18% Cu, 0.021% Mo and 0.02 g/t Au) is located in Southern Armenia, Lesser Caucasus and belongs to the Tethyan metallogenic belt. The deposit is hosted by the Tertiary Meghri pluton, which is characterized by a long lasting Eocene to Pliocene magmatic, tectonic and metallogenic evolution.

The deposit is hosted by a monzonite intrusion (31.83 ± 0.02 Ma; Moritz et al., 2013) belonging to the Meghri composite pluton. After emplacement of the monzonite intrusion, the tectonic evolution of the Kajaran ore field was characterized by a specific succession of development of faults and fractures, which controlled further emplacement of magmatic rocks and mineralization.

Early activation of eastwest-oriented fractures along the northern exocontact of the monzonite intrusion and roughly northsouth-oriented structures in the eastern part of the ore field, resulted in the emplacement of elongated zones of migmatites, which represent large apophyses of the monzonite. Further activity magmatic along the endocontact of the monzonite intrusion, resulted in the emplacement of isolated dikes of microsyenite and aplite (Tayan, 1984).

The earliest dike stage consists of porphyritic diorite dikes, located only in the eastern part of the Kadjaran ore field, within roughly northsouth- and northeast-oriented structures, which reveal local extension at this time, and lasting until the Lower Miocene. The same structures also controlled the emplacement of early spessartite dikes, and later abundant medium-grained granodioritic porphyry dykes.

The regional northwest-oriented Tashtun fault zone was active during the Lower Miocene, and was accompanied by the formation of a complex of 22 Ma-old porphyry granites. The Tashtun fault traces the contact between the 31.83 Ma-old host- monzonite and the 22 Ma-old porphyritic granite, and constitues the wesetrn limit of the Kadjaran deposit.

The magmatic evolution at the Kajaran ore field and deposit ends with the formation of thick, eastwest-oriented coarse-grained granodiorite-porphyry dikes. These dikes are interpreted to be genetically related to the 22 Ma-old porphyry granitoids (Moritz et at., 2013).

The above mentioned different structural controls of the different magmatic stages provide a basis to consider the Kajaran ore field as an area of increased long-lived magmatic and tectonic activity, which experienced a complex and multi-stage structural-geological evolution. The change of tectonic regime periodically resulted in repeated extension along the main.

The Kadjaran deposit is structurally controlled by a steeply dipping (65-85^0) orthogonal system of eastwest-, northsouth- and northeast-oriented (45-65^0) fractures. The major ore-bearing faults of the deposit host a stockwork mineralization, with veins ranging in thickness from a few mm up to 5 cm. They can attain a length up to a few tens of meters. They are predominantly shallow-dipping (25-40^0), rarely up to 60^0, they form parallel to sub-parallel oriented systems of veins.

At the Kadjaran deposit, the ore-enriched areas are zones sub-parallel to the eastwest-oriented fractures. In particular, they are located in areas where they crosscut steeply-dipping (70-85^0) eastwest-, northsouth- and northeast-oriented fractures. The dykes have played an important structural control on the location of mineralization.

Based on the available data, we conclude that the fracture system formed continuously during the entire duration of the formation of the Kajaran deposit.

Tectonic conditions varied between extension and compression. The long history of the formation of large zones of ruptures led to the development of a dense network of small fractures, favorable for the location of mineralization. The most pronounced mineralized areas occur along the bend of the Tashtun fault and in areas where the Tashtun fault intersects eastwest-oriented fracture zones.

REFERENCES

Moritz, R., Mederer, J., Ovtcharova, M., Spikings, R., Selby, D., Melkonyan, R., Hovakimyan, S., Tayan, R., Ulianov, A. & Ramazanov, V. 2013: Jurassic to Tertiary metallogenic evolution of the southernmost Lesser Caucasus, Tethys belt. In : Erik Jonsson et al. (eds), Mineral deposit research for a high-tech world, 12th SGA Biennial Meeting, 12-15 August 2013, Sweden, Uppsala, v. 3, p. 1447-1450.

Tayan, R. 1984: Features of development of fault structures of the Kajaran ore field. Proceedings of the Academy of Sciences of the Armenian SSR, Earth Sciences, V3, p.21-29. (in Russian with English abstract).

P 2.13

The gold potential of South East Greenland: new insights of the eastern extension of the > 150 km Nanortalik gold belt

Denis Martin Schlatter[1] & Joshua W. Hughes[2]

[1] *Helvetica Exploration Services GmbH, Carl-Spitteler-Strasse 100, CH-8053 Zürich (denis.schlatter@helvetica-exploration.ch)*
[2] *NunaMinerals A/S, Issortarfimmut 1, Postbox-790, DK-3900, Nuuk, Greenland*

In the past years high grade gold mineralizations have been found in quartz-veins of the Paleoproterozoic Nanortalik Gold Belt (NGB) on the Niaqornaarsuq peninsula (Fig. 1) in South West Greenland with samples of auriferous quartz with up to 2533 ppm Au (NunaMinerals announcement no. 14/2013). The rocks occurring on the Niaqornaarsuq peninsula are mainly dominated by granitoids (Hughes et al. 2014; Schlatter et al. 2013) and gold has not only been found in quartz but gold up to several ppm was also contained in hydrothermally altered granodiorites. The newly discovered gold prospect in South West Greenland is named Vagar after a Norse church located in the same area, has a size of 3 x 4 km and is found in granitoids of the Niaqornaarsuq peninsula (Fig. 1). Vagar comprises several large clusters with gold, each of the clusters are defined by highly anomalous stream sediment samples (with several samples >100 ppb Au) and in-situ rocks with >1 ppm gold. The findings at Vagar are of particular interest because the gold mine Nalunaq (Fig. 1) is in proximity of Vagar and validates the overall gold potential of the NGB.

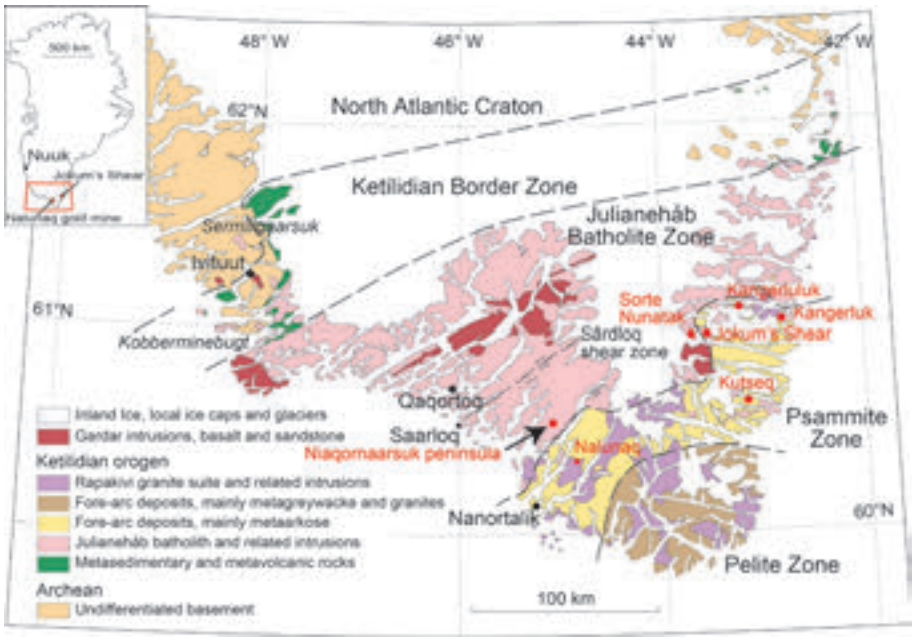

Figure 1. Schematic geological map of the Ketilidian orogen, South Greenland (modified after Chadwick and Garde 1996) showing the location of the exhausted Nalunaq gold mine and numerous gold occurrences. The black arrow indicates the location of the Vagar gold prospect.

The gold occurrences in South Greenland are located in a corridor trending roughly in a northeastern direction and the locus of the gold mineralizations is near the border of the granitoids of the Julianehåb batholith and the Psammite zone of the Ketilidian orogen (Fig.1). In this paper we discuss the gold potential of the eastern extension of the > 150 km NGB where several gold mineralizations have been found already in the 1990'ies in South East Greenland in Paleoproterozoic rocks (Stendal et al. 1997). Exploration efforts by the Geological Survey of Denmark and Greenland (GEUS) and the Greenlandic exploration company NunaMinerals have located gold mineralizations which could potentially become economic resources. For example at the Jokum's shear prospect (Fig. 1) reconnaissance profile sampling has yielded up to 3.1 m at 9.3 ppm gold hosted in hydrothermally altered mineralized and strongly sulfidized plutonic igneous rocks. The associated shear zone system is several tens of meter wide and can be followed over a 1.5 km strike length. The outcrops that have yielded gold were covered by a retrieving glacier and have only been exposed during the last two decades and were not accessible at the time when GEUS has mapped and investigated the area. Geochemical gold and trace element analyses were completed from more than 100 samples from the gold mineralized shear zone at Jokum's shear together with a few samples analysed for whole rock major and trace elements. These geochemical analyses assisted the classification of the host rocks and allowed to determine the trace elements that were added to the rock during the "gold stage"

alteration. The new gold showings at Jokum's shear are particularly interesting because the shear zone that contains the gold mineralizations strikes in a north easterly direction and possibly is continuous for over 25 km if it can be demonstrated that the same shear zone terminates on the South East coast at Kangerluluk where shear hosted gold zones occur (Fig. 1). It is shown from a few other gold mineralizations in South East Greenland that gold can also be hosted in metavolcanic rocks (Fig. 1; Kangerluluk) and in mafic rocks (Fig. 1; Kutseq). Therefore a variety of host rocks and settings should be targeted in South East Greenland for gold exploration. Especially hydrothermally altered shear zones near the Archean North Atlantic Craton – Paleoaproterozoic Julianehåb batholith boarder and locations at the easternmost extension of the NGB represent good underexplored gold targets.

REFERENCES

Chadwick, B. & Garde, A.A. (1996) Palaeoproterozoic oblique plate convergence in South Greenland: a reappraisal of the Ketilidian Orogen. Geol Soc Spec Publ 112:179-196

Hughes, J.W., Schlatter, D.M., Berger A. & Christiansen O. 2014: The Paleoproterozoic Nanortalik Gold Belt – a previously unrecognised Intrusion Related Gold System (IRGS) Province in South Greenland. Applied Earth Science (Trans. Inst. Min. Metall. B) 2013 VOL 122 NO 3: 156-157

Schlatter, D.M., Berger, A. & Christiansen, O. 2013: Geological, petrographical and geochemical characteristics of the granitoid hosted Amphibolite Ridge gold occurrence in South Greenland. Conference proceedings, "Mineral deposit research for a high-tech world." 12th Biennial SGA Meeting, Uppsala, Sweden, pp 1189-1192

Stendal, H., Mueller, W., Birkedal, N., Hansen, E.I. & Østergaard C. 1997: Mafic igneous rocks and mineralisation in the Palaeoproterozoic Ketilidian orogen, South-East Greenland: project SUPRASYD 1996. Geology of Greenland Survey Bulletin 176: 66-74

P 2.14

Les minéralisations à Pb-Zn-F de la province fluorée tunisienne : cas du Jebel Mecella

Jaloul Bejaoui (*), (**), et Salah Bouhlel (**)

(*) Institut supérieur des sciences et des technologies de l'énergie de Gafsa, Tunisie
(**) Laboratoire de Biotechnologie et Valorisation des Bio-Géoresources, Technopole Sidi Thabet et Faculté des Sciences de Tunis, Université de Tunis El Manar, 2092 Tunis

Corresponding author: bjaoui_geo@yahoo.fr

Le gisement du F-Ba-Zn-(Pb) du Jebel Mecella est localisé à 60 Km au Sud de Tunis. Il est limité au Nord par Jebel Ressas et au Sud par Jebel Zaghouan. Le massif du Jebel Mecella est marqué par des affleurements allant du Trias au Miocène. Notre zone d'étude est localisée à l'Ouest du Massif, qui est caractérisée par des terrains crétacés et jurassiques (calcaires para-récifaux de la formation Ressas : Kimméridgien-Tithonien). A Jebel Mecella la minéralisation est déposée dans un système karstique le long de l'inconformité Tithonien-Crétacé inférieur. Cette karstification semble être guidée par la fracturation, qui s'étale et affecte presque la totalité du massif du Mecella. Les remplissages minéralisés intra-calcaires dépendent essentiellement du développement en profondeur des phénomènes karstiques au sein de la roche encaissante. Les calcaires jurassiques constituent des lambeaux en contact tectonique avec des séries marno-calcaires de l'Hauterivien (Crétacé Inférieur). Vers l'Est nous remarquons la présence d'une faille de direction N30, cette faille est jalonnée par du Trias. Au Sud de la mine du Jebel Mecella, les travaux miniers montrent que le contact Tithonien-Crétacé inférieur (Hauterivien) et matérialisé par une surface d'inconformité. La paragenèse minérale est simple et elle est formée par la fluorine, barytine, sphalérite, galène et le quartz.

Les températures d'homogénéisations des inclusions fluides primaires aqueuses (L+V) dans les fluorines sont comprises entre 116°C et 160°C et des salinités variant de 17 % poids équiv. NaCl et 20,5 % poids équiv. NaCl. Les températures d'homogénéisations des inclusions fluides aqueuses (L+V) dans la sphalérite varient de 129°C à 145°C et des salinités comprises entre 14 % poids équiv. NaCl et 18 % poids équiv. NaCl. Le modèle de dépôt proposé est un modèle de mélange de deux fluides est le long de l'inconformité jurassique/crétacé, l'un est caractérisé par une température modérée (130°C) et une salinité de (20 % poids équiv. NaCl) et un fluide à températures (variant de 120°C à 140°C) et des salinités de 15 % poids équiv. NaCl à 20 % poids équiv. NaCl) (Bejaoui, 2012) et (Bejaoui et al., 2013).

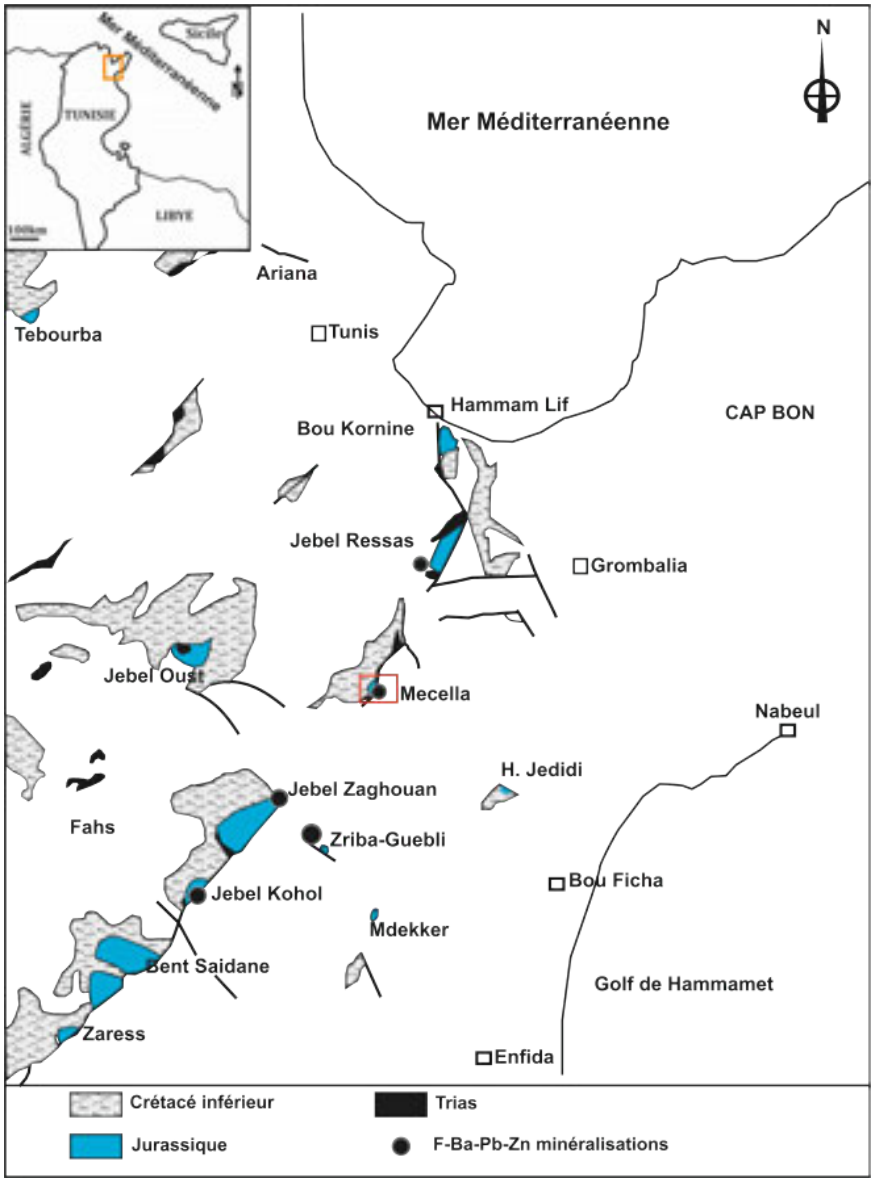

Fig.1 Localisation du gisement du Jebel Mecella dans la dorasle tunisienne (Adopté de Bouhlel et al., 1988).

RÉFÉRENCES

Bejaoui. J (2012) - Géologie, Minéralogie, Eléments en traces Inclusions Fluides, Isotopes et Modélisation Génétique des Gisements à Pb-Zn et ou F, Ba de la Tunisie centro-septentrionale (Fedj Hassène, El Hamra, Ajered, El Kohol, Mecella, El Mokta et M'Tak). Thèse doct., Univ. Tunis II, 260pp.

Bejaoui. J, Bouhlel S and Donatella B (2013) - Geology, mineralogy and fluid inclusions investigation of fluorite deposit at Jebel at Kohol, Northern Tunisia, di Mineralogia (2013), 82, 2, 217-237

Bouhlel S., Fortuné J. P., Guilhaumou N. et Touray J.C (1988) - Les minéralisations stratiformes à F-Ba de Hammam Zriba-Jebel Guebli (Tunisie nord-orientale) : l'apport des études d'inclusions fluides à la modélisation génétiques. Miner. Deposita, 23, 166-173.

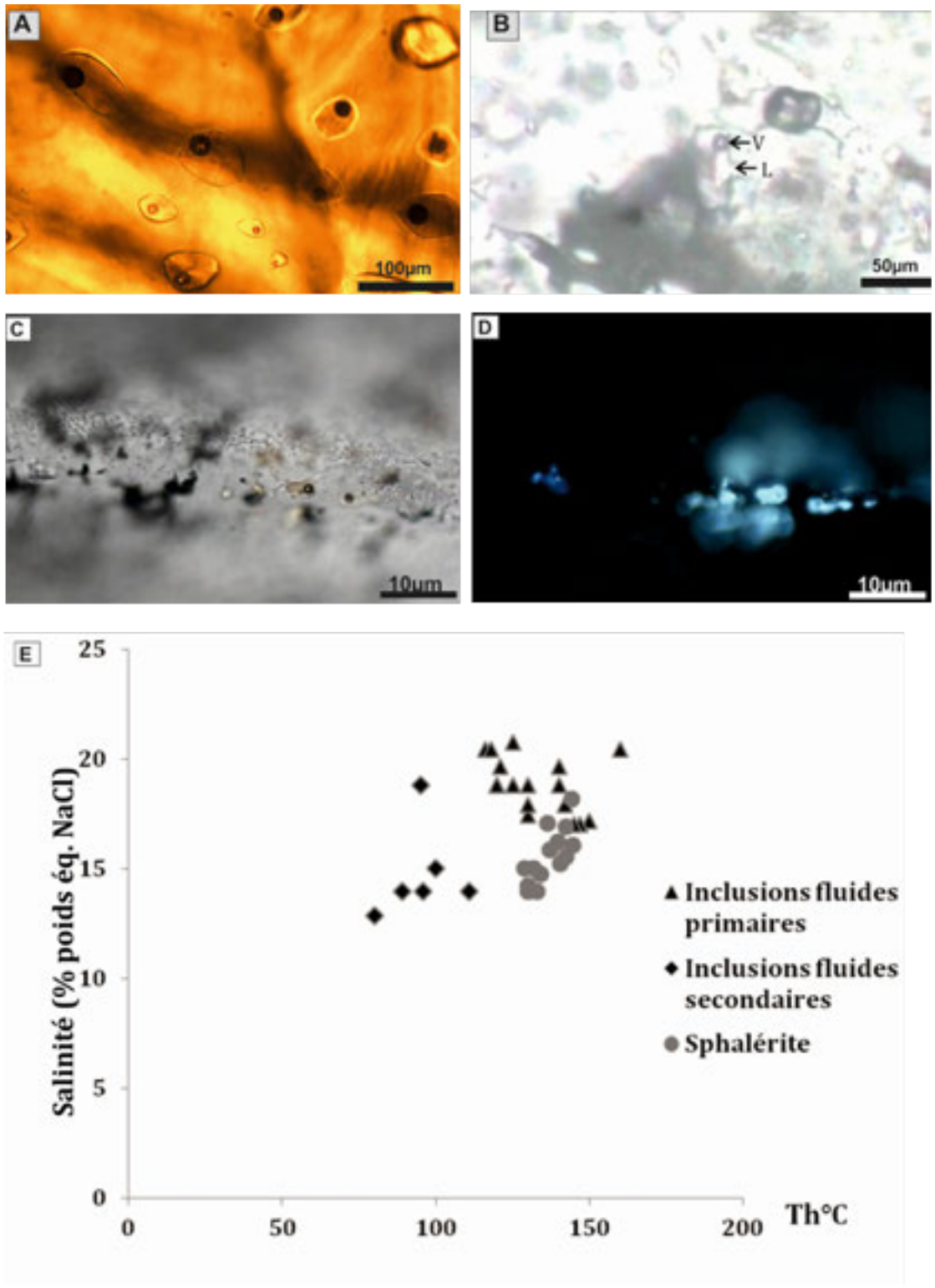

Fig. 2. (1) Inclusions fluides primaires isolées piégées dans la fluorine (A) ; (B) Inclusions fluides gazeuses à CO_2 gaz ; Microphotographies en lumière transmise (C) et en fluorescence (D) et (E) Diagramme binaire Th-Salinité des inclusions fluides primaires et secondaires (L+V) piégées dans la fluorine.

P 2.15

Le district minier à Pb-Zn-Ba du Jebel Hamra-Jebel Ajered (Tunisie centrale) : Géologie, Minéralogie, Inclusions Fluides et Isotopes.

Jaloul Bejaoui ([1]), ([2]), et Salah Bouhlel ([1])

(1) Institut supérieur des sciences et des technologies de l'énergie de Gafsa, Tunisie
(2) Laboratoire de Biotechnologie et Valorisation des Bio-Géoresources, Technopole Sidi Thabet et Faculté des Sciences de Tunis, Université de Tunis El Manar, 2092 Tunis

Corresponding author: bjaoui_geo@yahoo.fr

Le district minier de Pb-Zn-Ba du Jebel Hamra-Jebel Ajered est situé dans un massif de calcaire aptien, situé au centre-ouest de la Tunisie, près de la frontière algéro-tunisienne, à une cinquantaine de kilomètres de la ville de Kasserine et à 290 km de Tunis (Figure 1). Ces massifs renferment un champ de corps minéralisés, où le minerai est formé par la galène et la sphalérite dans une gangue de barytine. Ces minéralisations font partie du district algéro-tunisien à Pb-Zn-Ba encaissées dans des calcaires de la plateforme aptienne de Kasserine-Tebessa, incluant aussi les gisements de Bou Jaber, Slata, Ajered, Chambi, Trozza en Tunisie et Mesloula, M'Zouzia, Bel Kfif en Algérie. Ce district de Pb-Zn-Ba du Jebel Hamra-Jebel Ajered est formé par des gîtes dispersés dans l'ensemble des massifs aptiens.

Dans ce travail nous présentons une étude géologique, minéralogique, pétrographique des minerais. La partie géochimique comportera une étude microthermométrique et une analyse isotopique du soufre et de Pb.

Les minéralisations du **Jebel Hamra** sont du type stratabound, pénéconcordants le long de l'inconformité Apto-Albienne, mais discordant sur les strates des carbonates aptiens (Figure 2). La paragenèse est simple, constituée par la succession suivante : chalcopyrite (traces), sphalérite, galène et de la barytine.

L'étude microthermométrique des inclusions fluides primaires aqueuses piégées dans la sphalérite sont caractérisées par des températures d'homogénéisation variant de 110 °C à 152 °C et des salinités de l'ordre de 14 % poids équiv. NaCl à 19 % poids équiv. NaCl avec une moyenne à 17 % poids équiv. NaCl. Les valeurs de $\delta^{34}S$ de sphalérite et galène variant de -3 à 6,3 ‰ CDT et la présence des évaporites triasiques conduisent à proposer une source triasique du soufre. Les isotopes du soufre sont compatibles avec une réduction des sulfates triasique par des processus de réduction thermochimique (TSR) sous des conditions de températures variant entre 150 °C et 200 °C et en présence de matière organique abondante.

Les minéralisations de P-Zn-(Ba) du **Jebel Ajered** sont caractérisées par des corps minéralisés sont lenticulaires en remplissage des poches karstiques qui affectent les calcaires silicifiés et dolomitisés de l'Aptien supérieur (Formation Serdj) (Figure 2). (i) Les inclusions fluides piégées dans la sphalérite montrent des températures d'homogénéisations entre 126°C et 139°C et des températures de fin de fusion entre -14,5°C et -11°C et qui correspondent à des salinités entre 15 % poids équiv. NaCl et 18 % poids équiv. NaCl. (ii) Les inclusions fluides piégées dans le quartz associé à la sphalérite donnent des valeurs de températures d'homogénéisations entre 128°C et 147°C et des salinités comprises entre 18,7 % poids équiv. NaCl et 21,5 % poids équiv. NaCl. (iii) Les inclusions fluides piégées dans le quartz géodique du signal s'homogénéisent en phase liquide à des températures d'homogénéisations T_h variables entre 155 °C et 170 °C et des salinités qui sont comprises entre 18,7 % poids équiv. NaCl et 21,5 % poids équiv. NaCl. Les différences enregistrées au niveau des températures d'homogénéisations mesurées dans la gangue « quartz » et la sphalérite, montrent que la précipitation de la sphalérite a été effectuée à partir de mélange de deux fluides caractérisés par des températures et des salinités différentes. Les analyses de la composition isotopiques de $^{206}Pb/^{204}Pb$, $^{208}Pb/^{204}Pb$ et $^{207}Pb/^{204}Pb$ dans des échantillons de galène prélevés des minerais karstiques montrent respectivement les valeurs suivantes ; 18,9102 à 18,8819, 15,6710 à 15,6720 et 38,7840 à 38,8029. Les compositions isotopiques de plomb du Jebel Ajered et de Jebel Hamra se localisent dans le même champ pour la majorité des gisements de Pb-Zn de Tunisie et elles montrent une similitude avec les compositions isotopiques de Plomb de la Croûte Supérieure. Les études minéralogiques et géochimiques des deux gisements du Jebel Hamra et Jebel Ajered montrent une grande ressemblance dans les paragenèses minérales. La synthèse et l'interprétation de l'ensemble de nos données sur ce district minier de Pb-Zn-Ba nous ont permis également, de faire un rapprochement de ce dernier avec des gisements de type Mississippi Valley.

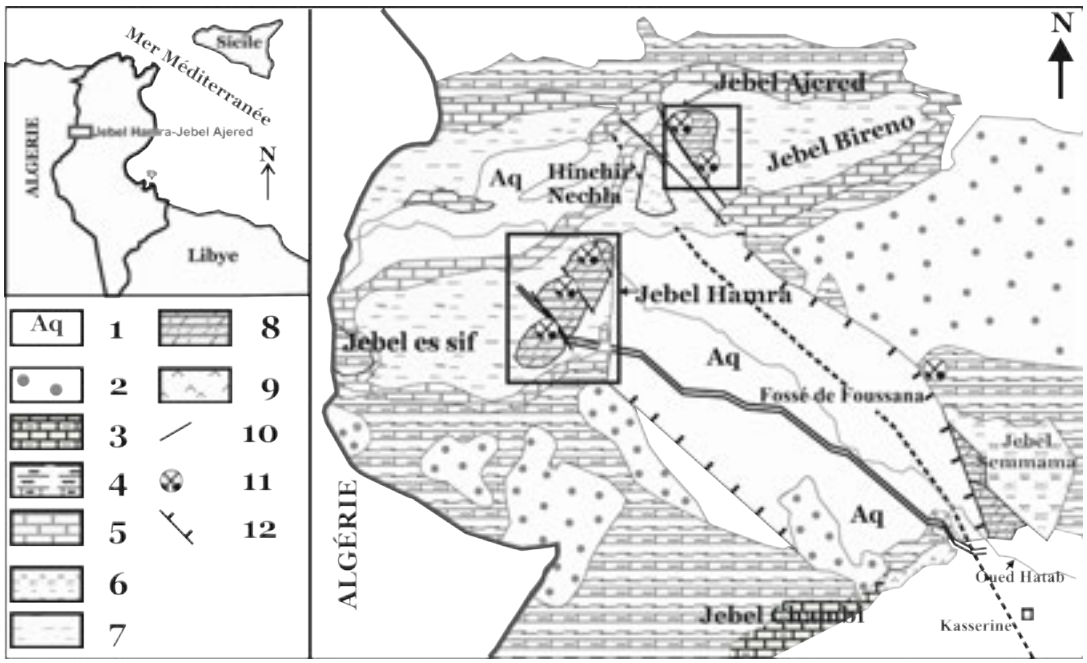

Figure 1 : Localisation du district minier Jebel Hamra-Jebel Ajered dans un extrait de la carte géologique de la Tunisie au 1/500 000. (1) Quaternaire : Alluvions récents et actuels; (2) Miocène supérieur : alternances de grés et des argiles; (3) Sénonien supérieur : calcaires à intercalations d'argiles; (4) Sénonien inférieur : marnes à intercalations calcaires de la formation Kef; (5) Turonien : calcaires de la formation Bireno; (6) Cénomanien supérieur à Turonien : marnes, marno-calcaires et calcaires en plaquettes; (7) Albien à Cénomanien : marnes et calcaires de la formation Fahdène; (8) Aptien : calcaires récifaux et des dolomies de la formation Serdj; (9) Trias : argiles, dolomies et évaporites; (10) Failles; (11) Minéralisations à Pb-Zn-(Ba) et (12) Coupe géologique.

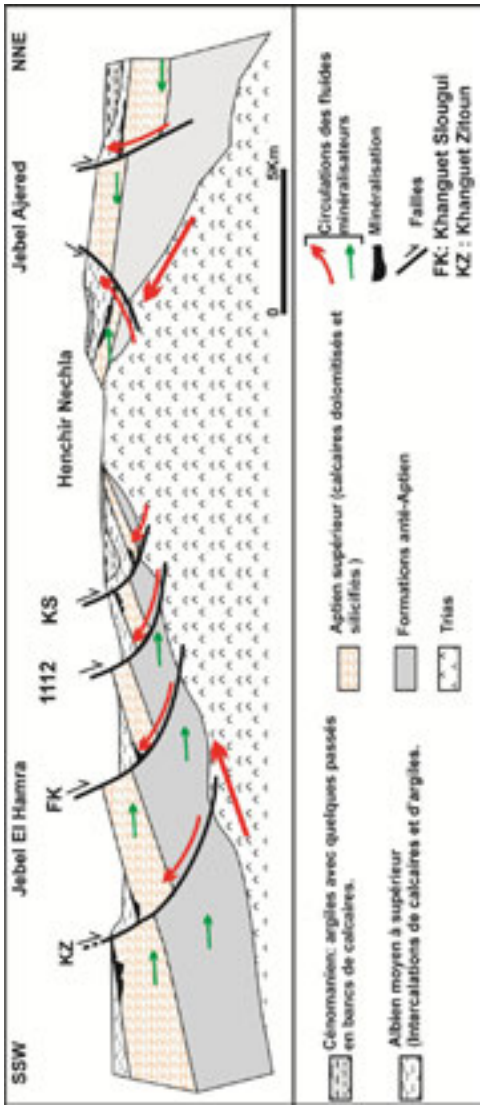

Figure 2 : Projection de la localisation de la minéralisation et la circulation des fluides hydrothermaux sur une coupe structurale à travers le district Jebel Hamra-Jebel Ajered

P 2.16

First evidence of multiple porphyry events in the Cerro de Pasco polymetallic district, central Peru

Bertrand Rottier[1],Kalin Kouzmanov[1], Vincent Casanova[1], Ronner Bendezú[2], David Cuéllar[2], Lluís Fontboté[1]

[1] *Earth and Environmental Sciences, University of Geneva (Bertrand.Rottier@unige.ch)*
[2] *Volcan Compania Minera S.A.A., Av. Gregorio Escobedo 710, Lima*

Cerro de Pasco, part of the Miocene metallogenic belt of central Peru, is one of the largest known epithermal base metal deposits. The deposit is formed along the eastern margin of a diatreme-dome complex emplaced in the Mid-Miocene. We report the first evidence of multiple porphyry events at Cerro de Pasco.

Hornfels clasts with typical A and B quartz-molybdenite porphyry veins (Fig. 1A) were found incorporated in a magmatic breccia intersected by holes drilled in the southeast part of the diatreme. The magmatic breccia (dacitic in composition) crosscuts the phreatomagmatic breccia of the diatreme, known as Rumiallana Agglomerate (Baumgartner et al., 2009).

Considering the geochronology established by Baumgartner et al. (2009) and assuming that the magmatic breccia is coeval with or very close in age to the Rumiallana Agglomerate, the Mo porphyry mineralization could have taken place around 1 m.y. prior to the epithermal base metal mineralization. Similar time gaps between porphyry and epithermal base metal mineralizations have been reported in other districts in central Peru. Hornfels clasts are fine-grained (Fig. 1A); most of the them are affected by high-temperature K-alteration marked by K-feldspar-biotite-andalousite-albite assemblage, and in some cases overprinted by lower-temperature phyllic or argillic alteration marked by kaolinite-dickite-(illite) assemblage.

Around 20% of the hornfels clasts are crosscut by 1 - 10 mm thick quartz veins. The veins are sulfide-poor (<<1%), the main sulfides being pyrite, molybdenite, and chalcopyrite. SEM-CL images reveal only one quartz generation, highly luminescent with subtle subrounded oscillatory growth zoning (Fig. 1C), typical of high temperature quartz (>500°C).

In addition, direct evidence of porphyry-style mineralization at surface has been found in the central part of the diatreme in a tiny outcrop (approximately 12 x 5 m, coordinates 361389E, 8820680N) of andesitic plug-like body crosscutting the diatreme dome complex. The porphyryrtic andesite is affected by a network of quartz-magnetite-chalcopyrite-pyrite porphyry style veinlets, up to 1 cm in thickness (Fig. 1D). Crosscutting relationship indicates that the porphyry plug and the subsequent stockwork mineralization postdate the diatreme-dome complex. The andesite porphyry is affected by pervasive chlorite-epidote-magnetite alteration. The magnetite-chalcopyrite-pyrite veins are widespread and locally very dense,

up to 20 veinlets per square meter. The veins are generally thin: from <1 mm to 2 cm. Microscopic observation reveals high chalcopyrite/pyrite ratios, with up to 5% of chalcopyrite, both sulfides being affected by supergene alteration (Fig. 1E). SEM-CL images of the veins reveal two generation of quartz (Fig. 1F), a high-luminescence resorbed quartz (qtz-1), with a late low-luminescence quartz associated with the chalcopyrite precipitation (qtz-2).

Moreover, tens of mineralized porphyry fragments enclosed within E-W-trending quartz-monzonite porphyry dykes were observed up to more than 1 km west from the outcrop described above. The fragments contain quartz-magnetite-chalcopyrite-pyrite veinlets generally associated with K alteration (biotite, K feldspar).

These new observations are the first field evidence of the presence of porphyry mineralization in the Cerro de Pasco district. These porphyry mineralizations occur before and after the diatreme-dome complex indicating that Cerro de Pasco is long-lived mineralizing system (>1 My). Further investigation are in progress to understand the genetic link between the multi-stage porphyry and epithermal base metal mineralization.

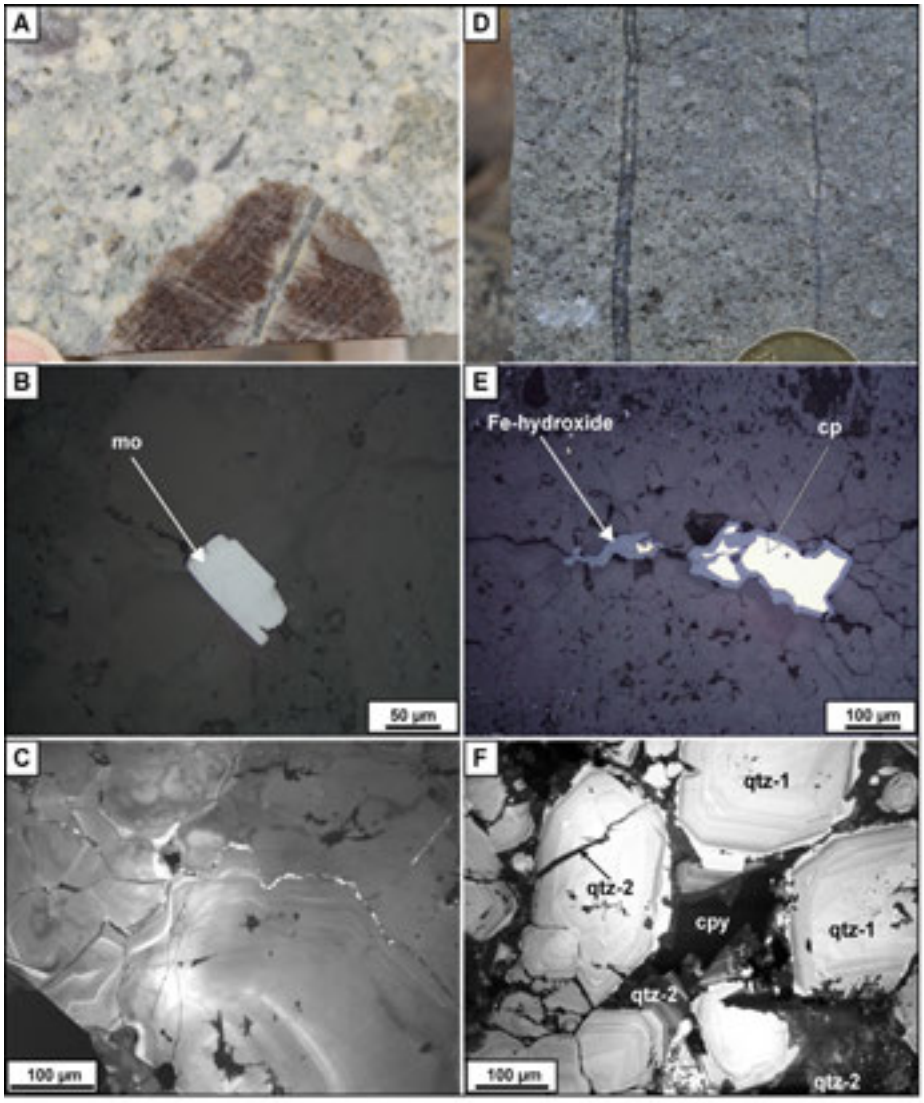

Figure 2. A,B,C) A:hornfels clast hosted in magmatic breccia crosscut by quartz-molybdenite porphyry veins B: Reflected-light photography of the vein C: SEM-CL images of the vein. D,E, F) D:andesitic porphyry crosscut by quartz magnetite-chalcopyrite-pyrite veins, E: Reflected-light photography of one vein F: SEM-CL images of one vein

REFERENCES

Baumgartner R., Fontboté L., Spikings R., Ovtcharova M., Schneider J., Pace L., Gutjahr M. 2009: Bracketing the age of magmatic-hydrothermal activity at the Cerro de Pascoepithermal polymetallic deposit, central Peru: a U-Pb and $^{40}Ar/^{39}Ar$ study. Economic Geology, 104, 479-504.

Project supported by SNF grant 146353 and Volcan Cia. Minera.

P 2.17

Petrography and geochemistry of the Cusín and Cubilche volcanoes (Interandean Valley, Ecuador)

Elisa Tamagnone Cosmelli[1]

[1] *Section of Earth and Enviromental Sciences, University of Geneva, Rue de Maraîchers 13, CH-1205 Genève*

The Cusín and the adjacent smaller Cubilche volcanoes (the latter with two satellite edifices, Planchaladera crater and Cunru dome) are located in the Interandean Valley between the Western and the Eastern Cordillera of the Northern Andes of Ecuador. Together with the frontal arc volcanoes of Pilavo, Yanaurcu, and Huanguillaro-Chachimbiro situated to the NW they form a NW-SE alignment of volcanic edifices perpendicular to the trench, situated between 0° and 0°30'N. The frontal arc volcanoes of this transect (Pilavo, Yanaurcu, and Huanguillaro-Chachimbiro) have already been the object of previous studies (e.g., Chiaradia et al. 2011, Beguelin, 2014), which have shown the possible occurrence of systematic across-arc geochemical changes. The investigation of these additional 4 volcanic edifices in conjunction with the previously investigated ones aims to reconstruct geochemical changes of closely spaced volcanic edifices along a 50-km long across-arc transect and to investigate the variability of petrogenetic processes at adjacent volcanic edifices. In order to realize this aim we plan to carry out petrography, mineral chemistry and whole rock geochemistry (major and trace elements as well as radiogenic isotopes) on selected rocks from the 65 samples collected during a field campaign last June. $^{40}Ar/^{39}Ar$ dating will be also carried out on rocks of the 4 volcanic edifices to assess the temporal scale of geochemical variability at adjacent edifices. Finally, the study of these volcanoes and of their numerous xenoliths is also expected to contribute to understand the geology of the basement in the Interandean Valley, which is poorly known because covered by Tertiary to Quaternary volcanic and volcaniclastic rocks.

REFERENCES

Chiaradia, M., Müntener, O., Beate, B. 2011: Enriched basaltic andesites from mid-crustal fractional crystallization, recharge, and assimilation (Pilavo volcano, Western Cordillera of Ecuador). Journal of Petrology, 52, 1107-1141.

P 2.18

Mineralogy and cultural heritage – introducing QEMSCAN® automated technology to the study of ancient artefacts

Branimir Šegvić[1], Annette Süssenberger[1], Marina Ugarković[2], Andrea Moscariello[1]

[1] *Section des sciences de la Terre et de l'environnement, Université de Genève, Rue de Maraîchaire 13, CH-1205 Genève (branimir.segvic@unige.ch)*
[2] *Institute of Archaeology, Ljudevita Gaja 32, HR-10000 Zagreb*

The FEI QEMSCAN® Quanta 650F device has recently been installed at the Rock-Typing Laboratory at the University of Geneva. The instrument is essentially based on automated acquisition of SEM-EDS spectra that integrated yield the high-quality mineralogical mapping of measured samples. The method was originally developed about a decade ago for the purposes of ore processing industry needing rapid and fully quantified mineralogical data. Despite just a few existing laboratories using this technology in publically funded research institutions, Geneva being the 2nd in continental Europe, the past few years saw a diversification of QEMSCAN® technology application ranging from mining and oil and gas research to forensic studies and archaeology. In archaeological research in particular exists only a few studies using automated mineralogy approach. Therefore, our aim is to discuss some of the advantages and limitations of its application by presenting preliminary results on the research on Hellenistic ceramics.

The striking advantage of QEMSCAN® technology when compared to any earlier petrographic method is the possibility of performing systematic mineralogical mapping of the whole sample area thus offering a clear visual understanding of the sample texture (Fig. 1.). The image resolution depends on the spot spacing where at each point an EDS spectrum is taken and compared to the available spectra databases assigning the related point to certain mineral or compositional grouping. Modal mineralogy is normally presented in terms of area percentages (Fig. 1.), with additional possibilities to

be shown like the mean size of particular entry, preferential mineral associations, distribution of densities, etc.

In ceramic studies such information are indispensable for several reasons. Firstly, a comprehensive understanding of the clayey matrix composition is provided, elucidating the type of raw material used and the way the pottery paste was prepared. In the example shown, the matrix is predominantly Ca-illitic with some scattered presence of chlorite-like pixels. Furthermore, two types of isometric inclusions are present – first being composed of the same clay type characterised by a relative reduced pore content, whilst the second type essentially consists of smectite. This allows us to define the ceramic raw material as illitic clay with some Ca to Fe/Mg-rich component contamination. Alternatively, the whole matrix is consisted of mixed-layered clays. Inclusions are interpreted to be linked to the paste preparation artefacts (first type), or rather as features of baking paste optimisation (second type). The following line of inquiry supported by QEMSCAN® data consists of the precise study of mineral inclusion content, especially the one on heavy minerals, and some key

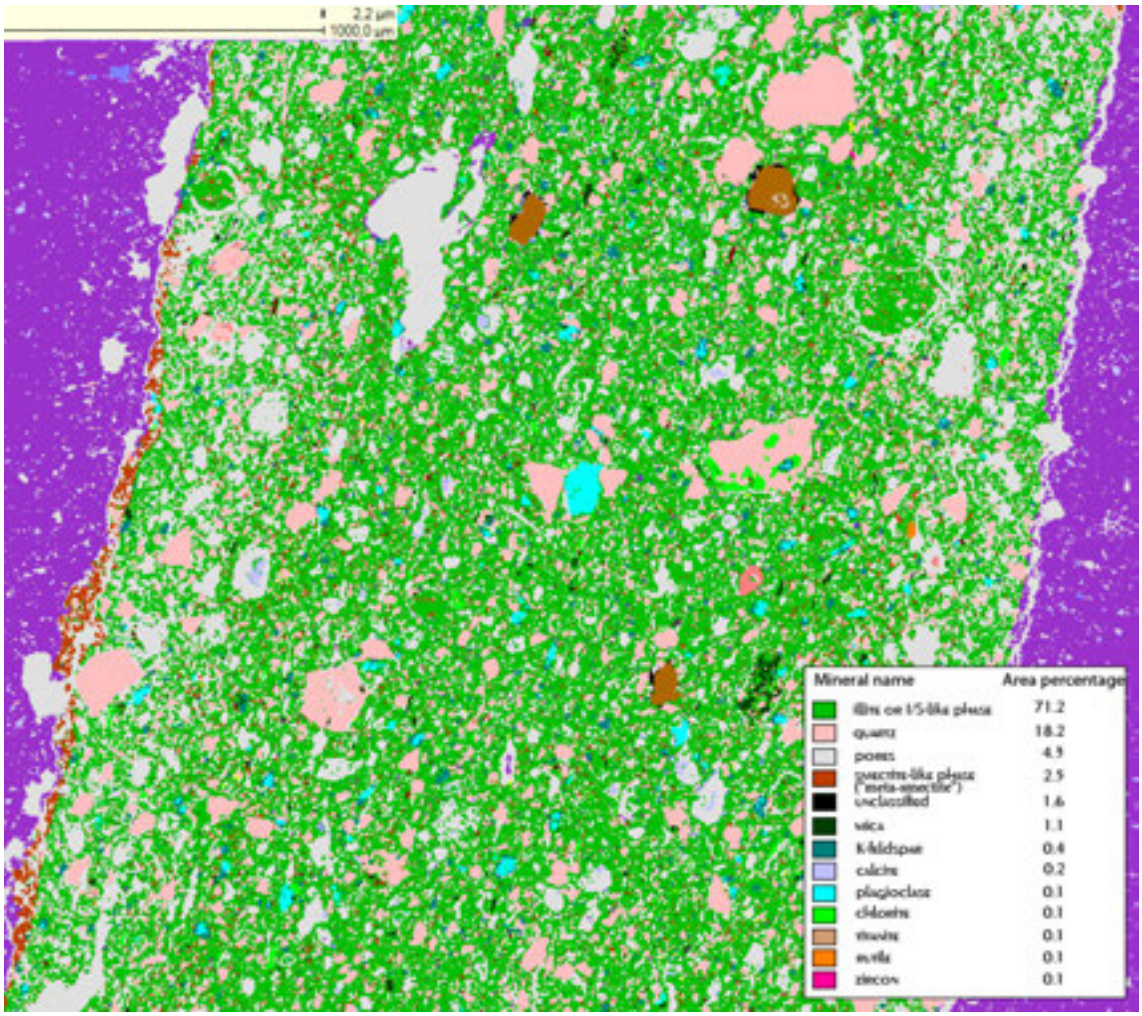

Figure 1. The ceramic potsherd QEMSCAN® image showing the high-resolution mapping based on automated EDS spectra acquisition. Measurement conditions: 15 kV acceleration voltage and 2.5 µm acquisition step.

silicates, such as quartz and feldspars, which are important for provenance analyses. The third important piece of acquired data is the quantification of microporosity. Namely, any imaged areas not classified as minerals are pores (based on BSE level threshold data). In the potsherd depicted (Fig. 1.), a secondary microporosity is well developed, which is associated with the occurrence of reticular clay matrix. This is an indication of several hours of firing at temperatures attaining up to 800°C.

In general, important aspects of automatisation applications to archaeological science and material research have been shortly addressed. There are, however, some limitations one needs to be aware of. Minerals of same chemistry but different mineralogy cannot be distinguished. Those of similar chemistry (clay minerals, pyroxenes, amphiboles, etc.) should be separated with caution. Spectra of thermally processed and metastable phases are frequently not uniform and are, therefore, not defined. To overcome some of these obstacles, a detailed work on building up synthetic and/or standard-derived EDS spectra database is required, along with the combination of QEMSCAN® results and other techniques, in particular X-ray diffraction and electronic microanalysis.

P 2.19

The Miocene Mariño Formation (Central Argentinian foreland, Mendoza region): a high-resolution integrated study of sedimentary and paleoenvironmental responses to tectonic and climatic forcing

Gabriel Hunger [1], Dario Ventra [1], Gonzalo Veiga [2], Andrea Moscariello [1]

[1] *Earth and Environmental Sciences, University of Geneva, rue des Maraichers 13, 1205 Geneva, Switzerland (gabriel.hunger@unige.ch)*
[2] *Centro de Investigaciones Geológicas, Universidad Nacional de La Plata - CONICET, Argentina*

Numerous studies relate foreland-basin infill to allogenic forcing, but to date only a few have been able to clearly disentangle the relative roles of tectonics and climate on long-term deposition. Here we present preliminary observations on the continental sedimentology and stratigraphy of the Central Argentinian Foreland near Mendoza. The basin comprises a thick (over 4 km), almost complete sedimentary infill recording local environmental change from the late Oligocene to the Quaternary, during active Andean orogeny.

The Mariño Formation comprises a large part of the Neogene sediments in the Central Argentinian Foreland, dating from ~15.7 to 12.0 Ma and extending over almost 1100 m in stratigraphy. It is extensively exposed as the surface expression of folds related to Plio-Pleistocene uplift of the Precordillera. The formation comprises a continuous stratigraphic record of aeolian and ephemeral fluvial systems developed during the uplift of the Principal Cordillera in an arid to semiarid climate context. The basal part is characterized by the frequent intercalation of aeolian and fluvial deposits, followed vertically by the stacking of fluvial deposits with highly differentiated facies associations and architectures. This stratigraphic picture suggests the interaction of different allogenic controls in the region, namely climate change and tectonics.

This project aims to provide a detailed reconstruction of paleoenvironmental dynamics and to unravel the relative roles of climate and tectonics through a high-resolution, integrated compositional and sedimentological analysis of the Mariño Formation. The main objectives are: to improve the current chronological framework by magnetostratigraphy; to obtain chemostratigraphic logs for sediment elemental composition (in order to detect geochemical signatures of allogenic controls); to track changes in sediment provenance and relative information on magmatism and exhumation in the uplifting Andes; and to recognize the effects of different allogenic drives on sedimentary processes and local environmental change.

Part of the research consists of a multidisciplinary compositional study of 400 m-thick succession which comprises significant environmental (aeolian to fluvial) transitions. Our approach consists of high-resolution petrography (based on conventional thin section, XRD and QEMScan technology), heavy-minerals analysis, geochemistry (major and trace elements by XRF and LA-ICP-MS), radiogenic isotope analysis (Sr, Nd, Pb by MC-ICP-MS), U-Pb dating of detrital zircon, magnetostratigraphy and palynology. A first field campaign provided a detailed stratigraphic and facies architectural framework; sampling was conducted along multiple transects (logged as continuous vertical sections).

The exceptional lateral exposure and the possibility to develop stratigraphic correlations calibrated with quantitative analytical approaches will constrain the relative role of different allogenic processes and offer insights for understanding similar sedimentary complexes in the subsurface.

P 2.20

GEMSFITS: A Code For Input Parameter Optimization Of Chemical Thermodynamic Models

George D. Miron[1], Dmitrii A. Kulik[2], Svitlana V. Dmytrieva[3], Thomas Wagner[4]

[1] *Institute of Geochemistry and Petrology, ETH Zurich, Switzerland (dan.miron@erdw.ethz.ch)*
[2] *Laboratory for Waste Management, Paul Scherrer Institut, Switzerland*
[3] *Institute of Environmental Geochemistry, Kiev, Ukraine*
[4] *Department of Geosciences and Geography, University of Helsinki, Finland*

The GEMSFITS code package is a tool for regressing internally consistent input parameters of chemical thermodynamic models against experimental data, and for performing various inverse modeling tasks (e.g. thermogeobarometry). This has many applications for more accurate and robust modeling of complex multicomponent-multiphase geochemical systems. The new code is more general and has a much broader scope than its earlier prototype (Hingerl et al., 2014) aimed at fitting interaction parameters of thermodynamic activity models only. The GEMSFITS code includes the GEMS3K chemical solver (Kulik et al., 2013) – a Gibbs energy minimization kernel of GEM Software that includes the TSolMod library (Wagner et al., 2012) of equations of state and activity models of solution phases (fluid mixtures, aqueous solutions, solid solutions etc.). For parameter fitting, GEMSFITS code uses a robust open-source library NLopt (http://ab-initio.mit.edu/wiki/index.php/NLopt) for nonlinear optimization, providing easy selection between several algorithms (global, local, gradient-based). Statistical evaluation of results is performed by calculating summary statistics, sensitivities of measured data and parameters, correlation coefficients, and confidence intervals using Monte Carlo simulations. The code can take advantage of parallelization, which substantially decreases the computing time required to complete a fitting task when a large number of experiments and parameters are involved.

GEMSFITS code can import, manage and query extensive sets of experimental data stored in database files in the industry-winning NoSQL BSON format. Due to the flexibility of NoSQL database, which does not need a priori knowledge of data structure, many types of experimental data can be inserted, describing various experimental properties such as (but not limited to): chemical composition of experimental systems, measured phase compositions (e.g. solubility data), measured phase properties (e.g. density) temperature and pressure, osmotic coefficients, activities/fugacities of components,etc.

GEMSFITS is equipped with a simple graphical user interface (GUI) that allows creating a project for fitting tasks, managing the experimental data base (create, edit, delete entries), running the fitting task, and analyzing the results. In a project, any number of fitting tasks (variants) can be created, edited (in JSON format) and stored in the database. Multiple parameters can be fitted simultaneously against selected experimental properties, augmented with several options for data weighting, parameter bounds and constraints, and statistical methods.

Results (parameters, sensitivity data, statistics) can be stored in database, viewed and plotted on XY plots using the GUI. The practical utility and efficiency of GEMSFITS is demonstrated by application examples of typical classes of problems and combinations that include fitting of parameters of thermodynamic mixing models, optimization of standard state Gibbs energies of aqueous species and solid-solution end-members, thermobarometry and inverse titrations. GEMSFITS codes (Miron et al., 2014) will be made freely distributable and open-source, as part of the GEM Software collection (http://gems.web.psi.ch).

REFERENCES

Hingerl, F.F., Kosakowski, G., Wagner, T., et al. 2014: GEMSFIT: a generic fitting tool for geochemical activity models, Computational Geosciences, 18, 227-242.

Kulik, D.A., Wagner, T., Dmytrieva, S.V., et al. 2013: GEM-Selektor geochemical modeling package: revised algorithm and GEMS3K numerical kernel for coupled simulation codes, Computational Geosciences 17, 1-24.

Wagner, T., Kulik, D.A., Hingerl, F.F., Dmytrieva, S.V. 2012: GEM-Selektor geochemical modeling package: TSolMod library and data interface for multicomponent phase models, Canadian Mineralogist, 50, 1173-1195.

Miron G.D., Kulik D.A., Dmytrieva S.V., Wagner T. (2014) Applied Geochemistry, in review.

P 2.21

Petrographic and sedimentologic examinations of river gravel from the 'Kleine Wiese' river, Black Forest (D)

Touzin Marc Andre[1], Franz Leander[2], Wetzel Andreas[1],

[1] *Institute of Mineralogy and Petrography, University of Basel, Bernoullistrasse 32, CH-4056 Basel (marc.touzin@stud.unibas.ch)*
[2] *Institute of Geology and Paleontology, University of Basel, Bernoullistrasse 32, CH-4056 Basel*

As part of a comprehensive petrological as well as sedimentological study of the deposit gravel of the Rhine River and its tributaries the University of Basel, this investigation focusses on the Kleine Wiese river. The 25,1 km long Kleine Wiese drains part of the southern Black Forest (Baden-Wuerttemberg, Germany).

The gravel was sampled at eight locations faking into account the surrounding geology. Sampling began at the river´s headwaters at the south facing slope of the Belchen downstream to its mouth in Langenau where the river flows into the 'Grosse Wiese'. 152 pebbles were macroscopically studied and 33 thin sections, in addition to gather information about the mineral composition, the rock fabric and to draw conclusions on the formation of the specific gravel deposit.

Furthermore, for a sedimentological analysis, the frequency of particular pebbles in addition to their sphericity and roundness were measured. Important is the interplay between the petrographic and the sedimentologic data to understand transport processes and their effects on the gravel composition. Based on the existing map material from Metz and Rein (1957), the gravel types were assigned to the geological units within the catchment area. Glaciers could also have a strong influence on the entire river valley. According to the maximum snowline during the last glacial period, glaciers could have prograded down to 500 meters above sea level, which approximately corresponds to Langensee between Tegernau and Neuenweg. These glacial processes could have transported some components from the Badenweiler-Lenzkirch-Zone, one of the four main units of the Black Forest, into the Kleine Wiese riverbed.

These five geological units are found along the river. (1) Within the rivers headwater close to the town of Neuenweg, a massive intrusive rock called 'Granit of Münsterhalden', formally known as 'Belchengranit' crops out. Granitic samples collected at this first point had a uniform medium-grained texture. (2) Right next to Neuenweg, at sample point two, well-rounded conglomerates appear. They consist of migmatic gneisses, Upper Devonian greywacke and argillaceous shale.

Furthermore, several pieces of fine-grained granitic dike gravel, subordinate medium grained granitic gravel as well as well-rounded greywacke gravel, together with construction waste was found. According to the geological map of Metz and Rein (1957), these conglomerates formed during Lower Carboniferous basin uplift. (3)-(6) These sample points are located amidst a geological unit called 'syntexite complex of Mambach'. It is made up of a complex association of gneisses, granitic and lamprophyre dikes. Bordering on the conglomerates up north, some collected gravel contained deformed mylonitic rocks, coarse-grained rhyolitic rocks and quartz-monzonites. (7) At this location the so-called 'Marlsburger Granit' dominates within the gravel; this granite crops out nearby. This granite reveals a grey to brown-red colour and a medium-grained, unoriented texture. In some cases, porphyric orthoclase crystals occurred. (8) Sample point eight included red sandstone of Lower Triassic age. All collected sandstone samples had a well-rounded shape because of their low durability. An increased number of quartz gravels indicate quarz vein to occur nearly.

Surprisingly the Kleine Wiese provides a dominance of igneous gravel compared to metamorphic gravel even though it is located in a syntexite area. One reason for this could it be the high weathering resistance of the former rocktype.

Using a plot of roundness of the gravel vs. distance from the river head after Krumbein, and Sloss (1963) it is possible to classify the sedimentological maturity and to provide a rough estimation of the haul distance. As expected the roundness increases with distance to the river headwater. The approximate nominal diameter as well as the sphericity produces the same results.

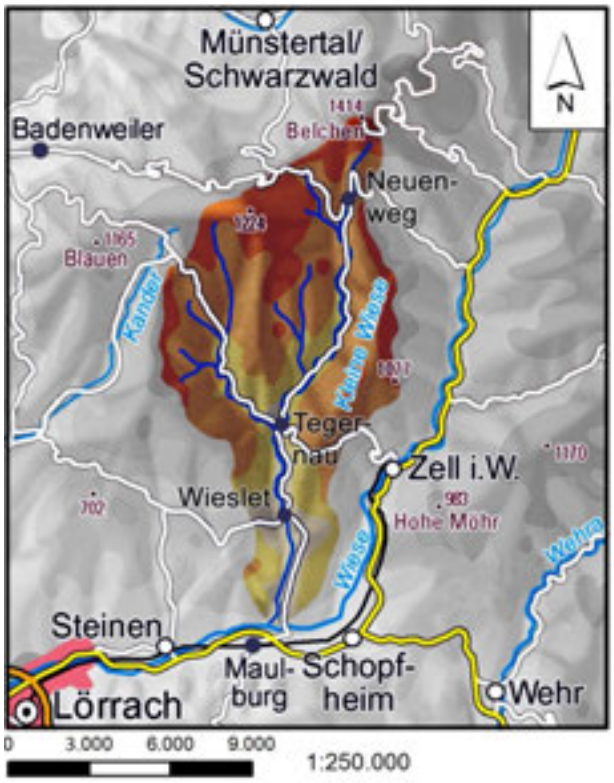

Figure 1: Catchment area and tributaries of the 'Kleine Wiese'(modified acc. to the automated real estate map (ALK) stand 12.10.2012)

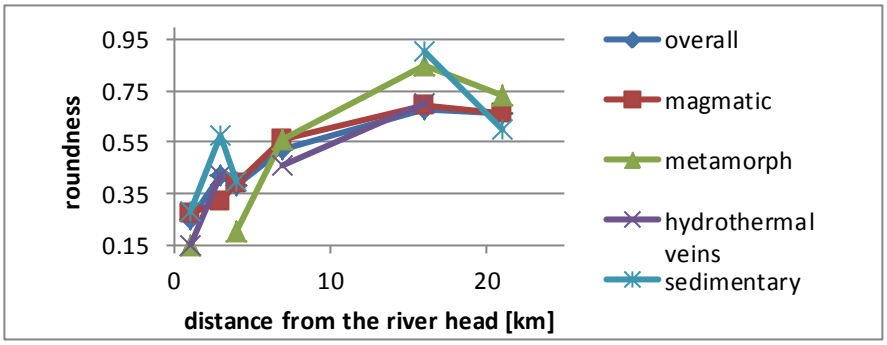

Figure 2: Diagram showing increasing roundness of gravel samples with distance to the riverhead

REFERENCES

Krumbein W.C., and Sloss L.L. 1963: Stratigraphy and Sedimentation. Freeman, San Francisco, 660 pp. Landesamt für Geoinformation und Landentwicklung Baden Württemberg automated real estate map (ALK) Stand: 12.10.2012

Metz & Rein 1957: Geologisch-petrographische Übersichtskarte des Südschwarzwaldes Massstab 1:50'000.

3. Magma fluxes and their effect on crustal growth, magma chemistry and dynamics of volcanic eruptions

Olivier Bachmann, Luca Caricchi

TALKS:

3.1 Bagheri G., Rossi E., Bonadonna C.: Aggregation of Volcanic Particles: Physical Constraints Provided by Field and Numerical Investigations

3.2 Hauser, A., Bussy, F.: Mechanism for development of fine-scale rhythmic magmatic layering in the centre of an incrementally built complex (Punta Falcone, Sardinia)

3.3 Leuthold, J., Blundy, J.D.: Cr-Spinel as an Indicator of Cumulates Partial Melting and Liquid Hybridization

3.4 Reubi, O., Cooper, L., Dungan, M.D., Bourdon, B.: ^{226}Ra-^{230}Th disequilibria in magmas from Llaima and Lonquimay volcanoes, Chile: On the roles and rates of subvolcanic magmatic processes.

3.5 Rochat L., Pilet S., Abe N.: Garnet Xenocryst In a Petit Spot Lava: Recycling Or Direct Formation In Oceanic Lithosphere?

3.6 Tornare E., Bussy F., Pilet S.: Magma differentiation during magma rise in the plumbing system of an ocean island volcano, Fuerteventura, Canary Islands

POSTERS:

P 3.1 Bakker R., Lupi M., Frehner M.: Effects of rapid icecap melting on a shallow magma chamber: A multi-discplinary case study of Snæfellsjökull volcano, Western Iceland

P 3.2 Bellver-Baca M.-T., Chiaradia M., Beate B.: Magmatic and time-scale factors controlling the association of porphyry type-deposits with high Sr/Y magmas

P 3.3 Caricchi, L., Simspon, G., Schaltegger, U.: Magma Fluxes and the long-term chemical evolution of magmatic systems

P 3.4 Chabbey B., Rapin T., Pilet S.: Petrological Evolution of Fogo island (Cape-Verde)

P 3.5 Dominguez L., PioliL., Bonadonna C., Connor C.B.: Dynamics of Volcanic Pulsatory Activity

P 3.6 Guinand A., Caricchi L.: Relationship between magma chemistry and eruptive dynamica at selected eruption of Cotopaxi volcano

P 3.7 Hartung E., Caricchi L., Floess D., Wallis S., Harayama S.: Melt segregation and assembly of the youngest exposed magma chamber in the world: Takidani Pluton (Japan)

P 3.8 Hunziker D., Burg J.-P., von Quadt A.: Early Cretaceous MORB-type to Late Cretaceous subduction-related magmatism recorded in the geochemical variability of lavas, North Makran Ophiolites, SE Iran

P 3.9 Régnier A., Caricchi L., Londoño J-M., Mendez R.: Cerro Machin a highly explosive volcano showing signs of unrest

P 3.10 Ricchi E., Caricchi L., Bindeman I., Wotzlaw J.: Duration of Volcanic Unrest Preceding a Super-Eruption

P 3.11 Schmid R., Franz L., Rahn M., Gautheron C., de Capitani C.: Petrography and geochronology of phonolites of the Hegau volcanic field, SW Germany

P 3.12 Stoppa L., Kutterolf S., Rausch J., Grobéty B.: Tephra chronostratigraphy of the Malpaisillo Volcanic Complex (central-western Nicaragua)

3.1

Aggregation of Volcanic Particles: Physical Constraints Provided by Field and Numerical Investigations

Gholamhossein Bagheri[1], Eduardo Rossi[1], Costanza Bonadonna[1]

[1] *Départment de Minéralogie, University of Geneva, Rue de Maraîchaire 13, CH-1205 Genève (gholamhossein.bagheri@unige.ch)*

The characterization and parameterization of both sedimentation and aggregation of volcanic particles is necessary for an accurate description of the sink term in numerical models of tephra dispersal used for the evaluation of tephra hazards. Nonetheless, our understanding of particle fallout in various eruptive and atmospheric conditions is still limited mostly due to the lack of direct observations. A comparative investigation of sedimentation and aggregation of volcanic particles is here presented based on field experiments and numerical simulations. Field experiments are based on detailed observations of particle fallout during Vulcanian explosions and ash emissions at Sakurajima volcano (Japan) on August 3, 2013. Column height was up to about 3 km above sea level and the cloud spread with average velocity of about 7 ms-1 toward southeast direction. Aggregates that fell at a distance of about 4 km from the vent were filmed with a high-speed and high-resolution camera before depositing on collection glasses. In order to preserve and analyze particle aggregates with the Scanning Electron Microscope, collecting glasses were covered with a special adhesive tape. Dedicated trays were also used to collect the depositing tephra at five-minute intervals to investigate both accumulation rate and particle size. CILAS grain size analysis showed that mode of particles deposited on the ground decreased with time from 550 µm to 250 µm at the reference location. Aggregate size ranged between 400 and 900 µm (based on video analysis) and they mostly consist of a single or multiple particles acting as nuclei with diameter between 200 and 800 µm coated with ash particles (<90 µm). Also aggregate size decreased with time during fallout and aggregate typology changed from mostly coated particles to ash clusters. Aggregation significantly affected particle residence time in the spreading cloud by changing the associated settling velocity. Based on numerical constraints, aggregates were thought to be formed within the rising plume or at the corner with the horizontal cloud and within 200 seconds of the onset of the eruption.

3.2

Mechanism for development of fine-scale rhythmic magmatic layering in the centre of an incrementally built complex (Punta Falcone, Sardinia)

Anne-Cécile Hauser[1], François Bussy[1]

[1] *Institut des Sciences de la Terre, University of Lausanne, Géopolis, CH-1015 Lausanne (anne-cecile.hauser@unil.ch)*

The gabbroic complex of Punta Falcone has a prominent vertical structure due to incremental emplacement of 5-6 magma pulses of 20-60 m thickness. Its symmetrical geometry and the nature of contacts between the different cooling units show that the outer units where emplaced first and that new injections took place in the centre of pre-existing units. One of the latest units in the centre of the intrusion shows vertical centimetre-scale rhythmic magmatic layering. Layering is roughly parallel to the contacts between the different units and diminishes in intensity from the borders of the unit inwards while its spacing remains constant (2.5 – 3 cm).

The liquidus phase, a high-An plg (An_{80-90}), occurs in both dark and white layers and shows no preferred orientation. Pyroxene and amphibole crystallizing after plg are present only in the dark layers, whereas late minerals (plg-rims of about An_{50} and interstitial qtz) are present only in the white layers. Px and amph have the same textures: they form up to 1cm big poikilitic grains enclosing the early euhedral high-An plg cores. Rare, somewhat more evolved borders on plg cores included in mafic phases occur towards the border of the latter. Plg crystals half-included in mafic phases have An_{50} rims only on the outside. Amph show a wide range of composition: some of them formed peritectically, others crystallized directly from the liquid. These chemical and textural observations indicate that px and amph crystallize at about the same time, rapidly and over a small T-interval. This leads to an increase in crystallinity by about 30 vol%, locks up the system and is thus the crucial moment for the development of layering.

We propose that after emplacement of the plg-bearing magma a first dark layer forms by rapid nucleation and crystallization of pyroxenes and amphiboles along a well-defined temperature plane. This leads to the development of a depleted zone next to it in which nucleation and further crystallization of mafic minerals is suppressed and which will eventually form a white layer. As cooling proceeds to a still un-depleted part, the cycle begins again and a new dark layer forms.

The constant spacing of layering from the borders inwards requires a regularly advancing temperature front. Numerical thermal modelling shows that this is possible thanks to preheating of the system by injection of the earlier magma pulses and the important amount of latent heat supplied during crystallization of the mafic phases. Preheating of the system also below emplacement level allows for the absence of nuclei of pyroxene and amphibole before injection. Decrease in intensity of layering is probably due to the flattening of the thermal gradient and the resultant widening of the zone comprised in the temperature interval in which pyroxene and amphibole crystallize.

3.3

Cr-Spinel as an Indicator of Cumulates Partial Melting and Liquid Hybridization

Julien Leuthold[1], Jon D. Blundy[1]

[1] *School of Earth Sciences, University of Bristol, BS8 1RJ Bristol, United Kingdom (julien.leuthold@bristol.ac.uk)*

The Rum Layered Intrusion (Scotland) was emplaced 60.53 ± 0.08 Ma ago (Hamilton et al. 1998), in response to the proto-Iceland plume (Saunders et al. 1997). The Unit 9 gabbro cumulates were successively intruded by olivine-phyric picritic sills. Reactive liquid flow produced clinopyroxene-poor gabbro, troctolite and dunite restite, and expelled melt crystallized to form gabbro with poikilitic clinopyroxene and Cr-spinel-rich anorthosite (Leuthold et al. 2014). The Cr-spinel origin is strongly debated (e.g. O'Driscoll et al. 2009).

We have run one atmosphere, fO_2-controlled equilibrium experiments of the Rum parental picritic parental liquid (Upton et al. 2002). At NNO-0.8 conditions, Cr- spinel saturates from 1360°C, olivine from ~1330°C, plagioclase from 1240°C and clinopyroxene from 1220°C, systematically ~40°C above MELTS calculations. Natural Cr- spinel grains have a higher Cr/(Cr+Al+Fe^{3+}) ratio (~0.51 to 0.03) than grains crystallized along the picrite NNO-0.8 liquid line of descent (0.38 to 0.06). Fe^{3+}-rich spinel is abundant (~1 vol%) at NNO+1, and Al-rich spinel occurs as trace at NNO-3. In picrite-troctolite hybrid experiments, plagioclase (~An86) saturates from 1280°C and clinopyroxene from 1200°C. Al- spinel crystallizes at high temperature, and gets more Cr-rich upon cooling, reaching the highest measured Cr/(Cr+Al+Fe^{3+}) ratio of ~0.44 at 1225°C, falling to 0.09 at 1200°C. Plagioclase and clinopyroxene stability plays a major role in spinel composition. Increasing the pressure or the parental magma water content would delay plagioclase saturation and result in spinel with lower Cr/Al ratio.

We deduce that Unit 9 peridotite, troctolite, anorthosite and also gabbro and poikilitic gabbro Cr-rich spinel did not crystallize from the Rum parental picritic liquid. Instead, they crystallized from a hybrid liquid produced by the mixing of invading picritic liquid with a partially molten plagioclase ± clinopyroxene-rich cumulate, leaving an olivine-rich residue/cumulate.

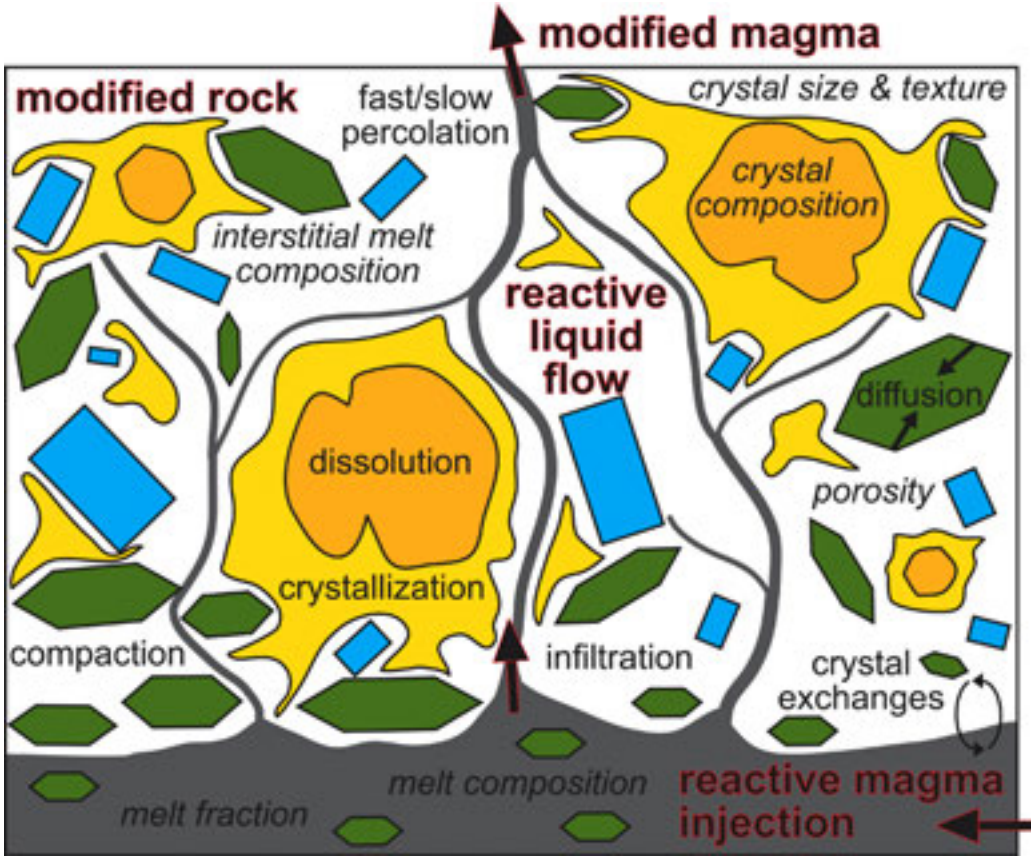

Figure 1. Schematic representation of the various effects of 'reative liquid flow' process that might occur in a crystal mush, in response to the migration of chemically and/or physically distinct magma. See Leuthold et al. (2014) for details.

REFERENCES

Hamilton, M.A., Pearson, D.G., Thompson, R.N., Kelly, S.P. & Emeleus, C.H. 1998: Rapid eruption of Skye lavas inferred from precise U-Pb and Ar-Ar dating of the Rum and Cuillin plutonic complexes, Nature, 394, 260-263.

Leuthold, J., Blundy, J.D., Holness M.B. & Sides, R. 2014: Successive episodes of reactive liquid flow through a layered intrusion (Unit 9, Rum Eastern Layered Series, Scotland), Contributions to Mineralogy and Petrology, 167:1021.

O'Driscoll, B., Donaldson, C.H., Daly, J.S. & Emeleus, C.H. 2009: The roles of melt infiltration and cumulate assimilation in the formation of anorthosite and a Cr-Spl seam in the Rum Eastern Layered Intrusion, NW Scotland; Lithos, 111, 6-20.

Saunders, A.D., Fitton, J.G., Kerr, A.C., Norry, M.J. & Kent, R.W., 1997: The North Atlantic igneous province. In Mahoney, J.J. & Coffin, M.F. (ed) Large igneous provinces: Continental, oceanic, and planetary flood volcanism, American Geophysical Union, Washington, 45-93.

Upton, B.G.J., Skovgaard, A.C., McClurg, J., Kirstein, L., Cheadle, M. & Emeleus, C.H., Wadsworth W.J., Fallick A.E. 2002: Picritic magmas and the Rum ultramafic complex, Scotland; Geological Magazine, 139, 437-452.

3.4

^{226}Ra-^{230}Th disequilibria in magmas from Llaima and Lonquimay volcanoes, Chile: On the roles and rates of subvolcanic magmatic processes.

Olivier Reubi[1], Lauren Cooper[2], Mike Dungan[3], Bernard Bourdon[4]

[1] *Inst. des Sciences de la Terre, Université de Lausanne, Switzerland*
[2] *Inst. of Geochemistry and Petrology, ETH Zurich, Switzerland*
[3] *Dept. of Geological Sciences, University of Oregon, USA;*
[4] *Laboratoire de Géologie de Lyon, Ecole Normale Supérieure de Lyon, France.*

^{226}Ra excesses in mafic arc magmas are generally attributed to recent (< 8 kyr) addition of slab-fluid to the mantle wedge and/or mantle melting. Preservation of ^{226}Ra-^{230}Th disequilibria from such sources requires short crustal residence times (<< 8 kyr) for these magmas. The correlation between ^{226}Ra excesses and ^{10}Be/Be previously observed for magmas from the Chilean Southern Volcanic Zone (SVZ) contributed to the view that recent slab-fluid additions causes ^{226}Ra excesses in arc magmas[1]. Our extensive dataset for Llaima (n=28) and Lonquimay (n=7) volcanoes (SVZ) shows variations in (^{226}Ra/^{230}Th) for each volcano, and in some cases within single eruptions. These variations span almost the entire SVZ range, thus questioning the pertinence of mantle-derived (^{226}Ra-^{230}Th) models.

Llaima and Lonquimay volcanoes differ in terms of their petrology and magmatic evolution. Llaima magmas (51 to 55 wt% SiO_2) are predominantly crystal-rich and carry conspicuous evidence for magma mixing and AFC processes. ^{238}U and ^{231}Pa excesses and incompatible trace element ratios are correlated and can be accounted for by up to 20% assimilation of basement plutonic rocks[2]. Crustal contamination had a secondary influence on ^{226}Ra-^{230}Th disequilibria. Magmas with the highest AFC contribution have ^{226}Ra-^{230}Th close to equilibrium, implying that (^{226}Ra-^{230}Th) are mostly affected by either differentiation on time scales of ~8 kyr, or more likely, mixing with mush bodies >8 kyr old. The relative influence of crustal assimilation and fractional crystallization varies from flow to flow, suggesting a spatial control and implying that the subvolcanic magmatic system comprises distinct magma pathways in which the magma residence time and injection rates vary significantly.

Lonquimay magmas (52 to 64 wt% SiO_2) are crystal-poor. Their evolution was controlled by fractional crystallization with limited crustal contamination. (^{226}Ra-^{230}Th) ranges from moderate ^{226}Ra excesses to small deficits, and are negatively correlated with Ba/Th and MgO. These observations are difficult to reconcile with only slab-fluid addition and mantle melting. We posit that this (^{226}Ra-^{230}Th) range results from diffusive Ra-exchange between young recharge melts and a old crystal mush bodies in the conduit system. A process further suggested by the ^{238}U-^{230}Th ages of the few crystals present that outdate the relative U-series ages of the melts by tens of kyr[3]. The time scale of differentiation (to 63 wt% SiO_2) is constrained by the ^{231}Pa and ^{226}Ra excesses to be <5 kyr.

(^{226}Ra-^{230}Th) in historical magmas at Llaima and Lonquimay reflect modification of mantle-derived signatures by open-system magmatic processes in the crust. The U-series dataset nevertheless provides valuable constraints on the maximal duration of the magmatic processes at play. Preservation of ^{226}Ra excesses in erupted magmas still requires the time span between mantle melting and eruption, including the time scale of differentiation, to be several kyr, at most, for some magma batches. However, the residence times of magma batches and crystals in the subvolcanic magmatic system is commonly in the tens of kyr range. This suggests that these magmatic systems are characterized by relatively short residence and differentiation times in the lower crust and frequent interaction between young recharge melts and older crystal-rich magmas or mush bodies in the upper crust.

REFERENCES

1 Sigmarsson et al., 2002, Earth and Planet. Sc. Lett. 196, 189-196.
2 Reubi et al., 2011, Earth and Planet. Sc. Lett. 303, 37-47.
3 Zellmer e al., 2014, GSL special publication 385, 185-208.

3.5

Garnet Xenocryst in a Petit Spot Lava: Recycling or Direct Formation in Oceanic Lithosphere?

L. Rochat[1], S. Pilet[1], N. Abe[2]

[1] Institute of Earth Science, University of Lausanne, CH-1015 Lausanne.
[2] Jamstec, Yokosuka-city, Kanagawa 237-0061, Japan.

Xenoliths and xenocrysts present in *petit spot* lavas can provide information on the nature and processes occurring in the oceanic lithosphere. *Petit spot* volcanoes have been discovered on the undergoing Pacific plate east of Japan and represent small-scale seamounts formed by the extraction of low-degree melts from the base of the lithosphere in response to plate flexure and/or crack propagation (*1-3*). Here, we report the discovery of a garnet xenocryst present in a petit spot sample from east of Japan. The xenocryst is pyrope-rich (Py_{60}, Gr_{20}, Al_{16}), has low Cr (0.07-0.21) and Ti (0.06-0.17) contents, depleted LREE, a slight positive Eu anomaly and flat HREE with primitive mantle normalized values of around one.

The presence of garnet xenocryst in petit spot lavas can be explained as a disaggregated garnet-peridotite coming from the oceanic lithosphere. But, such garnet should have higher Mg# and Cr content than observed in our sample. Garnet in oceanic lithosphere could also be linked to the presence of garnet-pyroxenite. Mantle pyroxenite as xenoliths are frequently interpreted as subducted oceanic crust (eclogite). Although we cannot exclude this hypothesis, the presence of eclogite in the Pacific oceanic lithosphere, at petit spot emplacement, would require long transport time without melting at the mid-oceanic ridge. In addition, the pyrope content of the xenocryst is relatively high and the HREE are low compared to garnet from typical eclogites.

Garnet-pyroxenite could also form by direct crystallization from a melt percolating through the lithosphere. However, the REE pattern of the garnet xenocryst excludes direct crystallization from a basaltic melt. We hypothesize, in order to explain the major and trace element composition of this garnet, that it is formed by subsolidus reaction of ol-pl-cpx cumulates during the cooling of the lithosphere at constant pressure (~1-1.5 GPa). This cumulate is interpreted to have formed during the percolation and differentiation of basaltic melts in the periphery of a mid-oceanic ridge. The presence of this garnet xenocryst supports the hypothesis that oceanic lithosphere is re-enriched by metasomatic processes in periphery of mid-ocean ridges (4-7).

REFERENCES

1. N. Hirano et al., Volcanism in response to plate flexure. Science 313, 1426 (2006).
2. G. A. Valentine, N. Hirano, Mechanisms of low-flux intraplate volcanic fields-Basin and Range (North America) and northwest Pacific Ocean. Geology 38, 55 (2010).
3. D. M. Buchs et al., Low-volume intraplate volcanism in the Early/Middle Jurassic Pacific basin documented by accreted sequences in Costa Rica. Geochemistry Geophysics Geosystems 14, 1552 (2013).
4 A. N. Halliday et al., Incompatible Trace-Elements in Oib and Morb and Source Enrichment in the Sub-Oceanic Mantle. 133, 379 (1995).
5. G. N. Hanson, Geochemical evolution of the suboceanic mantle. J. Geol. Soc. Lond. 134, 235 (1977).
6. Y. L. Niu, M. J. O'Hara, Origin of ocean island basalts: A new perspective from petrology, geochemistry, and mineral physics considerations. J. Geophys. Res.-Solid Earth 108, (2003).
7. S. Pilet, M. B. Baker, O. Muntener, E. M. Stolper, Monte Carlo Simulations of Metasomatic Enrichment in the Lithosphere and Implications for the Source of Alkaline Basalts. Journal of Petrology 52, 1415 (2011)

3.6

Magma differentiation during magma rise in the plumbing system of an ocean island volcano, Fuerteventura, Canary Islands.

Tornare Evelyne[1], Bussy François[1], Pilet Sébastien[1]

[1] *Institut des Sciences de la Terre, Géopolis, University of Lausanne, CH-1015 Lausanne, Switzerland*

In volcanic settings magmas are usually thought to travel through the crust along vertical dikes or channels with potential stagnation stages in magmatic reservoirs like sills. Magma differenciation and mixing processes are considered to occur mainly during stagnation stages. Here we consider differentiation processes to occur mainly in vertical dikes or crystal-rich channels during magma ascent as illustrated by a clinopyroxenite intrusion (PX1) in the root zone of an eroded ocean island volcano.

PX1 is composed of gabbros and clinopyroxenites which are almost all cumulative. The mafic host-rock of PX1 shows evidences for a very intense contact metamorphism leading to partial melting (ca. 1000°C, Hobson *et al.*, 1998). This records a high heat flux which required a sustained melt flux over a long time. Field observations show vertical layering at all scales, from pluton to outcrop to thin section scale. This cumulative body doesn't represent a shallow level, long-lived and convective magma chamber, but a zone of metre to decametre-scale melt channels, through which magma travelled.

Many clinopyroxenites are characterized by a coarse-grained texture and crystal zoning. Resorbed features and reverse rim zoning are interpreted as evidence of percolation of successive magma pulses through a clinopyroxenitic mush, which led to crystal coarsening.

We interpret the coarse-grained clinopyroxenites as crystal-rich magma channels, through which sustained magma fluxes travelled to the surface over a long period of time, thus generating the contact aureole. On the other hand, gabbro bands are interpreted as sluggish magma pulses emplaced in a cooler environment during the waning stages of magmatic activity.
We propose a model of magma differentiation by dynamic fractionation during magma ascent in vertical channels. This model assumes fractional crystallization of continuously rising magmas all along their way to the surface through phenocryst accumulation and crystal-melt interaction processes. This model suggests a new hypothesis to understand the plumbing system of basaltic volcanoes and open perspective to explain the generation of cumulatives lavas.

REFERENCES

Hobson, A., Bussy, F., Hernandez J. 1998: Shallow-Level Migmatization of Gabbros in a Metamorphic Contact Aureole, Fuerteventura Basal Complex, Canary Islands, Journal of Petrology, 39, 1025-1037.

P 3.1

Effects of rapid icecap melting on a shallow magma chamber: A multi-discplinary case study of Snæfellsjökull volcano, Western Iceland

Richard Bakker[1], Matteo Lupi[1], Marcel Frehner[1]

[1] *ETH Zürich, ERDW, Geological Institute, Sonneggstrasse 5, CH-8092*

The most dramatic effect of global warming is the water level rise due to rapid melting of ice sheets. However, recent studies suggest that accelerated glacial retreat and associated viscoelastic relaxation of the mantle may enhance upwelling of magmatic fluids through the litoshpere (e.g. Hooper et al., 2011). Here, we investigate whether, also at short geological timescales, shallow magmatic systems may be affected by rapid melting of ice caps. As a case study, we chose the Snæfellsjökull volcanic system in western Iceland, whose ice cap is rapidly melting with 1.25 $m_{w.e./}$year (Jóhannesson et al., 2011). To investigate the role of deglaciation in promoting volcanic unrest we use a cross-disciplinary approach integrating geophysical field data, laboratory rheological rock tests, and numerical finite-element analysis.

Initial results from seismic data acquisition and interpretation in 2011 show seismic activity (occasionally in swarm sequences) at around a depth range of 8–13 km (Fuchs et al., 2013), indicating the presence of a magmatic reservoir in the crust. In addition, a temporary seismic network of 21 broad-band stations has been deployed in spring 2013 and continuously collected data for several months, which will help better constrain the subsurface geometry.

During summer 2013 we collected samples of Tertiary basaltic bedrock from the flanks of Snæfellsjökull, which we assume to be representative for the subsurface volcanic system. Cores drilled from these samples were tri-axially deformed in a Paterson-type apparatus at a constant strain rate of 10^{-5} s^{-1}, a confining pressure of 50 MPa (i.e., ~2 km depth), and a temperature ranging from 200 °C to 1000 °C (i.e., various proximities to magma chamber). We observe a brittle ductile transition between 800 and 900 ˚C. From the obtained stress-strain curves the static Young's modulus is calculated to be around 35 (±2) GPa, which is not significantly influenced by increasing temperatures up to 800 °C. Beyond the elastic domain, cataclastic shear bands develop, accommodating up to 7% strain before brittle failure. In the ductile cases we observe a gradual hardening after an intial elastic phase.

The subsurface geometrical constraints from geophysical field data and the rheological parameters from laboratory testing are fed into a numerical finite-element model solving for the pressure in the magma chamber and the stress field in the surrounding basement rock before and after the retreat of an assumed 200 m thick ice cap. Preliminary results (see figure 1) show that ice unloading has two effects. First, it leads to significant stress release at shallow depths in the volcanic edifice, possibly resulting in a destabilization of the flanks, which in turn leads to further unloading of the volcanic cone by means of landslides. Second, the pressure change around the magma chamber is in the order of 0.5 MPa. This may be sufficient to induce volatile exsolution and accelerated pressurization of the magmatic reservoir, ultimately leading volcanic unrest, in particular in critically stressed environments prior to glacial retreat.

We point out ice cap melting as a possible mechanism for triggering volcanic unrest of shallow magmatic systems.

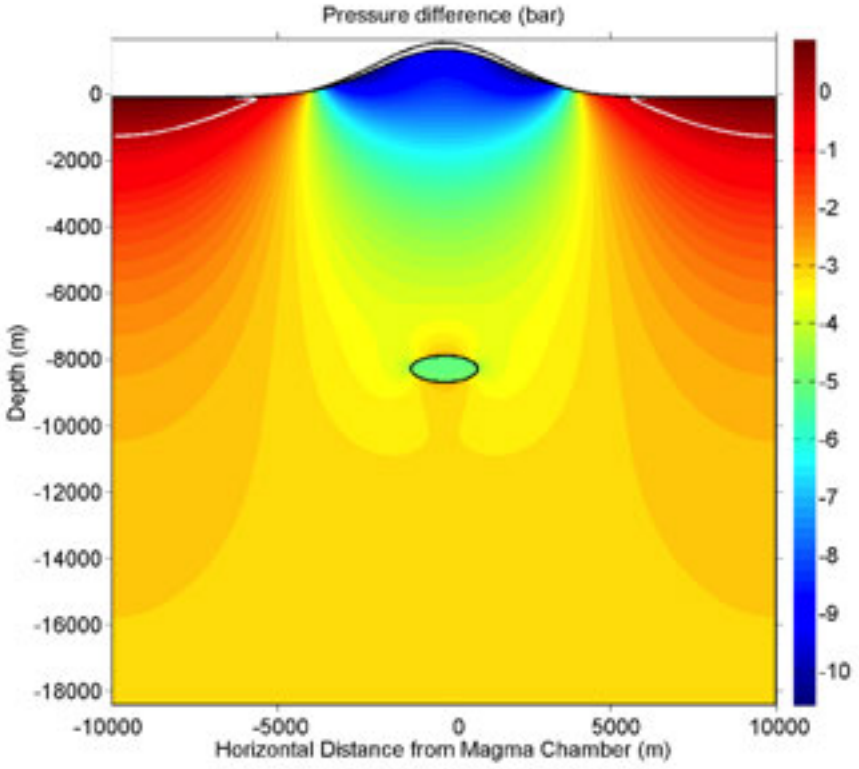

Figure 1. Calculated pressure difference inside the volcanic edifice. The white line illustrates the where the pressure difference is zero.

REFERENCES

Fuchs, F., Lupi, M., Jakobsdóttir, S.S., Thordarson, T., & Miller, S.A., 2013: Seismicity observed under the Snæfellsjökull volcano, JÖKULL No. 63, 105-112

Hooper, A., Ófeigsson, *B.*, Sigmundsson, F.,Lund, B., Einarsson, P., Geirsson, *H.* & Sturkell, E. 2011:, Increased capture of magma in the crust promoted by ice-cap retreat in Iceland, Nature Geoscience, Vol. 4, 783–786.

Jóhannesson, T., Björnsson, H., Pálsson, F., Sigurðsson, O. &Þorsteinsson, Þ. 2011: LiDAR mapping of the Snæfellsjökull ice cap, western Iceland. JÖKULL No. 61, 19-32

P 3.2

Magmatic and time-scale factors controlling the association of porphyry type-deposits with high Sr/Y magmas

María Teresa Bellver-Baca[1], Massimo Chiaradia[1], Bernardo Beate[2]

[1] *Earth and Environmental Sciences Section, Faculty of Sciences, Geneva University. Rue des Maraîchers 13 – 1205 Geneva – Switzerland. (MariaTeresa.BellverBaca@unige.ch; Massimo.Chiaradia@unige.ch)*
[2] *Departamento de Geología, Escuela Politécnica Nacional, Quito, Ecuador.*

Porphyry systems (including porphyry deposits *sensu stricto*, skarn, carbonate-replacement deposits and high and intermediate sulfidation epithermal deposits) supply most of the copper and significant gold to our economy (Sillitoe, 2010). During the last 20 years detailed petrological and geochemical studies have shown that high Sr/Y magmas, also known as adakite-like magmas, play an important role to form giant Cu-Au porphyry mineralisation (Thièblemont et al., 1997; Cooke et al., 2005; Chiaradia et al., 2009; Richards, 2011).

Adakite-like magmas are characterized by high Sr/Y (>40) and La/Yb (>20) ratios (induced by crystal fractionation of amphibole±garnet and suppression of plagioclase fractionation), high water (> 4 wt.%) and S contents (> 1000 ppm). The Ce^{4+}/Ce^{3+} ratios in zircons associated with these magmas indicate, together with amphibole compositions, high oxygen fugacities (>FMQ), increasing with time and reaching peak values at the mineralisation time (Chelle-Michou, 2014). Adakite-like rocks associated with porphyry-type deposits are most likely formed by mid- to lower crustal magmatic processes (crystal fractionation of amphibole, clinopyroxene±garnet, magma recharge and mixing, partial melting and assimilation) during compressive events leading to crustal thickening (e.g., Chiaradia et al., 2009, Richards, 2011). These magmatic processes last several millions of years (>1-6 Ma) during which magmas display a systematic transition from non-adakitic to adakite-like signatures (e.g., Yanacocha, Peru; El Teniente and Los Pelambres, Chile; Coroccohuayco and Antapaccay, Peru; Altar, Argentina). In this context, porphyry systems occur in the final stages of such magmatic cycles in association with the high Sr/Y (adakite-like) signatures.

In contrast, magmatic cycles with a similar systematic increase of Sr/Y values through a much shorter time of few hundreds of thousands of years are apparently barren.

It would seem therefore that the time factor, coupled with the high-pressure (mid-crustal) magmatic evolution, plays a prominent role in the association of high Sr/Y magmatic rocks with major porphyry systems. In the frame of the current project we will investigate in detail the role of the time factor in the generation of magmatic systems favourable to the formation of porphyry systems through the comparison of two systems with a similar increase of Sr/Y ratios through different timescales (Fig. 1 a, b): the ~6 Ma long magmatic system of the Yanacocha district (northern Peru), associated with world-class high sulfidation Au-Cu mineralization, and the ~0.4 Ma long barren Chachimbiro complex (northern Ecuador). Systematic whole rock and mineral chemistry investigations on the two systems accompanied by radiometric dating (U-Pb in zircon, $^{40}Ar/^{39}Ar$ on amphibole and biotite, and ^{14}C on wood remains of pyroclastic flows) will allow us to reconstruct a detailed temporal geochemical and petrological evolution of the two systems which will be the basis for understanding similarities and differences between them and to formulate detailed hypotheses about the role of the length of magmatic cycles in the generation of major porphyry-type deposits.

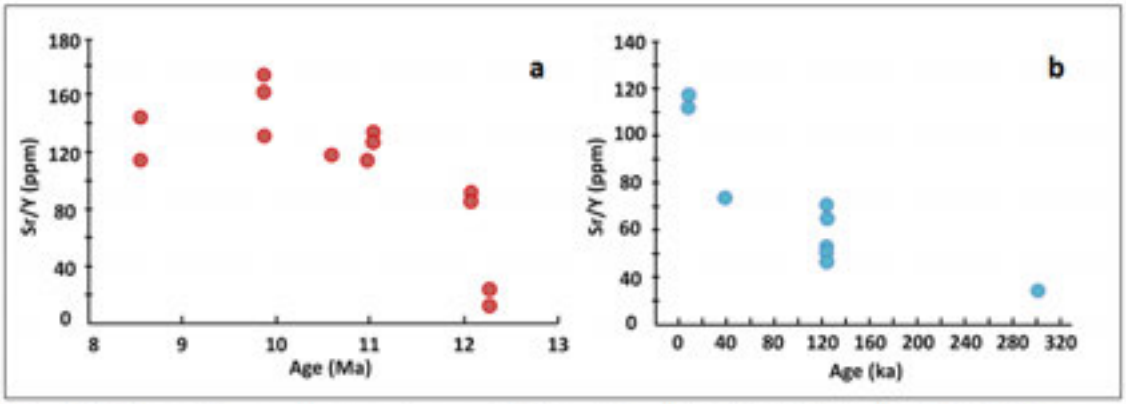

Fig 1. Sr/Y variations with respect age in Yanacocha district (a) (Chiaradia et al., 2009) and Chachimbiro complex (b) (Chiaradia, unpublished data).

REFERENCES
Chelle-Michou, C. 2014: Geochronologic and Petrologic Evolution of the Magmatic Suite Associated with the Eocene Coroccohuayco Deposit, and its Role in the Genesis of the Associated Cu(-Au) Porphyry-skarn Mineralization, Timtaya District, Peru. Terre et Environnement, 127, 192 pp. ISBN 978-2-940472-28-4.
Chiaradia, M., Merino, D., Spikings, R. 2009: Rapid transition to long-lived deep crustal magmatic maturation and the formation of giant porphyry-related mineralization (Yanacocha, Peru). Earth and Planetary Science Letters, 288, 505-515.
Cooke, D., Hollings, P., Walshe, J.L. 2005: Giant porphyry deposits: characteristics, distribution, and tectonic controls. Economic Geology, 100, 801-818.
Richards, J.P. 2011: High Sr/Y arc magmas and porphyry Cu±Mo±Au deposits: just add water. Economic Geology 106, 1075-1081.
Thiéblemont D., Stein G, and Lescuyer J. L. 1997: Gisements épithermaux et porphyriques: la connection adakite. Comptes Rendus Acad.Sci. Paris 325,103-109.

P 3.3

Magma Fluxes and the long-term chemical evolution of magmatic systems

Luca Caricchi[1], Guy Simspon[1], Urs Schaltegger[1]

[1] *Section of Earth and Environmental Sciences, University of Geneva, Rue de Maraîchaire 13, CH-1205 Genève*

Magmatic reservoirs that feed explosive volcanic activity at the surface are constructed by the periodic injection of magma into the upper crust. The long-term magma flux controls the thermal evolution of these magmatic reservoirs and therefore the chemistry and physical characteristics of eruptible magma (<50vol.% crystals) present in subvolcanic magma chambers.

Using numerical modelling we explored the thermal evolution of magmatic systems characterised by different long-term magma fluxes. The calculations show that eruptions of rhyolitic compositions can only occur after a stage of prolonged thermal maturation of the magmatic reservoir (lasting a few hundredths of thousands of years). The probability of eruptions with rhyolitic compositions increases substantially once the injection of magma into the magmatic reservoir ceases, which would imply that rhyolitic eruptions (not produced by partial melting of continental crust) are most likely to occur during the waning (not waxing) stages of magmatic activity. These results can be applied to retrieve the long-term flux of magma in volcanic systems characterised by different trend of evolution of magma chemistry with time.

P 3.4

Petrological Evolution of Fogo island (Cape-Verde)

Benjamin Chabbey[1], Timothé Rapin[2], Sébastien Pilet[2]

[1] *Section of earth and enviromental sciences, Univesity of Geneva, Rue de Maraîchers 13, CH-1205 Genève (chabbeb0@etu.unige.ch)*
[2] *Institut of Earth Science, University of Lausanne, Geopolis, CH-1015 Lausanne*

The Cape-Verde oceanic islands, in the central Atlantic, are typical intraplate volcanism interpreted as a trace of a mantle plume. Constant volcanism activities have been observed there since over 17 Ma (Mitchell et al., 1983 ; Holm et al., 2008). The activity has migrated from East to West and is nowadays observed on the island of Fogo and Brava. The emitted magmas are characterized by alkali composition going from basanite to alkali basalt, which are enriched in Sodium and Potassium, and depleted in Silica.

Different studies based on Sr, Nd and Pb in the basaltic island of Cape-Verde has shown that the sources of the emitted magmas varies from an island to another (Escrig et al., 2005 ; Holm et al., 2006), and that for a given island those sources are composed of several mantle component. However, the size of those components and their spatial distribution in the mantle isn't constrained.

Two of the most often invoked processes proposed to explain the generation of alkali magmas are, on one hand, the fusion of peridotite/pyroxenite in presence of CO_2, and, on the other hand, the fusion of metasomatised lithospheric mantle (Herzberg, 2007 ; Pilet et al., 2008).

The caldera created by the collapse of the former Monte Amarello stratovolcano (Elsworth et al., 1999) on the island of Fogo exposed a 400 meters height cliff. This cliff represents a unique opportunity to study the variation of compositions of magmas emitted during a relatively constrained period of time. This should allow the investigation of the variability of the sources composition and their evolution during time.

Here, we report initial data on 95 alkaline lavas sampled on a cross section of this caldera trough a via ferrata. Most of the rocks show olivine + cpx phenocrysts in various proportion, amphibole are rare in opposite to recent eruption of Pico del Fogo which show abundant amphibole phenocrysts and megacrysts. The MgO content of the caldera lavas ranges from 3 to 14 wt. % while their SiO_2 content varies from 37 to 47 wt.%. Future analyses (trace-elements and mineral analyses) will allow to evaluate the cyclicity associated to alkaline volcano evolution and will allow to constrain the mechanism of differentiation. Radiogenic isotopes data will also be analysed on a selection of lava in order to evaluate the evolution of the sources and the potential role of the lithosphere.

REFERENCES

Herzberg (2007) Food fro a Volcanic Diet, Science 316 : 378-379.

Escrig, S., Doucelance, R., Moreira, M. and Allegre, C.J., 2005. Os isotope systematics in Fogo Island: Evidence for lower continental crust fragments under the Cape Verde southern islands. Chem. Geol. 219: 93-113.

Holm, P.M. et al., 2008. An Ar-40-Ar-39 study of the Cape Verde hot spot: Temporal evolution in a semistationary plate environment. J. Geophys. Res. 113: B08201

Holm, P.M. et al., 2006. Sampling the cape verde mantle plume: Evolution of melt compositions on Santo Antao, Cape Verde Islands. J. Petrol. 47: 145-189.

Pilet, S., Baker, M.B. and Stolper, E.M., 2008. Metasomatized lithosphere and the origin of alkaline lavas. Science 320: 916-919.

Elsworth, D., Day, S.J., 1999. Flank collapse triggered by intrusion: the Canarian and Cape Verde Archipelagoes. Journal of Volcanology and Geothermal Research 94: 323-340.

P 3.5

Dynamics of Volcanic Pulsatory Activity

Lucia Dominguez[1], Laura Pioli[1], Costanza Bonadonna[1] & Charles B Connor[2]

[1] *Département de Sciences de la Terre, Université de Genève, Rue de Maraîchers 13, CH – 1025 (Lucia.Dominguez@etu.unige.ch, Laura.Pioli@unige.ch, Costanza.Bonadonna@unige.ch)*
[2] *Departement of Geology, University of South Florida, 4202 E. Fowler Avenue, NES 107 Tampa, Fl 33620-5550 USA (cconnor@cas.usf.edu)*

Volcanoes are complex and dynamic systems controlled by the interaction of many processes, whose relations are often non-linear and stochastic. However, these complex systems are not unconstrained and eruptions can show systematic evolutionary trends as well as periodic behaviour which can be examined in terms of *failure time* through *duration analysis*, better know as survival analysis. In this study we focus on the dynamics of pulsatory explosive activity and analyse the unsteadiness of the time interval between single pulses of Strombolian, violent Strombolian and Vulcanian explosions. In particular, we focus on data for the explosive eruptions of Cerro Negro (Nicaragua, 1995), Eyjafjallajökull (Iceland, 2010), Etna (Italy, April and July 2012), Santiaguito (Guatemala, 2003), Sakurajima (Japan, 1973 to 1979 and 2009 to 2013) and Soufrière Hills (Montserrat, 1997 to 2010). The unsteady behaviour of these eruptive styles cannot be defined based on their deposits, as the time scale of periodicities cannot be quantified through the stratigraphic record. As a result, classification of eruption style based on the deposit features cannot capture the complexity of unsteady activity. Instead, we characterize the source dynamics based on a statistical analysis of the *repose interval*, its periodicity and distribution over time, which is viewed as the surface manifestation of system failure. The repose interval is defined as the time elapsed between the onsets of two consecutive pulses, during a certain period of one pulsating eruption. Dynamics of unsteady activity can be related to the frequency and regularity of the system based on the Log-logistic model which describes the processes controlling the probability of system failure as being due to competing processes at different time-scales, influencing the probability of explosion over time. Here we propose to correlate the Log-logistic parameters, μ and s, in terms of frequency and regularity of the system which are mainly controlled by the magma viscosity, permeability and fracture structures, magma feeding rate, plumbing system, vent opening, reservoir depth, conduit geometry and tectonic environment. We highlight the application of these relationships and the common features that can aid in the classification of pulsatory explosive activity based on source dynamics.

REFERENCES

Watt, S. F. L., Mather, T. A., & Pyle, D. M. 2007: Vulcanian explosions cycles: Patterns and Predictability. Geology, 35 (9): 839-842.

Varley, N., Johnson, J., Ruiz, M., Reyes, G., & Martin, K. 2006: Applying statistical analysis to understanding the dynamics of volcanic explosions. In Statistics in Volcanology, 57-76. Geological Society for IAVCEI.

Connor, C.B., Sparks, R.S.J., Mason, R. M., Bonadonna C., Young, S. R. 2003: Exploring links between physical and probabilistic models of volcanic eruptions: The Soufrière Hills volcano, Montserrat. Geophysical Research Letters, 30, 13, 1701.

P 3.6

Relationship between magma chemistry and eruptive dynamica at selected eruption of Cotopaxi volcano

Guinand A., Caricchi L.,

Cotopaxi, located in Ecuador, is one of the highest active volcanoes (5897m above sea level) in the world and one of the most dangerous in Ecuador. Four different eruptions (layer 5, 3, 2 and 1) for which the relationships between eruptive products and eruptive dynamics have been already investigated at the University of Geneva, were selected for this study. The target of this study is to establish the link between the eruptive dynamics and the petrological characteristics of the erupted products.

The products of the four eruptions were analyzed using X-ray fluorescence, electron microprobe, laser ablation inductively coupled Mass spectrometry to measure major and trace elements concentrations in whole rock and single minerals. Crystal size distribution and geochemical modeling, in combination with thermo-barometry were performed to identify the pre-eruptive processes and timescales for the four eruptions of interest. The eruptive products are basaltic-andestites and andesites (SiO_2 ~ 56-60 wt %). Major and trace elements vary within a very restricted range and the only deposit showing notable differences is layer 3 associated to the second eruptive event we studied.

The results suggest that the plumbing system of the volcano is composed of two magmatic reservoirs located at depth of about 30 and 15 km depth. Most of the fractionation of the products seems to occur in the deep-seated magma chamber and magmas spend about 40-50 years within the shallower reservoir before before erupting.

P 3.7

Melt segregation and assembly of the youngest exposed magma chamber in the world: Takidani Pluton (Japan)

Eva Hartung[1], Luca Caricchi[1], David Floess[1], Simon Wallis[2], Satoru Harayama[3]

[1] *Section of Earth and Environmental Sciences, University of Geneva, Rue de Maraîchers 13, CH-1205 Geneva (eva.hartung@unige.ch)*
[2] *Department of Earth and Planetary Science, University of Nagoya, Japan*
[3] *Department of Geology, Shinshu University, Matsumoto, Japan*

Segregation of residual melt from partially crystallized magmas is a process of paramount importance for the chemical evolution of magmas and the construction of reservoirs of potentially eruptible magma. In this study we investigate the Takidani pluton, one of the youngest exposed plutons on Earth (about 1Ma). This chemically zoned magmatic body is located within the active Norikura Volcanic Chain in the Northern Japan Alps and associated with large dacitic to rhyolitic deposits (Nyukawa Pyroclastic Flow Deposit and Ebisutoge-Fukuda tephra). Our study focuses on the physical processes responsible for the extraction of residual melt from a crystallizing magma and the construction of the subvolcanic reservoirs that fed large silicic eruptions.

Detailed structural mapping and sampling along four transects from the base to the top of the pluton were carried out along with a magnetic susceptibility survey. Our preliminary results indicate that the pluton was assembled by multiple intrusions. The pluton can be broadly separated into three distinct lithological units: 1) fine grained granite; 2) equigranular granodiorite that locally grades into either porphyritic granodiorite or granite towards the roof of the intrusion; and 3) mafic granodiorite. Units 1) and 2) form the core of the intrusion and together represent about 70% of the total volume of the pluton. Our results show that the equigranular granodiorite is internally inhomogeneous with felsic lenses of lower magnetic susceptibility. The magnetic susceptibility decreases gradually towards the roof of the pluton reaching its lowest value within leucrocratic porphyritic units. Higher magnetic susceptibility values at the contact with the roof correspond to a slightly more mafic porphyritic unit. Melt segregation and evolution of the Takidani Granodiorite are being further investigated using bulk rock and mineral chemistry (EMPA and LA-ICP-MS) together with anisotropy of magnetic susceptibility.

P 3.8

Early Cretaceous MORB-type to Late Cretaceous subduction-related magmatism recorded in the geochemical variability of lavas, North Makran Ophiolites, SE Iran

Daniela Hunziker[1], Jean-Pierre Burg[1], Albrecht von Quadt[2]

[1] *Geologisches Institut, ETH Zürich, Sonneggstrasse 5, CH-8092 Zürich (daniela.hunziker@ethz.ch)*
[2] *Institute for Geochemistry und Petrology, Clausiusstrasse 25, CH-8092 Zürich*

The North Makran Ophiolites represent a remnant of the Alpine-Himalayan Tethys Suture which is still scarcely known. Field observations combined with petrographical and geochemical investigations show a wide chemical and temporal range of lava types. 1) Tholeiitic lavas (older than 125Ma) are melt products of the ophiolitic diabases; their geochemistry suggests formation in a marginal basin; 2) alkaline lavas (older than Valanginian) spilled on an extensional continental margin; 3) alkaline to tholeiitic lavas (older than Barremian) unconformably covered the North Makran Ophiolites during further opening of the marginal basin; 4) Younger (Late Cretaceous) basaltic to andesitic lavas with Island Arc Tholeiite chemistry and Nb and Ta anomalies unconformably cover all previous rocks in an arc or fore-arc domain; 5) calc-alkaline basaltic to dacitic lavas associated with Late Cretaceous to Eocene deep sea sediments exposed in tectonic windows below the ophiolites.

These five lava types represent two major magmatic events: (i) Early Cretaceous continental rifting/ opening of a marginal basin (types 1, 2 and 3) and (ii) subduction in the Late Cretaceous and Eocene, when the North Makran marginal basin became part of the arc/fore-arc region (types 4 and 5). εNd(t) values change from 7.4 to 2.6; younger lavas correspond to lower values, which is related to a subduction component.

The chemical change in the lavas, coupled with the evolution of the deposition environment from deep sea to shallow water with time, record the geodynamic evolution of North Makran where marginal extension with MORB-type volcanism was followed by subduction related magmatism.

P 3.9

Cerro Machin a highly explosive volcano showing signs of unrest

Antoine Régnier[1], Luca Caricchi[1], John Makario Londoño[2], Ricardo Mendez[2]

[1] *Section of earth and enviromental sciences, Univesity of Geneva, Rue de Maraîchers 13, CH-1205 Genève*
[2] *Servicio geológico Colombiano, Avenida 12 de Octubre, Manizales, Colombia*

Cerro Machin is a volcano located in the central cordillera of Colombia, 17km from Ibague, where 500'000 people are living. This volcano has erupted at least 5 times during the last 10'000 years and each eruption has been classified plinian to ultraplinian with Volcanic Explosivity Index 5 (VEI 5, Thouret et al, 1995). Carbon dating on trees embedded in pyroclastic deposits indicates that eruptions occur with a recurrence rate of about 1000 years. The last eruption occurred ~900 years ago and in the last 15 years multiple monitoring parameters have highlighted the reactivation of this volcanic system (Mendez et al., 2002 ; Laegger et al., 2013).

Machin is a volcano with a 2.4km diameter caldera and 150m height pyroclastic rim. Two dacitic domes showing signs of fumarolic activity are present within the crater rim. However, no study has previously characterised the past activity of the volcano from a volcanological and petrological point of view. This knowledge is fundamental to determine the most likely eruption that will occur at Cerro Machin in the future. Essential for this is to determine the depth of the magma chamber, through the amphibole geobarometry, ascent rate and residence time of magma within the subvolcanic magma chamber using crystal size distribution on plagioclase. These parameters will potentially allow us to determine the time available between the escalation of the volcanic crisis and the eruption. The analyses of geophysical data collected with the currently present monitoring instrument permit to identify two zones with a high volcano-tectonic (VT) seismic activity, one at 3km under the vent and another one 20km depth at the south-east of Machin volcano. One of the goals of the project is to describe the general petrology of the eruptions and particularly the 3'600BP, which was the largest of the system. This work will be compared with the petrological study on the eruption of 15th June 1991 of Pinatubo, which has a similar dacitic composition to Cerro Machin (Scaillet & Evans, 1999).

REFERENCES

Laeger, K., Halama, R., Hansteen, T., Savov, I. P., Murcia, H. F., Cortés, G. P., & Garbeschönberg, D. (2013). Crystallization conditions and petrogenesis of the lava dome from the ~900 years BP eruption of Cerro Machin Volcano, Colombia. Journal of South American Earth Sciences, 48, 193-208.

Méendez, R. A. (2002). Evaluación de la amenaza volcánica potencial del Cerro Machin (departamento del Tolima, Colombia).

Scaillet, B., & Evans, B. W. (1999). The 15 June 1991 eruption of Mount Pinatubo. Phase equilibria and Pre-eruption P-T-fO_2-fH_2O conditions of the dacite magma. Journal of Petrology, 40(3), 381-411.

Thouret, J. C., Cantagrel, J-M., Robin, C., Murcia, A., Salinas, R., Cepeda, H. Quaternary eruptive history and hazard-zone model at Nevado del Tolima and Cerro Machin volcanoes, Journal of Volcanology and Geothermal research 66 (1-4), p. 397-426

P 3.10

Duration of Volcanic Unrest Preceding a Super-Eruption

Emmanuelle Ricchi1, Luca Caricchi1, Ilya Bindeman2, Joern Wotzlaw1

[1] *Section of Earth and Environmental Sciences, University of Geneva, Rue de Maraîchers 13, CH-1205 Genève (ricchi0@etu.unige.ch)*
[2] *Department of Geological Sciences, University of Oregon, Eugene, OR 97403-1272*

The Heise volcanic field is the most recent cycle of the volcanism associated to the Yellowstone hotspot track. Geochemical and geochronological studies of the Kilgore Tuff, the largest eruption produced by the Heise volcanic field, suggest that this supereruption was preceded by the assembly of separated reservoirs of eruptible magma (Wotzlaw, 2014). The buoyancy associated to this process may have been sufficient to trigger the eruption (Caricchi et al., 2014, Wotzlaw et al., 2014). Geophysical imaging of the present day Yellowstone magmatic system also shows the existence of several isolated melt-rich regions within a highly crystallised magmatic mush (Miller and Smith, 1999). Therefore, the sequence of events that preceded the eruption of the Kilgore Tuff may be an appropriate proxy for a future Yellowstone supereruption.

While the most recent studies suggest that the assembly of multiple reservoirs may typically precede supereruptions (Ellis et al., 2014; Wotzlaw et al., 2014), the time-interval between the merging and the eruption remains unclear.

The main target of my study is to determine the time interval between the connection of the different magma batches and eruption. This will be carried out by chemical analyses and diffusions modelling on sanidines and pyroxenes minerals that have been erupted during the Kilgore Tuff eruption.

We will first characterise the major and trace element composition of the Kilgore Tuff along high spatial resolution profiles and combine this data with detailed mineral chemistry. This data are being currently acquired and will serve to select the crystals on which to acquire chemical profiles and perform the diffusion modelling.

REFERENCES

Caricchi, L., Annen, C., Blundy, J., Simpson, G., Pinel, V., 2014, Frequency and magnitude of volcanic eruptions controlled by magma injection and buoyancy: Nature Geoscience, v.7, p.126-130, doi: 10.1038/ngeo2041

Ellis, B.S., Bachmann, O. & Wolff, J.A., 2014. Cumulate fragments in silicic ignimbrites: The case of the Snake River Plain. Geology, 42(5), pp.431–434.

Miller, D.S. & Smith, R.B., 1999. P and S velocity structure of the Yellowstone volcanic field from local earthquake and controlled-source tomography. Journal of Geophysical Research, 104(B7), pp.15105–15–121.

Wotzlaw, J.F., Bindeman, I.N., Watts, K.E., Schmitt, A.K., Caricchi, L., Schaltegger, U., 2014, Linking rapid magma reservoir assembly and eruption trigger mechanisms at evolved Yellowstone-type supervolcanoes: Geology, doi: 10.1130/G35979.1.

P 3.11

Petrography and geochronology of phonolites of the Hegau volcanic field, SW Germany

Ramon Schmid[1], Leander Franz[1], Meinert Rahn[2], Cécile Gautheron[3] & Christian de Capitani[1]

[1] *Mineralogisch-Petrographisches Institut, Universität Basel, Bernoullistrasse 30, CH-4056 Basel (ramon.schmid@stud.unibas.ch)*
[2] *Eidgenössisches Nuklearsicherheitsinspektorat ENSI, Industriestrasse 19, CH-5200 Brugg*
[3] *UMR GEOPS-CNRS-UPS 8148, Université Paris Sud, F-91405 Orsay*

A petrographic characterization and (U-Th)/He-dating of the six major phonolites of the Hegau volcanic field was performed and the results compared to previous studies. The Hegau volcanic field is situated near Singen (South-West Germany) between Lake Constance, Canton Schaffhausen (CH) and the Danube river. Investigations focused on the known six conoid phonolitic mountains Hohentwiel (HT), Gönnersbohl (GB), Staufen (ST), Hohenkrähen (HK), Mägdeberg (MB) and Schwindel (SC). Between two and six samples were taken at each location and described in thin-section. Apatite single grain samples from the locations HT, GB, ST and HK were found suitable for (U-Th)/He-dating, while the locations MB and SC did not provide apatites of sufficient quality. Geochronological analyses were performed at UMR GEOPS, Université Paris Sud.

Thin-sections of the phonolites can texturally be described as hypocrystalline porphyritic, with porphyritic phases including euhedral sanidine, pseudomorphs of nosean and subhedral aegirine-augite. They lie in a tight matrix of the same phases enhanced by biotite and altered material (former glass). Both porphyritic crystals and matrix are homogeneously distributed and commonly show a trachytic flow fabric. In addition, likewise arranged vacuoles filled with zeolite, carbonate and/or apatite are observed. The rocks underwent strong post-magmatic hydrothermal alteration, which is best expressed by the presence of nosean pseudomorphs, glass alteration to clay minerals, zeolite and/or carbonate as well as alteration of biotite. The phonolites contain multiple generations of apatite, which occur as inclusions in primary phases (early crystallisation), are found as porphyritic phases in the matrix (intermediate crystallisation) as well as in late vacuoles (post-magmatic hydrothermal crystallisation). The generally assumed sequence of magmatic crystallisation is nosean – aegirine-augite – sanidine – biotite – matrix minerals. All samples can be classified as nosean phonolites, in line with previous studies. In present samples nosean was the only representative foide mineral, whereas Lippolt et al. (1963) also described haüyn, and nepheline was found in the matrix by Keller (1984). It is likely that the observed absence of other foide minerals than nosean was mainly due to the degree of alteration in the samples investigated.

(U-Th)/He-ages of the four phonolites HT, GB, ST and HK (between 2 and 4 single grain ages per sample) can be combined to a mean age of 11.3±1.9 Ma (1σ). The phonolitic samples show different single grain age reproducibility and therefore different standard deviation for the mean age (cf. fig. 1). It is interesting to note that there seems to be a correlation between the dimension of the phonolitic intrusion and the uncertainty of the calculated (U-Th)/He-ages. This could indicate grain age variation within single phonolitic intrusive bodies due to multiple phonolitic eruptions and/or He age reset by hydrothermal activity. Previous studies on the Hegau volcanism suggested phonolitic activity to be the youngest magmatic phase in the Hegau, occuring between 9.5 and 8.6 Ma (Lippolt et al., 1963; Staesche et al., 1995). As shown in figure 1 our results are in line with fission track data which provided ages between 10.6 and 11.6 Ma (Rahn & von der Handt, 2013). We therefore conclude that the phonolitic episode of volcanism in the Hegau occurred earlier than previously assumed.

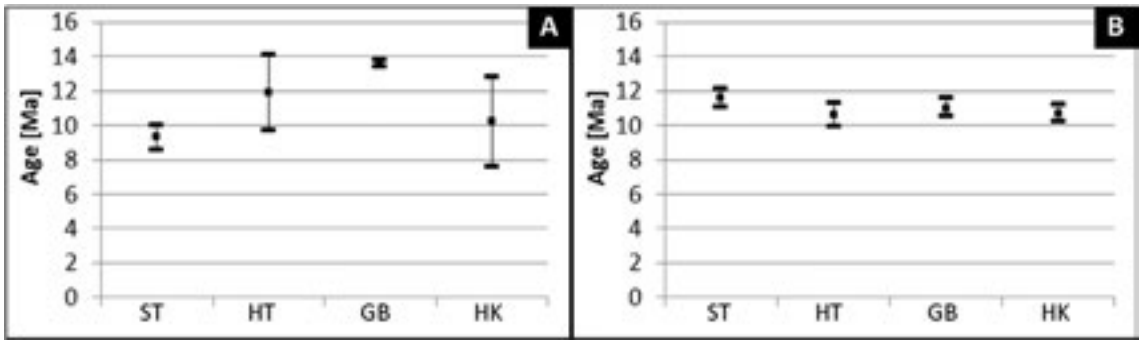

Figure 1. Compared mean ages with 1σ-standard deviation by location (Staufen (ST), Hohentwiel (HT), Gönnersbohl (GB) & Hohenkrähen (HK)) determined by (A) (U-Th)/He and (B) fission-track analysis.

REFERENCES
Keller, J. 1984: Der Jungtertiäre Vulkanismus Südwestdeutschlands: Exkursionen im Kaiserstuhl und Hegau. Fortschr. Miner. 62, 2-35.
Lippolt, H.-J., Gentner, W. & Wimmenauer, W. 1963: Altersbestimmungen nach der Kalium-Argon-Methode an tertiären Eruptivgesteinen Südwestdeutschlands. Jh. geol. L. Amt Baden-Württ. 6, 507-538.
Rahn, M. & von der Handt, A. 2013: Tracing the time-resolved magmatic evolution of the Hegau volcanic field (Southern Germany) through apatites. Goldschmidt2013 Conference Abstracts 2020.
Staesche, A., Hegner, E. & Satir, M. 1995: The genetic relationship of melilitites and phonolites, Hegau volcanic field, S-Germany. European Journal of Mineralogy 7, 236.

P 3.12

Tephra chronostratigraphy of the Malpaisillo Volcanic Complex (central-western Nicaragua)

Line Stoppa[1], Steffen Kutterolf[2], Juanita Rausch[1] & Bernard Grobéty[1]

[1] *Department of Geosciences, University of Fribourg, Ch. Du Musée 6, CH-1700 Fribourg (line.stoppa@unifr.ch)*
[2] *GEOMAR Helmholtz Centre for Ocean Research, Wischhofstrasse 1-3, D-24148 Kiel*

The Malpaisillo Caldera is part of the Central American Volcanic Arc (CAVA) that is the result of the Cocos plate subducting beneath the Caribbean plate. The ca. 10 km-wide Malpaisillo Caldera is situated ca. 40 km northwest of Managua, the capital of Nicaragua (Fig. 1A), where ca. one third of the country's population resides. It is, interpreted to be older than 200'000 yr BP based on geological mapping in this area (Van Wyk de Vries 1993). It represents one of the largest – or possibly the largest – caldera structure in central western Nicaragua and most likely hosted also the largest eruptive event in that region. Surprisingly, the eruptive products of the Caldera have not been studied in detail so far. The goal of the current study is to examine and map the eruptive products emitted by the Malpaisillo Caldera and thus, extend the existing tephra chronostratigraphy of the country (summarized in Kutterolf et al. 2007). The results of this study aim also to contribute to a better understanding of the evolution of explosive Nicaraguan volcanoes since the Pleistocene and therefore also to a more reliable volcanic hazard assessment in the highly vulnerable country of Nicaragua.

A detailed field work was carried out to establish stratigraphic correlations of the volcanic deposits exposed in the surroundings of the Malpaisillo Caldera. A total of 58 proximal to distal outcrops, consisting of a mixture of ignimbrite, fallout and surge deposits were logged and described (Fig. 1A, B). Field-based correlations were refined and complemented with geochemical analysis of pumice sampled from the different deposits. The concentrations of major elements - determined by EMP - and trace elements - measured with LA-ICP-MS – of 61 samples show that the Malpaisillo deposits are characterized by a calk-alkaline (medium- to high-K: K_2O = 2.2-4.0 wt. %), rhyolitic composition that differ from all other volcanic products known in Nicaragua (Kutterolf et al. 2008). Based on major and trace element concentrations, the Malpaisillo deposits clearly build a separate new compositional group, which consists of up to eight subgroups (Fig. 1C).

Geochemical evidences combined with field observations suggest thus that the Malpaisillo Caldera was the source of at least six individual, large-volume, eruptive phases or eruptions (A-F in Fig. 1), some of which are separated by paleosols. Ar-Ar dating on feldspars picked from two samples will hopefully reveal the exact stratigraphic position of the Malpaisillo eruptive products within the Nicaraguan eruptive succession.

The new findings on the Malpaisillo Caldera facilitate to establish a new large volcanic complex in the Pleistocene (namely Malpaisillo Volcanic Complex) in Central Western Nicaragua, justified by its distinct geochemical signature and the regional distribution of its eruptive products. In the following this allows also the definition of a new tephrostratigraphic formation in Nicaragua: the Malpaisillo Formation.

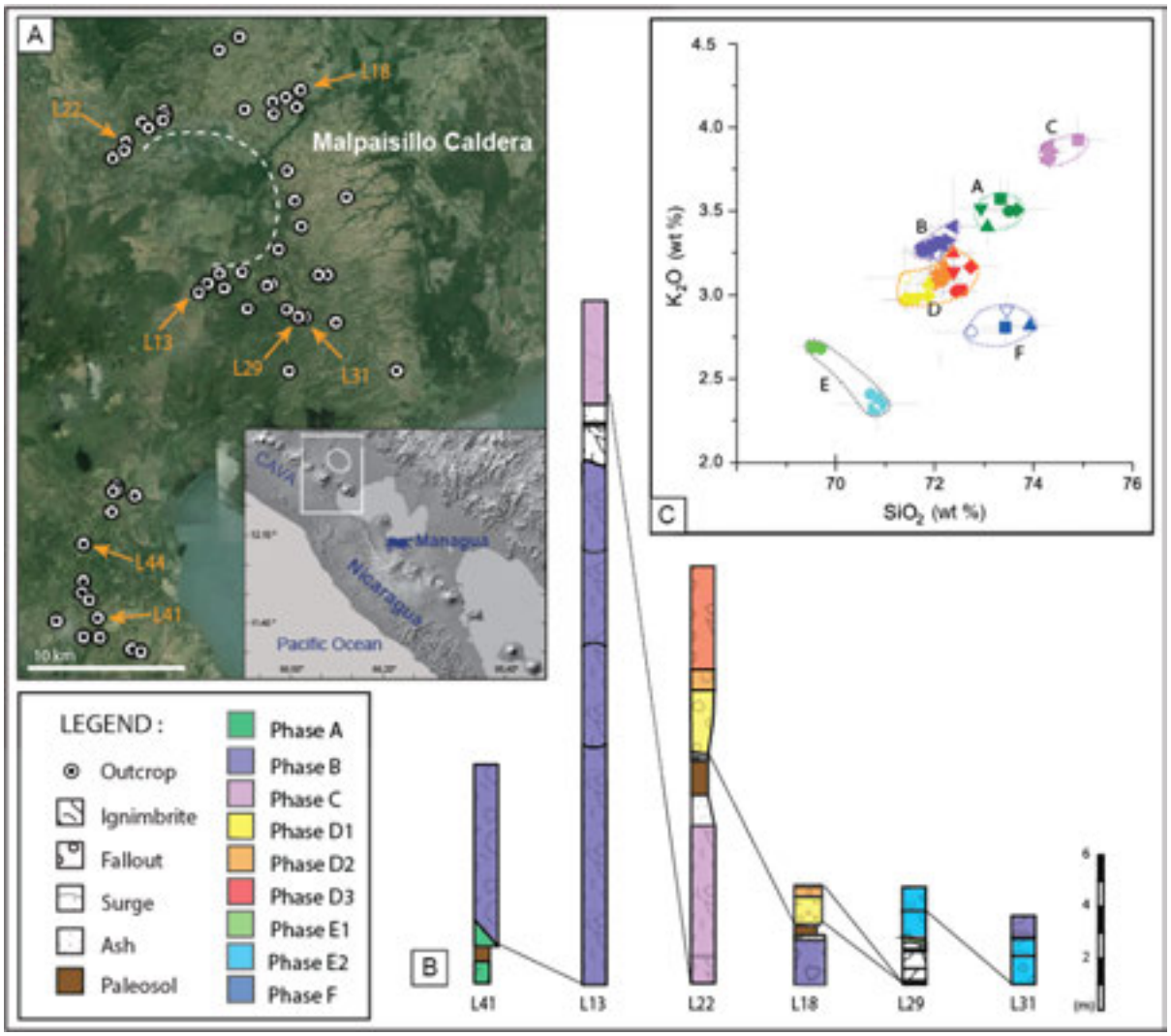

Fig. 1 : A) Satellite image (http://www.earth.google.com) showing the Malpaisillo Caldera (dashed line) and the outcrops studied (dots). Inset map: Digital Elevation Model of central-western Nicaragua showing the location of the study area. B) Field- and geochemical-based correlation of selected stratigraphic sections. The sites were the stratigraphic sections were logged, are showed in Fig. 1A. C) SiO_2 vs. K_2O diagram showing the different geochemical groups (A-F) identified within the Malpaisillo Formation. The colours of the stratigraphic sections correspond to the colours of the geochemical groups.

REFERENCES

Kutterolf, S., Freundt, A., Peréz, W., Wehrmann, H. & Schmincke, H.-U. 2007: Late Pleistocene to Holocene temporal succession and magnitudes of highly-explosive volcanic eruptions in west-central Nicaragua. J Volcanol Geotherm Res, 163, 55-82.

Kutterolf S, Freundt A, Peréz W, Mörz T, Schacht U, Wehrmann H & Schmincke H-U (2008) The Pacific offshore record of Plinian arc volcanism in Central America, part 1: Along-arc correlations. Geochem Geophys Geosyst. 9 (2).

Van Wyk de Vries, B. 1993: Tectonics and magma evolution of Nicaraguan volcanic systems. Doctoral Thesis. Open University,Milton Keynes, 328 pp.

4. Palaeontology

Lionel Cavin, Damien Becker, Christian Klug

Swiss Geological Survey – swisstopo,
Schweizerisches Komitee für Stratigraphie,
Naturhistorisches Museum Bern,
Schweizerische Paläontologische Gesellschaft,
Kommission des Schweizerischen Paläontologischen Abhandlungen (KSPA)

TALKS:

4.1 Aguirre-Fernández, G., Carrillo-Briceño, J. D., Sánchez, R., Jaramillo, C., Sánchez-Villagra, M. R.: Fossil whales and dolphins (Cetacea) from the Miocene of Venezuela and Colombia

4.2 Anquetin J.: A new diverse turtle fauna in the late Kimmeridgian of Switzerland

4.3 Bagherpour B., Bucher H., Brosse M., Baud A., Frisk Å., Guodun K.: Tectonic control on the deposition of Permian-Triassic boundary microbialites in the Nanpanjiang Basin (South China)

4.4 Carrillo J. D., Carlini A. A., Jaramillo C., Sánchez-Villagra M. R.: New fossil mammals from the northern neotropics (Urumaco, Venezuela, Castilletes, Colombia) and their significance for the new world diversity patterns and the Great American Biotic Interchange

4.5 Costeur L., Mennecart B., Rössner G.E., Azanza B.,: Inner ear in earyl deer

4.6 Hiard F., Métais G., Goussard F.: On the "thumb" of anoplotheriins: a 3D comparative study of the hand of *Anoplotherium* and *Diplobune*.

4.7 Klug C., Hoffmann R.: The origin of the complexity of ammonoid sutures

4.8 Koppka, J.: The oysters (Ostreoidea, Bivalvia) of the Reuchenette Formation (Kimmeridgian, Upper Jurassic) in Northwestern Switzerland

4.9 Leuzinger L., Kocsis L., Billon-Bruyat J.-P., Spezzaferri S.: Taxonomy and biogeochemistry of a new chondrichthyan fauna from the Swiss Jura (Kimmeridgian): an unusual isotopic signature for the hybodont shark *Asteracanthus*

4.10 Maridet O., Costeur L., Schwarz C., Furió M., van Glabbeek F. M., Hoek Ostende L. W.: Comparison of the bony labyrinths of some extant and fossil hedgehogs (Erinaceomorpha, Mammalia): evolutionary and paleoecological implications

4.11 Meier M., Bucher H., Ware D.: The diversity and phylogenetic bottleneck of ammonoids across the end-Permian mass extinction

4.12 Pérez-Asensio J.N., Samankassou E., Jiménez-Moreno G., Larrasoaña J.C., Mata P., Civis J.: Late Miocene-early Pliocene benthic foraminiferal assemblages from the La Matilla core, lower Guadalquivir Basin (SW Spain)

4.13 Pirkenseer C., Rauber G.: The «Cyathula-Bank», a regional stratigraphic unit at the interface between two tectonic and sedimentological provinces.

4.14 Schaefer K., Billon-Bruyat J.-P.: The crocodilian *Steneosaurus* cf. *bouchardi* in the Kimmeridgian of Switzerland

4.15 Ware D., Bucher H., Schneebeli-Hermann E.: The Dienerian (Early Triassic) ammonoid diversity crisis: timing and environmental proxies from the northern Indian margin

POSTERS:

P 4.1 Becker, D, Dini, M., Scherler, L.: Woolly rhinoceros from the Pleniglacial of Ajoie (Jura Canton, Switzerland): anatomical description and ecological implications

P 4.2 Minwer-Barakat R., Marigó J., Costeur L. Engesser, B.: New primate material from the Middle Eocene Swiss Site Verrerie de Roches

P 4.3 Marchegiano M., Gliozzi E., Buratti N., Ariztegui D., Cirilli S.: Environmental change in central Italy since the Late Pleistocene. The Lake Trasimeno ostracod record.

P 4.4 Püntener C., Anquetin J., Billon-Bruyat J.-P.: A new species of the coastal marine turtle *Thalassemys* Rütimeyer 1873 from the Kimmeridgian of the Swiss Jura Mountains

P 4.5 Savary V., Mennecart B.: Testing the EBSD Method on Mammal Enamel

4.1

Fossil whales and dolphins (Cetacea) from the Miocene of Venezuela and Colombia

Gabriel Aguirre-Fernández[1], Jorge D. Carrillo-Briceño[1], Rodolfo Sánchez[2], Carlos Jaramillo[2], Marcelo R. Sánchez-Villagra[1]

[1] *Paläontologisches Institut und Museum, Universität Zürich, Karl-Schmid-Strasse 4, 8006 Zürich (gabriel.aguirre@otago.ac.nz)*
[2] *Center for Tropical Paleoecology, Smithsonian Tropical Research Institute, Balboa, Ancón, Panama, 0843- 03092, Panama*

There is an increasing interest on deep-time patterns of the latitudinal biodiversity gradient and their role in predicting the effects of future climate change (Mannion et al., 2014). Databases such as the Paleobiology Database (http://paleobiodb.org/) are widely used as tools to study past diversity and are constantly updated by a dedicated scientific community. But, as a general case, there is a latitudinal research effort bias towards Northern collections. The past diversity of fossil cetaceans (whales and dolphins) is globally biased by a greater collection and research effort in the Northern Hemisphere (Uhen, 2010). The past diversity of cetaceans in the Americas is strongly linked to collection effort in USA and NW Mexico (Figure 1). Contrastingly, a relationship between generic diversity and outcrop area (marine formations as a proxy) is less obvious (Figure 1).

Recent prospection in Colombian and Venezuelan Neogene localities have yielded six new specimens of cetaceans collected from three different formations: 1) two possible inioids from the Urumaco Formation (Late Miocene, Western Venezuela); 2) a possible squalodelphinid from the Querales Formation (Early to Middle Miocene, Western Venezuela); and 3) a small odontocete, an inioid, and a mysticete from the Castilletes Formation (Early Miocene, Northern Colombia). Previously reported cetaceans from Venezuela include some squalodelphinids (Cantaure and Castillo Formations, both Early Miocene), and an indeterminate mysticete (Punta Gavilan Fm, Early Pliocene). Ongoing preparation and study of the material presented here offers a unique opportunity to better understand the fauna from poorly-prospected northern Neotropical localities.

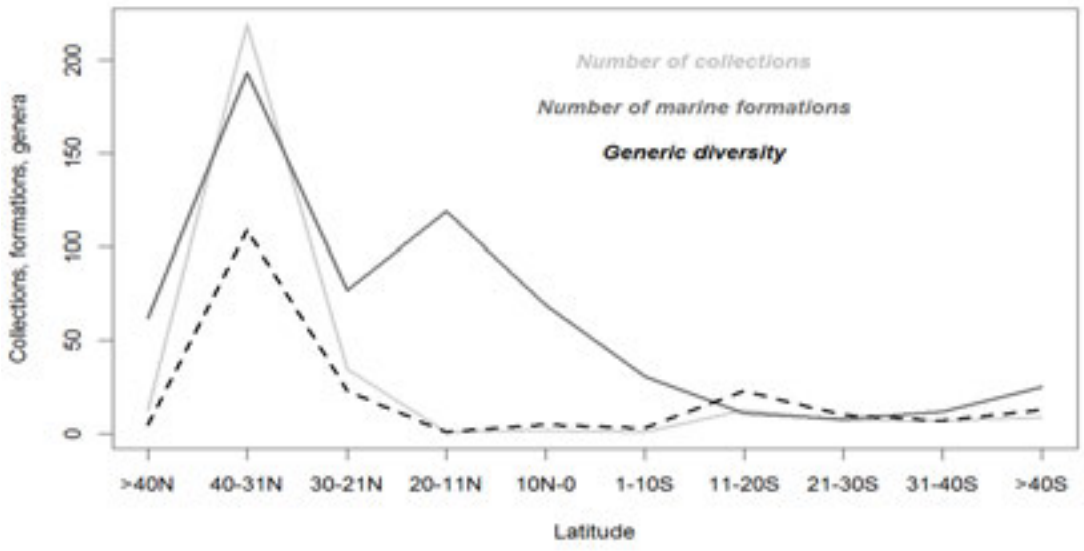

Figure 1. Latitudinal gradient of generic diversity of Neogene cetaceans in the Americas compared to number of collections and number of marine formations (as a proxy of outcrop area). Data taken from paleobiodb.org (see Uhen, 2014).

REFERENCES

Mannion, P. D., Upchurch, P., Benson, R. B. J. & Goswami, A. 2014: The latitudinal biodiversity gradient through deep time. Trends in Ecology & Evolution, 29 (1), 42-50.

Uhen, M. D. 2010: The Origin(s) of Whales. Annual Review of Earth and Planetary Sciences, 38 (1), 189–219.

Uhen, M. D. Online systematics archive 9, Cetacea. [parameters: Cetacea; Eocene–Pliocene; North America, South America]. Retrieved on 12.05.2014 from www.paleobiodb.org.

4.2

A new diverse turtle fauna in the late Kimmeridgian of Switzerland

Anquetin Jérémy

Section d'archéologie et paléontologie, Office de la culture, République et Canton du Jura, Porrentruy, Switzerland (j.anquetin@gmail.com)

During the Kimmeridgian and the Tithonian (Late Jurassic), Europe was the theater of the diversification of numerous coastal eucryptodiran turtles (Plesiochelyidae, Thalassemydidae, and Eurysternidae). Most turtle assemblages were discovered during the 19th century. The best localities and horizons include the Kimmeridge Clay of England, the Turtle Limestone of Solothurn, Switzerland, and the lithographic limestones of Bavaria, Germany. Despite the abundance of material, these faunas have been scarcely studied during the 20th century. Historically, Solothurn is the richest turtle locality for the Kimmeridgian (Bräm, 1965; Meyer and Thüring, 2009), with several hundreds shell remains and six valid species (Anquetin et al., 2014). The presence of six more or less closely related, relatively large coastal marine turtles in the same paleoenvironment is remarkable in terms of paleobiodiversity. For comparison, there are currently only eight species of marine turtles worldwide.

Here, we report an even more diverse turtle assemblage from late Kimmeridgian deposits in the vicinity of Porrentruy, Canton Jura, Switzerland. These turtles were discovered by the PAL A16 team during controlled excavations along the course of the A16 Transjurane motorway. The PAL A16 Kimmeridgian turtle collection includes about 80 sub-complete shells, five crania, four mandibles, and thousands of isolated remains. The description of this rich assemblage is still ongoing, but the presence of at least eight distinct taxa has already been recognized. Three of these are also present in the Solothurn assemblage: *Plesiochelys etalloni*, *Thalassemys moseri*, and *Tropidemys langii*. As in Solothurn, *Plesiochelys etalloni* is the most abundant species in Porrentruy. Interestingly, the second most abundant species is *Thalassemys moseri*, for which only two partial shells are known in Solothurn. *Tropidemys langii* is represented by several articulated shells, providing new insights into the anatomy of this characteristic plesiochelyid turtle (Püntener et al., 2014).

Remarkably, the rest of the Porrentruy assemblage differs from that of Solothurn. Thalassemydidae are represented by a new species of *Thalassemys* (see Poster by Christian Püntener). At least two species of Eurysternidae are present: *Solnhofia* aff. *parsonsi* and *Eurysternum* sp. *Solnhofia* aff. *parsonsi* is notably characterized by a short snout, whereas the Tithonian holotype of *Solnhofia parsonsi* is characterized by an elongated snout. Whether this is a distinct species or a morph of the same species will be further investigated. A skull from Solothurn initially referred to *Solnhofia parsonsi* may actually belong to this new form. The presence of numerous remains of *Eurysternum* sp. in Porrentruy is remarkable as eurysternids are rarely abundant in plesiochelyid-dominated assemblages. Plesiochelyidae are further represented by several additional taxa. A large, complete shell that exhibits several unusual features probably represents a new taxon. A few specimens, including a previously reported trampled shell (Billon-Bruyat et al., 2012), may be provisionally assigned to *Craspedochelys* sp. And finally, two additional taxa can be identified based on cranial material. One is a distinct, undetermined plesiochelyid that might correspond to one of the shell-based taxa. The other is identified as a new species of *Portlandemys*, a form previously only known in the Tithonian of the Isle of Portland, England.

The turtle localities around Porrentruy are slightly older (end of *Cymodoce* zone and *Eudoxus* zone) than the Turtle Limestone of Solothurn (*Autossiodorensis* zone). This short difference in age may explain some discrepancies between the two faunas, but other factors also probably played a part. The paleoenvironments must have been different, as apparent from the lithology and the presence of eurysternids. Some ammonites and sharks, as well as ostracods, also reveal the existence of a boreal signal in the Porrentruy fauna. Turtles may also reflect this influence, as suggested by the presence of *Portlandemys* sp.

The description of this rich new turtle assemblage in months and years to come, coupled with the long overdue taxonomic reassessment of Late Jurassic eucryptodires at the European scale, will provide a better understanding of the diversity and paleobiogeography of these coastal turtles, which represent the oldest documented radiation of these reptiles into marine environments. The first results suggest that European turtle faunas were more homogeneous than previously thought.

REFERENCES

Anquetin, J., Püntener, C. & Billon-Bruyat, J.-P. 2014: A taxonomic review of the Late Jurassic eucryptodiran turtles from the Jura Mountains (Switzerland and France). PeerJ, 2, e369.

Billon-Bruyat, J.-P., Marty, D., Bocat, L. & Paratte, G. 2012: Under the feet of sauropods: a trampled coastal marine turtle. Abstract, Fourth Symposium on Turtle Evolution 2012, University of Tübingen, Germany.

Bräm, H. 1965: Die Schildkröten aus dem oberen Jura (Malm) der Gegend von Solothurn. Schweizerische Paläontologische Abhandlungen, 83, 1–190.

Meyer, C. A. & Thüring, S. 2009: Late Jurassic marginal marine ecosystem of the Southern Jura Mountains. In: Billon-Bruyat, J.-P., Marty, D., Costeur, L., Meyer, C. A. & Thüring, B., eds. Abstracts and Field Guides, 5th International Symposium on Lithographic Limestone and Plattenkalk, Actes 2009 bis de la Société jurassienne d'émulation. Porrentruy, Switzerland, 130–141.

Püntener, C., Billon-Bruyat, J.-P., Bocat, L., Berger, J.-P. & Joyce, W. G. 2014: Taxonomy and phylogeny of the turtle *Tropidemys langii* Rütimeyer, 1873, based on new specimens from the Kimmeridgian of the Swiss Jura Mountains. Journal of Vertebrate Paleontology, 34, 353–374.

4.3

Tectonic control on the deposition of Permian-Triassic boundary microbialites in the Nanpanjiang Basin (South China)

Borhan Bagherpour[1], Hugo Bucher[1], Morgane Brosse[1], Aymon Baud [2], Åsa M. Frisk[1,2] and Kuang Guodun[4]

[1] *Paläontologisches Institut der Universität Zürich, Karl Schmid-Strasse 4, 8006 Zürich, Switzerland (borhan.bagherpour@pim.uzh.ch)*
[2] *Geological Museum, Lausanne University, Quartier UNIL-Dorigny, Bâtiment Anthropole, CH-1015 Lausanne, Switzerland*
[3] *Palaeobiology, Department of Earth Sciences, Uppsala University, Villavägen 16, 753 36 Uppsala, Sweden*
[4] *Guangxi Bureau of Geology and Mineral Resources, Jiangzheng Road 1, 530023 Nanning, China*

In most shallow water successions from northwestern Guangxi and southern Guizhou, the Permian-Triassic boundary separates the Late Permian Heshan Fm. from the Early Triassic Luolou Fm. The Late Permian Heshan Formation consists of thick-bedded skeletal limestone with chert nodules and occasional ash layers. The abundant and diversified benthic fauna of the Heshan Fm. includes siliceous sponges, calcareous algae, corals, gastropods, foraminifera, bivalves, brachiopods, bryozoans, and crinoids. The last preserved bed of the Heshan Formation is often an ash layer. The base of the Early Triassic Luolou Formation shows the development of a microbialite unit, ranging from 3.5m to 9.5m in thickness.

Before the onset of microbial deposition, five successive events are recognized:

1. Deposition of an ash layer
2. Deposition of a high-energy grainstone with Late Permian reworked fauna (mainly foraminifera)
3. Deposition of a thin clotted microbialite bed on top of an erosional surface (wavy bedding plane underlined by iron oxide and with bioerosion cutting through 2)
4. Occasional deposition of a second, high-energy grainstone bed containing a Late Permian reworked fauna
5. Deposition of main microbialite episode

High resolution $\delta^{13}C_{carb}$ record across this succession shows that the main negative jump of ca. 1 per mil occurs between 1 and 2. No negative spikes comparable to those known from deeper water or expanded records are recovered. This indicates the presence of a substantial gap between 1 and 2. Moreover, the last preserved bed below this gap is usually an ash layer, which opens the possibility that any younger limestone layers of the Heshan Fm. may have been chemically and/or mechanically removed.

Macrostructure of the microbialite is mostly tabular in the lower half and dome shaped or columnar in the upper half. Shelly lenses yielding highly diversified benthic faunas may occasionally be trapped between the domes. This change of microbialite facies reflects a moderate drowning of the platform. Predominant mesostructures include layered stromatactis-type, fenestral, labyrinthic, spotted, and vesicular structures in the lower half of the microbialite unit and digitated structure in the upper half.

In all studied sections, the microbialite unit is directly capped by a greywacke whose thickness varies from a few cm up to 6 m. The base of this greywacke locally contains decimetric lenses of brecciated microbial limestone. Deposition of this greywacke and enclosed breccias indicates a sudden drowning of the platform. This tectonic phase is also responsible for the cessation of the deposition of the microbialites. The next overlying deeper water succession consists of laminated black shales and occasional thin-bedded micritic limestone yielding a conodont fauna of late Griesbachian age. This age constraint and the presence of a significant gap at the base suggest that deposition of the microbial unit took place in less than 1 Myr, a duration which was directly under synsedimentary tectonic control.

4.4

New fossil mammals from the northern neotropics (Urumaco, Venezuela; Castilletes, Colombia) and their significance for the new world diversity patterns and the Great American Biotic Interchange

Juan D. Carrillo[1], Alfredo A. Carlini[2], Carlos Jaramillo[3] & Marcelo R. Sánchez-Villagra[1]

[1] *Paleontological Institute and Museum,University of Zurich, Karl Schmid-Strasse 4, CH-8006 Zurich (juan.carrillo@pim.uzh.ch)*
[2] *División de Paleontología de Vertebrados, Facultad de Ciencias Naturales y Museo, Universidad Nacional de La Plata, Paseo del Bosque s/n, B1900WFA La Plata, Argentina*
[3] *Smithsonian Tropical Research Institute, 9100 Panama City PL, Washington DC, 20521-9100, USA*

The Great American Biotic Interchange (GABI) refers to the faunal exchange between North and South America around the time of closure of the Central American Seaway, an event that modified the mammal fauna of both continents. Unfortunately, current hypotheses about diversity dynamics during this migration event have been mostly based on data from temperate sites. We present new data from the Urumaco sequence in Venezuela and from new sites at the Guajira Peninsula, northeastern Colombia, which together comprise a sequence of faunas expanding from the early Miocene to the early Pliocene. These faunas, due to their age and geographical location, serve to characterize the Neotropical mammal community before and after GABI's migrational intervals. Studies of several taxonomic groups involve different teams of researchers. In Urumaco the greatest diversity of mammals is in the xenarthrans, with at least 20 species representing Mylodontids, Megalonychids, Megatherines, Glyptodontids, Pampatherids and Dasypodids. Different species provide insights into the re-ingression from North America, taxonomic affinities with megalonychids otherwise present in the Caribbean islands, and the record in these northern latitudes of 'basal' forms recorded in earlier deposits of higher latitudes of the continent. Among rodents, the revision of both new dental and postcranial remains and their variation revealed that several species must have existed, including Phoberomys pattersoni, Eumegamys sp., and Neoepiblema sp. Among the 'meridiungulata', cranial remains of toxodonts suggest the presence of forms with plesiomorphic features unexpected for animals at this geological age. Astrapotheres include cranial remains from Castilletes representing the oldest record of Uruguaytheriinae in the tropics. The oldest procyonid carnivores from the northern neotropics are recorded based on dental remains, from Castilletes and Urumaco (San Gregorio Fm.), both of affinities with genera recorded so far from Argentina. We complement field data by compiling and analyzing the composition of late Neogene mammal assemblages in the Americas by computing the percentage of both native and migrational faunas across a latitudinal gradient. Migrations started in the late Miocene (~10 Ma), but most exchange occurred after the early Pliocene (~5 Ma). In tropical South America migrants are first recorded in the Pliocene, whereas in temperate South America there are some records of North American migrants during the late Miocene and Pliocene, but is not until the Pleistocene when migrants became common.

Figure 1. Artistic representation of *Phoberomys* pattersoni. A giant (XX kg) rodent recorded in Urumaco, late Miocene, Venezuela. Artwork by Jorge González. Taken from Sánchez-Villagra et.al. (2010).

REFERENCES

Sánchez-Villagra, M. R. Aguilera, O. A. Carlini, A. A (eds). 2010: Urumaco and Venezuelan Paleontology. The Fossil Record from the Northern Neotropics. Indiana University Press. Bloomington and Indianapolis. USA.

Woodburne, M. O. 2010: The Great American Biotic Interchange: Dispersal, tectonics, climate, sea level and holding pens, Journal of Mammalian Evolution, 17, 245-264.

4.5

Inner ear in early deer

Loïc Costeur[1], Bastien Mennecart[2], Gertrud Rössner[3] & Beatriz Azanza[4]

[1] *Naturihistorisches Museum Basel, CH-4001 Basel (loic.costeur@bs.ch)*
[2] *UMR 7207 CNRS-MNHN-UPMC, 8 rue Buffon, 75005 Paris, France*
[3] *Bavarian State Collections of Palaeontology and Geology, Richard-Wagner-Str. 10, 80333 Munich, Germany*
[4] *University of Zaragoza, Ciencias de la Tierra,*

Deer (family Cervidae) are a diverse group of even-toed mammals with currrently 5 tribes comprising about 50 species Their evolutionary history spans the last 20 million years. Morphologically speaking, all deer are united by the presence of antlers (except in the Chinese water deer where they were secondarily lost). The identification of a fossil deer is thus made easier when antlers are preserved. So far, the earliest representatives of deer were found in the Early Miocene of Europe with *Procervulus*, *Acteocemas* or *Ligeromeryx* from MN3 localities (around 19 Myrs). These taxa show dichotomously forked antlers and a new specimen from Switzerland (Rössner et al. 2014) attributed to *Acteocemas* documents the first early cervoid with protoburr-and-pearls-bearing antlers of the dicrocerine lineage, close to muntjacs. Another shared character with muntjacs of all these early cervids are elongate, sabre-like upper canines.

A debate has arose in the last twenty years as to wether the Muntiacinae lineage was already established in the Middle Miocene with *Euprox* (about 15 Myrs old) as postulated by Azanza (1993). This hypothesis would push back the divergence time of the crown Cervidae in the Early to Middle Miocene while molecular data indicate an origin rather in the Late Miocene, several million years later (Miyamoto et al., 1990; Pitra et al., 2004, Gilbert et al. 2006). *Euprox* has muntjak-like antlers, but the latter authors regard them as basal, phylogenetically uninformative, and prefer to keep this taxon outside the Muntiacini clade. Azanza et al. (2013) question the sister relationship of Muntiacini with Cervini and rather postulate that muntiacines are the sister group to Cervini and Capreolini, with probable stem Munticinae in the Middle Miocene such as *Eurpox*.

We add information to this discussion using characters of the inner ear which has been shown to yield significant phylogenetical information in other groups of mammals (i.e., in all placentals in Ekdale, 2013 or more specifically in primates, Gunz et al., 2012). Using high resolution x-ray computed tomography we scanned several Early to Middle Miocene "stem Cervidae" including *Procervulus*, *Heteroprox*, *Dicroceros* or indeterminate early deer (isolated petrosals) and compare the 3D-reconstucted shape of their inner ear to that of the five living clades. Fossil and extant deer all share a posterior limb of the lateral semi-circular canal entering the vestibule in or slightly above the ampulla of the posterior semi-circular canal, a different state than in most other ruminants. The canals in fossil species are long and largely extend above the common crus, a situation seen in the living tribe Cervini; the posterior canal is less expanded in the other tribes. The position and orientation of the cochlea close to the vestibule recalls the situation seen in. The massiveness of the cochlear basal turn in *Procervulus* or *Heteroprox* is a basal trait also present in other ruminant lineages. *Heteroprox* has a lateral canal entering the vestibule in the posterior ampulla somewhat anteromedially recalling the condition in *Odocoileus* (Odocoileini). The condition in the early deer from Chilleurs (MN3) is close to that in *Axis* (Cervini) or *Muntiacus* (Muntiacini), where both the lateral and posterior canals meet before the posterior ampulla, mimicking the basal condition of a secondary common crus seen in the earliest artiodactyls (e.g., *Diacodexis*, Orliac et al., 2012). The common area is nonetheless much smaller than a true secondary common crus and both canals are still recognizable despite their junction. The inner ear of *Procervulus* from Rauscheröd (MN4) shows very close canals, but not attached. *Dicroceros* has an angle of the posterior and anterior canals less than 90° close to *Muntiacus* condition but the entry of the lateral canal is closer to that of *Odocoileus* or *Heteroprox* than to that of *Muntiacus* or *Procervulus*.

To summarize, *Procervulus*, *Heteroprox* and *Dicroceros* have inner ears that look more like those of crown deer than like that of other extant ruminants or known fossil representatives of crown ruminants. The earliest crown Cervidae may thus be found earlier than usually accepted by molecular phylogenies (i.e., around 10.7 My), i.e., at least in the Middle Miocene

around 14-15 Myr such as already postulated by Azanza (1993) on the basis of antlers. The antlers without burr of *Procervulus* still leave this taxon in stem cervids. Its primitive-looking but deer-like inner ear confirms this position. The newly found antlers in the Early Miocene of Switzerland, testifying to a second stem lineage early in the Miocene, hint at a radiation in stem cervids.

REFERENCES

Azanza ,B. 1993: Sur la nature des appendices frontaux des cervidés (Artiodactyla, Mammalia) du Miocène inférieur et moyen. Remarques sur leur systématique et leur phylogénie. Comptes Rendus de l'Académie des Sciences Paris II, 316, 1163-1169.

Azanza, B., Rössner, G.E. & Ortiz-Jaureguizar, E. 2013: The early Turolian (late Miocene) Cervidae (Artiodactyla, Mammalia) from the fossil site of Dorn-Dürkheim 1 (Germany) and implications on the origin of crown cervids. Palaeodiversity and Palaeoenvironments, 93, 217-258.

Ekdale, E.G. 2013: Comparative Anatomy of the Bony Labyrinth (Inner Ear) of Placental Mammals. PLoS ONE, 8(6), e66624.

Gilbert, C., Ropiquet, A. & Hassanin A. 2006: Mitochondrial and nuclear phylogenies of Cervidae (Mammalia, Ruminantia): Systematics, morphology, and biogeography. *Molecular Phylogenetics and Evolution* 40(1),101-117.

Gunz, P. Ramsier, M., Kuhrig, M., Hublin, J.-J. & Spoor F. 2012: The mammalian bony labyrinth reconsidered, introducing a comprehensive geometric morphometric approach. Journal of Anatomy, 220, 529-543.

Miyamoto, M.M., Kraus, F. & Ryder, O.A. 1990: Phylogeny and evolution of antlered deer determined from mitochondrial DNA sequences. Proceedings of the National Academy of Sciences USA, 87, 6127-6131.

Orliac, M., Benoit, J. & O'Leary, M.A. 2012: The inner ear of *Diacodexis*, the oldest artiodactyl mammal. Journal of Anatomy, 221(5), 417-426.

Pitra, C., Fickel, J., Meijaard, E. & Groves, P.C. 2004: Evolution and Phylogeny of Old World deer. Molecular Phylogenetics and Evolution, 33, 880-895.

Rössner, G.E., Azanza, B., Jost, J. & Costeur, L. 2014: New evidence of early cervids and phylogenetic implications. Annual Meeting of the Society of Vertebrate Paleontology.

4.6

On the "thumb" of anoplotheriins: a 3D comparative study of the hand of *Anoplotherium* and *Diplobune*.

Florent Hiard[1], Grégoire Métais[2] & Florent Goussard[2]

[1] *Department of Geosciences – Earth Sciences, University of Fribourg, Chemin du Musée 6, CH-1700 Fribourg (florent.hiard@unifr.ch)*
[2] *UMR 7207 CR2P CNRS, Muséum d'Histoire Naturelle, 8 rue Buffon, CP38, 75231 Paris Cedex 05, France*

Anoplotheriinae is an unusual clade of European artiodactyls that existed from the Middle Eocene to the earliest Oligocene characterised by a number of singular postcranial features (e.g. Sudre 1983, Hooker 2007). The notable presence of a well-developed digit II with an uncommon orientation in the fore- and hindlimbs is known at least for the taxa *Anoplotherium* and *Diplobune* but the functionality and utility of this toe have been discussed at least since the middle of the 19th century (Gervais 1848-1852).

We present here a new anatomical description and comparison of the carpals, the metacarpals bones and the phalanges of *Anoplotherium* and *Diplobune* and provide three-dimensional reconstruction of well-preserved specimens of the both taxa to model the mobility of the hand (Fig.1).

This study underlines several significant differences between both taxa, especially in the arrangement of the carpal bones. For instance, the lunate bone of *Diplobune* is more deeply inserted between the hamate and the capitate bones than in *Anoplotherium*, limiting the possibility of lateral movement in the wrist. A second difference is that the articular surface of the trapezoid bone with the scaphoid is more extended in *Diplobune* than in *Anoplotherium*, allowing a higher mobility of the digit II in the former.

The results of this study confirm the possibility of an arboreal lifestyle for *Diplobune*, as already supposed by Sudre (1983). The paleoecology of *Anoplotherium* remains unclear. Even if we accept that *A. commune*, which has a reduced digit II, was in fact the female of *A. latipes*, which presents a well-developed digit II, as proposed by Hooker (2007), it seems improbable that this structure is a sexually dimorphic adaptation for bipedal browsing as he also proposed, given that the teeth show the same type of morphology and wear. We suggest instead that digit II, with his claw-like hoof, was competitively used in male-to-male combats.

Figure 1. 3D reconstruction of MNHN-GY752 *Diplobune secundaria*. A, Dorsal view. B, Dorso-medial view. C. Medial view. Scale bar: 20 mm.

REFERENCES

Gervais, P. 1848-1852: Zoologie et Paléontologie françaises (animaux vertébrés) ou Nouvelles Recherches sur les Animaux Vivants et Fossiles de la France, Tome II. Arthus Bertrand, Paris 46 pp.

Hooker, J.J. 2007: Bipedal browsing adaptations of the unusual Late Eocene-earliest Oligocene tylopod *Anoplotherium* (Artiodactyla, Mammalia), Zoological Journal of the Linnean Society, 151, 609-659.

Sudre J. 1983: Interprétation de la denture et description des éléments du squelette appendiculaire de l'espèce Diplobune minor (Filhol 1877): apports à la connaissance de l'anatomie des AnoplotheriinaeBonaparte 1850. In: Actes du Symposium Paléontologique G. Cuvier (Ed. By Buffetaut, E, Mazin, J.M. & Salmon, E.), Montbéliard, pp. 439-458.

4.7

The origin of the complexity of ammonoid sutures

Christian Klug[1] & René Hoffmann [2]

[1] *Paläontologisches Institut und Museum, University of Zurich, Karl Schmid-Strasse 6, CH-8006 Zurich, Switzerland (chklug@pim.uzh.ch)*
[2] *Ruhr-Universität Bochum, Department of Earth Sciences, Institute of Geology, Mineralogy, and Geophysics, Bochum, Germany*

Ranging from simple to complex, the folded septa of the phragmocone characterize the ammonoid clade and contribute much to their aesthetic appearance. However, many contradicting opinions and models on septum formation and as explanation for the evolution and function of sutural complexity and septal frilling have been published. The most important existing hypotheses are the Viscous Fingering Model, the Tie-Point Model and the application of the Reaction Diffusion Model to the morphogenesis of ammonoid septa.

We present a compound model including a revised chamber formation cycle. This model incorporates a series of older models and new thoughts and explanations. Notably, information from phylogenetic and developmental transformations have contributed much to our understanding of the morphogenesis of ammonoid septa. To begin with, it has to be understood that the ammonoid septum is derived from very simple, nearly hemispherical septa with central septal perforation of orthocerids. Lateral compression mechanically caused the formation of lateral lobes. In the course of the evolution of the Bactritida, the siphuncle shifted to a ventral position, leading to the formation of a ventral lobe.

Already with the Bactritida, the first forms with slightly curved shells evolved. These forms gave rise to such with shells, which comprise over one whorl, the first ammonoids. This increase in coiling in combination with the ventral siphuncle caused a dorsoventral imbalance that lead to a dorsoventral assymmetry of the lateral lobe. With tighter coiling, the whorls began to touch and eventually overlap, thus introducing the dorsal or internal lobe. At a slightly later point in ammonoid evolution, a change in chamber pressure during septum formation is documented in inflexions of the septum. Ultimately, complexity is increased by a more and tighter coiling in combination with a reduction in embryonic shell size. Apparently, the septal mantle, which is responsible for mineralisation of the septum, kept the overall morphology of the preceding septum to a large extend and the increase in whorl section diameter than contributed to increasing complexity. Thus, many aspects of septum morphogenesis can be explained by simple mechanics rather than genetic heredity.

4.8

The oysters (Ostreoidea, Bivalvia) of the Reuchenette Formation (Kimmeridgian, Upper Jurassic) in Northwestern Switzerland

Jens Koppka[1]

[1] *Office de la culture, Section d'archéologie et paléontologie, Hôtel des Halles – CP 64, CH-2900, Porrentruy (jens.koppka@jura.ch)*

During the construction of the Transjurane highway (A 16) in Northwestern Switzerland rich Late Jurassic invertebrate faunas have been discovered in the Reuchenette Formation by members of the "Section d'archéologie et paléontologie" (Paléontologie A 16). Bivalves are the most frequent finds among the invertebrates. Several oyster species have been found and collected in large quanteties in the area north of Courtedoux (Canton Jura, Ajoie), especially in the Lower Kimmeridgian "Banné Marls" (*Cymodoce* Zone) and younger strata as the "Lower *Virgula* Marl" (Upper Kimmeridgian, *Eudoxus* Zone). The review of the oysters is the first part of a taxonomic revision of the high diverse Kimmeridgian bivalve associations found in the Reuchenette Formation. Most of these bivalves have been described in the 19th century in two monographies published by Contejean (1859) and Thurmann & Etallon (1861-1864), but most of the fauna remained literally untouched by subsequent authors for 150 years.

In the revision prepared by the author (Koppka 2014 (subm.)) eight oyster species characterizing the northern Helvetic shelf system are described, new classified and discussed in detail, including a documentation of their high intraspecific variabilty and palaeoecology. The species are: *Circunula* n. gen. *cotyledon* (Contejean, 1859) (Gryphaeidae, ?Pycnodonteinae),

Nanogyra (*Nanogyra*) *nana* (J. Sowerby, 1822), *Nanogyra* (*Palaeogyra*) *reniformis* (Goldfuss, 1833), *Nanogyra* (*Palaeogyra*) *virgula* (Deshayes, 1831) (Gryphaeidae, Exogyrinae), *Helvetostrea* n. gen. *sequana* (Thurmann & Etallon, 1862) (Flemingostreidae, Crassostreinae), *Praeexogyra dubiensis* (Contejean, 1859), *Praeexogyra monsbeliardensis* (Contejean, 1859) (Flemingostreidae, Liostreinae), and *Actinostreon gregareum* (J. Sowerby, 1815) (Arctostreidae, Palaeolophinae). The genera *Circunula* and *Helvetostrea* are proposed as new. *Nanogyra* Beurlen, 1958 is divided into 2 subgenera, all species with developed chomata belonging to *Nanogyra (Palaeogyra)* Mirkamalov, 1963 the remaining to *Nanogygra* sensu stricto.

The early shell ontogeny in general and the generic characters of *Praeexogyra* are revisited. Larval shells respectively their moulds are shown for six species: *N. nana*, *N. reniformis*, *N. virgula* and for comparison also *N.* cf. *auricularis*, *Praeexogyra* cf. *sandalinoides* (de Loriol, 1901) and *Actinostreon marshii* (J. Sowerby, 1814). All of them share a "*Crassostrea*"-like prodissoconch morphology, suggesting a planktic-planktotrophic mode of development.

The observed species were adapted to different niches on a shallow marine carbonate platform. *Circunula* n. gen. *cotyledon* is a typical early settler of hardgrounds but occurs as well in subtidal soft-bottom environments attached to large shells. *Nanogyra* (*N.*) *nana* was found attached to apparently all kinds of biogenous hard and soft substrates including algal stems and thalli; it is regularly distributed in calm to moderate energetic shallow marine palaeoenvironments. *Nanogyra (P.) reniformis* frequently attached hidden on the interior of empty bivalve shells. *Nanogyra (P.) virgula* was a proliferous secondary soft-bottom dweller of shallow marine marls and lime muds; the species is often found concentrated in widely distributed (par)autochthonous lumachelles ("*virgula* marls" of authors). *Praeexogyra dubiensis* and *P. monsbeliardensis* occur in marly, shallow marine palaeoenvironments. *Praeexogyra dubiensis* appears to have preferred attachment to small objects in a moderately energetic facies; in the study area it is also associated with algal meadows; *P. monsbeliardensis* was preferentially gregarious in a somewhat deeper and calmer palaeoenvironment. The strongly chambered and probably fast growing *Helvetostrea* n. gen. *sequana* was adapted to dynamic shallow marine, marly habitats; it is frequently found associatiated with corals and forming ostreoliths or small oyster buildups. *Actinostreon gregareum* usually lived gregariously but was also able to attach to algae on soft substrates (see Fig. 1); the species is known from calm marly to higher energetic coralline palaeoenvironments.

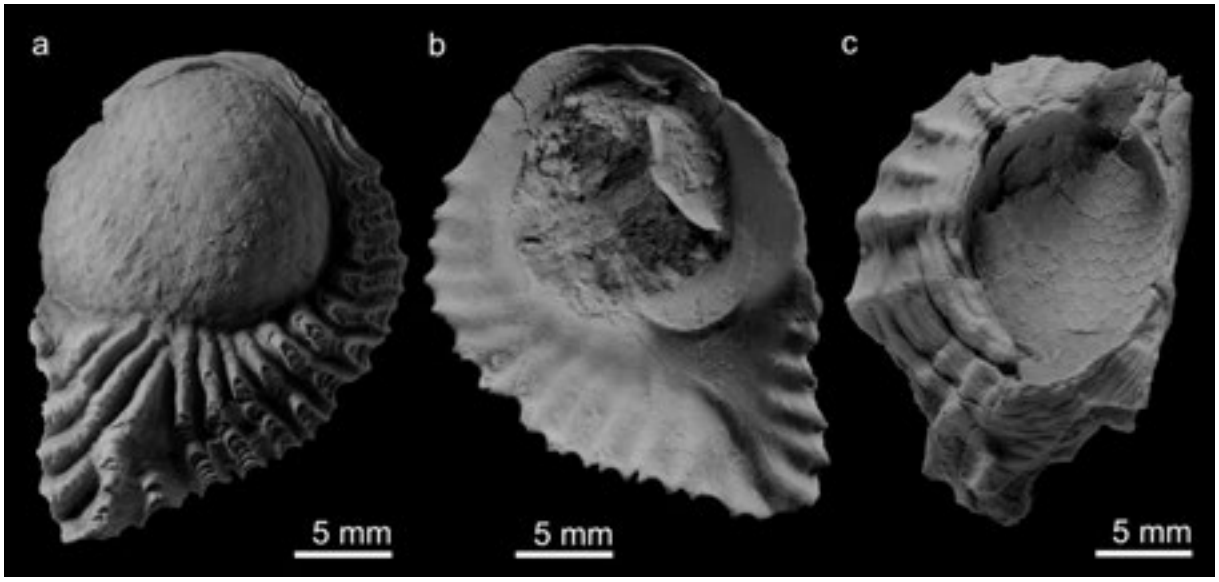

Figure 1. *Actinostreon gregareum* (J. Sowerby, 1815), Vâ Tche Tchâ close to Courtedoux, Banné Marls, Lower Kimmeridgian. a: right valve (CTD-VTT001-1173), exterior view, xenomorph after the calcareous algae *Goniolina geometrica*, b: same as a, interior view; c: left valve (CTD-VTT001-1602), exterior view, with imprint of bioimmured *Goniolina*.

REFERENCES

Contejean, C.H. 1859: Étude de l'étage Kimméridien dans les environs de Montbéliard et dans le Jura, la France et l'Angleterre. Mémoires de la Société d'Émulation du Doubs, Year 1858, 352 pp.

Koppka, J. 2014: Revision of the Bivalvia from the Upper Jurassic Reuchenette Formation, Northwest Switzerland – Ostreoidea. Zootaxa. (submitted)

Thurmann, J. & Etallon, A. 1861-1864: Lethea Bruntrutana ou Études paléontologiques et stratigraphiques sur le Jura Bernois et en particulier les environs de Porrentruy. Denkschriften der Schweizerischen Naturforschenden Gesellschaft, 18, 1-146 (1861), 19, 147-354 (1862), 20, 355-500 (1864).

4.9

Taxonomy and biogeochemistry of a new chondrichthyan fauna from the Swiss Jura (Kimmeridgian): an unusual isotopic signature for the hybodont shark *Asteracanthus*

Léa Leuzinger1,2, László Kocsis3,4, Jean-Paul Billon-Bruyat2, Silvia Spezzaferri1

[1] *Institut de Géologie, Université de Fribourg, Chemin du Musée 6, 1700 Fribourg*
[2] *Paléontologie A16, Office de la culture de la République du Canton du Jura, Hôtel des Halles, 2900 Porrentruy*
[3] *Institut des Sciences de la Terre, Université de Lausanne, Quartier UNIL-Mouline, Bâtiment Géopolis, 1015 Lausanne*
[4] *Geoscience Department, University of Brunei Darussalam*

Remains of sharks, rays and chimaeras (class Chondrichthyes) are very common in Jurassic deposits. Especially chondrichthyan teeth are abundant due to their high resistance to mechanical and chemical alteration. Besides their taxonomic value, they are an ideal material for stable isotope analyses and are widely used as a palaeoenvironmental proxy. Since most chondrichthyans continuously grow and replace their teeth – in isotopic equilibrium with the surrounding water – the isotopic signal recorded in pristine teeth is directly related to the sea water isotopic composition at the time they formed. We report a new chondrichthyan association, in both taxonomic and biogeochemical perspectives. More than 2000 fossils were discovered in Kimmeridgian deposits of Ajoie (Canton Jura, Switzerland), during the building of the Transjurane highway (A16) in the framework of controlled excavations led by the Paléontologie A16, between 2000 and 2011.

The evolution history of sharks in the Late Jurassic is characterized by the expansion of modern forms, causing the decline of hybodonts, or "primitive" sharks, in the marine realms. With a strong dominance of rays and hybodonts (~50% and 40% of the material, respectively), our assemblage clearly differs from neighbouring late Jurassic associations from southern Germany or France, where hybodonts are scarce or absent. This suggests a relatively isolated environment still favourable to primitive sharks in the Ajoie region. It is also noteworthy that the modern shark *Corysodon* (Neoselachii) is reported for the first time in Switzerland.

Oxygen isotopic compositions of phosphate from apatite were measured in chondrichthyans (teeth), as well as in associated remains of turtles (osteoscutes) and of bony fish Pycnodontiformes (teeth) for comparisons. The isotopic values of Pycnodontiformes and *Asteracanthus* indicate distinct living environments, however both taxa are found in the same deposits. While the Pycnodontiformes' data are consistent with marine conditions, the results from the hybodont shark *Asteracanthus* indicate a brackish environment. Considering the absence of transport related marks on the analyzed teeth (*e.g.* damage from reworking), we suggest a marine lifestyle combined with excursions into estuaries or rivers for the hybodont shark *Asteracanthus*.

Our results are consistent with the presence of freshwater on the platform, as suggested by turtle and crocodilian biogeochemistry (Meyer et al. 2012), as well as inferred from the presence of sauropod dinosaur footprints and woods (Philippe et al. 2010). However, the location of the freshwater-influenced environment recorded in *Asteracanthus* remains questionable (on this platform?). This is the first biogeochemical evidence of freshwater influenced conditions for the large, durophagous shark *Asteracanthus*, classically considered as marine for more than 150 years (Agassiz 1837). Interestingly, the presence of *Asteracanthus* remains in Purbeck and Wealden of southern England (Woodward 1895) suggested a tolerance to brackish waters, without further evidence. Compared to previously published biogeochemical data and faunal composition of French and British Jurassic localities, our results represent so far a unique isotopic signature for *Asteracanthus*.

REFERENCES

Agassiz, L. 1837. Recherches sur les poissons fossiles, Tome III. Neuchâtel: Imprimerie de Petipierre, 5, 383 pp. (Text), Plates A-S and 1-47 (Atlas).

Leuzinger, L. 2013: Systematics and biogeochemistry of a new chondrichthyan fauna: implications for the palaeoecological reconstruction of a shallow-water platform (Late Jurassic, Swiss Jura). *Master's Thesis, University of Fribourg, Switzerland*, 134 pp.

Meyer, C. A., Billon-Bruyat, J.-P., Lécuyer, C., & Bocat, L. 2012: Oxygen isotope compositions of Late Jurassic turtles in Europe: new data from Switzerland and Germany. Symposium on Turtle Evolution, University of Tübingen, Germany. Program and abstracts, p. 30.

Philippe, M, Billon-Bruyat, J.-P., Garcia-Ramos, J. C., Bocat, L., Gomez, B., & Piñuela, L. 2010: New occurences of the wood *Protocupressinoxylon purbeckensis* FRANCIS: implications for terrestrial biomes in southwestern Europe at the Jurassic/Cretaceous boundary. Palaeontology, 53(1), 201-214.

Woodward, A. S. 1895: *Catalogue of fossil fishes in the British*, Part III. British Museum of Natural History, 544 pp.

4.10

Comparison of the bony labyrinths of some extant and fossil hedgehogs (Erinaceomorpha, Mammalia): evolutionary and paleoecological implications

Maridet Olivier[1], Costeur Loïc[2], Schwarz Cathrin[3], Furió Marc[4], van Glabbeek Flora M.[5], Hoek Ostende Lars W. [5]

[1] *Jurassica Museum, route de Fontenais 21, CH-2900 Porrentruy (olivier.maridet@jurassica.ch)*
[2] *Geowissenschaften Abt., Naturhistorisches Museum Basel, Augustinergasse 2, CH-4001 Basel.*
[3]Paläontologie Abt., Universität Wien, Althanstrasse 14, A-1090 Vienna.
[4]Institut Català de Paleontologia, Universitat Autònoma de Barcelona, c/ de les Columnes, s/n, SP-08193 Barcelona.
[5] *Naturalis Biodiversity Center, Darwinweg 2, NL-2333 Leiden.*

Family Erinaceidae comprises the spiny hedgehogs (Erinaceinae) and the hairy hedgehogs (Galericinae). Although the extant members of this family are well-known, their phylogenetic relationships and their position among the phylogeny of mammals, especially among Eulipotyphla, remain controversial (Meredith et al. 2011; Bininda-Emonds et al. 2007; He et al. 2012). Furthermore, the evolutionary history of Erinaceidae, especially the separation between the two extant subfamilies remains poorly understood. Extant spiny and hairy hedgehogs also differ in their ecological traits. The spiny hedgehogs are strictly ground-dwelling living in temperate or sub-desertic environnements whereas hairy hedgehogs live in tropical forests and are slighly more agile, giving them the possibility to climb small obstacles.

Thanks to high-resolution computed tomography it is now possible to virtually study the inner morphology of skulls in a non-destructive way. The bony labyrinth is constituted of the organs of hearing and balance and is situated within the petrosal bone. It is a fine and complex network of canals known to bear meaningful systematic and phylogenetic information (Ni et al. 2012; Ekdale 2013). We reconstruct here for the first time the bony labyrinth of several exant and fossil hedgehogs.

A tentative cladistic analysis is performed based on the morphology of the bony labyrinth, in order to asses the potential contribution of these characteriscs to our understanding of Erinaceidae evolutionary history. The phylogeny confirms that Soricidae constitute a primitive clade with regard to Erinaceidae, and that all fossil and extant taxa ascribed to the Erinaceinae form indeed a monophyletic and apomorphic clade. However, all taxa previously ascribed to Galericinae seem to constitute a polyphyletic clade.

The three semi-circular canals constitute the center of balance within the bony labyrinth. For instance, thinner canals indicate a more accurate sense of balance allowing a more agile mode of locomotion. This difference is obvious when comparing extant spiny and hairy hedgehogs, however several fossil forms of spiny hedghogs display thin semi-circular canals (*e.g. Amphechinus*, Figure 1) thus indicating that the strict ground-dwelling locomotion is not characteristic of the Erinaceinae subfamily, but rather indicating a recent ecological evolution within this monophyletic clade.

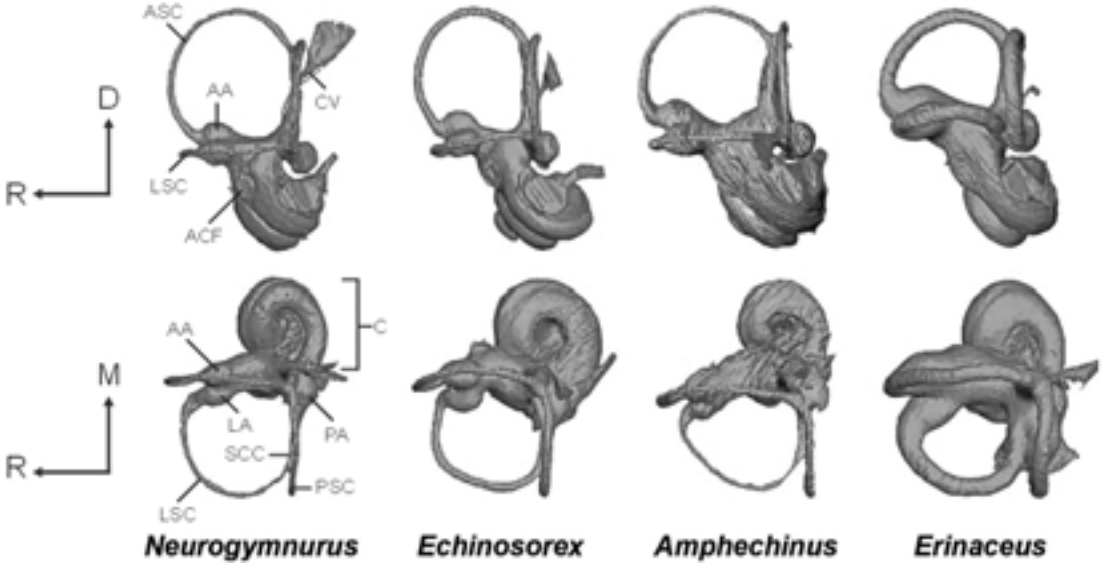

Figure 1. Reconstruction of the bony labyrinths for: *Neurogymnurus cayluxi* Filhol, 1877 (Galericinae, Early Oligocene, France); *Echinosorex gymnura* Raffles, 1822 (Galericinae, Sumatra, extant); *Amphechinus edwardsi* (Filhol, 1879) (Erinaceinae, Early Miocene, France), *Erinaceus europaeus* Linnaeus, 1758 (Erinaceinae, Switzerland, extant). Orientations: **R**. Rostral , **D**. Dorsal, **M**. Medial. Abbreviations: **C**. Cochlea, **ASC**. Anterior Semicircular cannal, **LSC**. Lateral semicircular canal, **PSC**. Posterior semicircular canal, **AA**. Anterior ampula, **LA**. Lateral ampula, **PA**. Posterior ampula, **CV**. Conduct of vestibule, **SCC**. Secondary crus commune, **ACF**. External aperture of the cochlear fossula.

This preliminary analysis emphasizes the potential of inner ear morphology to better understand the evolutionary history of Erinaceidae. Further analyses including more taxa and taking into account the morphology of the petrosal bone and the dentition will be necessary to fully understand the differentiation between the two extant subfamilies and the evolution of their ecology traits.

REFERENCES

Meredith, R.W., et al. 2011: Impacts of the cretaceous terrestrial revolution and KPg extinction on mammal diversification. Science, 334, 521-524.

Bininda-Emonds, O.R.P., et al. 2007: The delayed rise of present-day mammals. Nature, 446, 507-511.

He, K., et al. 2012: An Estimation of Erinaceidae Phylogeny: A combined analysis approach. PLoS ONE, 7(6), e39304.

Ni, X., et al. 2012: Imaging the inner ear in fossil mammals: High-resolution CT scanning and 3-D virtual reconstructions. Palaeontologia Electronica, 15(2), 18A.

Ekdale, E. 2013: Comparative anatomy of the bony labyrinth (inner ear) of placental mammals. PLoS ONE, 8(6), e66624.

4.11

The diversity and phylogenetic bottleneck of ammonoids across the end-Permian mass extinction

Maximiliano Meier[1], Hugo Bucher[1] & David Ware[1]

[1] *Paläontologisches Institut, University of Zürich, Karl-Schmid-Strasse 4, CH-8006 Zürich (maximiliano.meier@pim.uzh.ch)*

Xenodicids have long been recognized to survive the Permian-Triassic boundary mass extinction and to represent the long ranging stem group of the Early Triassic explosive radiation of ammonoids. Despite the general lack of adequate sections providing a complete, gap-free Permian-Triassic boundary ammonoid record (Tozer 1969), pioneers such as Griesbach and Diener already noticed similarities between late Permian and Early Triassic very evolute and morphologically simplified ammonoids. Kummel (1970) also argued that xenodiscids were Permian-Triassic boundary-crossers and stressed that these early Griesbachian evolute ammonoids represent an extremely plastic stock directly related to the late Permian forerunner *Xenodiscus*.

However, since the beginning of the 20th century, emphasis has been repeatedly put on the dissimilarities among xenodiscids with the pervasive aim of gaining higher biostratigraphic resolution. This resulted in taxonomic over-splitting and synonyms at the species, genus and family levels. Overlooked patterns of intraspecific variability also generated a significant bias in terms of diversity pattern at the base of the Early Triassic (Griesbachian).

The Griesbachian record from northeastern Greenland offers a rare and well preserved faunal succession. It includes, in stratigraphic order, the *Hypophiceras triviale*, *H. martini*, *Metophiceras subdemissum*, *Ophiceras commune* and *Wordieoceras decipiens* zones. Extensive and intensive bedrock-controlled sampling yielding numerous specimens per fossiliferous layers allows utilizing a biometric "population" approach of ontogenetic trajectories. Among the taxa from these zones, three xenodiscid genera are here of particular interest: *Metophiceras, Hypophiceras* and *Tompophiceras*. Their intraspecific variability is thoroughly investigated, leading to a revised taxonomy and new phylogenetic hypotheses. Together with new xenodiscid material from Oman and Spiti, this work aims at unravelling the phylogenetic link between xenodiscids and the basal Triassic iconic ophiceratids. Ophiceratids, the first typical Triassic clade, display many resemblances with some xenodiscids in terms of shell shape, but are considered to have a 6 lobed suture line instead of 5 lobed one as is the case of xenodiscids (Tozer 1969). Further studies of suture ontogeny should clarify the evolutionary relations during the ammonoid diversity and phylogenetic bottleneck around the Permian-Triassic boundary.

REFERENCES

Kummel, B. 1970: Ammonoids from the Kathwai Member, Mianwali Formation, Salt Range, West Pakistan. In: Kummel, B., Teichert, C. (Eds.), Stratigraphic Boundary Problems: Permian and Triassic of West Pakistan. Department of Geology Special Publication, vol. 4. University Press of Kansas, pp. 177-192.

Tozer, E.T., Xenodiscacean Ammonoids and their bearing on the discrimination of the Permo-Triassic boundary. GEOLOGICAL MAGAZINE, Vol. 106, No. 4, July-August, 1969, pp. 348-361.

4.12

Late Miocene-early Pliocene benthic foraminiferal assemblages from the La Matilla core, lower Guadalquivir Basin (SW Spain)

José N. Pérez-Asensio[1], Elias Samankassou[1], Gonzalo Jiménez-Moreno[2], Juan C. Larrasoaña[3], Pilar Mata[3] & Jorge Civis[3]

[1] *Section of Earth and Environmental Sciences, University of Geneva, Rue des Maraîchers 13, CH-1205, Geneva, Switzerland (Noel.PerezAsensio@unige.ch)*
[2] *Departamento de Estratigrafía y Paleontología, Universidad de Granada, Fuente Nueva s/n, 18002, Granada, Spain*
[3] *Instituto Geológico y Minero de España, Calle Ríos Rosas 23, 28003, Madrid, Spain*

Benthic foraminiferal assemblages have been studied in the lower part of the 276 m-long La Matilla core from the lower Guadalquivir Basin (SW Spain) that covers the late Miocene (Messinian) and early Pliocene (Zanclean). This part of the core encompasses marine sediments from the Messinian Arcillas de Gibraleón Formation, which consists mostly of greenish-bluish clays, and from the Zanclean Arenas de Huelva Formation including silts and sands. Forty samples were collected each 3 m along the interval from 257 to 150 m. Benthic foraminifera from the size fraction >125 µm were identified and counted until reaching at least 300 individuals. Furthermore, we calculated the relative abundance of species and several diversity indices, including number of taxa, Shannon index, evenness and species dominance. Benthic foraminiferal assemblages were established by means of Q-mode principal component analyses (PCA). In addition, benthic foraminifera were classified according to their microhabitat preferences. The planktonic/benthic ratio (P/B ratio), sand content and total number of benthic foraminifera per gram of dry sediment (N/g) were also calculated. Finally, Pearson correlation coefficients were used to quantify the relationships between all the metrics used in this study.

Five benthic foraminiferal assemblages have been identified in the studied interval. The distribution of these assemblages shows changes in paleobathymetry, productivity and oxygen content. In the lower part of the studied section, between 267 and 204 m, the dominance of the *Brizalina spathulata*, *Cibicidoides pachydermus* and *Uvigerina peregrina* s.l. assemblages indicates an outer shelf-slope setting. The upper part of the studied section, from 204 to 150 m, is characterized by the *Nonion fabum* and *Cassidulina laevigata* assemblages, which suggests an outer shelf environment. Therefore, a sea-level drop from the slope to the outer shelf is recorded during the late Miocene-early Pliocene. The slight increase in the sand content of the episodic sand inputs observed in the core is also consistent with the shallowing-upward trend. This sea-level lowering is also recorded in the Montemayor-1 core, located closer to the northwestern margin of the basin, and in the Atlantic side of the Rifian corridors (Pérez-Asensio et al. 2012; Jiménez-Moreno et al. 2013). Hence, this sea-level lowering has, at least, regional significance.

Concerning changes in productivity and oxygenation, the lowermost part of the studied interval, between 267 and 225 m, shows an alternation between the *Cibicidoides pachydermus* and *Uvigerina peregrina* s.l. assemblages, which can be interpreted as a moderately oxygenated mesotrophic environment with cyclic inputs of labile organic matter related to repeated upwelling events (Pérez-Asensio et al. 2012, 2014). This increased productivity during upwelling events is mirrored in higher abundances of shallow infaunal taxa, while less productivity is marked by more epifaunal-shallow infaunal taxa. Furthermore, these 2 assemblages show positive and negative correlations with the number of taxa and Shanon index, and dominance, respectively. Hence, these mesotrophic assemblages have a high diversity and low dominance suggesting low environmental stress. The uppermost part of the lower interval, from 225 to 204 m, is characterized by the *Brizalina spathulata* assemblage, which includes *Stainforthia complanata* as secondary species. This assemblage shows the highest abundance of deep infaunal taxa (up to 55%) along the studied interval and coincides with a period of low diversity and high dominance. Both species can thrive in environments with very low oxygen content and high organic carbon input. Hence, this assemblage inhabited the most eutrophic environment with the lowest oxygen content, which might be related to strong stratified water column conditions. Such particular eutrophic conditions have not been reported in more marginal areas of the basin (Pérez-Asensio et al. 2012). Finally, the upper part of the studied interval (204-150 m) exhibits an alternation between the *Nonion fabum* and *Cassidulina laevigata* assemblages. The presence of *Nonion fabum* assemblage with *Bulimina elongata* as associated taxa points to low oxygen eutrophic conditions with supply of continental degraded organic matter derived from river run-off (Pérez-Asensio et al. 2012). A lower diversity, higher dominance and more intermediate infaunal taxa are observed in the upper part of the studied interval indicating a gradual increase of the riverine discharge due to shallowing and/or increased humidity during the latest Miocene-lowest Pliocene. The mesotrophic *Cassidulina laevigata* assemblage and its secondary species *Spiroplectinella wrightii* are indicative of marine organic matter supply and moderate oxygenation, and mark freshwater-marine transitional conditions (Pérez-Asensio et al. 2012). This assemblage shows low abundance of intermediate infauna and high abundance of epifauna-shallow infauna pointing to less environmental stress compare to the *Nonion fabum* assemblage. Repeated riverine influence in the outer shelf could be controlled by low amplitude cyclic sea-level changes and/or enhanced rainfall during humid periods.

REFERENCES

Jiménez-Moreno, G., Pérez-Asensio, J.N., Larrasoaña, J.C., Aguirre, J., Civis, J., Rivas-Carballo, M.R., Valle-Hernández, M.F. & González-Delgado, J.A., 2013: Vegetation, sea-level and climate changes during the Messinian salinity crisis. Geol. Soc. Am. Bull., 125, 432-444.

Pérez-Asensio, J.N., Aguirre, J., Schmiedl, G. & Civis, J. 2012: Messinian paleoenvironmental evolution in the lower Guadalquivir Basin (SW Spain) based on benthic foraminifera. Palaeogeogr. Palaeoclimatol. Palaeoecol., 326-328, 135-151.

Pérez-Asensio, J.N., Aguirre, J., Schmiedl, G. & Civis, J. 2014: Messinian productivity changes in the northeastern Atlantic and their relationship to the closure of the Atlantic-Mediterranean gateway: implications for Neogene palaeoclimate and palaeoceanography. J. Geol. Soc. London, 171, 389-400.

4.13

The «Cyathula-Bank», a regional stratigraphic unit at the interface between two tectonic and sedimentological provinces

Claudius Pirkenseer[1], & Gaëtan Rauber[1]

[1] *Office Cantonal de la Culture, Paléontologie A16, Rue de la Chaumont 13, CH-2900 Porrentruy (claudius.pirkenseer@jura.ch, gaetan.rauber@jura.ch)*

During the last two decades the study of the Cenozoic deposits of the so-called "Jura-Molasse" re-intensified due to the construction of the highway A16, stimulating more complex interpretations of the palaeogeographic situation and lateral facies changes. Still, some lithological units like the "Cyathula-Bank/Mergel" remain poorly understood.

The "Cyathula-Bank" (after *Crassostrea cyathula*) in the area between Basel and Laufen has been interpreted as a marker bed subdividing the Late Rupelian Molasse alsacienne (equiv. to upper Cyrenenmergel, lower Niederroedern Formation in Fig. 1), possibly representing a short-term transgressive event within the final regressive phase of the Ru-3 sequence. The "Cyathula-Mergel" in the Delémont area has been interpreted as basin-marginal stratigraphic equivalent to the Cyrenenmergel of the southern Upper Rhine Graben. The preliminary analysis of cores drilled in the Delémont Basin however show the occurrence of a well-defined, densely packed *cyathula*-bearing (coquina) sandstone level at the base of a condensed, 5 to 20 m thick marine series equivalent to the much thicker Serie grise (mainly Meletta-Schichten and Cyrenenmergel) of the Upper Rhine Graben. The thickness of the oyster-bearing levels varies from beds > 5 m (DEL1), patches (Retzwiller) to scattered specimens (Dornachbrugg-1, DP-202, Allschwil-2) or absence (Laufen).

This stratigraphical disparity of occurrences of oysters either during the transgressive or regressive phase of the Serie grise requires a new definition of this lithological unit. A plausible solution represents the interpretation of the "Cyathula-Bank" as an estuarine / deltaic, laterally limited, repetitive regional facies related to fast palaeoenvironmental changes of the extensive prograding Molasse alsacienne-river system. The northward-directed development of the latter and the complex regional palaeogeography in the late Rupelian may explain the scattered occurrences through time and space. The arrival of fluviatile sediments from the Molasse Basin to the southeast is not isochronous and clearly evidenced by changes in other faunal assemblages (autochthone vs. allochthone, marine vs. freshwater), heavy mineral associations (spectrum change) and sedimentological features (disconformity, increase in coarse clastic sediments, point bars).

The occurrence of oyster beds at the base of the marine series in the Delémont basin raises the question about the supposedly uniform timing of the initial transgression (Ru2 transgression) in the different subbasins at the southern end of the Upper Rhine Graben in the late Rupelian.

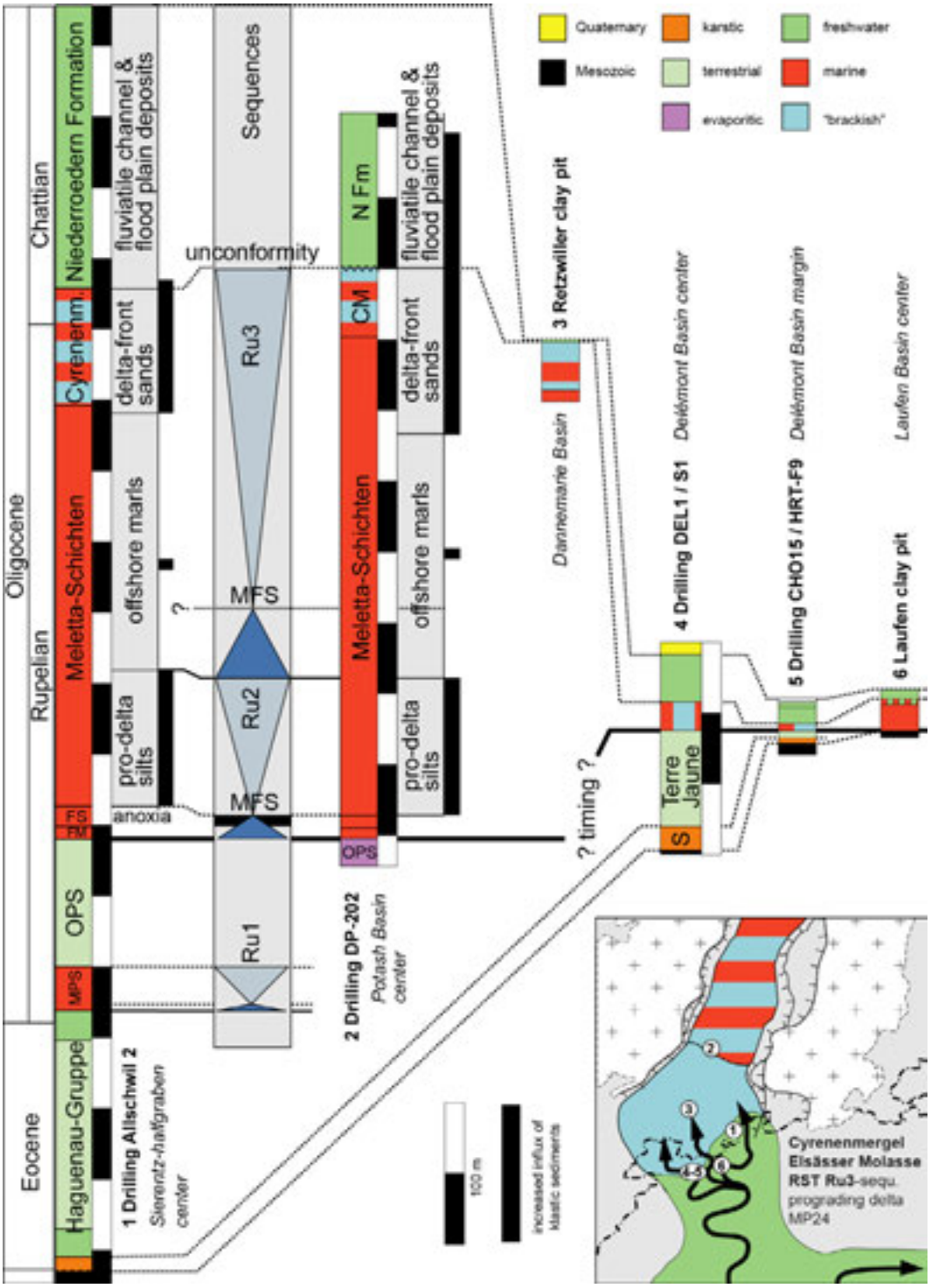

Figure 1. Sediment thickness and correlation between sections in different subbasins in the southernmost Upper Rhine Graben. The small inset indicates localities and the palaeogeography at the interface between the URG and the Molasse Basin during the latest Rupelian. Occurrences of *Crassostrea cyathula*: 1 isolated specimens in CM, 2 isolated specimens in CM, 3 small bioherms in CM, 4 bed of around 5 m at the transgressive surface, 5 bed 50 cm at the transgressive surface, 6 not recorded. (CM = Cyrenenmergel, FS = Fischschiefer, FM = Foraminiferenmergel, S = Siderolithikum)

4.14

The crocodilian *Steneosaurus* cf. *bouchardi* in the Kimmeridgian of Switzerland

Schaefer Kévin, Billon-Bruyat Jean-Paul

Section d'archéologie et paléontologie, Office de la Culture, République et Canton du Jura, Hôtel des Halles, 2900 Porrentruy (kevin.schaefer@jura.ch)

Between 2000 and 2011, more than 500 isolated teeth and more than 170 isolated bones but also 3 skeletons of Thalattosuchia (Crocodylia, Mesosuchia), a suborder of Mesozoic marine crocodilians, have been discovered in the Canton Jura. Those remains have been found during controlled excavations along the future path of the A16 motorway (Transjurane). A preliminary study of the dentition - mainly based on isolated teeth - has shown that the crocodilian fauna consists of four genera, the teleosaurids *Steneosaurus* and *Machimosaurus* and the metriorhynchids *Metriorhynchus* and *Dakosaurus* (Schaefer 2012a, b). Most of the remains belong to *Steneosaurus*, a long-snouted form. It is represented in the Canton Jura by two species: *S*. cf. *jugleri*, a longirostrine species, and *S*. cf. *bouchardi*, a mesorostrine species.

Here, we report a nearly complete isolated mandible, with both *in situ* and associated teeth, and 34 isolated teeth referred to *Steneosaurus* cf. *bouchardi*. The mandible and most of the isolated teeth come from the upper Kimmeridgian *Eudoxus* ammonite zone, whereas some isolated teeth come from the upper Kimmeridgian *Acanthicum* and lower Kimmeridgian *Divisum* zones.

Comparisons with mandibles and a skeleton of *Steneosaurus* cf. *jugleri* allow to clarify dental and jaw differences between the two species of *Steneosaurus*. The teeth of *S*. cf. *bouchardi* are more massive with a "height/mesio-distal diameter" ratio lower or equal to 3, whereas in *S*. cf. *jugleri* the same ratio is greater of equal to 3, in addition the teeth are more gracile in shape. The mandible of *S*. cf. *bouchardi* is more massive, the alveoli are larger and circular in shape instead of being compressed. Moreover the "symphisis *versus* total mandible length" ratio is *ca*. 56.5%, instead of at least *ca*. 66.6% in *S*. cf. *jugleri*.

Steneosaurus bouchardi differs from other Late Jurassic *Steneosaurus* species in having a more massive skull (Vignaud 1995). It is known from two French specimens: a partial skull and mandible from the upper Kimmeridgian (*Autissiodorensis* zone) of the Boulonnais and a partial skull from the lower Kimmeridgian (*Baylei* zone) of Normandie (Sauvage 1874, Buffetaut & Makinsky 1984). The reported material with its massive mandibule and dentition, is very close to *S. bouchardi*. However, a detailled comparison with the remains from France is precluded: the material from the Boulonnais is lost and the skull from Normandie belongs to a private collection.

Thus, the reported remains from the Canton Jura could be the only available material for *S. bouchardi*. It should alse be noted that our team has recently discovered a skeleton (including the skull, mandible and many postcranial bones) related to *S. bouchardi*. Its description would confirm the identification at the species level.

REFERENCES

Buffetaut, E., Makinsky, M. (1984): Un crâne de *Steneosaurus* (Crocodylia, Teleosauridae) dans le Kimméridgien de Villerville (Calvados). *Bulletin trimestriel de la Société Géologique de Normandie et des Amis du Muséum du Havre* 71, 19-24.

Sauvage, H.-E. (1874): Mémoire sur les Dinosauriens et les Crocodiliens des terrains jurassiques de Boulogne-sur-Mer. *Mémoires de la Société Géologique de France* 10(2), 1-58.

Schaefer, K. 2012a: Variabilité de la morphologie dentaire des crocodiliens marins (Thalattosuchia) du Kimméridgien d'Ajoie (Jura, Suisse). Unpublished master thesis, University of Fribourg, 111 pp.

Schaefer, K. 2012b: Variability of the dental morphology in marine crocodilians (Thalattosuchia) from the Kimmeridgian of Ajoie (Jura, Switzerland). Abstract, 10th Swiss Geoscience Meeting 2012, Bern, p. 212-213.

Vignaud P. (1995): Les Thalattosuchia, crocodiles marins du Mésozoïque: systématique phylogénétique, paléoécologie, biochronologie et implications paléogéographiques. Unpublished doctoral thesis, University of Poitiers (France), 271 pp.

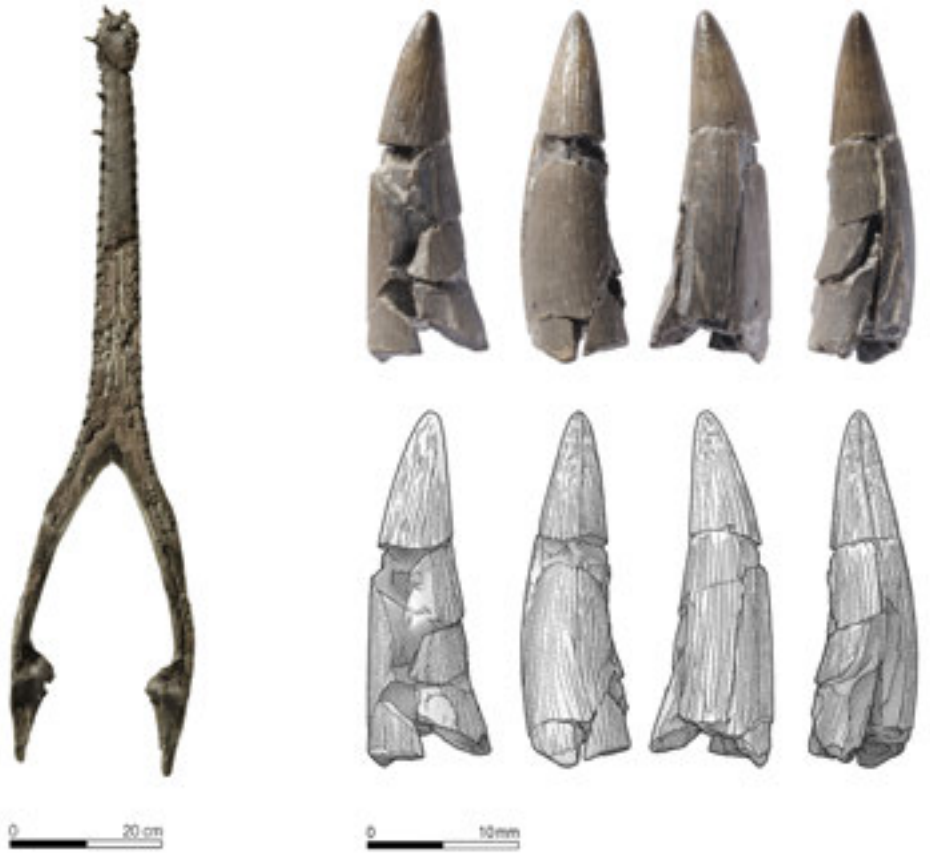

A B

Figure 1. *Steneosaurus* cf. *bouchardi* (late Kimmerdigian, Courtedoux, Swiss Jura). A: mandible TCH006-1439, in dorsal view. B: example of a tooth associated with the mandible in - from left to right - lingual, mesio-distal, labial and mesio-distal views (photographs and corresponding drawings).

4.15

The Dienerian (Early Triassic) ammonoid diversity crisis: timing and environmental proxies from the northern Indian margin

David Ware[1], Hugo Bucher[1] & Elke Schneebeli-Hermann[1]

[1] *Paläontologisches Institut und Museum der Universität Zürich, Karl Schmid-Strasse 4, CH-8006 Zürich, Switzerland (david.ware@pim.uzh.ch; hugo.fr.bucher@pim.uzh.ch)*

Following the recent revision of the taxonomy and biostratigraphy of Dienerian ammonoids from the Salt Range (Pakistan) and from Spiti (Northern India), a new high resolution biozonation based on the Unitary Association (UA) method is constructed for the Dienerian of the Northern Indian Margin (NIM). It includes 12 UA-zones and leads to subdivide the Dienerian into three parts (early, middle and late). This new scheme strongly contrasts with all previously established Dienerian biozonation. For example, Tozer (1994) divided the Dienerian stage of Canada it into two parts (early and late) and recognised only 4 sub-zones, grouped into two zones. Correlation of this new scheme outside the NIM is made difficult by the emergence of a latitudinal differenciation during theDienerian, which indicates a substantial paleobiogeographic change from the cosmopolitan distribution of the preceeding Griesbachian faunas.

The corresponding diversity analyses, coupled with results previously obtained for the early Smithian of the same margin, highlight the four following phases: (1) a first modest diversity high in the early Dienerian; (2) a protracted diversity low spanning the middle Dienerian; (3) a slow increase of diversity during the late Dienerian, and (4) a sustained diversificati-

on in the early Smithian. Turnover rates are very high during the whole interval, and the boundaries between early-middle and middle-late Dienerian are underlined by complete renewals of the faunas. The low diversity in the middle and early late Dienerian is associated with a global anoxic event and warmer temperatures than during early Dienerian and early Smithian times. Together with the end-Smithian extinction, middle and late Dienerian times witnessed the two most severe diversity demises of Early Triassic ammonoids. The middle Dienerian of the NIM (Salt Range) is also characterized by a spore spike similar to that previously documented at the end-Permian (Schneebeli-Hermann et al. 2014), thus emphasizing a marked and simultaneous deterioration of both terrestrial and marine environments. This pattern stands in strong contrast with the general view of a protracted or stepwise recovery following the end-Permian mass extinction.

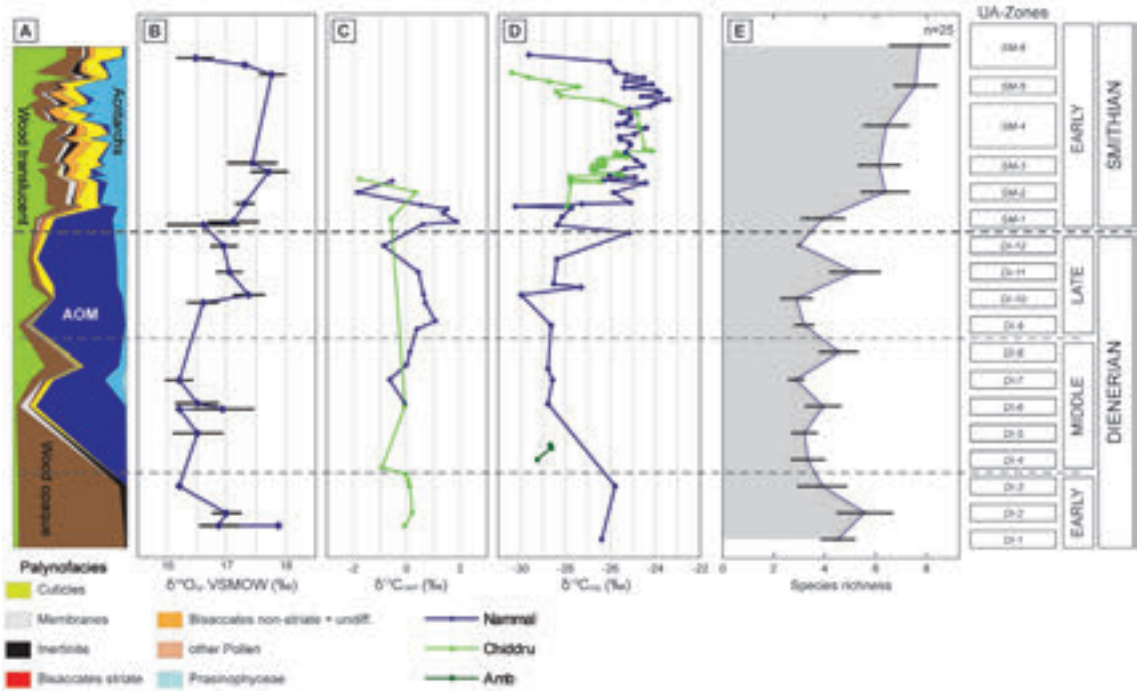

Figure 1. Comparison of the biodiversity signal with palaeoenvironmental proxies: [A] Palynofacies of the Nammal Nala section (modified after Hermann et al. 2011); AOM = Amorphous Organic Matter [B] Oxygen isotopes from Nammal Nala section (modified after Romano et al. 2013); [C] Carbonate carbon isotopes from Chiddru and Nammal (modified after Hermann et al., 2011) ; [D] Organic carbon isotopes from Chiddru and Nammal (modified after Hermann et al. 2011) and from Amb (modified after Schneebeli-Hermann et al. 2012); [E] Rarefied species richness curve and associated 95% confidences intervals for the Northern Indian Margin.

REFERENCES

Hermann, E., Hochuli, P.A., Méhay, S., Bucher, H., Brühwiler, T., Ware, D., Hautmann, M., Roohi, G., ur-Rehman, K. & Yaseen, A. 2011: Organic matter and palaeoenvironmental signals during the Early Triassic biotic recovery: The Salt Range and Surghar Range records. Sedimentary Geology 234, 19-41.

Romano, C., Goudemand, N., Vennemann, T.W., Ware, D., Schneebeli-Hermann, E., Hochuli, P.A., Brühwiler, T., Brinkmann, W. & Bucher, H. 2013: Climatic and biotic upheavals following the end-Permian mass extinction. Nature geosciences 6, 57-60.

Schneebeli-Hermann, E., Kürschner, W.M., Hochuli, P.A., Bucher, H., Ware, D., Goudemand, N. & Roohi, G. 2012: Palynofacies analysis of the Permian–Triassic transition in the Amb section (Salt Range, Pakistan): Implications for the anoxia on the South Tethyan Margin. Journal of Asian Earth Sciences 60, 225-234.

Schneebeli-Hermann, E., Kürschner, W.M., Bomfleur, B., Hochuli, P.A, Ware, D., Roohi, G. & Bucher, H. 2014: Vegetation history across the Permian-Triassic boundary in Pakistan (Amb section, Salt Range), Gondwana Research, http://dx.doi.org/10.1016/j.gr.2013.11.007.

Tozer, E.T. 1994: Canadian Triassic Ammonoid Faunas. Bulletin of the Geological Survey of Canada 467, 1-663.

P 4.1

Woolly rhinoceros from the Pleniglacial of Ajoie (Jura Canton, Switzerland): anatomical description and ecological implications

Damien Becker[1,2], Mélina Dini[3], Laureline Scherler[4]

[1] *Jurassica Museum, route de Fontenais 21, CH-2900 Porrentruy (damien.becker@jurassica.ch)*
[2] *Section d'archéologie et paléontologie, Office de la culture, République et Canton du Jura, Hôtel des Halles, CH-2900 Porrentruy*
[3] *Département des Géosciences, Université de Fribourg, Chemin du Musée 6, CH-1700 Fribourg*
[4] *Institut des Sciences de l'Evolution, Place Eugène Bataillon, Université de Montpellier 2, F-34095 Montpellier*

The Ajoie region (N-W Switzerland) is dotted with numerous dolines, whose Quaternary fillings have regularly yielded megafauna remains dated from the Pleniglacial. The fossil specimens have been transported by biological (predators or scavengers) or physical (solifluction, withdrawing) processes resulting in sorting, abrasion, weathering and concentration of bones and teeth. The mammalian assemblages are dominated by grazing mega- and large herbivores. Previous studies showed that their preferred biotope was open, with low grassy vegetation and tall herbs, but there were also patches with bushes, dwarf shrubs, and scattered trees. There were both fairly damp ground with well-developed soils and drier, somewhat rocky surfaces. This natural environment of wooded tundra-steppe probably developed during relatively temperate interstadials that marked the Pleniglacial (Becker et al. 2009, 2013).

Based on comparative anatomy within late Quaternary Rhinocerotidae, the referred remains are attributed to the classical woolly rhinoceros *Coelodonta antiquitatis*. A detailed ecomorphological analysis underlines a grass-dominated mixed feeder in open habitats of a robust anatomical type. Also, a selective mortality of populations, dominated by breastfed juveniles and young adult and excluding old individuals, is observed on the base of dental wear analysis (Figure 1). Within the local periglacial context in North Alpine domain, woolly rhinoceros from the Pleniglacial of Ajoie seem to be in decline resulting from interspecific competition, low ecological tolerance, probably to the seasonality, and social behaviour rather solitary or in small groups. These results observed at regional scale could illustrate the mechanism of disappearance of woolly rhinoceros occurring in all Northern Eurasia during the terminal Late Glacial (Kuzmin 2010; Stuart & Lister 2012).

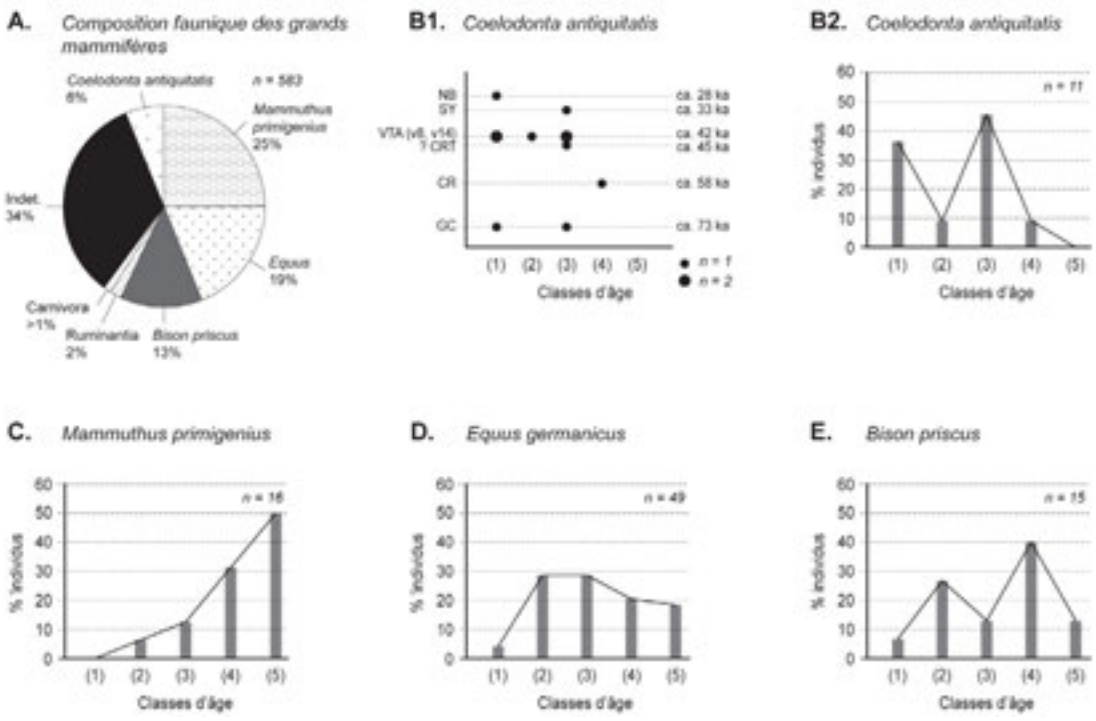

Figure 1. Faunal composition of large mammals recorded in the Ajoie (N-W Switzerland) during the Pleniglacial (**A.**). Mortality histogram of *Coelodonta antiquitatis* d'Ajoie (**B1.**) and age class *vs* remain number distribution per site (**B2.**). Mortality histogram of *Mammuthus primigenius* (**C.**), *Equus germanicus* (**D.**) and *Bison priscus* (**E.**) d'Ajoie (modified after Rothen et al. 2012 and Savoy et al. 2013).

REFERENCES
Becker, D., Aubry, D. & Detrey, J. 2009: Les dolines du Pléistocène supérieur de la Combe de « Vâ Tche Tchâ » (Ajoie, Suisse): un piège à restes de mammifères et artefacts lithiques. Quaternaire, 20, 123-137.
Becker, D., Oppliger, J, Thew, N., Scherler, L., Aubry, D. & Braillard, L. 2013: Climat et écologie en Ajoie durant la seconde partie du Pléniglaciaire moyen weichsélien : apport des remplissages des dolines de Courtedoux–Vâ Tche Tchâ (Jura, Suisse). Annales Littéraires de l'Université de Franche-Compté, 916, and Cahier d'archéologie jurassienne, 21, 13-24.
Kuzmin, Y.V. 2010: Extinction of the woolly mammoth (*Mammuthus primigenius*) and woolly rhinoceros (*Coelodonta antiquitatis*) in Eurasia: review of chronological and environmental issues. Boreas, 39, 247-261.
Rothen, J., Becker D. & Berger, J.-P. 2012: Morphométrie des dents jugales du mammouth laineux (*Mammuthus primigenius*) découvertes dans les remplissages pléistocènes de dolines d'Ajoie (Jura, Suisse). Actes de la Société Jurassienne d'Emulation, Porrentruy, 114, 17-36.
Savoy, J., Scherler, L. & Becker, D. 2013: Variabilité morphologique et biométrique des dents d'*Equus germanicus* des dolines pléistocènes d'Ajoie (Jura, Suisse). Actes de la Société jurassienne d'Emulation, Porrentruy, 115, 17-36.
Stuart, A.J. & Lister, A.M. 2012: Extinction chronology of the wolly *Coelodonta antiquitatis* in the context of late Quaternary megafaunal extinctions in northern Eurasia. Quaternary Science Reviews, 51, 1-17.

P 4.2

New primate material from the Middle Eocene Swiss Site Verrerie de Roches

Raef Minwer-Barakat[1], Judit Marigó[2], Loïc Costeur[3] & Burkart Engesser[3]

[1] *Institut Català de Paleontologia Miquel Crusafont, 08193 Cerdanyola del Vallès, Barcelona, Spain (raef.minwer@icp.cat)*
[2] *Duke University, Department of Evolutionary Anthropology, 27708 Durham, NC, USA*
[3] *Naturhistorisches Museum Basel, CH-4001 Basel, Switzerland*

Excavations carried out in the seventies yielded abundant mammal material of the Middle Eocene Swiss site Verrerie de Roches (Jura, MP16). While Stehlin (1916) and Becker et al. (2013) described about 10 primate teeth from old and new material, the present study adds more than 70 primate teeth to the previously published material.
Most specimens correspond to the genus *Necrolemur* already described from Verrerie de Roches (Stehlin 1916, Becker et al., 2013). A preliminary observation of the material has allowed us to observe that it is smaller than the species *Necrolemur antiquus* and shows a less accentuated enamel wrinkling and less developed conules in the upper molars. On the other hand, it is similar in size and morphology to a still undescribed species from Sant Jaume de Frontanyà-1, north-eastern Spain (Minwer-Barakat et al., 2014). A second microchoerine belonging to genus *Pseudoloris* has been identified at Verrerie de Roches. The presence of this genus there was not known before. The teeth of this primate, much less abundant than *Necrolemur* at this site, seem to be larger than those of *Pseudoloris parvulus*, and probably similar in size to other species such as *Pseudoloris pyrenaicus*, only found in Spain up to date in Sant Jaume de Frontanyà-3. The similarities between the primates from Verrerie de Roches and Sant Jaume de Frontanyà seem to support previous hypotheses considering that the Pyrenean Basins were connected to central Europe during the Middle Eocene. Further study is needed to give a determination at the specific level for the two primates identified at Verrerie de Roches, but the discovery of this rich material already represents a very notable advance in the knowledge of the Swiss Palaeogene primate faunas.

REFERENCES
Becker, D., Rauber, G., Scherler, L. 2013: New small mammal fauna of late Middle Eocene age from a fissure filling at la Verrerie de Roches (Jura, NW Switzerland). Revue de Paléobiologie, 32(2), 433-446.
Minwer-Barakat, R., Marigó, J.& Moyà-Solà, S. 2014: New material of Necrolemur (Microchoerinae, Omomyidae, Primates) from the Middle Eocene of the Pyrennes (Northeastern Spain). American Journal of Physical Anthropology 153, 111.
Stehlin, H.G. 1916: Die Saugetiere des schweizerischen Eozäns, Critischer Catalog der materialien. *Caenopithecus–Necrolemur–Microchoerus–Nannopithex–Anchomomys–Periconodon–Amphichiromys–Hetero–Chiromys–*Nachträge zu *Adapis–*Schlussbetrachtungen zu den Primaten. Schweizerische Paläontologische Abhandlungen, 41, 1299-1552.

P 4.3

Environmental change in central Italy since the Late Pleistocene. The Lake Trasimeno ostracod record.

Marta Marchegiano[1], Elsa Gliozzi[2], Nicoletta Buratti[3], Daniel Ariztegui[1] & Simonetta Cirilli[3]

[1] *Earth & Environmental Sciences, University of Geneva, 13 rue de Maraîchers, 1205 Geneva, Switzerland (marta.marchegiano@unige.ch, daniel.ariztegui@unige.ch)*
[2]*Department of Science, University Roma Tre, Largo S. Leonardo Murialdo 1, 00146 Roma, Italy (elsa.gliozzi@uniroma3.it)*
[3] *Department of Geological Sciences, University of Perugia, Piazza Università 1, 06100 Perugia, Italy (stradott@unipg.it, simocir@unipg.it*

Long terrestrial records such as lacustrine sediments are excellent archives of paleoenvironmental information. While the tectonic evolution of central Italy has been largely studied, there is a clear paucity of paleoenvironmental and paleoclimatic records covering the middle-late Pleistocene. Lake Trasimeno is located in Central Italy (Umbria Region). Previous studies have shown that this presently very shallow (6m maximum water depth) and large lake (surface ~120km^2) was formed at the end of the early Pleistocene during a phase of general uplift in the area. As in most shallow water ecosystems, climate change plays a fundamental role in its evolution. Thus, Lake Trasimeno is an outstanding site to better understand the paleoenvironmental history of this area since the late Pleistocene.

A 175 m long sedimentary core was retrieved by the Geological Survey of the Umbria Region along the present southern shore of the lake (north of the Panicarola town). A multidisciplinary analysis of the lowermost 30 m is now in progress including physical properties, palynology, fossil remains, sedimentological and geochemical analyses. The sediments are relatively uniform comprising mostly green-gray clays with organic matter rich level, occasional sand intervals and evidence of oxidation layers probably caused by desiccation periods. TOC analyses reveal a low content of organic matter except for one level (from 29m to 29.52m) representing sapropel-like sediments. A preliminary age model based on two radiocarbon analysis and an estimation of sedimentation rate suggests that it is possible to bracket the age of the first 30 m of analyzed sediment core between around 140,000 and 21,000 yr.

Ostracod assemblages in lacustrine sediments provide an excellent tool for paleoenvironmental reconstructions. Despite that the Lake Trasimeno sediments are relatively uniform they contain ostracod remains showing distinctive changes. They are constantly present throughout the core except for the organic-rich level at the bottom and from 13 m to the uppermost part of the core that is sterile. The ostracod-rich interval is generally containing mature communities composed of adults and instars. On the whole, 16 species referable to 13 genera were collected (*Ilyocypris gibba, Candona neglecta, Candona angulata, Cypridopsis vidua, Heterocypris salina*, *Limnocythere* sp.2, *Limnocythere stationis, Darwinula stevensoni, Cyprideis* torosa, *Leptocythere* spp., *Fabaeformiscandona fabaeformis, Cyclocypris pigmea, Cyclocypris sp. Pseudocandona juv., Paralimnocythere sp.* and *Cypris subglobosa.*). Conspicuous changes in the abundance of these assemblages have been identified along the studied core alternating sections with very abundant ostracod remains with others with scant (or even null) individuals.

The recovering of species exclusives of certain intervals indicates substantial environmental variations. In particular, the section from 25.60 m to 23.50 m is characterized by a rich ostracod fauna and presence of halophilic species (*Cyprideis torosa and Leptocythere* spp) that suggests an increasing of TDS concentration

The presence of warm (*C. subglobosa*) and cool (*L. stationis*) indicators among ostracods matches very well the temperatures inferred from the marine isotopic curve. In particular, the warm species C. subglobosa inhabited the Trasimeno waters during the Eemian (5e) and the cool species L. stationis lived starting from the beginning of the first phase of the last glacial (isotopic stage 5a-4).

It appears also that the areal extension of the lake was climatically driven. In fact, during the warm and humid climatic phase of the isotopic stage 5, the Trasimeno Lake was wide and rather deep, whereas during the cool and arid stages 4-3 and 2 the lake level decreased drastically, reducing the extension of the lake. The delay observable between the maximum deepening of the lake and the maximum warm climatic phase is probably due to the feedback delay between the lacustrine system and the climate forcing.

P 4.4

A new species of the coastal marine turtle *Thalassemys* Rütimeyer 1873 from the Kimmeridgian of the Swiss Jura Mountains

Christian Püntener, Jérémy Anquetin & Jean-Paul Billon-Bruyat

Section d'archéologie et paléontologie, Office de la culture, République et Canton du Jura, Hôtel des Halles, 2900 Porrentruy, Suisse (christian.puntener@jura.ch)

The genus *Thalassemys* (Thalassemydidae) is represented by *T. hugii* from the Kimmeridgian of Solothurn, Switzerland (Rütimeyer 1873; Bräm 1965) and *T. marina* from the Tithonian of Schnaithaim, Germany (Fraas 1903). The holotype of the type species *T. hugii* consists of a relatively flat and large shell (the largest turtle in Solothurn) with associated postcranial remains. Only a few other remains of *T. hugii* were found in the Solothurn Turtle Limestone, where plesiochelyid turtles are much more abundant (Anquetin et al. 2014).

Excavations in the Kimmeridgian of the Porrentruy area, Jura, Switzerland, brought to light a rich and diverse turtle fauna. As in Solothurn, this new fauna is dominated by the Plesiochelyidae (Anquetin et al. 2014; Püntener et al. 2014). Recently, an almost complete shell was found in Porrentruy, showing several anatomical similarities with *T. hugii* : a relatively flat and large carapace; a strong widening of the first neural; presence of linear striations perpendicular to sutures; presence of costo-peripheral fontanelles; and presence of central and notably lateral plastral fontanelles. While these features allow a confident attribution of this specimen to *Thalassemys*, other features differ strongly from *T. hugii* : a thickening of the nuchal; wider vertebral scales; a proportionally larger plastron; a different shape and orientation of the xiphiplastron; and a wider angle between the scapular and acromion processes.

The reported specimen is interpreted as belonging to a new species of *Thalassemys*. It reveals that the Thalassemydidae were more diverse than previously thought during the Kimmeridgian. In order to better understand the palaeobiogeographic distribution of these Late Jurassic turtles, comparisons will be extended with two yet undescribed specimens of *Thalassemys* from the Kimmeridgian of England.

REFERENCES

Anquetin, J., Püntener, C. & Billon-Bruyat, J.-P. 2014: A taxonomic review of the Late Jurassic eucryptodiran turtles from the Jura Mountains (Switzerland and France). PeerJ 2, e369.

Bräm, H. 1965: Die Schildkröten aus dem oberen Jura (Malm) der Gegend von Solothurn. Schweizerische Paläontologische Abhandlungen 83, 1-190.

Fraas, E. 1903. *Thalassemys marina* E. Fraas aus dem oberen weissen Jura von Schnaitheim nebst Bemerkungen über die Stammesgeschichte der Schildkröten. Jahreshefte des Vereins für vaterländische Naturkunde in Württemberg 59, 72-104.

Püntener, C., Billon-Bruyat, J.-P., Bocat, L., Berger, J.-P. & Joyce, W. G. 2014: Taxonomy and phylogeny of the turtle *Tropidemys langii* Rütimeyer, 1873 based on new specimens from the Kimmeridgian of the Swiss Jura Mountains. Journal of Vertebrate Paleontology 34, 353-374.

Rütimeyer, L. 1873: Die fossilen Schildkröten von Solothurn und der übrigen Juraformation. Neue Denkschrift der allgemeinen schweizerischen naturforschenden Gesellschaft 25, 1-185.

P 4.5

Testing the EBSD Method on Mammal Enamel

Valentine Savary[1] & Bastien Mennecart[2]

[1] *Department of Geosciences – Earth Sciences, University of Fribourg, Chemin du Musée 6, CH-1700 Fribourg (valentine.savary@unifr.ch)*
[2] *UMR 7207 (CNRS, MNHN, UPMC), Muséum National d'Histoire Naturelle, 8 rue Buffon, CP 38, F-75231 Paris, France*

The microstructure of enamel, the hard outer tissue of teeth, is known to reflect phylogenetic relationships and dietary preferences in mammals (Ungar 2010). The enamel of mammals is organised in five levels of complexity (Koenigswald & Clemens 1992). The most basal of these is the crystallite level, which is formed by hydroxyapatite crystals in varying orientations. Until now, the organisation of enamel at all levels was studied only through visualisations and morphological descriptions (Stefen 1997, Maas & Dumont 1999), but quantitative methods have not yet been applied.

Here we are presenting a new quantitative method that characterizes the preferential orientation of hydroxyapatite crystals in enamal at the crystalite level using Electron Backscatter Diffraction (EBSD). For this purpose, teeth of extant mammals are heated to 1000° C to remove organic matter and to increase the size of the hydroxyapatite crystals they contain. The samples are then mechanically and chemically polished to enable obtaining orientational measurements of the crystallites across the entire enamel layer using a scanning electron microscope. The primary data is then converted into a crystal orientation map using the EBSD method. This highlights regional differences in preferential crystal orientation within a defined enamel area. These maps can secondarily be converted into pole figures.

As a first step we are quantifying the crystallite orientation of a broad sample of mammals (e.g. wolf, dog, fox, cat, badger) to test for inter- and intraspecific variation. We hope this method will one day allow further characterizing the phylogenetic relationships and ecological preferences of fossil mammals.

REFERENCES

Koenigswald, W. von, & Clemens, W. A. 1992: Levels of complexity in the microstructure of mammalian enamel and their application in studies of systematics, Scanning Microscopy, 6, 195-218.

Maas, M. C., & Dumont, E. R. 1999: Built to last: The structure, function, and evolution of primate dental enamel, Evolutionary Anthropology, 8, 133-152.

Stefen, C. 1997: Differentiations in Hunter-Schreger bands of carnivores. In: Tooth Enamel Microstructure (Ed. by Koenigswald, W. von & Sander, P. M.), A.A. Balkema, Rotterdam, p. 123–136.

Ungar, P. S. 2010: Mammal Teeth: Origin, Evolution and Diversity.The John Hopkins University Press, Batimore, 312 pp.

5. Stratigraphy in Switzerland - new data and developments

Alain Morard, Reto Burkhalter, Oliver Kempf & Ursula Menkveld-Gfeller

Swiss Commitee for Stratigraphy (SKS/CSS),
Swiss Palaeontological Society (SPG/SPS),
Swiss Geological Survey – swisstopo

TALKS:

5.1 Jordan P.: Gliederung der Trias, des Perms und des Karbons in der Nordschweiz

5.2 Reisdorf A. G., Hostettler B., Feist-Burkhart S., Waltschew A., Bläsi H., Jaeggi D., Deplazes G., Morard A., Menkveld-Gfeller U..: Litho-, Bio- and Chronostratigraphy of the Staffelegg Formation, Opalinus-Ton, Passwang Formation and Hauptrogenstein of the Mont Terri Rock Laboratory, Canton Jura, Switzerland.

5.3 Wohlwend S. & Weissert H.: New insigths from the northern Helvetic Seewen Formation (Eastern Switzerland) - Sedimentological and Chemostratigraphical correlation.

POSTERS:

P 5.1 Rauch A., Sartori M.: Stratigraphic and structural relationships between ophiolite body and sedimentary cover at Piz Mundin (Lower Engadine Window, GR, CH).

P 5.2 Morard, A.: Correlations beyond HARMOS: how, where, why?

5.1

Gliederung der Trias, des Perms und des Karbons in der Nordschweiz

Peter Jordan[1,2]

[1] *Geologisch-Paläontologisches Institut, University of Basel, Bernoullistrasse 32, CH-4056 Basel (peter.jordan@unibas.ch)*
[2] *Gruner Böhriner AG, Mühlegasse 10, 4104 Oberwil (peter.jordan@gruner.ch)*

Im Rahmen der Revision der stratigraphischen Einheiten der Schweiz (HARMOS) wurden die spät-paläozoischen und früh-mesozoischen Ablagerungen der Nordschweiz neu gegliedert.

Die Gliederung basiert auf älteren stratigraphischen Arbeiten und berücksichtigt die Neugliederung der entsprechenden Einheiten im angrenzenden süddeutschen Raum. Mangels aktueller Aufschlüsse beziehen sich die Typuslokalitäten auf ältere Aufnahmen von Profilen, die teilweise schon damals unvollständig waren und heute oft nicht oder nur beschränkt zugänglich sind. Alle Formationen wurden deshalb durchwegs auch anhand gekernter Strecken der Nagra-Tiefbohrungen definiert. Diese Referenzprofile sind umfangreich dokumentiert und dank Konservierung der Kerne der Wissenschaft für weitere Untersuchungen zugänglich. Zum besseren Verständnis wurden in zwei Formationen je ein Member definiert. Für eine Formation wird informell eine Gliederung vorgeschlagen. Die formelle Definition dieser Gliederung wie auch die Gliederung der übrigen Formationen wird späteren Bearbeitern überlassen.

Die Neugliederung ergibt sich aus Fig. 1. Dabei entspricht die Klettgau-Formation dem vormaligen «Mittlelkeuper» (ohne «Gipskeuper») inklusive «Rhät», welches neu als Belchen-Member definiert wird. Informell vorgeschlagen wird die Unterteilung der restlichen Formation in Hemmiken- (1. regressiver Zyklus: „Schilfsandstein“ - „untere bunte Mergel“), Gansingen- (2. Zyklus: „Gansingen Dolomit“ - „obere Bunte Mergel“), Seebi- (3. Zyklus: „Stubensandstein“) und Gruhalden-Member (4. Zyklus: „Knollenmergel“). Die Bänkerjoch-Formation ersetzt den «Gipskeuper». Die Schinznach-Formation beschreibt den Abschnitt vom «Hauptmuschelkalk» bis zur «Lettenkohle». Letztere wird neu als Asp-Member beschrieben. Die «Anhydritgruppe» wird zur Zeglingen-Formation und das «Wellengebirge» zur Kaiseraugst-Formation. Die Dinkelberg-Formation umfasst den «mittleren und oberen Buntsandstein».

Die Formationen des Perms und Karbons wurden kürzlich von Nitsch & Zerleder (2009) in ihrer typischen Ausprägung am Hochrhein neu definiert. Diese Formationen können zur Beschreibung der Verhältnisse im kleinen Ausstrichgebiet und in den Bohrungen der Nordschweiz übernommen werden. Dabei entspricht die Wiesental-Formation dem oft irrtümlich als «unterer Buntsandstein» oder «oberstes Rotliegendes» beschriebenen Abschnitt, der gemäss Nitsch & Zerleder (2009) mit der Zeichstein-Gruppe weiter nördlich korreliert werden kann. Die Weitenau-Formation fasst die Abfolge «Unterer Schuttfächer» – «Playa-Serie» – «Oberer Schuttfächer» (inkl. «diagonal geschichteter Sandstein») und die Weiach-Formation die darunter liegenden See- sowie älteren und jüngeren Flussablagerungen.

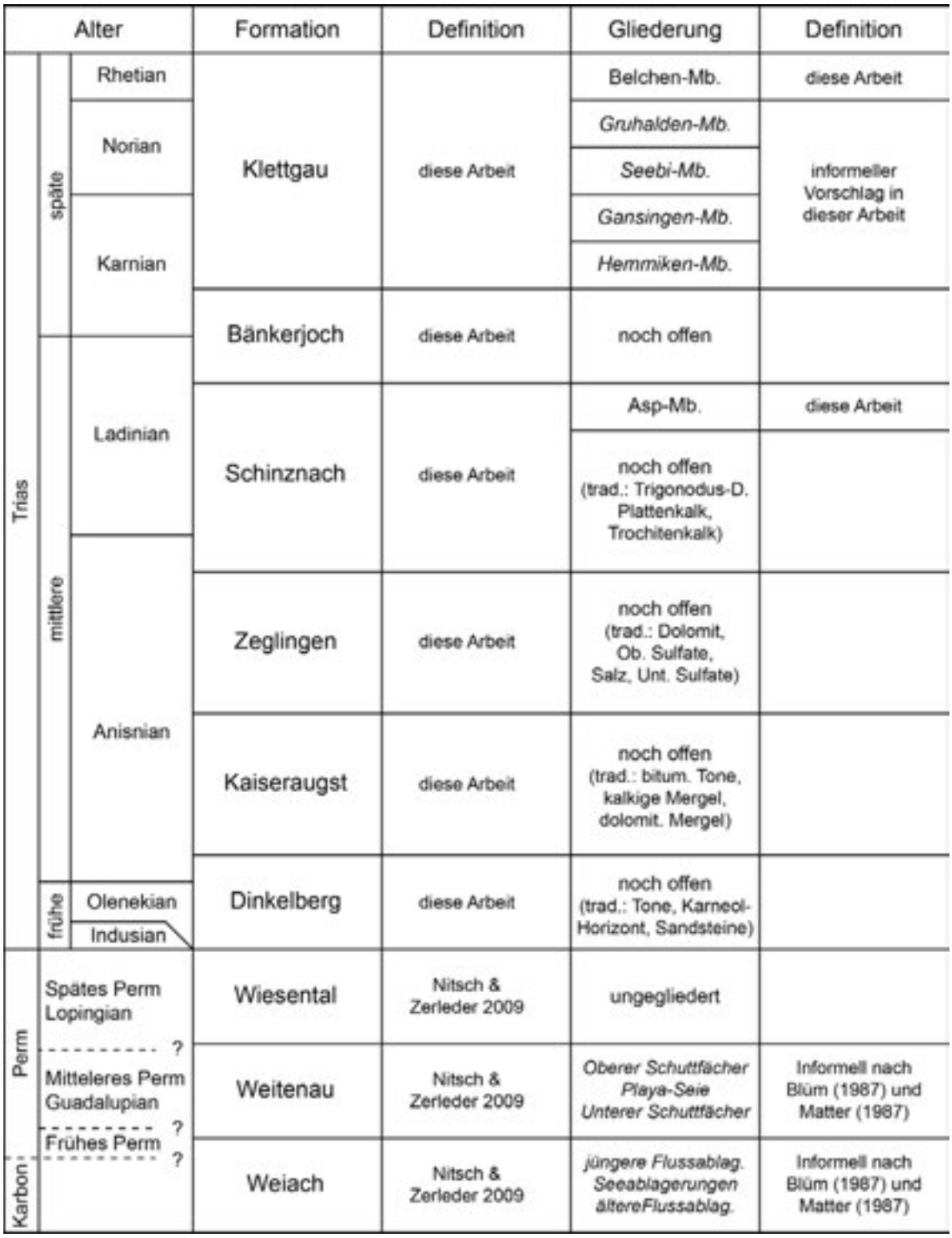

Figur 1. Gliederung der Trias, des Perms und des späten Karbons in der Nordschweiz

REFERENZ

Nitsch, E. & Zedler, H. (2009): Oberkarbon und Perm in Baden-Württemberg. – LGRB-Informationen, 22: 7–102; Freiburg i.Br.

5.2

Litho-, Bio- and Chronostratigraphy of the Staffelegg Formation, Opalinus-Ton, Passwang Formation and Hauptrogenstein of the Mont Terri Rock Laboratory, Canton Jura, Switzerland

Achim G. Reisdorf[1,2], Bernhard Hostettler[1], Susanne Feist-Burkhardt[3], Anton Waltschew[4], Hansruedi Bläsi[5], David Jaeggi[6], Gaudenz Deplazes[7], Alain Morard[8] & Ursula Menkveld-Gfeller[1]

[1] *Naturhistorisches Museum der Burgergemeinde, Bernastrasse 15, CH-3005 Bern*
[2] *Geologisch-Paläontologisches Institut, University of Basel, Bernoullistrasse 32, CH-4056 Basel (achim.reisdorf@unibas.ch)*
[3] *SFB Geological Consulting & Services, Odenwaldstrasse 18, D-64372 Ober-Ramstadt, Germany*
[4] *Nürnberg, Germany*
[5] *Institute of Geological Sciences, University of Bern, Baltzerstrasse 1 + 3, CH-3012 Bern*
[6] *Mont Terri Consortium, Swisstopo, Fabrique de Chaux, Rue de la gare 63, CH-2882 St-Ursanne*
[7] *Nagra, Hardstrasse 73, CH-5430 Wettingen*
[8] *Swiss Geological Survey, Federal Office of Topography swisstopo, Seftigenstrasse 264, CH-3084 Wabern*

In a collaborative project of swisstopo, NAGRA, and the Naturhistorisches Museum der Burgergemeinde Bern, new data on lithostratigraphy, biostratigraphy, and sedimentology were obtained at the Mont Terri rock laboratory. This multidisciplinary study was carried out on the core of borehole BDB-1, which was drilled in December 2013 and January 2014.

Starting at the lowermost part of the Hauptrogenstein, borehole BDB-1 intersected the Passwang Formation and the Opalinus-Ton. The drilling terminated at the topmost layers of the Rietheim Member (formerly "Posidonienschiefer") of the Staffelegg Formation. Several partial sections of the Passwang Formation (La Mâlcote section, Sous les Roches section) of the Mont Terri area are included in the study. These sections served as orientation during the drilling process and were used for the lithographic subdivision of the core (e.g., delimitation between the Passwang Formation and the Opalinus-Ton; identification of prominent beds of the Passwang Formation). They also provided valuable biostratigraphic data (ammonites).

The analysis of the sedimentological (micro- and macrofacies) and palaeontological contents made possible a stratigraphic classification of the Opalinus-Ton and the overlying and underlying formations in a detail never before achieved for the Mont Terri area. Biostratigraphic dating is based on ammonites, foraminifera, ostracods, and palynomorphs. The greatest biostratigraphic correspondence was found between ammonites and palynomorphs.

The facies, thickness, as well as litho- and chronostratigraphy of the studied formations have a greater correspondence with findings from the adjacent areas in France and Germany than with those occurrences farther eastward in northern Switzerland (e.g., Reisdorf et al. 2014). In this context it is especially remarkable that the lowest 30 meters of the ca. 130-meter-thick Opalinus-Ton in the Mont Terri rock laboratory can be assigned chronostratigraphically to the Late Toarcian. Moreover, several of the lithographic units defined in the type area of the Passwang Formation (Hauenstein, Hirnichopf, Waldenburg, and Rothenfluh Members) could not be identified in the Mont Terri area (Burkhalter 1996; Jordan et al. 2008), even though according to the biostratigraphic data, sediments of the same age as these were found.

REFERENCES

Burkhalter, R.M. 1996: Die Passwang-Alloformation (oberes Aalenien bis unteres Bajocien) im zentralen und nördlichen Schweizer Jura. Eclogae geologicae Helvetiae, 89(3): 875–934.

Jordan, P., Wetzel, A. & Reisdorf, A.G. 2008: Jurassic. Swiss Jura Mountains. In: The Geology of Central Europe. Volume 2: Mesozoic and Cenozoic (Ed. by McCann, T.). Geological Society, pp.: 880–889; London.

Reisdorf, A.G., Hostettler, B., Waltschew, A., Jaeggi, D. & Menkveld-Gfeller, U. 2014: Biostratigraphy of the Basal Part of the Opalinus-Ton at the Mont Terri rock laboratory, Switzerland. Technical Report TR2014-07, August 2014, SO (Sedimentology of the Opalinus-Ton), 23 pp. + appendix.

5.3

New insights from the northern Helvetic Seewen Formation (Eastern Switzerland) - Sedimentological and Chemostratigraphical correlation

Stephan Wohlwend[1] & Helmut Weissert[1]

[1] *Geologisches Institut, ETH Zürich, Sonneggstrasse 5, CH-8092 Zürich (stephan.wohlwend@erdw.ethz.ch)*

Three Cenomanian/Turonian pelagic limestone sections of Northern Tethyan origin were studied at high resolution to gain a better understanding of the highly variable sedimentation and oceanography during Late Cretaceous. They all belong to the northern Helvetic Seewen Formation (Churfirsten-Säntis nappe). These sections (Chäserrugg, 32 m; Strichboden, 16 m and Kamor, 29 m) were sampled in 10 cm spacing for sedimentological and stable carbon- and oxygen-isotope investigations. The new C-isotope stratigraphy shows that correlation with other reference curves of the Cenomanian and Turonian intervals is possible.

We document in all three sections in the lower Seewen Fm the isotopically defined OAE 2 during the Cenomanian/Turonian Boundary Event (CTBE). The distinct boundary intervall can be found in all sections in a different stratigraphic level because of a diachronous base of the pelagic Seewen Limestone. However the oceanographic response of the OAE2 can be traced by a glauconite/quarz rich sand layer from the Vorarlberg westward into the Churfirsten. We explain the sediment transport process by a ocean current intencification during the OAE2.
Further we show that the first and most prominent Red Seewen Limestone intervall, about 10m above the CTBE, allways occures at the same stratigraphic level during a sharp negative shift of the $\delta^{13}C$ record in the Middle Turonian. This reddish intervall can be traced throug the most distal Helvetic nappes from the Vorarlberg into the Central Switzerland area. In the Churfirsten the distribution of the Red Seewen Limestone is approximatly similar to the one of the deep water stromatolithes which can be found in the top of the underlaying Garschella Fm (Ouwehand 1987). Therefore, with all these informations (stromatolithes, ocean current and oxygen rich bottom water) a regional paleotopography model for the Churfirsten area can be reconstructed at the edge of the Helvetic shelf during the Late Cretaceous time.

REFERENCES

Ouwehand, P. 1987: Die Garschella-Formation ("Helvetischer Gault", Aptian-Cenomanian) der Churfirsten-Alvier Region (Ostschweiz) Sedimentologie, Phosphoritgenese, Stratigraphie. Dissertation an der Eidg. Technischen Hochschule Zürich.

P 5.1

Stratigraphic and structural relationships between ophiolite body and sedimentary cover at Piz Mundin (Lower Engadine Window, GR, CH)

Anna Rauch[1], Mario Sartori[1]

[1] *Section des sciences de la Terre et de l'environnement, University of Geneva, Rue de Maraîchaire 13, CH-1205 Genève (anna.rauch@etu.unige.ch)*

In the Lower Penninic units (Bündnerschiefer) of the Lower Engadine Window (Graubünden, Eastern Switzerland-Western Austria), several ophiolite bodies have been described in the literature. The largest ophiolite body, constituted exclusively of meta-pillow lavas, is situated in the centre of the window at Piz Mundin. Former alpine oceanic domains (especially the Valais Domain) still stimulate lively debates about their extension and timing. Moreover, very few metabasalts of alpine age associated to Lower Penninic units, and thus to the Valais Domain, are found within the Alps. Therefore, the metabasalts of the Mundin area and the overlying metasediments were investigated in order to expand the information related to the alpine ocean controversy. In this study, the stratigraphy of the area is analysed and compared to other Valais Domain occurrences of the Western Alps.

Based on detailed mapping and outcrop logging, a new stratigraphy is established. Generally, the sedimentary sequence is virtually in perfect correlation (in terms of lithology) with the typical Lower Penninic sequence, the 'Valais Trilogy', considered as Cretaceous to Tertiary in age. At the bottom of the sequence, a massive marble containing breccia-layers represents similar lithological characteristics as the *'Aroley Beds'*. A black schist with fine greenish-quartzite intercalations overlays the marble, very similar to the *'Marmontains Beds'*. Finally, the detrital input gets more important so that calcareous metasandstone beds dominate within a black schist matrix, which is also observed within the *'St. Christophe Beds'*. Curiously, the sequence rests partially on a siliceous, fissile purple schist, which is identified through geochemical data as radiolarian chert or clay deposit. In other parts of the area, the Valais Trilogy lies directly on the metabasalt. The lack of continuity of the radiolarites may have structural cause or it may represent an unconformity, the contact from metabasalt to metasediments being very likely stratigraphic. This is the first documentation of radiolarite deposits associated with typical Lower Penninic units. These new observations will have an impact on further alpine ocean domain analyses, provided that at some point in the future ages of the metabasalts or metaradiolarites can be determined.

P 5.2

Correlations beyond HARMOS: how, where, why?

Alain Morard[1]

[1] *Swiss Geological Survey (SGS), Federal Office of Topography swisstopo, Seftigenstrasse 264, CH-3084 Wabern*

Thanks to the scientific expertise and commitment of more than 40 experts, a new lithostratigraphic framework with standard legends is now available for the Geological Atlas of Switzerland 1:25 000 (see www.stratigraphie.ch for the description of the units and the correspondence with obsolete terminology). The next challenging task for the Swiss Geological Survey will be the nationwide application of these harmonised legends to the GIS datasets, and thus revising of all published map sheets and GeoCover datasets. This will simultaneously represent a large-scale test for the newly established lithostratigraphic chart.

Despite this major achievement, four fundamental correlation issues need to be further addressed:

- Lithostratigraphic correlation with the charts of neighbouring countries: Germany [DSK 2002], Austria [ÖSK 2004], Italy and France (work in progress). A number of lithostratigraphic terms are used in common (e.g. Allgäu-Fm.) and further correlations are already indicated as lateral equivalents in the Lithostratigraphic Lexicon of Switzerland (www.stratigraphie.ch).

- Incorporation of correlation criteria for subsurface geology: most of the distinguishing features of the lithostratigraphic units derive from field observations. Microscopic characteristics and other potential indicators (geochemistry, geophysics, …) need to be added to the definition of the units in order to set the corresponding lithostratigraphic boundaries in drill cores.

- Refinement of the bio/chronostratigraphic constraints: detailed biostratigraphic data, as well as precise age determinations with other relative and asolute dating methods, are needed to further constrain the time frame of the lithostratigraphic units. Only by the combination of descriptive lithostratigraphy and robust independent age determinations will it be possible to resolve controversial genetic interpretations (including sequence stratigraphy).

- Time-based correlations across the different tectonic domains and comparisons between the individual rock units (also in basement areas): this step will ultimately help improving the paleogeographic reconstructions for successive time intervals.

We are looking forward to the upcoming challenges and count on the valuable collaboration with the geoscientific community in the fields of regional geology and stratigraphy. Although the elaboration of a new lithostratigraphic framework led to the clarification of many correlation problems, it also raised a series of new questions and especially pointed out our lack of knowledge for some crucial places and time intervals.

REFERENCES

DSK (Deutsche Stratigraphische Kommission, Hrsg.) 2002: Stratigraphische Tabelle von Deutschland 2002. [see also http://www.bgr.de/app/litholex/]

ÖSK (Österreichische Stratigraphische Kommission und Kommission für die paläontologische und stratigraphische Erforschung Österreichs der Österreichischen Akademie der Wissenschaften) 2004: Stratigraphische Tabelle von Österreich 2004 (sedimentäre Schichtfolgen). [see also http://resource.geolba.ac.at/GeologicUnit.html]

6. Geophysics and Rockphysics

Marcel Frehner, Klaus Holliger

Swiss Geophysical Commission

TALKS:

6.1 Lengyel B., Turberg P., Baumgartner L.: Non-destructive 3D characterization of concrete alteration by X-ray micro-CT and correlation with petrographic and geotechnical properties

6.2 Madonna C., Pini R.: Moving across scales: An Assessment of X-ray CT to quantify reservoir rock properties

6.3 Michlmayr G., Chalari A., Clarke A., Breitenstein D., Wunderli H., Lehmann P., Fan L., Or D.: Fiber-optic based measurements of acoustic and microseismic emissions for early warning of rapid mass movements

6.4 Pellet C., Hilbich C., Python S., Daengeli S., Hauck C.: Quantitative estimation of ice and water content in mountainous terrains using ERT and RST measurements

POSTERS:

P 6.1 Bakker R.R., Violay M.E.S., Benson P.M., Vinciguerra S.C.: Volcanoes with carbonate basements: Understanding basement deformation and degassing phenomena

P 6.2 Hauck C., Hilbich C.: Applicability of petrophysical relationships to quantify subsurface ice and water contents from geophysical measurements in mountain and polar regions

P 6.3 Heck M., van Herwijnen A., Schweizer J., Fäh D.: Automatic detection of avalanches in seismic data using Hidden Markov Models

P 6.4 Lupi M., Kenkel J., Fuchs F., Ricci T., Suski B., Miller S.A.: Effects of remote earthquakes at the Nirano Mud Volcanic Field: Insights from geophysical studies

P 6.5 Shih P.-J. R., Frehner M.: Laboratory evidence for Krauklis wave resonance in fractures

P 6.6 Subramaniyan S., Madonna C., Quintal B., Saenger E. H.: Seismic attenuation in sandstones

P 6.7 Violay M., Burg J.-P.: Experimental measurements of dilatancy and permeability evolution during triaxial compression of micro-gabbro and implications for hydrothermal circulation at the mid ocean ridge

6.1

Non-destructive 3D Characterization of Concrete Alteration by X-ray micro-CT and Correlation with petrographic and geotechnical Properties

Barbara Lengyel[1], Pascal Turberg[2], Lukas Baumgartner[1]

[1] *Institut des sciences de la Terre, University of Lausanne, Quartier UNIL-Mouline, Bâtiment Géopolis, CH-1015 Lausanne (blengyel@unil.ch)*
[2] *Laboratoire des systèmes écologiques, Ecole polytechnique de Lausanne, EPFL ENAC IIE ECOS, GR B2 402 (Bâtiment GR), Station 2, CH-1015 Lausanne*

Concrete is a most important geomaterial as it is used for a large part in our buildings and infrastructures. According to Planetoscope (2012) its production is about 6 billion m^3 per year (190 m^3 each second) which makes it the most used manufactured material in the world. The alteration of concrete, tightly associated with the durability and security of our infrastructures, depends on its primary composition (Kovler & Roussel 2011; Bérubé 2001) but also on a wide range of environmental factors (mechanical solicitations, freezing-thawing cycles, alkali-aggregate reactions, etc.) (Swamy 1997). Hence, the contribution of geological or geological-related analysis to understand concrete alteration processes is required because this material is mainly composed of aggregates made of different minerals and rocks, the type and quality of which are important due to their influence on concrete behaviour.

In this study, high resolution X-ray Computed tomography (X-ray micro-CT) was used to image 3D different types of concrete cores in order to characterize their respective state of alteration. The global alteration index (GAI) developed by Christe et al. (2010) for natural cataclastic rocks was applied to the segmented X-ray CT images of these concrete cores and compared to the results of microstructural analysis on thin slices and of compression tests. Also, an internal attack of concrete by hydrochloric acid was carried out in laboratory to simulate artificial alteration through carbonate dissolution and its process was monitored along time by X-ray micro-CT imaging (4D monitoring).

Our first results show that X-ray CT imagery enables, without any destruction of the specimens, to characterize concrete internal features in terms of macroporosity, highly microporous cement paste, standard cement paste or aggregates. In particular, initial entrapped porosity as well as cracks are easily detected, characterised and quantified before and after mechanical testing.

Petrographic analyses on thin sections enabled to verify the physical meaning of the X-ray CT-based detected features, such as the highly microporous cement paste, the opening of the microcracks and the detachment halos around aggregates which all act as weakening parameters.

Despite the limited number of samples, a coherent relation between the GAI and the compressive strength of the concrete specimens is observed as the concrete compressive strength clearly decreases when the GAI increases. In this case, it logically means that the concrete with a higher porosity is less resistant. Moreover, the 4D monitoring of the acidic attack test led to dynamically show how the carbonated structure of the concrete was progressively altered.

These preliminary results demonstrate that GAI, based on XRCT imagery analysis, can be used to evaluate the degree of alteration of concrete and could thus lead to estimate its strength. In more general terms, X-ray CT analysis opens new perspectives to relate the quality of concrete with its mechanical properties. This method could probably be further applied to a wide range of problems related to the inspection and maintenance of concrete infrastructures.

REFERENCES

Bérubé, M.A. 2001: The Mineralogical and Petrographic Analysis of Concrete Aggregates, Journal of Mineralogy 53 (12), 45-47.

Christe, P., Turberg, P., Labiouse, V., Meuli, R. & Parriaux, A. 2010: An X-ray computed tomography-based index to characterize the quality of cataclastic rock samples, Engineering Geology (2011), 180-188.

Kovler, K. & Roussel, N. 2011: Properties of fresh and hardened concrete, Cement and Concrete Research 41, 775-792.

Planetoscope 2012 : Production mondiale de béton [Web page]. Available on www.planetoscope.com (consulted on 03.12.2014).

Swamy, R.N. 1997: Assessment and Rehabilitation of AAR-affected Structures, Cement and Concrete Composites 19, 427-440.

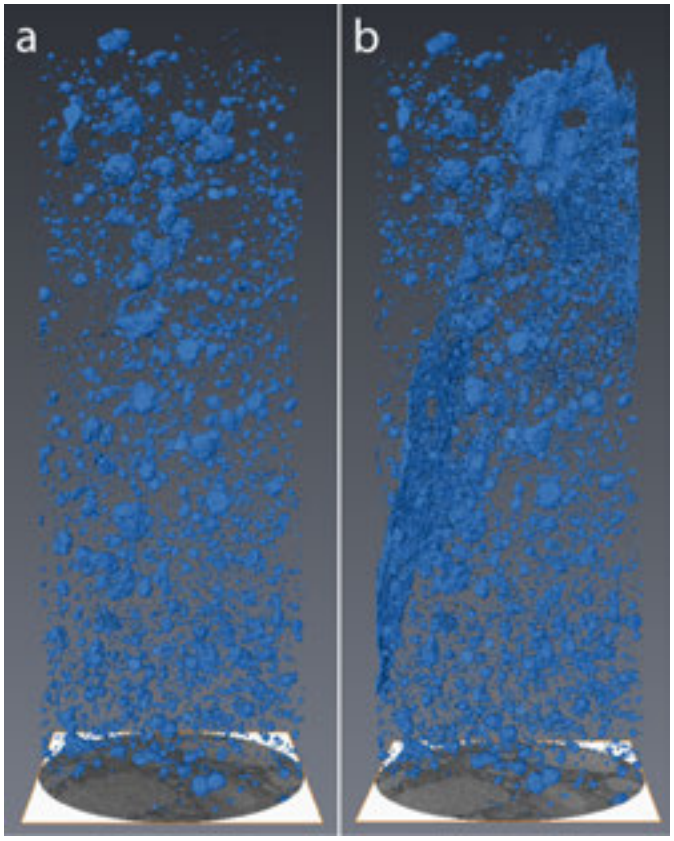

Figure 1. Volume rendering of the macroporosity (a) before and (b) after the mechanical test for the sample AR52-03-05. Diameter = 36.27 mm.

6.2

Moving across Scales: an Assessment of X-ray CT to quantify Reservoir Rock Properties

Claudio Madonna[1] & Ronny Pini[2]

[1] *Geological Institute, ETH Zurich, Sonneggstrasse 5, CH-8092 Zurich (claudio.madonna@erdw.ethz.ch)*
[2] *Petroleum Engineering Department, Colorado School of Mines, 1600 Arapahoe Street, Golden, CO 80401*

Making accurate predictions of fluid distribution within reservoir rocks requires making measurements at the full range of relevant spatial scales, thus covering all the steps from the pore- up to the continuum-scale. Imaging techniques have the potential to dramatically increase our ability to make such observations, but the gap existing between measurements performed at various scales has restricted our ability to fully take advantage of this technology. This "missing-scale" problem is the subject of this study. We have applied multidimensional Computed Tomography (CT) to quantify the porosity of rocks by using both medical- and synchrotron-based x-ray radiation, so as to produce images of the same sample with mm- and micron-resolution, respectively. Samples of Berea Sandstones have been used and the independently obtained 3D porosity reconstructions have been successfully compared in terms of both average and spatially distributed patterns. It is shown that this approach has a dual benefit: first, informed decisions can be made on the segmentation of the micron-resolved images, this process being a key component of any Digital Rock Physics application. At the same time, the establishment of experimental protocols that link pore- and core-scale observations provides the required point of departure for developing up-scaling approaches that capture the inherently complex heterogeneity of rocks.

6.3

Fiber-optic based measurements of acoustic and microseismic emissions for early warning of rapid mass movements

Gernot Michlmayr[1], Athena Chalari[2], Andy Clarke[2], Daniel Breitenstein[1], Hans Wunderli[1], Peter Lehmann[1], Linfeng Fan[1] & Dani Or

[1] *Departement of Environmental Systems Science, ETH Zürich, Universitätstrasse 16, CH-8092 Zürich (gernot.michlmayr@env.ethz.ch)*
[2] *Silixa Ltd., 230 Centennial Park, WD6 3SN Elstree (United Kingdom)*

Rapid mass movements such as landslides, rock falls or debris flows present important geomorphological processes that shape landscapes in hilly and mountainous terrain. At the same time rapid mass movements may become a serious threat for infrastructure and human life. Significant scientific effort has been made to investigate the physical mechanisms that govern the triggering of such events. In the context of mass release early warning the understanding of triggering processes bears a great value for natural hazard protection. In this work we seek to complement existing tools for investigation and early warning of mass movements with fiber-optic based acoustic emission measurements. This method allows to detect elastic waves as precursors of slope failure at a tremendous spatial resolution (10^-0 meter scale) along a fiber optical cable. Such elastic waves are often referred to as acoustic emissions (AE) respectively microseismicity (MS) and have frequencies in the range of 10^3 – 10^6 Hz. AE/MS are released from micro-failure events that involve the formation of a shear zone and may culminate in slope collapse. A close relation between the accumulation of micro-failure and observed AE has been shown in earlier work (Michlmayr et al. 2013). Until recent the widespread application of conventional AE/MS technology was hampered by the restrictions imposed by strong signal attenuation in geologic materials, particularly in sediments and soils. Novel fiber-optic technology provides an unparalleled spatial resolution so that AE signals may be detected even if attenuation does not allow them to propagate far.

We triggered small landslides in an artificial channel (3m x 0.5m x 0.5m) filled with alluvial sediment by application of strong surface precipitation. Progressive failure development was monitored using hydrological measurements, piezoelectric AE sensors and fiber-optic AE monitoring. Video cameras were installed for visual inspection of material surface deformations. Our tests provide us with detailed insights of the failure development and its hydrological and acoustic signature. AE captured at different locations within the material are attributed to the propagation of a slip surface. Gradual surface deformation and an increasing water saturation of the material preceded the landslide event. Such phases of creep were marked by an elevated acoustic emission activity. At the imminence of terminal failure we typically observed water saturation at the channel bottom and a dramatic acceleration of generated AE signals.

Morphological and hydrological observations of the material confirmed a realistic failure process in our experimental setup. Time-lapse photography revealed significant creep deformation prior to failure events even before hydrological priming of the material was completed and the system was prone to landslide release. Fiber-optic AE measurements deliver a possibility to detect elastic waves as indications of ongoing failure at a high spatial resolution. Fiber-optic and conventional acoustic emission measurements both delivered a consistent picture of the failure mechanism.

We found that novel fiber-optic acoustic emissions measurements may provide a powerful means for the detection, early-warning and investigation of landslides and other rapid mass movements. Complementing existing monitoring technologies this method may become an important building block for natural hazard prevention and research.

REFERENCES

Michlmayr, G., Cohen, D. & Or D. 2013: Shear-induced force fluctuations and acoustic emissions in granular material, Journal of Geophysical Research-Solid Earth, 118/12, 6086-6098.

6.4

Quantitative estimation of ice and water content in mountainous terrains using ERT and RST measurements

Cécile Pellet[1], Christin Hilbich[1], Samuel Python[1], Susanne Daengeli[1] & Christian Hauck[1]

[1] *Department of Geosciences, University of Fribourg, Chemin du Musée 4, CH-1700 Fribourg (cecile.pellet@unifr.ch)*

The use of geophysical methods in the field of permafrost research is well established and crucial since it is the only way to infer the composition of the subsurface material. Since geophysical measurements are indirect, ambiguities in the interpretation of the results can arise, hence the simultaneous use of several methods (e.g. electrical resistivity tomography and refraction seismics) is often necessary.

The so-called four-phase model, 4PM (Hauck et al., 2011) constitutes a further step towards clarification of interpretation from geophysical measurements. It uses two well-known petrophysical relationships, namely Archie's law and an extension of Timur's time-averaged equation for seismic P-wave velocities, to quantitatively estimate the different phase contents (air, water and ice) in the ground from tomographic electric and seismic measurements. This model depends on several parameters, the most sensitive and difficult to assess being the porosity. Two approches are currently used to solve the model: (1) assumption of a porosity model from borehole logs or expert knowledge which is then used for the calculation of the remaining phase contents or (2) assumption of unfrozen conditions where applicable, solving for the remaining three phases (water, air, rock, the so-called 3-phase model), and using the obtained porosity distribution as input parameter for a subsequent application of the full 4PM.

In this study we will present the application of the 4PM with different porosity models to several study areas distributed accross the western Alps and the Jura mountains. To test the accuray of the model in various situations, we selected six locations (Schilthorn, Stockhorn, Cervinia, Gemmi, Dreveneuse and Frétaz) with very different surface and subsurface properties as well as ground thermal regimes. The datasets used here were collected as part of the SNF-project SOMOMOUNT, which among others aims at using innovative geophysical methods to determine the spatial distribution of unfrozen water content in the ground, as well as monitoring its temporal evolution. Therefore, spatial and temporal soil moisture datasets are available at each location within SOMOMOUNT and were used as validation for the model.

REFERENCES

Hauck, C., Böttcher, M., & Maurer H. 2011: A new model for estimating subsurface ice content based on combined electrical and seismic data sets. The Cryosphere, 5(2), 453-468.

P 6.1

Volcanoes with carbonate basements: understanding basement deformation and degassing phenomena.

Richard Bakker[1], Marie Violay[1], Philip Benson[2] and Sergio Vinciguerra[3]

[1] *ETH Zürich, ERDW, Structural Geology and Tectonics group, Rock Deformation Laboratory. Sonneggstrasse 5, CH-8092. (richard.bakker@erdw.ethz.ch)*
[2] *University of Portsmouth, School of Earth and Environment. Burnaby Building, Burnaby Road, UK-PO1 3QL*
[3] *University of Leicester, Department of Geology. University Road, Leicester UK - LE1 7RH / British Geological Survey. Nicker Hill, Keyworth, Nottingham UK-NG12 5GG*

The physical properties of volcanic basement lithologies are of great importance in understanding edifice stability (Van Wyk de Vries and Borgia, 1996). Several studies have focussed on carbonate rocks, since they form basements of many volcanoes around the world (see Heap et al., 2013, and references therein). At high temperatures, calcite alteration reactions may occur (>500 ˚C, Rodriguez-Navarro et al., 2009), whereby CaO and CO_2 are produced. Excess CO_2 can increase pore pressures in the system and promote failure of the country rock. These processes are controlled by the amount of CO_2 released and the intrinsic permeability, determining how "easily" the gas can escape from the rock itself.
Previous work has focussed on the deformation of carbonates at high temperatures at room pressure. Here, UCS tests were performed where the CO_2 produced in the sample was able to escape from the experiment (Mollo et al., 2011 and Heap et al., 2013). This study indicated that decarbonatization reactions and resulting microstructure strongly influence the yield point, the peak strength and the deformation behaviour at higher strain. Post-test XRD analysis showed the occurrence of the mineral Portlandite, a reaction product of CaO with water from humidity.
Here, we investigate the effect of calcite alteration on the mechanical strength at high temperature and confinements of relevance for volcanic basements. To this end, we use a Paterson type tri-axial pressure vessel, fitted with a pore pressure system. We recreate pressure and temperature (PT) conditions representative of 2-4 km (i.e. P_c = 50 - 100 MPa resp. and T from 200 to 800 ˚C), and deform samples at a constant experimental strain rate of 10^{-5} s^{-1} under drained (permitting free degasing) and undrained conditions (constant volume). In addition, we monitored the gas release by keeping the pore pressure constant and adjusting the internal volume of the system accordingly. Permeability measurements were conducted using the transient step method (Brace et al., 1968).

Mechanical results indicate brittle behaviour up to 300 ˚C. At higher temperatures the deformation becomes macroscopically ductile. In the ductile field the strength is dependent on strain rate temperature. We observe a significant difference in strength between vented and unvented conditions when decarbonatization is active (i.e. at T> 500 ˚C, Rodriguez-Navarro, 2009). However a relative small amounts of gas release is measured, and the effect decreases with increasing temperatures up to the 600-800 ˚C range. Permeability measurements show that permeability drops irreversibly with increasing temperatures (figure 1). XRD analysis of post-test samples show no significant Portlandite peaks, indicating that decarbonatization reaction was limited.

We conclude that at elevated temperatures and confinements, degassing is enabled, but significantly limited because of permeability reduction, which in itself is likely caused by hydrostatic compaction. This new experimental evidence suggests that strength reduction due to decarbonatization reactions are negligible at relevant PT conditions.

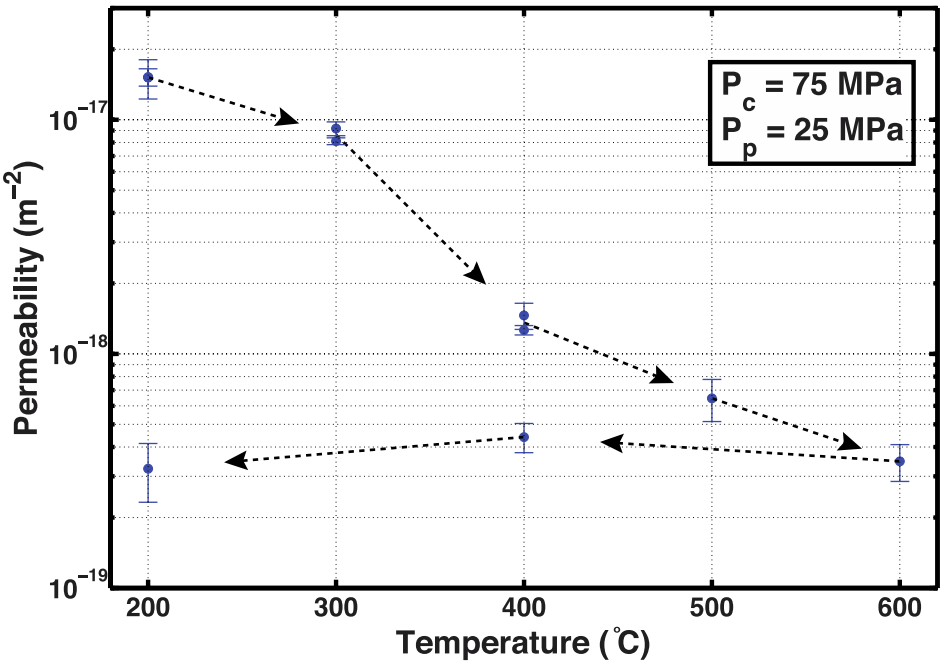

Figure 1. Results of permeability measurements at different temperatures. All measurements at an effective pressure of 50 MPa.

REFERENCES

Brace, W.F., Walsh, J.B. & Frangos W.T. 1968: Permeability of granite under high pressure. Journal of Geophysical Research. 73 (6) 2225–2236.

Chiodini, G., Caliro, S., Aiuppa, A., Avino, R., Granieri, D., Moretti, M. and Parello, F., 2011: First $^{13}C/^{12}C$ isotopic characterisation of volcanic plume CO2, Bulletin of Volcanology,

Heap, M. J., , S. Mollo, S. Vinciguerra, Y. Lavallée, K.-U. Hess, D.B. Dingwell, P. Baud, G. Iezzi, 2013: Thermal weakening of the carbonate basement under Mt. Etna volcano (Italy): Implications for volcano instability, Journal of Volcanological and Geothermal Research, Volume 250, Pages 42–60.

Mollo, S., Vinciguerra, S., Iezzi, G., Iarocci, A., Scarlato, P., Heap, M. J. and Dingwell, D. B., 2011: Volcanic edifice weakening via devolatilization reactions, Geophysical Journal International, Volume 186, Pages 1073- 1077

Rodriguez-Navarro, C., Ruiz-Agudo, E., Luque, A., Navarro, A.B. and Ortega-Huertas, M., 2009: Thermal decomposition of calcite: mechanisms of formation and textural evolution of CaO nanocrystals. Am. Mineral., 94, 578–593.

Van Wyk De Vries, B. and Borgia, A. 1996: The role of basement in volcano deformation. Geol. Soc. London, Special Publications, 110, Pages 95-110.

P 6.2

Applicability of petrophysical relationships to quantify subsurface ice and water contents from geophysical measurements in mountain and polar regions

Christian Hauck[1], Christin Hilbich[1]

[1] *Department of Geosciences, University of Fribourg, Chemin de Musée 4, 1070 Fribourg, Switzerland (christian.hauck@unifr.ch)*

Petrophysical relationships, using e.g. electrical resistivity, permittivity or seismic velocities, are widely used in exploration, but also hydrogeophysics to quantify the physical properties of the subsurface, especially regarding porosity and water content. Input data are obtained from borehole logs, cross-borehole electric, electromagnetic and seismic measurements or from surface-based measurements, usually in a 2- or 3-dimensional tomographic set-up. In a monitoring context, these approaches may yield estimates of water content or contaminant changes, which are often needed in environmental or engineering studies.

Recently, attempts have been made to use electrical resistivity (from Electrical Resistivity Tomography (ERT) measurements) and P-wave velocities (from Refraction Seismic Tomography) together with standard petrophysical relationships to quantify the subsurface ice content in permafrost regions (Hauck et al. 2011). This approach can be useful also for the long-term monitoring of climate change induced permafrost thawing, and the anticipated potential increase of slope instabilities due to various permafrost related degradation phenomena. Currently, automated continuous ERT measurements are employed to investigate temporal changes of ground ice content (Hilbich et al. 2011), but without quantitative estimates of ground ice loss.

In this contribution we would like to discuss the applicability of using various petrophysical relationships for the monitoring of ground ice and water content in mountainous and polar regions. The so-called 4-phase model approach of Hauck et al. (2011) uses two well-known relationships, namely Archie's Law and an extended Wyllie formula for electrical resistivities and P-wave velocities, respectively. However, the specifics of (partly) frozen environments, i.e. the presence of three different electrically resistive constituents (rock, ice, air, but to a varying degree) are not taken into account in standard mixing rules such as Archie's Law. Similarly, the often found similarity of electrical and elastic properties of (high mountain) permafrost materials make the differentiation between ice and rock challenging.

We will focus on potential improvements using (a) electrical mixing rules which take the conductivity of the rock matrix into account and (b) iterative procedures using time-lapse electrical and seismic data to determine the temporally invariant variables in the model (e.g. porosity, cementation factor, P-wave velocity of the rock material).

Geophysical field data together with ground temperature and water content data for validation will be presented from various permafrost field sites in the Swiss Alps in the context of the current SNF-projects TEMPS (The evolution of mountain permafrost in Switzerland) and SOMOMOUNT (Soil moisture in mountainous terrain and its influence on the thermal regime in seasonal and permanently frozen terrain). Additional 15-year long geophysical monitoring results since 1999 are presented for the long-term permafrost monitoring site Schilthorn, Berner Oberland.

REFERENCES

Hauck, C., Böttcher, M. & Maurer, H. 2011: A new model for estimating subsurface ice content based on combined electrical and seismic data sets. The Cryosphere 5, 453–468.

Hilbich, C., Fuss, C. & Hauck C. 2011: Automated Time-lapse ERT for Improved Process Analysis and Monitoring of Frozen Ground. Permafrost and Periglacial Processes 22, 306-319.

P 6.3

Automatic detection of avalanches in seismic data using Hidden Markov Models

Matthias Heck[1], Alec van Herwijnen[1], Jürg Schweizer[1], Donat Fäh[2]

[1] *WSL Institute for Snow and Avalanche Research SLF, Flüelastrasse 11, CH-7260 Davos Dorf (matthias.heck@slf.ch)*
[2] *Swiss Seismological Service (SED), Sonneggstrasse 5, CH-8092 Zürich*

Avalanche forecasting relies heavily on meteorological data as well as avalanche observations. While during the last decades the availability of meteorological data has greatly increased, avalanche activity data are still obtained through visual observation of potential avalanche areas. During times of bad visibility or at night, it is therefore not possible to estimate the level of avalanche activity. The goal of this work is to develop a system capable of automatically detecting avalanches in a continuous stream of seismic data.

We explored the seismic data of a string of six vertical component geophones in a known avalanche area above Davos, Switzerland. Manual inspection of the data revealed numerous avalanches in the seismic data. To automate the detection process, we used a Hidden Markov Model (HMM) [Hammer et al. 2012, 2013], a statistical pattern recognition tool used for speech recognition.
Using initially a small dataset, we were able to detect all manually identified avalanches during a two hour period of intense wet-snow avalanche activity in the spring of 2010, suggesting excellent model performance with a very low false alarm rate. Furthermore, we were able to detect six more avalanches, which were not identified with observational methods.
However, when using the same HMM on data from different years, model performance was rather poor with false alarm rates up to 80%. The reasons, why the HMM did not provide stable results may be due to different geophone setups over the years. In addition, different types of avalanches (dry and wet snow) will require a more diverse training set.
Though the HMM method is tailored to detect rare and highly variable events, the variability of signals generated by avalanches requires a substantial training set to obtain acceptable detection accuracy. To improve model perfomance, we will feed the model more avalanche training events as well as events from the main sources of environmental noise.

REFERENCES

Hammer, C., Beyreuther, M., Ohrnberger, M. 2012: A seismic-event spotting system for volcano fast-response systems. Bulletin of the Seismological Society of America. 102(3): 948-960.

Hammer, C., Ohrnberger, M. & Fäh, D. 2013: Classifying seismic waveforms from scratch: a case study in the alpine environment. Geophysical Journal International, 192: 425-439.

P 6.4

Effects of remote earthquakes at the Nirano Mud Volcanic Field: insights from geophysical studies

Matteo Lupi[1], Johannes Kenkel[2], Florian Fuchs[2], Tullio Ricci[3], Barbara Suski[4] (4), Stephen A. Miller[5]

[1] *ETH Zürich, Geological Institute, Zürich, Sonneggstrasse 5, CH (matteo.lupi@erdw.ethz.ch)*
[2] *Geophysics/Geodynamics, Steinmann Institute, University of Bonn, Bonn, DE*
[3] *Instituto Nazionale di Geofisica e Vulcanologia, Sezione di Roma, IT*
[4] *MEMSFIELD - MEMS and Nano-Technologies Consultancy, FR*
[5] *Centre for Hydrogeology and Geothermics. University of Neuchatel, Nuchatel, CH*

Mud volcanoes are often characterized by elevated fluid pressures that deviate from hydrostatic conditions.
This near-critical state makes mud volcanoes particularly sensitive to external perturbations and an ideal natural laboratory to test the effects of dynamic stress generated by remote seismic events. We use the Nirano Mud Volcanic System, Italy, as a natural laboratory to test if and how distant earthquakes may affect such geological systems.

We first characterized the subsurface with geoelectrical methods to investigate fluid distribution in the subsurface. Then we deployed a broadband seismic station inside the Nirano Mud Volcanic System to understand the typical seismic signal generated at depth.

Seismic records show a background noise below 2 s period, sometimes interrupted by repeated rhythmic high-frequency pulses that last from several minutes to hours. During such a period, each high-frequency pulse lasts approximately 20 s and individual pulses are separated by intervals of low frequency noise lasting from 40 s to 180 s. We identify such periods of high frequency (rhythmic) signals irregularly throughout our dataset, with no distinction between day or night hours.

In the late June 2013 the aftershocks of the M5.3 Garfagnana earthquake (21st of June 2013) were still on-going and we recorded a M4.4 event on the 30th of June, approximately 60 km from our station. The earthquake, dominated by frequencies between 1 Hz and 2 Hz, caused a maximum vertical and horizontal displacement at the surface of 0.7 mm and 0.48 mm, respectively. Before the earthquake, the frequency band between 10 Hz and 20 Hz was dominated by weaker signals while after the earthquake the same frequency band was characterized by much more intense signals. The excitement of these higher frequencies lasted for less than 20 minutes with possibly few locally induced microseismic events towards the end of this period.

Our study points out the subsurface structure of the Nirano Mud Volcanic Field and highlights the effects of incoming seismic energy in environments characterised by near-critical conditions at depth.

P 6.5

Laboratory evidence for Krauklis wave resonance in fractures

Pei-Ju Rita Shih[1], Marcel Frehner[1]

[1] *Geological Institute, ETH Zurich, Sonneggstrasse 5, CH-8092 Zurich*
(pei-ju.shih@erdw.ethz.ch, marcel.frehner@erdw.ethz.ch)

Understanding fluid-saturated reservoir rocks is essential for the applications of, for example, CO_2-sequestration, hydrocarbon exploration, or underground nuclear waste disposal. Seismic waves are influenced by the fluids in reservoir rocks, leading to dispersion and frequency-dependent attenuation (Biot, 1962). A reliable rock characterization can be obtained if the effects of fluids filling the pore and fracture space on the seismic response are well understood.

The Krauklis wave is a unique seismic waveform, which is bound to fluid-filled fractures and propagates along such fractures. It is highly dispersive with low phase velocity at low frequency (Korneev, 2008). It is expected to be able to resonate and emit seismic signals with a signature frequency. This resonant behavior should lead to strong frequency dependence for seismic body waves, enabling the identification of Krauklis wave-related signals in the coda of recorded seismograms (Korneev, 2008). Aki et al. (1977) and Chouet (1996) used this resonance behavior in interpreting volcanic tremor to show the potential of volcanic eruption forecasting. Identifying the characteristics of Krauklis waves in recorded seismograms might be one of the keys to reveal fracture-related petrophysical parameters of reservoirs.

Several theoretical studies have demonstrated analytically the dispersion behavior of Krauklis waves in infinitely long and straight fractures (e.g., Korneev, 2008). However, purely analytical methods cannot reveal the realistic fracture geometries or finite-length fractures. Therefore, we combine numerical modeling results with laboratory experiments to study and visualize fracture-related effects on seismic wave propagation in reservoir rocks. Frehner (2014) demonstrated that the initiation of Krauklis waves depends significantly on fracture orientation and on the incident wave mode. Moreover, Krauklis waves generated by an incident S-wave might carry more information about the fracture. For laboratory studies, we simulate similar conditions for a homogenous medium (i.e., plexiglas) as in the numerical experiments. We record the signals obtained from propagating ultrasonic waves along samples with and without a fracture which is inclined at an angle of 45°.

The preliminary experimental results of an incident S-wave indicate that the fracture indeed leads to resonance effects. Figure 1a) and 1b) present the spectrograms of receiver time signals of the intact sample and the fractured sample, respectively, at a source frequency of 1 MHz. The presence of the fracture seems to trigger a possible resonance at low frequencies. Figure 1b) indicates a persistent low-frequency signal (150 µs onwards). The average frequency of this fracture-related effect is approximately at 0.1 MHz. The laboratory results are in line with numerical studies (Frehner, 2014) even though there is a slight difference between the experimental setup and the numerical setup. By comparing numerical modeling (Frehner and Schmalholz, 2010; Frehner, 2014) and experimental results we aim to extract information about the fractures from the recorded seismic signals.

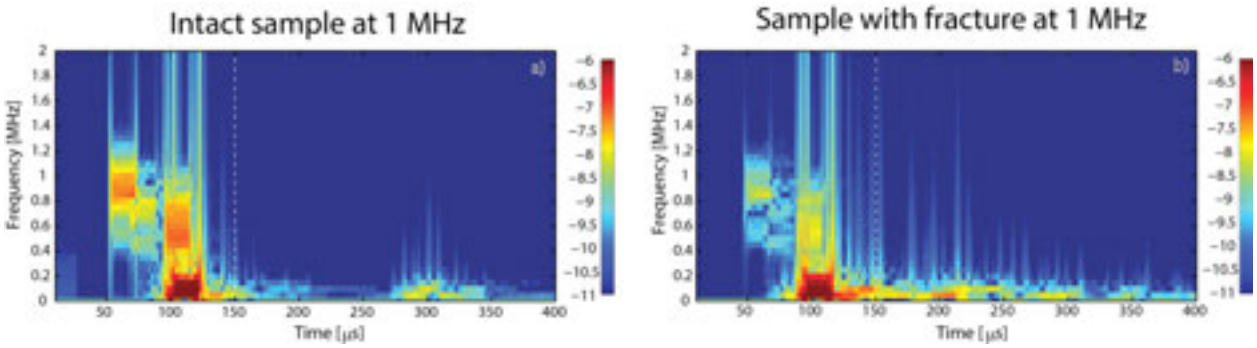

Figure 1. Spectrograms of receiver time signal of an S-wave propagating through a) the intact sample and b) the fractured sample with a source frequency of 1 MHz.

REFERENCES

Aki K., Fehler M. and Das S., 1977: Source mechanism of volcanic tremor: Fluid-driven crack models and their application to the 1963 Kilauea eruption, Journal of Volcanology and Geothermal Research 2, 259–287.

Biot, M.A. 1962: Mechanics of deformation and acoustic propagation in porous media, Journal of Applied Physics 33, 1482–1498.
Chouet B.A., 1996: Long-period volcano seismicity: Its source and use in eruption forecasting, Nature 380, 309–316.
Frehner M., 2014: Krauklis wave initiation in fluid-filled fractures by seismic body waves, Geophysics 79, in press, doi:10.1190/GEO2013-0093.1.
Frehner M. and Schmalholz S.M., 2010: Finite-element simulations of Stoneley guided-wave reflection and scattering at the tips of fluid-filled fractures, Geophysics 75, T23–T36.
Korneev V., 2008: Slow waves in fractures filled with viscous fluid, Geophysics 73, N1–N7.

P 6.6

Seismic attenuation in sandstones

Shankar Subramaniyan[1], Claudio Madonna[1], Beatriz Quintal[2], Erik H. Saenger[1]

[1]*ETH Zurich, Department of Earth Sciences, Sonneggstrasse 5, CH-8092 Zurich (shankar.subramaniyan@erdw.ethz.ch, claudio.madonna@erdw.ethz.ch, erik.saenger@erdw.ethz.ch)*
[2] *University of Lausanne, Applied and Environmental Geophysics Group, Quartier UNIL-Mouline, Géopolis, CH-1015 Lausanne (beatriz.quintal@unil.ch)*

Over the past years, seismic attenuation has been studied in the laboratory using several techniques, i.e. resonant bar, forced oscillation, ultrasonics (Subramaniyan et al. 2014). The forced oscillation method allows attenuation to be measured over a frequency range (1-100 Hz) similar to that used in the oil industry for exploration. Theoretically, there exist several physical mechanisms that cause attenuation, either due to rock matrix anelasticity or due to flow of viscous fluid in the pore space. Equations governing such mechanisms relate the magnitude of attenuation to rock/fluid properties such as porosity, permeability and fluid viscosity. Hence, understanding the frequency and saturation dependence of attenuation can shed light on the dominant mechanisms, in turn allowing us to relate attenuation to rock and fluid properties.

Sandstones have been extensively studied owing to their relatively simple granular structure and to how well these rocks have been characterized. Once the mechanisms involved in sandstones are well understood, the investigation can be further extended to more complicated rocks. Only recently, Tisato & Quintal (2013) verified that patchy saturation can explain the frequency-dependent component of seismic attenuation measured in the laboratory for partially saturated Berea sandstone at room pressure and temperature. Currently, attenuation measurements are being carried out on two different Fountainebleau samples. They represent two extremes (high and low) in terms of permeability and porosity. We employ the Seismic Wave Attenuation Module (Madonna & Tisato 2013) to measure seismic attenuation in these samples for different saturation degrees (90% and 100% water) and under three different confining pressures (5, 10, 15 MPa). Preliminary results from these investigations will be discussed.

REFERENCES

Madonna, C. & Tisato, N. 2013: A new seismic wave attenuation module to experimentally measure low-frequency attenuation in extensional mode. Geophysical Prospecting, doi: 10.1111/1365-2478.12015.
Subramaniyan, S., Quintal, B., Tisato, N., Saenger E. H. & Madonna, C. 2014: An overview of laboratory apparatuses to study seismic attenuation in reservoir rocks, Geophysical Prospecting, doi: 10.1111/1365-2478.12171.
Tisato, N., & Quintal, B. 2013: Measurements of seismic attenuation and transient fluid pressure in partially saturated Berea sandstone: evidence of fluid flow on the mesoscopic scale. Geophysical Journal International, doi: 10.1093/gji/ggt259.

P 6.7

Experimental measurements of dilatancy and permeability evolution during triaxial compression of micro-gabbro and implications for hydrothermal circulation at the mid ocean ridge.

Violay M.[1], Burg J.P[1].

[1] *ETH D-ERDW, Sonnegstrasse, 5 CH-8092, Zürich, Switzerland*

The brittle to ductile transition in rocks may strongly influence their hydraulic properties (i.e. permeability, porosity) and the depth and temperature ranges in which hydrothermal fluids may circulate. To examine this transition in the context of the crust of Iceland, we conducted deformation experiments on a natural micro-gabbro sampled (initial porosity < 3%) submitted to oceanic crust conditions (temperature from 400 °C to 950 °C, pressure of 130 MPa, and pore fluid pressure of 30 MPa). Dilatancy and permeability were measured during deformation. The dilatancy method consisted in monitoring the volume of pore fluid that flows into or out of the sample at constant pore pressure. Permeability was measured by transient pressure pulse method. Mechanical and micro-structural observations at experimental constant strain rate of 10^{-5} s^{-1} indicate that the microgabbro was brittle and dilatant up to 600 °C. Extrapolation of these results to the Iceland oceanic crust conditions predicts that hydrothermal fluids might circulate, at least transiently, through the basaltic crust down to 5 to 7 km depth. At these depths and temperatures, fluids are in the supercritical state. Such fluids have been recently recognized to be of important industrial interest, in particular for geothermal energy.

7. Geothermal Energy, CO_2 Sequestration and Shale Gas

Lyesse Laloui, Larryn Diamond, Paul Bossart

Swiss Geothermal Society,
Swiss Association of Energy Geoscientists (SASEG)

TALKS:

7.1 Adams A., Aschwanden L., Ramseyer K., Diamond L. W., Bläsi H.: Facies analysis and correlation of the middle Triassic Swiss carbonate ramp: Relation to current aquifer properties of the Upper Muschelkalk

7.2 Alt-Epping P., Diamond L.W.: Fluid-rock reactions arising from CO_2 injection into the U. Muschelkalk aquifer in N-Switzerland – insights from coupled numerical simulations

7.3 Clerc N., Rusillon E., Moscariello A.: Structural and Reservoir Rock Typing Characterisation of the Greater Geneva Basin for Geothermal Resource Assessment

7.4 Favero V., Ferrari A., Laloui L.: Effect of temperature on the mechanical behaviour of shales

7.5 Hu L., Brauchler R., Alt-Epping P., Tatomir A., Sauter M., Bayer P.: Application of time-lapse pressure tomography to characterize CO_2 plume evolution in a deep saline aquifer: a numerical study

7.6 Li C., Laloui L.: Coupled effects in carbon dioxide injection into a deep aquifer

7.7 Makhnenko R., Laloui L.: Characterization of host and caprock geomechanical properties for safe geological carbon dioxide storage

7.8 Miller S.A.: Modeling enhanced geothermal systems and the essential nature of large-scale changes in permeability at the onset of slip

7.9 Miskovich I., Basavarajappa M.: Peridynamic Formulation of Hydraulic Fracture Propagation and Branching in Shales

7.10 Moscariello A., Chelle-Michou C., Clerc N., Do Couto D., Rusillon E.: Regional Research for Geothermal Resources in Western Switzerland.

7.11 Nussbaum C., Manceau J.C., Trémosa J., Audigane P., Claret F., Lettry Y., Fierz T., Kikuchi T.: 1:1 scale wellbore experiment for a better understanding of well integrity in the context of CO_2 geological storage, Mont Terri underground rock laboratory

7.12 Scott S., Driesner T., Weis P.: Geologic factors controlling the development supercritical fluid resources in geothermal systems

7.13 Thien B., Kosakowski G., Kulik, D.: What key factors control the rock alteration in Icelandic hydrothermal systems?

7.14 Vouillamoz N., Abednego M., Wust-Bloch G.-H., Mosar, J.: Subsurface fault mapping by nanoseismic monitoring in the Fribourg area (Switzerland)

7.15 Wanner C., Peiffer L., Sonnenthal E., Spycher N. Iovenitti J., Kennedy B.M.: Reactive transport modeling of the Dixie Valley geothermal area: insights on flow and geothermometry

POSTERS:

P 7.1 Aschwanden L., Adams A., Diamond L.W., Mazurek M., Ramseyer K.: Reservoir properties of the Middle- and Upper Muschelkalk carbonate aquifer at Schlattingen, NE-Switzerland

P 7.2 Gischig, V., Preisig, G.: Pros and Cons of Hydraulic Fracturing and Hydraulic Shearing for Deep Reservoir Stimulation

7.1

Facies analysis and correlation of the middle Triassic Swiss carbonate ramp: Relation to current aquifer properties of the Upper Muschelkalk

Arthur Adams[1], Lukas Aschwanden[1], Karl Ramseyer[1], Larryn W. Diamond[1], Hansruedi Bläsi[1]

[1] *Institut für Geologie, Baltzerstrasse 1+3, 3012 Bern, Switzerland (arthur.adams@geo.unibe.ch)*

The Upper Muschelkalk is one of the major deep saline aquifers in the Molasse Basin beneath northern Switzerland. It is currently under evaluation for its potential for geothermal energy production and for gas storage (whether permanent sequestration of CO_2 or seasonal storage of methane). It is well known that aquifer properties are in part determined by the type and distribution of sedimentary facies within the reservoir. Within this context we have analysed the facies in drill cores of the Upper Muschelkalk from boreholes at Benken, Schlattingen and Weiach in the NE of Switzerland. High resolution logging revealed nine lithofacies assemblages (LFA) along with 14 lithofacies. The cores were examined sedimentologically and petrographically in order to assess the aquifer properties and architecture of the ramp.

The Upper Muschelkalk (Anisian/Ladinian) was originally sedimented as a gently inclined epeiric carbonate ramp on the eastern reaches of the Upper Muschelkalk Sea in the German basin. The lithofacies distribution indicates a transgressive - regressive ramp evolution in all three studied sections, with environments ranging from: (1) a supratidal evaporitic flat; (2) deep crinoidal mounds; (3) a storm influenced mid-ramp; (4) shelly and ooid shoals; and (5) a backshoal lagoon. The initial transgression deposited thickly bedded, nodular mudstones dominated by crinoidal debris, which were further overlain by regressive tempestite-dominated mid-ramp facies. Tempestite evolution closely followed the model proposed by Aigner (1985) as the ramp progressively shallowed. Mid-ramp tempestites were overlain by shelly shoal bodies and sheltered backshoal lagoonal sediments of the Trigonodus Dolomit formation. Dolomitization increased upwards through the sections occurring in two stages: an evaporation-driven dolomitization process followed by burial dolomitization in moldic pore spaces.

LFA are easily correlated over several kilometers across all three drill cores and show a similar ramp development. Individual tempestites are readily correlatable over kilometers due to their sheet-like geometries, showing the evolution of waning energy conditions into the basin. All five dolomite generations can be identified in two of the examined cores and they bear great similarities with the dolomitization in the German basin. Dolomitization is shown to have caused large increases in porosity via dissolution of anhydrite and bivalves. Porosity has been determined to be closely related to facies and early diagenetic processes.

The results demonstrate that the sedimentology and diagenesis of the Swiss carbonate ramp in the NE of the Swiss Molasse Basin is very similar to the well-studied German carbonate ramp. The lateral continuity of certain facies permits modest extrapolation of the aquifer properties outside the area of boreholes. Ongoing research on other borehole samples will expand the facies model and test the degree to which extrapolations can be made with confidence.

REFERENCES

Aigner, T. 1985: Storm Depositional Systems; Dynamic stratigraphy in Modern and Ancient Shallow-Marine Sequences. Springer-Verlag, Berlin, Heidelberg, New York, Tokyo, 174 pp.

7.2

Fluid-rock reactions arising from CO_2 injection into the U. Muschelkalk aquifer in N-Switzerland – insights from coupled numerical simulations

Alt-Epping Peter[1], Diamond Larryn W.[1]

[1] *Rock–Water Interaction Group, Institute of Geological Sciences, University of Bern, Baltzerstrasse 3, CH-3012 Bern, Switzerland (alt-epping@geo.unibe.ch)*

A study by Chevalier et al. (2010) has identified several deep saline aquifers in the Swiss Molasse Basin, which may potentially be used as reservoirs to store industrial CO_2. One of the aquifers considered a possible injection target is the Trigonodus Dolomite of the Upper Muschelkalk formation. To further evaluate its storage capacity, injectivity and long-term isolation performance, predictive numerical simulations have been carried out, constrained by experimental and observational data. These simulations assess the implications of CO_2 injection into a carbonate aquifer in terms of porosity/permeability changes and a possible injectivity loss. Furthermore, the dynamics of the CO_2 plume, the ensuing fluid-fluid and fluid-rock reactions and mechanisms of chemical CO_2 trapping are evaluated.

Numerical simulation of CO_2 injection and of the post-injection dynamics of the CO_2 plume is a challenging task owing to the complexity and coupled nature of the physical and chemical phenomena. During and shortly after injection, the immiscible CO_2 displaces the formation brine in a drainage-like process and migrates laterally and upward away from the injection wells, due to buoyancy forces. Once injection stops, CO_2 continues to migrate upward and displace water at the leading edge of the plume, while at the trailing edge water displaces CO_2 in an imbibition-like process. A trail of residual, immobile CO_2 is left behind the plume. The residual CO_2 and the CO_2 at the plume/brine interface slowly dissolves into the formation water, altering its chemical composition and density.

To assess the implications of CO_2 injection into the Upper Muschelkalk of the Swiss Molasse Basin critical properties and their spatial variability need to be known. The most important of these properties are the porosity and the permeability of the rock. The porosity of the rock determines the overall CO_2 storage capacity. The permeability controls the injectivity of CO_2, the dynamics of the CO_2 plume and its size and shape. Unfortunately, for the Upper Muschelkalk porosity and permeability data are available only from core samples such that predictions of the regional scale behaviour of the CO_2 plume are still associated with uncertainty. Laboratory measurements on core samples of the Trigonodus Dolomite indicate a heterogeneous distribution of porosity (values in the range of 3 - 24%) and permeability (1.6e-18 m^2 – 5.6e-15 m^2).

We use the code PFLOTRAN (Hammond & Lichtner, 2010; Hammond et al. 2011) to conduct simulations of CO_2 injection into the Trigonodus Dolomite on spatial scales ranging from sample (cm) to regional scale (100 km). Simulations suggest that upon arrival of the CO_2 plume a decrease in *pH* leads to the dissolution of primary carbonate minerals while anhydrite precipitates. The mineral quantities involved in dissolution-precipitation reactions are small and the ensuing porosity/permeability changes are insignificant.

As there is no potential for trapping CO_2 in secondary minerals, solubility trapping, i.e. the dissolution of supercritical CO_2 into the aqueous phase, is the only chemical trapping mechanism that occurs in the Trigonodus dolomite. The efficiency of solubility trapping is slightly dependent on the pre-injection pCO_2 of the brine. However, it is strongly dependent on the permeability and the permeability distribution of the aquifer, as the permeability controls the shape and size of the plume and therefore the contact area between the plume and the formation water (Fig. 1).

One peculiarity of the Upper Muschelkalk, with implications for the dynamics of the CO_2 plume, is its regionally uniform dip to the SE of some 2°. Regional-scale simulations suggest that this dip results in plume velocities on the order of 0.5 m/year. This implies, for instance, that following the injection of 1 Mio tons of CO_2 within one year, the CO_2 plume may move several tens of kilometres before all injected CO_2 has dissolved into the brine. This up-dip movement of the plume points to the need to ensure that the Gipskeuper overlying the Trigonodus Dolomite is an effective seal to prevent the leakage of CO_2 into overlying freshwater aquifers.

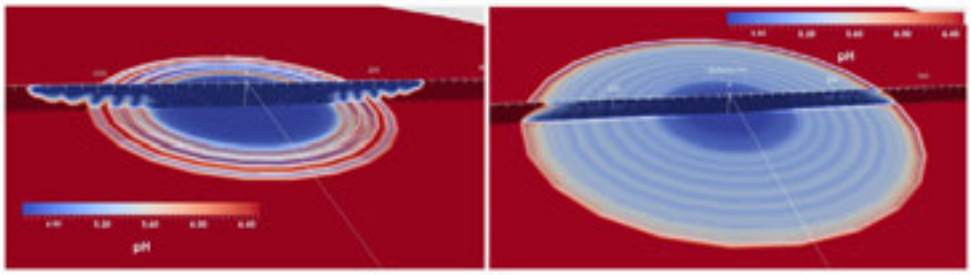

Figure 1: Vertical and horizontal sections through a CO_2 plume (marked by a low *pH*) in a cylindrical domain with homogeneous permeabilities of 1e-15 m^2 and 5e-15 m^2 (left and right panel, respectively). The permeability has a strong effect on the plume size and hence the efficiency of solubility trapping. Note the fingering at the edge of the plume arising from subtle density changes of the brine upon CO_2 dissolution.

REFERENCES

Chevalier, G., Diamond, L. W. & Leu, W. 2010: Potential for deep geological sequestration of CO_2 in Switzerland: a first appraisal. Swiss Journal of Geosciences 103 (3)

Hammond G.E., Lichtner, P.C. & Rockhold, M.L. 2011. "Stochastic Simulation of Uranium Migration at the Hanford 300 Area." Journal of Contaminant Hydrology 120-121:115-128

Hammond G.E. & Lichtner, P.C. 2010. "Field-Scale Model for the Natural Attenuation of Uranium at the Hanford 300 Area using High Performance Computing." Water Resources Research 46:Paper No. W09527

7.3

Structural and Reservoir Rock Typing Characterisation of the Greater Geneva Basin for Geothermal Resource Assessment

Nicolas Clerc[1], Elme Rusillon[1], Andrea Moscariello[1]

[1] *Earth and Environmental Sciences, University of Geneva, 13 rue des Maraîchers, CH-1205 Geneva (nicolas.clerc@unige.ch)*

A large, multistage program called "GEothermie 2020", aiming at developing the deep geothermal energy resources of the trans-border (Swiss-French) Greater Geneva Basin, has been launched by the Canton of Geneva.

In this framework, two research projects have been initiated to study the subsurface geology of the region focusing on both geothermal and hydrothermal energy exploration. The first project aims at characterising facies distribution, petrophysical and thermal properties of the sedimentary sequence ranging from Permo-Carboniferous to Lower Cretaceous units. The second project investigates the basin structural evolution, fault-related fractures and their geometrical characteristics and properties. This information will be integrated in 3D geological models derived from 2D seismic lines and well data, to build a predictive model of reservoir characteristics across the Greater Geneva Basin.

Detailed rock typing description from petrophysical well measurements and laboratory analysis of core and outcrop samples (facies and micro-facies description; geochemical, petrophysical and thermal properties measurements) are being carried out in order to assess the lateral variations of facies and their reservoir properties. Fracture analysis from outcrops and core data are also being studied in order to develop mechanical-stratigraphic models of target reservoir units.

Regional facies mapping based on reconstruction of depositional environment evolution through time, as well as insights on structural evolution of the basin help to understand better the distribution of productive reservoir facies and fractured zones within the study area. These elements will be key geological parameters for the successful development of geothermal energy in the Greater Geneva Basin.

7.4

Effect of temperature on the mechanical behaviour of shales

Valentina Favero[1], Alessio Ferrari[1] & Lyesse Laloui[1,2]

[1] *Ecole Polytechnique Fédérale de Lausanne (EPFL), School of Architecture, Civil and Environmental Engineering (ENAC), Laboratory for Soil Mechanics (LMS), EPFL-ENAC-LMS, Station 18, CH-1015 Lausanne, Switzerland. (valentina.favero@epfl.ch; alessio.ferrari@epfl.ch; lyesse.laloui@epfl.ch)*

[2] *King Abdulaziz University, Jeddah, Saudi Arabia*

The involvement of shales in many energy-related fields in the last decades has led to the need to study their thermo-mechanical behaviour and to pay particular attention to the analysis of the volumetric behaviour and porosity change at different temperatures and different stress conditions. This is mainly due to the great depth involved (several hundred meters), as in the case of the shale gas extraction and of the EGS technology, or to the high thermal load forseen (up to 100°C), as in the context of nuclear waste disposal. In addition, thermal changes can be induced in the shale formation by the injection of drilling and fracturing fluids at great depth where much greater temperatures respect to the one of the injected fluid are encountered. As a consequence, the understanding of the effect of temperature variations on the mechanical behaviour of the shale formation is of primary significance.

This paper describes the development, setting up and calibration of a high pressure- high temperature oedometer cell which allows the analysis of the 1D volumetric behaviour of shales at high temperatures (up to 100°C) and high stresses (up to 100MPa). An experimental investigation has been carried out in order to characterize the thermo-mechanical behaviour of shales under different thermo-mechanical stress paths which include mechanical loading and unloading at different constant temperatures (up to 80°C) and heating-cooling phases at constant vertical effective stresses and at different values of overconsolidation ratio (OCR).

Selected results are presented for the Opalinus Clay shale from the Mont Terri URL in the northern region of Switzerland. The initial saturation of the material is carried out limiting the vertical expansion while the heating and cooling phases are performed with a slow rate in order to ensure the dissipation of the excess pore water pressure. The analysis of the results allows the assessment of the effects of temperature on the evolution of the yield limit, on the compressibility and on the 1D volumetric behaviour of the shale.

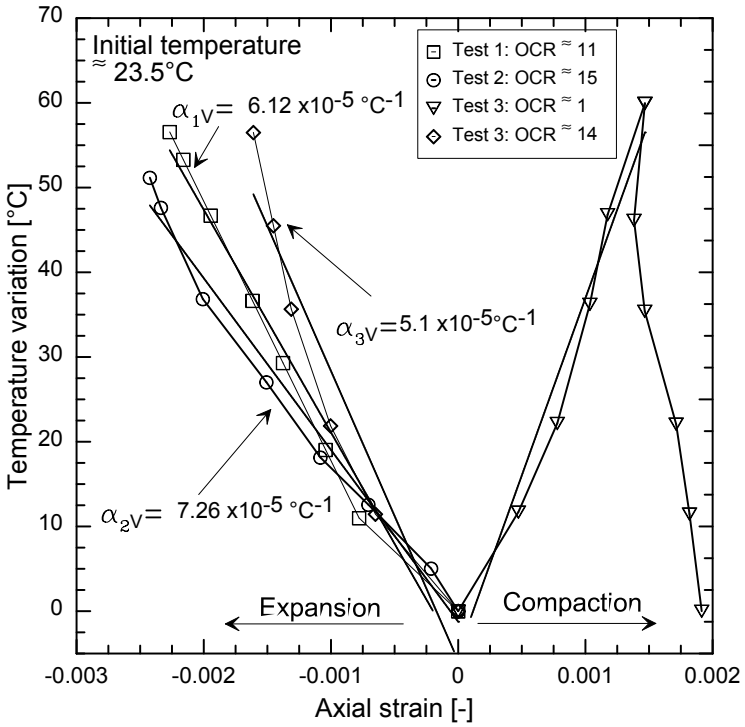

Figure 1. Volumetric behaviour of Opalinus Clay from the Mont Terri URL during heating at different value of overconsolidation ratio.

REFERENCES

Ferrari A,Laloui L. Advances in the testing of the hydro-mechanical behaviour of shales. In: Laloui L, Ferrari A, editors. Multiphysical Testing of Soils and Shales.Springer; 2012, p.57-68.

Ferrari, A., Favero, V., Manca, D. and Laloui L. 2013. Volumetric behaviour and consolidation analysis of shales at high confining stresses. 47th US Rock Mechanics / Geomechanics Symposium, San Francisco,USA, 23-26 June 2013.

7.5

Application of time-lapse pressure tomography to characterize CO_2 plume evolution in a deep saline aquifer: a numerical study

Linwei Hu[1], Ralf Brauchler[2], Peter Alt-Epping[3],Alexandru Tatomir[4], Martin Sauter[4], Peter Bayer[1]

[1] *Geological Institut, ETH Zurich, Sonneggstrasse 5, CH-8092 Zurich (linwei.hu@erdw.ethz.ch)*
[2] *AF-Consult Switzerland Ltd, Täfernstrasse 26, CH-5405 Baden*
[3] *Institute of Geological Sciences, University of Bern, Baltzerstrasse 3, CH-3012 Bern*
[4] *Geosciences Center, University of Göttingen, Goldschmidtstrasse 3, D-37077 Göttingen*

For characterization and monitoring of deep aquifers utilized for CO_2 sequestration, field methods are needed that are cost efficient, expressive and which give direct insight into the prevailing physical subsurface conditions. As an innovative approach, a time-lapse pressure tomography inversion procedure is suggested. In our study, it is applied to characterize CO_2 plume development in a modelled virtual deep saline aquifer. The introduced CO_2 affects the flow properties of the CO_2 and brine mixture depending on the CO_2 saturation. This is utilized in an eikonal-based hydraulic tomography framework, which allows for quantifying the apparent hydraulic diffusivity of the aquifer. Hydraulic pressure tomography creates streamline patterns by either injecting brine at different depths (sources) prior to full-scale CO_2 injection, or by injecting CO_2 in the two-phase (brine and CO_2) system during later stages of sequestration. The introduced pressure responses at given observation locations (receivers) are utilized for rapid and efficient eikonal-based inversion to reconstruct the heterogeneity of the subsurface with diffusivity tomograms. By a time-lapse strategy, through comparison between the derived diffusivity tomograms of the aquifer at different times, the evolution of the plume shape can ultimately be monitored.

7.6

Coupled effects in carbon dioxide injection into a deep aquifer

Chao Li[1] & Lyesse Laloui[1]

[1] *Laboratory of Soil Mechanics - Chair "Gaz Naturel" Petrosvibri, Swiss Federal Institute of Technology of Lausanne, EPFL - ENAC – LMS Station 18 CH-1015 Lausanne (chao.li@epfl.ch)*

CO_2 storage in deep aquifers is considered as a potential technology to reduce the greenhouse effects of CO_2. Practically, a large-volume (>1 Mt/year) of CO_2 could be injected into a system that consists of a highly porous host aquifer covered by a low-permeability sealing caprock. High-rate injection could result in the abrupt build-up of fluid pressures, deforming the aquifer and compromising the integrity of the caprock. In case the carbon dioxide injection temperature is lower than the storage formation a contractive behaviour is expected that could compromise the mechanical stability, being more likely to open new paths or re-open existing fractures.

The interaction between fluid overpressure, cooling effect and mechanical reaction within the host reservoir results in a complex coupled system. The understanding of these thermal-hydro-mechanical processes is crucial to secure the injection. We investigate numerically such coupled effects induced by CO_2 injection on aquifer stability and the related interactions with the caprock. The most significant physical processes and mechanical behaviours are highlighted within this study, which are suggested to be accounted for in future risk management of CO_2 storage projects.

7.7

Characterization of host and caprock geomechanical properties for safe geological carbon dioxide storage.

Roman Makhnenko[1] & Lyesse Laloui[1]

[1] *Soil Mechanics Laboratory - Chair ''Gaz Naturel'' Petrosvibri, École Polytechnique Fédérale de Lausanne, EPFL ENAC IIC LMS, GC – Station 18, CH-1015 Lausanne (roman.makhnenko@epfl.ch)*

Geologic CO_2 sequestration is considered to be the most promising technique to reduce the concentration of greenhouse gases in the atmosphere. Among all the storage options, deep saline aquifers have the greatest potential and due to their worldwide occurrence can play a major role in reduction of carbon dioxide emissions. In sedimentary basins at depths below 800 meters, CO_2 usually exists in supercritical condition ($scCO_2$), which means that its temperature and pressure are above 31.1° C and 7.4 MPa, respectively, and it has a liquid-like density (500-800 kg/m^3). Carbon dioxide then can dissolve in the *in-situ* fluids and be trapped stratigraphically under the low permeable cap rock and in pore space of the storage formation, as well as by reacting with minerals that form it. Injected CO_2 changes the local effective stresses and temperatures and thus can significantly deform the aquifer and the surrounding media. Therefore, for the proper assessment of safe geologic storage, thermo-hydro-mechanical characterization of possible host and caprock material has to be performed.

Sandstone reservoirs, which mostly are single-porosity systems, are usually considered as a host rock material. However, in some countries, including Switzerland (Chevalier et al. 2010), limestone aquifers are widespread and have to be examined for the possibility of storage. The injection of significant amounts of CO_2 into a limestone reservoir has to be carefully treated because it is usually a multiple-porosity system with wide permeability variations. Also, because of the dissolution reactions, large pores can be created in a calcite-rich limestone, which increases their permeability, but significantly decreases capillary trapping of carbon dioxide.

In order to study the possibility of CO_2 injection and storage in limestones, Calcarenite (Apulian limestone), which consists of 98% of calcite and has the porosity of 33%, was tested for full characterization of its poroelastic response. Drained, undrained, and unjacketed parameters were measured in hydrostatic and plane strain compression experiments (Makhnenko & Labuz, 2014). The dissolution effect was studied by using micro-imaging techniques and interpreted by the means of viscoporoelastic compaction-driven fluid flow behavior. The experiments aimed at rock-fluid interaction characterization when supercritical CO_2 is injected are currently in process.

Furthermore, Opalinus clay is considered to be a good representative of the caprock material for carbon dioxide storage in Switzerland (Chevalier et al. 2010). Analysis of the poromechanical behavior of the low-permeable shale is critical for anticipation and prevention of its failure and calculation of in-situ effective stresses Preliminary characterization of the poroelastic effect was done by measuring drained (Ferrari & Laloui, 2012) and unjacketed material parameters. The ongoing experiments are aimed at evaluating CO_2 permeability, breakthrough pressure, and retention properties of *in-situ* and remolded Opalinus clay.

REFERENCES

Chevalier, G., Diamond, L.W. & Leu, W. 2010: Potential for deep geological sequestration of CO_2 in Switzerland: a first appraisal. Swiss J. Geosci. 103, 427-455.

Makhnenko, R. & Labuz, J. 2014: Calcarenite as a possible host rock for CO_2 sequestration. In: Proceedings of 48th US Rock Mechanics/ Geomechanics Symposium, Minneapolis, MN, 1-4 June 2014, paper # 7559.

Ferrari, A. & Laloui, L. 2012: Advances in the testing of hydro-mechanical behaviour of shales. In: Multiphysical Testing of Soils and Shales (Ed. by Laloui, L. & Ferrari, A.). Springer Series in Geomechanics and Geoengineering, 57-68.

7.8

Modeling enhanced geothermal systems and the essential nature of large-scale changes in permeability at the onset of slip

Stephen A. Miller

Center for Hydrogeology and Geothermics (CHYN), University of Neuchâtel, Rue Armand 11, CH-2000 Neuchâtel

The permeability structure resulting from high fluid pressure stimulation of a geothermal resource is the most important parameter controlling the feasibility and the viability of Enhanced Geothermal Systems (EGS), yet is the most elusive to constrain. Linear diffusion models do a reasonably good job of constraining the front of the stimulated region because of the $t^{1/2}$ dependence of the perturbation length, but triggering pressures resulting from such models, and the permeability inferred using the diffusivity parameter, drastically underestimate both permeability and pressure changes. This leads to incorrect interpretations about the nature of the system, including the degree of fluid pressures needed to induce seismicity required to enhance the system. Here I use a minimalist approach to modeling, and show that all of the observations from Basel (Switzerland) fluid injection experiment are well matched by a simple model where the dominant control on the system is a large-scale change in permeability at the onset of slip. The excellent agreement between observations and these simplest of models indicates that these systems may be less complicated than envisaged, thus offering strategies for more sophisticated future modeling to help constrain and exploit these systems.

7.9

Peridynamic Formulation of Hydraulic Fracture Propagation and Branching in Shales

Ilija Miskovich[1], Manjunath Basavarajappa[1]

[1] *Department of Mining Engineering, Colleege of Mines and Earth Sciences, The University of Utah, 135 S 1460 E, Salt Lake City, UT 84112, USA (ilija.miskovic@utah.edu)*

Commercial exploitation of low-mobility shale gas reservoirs has been improved with multi-stage hydraulic fracturing of long horizontal wells. Favorable hydrocarbon exploitation from these reservoirs is correlated with large fracture surface area in contact with the shale matrix – this surface area being created by high rate and high volume injection of low viscosity water-based fluids. The environmental and economic implications of using large volumes of water are attracting considerable stakeholder and regulatory attention. Any and all of potential solutions for optimal shale gas extraction relate to characterizing mechanisms of transport phenomena and formation damage, which are generally associated with diffusive or mechanical interactions between treating fluid, formation fluid, and the formation rock itself. Successful representation and quantification of stimulation-triggered hydraulic and geomechanical processes within well-bore, reservoir, and caprock environments requires modeling approach that explicitly integrate these processes.

Currently used hydraulic fracture (HF) simulators are assuming very simplified, bi-planar fracture networks (King 2010), while in a real world scenarios hydraulically induced fractures are quite complex (Fisher et al. 2002). The reason for this is that today's HF models are based on the classical elasticity continuum mechanics, which cannot address problems with discontinuities characteristic for geomaterials. The local continuum theory is well established and has been applied successfully to numerous problems. However, due to the presence of spatial derivatives in the governing equations, the theory fails to address problems with discontinuities, for instance, formation or presence of microcracks or other defects in the material such as rock heterogeneity, in particular presence of planes of weakness.

Here we present a new peridynamic (non-local) model for hydraulic fracture propagation and branching in heterogeneous geomaterials, with specific focus on low-mobility shale gas reservoirs. In contrast to the local (classical) continuum theory, in which the state of a particle is only influenced by the particles in the immediate neighbors (grid cells), in the case of peridynamic theory, the state of a particle is influenced by particles located within a region of finite radius (Silling 2010). New model provides a unique capability for integrating and modeling the concepts of non-linearity in kinematic and ma-

terial response, rock fracture/damage, history dependence, and long range forces. Furthermore, by accounting for changes in material properties and surface and interfacial phenomena over multiple scales, from atomic- to continuum-scale, this model is aimed at producing high fidelity computer simulations and an accurate surrogate of hydraulically induced fractures in unconventional gas reservoirs.
This study shows the potential of peridynamics for analyzing the reservoir damage during the process of hydraulic fracturing. Development of new generation of HF models and simulators based on peridynamic theory, such as model presented in this study, provides a new basis for reservoir stimulation design and has potential to significantly improve our predictive capabilities for complex unconventional reservoirs.

As an example, we investigate the capabilities of the model on a shale block (near wellbore region) during both welbore perforation and fracture initiation with injected fluid velocities of 200 m/s and 400 m/s. A geometry of the shale block, which includes wellbore, was developed with CUBIT geometry generation toolkit. In this example, a central pairwise force function was introduced to describe the interior interactions between particles within definite distance. The total simulation time was 1 second with the time step of 10^{-6} sec. The numerical results show that hydraulically induced fractures in shale initiate and grow spontaneously as a part of the solution to the peridynamic equations of motion, and no special failure criteria or subsequent re-meshing are required (Fig. 1).

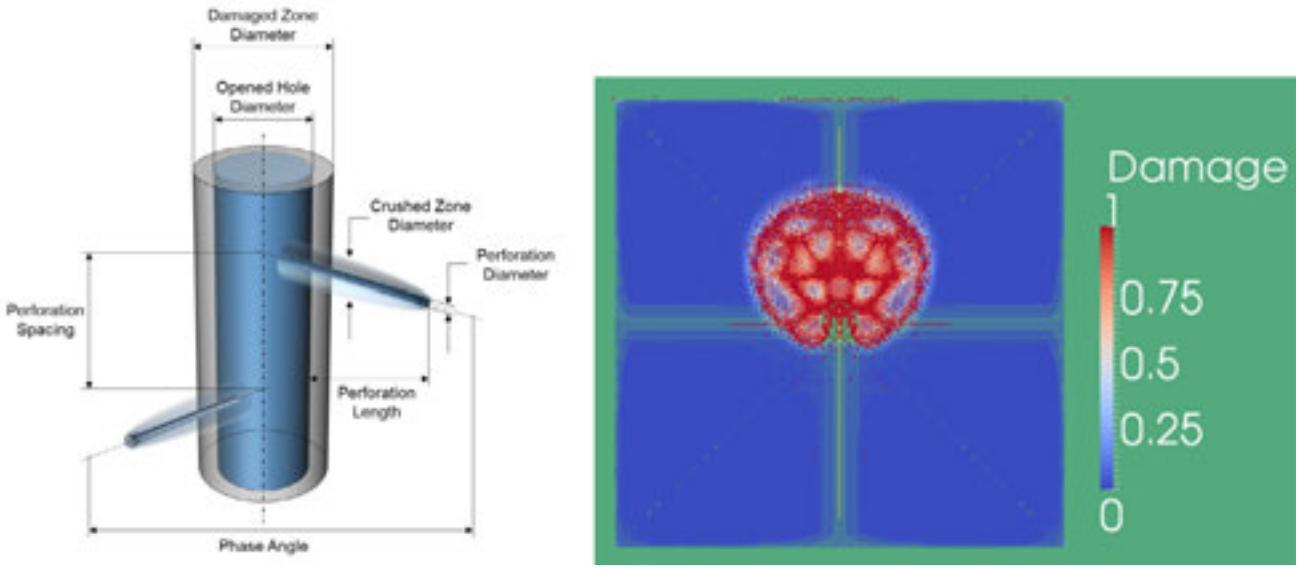

Figure 1. Perforation design (left) and map of fracture/damage propagation at fluid velocity of 400 m/s (right).

REFERENCES

King, G. 2010: Thirty years of gas shale fracturing: what have we learned? SPE Annual Technical Conference and Exhibition, 19-22 September, Florence, Italy.

Fisher, M. K., Wright, C. A., Davidson, B. M., Steinsberger, N. P., Buckler, W. S., Goodwin, A., & Fielder, E. O. 2005. Integrating Fracture Mapping Technologies to Optimize Stimulations in the Barnett Shale. SPE Production & Facilities, 20(02), 85-93.

Silling, S.A., Lehoucq, R.B. 2010. Peridynamic Theory of Solid Mechanics, In: Hassan Aref and Erik van der Giessen, Editor(s), Advances in Applied Mechanics, Elsevier, Volume 44, Pages 73-168.

7.10

Regional Research for Geothermal Resources in Western Switzerland.

Andrea Moscariello, Cyril Chelle-Michou, Nicolas Clerc, Damien Do Couto, Elme Rusillon,

Earth and Environmental Sciences, University of Geneva, 13 rue des Maraîchers, CH-1205 Geneva (andrea.moscariello@unige.ch)

A large regional scale evaluation of geothermal energy ressources is being carried out in Western Switzerland in the area ranging from the central Swiss Plateau (Neuchatel/Fribourg area) to the westermost part of Switzerland and the nearby surrounding France (Haute-Savoie and Ain Departments).

A large data set of 2D seismic lines from different surveys and vintage have been collected and integrated in a single data base which form the basis for the definition of the subsurface stratigraphy and the identification of regional variability of key geological formations calibrated by few deep borehole data. The latter span from the Permo-Carboniferous and Tertiary time period, including potential geothermal reservoirs such as the Palaeozoic sandstones, and the Jurassic and Cretaceous limestones.

A detailed mapping of fault systems is being carried out with specific focus on the deeply rooted lineaments which may allow connectivity between the cristalline basement and shallower stratigraphic formations. In particular, attention has been given to the lineaments controlling the Permo-Carboniferous extensional structures and their possible reactivation at later stages during the Alpine inversion and the present day tectonic regime as normal, inverse or transpressive faults.

Preliminary data of downhole temperatures from deep boreholes drilled in the study area in the 70s and 80s for hydrocarbon exploration have been analysed and suggest a gradient ranging between 25 and 30°C/km. This data have been used in jonction with regional Bouger-anomaly gravity maps and distribution of historical and recorded earth quakes epicenters.

Analysis of pervasive MVT-style mineralisations within intesily fractured Paleozoic rocks cored at ca 3000 m below the surface at the northern side of the Saleve Mountain (Humilly-2 well) are being investigated to reconstruct the temperature and timing of these processes and better understand the possible relationship with present-day heath flow.

The ongoing examination of these different data sets, despite the uncertainities of the various investigation techniques taken into account, aims to support further evaluation and risk assessment of the regional geothermal potential, and ultimately identify a number of most suitable prospects for geothermal exploration.

7.11

1:1 scale wellbore experiment for a better understanding of well integrity in the context of CO_2 geological storage, Mont Terri underground rock laboratory

Christophe Nussbaum[1], Jean-Charles Manceau[2], Joachim Trémosa[2], Pascal Audigane[2], Francis Claret[2], Yanick Lettry[3], Thomas Fierz[3] & T. Kikuchi[4]

[1] *SWISSTOPO, Seftigenstrasse 264, CH-3084 Wabern,*
[2] *BRGM, 3 avenue C. Guillemin 45060 Orléans Cedex 2, France*
[3] *SOLEXPERTS, Mettlenbachstr. 25, CH-8617 Mönchaltorf*
[4] *OBAYASHI Corporation, Shinagawa, Tokyo 108-8502, Japan*

In this study, we present a new experiment for following the evolution of the well integrity over time due to different changes in well conditions (pressure, temperature and fluids in contact with the well) in the context of CO_2 geological storage. A small section of a wellbore is reproduced in the Opalinus Clay of the underground rock laboratory of Mont Terri, Switzerland (caprock-like formation) at scale 1:1. This system has been characterized hydraulically and geochemically during three periods: initial state, after an increase in the well temperature and after replacing the fluid by synthetic pore water with dissolved CO_2. The characterization of the system includes both performing hydro-tests to quantify the hydraulic properties of the well and their evolution over time, and sampling the fluids to analyze the geochemical composi-

tion and changes. The results presented in this study confirm the ability of the chosen design to estimate the evolution of the well integrity over time.

The experimental setup has been designed as follows: a 2.3m long section of a wellbore is reproduced in the rock laboratory at scale 1:1 (5.5 '' casing and Ø198 mm borehole), using carbon steel for the casing and class G cement. As shown on Figure 1, below and above the well section, two different intervals have been designed for a continuous monitoring of the pressure and temperature conditions or for fluid injection and extraction (for fluid sampling for instance).

The experimental protocol contains several stages:

1 Drilling, relaxation and well completion (achieved end 2012, beginning 2013);
2 Initial state characterization (March 2013);
3 Temperature cycle in the system and characterization (April 2013 – December 2013);
4 Injection of pore water with dissolved CO_2 and tracers, and characterization (2014);
5- Overcoring of the system for mineralogical characterization (> 2015?)

The characterization of the initial state has been made during one month: a quasi-constant well effective permeability of 20 mD has been retrieved during this period both by two constant head tests (one at the beginning and one at the end of the observation period) and by steady state tests. The increase of the temperature of the lower interval (from the initial 16°C to 50°C) has led to a progressive decrease of effective well permeability down to 4×10^{-2} mD (i.e. 3 orders of magnitude decrease). The temperature was then decreased to 30 C to limit the effects of temperature. During this stage at 30 C, several high pressure increases have been imposed (magnitudes of respectively 3, 4, 6 and 8 bars). All of them show a significant increase in the effective well permeability after the pressure increase (the lowest increase was a 400% increase) and then a slow return to initial well effective permeability value. The same pressure tests were performed after replacing the bottom interval water with pore water and dissolved CO_2: four and five months after, an increase of the well effective permeability of 80% and 20% was observed respectively for a 8 bar and a 6 bar test.

The evolution of the effective well permeability in accordance with the abrupt changes of pressure that were imposed seems to indicate that the water flow occurs mostly at interfaces rather than through the cement matrix. This assumption is also suggested by the comparison between the observed evolution of the fluid composition in the two intervals before CO_2 was injected and the results of the reactive transport modeling: the small evolution of the fluid composition in the top interval cannot match a flow that would have reacted significantly with the cement by passing through the cement matrix. In addition, the quantitative estimation of the flow towards the caprock formation shows that this flow is likely to occur at the outside of the cemented sheath i.e. at the cement/caprock interface. Interestingly, the effects of the abrupt changes of pressure are significantly lowered after dissolved CO_2 was injected in the system. This could be a sign of carbonation occurring at the interfaces that would limit the flow even with high pressure changes. This needs to be confirmed notably with the results in terms of fluid composition changes and with the observation and characterization of mineralogical changes that are planned after the overcoring of the system.

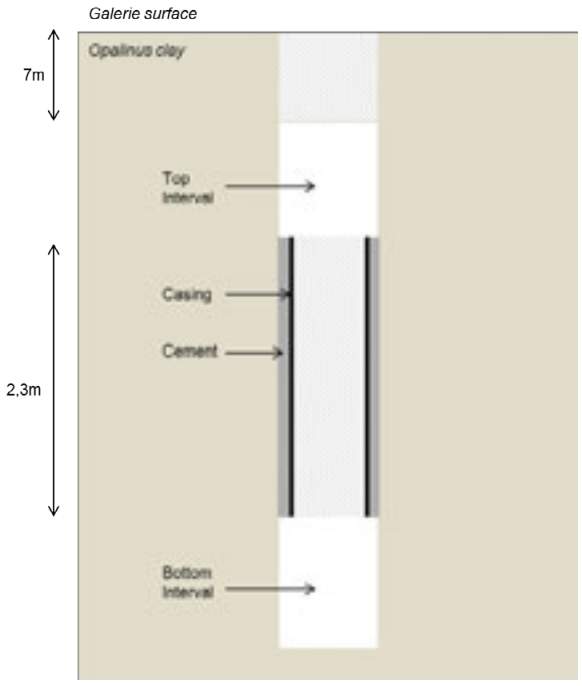

Figure 1. Concept of the experimentation with the two observation intervals (not to scale).

7.12

Geologic factors controlling the development of supercritical fluid resources in geothermal systems

Samuel Scott[1], Thomas Driesner[1], & Philipp Weis[1]

[1] *Institute of Geochemistry and Petrology, ETH Zürich, Clausiustrasse 25, CH-8092 Zürich*

It has long been known that conventional high-enthalpy geothermal systems are driven by the hydrothermal cooling of shallow intrusions. Recently, there has been increased interest in tapping supercritical fluid resources in geothermal systems, since such fluid reservoirs could provide a roughly order-of-magnitude greater potential for electricity production than conventional geothermal wells drilled to temperatures of 250-300 °C (Friðleifsson and Elders, 2005). The potential of supercritical geothermal reservoirs was demonstrated in 2010, when the Iceland Deep Drilling Project (IDDP) drilled into liquid magma at 2 km depth and encountered an overlying permeable, high-temperature (~450 °C) fluid reservoir capable of more than ~30 MWe of electricity production (Elders et al., 2014). However, a conceptual model describing the main factors governing the spatial extent and structure of target reservoirs and their relation to conventional high-enthalpy systems has remained elusive.

Here, we systematically investigate the role of rock permeability, the brittle-ductile transition temperature, and the depth of magma chamber emplacement on the development of supercritical fluid reservoirs. We use the numerical modeling code CSMP++ to model two-phase flow of compressible water around an intrusion. Results indicate that potentially exploitable supercritical fluid resources are an integral part of magma-driven geothermal systems occurring in rocks with a brittle-ductile transition temperature higher than ~400 °C, such as basalt (Figure 1). However, if the brittle-ductile transition temperature is near 360 °C, typical for quartz-bearing lithologies, supercritical fluids are nearly absent. Supercritical fluid is restricted to thin (approximately 10 to 100 m thick) reservoirs in high permeability (10^{-14} m^2) settings, whereas hotter and much more voluminous reservoirs can occur in less permeable (10^{-15} m^2) rocks. A shallow depth of intrusion (>3 km) also promotes hotter and more extensive supercritical fluid resources.

The systematic dependence of the size, location and hydrologic behavior of supercritical reservoirs on these factors aids the development of exploration models for different volcanic settings. In addition, by serving as the main agents of heat transfer at the interface of an intrusion and the overlying hydrothermal system, supercritical fluid reservoirs play a decisive role in determining the overall thermal histories of shallow intrusions and in shaping the overall character of hydrothermal systems.

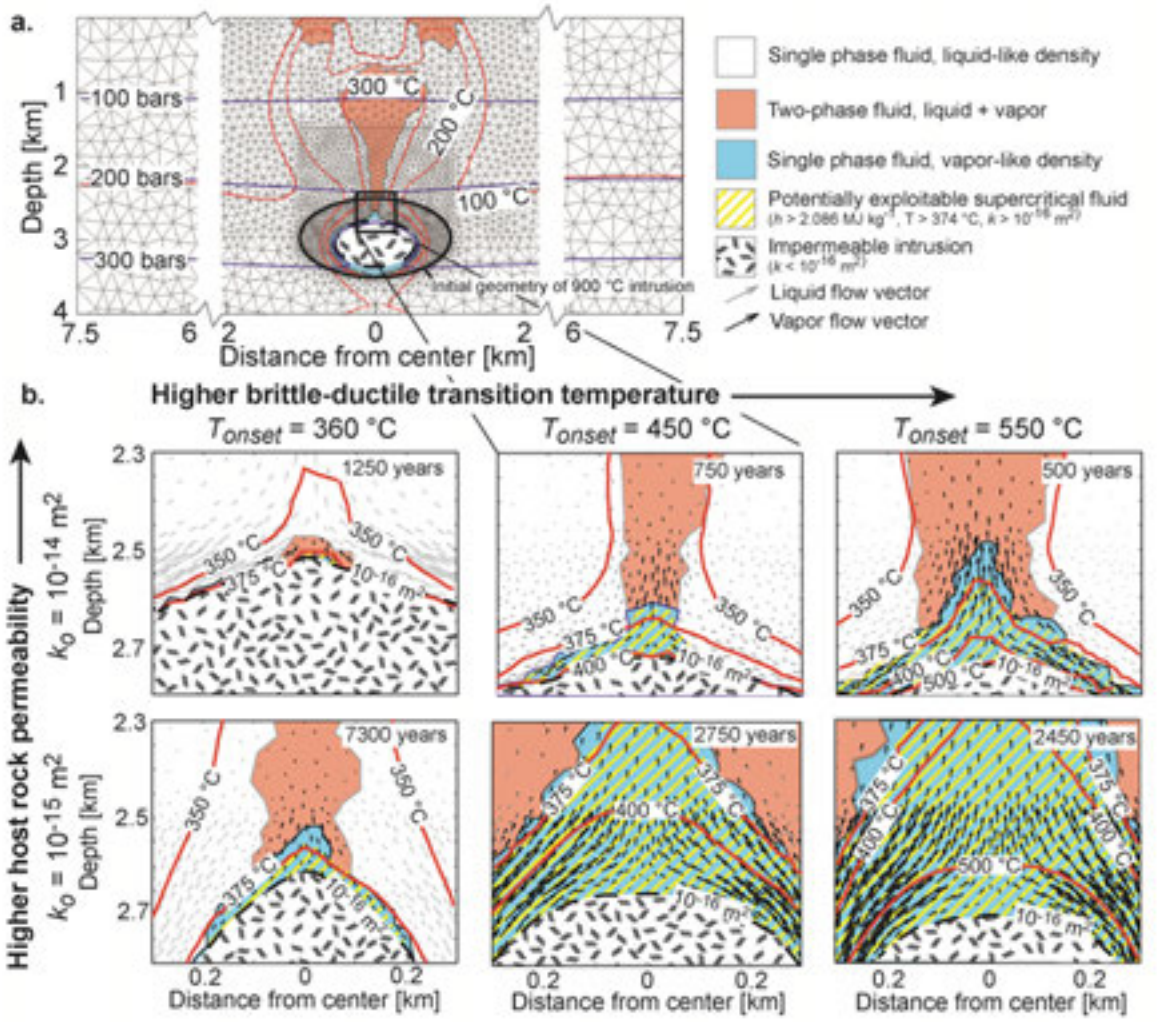

Figure 1. **a.** Typical large-scale thermal structure of a geothermal system, showing the initial geometry of the intrusion and the finite element grid. **b.** Snapshots showing fluid phase state distribution, temperature contours, liquid and vapor flow vectors around a cooling intrusion, under different conditions of host rock permeability and BDT temperature. Areas of potentially exploitable supercritical fluid (with a fluid enthalpy and temperature greater than the critical values, 2.086 MJ/kg and 374 °C, respectively) as well as the impermeable intrusion (with a permeability less than 10^{-16} m^2) are also shown.

REFERENCES

Elders, W. A., Friðleifsson, G. Ó., & Albertsson, A., 2014, Drilling into magma and the implications of the Iceland Deep Drilling Project (IDDP) for high-temperature geothermal systems worldwide: Geothermics, 49, 111-118.

Friðleifsson, G. Ó. & W. Elders, 2005, The Iceland Deep Drilling Project: a search for deep, unconventional geothermal resources, Geothermics, 34, 269-285

7.13

What key factors control the rock alteration in Icelandic hydrothermal systems?

Bruno M.J. Thien[1], Georg Kosakowski, & Dmitrii A. Kulik

Laboratory for Waste Management (LES), Nuclear Energy and Safety Research Department, Paul Scherrer Institut, CH-5232 Villigen
[1] *bruno.thien@psi.ch*

Mineralogical evolution of subsurface rocks, driven by fluid circulation in natural or enhanced hydrothermal systems, is likely to influence the long-term performance of geothermal power generation. Dissolution of primary minerals and precipitation of secondary phases may change the porosity. Porosity change is a key factor because it affects fluid circulation and solute transport, which, in turn, influence mineralogical alteration.

This study is part of the Sinergia COTHERM project (COmbined hydrological, geochemical and geophysical modeling of geotTHERMal systems) that is an integrative research project aimed at improving our understanding of the sub‐surface processes in magmatically‐driven natural geothermal systems. These are typically high enthalphy systems where a magmatic pluton is located at a few kilometers depth. These shallow plutons increase the geothermal gradient and trigger the circulation of hydrothermal waters with a steam cap forming at shallow depth.

Field observations suggest that active and fossil Icelandic hydrothermal systems are an intercalation of hyaloclasite layers with intrusive basalt layers. Hyaloclastites are usually found to be completely altered, whereas the basalts are typically rather fresh at the same location. With help of 1D and 2D reactive transport models (OpenGeoSys-GEM code), we investigated the reasons for this finding, by studying the mineralogical evolution of protoliths with different initial porosities at different temperatures and pressures, different leaching water composition and gas content, and different porosity geometries (i.e. porous medium versus fractured medium). From this study, we infer that the initial porosity of protoliths and volume changes due to their transformation into secondary minerals are key factors to explain the different alteration patterns observed in field studies. We also discuss the alteration time scales. The role of reactive surface area (variation) appears to be more important than that of kinetic rate constants.

7.14

Subsurface fault mapping by nanoseismic monitoring in the Fribourg area (Switzerland)

Naomi Vouillamoz[1], Martinus Abednego[1], Gilles-Hillel Wust-Bloch[2] & Jon Mosar[1]

[1] *University of Fribourg, Department of Geosciences, Earth Sciences, Chemin du Musée 6, CH-1700 Fribourg, Switzerland (naomi.vouillamoz@unifr.ch)*
[2] *Tel Aviv University, Department of Geophysics and Planetary Sciences, P.O.B. 39040, Tel Aviv, 69978, Israel*

We used nanoseismic monitoring (NM) techniques (Wust-Bloch & Joswig 2006, Joswig 2008) to characterize local microseismicity generated within the Fribourg area (Switzerland). NM takes advantages of mini-arrays and advanced signal processing techniques to optimize seismic event detection and location:
(1) SNR conditions are maximized by deploying portable small-aperture arrays in the direct vicinity of potential source zones. (2) Waveforms barely emerging from the background noise are analysed by visual event screening on continuous seismic sonograms. Sonograms are spectrograms, non-linearly scaled and auto-adaptive noise filtered that enhance the display of weak signal energy close to the noise threshold (Sick et al. 2012). (3) A Jackknifing approach which displays points of highest probability in space-time, is used for further identification and location of potential events. The interactive HypoLine software tests for initial signal coherence, backazimuth and slowness and then provides an innovative graphical interface for combined network- and array-mode location (Joswig, 2008).

The data used for the analysis was recorded by two portable mini-arrays (2009-2013) and complemented with SED (Swiss Seismological Service) continuous data from three nearby permanent stations (Figure 1). The use of NM techniques on

these datasets results in a) a significant increase in the number of events detected (282 vs 45) and b) a lowering of the detection threshold within the Fribourg area by ~0,8 magnitude, compared to the completeness magnitude of ECOS (Earthquake Catalog of Switzerland) (Figure 1, Histogram).

The new combined catalog (FRICAT) shows three main clusters of events (Figure 1, map and cross-sections). A first cluster corresponds to the Fribourg Lineament (Kastrup et al. 2007). The second cluster is located further south along the St-Sylvester structure. These two clusters corroborate well with subsurface fault zones interpreted by seismic imaging surveys (Interoil 2010). The third cluster (Fribourg Cluster) was previously undetected and includes low magnitude events generated under the city Fribourg. In the absence of seismic imaging surveys, these events cannot be associated to any known subsurface feature. However, their presence under an urbanized area is of considerable interest for natural or triggered seismic hazards.

Given the low seismicity rate and high ambient noise of the Fribourg area, these results emphasize the achievements of NM techniques to detect and evaluate weak seismicity (M_L down to -1.5) in noisy environments and its potential for seismic hazard assessment.

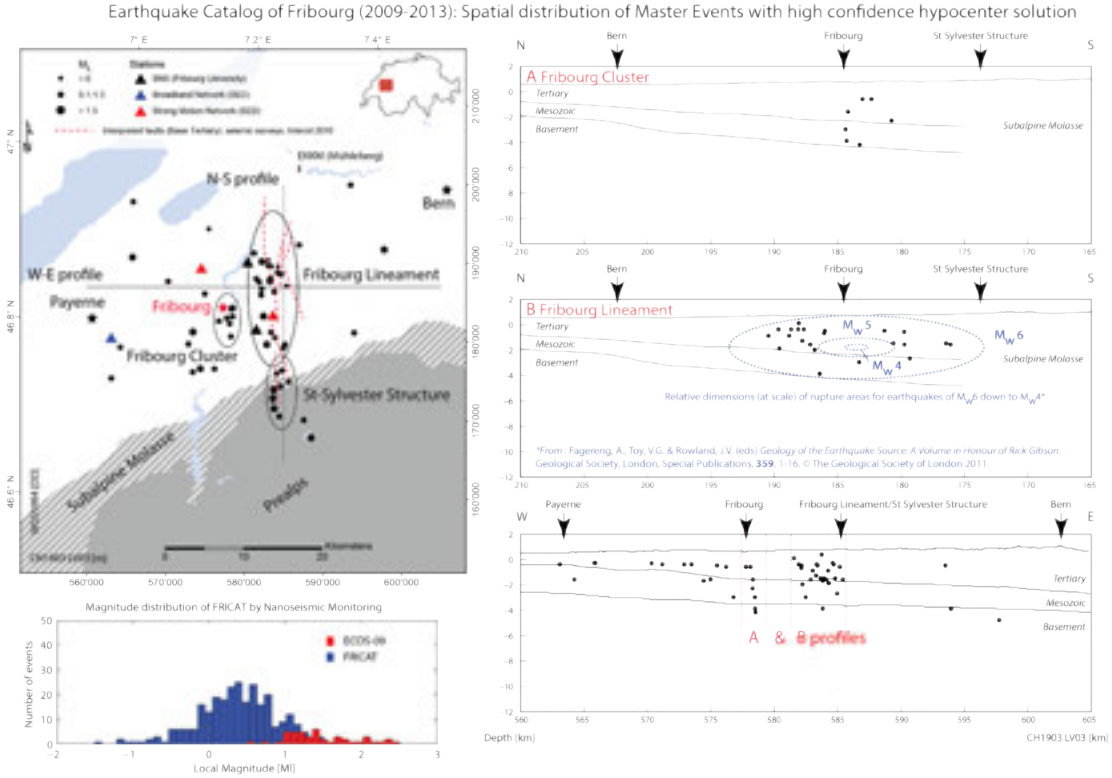

Figure 1. Left: Spatial distribution of master events with high confidence hypocenter solution (FRICAT 2009-2013). Right: Correpsonding NS and EW cross-sections. Bottom left: Magnitude distribution of the nanoseismic dataset (blue) and ECOS dataset (red).

REFERENCES

Interoil. 2010: 2D Seismic Interpretation in den Gebieten Payerne, Fribourg und Berner Seeland. Bericht vorbereitet von Interoil E&P Switzerland AG für die RESUN AG, Zürich.

Joswig, M. 2008: Nanoseismic monitoring fills the gap between microseismic networks and passive seismic. special topic, Leveraging Technology, first break 26, 117–124.

Kastrup, U., Deichmann, N., Fröhlich, A., Giardini, D. 2007: Evidence for an active fault below the northwestern Alpine foreland of Switzerland. Geophys. J. Int. (2007) 169 (3), 1273–1288.

Sick, B., Walter, M., Joswig, M. 2012: Visual Event Screening of Continuous Seismic Data by Supersonograms. Pure Appl. Geophys., 2012.

Wust-Bloch, G.-H. & Joswig, M. 2006: Pre-collapse identification of sinkholes in unconsolidated media at Dead Sea area by 'nanoseismic monitoring' (graphical jackknife location of weak sources by few, low-SNR records). Geophys. J. Int. (2006) 167, 1220-1232.

7.15

Reactive transport modeling of the Dixie Valley geothermal area: insights on flow and geothermometry

Christoph Wanner[1,2], Loïc Peiffer[1], Eric Sonnenthal[2], Nicolas Spycher[1], Joe Iovenitti[3], Burton Mack Kennedy[2]

[1] *Institute of Geological Sciences, University of Bern, Baltzerstrasse 1+3, CH-3012 Bern (christoph.wanner@geo.unibe.ch)*
[2] *Earth Sciences Division, Lawrence Berkeley National Laboratory,1 Cyclotron Road, Berkeley, CA 94720, USA*
[3] *Alta Rock Energy Inc.,Sausalito, CA, USA*

A 2D reactive transport model of the Dixie Valley geothermal area in Nevada, USA was developed to assess fluid flow pathways and fluid rock interaction processes. The model includes two major normal faults and the incorporation of a dual continuum domain to simulate the presence of a small-scale thermal spring being fed by a highly permeable but narrow fracture zone. Simulations were performed incorporating fluid flow, heat conduction and advection, and kinetic mineral-water reactions. Various solute geothermometry methods were applied to simulated spring compositions, to compare estimated reservoir temperatures with "true" modeled reservoir temperatures, for a fluid ascending the simulated fracture and cooling on its way to the surface.

Under the modeled conditions (cooling but no mixing or boiling), the classical Na-K(-Ca) geothermometers performed best because these are least affected by mineral precipitation upon cooling. Geothermometry based on computed mineral saturation indices and the quartz geothermometer were more sensitive to re-equilibration upon cooling, but showed good results for fluid velocities above ca. 0.1 m/d and a reactive fracture surface area 1-3 orders of magnitude lower than the corresponding geometric surface area. This suggests that such upflow rates and relatively low reactive fracture surface areas are likely present in many geothermal fields. The simulations also suggest that the presence of small-scale fracture systems having an elevated permeability of 10^{-12} – 10^{-10} m^2 can significantly alter the shallow fluid flow regime of geothermal systems. For the Dixie Valley case, the model implies that such elevated permeabilities lead to a shallow (less than 1 km) convection cell where superficial water infiltrates along the range front normal fault and connects the small-scale geothermal spring through basin filling sediments. Furthermore, we conclude that a fracture permeability on the order of 10^{-12} m^2 may lead to near surface temperature >100°C whereas a permeability of 10^{-10} m^2 is not realistic because this permeability led to extreme upflow velocities and to a short-circuit of the regional fault zone.

P 7.1

Reservoir properties of the Middle- and Upper Muschelkalk carbonate aquifer at Schlattingen, NE-Switzerland

Lukas Aschwanden[1], Arthur Adams[1], Larryn W. Diamond[1], Martin Mazurek[1], Karl Ramseyer[1]

[1] *Institute of Geological Sciences, University of Bern, Baltzerstrasse 1+3, CH-3012 Bern (lukas.aschwanden@geo.unibe.ch)*

In the Swiss Molasse basin (SMB), deep aquifers are one of the options under investigation for geothermal energy production and for storage of gas. Particularly the Middle Triassic carbonate rocks within the Middle- (Dolomit der Anhydritgruppe) and Upper Muschelkalk (Trigonodus Dolomit, Hauptmuschelkalk) show encouraging aquifer properties along the northern margin of the SMB. However, the mixed results obtained in exploration wells at Riehen and Schlattingen and the failed geothermal well at Triemli illustrate that the dimensions and distribution of porous and permeable zones within the aquifer are spatially heterogeneous and that current knowledge of the aquifer properties constitutes an insufficient basis for exploration. In this context a conceptual regional model of the Muschelkalk is required which helps to define the magnitudes and the 3D distribution of porosity and permeability throughout the basin.

This study provides a first step in this direction by focussing on one specific drill site, Schlattingen, which is located 10 km SSE of Schaffhausen. A detailed reservoir characterization has been conducted, including mineralogical, petrographic, structural, petrophysical and sedimentological analyses of the Muschelkalk core from Schlattingen. These findings will be complemented by ongoing studies at other nearby, deep boreholes (Benken, Weiach). The analyses of the Schlattingen core comprise a variety of laboratory methods including visual logging of the geometry and frequency of macroscopic rock pores and fractures, identification of environments in which the carbonates formed (facies analysis), measurements of porosity, permeability and ultrasonic p- and s-wave velocities (V_p, V_s) in bedding-parallel core plugs (representing the range of identified facies). Furthermore, the gamma-ray density and V_p were determined along the entire dry core using an automated Geotek Multi-Sensor Core Logger.

The results show that the Middle- and Upper Muschelkalk comprises nine lithofacies assemblages along with 14 lithofacies. The lithofacies distribution indicates a transgressive–regressive carbonate ramp evolution (Adams et al. this conference). The deposition environments range from (1) a backshoal lagoon at the top of the carbonate sequence, which changes into (2) shelly and ooid shoals, (3) storm influenced mid-ramp deposits, (4) deep crinoidal mounds and finally (5) supratidal evaporitic flats at the base of the sequence. The porosity and permeability of the carbonates is the sum of rock-matrix and fracture-network contributions. The matrix contribution is due to the early diagenetic history of the rock, determined largely by the initial depositional environment and early diagenetic processes. The dolomitized rocks of the backshoal lagoon and the shelly and ooid shoals show highly heterogeneous distribution of porosity and permeability with ranges of 0.5–21% and 1.6×10^{-18}–4×10^{-15} m^2, respectively. The calcareous, storm-influenced mid-ramp deposits and the deep crinoidal mounds show systematically lower values of 0.1–7% and 3.1×10^{-19}–2.8×10^{-16} m^2, respectively. The dolomitized rocks of the evaporitic flats at the base of the sequence again show higher values of 16.3–19.8% and 4.1×10^{-16}–4.8×10^{-16} m^2, respectively. The ultrasonic p- and s-wave velocities of the dolomitic facies range from 4505 to 6137 m/s and from 2604 to 3509 m/s, respectively. The calcareous facies show values of 4951–6280 m/s and 2852–3419 m/s, respectively. The p-wave velocities and gamma-ray densities measured along the entire core vary in the range of 2601–6086 m/s and 1.74–2.99 g/cm^3, respectively, reflecting the heterogeneous structure of the aquifer. However, macroscopically porous zones (e.g. dissolution features) can often be directly identified as distinct negative excursions in the logs of gamma-ray density and V_p, which make such logs a useful tool for investigations of the spatial distribution of porosity and permeability.

In addition to matrix porosity, a fracture network also makes an important contribution to total porosity at Schlattingen. The network is made up by sets of dilational joints that strike NNW and dip 70–90° ENE to WSW. The spacing of the joints is <1m and their spread in orientations implies that they intersect each other, forming an interconnected fracture network. A major portion of the fractures is likely to have formed in response to late-Neogene extensional faulting along the nearby Hegau-Bodensee graben.

This study demostrates that, at Schlattingen, the carbonate rocks within the Middle- and Upper Muschelkalk show favourable properties for geothermal energy exploitation or the geological storage of gas. The porosity and permeability of the carbonates is the sum of rock-matrix and fracture-network contributions. Since the matrix contribution is largely determined by the initial deposition environment (facies) and by early diagenetic processes, a useful exploration approach would be to investigate the regional extension of the key depositional facies. All the lithofacies assemblages recognized at Schlattingen can also be observed in cores from the Benken and Weiach wells and they show a similar ramp evolution. These correlations allow modest extrapolation of the aquifer properties outside regions probed by wells. On the other hand, the fracture-porosity contribution is largely determined by fractures which formed in response to the late-Neogene extensional faulting along the nearby Hegau-Bodensee graben and thus their abundance is likely to decrease with increasing distance from the graben.

P 7.2

Pros and Cons of Hydraulic Fracturing and Hydraulic Shearing for Deep Reservoir Stimulation

Valentin S. Gischig[1]1 & Giona Preisig[1]

[1] *EOAS – Geological Engineering, The University of Bristish Columbia, Vancouver BC, Canada (gischig@sed.ethz.ch)*
[1] *Now at: Swiss Competence Center on Supply of Electricity, ETHZ Zürich*

Hydraulic stimulation of deep reservoirs is an essential procedure for developing engineered/enhanced geothermal systems (EGS), but also in other Geo-energy contexts. The goal is enhancing permeability to such a degree that fluid flow rates within the reservoir are sufficiently high for an economically productive reservoir.

Two fracture stimulation mechanisms are distinguished that may occur concurrently during the hydraulic treatment: 1) During hydro-fracturing (HF) new tensile fractures are propagated from the borehole by means of a fluid pressure overcoming the minimal principle stress σ_3 plus the tensile strength T_0 of intact rock. In case of a pre-existing fracture oriented normal to σ_3 , the fracture can be opened by exceeding σ_3 only. Fluid injection is performed via small packed intervals for creating a stack of hydraulic fractures. 2) During hydro-shearing (HS), over-pressure induces slip along pre-existing fractures that are favourably oriented in the stress field for reactivation in shear. Such stimulation is usually performed in a large packed interval or in an open borehole. Which mechanism occurs predominantly during stimulation depends on the rock mass structure and in-situ stress field, but also on the orientation of discontinuities intersecting the open-hole section and thus being pressurized.

Both mechanisms also differ in how they affect fracture permeability. While permeability gained by HS is mostly irreversible due to rearrangement of asperity contacts accompanied with shear dilation, permeability enhanced during HF reduces nearly reversible after pressurization unless proppant is used to ensure permanent apertures. In this contribution, we critically discuss the pros and cons of both mechanisms regarding efficiency of enhancing permeability and the associated hazard of induced earthquakes based on literature review and numerical modelling.

We review literature that reports on how much permeability required for productive EGS reservoirs and how much permanent permeability can be gained by stimulation. We also compile information regarding the degree of seismicity induced during HF- or HS-dominated stimulation procedures, together with conceptual studies that reveal characteristics of seismicity associated with the two mechanisms.

Many observations and models indicate that HF may have a higher tendency of being aseismic, while felt seismic events are usually associated with HS. Further, we present a hydro-mechanically coupled fracture flow model that investigates, if and to what degree the stimulation strategy can be designed such that one of the two mechanisms is evoked and dominates over the other. It shows that HS may dominate in presence of larger persistent fractures nearly optimally-oriented in the stress field, even if HF is attempted in short packed intervals.

The model further demonstrates that stress transfer during HS promotes the development of permeability across an anisotropic layer of the stimulated rock instead of a large volume. Hence, the study sheds light onto the feasibility of creating productive EGS reservoirs in crystalline rock at several kilometres depths.

8. IODP and ICDP drilling for scientific research: major achievements from past and current drilling initiatives

Anneleen Foubert, Hendrik Vogel, Michael Strasser, Samuel Jaccard

SwissDrilling,
International Ocean Discovery Program IODP,
International Continental Scientific Drilling Program ICDP

TALKS:

8.1 Früh-Green G.L, Lang S.Q.: Serpentinization and Life: IODP Drilling at the Atlantis Massif

8.2 Kremer K., Usman M., Satoguchi Y., Nagahashi Y., Panieri G., Strasser M.: Timing of mass transport deposits at site C0018 (IODP Exp. 333)

8.3 Moscariello A., Camerlenghi A. and DREAM project: Uncovering a Salt Giant: Umbrella proposal of the Deep-Sea Record of Mediterranean Messinian Events (DREAM) multi-phase drilling project

8.4 Rüggeberg A., Raddatz J., Flögel S., Foubert A., Liebetrau V., Henriet J.-P., Dullo W.-C.: Cold-water coral reefs along the European continental margin through the Quaternary

POSTERS:

P 8.1 McCarthy A., & IODP Expedition 351 shipboard scientists: IODP Exp. 351 Izu-Bonin-Mariana (IBM) Arc: Scientific Objectives and Lithostratigraphy of Site U1438

P 8.2 Thomas C., Levy E., Grossi V., Neugebauer I., Antler G., Sivan O., Yechieli Y., Gavrieli I., Turchyn AT., Stein M., Brauer A., Ariztegui D. and the DSDDP Scientific Team.: Microbial influence on organic proxy in the Dead Sea sediment at the beginning of the Holocene

8.1

Serpentinization and Life: IODP Drilling at the Atlantis Massif

Gretchen L. Früh-Green[1] & Susan Q. Lang[1]

[1] *Institut für Geochemie und Petrologie, ETH Zürich, Clausiusstrasse 25, CH-8092 Zürich (frueh-green@erdw.ethz.ch)*

The Atlantis Massif, located at the inside corner high of the intersection of the Atlantis transform fault and the Mid-Atlantic Ridge at 30°N, is one of the best-studied oceanic core complexes (OCCs) and is the target of IODP drilling during Expedition 357 in late 2015. Drilling will address two exciting discoveries in ridge research: off-axis, serpentinite-hosted hydrothermal activity and carbonate precipitation, exemplified by the Lost City hydrothermal field, and the significance of tectono-magmatic processes in forming heterogeneous and variably serpentinized lithosphere as key components of slow spreading ridges. Serpentinization reactions at moderate- to low-temperatures result in alkaline fluids, which lead to precipitation of carbonate and brucite upon mixing with seawater, and are characterized by elevated concentrations of abiotic hydrogen, methane and low molecular weight hydrocarbons. These highly reactive systems have major consequences for lithospheric cooling, global geochemical cycles, carbon sequestration and microbial activity. However, little is known about the nature and distribution of microbial communities in subsurface ultramafic environments and the potential for a hydrogen-based deep biosphere in areas of active serpentinization and fluid circulation. The continuous flux of reduced compounds provides abundant thermodynamic energy to drive chemolithoautotrophy, however, carbon availability may be limited in these high pH environments and represent a challenge for microbial growth.

Here we review serpentinization processes as fundamental to understanding the evolution of oceanic lithosphere and discuss open questions related to the impact of serpentinization on the subsurface biosphere that are the motivations for IODP drilling. In particular, motivations for drilling the shallow subseafloor of the Atlantis Massif include: (1) exploring the extent and activity of the subsurface biosphere in young ultramafic and mafic seafloor; (2) quantifying the role of serpentinization in driving hydrothermal systems, in sustaining microbiological communities and in the sequestration of carbon in ultramafic rocks; (3) assessing how abiotic and biotic processes change with aging of the lithosphere and with variations in rock type; and (4) characterizing tectono-magmatic processes at OCCs and the evolution of hydrothermal activity associated with detachment faulting. Drilling will be carried out as a Mission Specific Platform (MSP) expedition and will use seabed rock drilling systems for the first time in the ocean drilling programs.

8.2

Timing of mass transport deposits at site C0018 (IODP Exp. 333)

Katrina Kremer[1], Mohamed Usman[1], Yasufumi Satoguchi[2], Yoshitaka Nagahashi[3], Giuliana Panieri[4]& Michael Strasser[1]

[1] *Geological Institute, ETH Zurich, Sonnegstrasse 5, 8092 Zurich (katrina.kremer@erdw.ethz.ch)*
[2] *Lake Biwa Museum (Geology), 1091 Oroshimo, Kusatsu, Shiga 525-0001, Japan*
[3] *Faculty of Symbiotic Systems Science, Fukushima University, 1 Kanayagawa, Fukushima 960-1296, Japan*
[4] *Department of Geology, UiT, The Arctic University of Tromsø, Dramsveien 201, 9037 Tromsø, Norway*

Submarine slides are gaining attention not only because of their catastrophic impacts, but also because their triggers (i.e earthquakes, rapid sedimentation, gas release, or clathrate dissociation etc) may represent geohazards themselves. Dating of the respective deposits, often reffered to as mass-transport deposits (MTDs) remains an important step in order to study the frequency of such large MTDs and to better understand their trigger mechanism. Although these MTDs can be imaged by seismic surveys, characterisation and dating of these deposits require scientific ocean drilling.

The aim of this study is to reconstruct the timing of five large MTDs at site C0018 (IODP Exp. 333) within a slope-basin in the outer forearc of the Nankai subduction zone, off the coast of SW Japan. The timing of the MTDs at C0018 is based on biostratigraphy and magnetostatigraphy combined with new tephrochronolgy, radiocarbon data and ^{18}O isotope-stratigraphy.

The ^{18}O data of planctonic foraminifera show a general decreasing trend above all studied MTDs. Isotope analysis of additional samples will be used to confirm this trend or not. In the case that this trend is confirmed, a relationship between MTDs, emplaced in an acitve tectonic setting, and climate cannot be excluded. The different processes/scenarios on how climate could act as trigger for these MTDs will be discussed in this study.

8.3

Uncovering a Salt Giant: Umbrella proposal of the Deep-Sea Record of Mediterranean Messinian Events (DREAM) multi-phase drilling project

Andrea Moscariello[1] and Angelo Camerlenghi[2] on behalf of the DREAM project team[3]

[1] *Earth and Environmental Sciences, University of Geneva, 13 rue des Maraîchers, CH-1205 Geneva (andrea.moscariello@unige.ch)*
[2] *OGS Istituto Nazionale di Oceanografia e di Geofisica Sperimentale, Borgo Grotta Gigante 42/C, OGS 34010 Sgonico, Trieste, Italy*

About 6 million years ago the Mediterranean Sea became an enormous saline basin where more than one million cubic kilometres of salt accumulated, locally exceeding a thickness of 3 km in the deep basins. This extreme, but geologically brief event (640 ka; the so-called Messinian salinity crisis MSC), changed the chemistry of the global ocean and had a permanent impact on both the terrestrial and marine ecosystems of a huge area surrounding the Mediterranean. Drilling the MSC salt giant represents a unique opportunity to understand the sedimentary history, stratigraphy, biosphere and fluid dynamics of a salt giant in a state close to its original depositional configuration, and to understand the responsiveness of a land-locked oceanic basin to planetary dynamics.

The MPD proposal "Uncovering a Salt Giant" originates from a series of workshops and international initiatives carried out since 2006, when riser-drilling technology was introduced in IODP in 2004. The proposal integrates in the overall objectives the goals of the MDP Proposal 798, (GOLD).

Four site-specific drilling proposals are conceived under this umbrella:
1. DREAM: Deep-Sea Records of the MSC;
2. Deformation and fluid flow in the MSC salt giant;
3. Probing the Salt Giant for its Deep Biosphere secrets;
4. Probing deep Earth and surface connections;

addressing four overarching questions:
1. What are the causes, timing and emplacement mechanisms of the MSC salt giant?
2. What are the factors responsible for early salt deformation and fluid flow across and out of the halite layer?
3. Do salt giants promote the development of a phylogenetically diverse and exceptionally active deep biosphere?
4. What are the mechanisms underlying the spectacular vertical motions inside basins and their margins?

A pre-proposal of the "Probing deep Earth and surface connections" (Rabineau et al.) proposal was approved by the SEP submitted in parallel with this MPD proposal.

Two deep basin sites (A-Sites) will be proposed, one each in the Western and Eastern Mediterranean basin, aiming at the recovery of the complete Messinian sequence. One of these, in the Western Basin, will be extended down to basement. Four intermediate basins sites are located at shallower water depths and target the recovery of MSC records to reconstruct a shallow-to-deep transect where the A-Sites are the basinal end-member.

Marginal basins sites, under consideration for ICDP, will obtain a continuous record of MSC deposits in order to provide a detailed stratigraphic correlation among a full land-deep basin transect.

Dream Project Team: Angelo Camerlenghi, Giovanni Aloisi, Sierd Cloetingh, Hugh Daigle, Gert DeLange, Rachel Flecker, Daniel Garcia-Castellanos, Zohar Gvirtzman, Christian Hübscher, Wout Krijgsman, Junichiro Kuroda, Johanna Lofi, Stefano Lugli, Agnès Maillard-Lenoir, Yizhaq Makovsky, Vinicio Manzi, Judith McKenzie, Terry McGenity, Andrea Moscariello, Marina Rabineau, Marco Roveri, Francisco Javier Sierro, Nicolas Waldmann… …….and many others.

8.4

Cold-water coral reefs along the European continental margin through the Quaternary

Andres Rüggeberg[1,2,3], Jacek Raddatz[2], Sascha Flögel[2], Anneleen Foubert[1], Volker Liebetrau[2], Jean-Pierre Henriet[3] & Wolf-Christian Dullo[2]

[1] *Department of Geosciences, University of Fribourg, Chemin du Museé 6, CH-1700 Fribourg (andres.rueggeberg@unifr.ch)*
[2] *GEOMAR Helmholtz Centre for Ocean Research Kiel, Wischhofstr. 1-3, D-24148 Kiel*
[3] *Renard Centre of Marine Geology, Department of Geology and Soil Sciences, Ghent University, Krijgslaan 281, S8, B-9000 Gent, Belgium*

Cold-water coral (CWC) reefs are marine benthic ecosystems acting as important hot spots of biodiversity and living resources. In the northeast Atlantic, the reefs form giant coral carbonate mound structures up to 300 m in height. The development of these coral carbonate mounds is controlled by environmental factors such as temperature, salinity, seawater density, current strength, food supply, sedimentation rate, and substrate availability – some of them paced by the Northern Hemisphere climate system since their development ~3 Myr ago (e.g., Freiwald, 2002; Rüggeberg et al., 2007; Raddatz et al. 2014). The aim of this study is to highlight the importance of seawater density for the CWC reefs along the European continental margin. Recent studies have shown that reefs thrive under present-day seawater densities (sigma theta, $_{\Theta}$) of ~27.5 ± 0.15 kg/m^3 (Dullo et al., 2008). This level is coherent with the position and stability of the thermocline for the carbonate mounds offshore the Irish margins (White and Dorschel, 2010). Stable and favourable environmental conditions including constant food supply by continuous or tidally controlled currents occur over longer time scales allowing CWCs to create large reef and mound ecosystems.

The possibility to reconstruct past seawater densities gives us the opportunity to determine past environmental water mass characteristics in comparison to the recent setting and interpret these in relation to CWC growth and carbonate mound development. Recent calibrations are based on salinity, temperature and stable oxygen isotope ratios of the seawater ($^{18}O_{sw}$) collected during several research cruises. The calculation of paleo-seawater densities at different time slices is based on calcitic $^{18}O_c$ values of epibenthic foraminifera (Lynch-Stieglitz et al., 1999), and has been tested for three drilled and cored coral carbonate mounds in the Porcupine Seabight, southwest off Ireland:

1. IODP Exp. 307 Site 1317 at Challenger Mound (Belgica Mound province),
2. Galway Mound (Belgica Mound province), and
3. Propeller Mound of the Hovland Mound province.

The results indicate that the development of CWCs building those carbonate mounds is closely linked to mid-depth bottom water densities. Thriving coral growth during the past 3 Myr is predominantly found at seawater densities (sigma-theta, $_{?}$) between 27.2 and 27.7 kg/m^3. In comparison to present-day conditions, the reconstructed $_{\Theta}$-values can be interpreted as the pycnocline at around 27.5 kg/m^3 serving as boundary layer on which horizontal currents develop to carry nutrients and possibly coral larvae.

To verify past seawater stratification at intermediate water depths, a compilation of existing $^{18}O_c$ data from DSDP, ODP and IODP sites combined with data from sediment cores are used to reconstruct paleo-seawater densities. At three latitudinal depth-transects (37°N, 51°N and 65°N) paleo-seawater densities of different periods in the Pleistocene have been determined for the upper 3000 m of water column. As example, using PMIP 2 Had-CM3M2 modelled temperature and salinity data of the Last Glacial Maximum, when no coral growth is reported at 51°N and 65°N, paleo-seawater densities for the latitudinal transects were determined. In comparison to the present-day data the Had-CM3M2 model data indicate a general freshening and cooling of the water masses resulting in slightly heavier $_{\Theta}$-values – confirming calculated $_{\Theta}$-values from $^{18}O_c$ data.

The determination of past seawater densities has great potential in paleoceanographic reconstructions of intermediate water mass dynamics. More time slices will be investigated to understand the cold-water coral carbonate mound development of the past 3 Myr in more detail. It also provides a tool to study the sensitivity of CWC ecosystems with respect to environmental changes and highlights the importance of pycnoclines as a controlling factor favoring CWC growth on carbonate mounds.

ACKNOWLEDGEMENTS
We thank the DFG for funding SPP IODP-ICDP Project INWADE (Du 129/48-1) and the international research network COCARDE (www.cocarde.eu). International modeling groups are thanked for providing their data and the LSCE for collecting and archiving the model data. PMIP 2 Data Archive is supported by CEA, CNRS and PNEDC.

REFERENCES

Dullo, W.-C., Flögel, S. & Rüggeberg, A., 2008: Cold-water coral growth in relation to the hydrography of the Celtic and Nordic European continental margin, Marine Ecology Progress Series, 371, 165-176.

Freiwald, A. 2002: Reef-forming cold-water corals. In: Ocean Margin Systems (Ed. by Wefer, G., Billett, D., Hebbeln, D., Jørgensen, B.B., Schlüter, M. & van Weering, T.). Springer Verlag, Berlin, Heidelberg, New York, pp. 365-385.

Lynch-Stieglitz, J., Curry, W.B. & Slowey, N., 1999: A geostrophic transport estimate for the Florida current from the oxygen isotope composition of benthic foraminifera, Paleoceanography, 14 (3), 360-373.

Raddatz, J., Rüggeberg, A., Liebetrau, V., Foubert, A., Hathorne, E.C., Fietzke, J., Eisenhauer, A. & Dullo, W.-Chr. 2014: Environmental boundary conditions of cold-water coral mound growth over the last 3 Million years in the Northeast Atlantic, Deep-Sea Research II, 99, 227-236.

Rüggeberg, A., Dullo, W.-Chr., Dorschel, B. & Hebbeln, D. 2007: Environmental changes and growth history of a cold-water carbonate mound (Propeller Mound, Porcupine Seabight), International Journal of Earth Sciences, 96, 57-72.

White, M. & Dorschel, B. 2010: The importance of the permanent thermocline to the cold water coral carbonate mound distribution in the NE Atlantic, Earth and Planetary Science Letters, 296, 395-402.

P 8.1

IODP Exp. 351 Izu-Bonin-Mariana (IBM) Arc: Scientific Objectives and Lithostratigraphy of Site U1438

Anders McCarthy[1] and IODP Expedition [351] shipboard scientists

[1] *Institute of Earth Sciences, Faculty of Geosciences and Environment, University of Lausanne, CH-1015 Lausanne (anders.mccarthy@unil.ch)*

Arc initiation and subduction inception are fundamental processes leading to arc magmatism and continental crust genesis. Within the past few decades, extensive investigation of the Izu-Bonin-Mariana (IBM) intraoceanic arc in the northwestern Pacific has helped constrain the age (~52 Ma) and site of subduction initiation along the Kyushu-Palau Ridge (KPR). The International Ocean Discovery Program (IODP) Expedition 351 (June-July 2014) targeted the Amami Sankaku Basin, adjacent to the KPR, where the pre-arc and nascent arc basement could be accessed by drilling. Two primary objectives of the expedition were to recover the sedimentological record overlying the oceanic crust as well as the oceanic crust itself in order to i) constrain the petrological and geochemical characteristics of the mantle prior to subduction ii) constrain the petrological and geochemical evolution of the nascent arc and iii) resolve the processes of subduction initiation and arc formation.

IODP Site U1438 recovered 160m of Neogene terrigenous, biogenic and volcanogenic mud and ooze interspersed with well-preserved vitric- and crystal-rich ash layers most likely related to the Ryukyu, Honshu and IBM volcanic arcs. These sediments overlie 1300m of volcaniclastic sedimentary rock dominated by tuffaceous sandstone and tuffaceous mudstone with minor tuffaceous breccia-conglomerate incorporating preserved basaltic to rhyolitic pebbles and pumice. The sedimentological record of Site U1438 provides an unprecedented look at the waxing and waning patterns of volcanogenic output of the IBM arc, particularly through the Paleogene from arc initiation (~52 Ma) through maturation and demise (~25 Ma) related to the eastward migration of the IBM arc and cessation of volcanic activity at the KPR. Underlying these arc-derived sediments is 150m of oceanic crust made up of well-preserved plagioclase-clinopyroxene aphyric to sparsely microphyric basaltic flows.

P 8.2

Microbial influence on organic proxy in the Dead Sea sediment at the beginning of the Holocene

Thomas C.1, Levy E.2, Grossi V.3, Neugebauer I.4, Antler G.5, Sivan O.2, Yechieli Y.7, Gavrieli I.7, Turchyn A.T.5, Stein M.6, Brauer A. 4, Ariztegui D.1, and the DSDDP Scientific Team.

[1] *Department of Earth Sciences, University of Geneva, Rue de Maraîchaire 13, CH- 1205 Genève, Switzerland*
[2] *Ben Gurion University of Negev, Beer Sheva, 84105, Israel*
[3] *Geology Laboratory of Lyon, University of Lyon I, 69622 Villeurbanne, France*
[4] *GeoForschungsZentrum, Potsdam, Telegrafenberg, 14473 Potsdam, Germany*
[5] *Cambridge University, Cambridge, United Kingdom*
[6] *Hebrew University of Jerusalem, Jerusalem, Israel.*
[7] *Geological Survey of Israel, Jerusalem, Israel.*

Paleoenvironmental reconstruction is among the main targets of the International Continental Drilling Program (ICDP)-sponsored Dead Sea Deep Drilling Project (DSDDP). During drilling of the Dead Sea in the winter 2010-2011, around 450 meters of core were retrieved and currently several multi-disciplinary studies are being performed to illuminate this almost continuous sedimentary record. Careful attention has been directed to understanding the microbial communities living in the hypersaline sediment and the potential impact they might have on biogeochemical cycles both in the lake and in the Dead Sea precursors. Studies have highlighted the potential for microbial activity in the lake, in spite of its hypersalinity, and the putative influence of microbial communities on the geochemical record, especially with respect to reconstruction of the carbon and sulfur cycles (Luz et al., 1997; Torfstein et al., 2005; Kolodny et al., 2005). More recently, geomicrobiological and geochemical studies with samples obtained during the DSDDP have revealed the potential for methane production (methanogenesis) in the subsurface; this can greatly impact the carbon isotope record in the subsurface and could skew any paleoenvironmental interpretation (Thomas et al., submitted). By combining carbon, sulfur and oxygen isotopes from the interstitial pore water and the surrounding sediment, including a lithological facies study and biomarker analysis, we highlight that the period following massive gypsum precipitation in the Dead Sea, at the onset of the Holocene, has been subject to major changes. At this time, variations in the level of the lake, accompanied by water mixing, have supposedly initiated intense microbial activity in the paleo-water column and probably within the sediment after its burial, as indicated by specific authigenic Fe-S mineralizations. Sulfur isotope evidence from the pore fluids suggests that these Fe-S precipitations may be microbial in nature. While no DNA could be extracted from this interval to allow a microbial diversity study, the retrieval, among other, of non-isoprenoid macrocyclic glycerol diethers potentially calls for the presence and influence of extremophiles involved in sulfur cycling (Baudrand et al., 2010). Current work will help unravel the extent of the biological impact on proxies that could be used for paleoclimatic studies. Additionally, this work highlights the importance of routinely implementing geobiological studies within the ICDP framework.

REFERENCES

Baudrand M., Grossi V., Pancost R. and Aloisi G. (2010) Non-isoprenoid macrocyclic glycerol diethers associated with authigenic carbonates. Org. Geochem. 41, 1341–1344.

Kolodny Y., Stein M. and Machlus M. (2005) Sea-rain-lake relation in the Last Glacial East Mediterranean revealed by $\delta^{18}O$-$\delta^{13}C$ in Lake Lisan aragonites. Geochim. Cosmochim. Acta 69, 4045–4060.

Luz B., Stiller M. and Talma A. S. (1997) Carbon dynamics in the Dead Sea. In The Dead Sea : The Lake and Its Setting (eds. T. M. Niemi, Z. Ben Avraham, and J. R. Gat). Oxford University Press, Oxford - New-York.

Thomas C., Ionescu D., Ariztegui D. and the DSDDP Scientific Party (submitted). Archaeal populations in two distinct sedimentary facies of the subsurface of the Dead Sea. Mar. Genomics.

Torfstein A., Gavrieli I. and Stein M. (2005) The sources and evolution of sulfur in the hypersaline Lake Lisan (paleo-Dead Sea). Earth Planet. Sci. Lett. 236, 61–77

P 8.3

Drilling modern to ancient continental spring carbonates – Comparison of facies and petrophysics from travertine cores in the Ballik area (Pleistocene, Denizli, Turkey) and Mammoth Hot Springs (Holocene, Yellowstone, USA)

Eva De Boever 1,2; Anneleen Foubert 2; Flavio S. Anselmetti 3; Jeroen Soete 1; Laura DeMott 4; Hannes Claes 1; Mehmet Özkul 5; Aurélien Virgone 6; Rudy Swennen 1; Bruce Fouke 4.

1 Department of Earth and Environmental Sciences, KU Leuven, Leuven, Belgium (eva.deboever@ees.kuleuven.be; eva.deboever@unifr.ch)
2 Department of Geosciences – Geology, University of Fribourg, Switzerland
3 Institute of Geological Sciences and Oeschger Centre for Climate Change Research, University of Bern, Switzerland
4 Institute of Genomic Biology and Department of Geology, University of Illinois at Urbana-Champaign, IL, USA.
5 Department of Geological Engineering, Pamukkale University, Denizli, Turkey.
6 TOTAL E&P Recherche Développement, Paris, France.

Continental microbial carbonate deposits gained recently interest due to their potential as reservoir rocks, e.g. for hydrocarbons. Travertine is a particular type of continental carbonate deposit that forms at hot springs. In these settings, the strong interplay of physico-chemical processes and micro-organisms along the downstream flow path influences the fast-precipitating carbonate fabric and its petrophysical properties. Diagenetic overprinting may, in addition, drastically affect the primary fabric and pore network.

The combined study of drill cores and time-equivalent, high-quality exposures in the ancient Faber quarry (Pleistocene, Denizli, Turkey) and the modern Mammoth Hot Springs system (Yellowstone, USA) allow direct 1D to 3D up-scaling. This offers a unique setting (1) to interpret depositional system evolution in terms of changing biological, physical, and chemical conditions and diagenetic imprints (cementation, alteration), and (2) to evaluate (facies-specific) parameters controlling the petrophysical and acoustic properties of these rocks.

This study used drill cores with a total length of 120 m from the Faber quarry, located in the northern flank of the Denizli Basin and incorporates preliminary observations of the Y-10 core (total length of 113 m; USGS, 1969; Chafetz and Guidry, 2003) transecting the modern to Holocene Mammoth Hot Spring (MHS) deposits. Core sections were described in detail and travertine fabrics were placed within a geobiological facies context. Representative sections of the Faber cores (+/- 60 m) have been logged for P-wave velocity and gamma ray density with a resolution of 1 cm (GEOTEK MSCL). Both cores were subsampled for microscopic observations and poroperm analyses.

In agreement with earlier observations, this study demonstrated the broad applicability of the five-fold travertine facies framework, proposed by Fouke (2011) both for modern and ancient deposits. Core sections from both areas documentthe presence of large-scale subhorizontally bedded facies intercalated with different levels of alluvial conglomerates and marly deposits at Faber and with volcanoclastic layers at MHS. Both travertine systems evolve into a domal build-up with increasingly more proximal deposits and repeated facies shifts.

For the Faber cores, porosity and permeability analyses on plugs (1.5 inch diameter) allowed calibrating porosity estimations based on the logged parameters. In agreement with Soete et al. (subm.) acoustic velocity variations in continental carbonates relate to geobody boundaries, in which the seismic expression is in function of porosity and pore types. In general, the results suggest that specific core transects allow to deduce the main vertical facies succession and evolution in spring carbonates. Acoustic and petrophysical properties, measured by physical logging of the calcitic Faber travertine cores provide a first measure for changes in the porosity and suggest a relation to pore structure and pore structure modifications.

ACKNOWLEDGMENTS: Funding for this project is provided by TOTAL E&P. Special thanks go to the quarry owners and managers in Turkey and the Yellowstone National Park Service as well as the CRC Denver staff for allowing access, sampling and providing data. PhDs. Dr. Hendrik Vogel is thanked for his assistance in acquiring the MSCL data (University Bern).

REFERENCES

Chafetz, H.S., Guidry, S.A., 2003: Deposition and diagenesis of Mammoth Hot Springs travertine, Yellowstone National Park, Wyoming, U.S.A. Canadian Journal of Earth Sciences, 40, 1515-1529.

Fouke, B.W., 2011: Hot-spring Systems Geobiology: abiotic and biotic influences on travertine formation at Mammoth Hot Springs, Yellowstone National Park, USA. Sedimentology 58, 170–219.

Soete, J.S., Kleipool, L.M., Claes, H., Claes, S., Hamaekers, H., Kele, S., Özkul, M., Foubert, A., Reijmer, J.J.G., Swennen, R., subm.: Acoustic properties in continental carbonates and their relation to porosity and pore types. Marine and Petroleum Geology.

9. Geomorphology

C. Graf, I. Gärtner-Roer, R. Delaloye, M. Keiler, N. Kuhn, C. Scapozza, J. Müller, C. Levy, F. Herman, B. Staub, S. Castelltort

Swiss Geomorphological Society

TALKS:

9.1 Bast A., Gärtner, H.: Eco-engineering in geomorphology: Sustainable prevention of surface erosion and superficial slope failures on hillslopes in alpine environments

9.2 Frank F., McArdell B. W., Huggel Ch.: The importance of erosion for debris flow runout modeling: examples from the Swiss Alps

9.3 Greenwood, P., Kuonen, S., Fister, W., Kuhn, N.J.: The possible influence of terracettes on surface hydrology of steep-sloping and subalpine environments

9.4 Grischott R., Kober F., Reitner J., Hippe K., Ivy-Ochs S., Hajdas I., Willett S.: Climatic and vegetation control on erosion during the Holocene – a 15 kyr Be-10 denudation rate record

9.5 Guerit L., Dominguez S., Castelltort S, Romano C., Henriquet M.: Evolution of a drainage network in collisional context - Insights from experimental modeling of the Southern Alps, New Zealand

9.6 Hohermuth B., Graf C.: Application of debris-flow simulations in practice

9.7 Kuhn N.J., Kuhn B., Gartmann A.: MarsSedEx I and II: Experimental investigation of gravity effects on sedimentation on Mars

9.8 Kummert M., Braillard L., Delaloye R.: Spatial and temporal variability of the sediment transfer processes at the front of the Gugla-Bielzug rock glacier (Mattertal, VS)

9.9 Litty C., Van Der Beek P., Baudin., M., Mercier J.,Robert X., Hardwick E: Tectonic Control on Topographic and Exhumational Segmentation of the Himalaya

9.10 Lombardo U.: Geomorphological evidence of Holocene neotectonics in Southern Amazonia

9.11 Madella A., Delunel R., Schlunegger F., Szidat S.: Along-strike changes in landscape architecture condition the mechanical coupling between hanging and subducting plates: An attempt to explain the absence of the Coastal Cordillera in the Andes of Northern Chile

9.12 Molnar P., Leonarduzzi E., Bennett G.: On the prediction of daily rainfall thresholds for the triggering of landslides and debris flows

9.13 Rabin M. , Sue C. , Champagnac J.-D. , Valla P. G. , Carry N. , Eichenberger U. , Bichet V., & Mudry J.: Neotectonics of a slow orogenic arc inferred from quantitative geomorphology: the Jura Mountains

9.14 Saletti M., Molnar P., Hassan M. A., Zimmermann A. E., Church M.: Temporal pattern and memory in sediment transport in a step-pool channel: an experimental study

POSTERS:

P 9.1 Boulicault L., Moscariello A., Sartori M., Ventra D., Moreau J.: Relations between Catchment Lithologies and Shallow Surface Morphologies of Three Alluvial Fans in the Rhône Valley (SW Switzerland).

P 9.2 Chen C., Castelltort S., Foreman B.: Sedimentary record of river response to climate change: example of the Paleocene-Eocene thermal maximum in the South-Pyrenean foreland basin, Spain

P 9.3 Cogez A., Meynadier L., Allègre C., Limmois D., Herman F., Gaillardet J.: Constraints on the role of tectonic and climate on erosion revealed by two time series analysis of marine cores around New Zealand

P 9.4 Costa A., Molnar P., Lane S.N., Bakker M.: Impact of river regulation on potential sediment mobilization

P 9.5 Cros X., Braillard L., Bochud M., Delaloye R.: Using accelerometers for the study of active rock glaciers kinematics and dynamics

P 9.6 Glover J., Kenner R.: Tracking terrestrial rockfalls on a rock glacier headwall at Piz Corvatsch, Switzerland

P 9.7 Heim L., Gärtner-Roer I., Purves R., Müller J.: Analysis and application of terrestrial laser scanning in a periglacial high mountain area, on the example of rock glacier Muragl, Upper Engadin, Switzerland

P 9.8 Kuhn N.J., Greenwood P., Kuhn B., Boardman J., Foster I., Meadows M.: The Great Karoo region of South Africa: A carbon source or sink?

P 9.9 Kummert M., Barboux C., Delaloye R.: Classifying torrential catchments according to the contribution of slope movements in the sediment supply to the channel: a pilot study in the lower Valais (Swiss Alps)

P 9.10 Mandal SK., Lupker M., Burg J.-P., Haghipour N., Christl M.: Low denudation preserves high topography in tectonically quiescent southern Peninsular India

P 9.11 Ruff A., Vieli A., Gärtner-Roer I., Jörg P.C.: Spatio-temporal quantification of geomorphological processes in the recently deglaciated area surrounding the Findelengletscher

P 9.12 Scapozza C., Ambrosi C.: "Via Soreda": a geotouristical trail in the hearth of the Parc Adula project

P 9.13 Strupler, M., Schwestermann, T., Hilbe, M., Anselmetti, F.S., Strasser, M.: A new high-resolution bathymetric map of Lake Zurich

P 9.14 Jalilian T., Gohroudi Tali M., Darvishi Khatooni J.: Distribution of sinkholes And their sensitivity to Falling in praw-bistoon calcareous masses

P 9.15 Xiao L., Fister W., Greenwood P., Hu Y., Kuhn N.J.: Potential fate of eroded SOC after erosion

9.1

Eco-engineering in geomorphology: Sustainable prevention of surface erosion and superficial slope failures on hillslopes in alpine environments

Alexander Bast[1], Holger Gärtner[1]

[1] *Swiss Federal Institute for Forest, Snow and Landscape Research WSL, Landscape Dynamics/Dendroecology, Zürcherstrasse 111, CH-Birmensdorf/ZH (alexander.bast@wsl.ch)*

In mountain environments many slopes are covered by coarse grained, glacial-, periglacial- or/and denudation-derived substrate. These slopes show a high geomorphic activity, are susceptible for surface erosion and superficial slope failures, as shallow landslides or debris flows, and can result in a high socio-economic hazard potential. This is especially true for slopes lacking a protecting vegetation cover. Regarding hazard prevention, ground eco-engineering gained in importance. This is related to a range of techniques, which can provide sustainable measures to protect erosion-prone hillslopes, or landforms in general.

Using plants for a sustainable erosion control demands a stable seedbed, providing appropriate water and nutrient supply. However, degraded alpine slopes are often unstable and the coarse-grained material shows a low retention capacity of water and nutrients. This hampers a fast and sustainable development of a protecting vegetation cover. Thus, the question arises what needs to be done to give planted saplings within eco-engineering projects maximum support developing their above- and belowground structures to promote slope stabilization. Laboratory experiments have shown a positive impact of mycorrhizal fungi inoculation on plant development and soil structure. Based on this, we intended to apply this approach on a field-experimental scale.

We established two eco-engineered test areas (with/without inoculum) located in the Eastern Swiss Alps. There we quantified fine-root development and soil aggregation at the end of three consecutive vegetation periods.

After the first vegetation period, at the mycorrhizal inoculated site, fine roots showed indeed a lower root length density compared to the non-mycorrhizal treated site, but the proportion of roots with thicker diameters tended to be higher. Contrary to expectations, aggregate stability was highest at the non-mycorrhizal treated site. At the end of the third vegetation period this pattern changed: Aggregate stability is then highest at the inoculated site and root length density increased. After a three-year growth development, the tendency to thicker root diameters at the mycorrhizal treated site, expected to occur after the first vegetation period, can be confirmed. In addition, we asserted that soil temperature seems to have a strong influence on fine root development and hence, on subsurface stability.

9.2

The importance of erosion for debris flow runout modeling: examples from the Swiss Alps

Florian Frank[1], Brian W. McArdell[1], Christian Huggel[2]

[1] *Swiss Federal Institute for Forest, Snow and Landscape Research WSL (florian.frank@wsl.ch)*
[2] *Department of Geography, University of Zurich*

Debris fans are characteristic Alpine landforms constructed by some combination of modern, historical and Holocene mass movements including rockfall, rock avalanches and debris flows. The geometry of debris-flow-dominated fans and their sediment deposits depend on the magnitude and frequency of the debris flows: relatively small and frequent debris flows (1000's of m^3 per event) are expected to produce generally steeper landforms than larger but much less frequent debris flows (on the order of 10^4 to a few 10^5 m^3 per event). The sudden onset of large and erosive debris flows has been observed recently in different catchments in Switzerland (Huggel et al., 2012).

In the Spreitgraben catchment (Canton Bern, Switzerland; catchment area 4 km^2) e.g. there has been a significant increase of the frequency of large debris flows. The cumulative magnitude of channel erosion since 2009 is on the order of several 10's of meters for several channel sections. Consequently the banks have become over-steepened and bank failure has led to channel widening.
In collaboration with cantonal authorities (Canton Bern, Switzerland) and private company (Geotest AG, Zollikofen, Switzerland), this PhD study was set up at WSL and University of Zurich with the goal to interpret the erosion produced by debris flows using a debris flow runout model. The RAMMS debris flow model solves the 2D shallow water equations of motion for granular flows and includes the Voellmy friction relation (Christen et al., 2012). A corresponding erosion model is based on generalization of field data of several debris flows measured at the Illgraben catchment, Valais, Switzerland (Schürch et al., 2011). The relationship between maximum shear stress and measured erosion was used to determine the maximum erosion depth. In additional, erosion sensor measurements are used to constrain the maximum erosion rate (Berger et al, 2011). The erosion model was corroborate using data of the 1st of July 2008 at the Illgraben.

Model testing was conducted for the large and highly erosive debris flow events at Spreitgraben, Switzerland in 2010 and 2011. The first results using the shear stress-based erosion model within the RAMMS software show that the model produces plausible erosion results. A significant advantage to including channel erosion is that the flow pattern is more realistic than in simulations where entrainment is not included. In particular, simulations without channel bed erosion show more lateral outflow from the channel where it has not been observed in the field. Therefore the erosion model may be especially useful for practical applications such as hazard analysis and mapping.
However, further events have to be modeled using the erosion model to do more testing and to establish more corroboration concerning slightly different debris flow channels and catchments.

REFERENCES

Berger, C., B. W. McArdell, and F. Schlunegger (2011), Direct measurement of channel erosion by debris flows, Illgraben, Switzerland, J. Geophys. Res., 116(F1), F01,002, doi:10.1029/2010JF001722.

Christen, M.; Bühler, Y.; Bartelt, P.; Leine, R.; Glover, J.; Schweizer, A.; Graf, C.; McArdell, B.W.; Gerber, W.; Deubelbeiss, Y.; Feistl, T. & Volkwein, A. 2012: Integral hazard management using a unified software environment: numerical simulation tool «RAMMS» for gravitational natural hazards. In: Koboltschnig, G.; Hübl, J.; Braun, J. (eds.) 12th Congress INTERPRAEVENT, 23-26 April 2012 Grenoble - France. Proceedings. Vol. 1. Klagenfurt, International Research Society INTERPRAEVENT. 77-86.

Huggel, Ch., Clague, J. J. and Korup, O. 2012: Is climate change responsible for changing landslide activity in high mountains? Earth surface processes and landforms, Volume 37, Pages 77-9.

Schürch, P.; Densmore, A.L.; Rosser, N.J.; McArdell, B.W. 2011: Dynamic controls on erosion and deposition on debris-flow fans. Geology 39: 827–830.

9.3

The possible influence of terracettes on surface hydrology of steep-sloping and subalpine environments

Philip Greenwood, Samuel Kuonen, Wolfgang Fister & Nikolaus J. Kuhn

Physical Geography & Environmental Change Research Group, Department of Environmental Sciences, University of Basel, Klingelbergstrasse 27, CH-4056 Basel (philip.greenwood@unibas.ch)

Alpine and mountain slopes represent important pathways that link high altitude grazing areas to meadows and rangelands at lower elevations. Given the often acute gradients associated with such environments, they potentially represent highly efficient runoff conveyance routes that facilitate the downslope movement of runoff and associated material during erosion events. Many such slopes host series of small steps, or `terracettes`. The position of terracette systems, usually juxtaposed across the natural downslope flow-path of non-complex yet steep slopes, lead us to hypothesise that their presence may influence typical hillslope processes by intercepting or capturing surface runoff during its downslope transit. Here we report preliminary results and some tentative conclusions from on-going work to explore this possibility. Google Earth was used to initially identify a ca. 400 m^2 area of well-developed terracette system situated on a west-facing slope with gradients ranging from 25-40o (46-84%). A digital elevation model (DEM) of a section of a terracette system was constructed using spatial data taken from a relevant excerpt of a topographic map. The DEM was then queried using a flow accumulation algorithm and the results were displayed in a Geographic Information System (GIS). The output data provided 'proof of concept' that terracettes are able to capture surface runoff. A series of rainfall / runoff simulations was then performed on the same section of terracettes. Results from both components of the investigation indicate that certain sections of a terracette system intercepted surface runoff and acted as preferential flow-pathways during runoff events. By contrast, and despite being subjected to intense rainfall, some sections of the same terracette system did not generate surface runoff. Based on these contrasting findings, we cautiously predict that areas where surface runoff was not generated may actually act as depositional sites, or retention zones, and could provide temporary storage for runoff-associated substances. Greater understanding of the exact influence of terracettes on surface hydrology in steep-sloping and subalpine environments could benefit the future management of grazing and rangelands in such areas.

9.4

Climatic and vegetation control on erosion during the Holocene – a 15 kyr Be-10 denudation rate record

Reto Grischott[1], Florian Kober[2], Jürgen Reitner[3], Kristina Hippe[4], Susan Ivy-Ochs[4], Irka Hajdas[4], Sean Willett[1]

[1] *Geologisches Institut, ETH Zurich, Sonneggstrasse 5, CH-8092 Zürich (reto.grischott@erdw.ethz.ch)*
[2] *NAGRA, Hardstrasse 73, 5430 Wettingen*
[3] *Geologische Bundesanstalt, Neulinggasse 38, AT-1030 Wien*
[4] *Labor für Ionenstrahlphysik, ETH Zürich, Otto-Stern-Weg 5, CH-8093 Zürich*

The influence of climate on erosion of alpine catchments has been sparsely understood due to the missing temporal or spatial resolution of archives and the quantification of processes. Sediment budget studies (Hinderer 2001)in the Alps show severalfold increased lateglacial denudation compared to the present being in line with the concept of paraglacial cycle (Church and Ryder 1972; Ballantyne 2002).

Here, we present results coupling a 15-ky record of cosmogenic ^{10}Be-derived paleo-denudation rates (n=42) from a 160 m Stappitz lake archive in the Austrian Alps (Seebach-Valley, 34 km^2) and a two-year timeseries of the modern stream. The age-depth chronology was established using ^{14}C dates and relative pollen-stratigraphy. Postdepositional correction for the core samples was not necessary due to sufficient shielding while deposited in a lake. Catchment mapping combined with glacial extents reconstructions revealed prominent lateglacial moraines which likely decoupled the sediment flux from upper valley flanks to the trunk stream since Younger Dryas. Thus, we interpret the denudational pattern as being dominated by the lower hillslopes for the Holocene. During this timeperiod the treeline was mostly on elevations similar to the lowest lateglacial moraines thus almost entirely covering the coupled slopes (Nicolussi et al. 2005). The portion of glacial remobilised sediment during the lateglacial transition was probably significantly mixed in with hillslope erosion thus the reflecting not true catchment erosion. The beginning of the Holocene shows decreasing denudation rates down to a minimum at 5 ky BP from 1.0 to 0.3 mm/yr. The transition from 5 to 3 ky BP is marked with increasing rates up to the level of the last 3 ky with 0.6 mm/yr, similar to the modern rate. Given the stratigraphy of the core, we attribute the rather low alpine denudation rates to the stabilising effect of vegetation on the hillslopes during the Holocene Thermal Optimum. Based on an assumed lag time, the denudation rates increase due to the cooler and wetter climate in the late Holocene which resulted in less vegetation and thus a lower treeline, more shallow debris-flows and periglacial activity. Our results suggest that in the study area climate exerts a first-order control on denudation by dictating vegetation on the hillslopes and efficient periglacial processes. Importantly, the state of coupling of sediment storage compartments e.g. glacial deposits to the trunk stream has to be considered otherwise nuclide concentrations might be solely a result of mixing. Furthermore, our data seem to contradict the concept of paraglacial cycle. Hence, denudation rate and sediment flux might be not as tightly coupled as commonly assumed.

REFERENCES

Ballantyne, C. K. (2002). Paraglacial geomorphology. Quaternary Science Reviews 21(18-19): 1935-2017.

Church, M. and J. M. Ryder (1972). Paraglacial sedimentation - A consideration of fluvial processes conditioned by glaciation. Geological Society of America Bulletin 83(10): 3059-&.

Hinderer, M. (2001). Late Quaternary denudation of the Alps, valley and lake fillings and modern river loads. Geodinamica Acta 14(4): 231-263.

Nicolussi, K., M. Kaufmann, G. Patzelt, J. van der Plicht and A. Thurner (2005). Holocene tree-line variability in the Kauner Valley, Central Eastern Alps, indicated by dendrochronological analysis of living trees and subfossil logs. Vegetation History and Archaeobotany 14(3): 221-234.

9.5

Evolution of a drainage network in collisional context - Insights from experimental modeling of the Southern Alps, New Zealand

Laure Guerit[1], Stéphane Dominguez[2], Sébastien Castelltort[1], Christian Romano[2], Maxime Henriquet[3]

[1] *Department of Earth Science, University of Geneva, Geneva, Switzerland (laure.guerit@unige.ch)*
[2] *University of Montpellier, Montpellier,France*
[3] *Ecole Normale Supérieure de Lyon, Lyon, France*

River networks are primary features of the Earth surface, and they are of main importance for many geomorphological processes. Understanding the processes that create and/or influence the evolution of river network, and thus, landscape evolution, is a motivating question. We work on the specific example of New Zealand, where the morphology of the Southern Alps is characterized on one side by short rivers generally perpendicular to the main divide, whereas on the other side, the rivers are large and rotated. It has been suggested that this specific pattern could result from the oblique collision that affects the South Island. We develop a laboratory experimental setup to investigate river pattern evolution over a doubly-vergent orogenic wedge growing in a context of oblique convergence. We use a rain-fall system to introduce erosion, sediment transport and river development. The evolution of this prism is fully recorded though space and time and we are able to follow the drainage deformation. The first results are in good agreement with previous models of river pattern deformation in New Zealand and suggest that the present-day river network morphology of the Southern Alps is strongly influenced by the regional tectonic regime.

9.6

Application of debris-flow simulations in practice

Benjamin Hohermuth[1], Christoph Graf[2]

[1] *Laboratory of hydraulics, hydrology and glaciology (VAW), ETH Zurich, HIA B 13, Hoenggerbergring 26, CH-8093 Zurich (hohermuth@vaw.baug.ethz.ch)*
[2] *WSL Swiss Federal Institute for Forest, Snow and Landscape Research, Zürcherstrasse 111, CH-8903 Birmensdorf*

Present-day numerical simulation tools allow detailed evaluation of hazard scenarios. Their use gained more importance in hazard and risk assessment in the last years. While the number of simulation tools has increased, there exists still the need for improving their application in practice, especcially for the intensive calibration of the input parameters and the interpretation and subsequent use of the simulation results.

The presented master thesis (Hohermuth, 2014) shows the application and limits of numerical debris-flow simulations for supporting the revision of the natural hazards protection concept at Plattenbach Vitznau (LU). Intensity maps and suggestions for the optimization of the design of mitigation measures are based on simulation results done by the software rapid mass movement system RAMMS v1.6.20 (Christen et al., 2010) which is developed at the Swiss Federal Insitute for Forest, Snow and Landscape Research WSL.

The sensitivity analysis and the comparison with existing intensity maps demonstrates the impact of the input data – surge volume, friction parameters and topography – on the reliability of the results. It was observed that surge volume and topography have a larger effect on the resulting intensity distribution than the rheological parameters. Figure 1 shows an example on how artefacts in the digital elevation model heavily affect the model results.

For scenarios with small debris fraction BASEMENT v2.3 a fluvial transport model developed at the laboratory of hydraulics, hydrology and glaciology VAW was used. The comparison of the two phase fluvial transport model with the single phase rheological model used in RAMMS showed limitations of each of these approaches. For large events the assumption of single phase flow holds and delivers plausible results while the two phase approach underestimates the debris velocity. The modelled debris deposits for a large event are compared in Figure 2. For events with high discharge in the stream and small debris fraction only the two phase approach delivers satisfying results.

Numerical simulations provide an objective base for the generation of intensitiy maps and help to assess the efectiveness of mitigation measures. The preparation of input data is crucial. Careful and reproducible interpration of simulation results is essential.

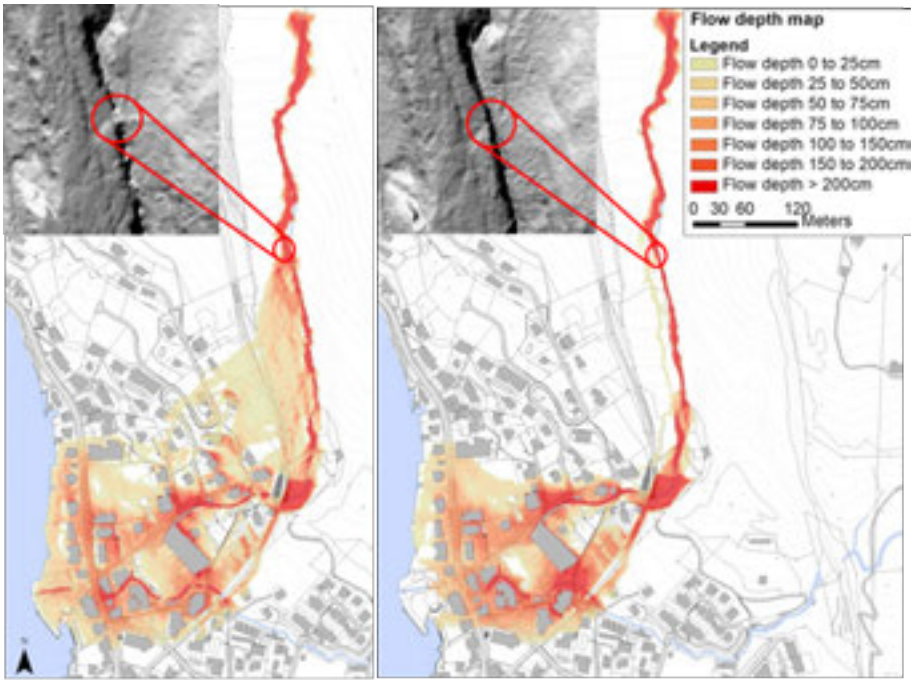

Figure 1. Flow depth for 10'000 m³ surge volume. Calculation based on the DEM from the surveying office Lucern (left and on a DEM calculated from the LIDAR point cloud using drainage enforcement (right).

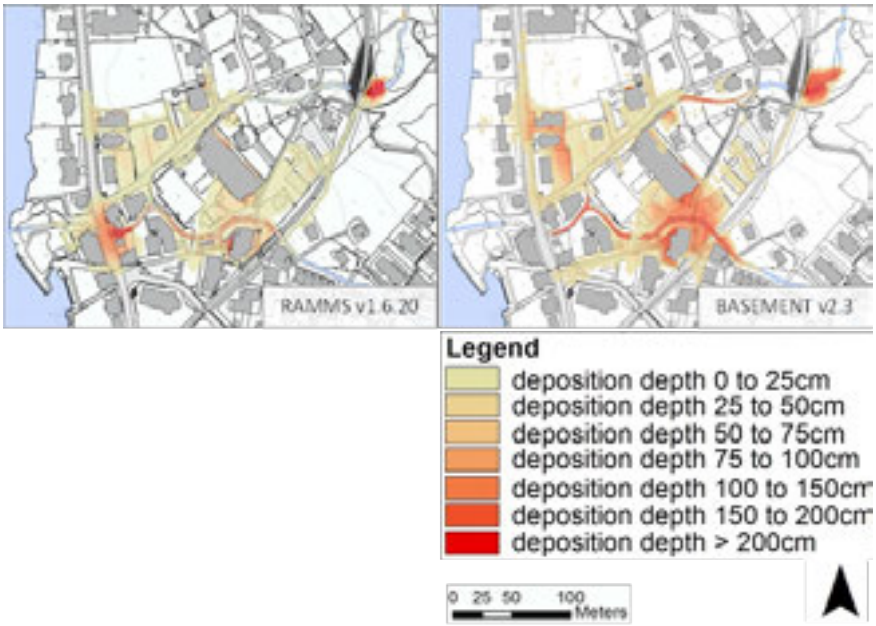

Figure 2: Comparison of debris deposits for a large event calculated using the single phase rheological model RAMMS v1.6.20 (left) and the two phase fluvial transport model BASEMENT (right).

REFERENCES

Christen, M., Kowalski, J., Bartelt, P., (2010). RAMMS: Numerical simulation of dense snow avalanches in three-dimensional terrain. Cold Regions Science and Technology, Vol. 63, 1-2, pp. 1 – 14

Hohermuth, B., (2014). Integrales Schutzkonzept Plattenbach Vitznau. Murgangsimulationen mit RAMMS. Masterarbeit FS 2014. VAW-WSL

9.7

MarsSedEx I and II: Experimental investigation of gravity effects on sedimentation on Mars

Nikolaus J. Kuhn, Brigitte Kuhn, Andres Gartmann

University of Basel, Physical Geography, Department of Environmental Sciences, Switzerland (nikolaus.kuhn@unibas.ch)

Sorting of sedimentary rocks is a proxy for the environmental conditions at the time of deposition, in particular the runoff that moved and deposited the material forming the rocks. Settling of sediment is strongly influenced by the gravity of a planetary body. As a consequence, sorting of a sedimentary rock varies with gravity for a given depth and velocity of surface runoff. Theoretical considerations for spheres indicate that sorting is less uniform on Mars than on Earth for runoff of identical depth. The effects of gravity on flow hydraulics limit the use of common, semi-empirical models developed to simulate particle settling in terrestrial environments, on Mars. Assessing sedimentation patterns on Mars, aimed at identifying strata potentially hosting traces of life, is potentially affected by such uncertainties. Using first-principle approaches, e.g. through Computational Fluid Dynamics, for calculating settling velocities on other planetary bodies requires a large effort and is limited by the values of boundary conditions, e.g. the shape of the particle. The degree of uncertainty resulting from the differences in gravity on Earth and Mars was therefore tested during three reduced-gravity flights, the MarsSedEx I and II missions, conducted in November 2012 and 2013. Nine types of sediment, ranging in size, shape and density were tested in custom-designed settling tubes during parabolas of Martian gravity lasting 20 to 25 seconds. Based on the observed settling velocities, the uncertainties of empirical relationships developed on Earth to assess particle settling on Mars are discussed. In addition, the potential effects of reduced gravity on patterns of erosion, transport and sorting of sediment, including the implications for identifying strata bearing traces of past life on are examined.

9.8

Spatial and temporal variability of the sediment transfer processes at the front of the Gugla-Bielzug rock glacier (Mattertal, VS).

Kummert Mario[1], Braillard Luc[1] & Delaloye Reynald[1]

[1] *Department of Geosciences/Geography, University of Fribourg, Chemin du Musée 4, CH-1700 Fribourg (name.surname@unifr.ch)*

Rock glaciers represent important sediment transfer agents in periglacial alpine hillslopes (Delaloye et al. 2010). Large volumes of rock debris originating from headwalls and moraines are slowly transported downward by permafrost creep. In the Alps, most rock glaciers can be considered as sediment traps, because the sediment output at their margin is usually small (Gärtner-Roer 2012). However, exceptions exist where a significant erosion rate can be observed at the front. In these cases, rock glaciers can act as the sediment source favoring the triggering of gravitative processes such as debris flows and rock falls.

The Gugla-Bielzug rock glacier is located on the orographic right side of the Matter Valley (Valais, Switzerland) and is characterized by a direct connectivity with the torrential network. Particularly high surface velocity (up to more than 8 cm/day in June 2013) have been recently measured by geodetic surveys and several debris flow events occurred over the past 2 years, spreading downward from the front of the rock glacier to the main valley. In this case, understanding which factors are controlling the erosion processes at the rock glacier front is essential to predict the triggering of debris flow.

This contribution presents results from a two-year survey at the Gugla-Bielzug rock glacier. The aim of the study is to assess the spatial and temporal variability of the sediment transfer processes at the front of the rock glacier and in the underlying gully. In order to get this information, we applied a combination of different methods including observations (webcam images), geodetic surveys (DGPS), and remote sensing (photogrammetry, terrestrial LiDAR).

The results point out the major role of water availability in the erosion of the rock glacier front and illustrate the link between the sediment yield and the creep velocity. Additionally, the terrestrial laser scanning data allow to assess the volumes and the spatial distribution of the sediment transfer processes.

REFERENCES

Delaloye, R., Lambiel, C., Gärtner-Roer, I. (2010). Overview of rock glacier kinematics research in the Swiss Alps. Seasonal rhythm, interannual variations and trends over several decades. Geogr. Helv., 65: 2, 135–145.

Gärtner-Roer, I. (2012). Sediment transfer rates of two active rockglaciers in the Swiss Alps. Geomorphology, 167-168, 45-50.

9.9

Tectonic Control on Topographic and Exhumational Segmentation of the Himalaya

Camille Litty1,2, Peter Van Der Beek1, Mallory Baudin1, Jonathan Mercier1, Xavier Robert1 and Elisabeth Hardwick1

(1) University of Grenoble, ISTerre, Grenoble, France, (2) Universität Bern, Institute of Geological Sciences, Berne, Switzerland

Although the Himalayan range is commonly presented as cylindrical along-strike, geological structures, topography, precipitation, and exhumation rates as recorded by low-temperature thermochronology data all vary significantly from west to east. In particular, segments of the belt that are characterized by a clear topographic step between the Lesser and Higher Himalaya, associated with a peak in precipitation and focused exhumation (e.g. central Nepal, Himachal Pradesh) alternate with segments where the topography increases more linearly to the north, precipitation peaks at lower elevations and exhumation rates appear to be lower (e.g. western Nepal, Bhutan). The potential climatic or tectonic controls on these spatially variable topographic, precipitation and exhumational patterns have been widely discussed in recent years but remain unclear.

Thermo-kinematic modelling predicts that the geometry of the main Himalayan detachment (in particular the presence or absence of a major mid-crustal ramp) strongly controls the kinematics, exhumation and topography of the orogen. Where a major crustal ramp is present, the topography shows a steep gradient that focuses exhumation and orographic precipitation whereas the topography is gentler and exhumation less focused in the absence of a ramp. We test this prediction by comparing the pattern of topography, river incision and long-term exhumation in central Nepal, where a major crustal ramp has been imaged by geophysical methods, with new results from the remote Karnali River transect in far western Nepal, where a ramp is predicted to be absent or minor. Our results therefore imply that along-strike climatic variations in the Himalaya respond to tectonics rather than driving it. The presence or absence of a mid-crustal ramp may be due to inherited structures on the underthrusting Indian Plate or, alternatively, may reflect transient behaviour of the accreting Lesser Himalayan thrust stack, which may oscillate between frontal accretion (without a ramp) or basal accretion in the presence of a ramp.

9.10

Geomorphological evidence of Holocene neotectonics in Southern Amazonia

Umberto Lombardo[1]

[1] *Geographisches Institut, University of Bern, Hallerstrasse 12, CH-3012 Bern (lombardo@giub.unibe.ch)*

The Llanos de Moxos (LM), located between the central Andes and the Brazilian Shield, is one of the largest seasonally flooded savannahs of South America. Covering most of Southern Amazonia, this region includes the transition between the rainforest and the savannah and is, therefore, a preferential area to study past changes in the size and dynamics of the Amazon rainforest (Mayle et al., 2000). Paleoecological reconstructions are key in order to understand the origins of modern landscapes and the potential changes they could undergo in the future due to climate change. Up to now, paleoecological reconstructions in southern Amazonia have been based primarily on pollen and charcoal archives from lake cores. Most studies point towards climate and pre-Columbian human impact as having shaped the evolution of the landscape during the Holocene, implicitly assuming that other factors, such as neotectonics, did not play an important role.
My research suggests that neotectonics was a key factor behind the formation of the modern landscape of the LM and past inundation patters during the Holocene. It uses both new and published data based on the analysis of remote sensing imagery and extensive field work in the LM. The study of the region's modern and paleorivers, ria lakes, paleosols and topography provides a strong case in favour of the thesis that the northern part of the LM constitutes the southern margin

of the Fitzcarrald arch (Figure 1) and that it has experienced uplift during the Holocene. The evidence suggests that at least two uplift events took place: a first uplift, which caused the formation of Lake Oceano, and a second uplift, which formed Lake Rogaguado. These two events appear to be linked to the knickpoints observed near the towns of Guayaramerín and Puerto Siles respectively. A 130 cm long sedimentary core extracted from the bottom of Lake Rogaguado shows a terrestrial phase at the bottom, which predated the formation of the lake, followed by a lacustrine phase. These two phases are separated by a clay layer which could be the result of a quick depositional event linked to the uplift. Radiocarbon ages from both phases indicate that the lake formed around 6k cal years BP (Lombardo, 2014). Data suggests that the back water effect due to these uplifts transformed the region's major rivers in seasonal ria lakes, causing the deposition of thick organic clay layers along the Beni, Mamoré and Madre de Dios river banks.

The central and southern part of the LM have a different sedimentary setting, where the subsiding foreland basin of the central Andes creates the accommodation space for the formation of distributive fluvial systems (DFS). Two of these DFS, the one deposited by a paleo Grande River (Lombardo et al., 2012) and the one deposited by the Maniqui River, have been extensively surveyed and cored at several locations. Radiocarbon ages of soils buried by these alluvia indicate that the central and southern LM experienced extensive deposition of fluvial sediments throughout the Holocene.

I argue that neotectonic episodes could have dramatically changed the drainage of the Llanos, determining its flooding regime, soil properties and forest-savannah ecotone. These results stress the need for geomorphologists, paleoecologists and archaeologists to take into account neotectonics when reconstructing the region's past.

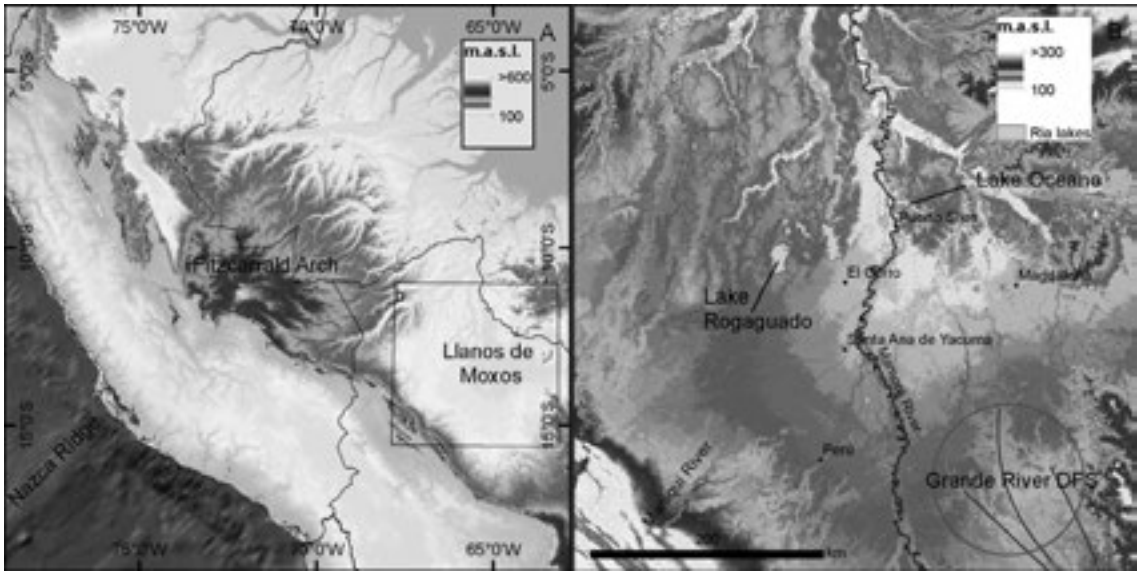

Figure 1. Geological setting of the LM. In B the LM are shown together with the location of the study sites cited in the text.

REFERENCES

Lombardo, U. 2014: Neotectonics, flooding patterns and landscape evolution in southern Amazonia. Earth Surf. Dynam. Discuss., 2(2), 635-679.

Lombardo, U., May, J.-H., Veit, H. 2012: Mid- to late-Holocene fluvial activity behind pre-Columbian social complexity in the southwestern Amazon basin. The Holocene, 22(9), 1035-1045.

Mayle, F.E., Burbridge, R., Killeen, T.J. 2000: Millennial-scale dynamics of southern Amazonian rain forests. Science, 290(5500), 2291-2294.

9.11

Along-strike changes in landscape architecture condition the mechanical coupling between hanging and subducting plates: An attempt to explain the absence of the Coastal Cordillera in the Andes of Northern Chile

Andrea Madella[1], Romain Delunel[1], Fritz Schlunegger[1], Sönke Szidat[2]

[1] *Institut für Geologie, Universität Bern, Baltzerstrasse 1+3, CH-3012 Bern (andrea.madella@geo.unibe.ch)*
[2] *Departement für Chemie und Biochemie, Universität Bern, Freiestrasse 3, CH-3012 Bern*

The western Andean margin of Peru and northern Chile comprises the Coastal Cordillera near the Pacific coast, the volcanic arc that delineates the western margin of the Altiplano Plateau, and the Western Escarpment that links the Altiplano with the Coastal Cordillera. This architecture is remarkably constant along the entire Andean margin. An exception, however, is present near Arica at 21°S where the Andes change their strike direction by c. 45° from NW-SE to N-S. There, a Coastal Cordillera is completely absent over a lateral width of circa 50 km, which has posed a substantial problem in the geodynamic interpretations of this mountain range. Here, we investigate the post-Oligocene landscape evolution in Northernmost Chile and Southernmost Peru. We particularly focus on the Coastal Cordillera and on the related unsolved and poorly documented problem of the missing range at the latitude near Arica, where the Andes form a c. 45°-large bend. We discuss the implications of along-strike unhomogeneity in coastal uplift in terms of continental basin evolution and sediment discharge into the trench, analyzing the possible consequences at the subduction interplate boundary. In order to do this, we compile structural data from the literature and complement this dataset with new observations on orthophotos, which we relate to the erosional history of the Andean landscape within a detailed chronological and stratigraphic framework. We finally combine this information with data about the offshore and onshore pattern of seismicity, which ultimately allows us to determine along-strike changes in the coupling relationships between the hanging South American continental plate and the subducting Nazca oceanic plate. The results show that a climate-driven sediment starvation in the trench West of the central Andes has most likely increased the friction at the interplate boundary, which in turn can be invoked to explain a renewed phase of uplift at least during the Quaternary, and even longer (Lamb & Davis 2003). Nevertheless, near Arica, the absence of a sediment barrier at the coast since 2.7 My and possibly earlier, combined with the amphitheater-shaped topography of the Western Andes at this latitude, has resulted in a three times higher sediment discharge in this area compared to the regions farther south and north. We interpret that the larger supply of sediment along this reach could have reduced the friction at the interface between the hanging and subducting plates, keeping the uplift push at lower levels and the Coastal Cordillera submerged below Arica. In addition we speculate that the postulated low-friction anomaly might explain the lower frequency of large subduction earthquakes in the area.

REFERENCES

Lamb, S., & Davis P. 2003: Cenozoic climate change as a possible cause for the rise of the Andes, Nature, 425, 792-797.

9.12

On the prediction of daily rainfall thresholds for the triggering of landslides and debris flows

Peter Molnar[1], Elena Leonarduzzi[1], Georgina Bennett[2]

[1] *Institute of Environmental Engineering, ETH Zürich, Stefano-Franscini-Platz 5, CH-8093 Zürich (molnar@ifu.baug.ethz.ch)*
[2] *Department of Geological Sciences, University of Oregon, Eugene, Oregon, USA*

Rainfall is a key triggering variable for many natural hazards in Alpine environments, most notably floods, landslides and debris flows. The simplest predictive models of landslides and debris flows identify the minimum rainfall intensity that led to events, and develop rainfall intensity-duration threshold curves (Guzzetti et al. 2008). Although widely used, this approach does not allow for a clear assessment of prediction accuracy and errors. In this paper we first present a method for an objective selection of daily rainfall thresholds which led to landslides across Switzerland, and second we show that a more physically-informed modelling approach can explain the variability in daily rainfall which generates debris flows on a catchment scale.

In Switzerland the WSL has been systematically collecting information on flood and mass movement damage since 1972 (Hilker et al. 2009). We extracted 2497 landslides with known locations from this dataset and studied the properties of their triggering rainfall events from the new gridded MeteoSwiss dataset RhiresD. A daily rainfall threshold R* was found by minimizing both false positive and negative predictions (Type I and II errors) in the period 1972-2012. This allows us to generate probability maps of triggering daily rainfall (Figure 1) which can be used for landslide vulnerability assessment.

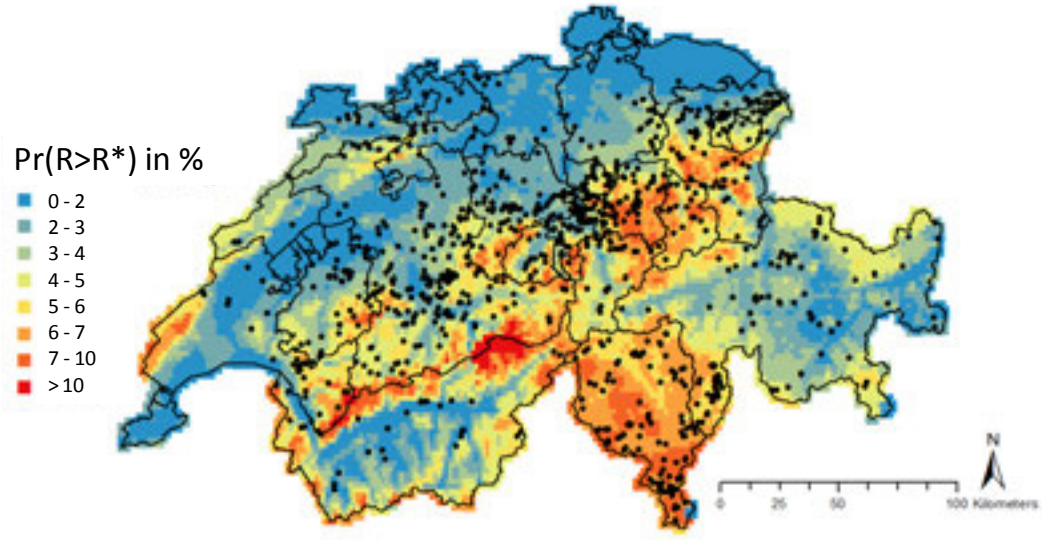

Figure 1. The probability of exceeding a daily rainfall threshold of R*=22 mm/d across Switzerland estimated for the period 1961-2012 from the gridded precipitation dataset RhiresD (MeteoSwiss). Points show a selection of 969 landslides from the WSL Landslide Dataset.

Although useful as an indicator, a constant daily rainfall triggering threshold cannot capture all events correctly due to stochasticity in triggering, initial conditions, system nonlinearities. There is ample evidence for this in the field (e.g. Schneuwly-Bollschweiler & Stoffel 2012). This observed variability in rainfall triggering can however be predicted by physically-based models combined with stochastic forcing. As an example we show the variability in daily rainfall depths that led to debris flows in the Illgraben catchment simulated with the probabilistic sediment cascade model SedCas (Bennett et al. 2014).

Figure 2 shows the SedCas prediction of the statistical distribution of daily rainfall which led to debris flows when the catchment sediment supply and storage history are accounted for, together with the hydrological dynamics (Figure 2a), and a drop in performance when the hydrological part of the model which simulates transient soil moisture is turned off and all rainfall becomes runoff (Figure 2b). The second case corresponds to a constant rainfall threshold approach modulated by sediment availability. We conclude that it is the history of sediment supply and transport together with landscape susceptibility to erosion and triggering rainfall that determine the likelihood of mass transport events. Predictive models should be built to account for this uncertainty.

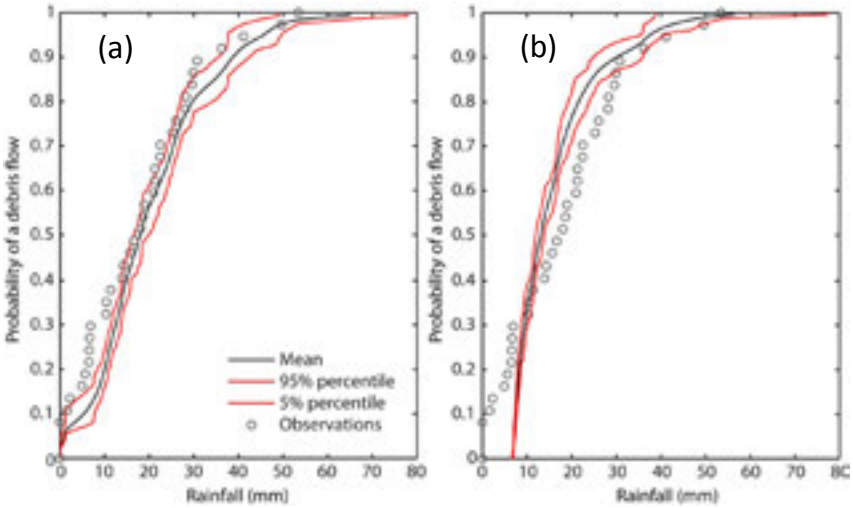

Figure 2. Probability of daily rainfall triggering a debris flow in the Illgraben with the SedCas model with the hydrological component turned on in (a) and off in (b) with 95% uncertainty bounds, compared with observed rainfall during 36 debris flows in the period 2000-2009 (points) (from Bennett et al. 2014).

REFERENCES
Bennett, G., Molnar, P., McArdell, B.W. & Burlando, P. 2014: A probabilistic sediment cascade model of sediment transfer in the Illgraben, Water Resour. Res., 50, doi:10.1002/2013WR013806.
Guzzetti, F., Peruccacci, S., Rossi, M. & Stark, C. P. 2008: The rainfall intensity-duration control of shallow landslides and debris flows: an update, Landslides, 5, 3-17.
Hilker, N., Badoux, A. & Hegg, C. 2009: The Swiss flood and landslide database, Nat. Hazards Earth Syst. Sci., 9, 913-925.
Schneuwly-Bollschweiler, M. & Stoffel, M. 2012: Hydrometeorological triggers of periglacial debris flows in the Zermatt valley (Switzerland) since 1864, J. Geophys. Res., 117, F02033.

9.13

Neotectonics of a slow orogenic arc inferred from quantitative geomorphology: the Jura Mountains.

Rabin M. [1], Sue C. [1], Champagnac J.-D. [2], Valla P. G. [3], Carry N. [1], Eichenberger U. [4], Bichet V. [1], & Mudry J. [1]

[1] *Chrono-environnement Laboratory, UMR 6249. University of Franche-Comté, 16 route de Gray 25000 Besançon. France (mickael.rabin@univ-fcomte.fr) (christian.sue@univ-fcomte.fr) (vincent.bichet@univ-fcomte.fr) (nicolas.carry@univ-fcomte.fr) (jacques.mudry@univ-fcomte.fr)*
[2] *Geologisches Institut. ETH-Zürich Sonneggstrasse 5 8092 Zürich. Switzerland (jean-daniel.champagnac@erdw.ethz.ch)*
[3] *Institute of Earth Surface dynamics. University of Lausanne, CH-1015 Lausanne (Pierre.Valla@unil.ch)*
[4] *ISSKA, 68 rue de la Serre CH-2301 La Chaux-de-Fonds. Switzerland (urs.eichenberger@isska.ch)*

The Jura has been well studied from a structural point of view, but still remains the source of debates, especially regarding its current and recent tectonic activity. It is deemed to be always in a shortening state according to geomorphologic and stress/strain data, «container-title»:»Tectonophysics»,»page»:»381-406»,»volume»:»321»,»issue»:»4»,»source»:»ScienceDirect »,»abstract»:»Recently completed in situ stress measurements using the borehole slotter at 33 new test sites within the Swiss and French Jura Mountains, combined with previously published stress data, allow a detailed description of the contemporary state of stress in this fold-and-thrust belt and the adjacent foreland. Five stress provinces can be recognized, with two different general orientations of maximum horizontal stress SH: (1but geodetic studies available on the Jura involve disagreement between authors.

Quantitative morphotectonic approaches have been increasingly used since a couple of decades to infer relationships between climate and tectonics in landscape evolution. In this study, we propose to apply morphometric tools to calcareous bedrock in a slowly deformed mountain belt (Jura Mountains). In particular, we used watersheds metrics determination and associated river profiles analysis to quantify the degree and nature of the equilibrium between the long term tectonic forcing and fluvial erosion processes. We present a systematic analysis of river profiles applied to the main drainage systems of the Jura.
Our morphometric results reveal abnormal longitudinal profiles, which are controlled by tectonic and/or karst forcing. Evaluating the relative contributions of tectonics and karst influence on the destabilization of river profiles is challenging and appears still unresolved. However, we managed to isolate morphometric signals (i.e. knickpoints or prominent knickzones along the river profiles) which are correlated with major tectonic structures along the Jura arc. Results suggest recent tectonic activity along both the internal and external ranges of the Jura. This activity seems to be located along E-W oriented structures and could correspond to folds and thrusts still recently active. However, slope destabilization, as well as rock softening due to tectonic crushing, which both occur along thrust faults can also led to disturbed river profiles. Further investigations coupling DEM analysis and detailed field observations are required to fully evaluate the tectonic imprint on the Jura landscape morphology.

9.14

Temporal pattern and memory in sediment transport in a step-pool channel: an experimental study

Matteo Saletti[1], Peter Molnar[1], Marwan A. Hassan[2], André E. Zimmermann[3], Michael Church[2]

[1] *Institute of Environmental Engineering, ETH Zürich, Stefano-Franscini-Platz 3, CH-8093 Zürich (saletti@ifu.baug.ethz.ch)*
[2] *Department of Geography, University of British Columbia, Vancouver, Canada*
[3] *Northwest Hydraulic Consultants, North Vancouver, BC, Canada*

In this work we analyze the complex dynamics of sediment transport and bed morphology in steep streams with experimental data. We use a dataset of 32 experiments in a steep flume with natural sediment conducted at UBC, Canada (Zimmermann, 2009). In every experiment, high resolution (1 sec) time series of sediment transport at the outlet of the flume for different grain size classes were measured for different combinations of sediment input rates, discharges, and flume slopes. We use this data to explore the temporal patterns of sediment transport as a function of grain size, searching for evidence of pulses in sediment transport connected to step collapsing events.

We focussed on the "long recovery" in the system, i.e. long periods of adjustment with no sediment feed. In the experiments, in the first phase sediment was fed into the system allowing the bed structures (steps) to form. Subsequently the feed was shut down and the water discharge was proportionally increased. In this phase we divided the signal into segments of constant water discharge and we analyzed the statistical properties of total and fractional transport rate at the channel outlet. The results show that the relation between instantaneous discharge and sediment transport is not trivial and exhibits large variability (Figure 1). This is because the sediment on the bed is well packed and armored within the step structures, and as a result sediment transport is limited by the stability of steps and supply of sediment, and not discharge alone. Consequently, the concept of transport capacity limitations in steep mountain streams is not likely to be valid.

We characterized and quantified the memory in sediment transport rates by estimating the autocorrelation coefficient for different time lags from transport data for different grain sizes. Our results show that the structure of memory in the instantaneous transport rate is both a size-dependent and magnitude-dependent phenomenon: temporal autocorrelation is stronger for small grain size fractions and when the average sediment transport rate is large (Figure 2). We argue that the dropoff in the autocorrleation coefficient with lag time reflects the memory scale of the system which connects morphological variations (e.g. step collapse or other sediment pulses) with actual transport stochasticity (e.g.fluctuations in bed shear stress) at various timescales.

Step-pool systems are not ubiquitous and they require the right combination of transport stage, channel width and sediment supply to exist (Church & Zimmermann, 2007, Zimmermann et al., 2010). Our results give a physical explanation for the extreme and isolated sediment pulses, connecting them to sudden collapses of bed structures. The experimental results have connections to natural streams where channels have been shown to respond at different timescales to changes in sediment supply (Hassan & Zimmermann, 2012).

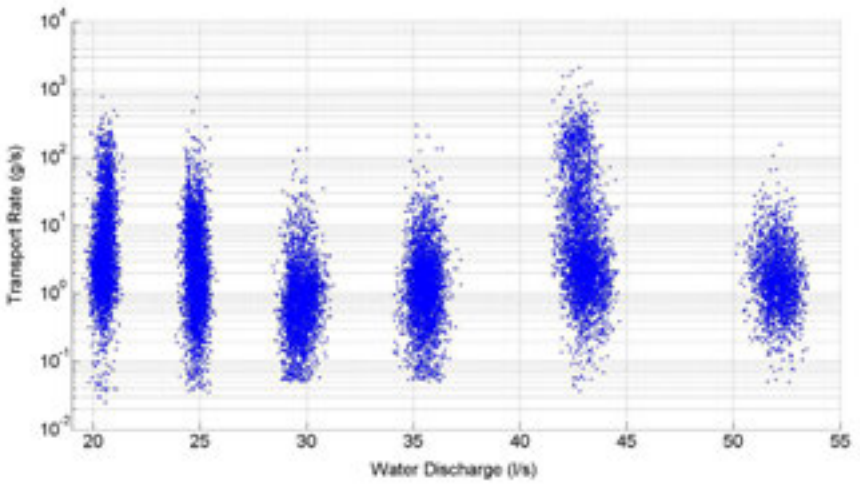

Figure 1. Total instantaneous sediment transport rate as a function of water discharge during the "long recovery" phase in 6 increments of flow.

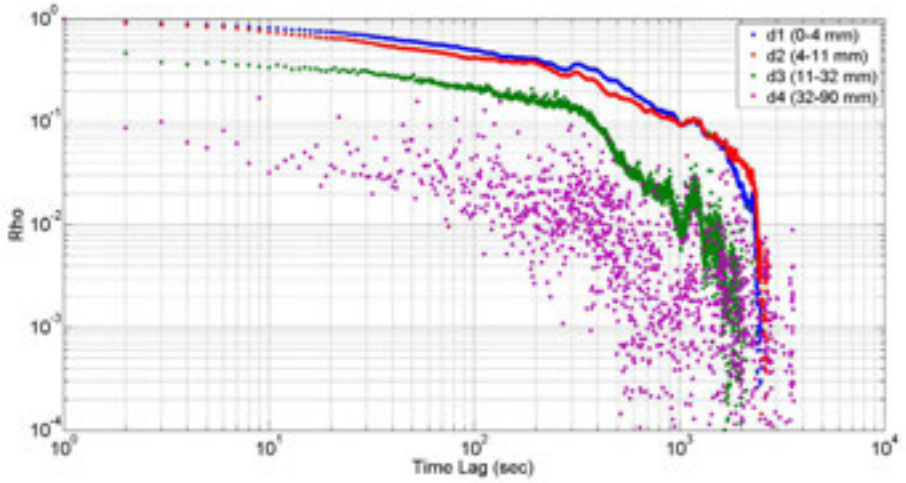

Figure 2. Autocorrelation coefficient in instantaneous sediment transport rates against time lag for different grain sizes.

REFERENCES

Church, M., & Zimmermann, A.E. 2007: Form and stability of step-pool channels: Research progress. Water Resources Research, 43, 1–21.

Hassan, M.A. & Zimmermann, A.E. 2012: Channel Response and Recovery to Changes in Sediment Supply, in Gravel-Bed Rivers: Processes, Tools, Environments (eds M. Church, P. M. Biron and A. G. Roy), John Wiley & Sons, Ltd, Chichester, UK.

Zimmermann, A.E. 2009: Experimental investigations of step-pool channel formation and stability, Ph.D. thesis, 359 pp, Univ. of British Columbia, Vancouver, B. C., Canada

Zimmermann, A.E., Church, M. & Hassan, M.A., 2010: Step-pool stability: Testing the jammed state hypothesis. Journal of Geophysical Research, 115(F2).

P 9.1

Relations between Catchment Lithologies and Shallow Surface Morphologies of Three Alluvial Fans in the Rhône Valley (SW Switzerland).

Lise Boulicault[1], Andrea Moscariello[1], Mario Sartori[1], Dario Ventra[1], Julien Moreau[2]

[1] *Department of Earth and Environmental Sciences, University of Geneva, Rue des Maraîchers 13, 1205 Genève, Suisse (lise.boulicault@etu.unige.ch, andrea.moscariello@unige.ch, mario.sartori@unige.ch, darioven@hotmail.com)*
[2] *Department of Geosciences and Natural Resource Management, Section of Geology, University of Copenhagen, Øster Voldgade 10, 1350 København, Denmark (julien.moreau@ign.ku.dk)*

The surface topography of the Rhône Valley in southwestern part of Switzerland comprises numerous tributaries alluvial fans issued by lateral relief. The morphodynamic evolution of these Quaternary fans is complex and primarily controlled by their catchment properties (morphology, bedrock lithology, etc.).

In this study, we focus on the comparison of three fan-catchment systems in the valley, namely the Abboyeu, the Losentse and the Illgraben. Our objectives are: (1) to describe the present-day morphology and stratigraphic architecture of the fans; (2) to verify possible correlations between the fans depositional mechanisms and catchment lithology; and (3) based on the common assumption that vegetation may hinder surface erosion, to test the qualitative sensibility of the fan's activity in function of surface and typology variations of the vegetation cover in the catchments.

Field observations include the measurement of sedimentary logs and acquisition of shallow-subsurface profiles by Ground Penetrating Radar (GPR). Grain-size and petrographic analyses are carried out on sediment samples from each fan and compared with catchment geological maps. Comparisons show that in spite of differences in catchment bedrock, all fans are aggraded by the stacking of sedimentary gravity flow deposits, unconfined waterflow (sheet-flows) deposits and streamflow (waterlaid) deposits.

Predictive models of petrographic spectra of eroded material were computed for each catchment, integrating such parameters as bedrock lithologies, topography and vegetation type (forests and grassland). Considering the protective role of vegetation, these predictive models estimate the relative percentage of each catchment lithology which will potentially be eroded in situations of reduced vegetation cover. If validated such petrographic spectra could be used to identify the signatures of fluctuations in the past vegetation cover distribution inferred by the stratigraphical variation of lithological composition of fan deposits.

P 9.2

Sedimentary record of river response to climate change: example of the Paleocene-Eocene thermal maximum in the South-Pyrenean foreland basin, Spain

Chen Chen[1], Sebastien Castelltort[1], Brady Foreman[2]

[1] *Section des Sciences de la Terre et de l'Environnement, Université de Genève, Rue des Maraîchers 13, CH-1205 Genève, Suisse (chen.chen@unige.ch, sebastien.castelltort@unige.ch)*
[2] *University of Wyoming, Department of Geology & Geophysics, Laramie, WY, USA*

The "Paleocene-Eocene Thermal Maximum" (PETM), is understood to be an extreme global warming event that occurred about 56 million years ago and during which, global annual temperatures are estimated to have increased by 5-8°C. An outstanding question is: in addition to the global increase in temperature, how has precipitation been perturbed during the event, and how have surface processes responded?

In the southern Spanish Pyrenees, the Paleocene succession of the Tremp-Graus basin is made up of the Talarn (Danian) and Esplugafreda (Thanetian) red bed formations. The Esplugafreda section is composed of approximately 250m of reddish paleosols and contains numerous channel-like bodies of calcareous conglomerates, which are interpreted as braided channels. The Esplugafreda formation is overlain by the Claret Conglomerate—an extensive sheet-like unit which ranges in thickness between 1m and 4m of clast-supported calcareous conglomerate and pebbly calcarenites and is interpreted mark the beginning of the Eocene. The Claret conglomerate is thus proposed to be a witness of river response to a dramatic climate change, in the form of the transformation of a braided river and floodplain system into an enormous conglomeratic braided plain (formed over at least 2000km^2 conservatively) indicating dramatic change in the hydrologic cycle. The conglomerate unit ends abruptly and is overlaid by fine-grained yellowish soil which mainly made up of silty mudstones with abundant small size carbonate nodules suggesting another shift in the hydrological cycle after the PETM.

Here we first present channel width/depth and grain size data collected in the southern Pyrenees (Tremp, Aren, and Serraduy sectors) in order to document river response during the climate change assumed to have occurred during the PETM. Secondly, we present preliminary results of experiments investigating river response to water discharge and sediment supply variations in a flume tank at the Surface Dynamics Laboratory of the University of Geneva. Our principal objective is to discuss the possible precipitation perturbations at the PETM and how these are transferred into the rock record of river response.

P 9.3

Constraints on the role of tectonic and climate on erosion revealed by two time series analysis of marine cores around New Zealand

Antoine Cogez[1,2], Laure Meynadier[1], Claude Allègre[1], Delphine Limmois[1], Frédéric Herman[2] & Jérôme Gaillardet[1]

[1] *Institut de Physique du Globe de Paris, Université Paris Diderot, 1 rue Jussieu, 75005 Paris (France)*
[2] *Université de Lausanne, Institut de la Dynamique des Surfaces Terrestres, Quartier Unil-Mouline, Bâtiment Geopolis, CH-1015 Lausanne (Switzerland)*

Physical and chemical weathering govern rocks and chemical elements cycles at the Earth surface. The importance of climate and tectonics has been identified but their relative influence still needs to be investigated. We address this question by studying neodymium (Nd) isotopic composition time series in two sediment cores located on the eastern and western sides of New Zealand. The current and past climatic and oceanographic settings of this region have been already well studied, providing the underlying framework. Both detrital and authigenic phases of the sediment can be measured to decouple oceanic from continental contributions.

The results show glacial-interglacial variations of the authigenic signal, with larger amplitudes for the eastern core. We propose that continental erosion on the South Island controls Nd isotopes records in both cores. Mixing calculations show that Nd discharge was 2 to 10 times higher during glacial times than during interglacials on the eastern side, whereas these variations are almost negligible on the western side. We suggest that higher physical erosion during glacial on the East, with sediments characterized by higher specific area that can be easily weathered, are due to larger ice volumes and fluxes during glacial periods. The steady rates on the western side imply that they are rather controlled by rock uplift rates. The temporal relationship between climatic indicators like oxygen isotopes and the Nd isotopic composition shows non linear response of the erosion-weathering to climate forcing. Those results contrast with previous studies using the same tracer, that showed stronger erosion and weathering over Himalaya during interglacial periods. This study illustrates the complexity of erosion and weathering responses to climatic and tectonic forcings.

P 9.4

Impact of river regulation on potential sediment mobilization

Anna Costa[1], Peter Molnar[1], Stuart N. Lane[2], Maarten Bakker[2]

[1] *Institute of Environmental Engineering, ETH Zürich, Stefano-Franscini-Platz 3, CH-8093 Zürich (costa@ifu.baug.ethz.ch)*
[2] *Institute of Earth Surface Dynamics, University of Lausanne, CH-1015 Lausanne*

The upper Rhône basin (upstream of Lake Geneva) has been heavily affected by human activities during the last century. The most evident impacts are related to river regulation, specifically flow impoundement, flow abstraction and channelization. In the last century and mainly since 1960, several large dams have been built along the main tributaries of the Rhône River, resulting in the water storage of a volume equal to 20% of the total annual river flow. The dams are part of hydropower systems which abstract water from streams and transfer it through complex networks (intakes, tunnels and pumping stations) to the reservoirs. Hydropower production leads to regulated flow in the Rhône: mostly an increase of winter flows, a reduction of summer flows (Figure 1), and a decrease of flood peaks. The sediment supply into Lake Geneva has decreased following dam construction (Loizeau & Dominik, 2000) due to the storage of sediment in upstream reservoirs, in rivers with reduced sediment transport capacity due to flow abstraction, and due to the development of sediment mining. Our hypothesis is that streamflow regulation itself has dramatically impacted the sediment transport dynamics of the system.

We investigate the impacts of flow regulation on the sediment transport regime, by analysing the effects on potential sediment transport capacity (bedload). By the use of different bedload transport formulae (Meyer-Peter Müller, Rickenmann, Smart and Jaeggi), the potential sediment transport capacity is computed at Port du Scex, a hydrometric station located on the Rhone River just upstream of Lake Geneva. Potential sediment mobility occurs when the applied bed shear stress exceeds a critical value, $\tau>\tau_c$. The applied bed shear stress is computed as $\tau=\rho g h S$, with water depth (h) measured from rating curves. We obtain an estimate of the energy slope (S) from the analysis of the river cross section, assuming uniform flow. The critical value of bed shear stress τ_c is computed using empirical formulae as a function of the grain diameter (d_s). To identify the grain size-dependent effects of streamflow regulation, computations are applied to different grain sizes taken from grain size distributions of river bed sediment.

The results in Figure 2 show that flow regulation has indeed resulted in higher potential mobility of finer grain sizes due to winter flow increases, but not for the coarsest fractions which are mobilized only during summer high flows. Although the analysis is constrained to potential mobility conditions only, and does not account for sediment supply (e.g. flushing, bed and bank erosion, etc.), we nevertheless consider the results as a first order approximation of the changes in sediment dynamics due to river regulation in this Alpine catchment. Analyzing several stations along the main Rhône River and its tributaries will allow us to construct the spatial connectivity of seasonal sediment mobility along the river system. In future work we will also concentrate on fine suspended sediment transport and supply.

The present work is part of the research project SEDFATE funded by the SNF Sinergia Programme, which aims at quantifying the human impacts on the observed reduction of suspended sediment inflows to Lake Geneva.

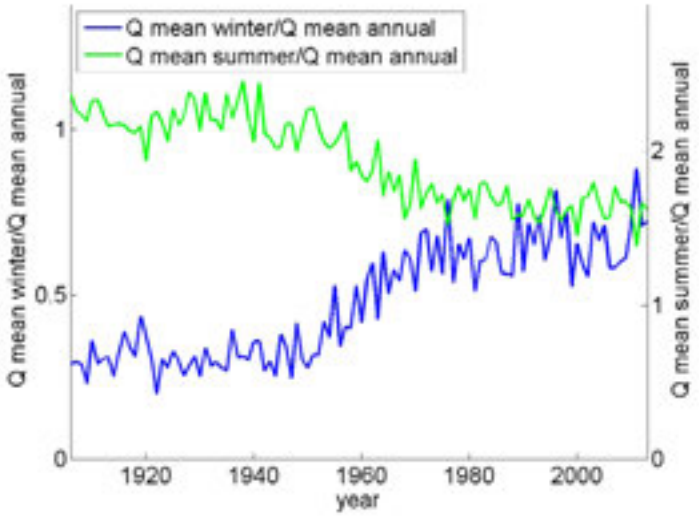

Figure 1. Relative mean winter and mean summer discharge time series at Port du Scex.

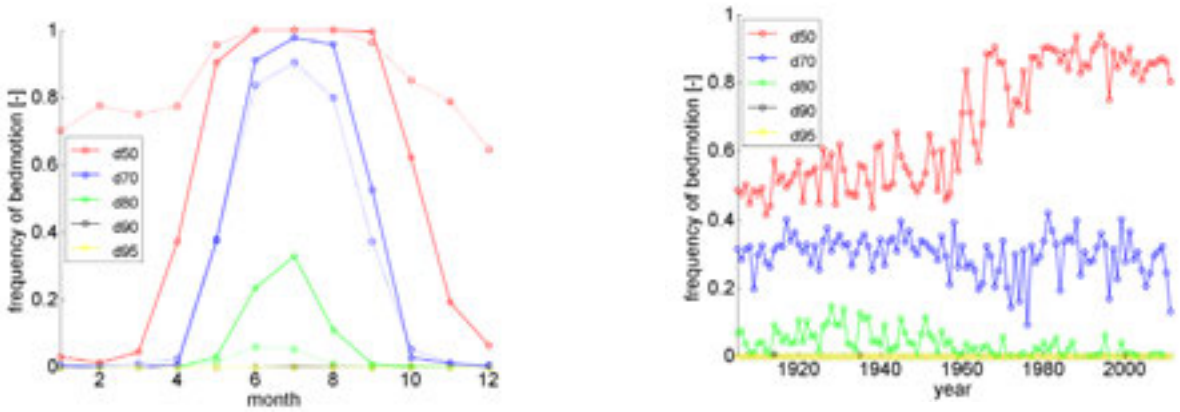

Figure 2. The estimated annual frequency of bedload motion for different grain sizes at Port du Scex per year (left) and monthly (right), before (full line) and after (dashed line) dam construction which mostly took place between 1955-1970 (Gillioz, 2012).

REFERENCES
Gillioz, A. 2012: Frequency of theoretical bedload transport in the Rhone river and in some of its tributaries with evaluation of dam impact, MSc Thesis, ETH Zürich, 61pp.
Loizeau, J.-L. & Dominik, J. 2000: Evolution of the Upper Rhone River discharge and suspended sediment load during the last 80 years and some implications for Lake Geneva, Aquatic Sciences, 62, 54-67.

P 9.5

Using accelerometers for the study of active rock glaciers kinematics and dynamics

Xavier Cros[1], Luc Braillard[1], Martin Bochud[2], Reynald Delaloye[1]

[1] *Department of Geosciences/Geography, University of Fribourg, Chemin du Musée 4, CH-1700 Fribourg (name.surname@unifr.ch)*
[2] *GeoAzimut Sàrl, Rte de la Fonderie 8, CP 145, 1705 Fribourg*

Rock glaciers kinematics and dynamics have been studied in Switzerland since the 1970s using different methods such as photogrammetry, GPS measurements campaigns, permanent GPS stations, InSAR surveying and Webcams images.

We present here the basic principles and the first results of a new technique that uses accelerometers, which, combined with GPS measurements campaigns and permanent GPS stations, has the potential to better understand the short-term movements of boulders present on rock glacier surfaces.

Our test site is the Tsarmine rock glacier in the Swiss Alps (Valais, elevation of 2460-2680 m asl.) which is studied since 2004 (GPS measurements, one permanent GPS station, Lidar, photogrammetry, Webcam images).

The components we use are 3-axis accelerometers from the new generation type such as those present in portable electronic devices. Their low price and small size allow using numerous units to cover large areas of the rock glacier. The accelerometers that are fixed on surface boulders measure angle variations relative to gravity in order to detect the movement of the boulders. From a technical point of view, the accelerometers send the data to a controller by way of a radio communication. The controller saves the data onsite on a memory card and transmits them to a webserver via a GSM communication. Calculating angle variations of accelerometers out of those data, we can detect slow moving tilts of boulders and analyse the rock glacier surface's behaviour within a short time-scale.

The main objective of this project is to study the links that exist between the movements of the different boulders equipped with an accelerometer and the known velocities from the permanent GPS station.
Another goal is to test and validate this system onsite.
The surveillance of slope instabilities is a possible development of the system.

P 9.6

Tracking terrestrial rockfalls on a rock glacier headwall at Piz Corvatsch, Switzerland

James Glover, Robert Kenner

Snow and Permafrost, WSL Institute for Snow and Avalanche Research SLF, Flüelastrasse 11, CH-7260 Davos Dorf. (glover@slf.ch)

A history of rockfall events has been revealed from anual terrestrial laser scanning and change analysis of a rock glacier head wall close to Piz Corvatsch in Switzerland which has been conducted since 2011. The rock wall is divided by a large central couloir containing a considerable amount of potentially frozen scree which represents the main origin of rockfall activity during the observation period. The rockfall deposit zone extends from the base of the central gully and over two rock glaciers at the foot of the rock wall. The measurement methods applied to produce the change maps are similar to those described in Kenner et al (2013). Rockfall release zones, rockfall impact craters and the corresponding rockfall deposits are all visible when computing the derived differences (DSM) between anual laser scans. Mapping these features has provided a data set characterising the rockfall runout zone and has permitted an assessment of the rockfall runout dynamics onto the rock glacier below. Rockfall runout paths were traced by linking consecutive rockfall impact craters based on crater morphology identified in the change maps. Assuming a parabolic trajectory between impact craters, estimations of rockfall runout velocites and jump heights are made (Volkwein, et al., 2011). Additional rockfall features are also evident in the change maps such as rock fragmentation and rock runout mode (rolling, sliding, rock orientation and jumping). The deposit maps and estimates of runout dynamics have allowed a cross validation of a three-dimensional rigid-body rockfall model RAMMS::Rockfall (Leine, et al., 2013) which could be applied to back calculate the rockfall events in the area.

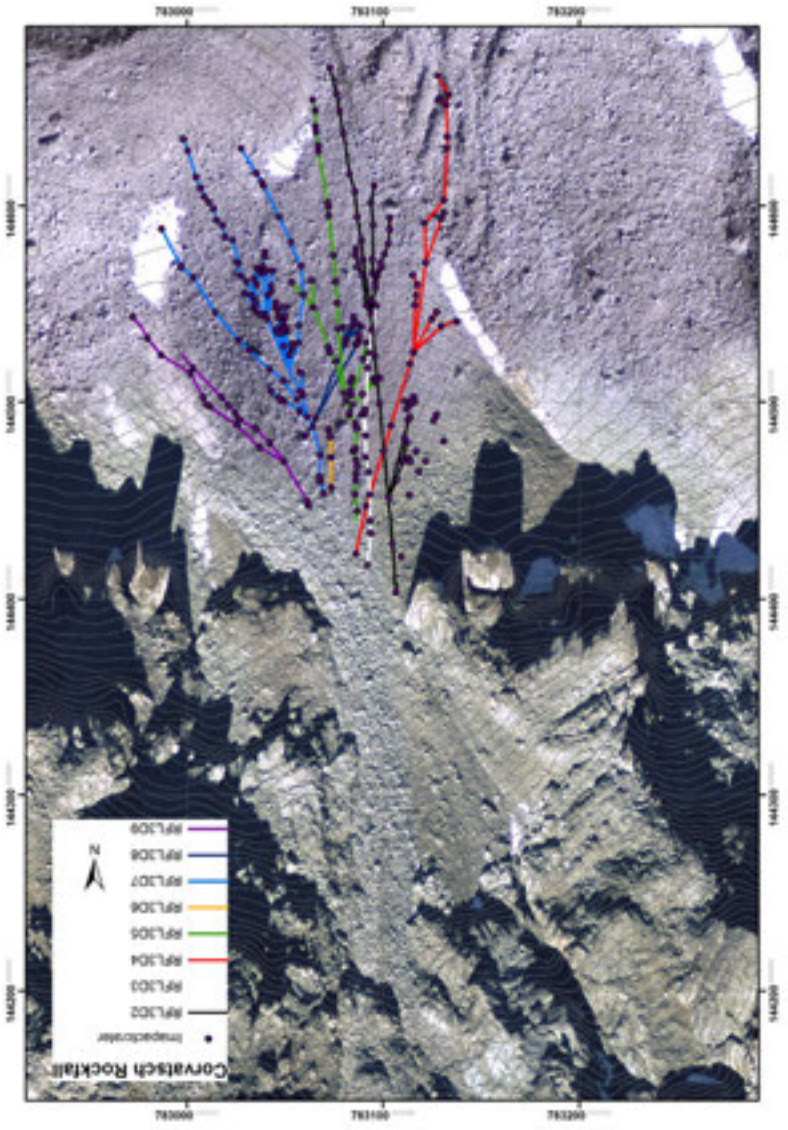

Figure 1. Mapped rockfall paths from 2011 to 2012 beneath the Piz Corvatch rock glacier headwall.

REFERENCES

Kenner, R.; Phillips, M.; Danioth, C.; Denier, C.; Thee, P. & Zgraggen, A. Investigation of rock and ice loss in a recently deglaciated mountain rock wall using terrestrial laser scanning: Gemsstock, Swiss Alps, Cold Regions Science and Technology , 2011, 67, 157 - 164

Leine, R., Schweizer, A., Christen, M., Glover, J., Bartelt, P., and Gerber, W. (2013). Simulation of rockfall trajectories with consideration of rock shape. multibody System Dynamics, pages 1-31.

Volkwein, A., Schellenberg, K., Labiouse, V., Agliardi, F., Berger, F., Bourrier, F., Dorren, L. K. A., Gerber, W., and Jaboyedo_, M. (2011). Rockfall characterisation and structural protection - a review. Natural Hazards and Earth System Science, 11(9):2617{2651.

P 9.7

Application and analysis of terrestrial laser scanning in a periglacial high mountain area

Luca Heim, Isabelle Gärtner-Roer, Ross Purves, Johann Müller

Department of Geography, University of Zurich, Winterthurerstrasse 190, CH-8057 Zurich, Switzerland (contact: luca.heim@geo.uzh.ch)

In order to monitor variation of mass transportation in high mountain regions for geomorphologically significant forms such as rock glaciers and deep-seated slope failures, periodic measurements of land surface form can be applied. Remote sensing techniques have become essential tools if we are to better understand variation in mass transport, and the link to process, in high mountain areas (Kääb, 2002). Beside classical methods, such as photogrammetry, the technique of laser scanning, both airborne and terrestrial, is an established method for purposes of geomorphological assessments (Armesto et al. 2008).

This paper examines the application of terrestrial laser scanning (TLS) in a high mountain environment on the research object of rock glacier Muragl, situated in the Upper Engadin, Switzerland. The processing procedure includes the co-registration of TLS point clouds, the processing of digital elevation models (DEM) with cell sizes of 1m and 0.5m, the development of grayscaled Tiffs, and finally the determination of horizontal and vertical displacement rates by applying the image correlation software CIAS. The latter software is based on the identification of correpsonding grayscale pixel values by application of a double cross-correlation function (Kääb 2002). Based on repeated orthophotos, this method has already been applied for Muragl rock glacier in 2000 (Kääb & Vollmer 2000) and is now adapted with TLS data for the first time. The current study focuses on an evaluation of the resulted length and height changes by consulting additional literature and data. Furthermore, the suitability of the TLS technique, concerning the high mountain environment, as well as the present procedure are assessed.

The observed time span covers one entire year and includes four snapshots of the rock glacier surface. Hence, the displacements are determined for three individual periods, indicating monthly (July 13 to August 13), seasonal (July 13 to October 13) and annual variations (July 13 to July 14).

Distinct velocity patterns as well as vertical changes are quantified and presented in terms of permafrost-related mass movement processes.

Overall, the TLS technique can be regarded as feasible method for purposes of investigating or monitoring high mountain environments. Exemplarily, measured changes of 0.5m within the area of the lower part are evaluated as reasonable, compared to reference data. However, specific characteristics, such as the horizontal measurement perspective or the point spacing, have to be considered as it entails the occurrence of data voids. With respect to standard deviations of around 10cm due to the co-registration, especially displacements within the range of 0 to 0.1m have to be assessed critically.

REFERENCES

Armesto, J., Ordóñez, C., Alejano, L., Arias, P. 2009: Terrestrial laser scanning used to determine the geometry of a granite boulder for stability analysis purposes, Geomorphology, 106, 271-277.

Kääb, A. & Vollmer, M. 2000: Surface Geometry, Thickness Changes and Flow Fields on Creeping Mountain Permafrost: Automatic Extraction by Digital Image Analysis, Permafrost and Periglacial Processes, 11, 315-326.

Kääb, A. 2002: Monitoring high-mountain terrain deformation from repeated air-and spaceborne optical data: examples using digital aerial imagery and ASTER data, ISPRS Journal of Photogrammetry and remote sensing, 57, 39-52.

P 9.8

The Great Karoo region of South Africa: A carbon source or sink?

Nikolaus J. Kuhn [1], Philip Greenwood[1], Brigitte Kuhn [1], John Boardman [2], Ian Foster [3], Mike Meadows [4]

[1] *Department of Environmental Sciences, University of Basel, Switzerland (nikolaus.kuhn@unibas.ch)*
[2] *Environmental Change Institute, University of Oxford, UK*
[3] *School of Science and Technology, University of Northampton, UK*
[4] *Department of Environmental and Geographical Science, University of Cape Town, South Africa*

Work undertaken in the seasonally arid upland areas of the Great Karoo region of South Africa has established a link between land degradation and overgrazing that began approximately 200 years ago when European farmers first settled the area. In response to changing land use, coupled with shifting rainfall patterns, parts of the landscape are now characterised by badlands on footslopes of valley-sides and complex gully systems on valley floors. Limited precipitation and agricultural intensification, particularly from around the 1920s onwards, resulted in a growing demand for water, and led to the construction of many small reservoirs, most of which are now in-filled with sediment. Whilst the deposited material has provided a means of linking catchment-scale responses to land use changes over the last ca. 100 years, the influence of land degradation on erosion and deposition of soil-associated carbon (C) has received only limited attention. Despite a reversion to extensive agriculture and reduced livestock densities in certain areas, limited vegetation regrowth suggests that soil rehabilitation will be a long-term process. This communication presents preliminary results from an investigation to determine whether land degradation in the Karoo has resulted in a shift from a net sink of C to a net source of C. Sediment deposits from a silted-up reservoir in a small dry valley system was analysed for varying physico-chemical parameters. Total Carbon (TC) content was recorded and the sharp decrease in total C content with decreasing depth suggests that land degradation during and after post-European settlement probably led to accelerated erosion of the relatively fertile surface soils, and this presumably resulted in the rapid in-filling of reservoirs with carbon-rich surface material. Overall, the results indicate a sharp decline in soil organic matter (SOM) of eroded material, presumably as a consequence of land degradation. This suggests that in landscapes such as the overgrazed drylands of the Karoo, the C sink effect caused by soil erosion is now much smaller than at the onset of overgrazing leading to accelerated erosion. Such a loss of C sinks on degraded rangeland soils raises the question whether past soil erosion may have had a greater attenuating effect on GHG emissions than modeled scenarios of present emissions suggest.

P 9.9

Classifying torrential catchments according to the contribution of slope movements in the sediment supply to the channel: a pilot study in the lower Valais (Swiss Alps)

Mario Kummert[1], Chloé Barboux[1] & Reynald Delaloye[1]

[1] *Department of Geosciences/Geography, University of Fribourg, Chemin du Musée 4, CH-1700 Fribourg (name.surname@unifr.ch)*

In mountainous areas such as the Alps, the steepness of the slopes and the high elevations emphasize the development of mass movements such as rock glaciers, landslides or sagging. These processes participate in the so-called sediment cascade (Caine 1974) by transferring large amounts of rock debris downward. In some cases, the sediment yield at the margin such slope movement can be significant. When a sedimentary connectivity exists between the moving landforms and torrential channels, this sediment yield may influence the triggering of hazardous gravitative processes such as debris flow.

Catchments in which slope movements are connected to the torrential network are characterized by a potentially unlimited debris supply to the channels, inducing a potentially long term torrential activity. More importantly, any change in the slope movements behavior (e.g., changes in velocity) can modify the frequency-magnitude relation of debris flow events. As an example, the recently observed acceleration of several rock glaciers in the Swiss Alps (e.g., Roer et al. 2008, Delaloye et al. 2013) could lead to the increase of torrential activity. Because of this relation between the torrential activity and slope movements, the detection and the monitoring of these particular catchments could help to predict the evolution of the torrential activity and to plan mitigation strategies.

In this context, a methodology to locate, classify and describe catchments in which slope movements are connected to the torrential network has been developed. In a first step, catchments are classified given their torrential activity and the presence of moving landforms connected to the channels. In a second step, the past and current state of the slope movements (velocity, morphology, sediment yield) is assessed for the catchments classified as a priority. The methodology reposes on a simple analysis of aerial images, DEM and two DInSAR-based slope movement inventories covering two different time period (90's and late 2000's), and was applied recently on a test area in the lower Valais (western Swiss Alps). This contribution intends to present the methodology and the first results.

REFERENCES

Caine, N. (1974). The geomorphic processes of the alpine environment. In°: Ives, J.D., Barry, R.G. (Eds.). Arctic and Alpine Environments. Methuen, London, 721-748.

Delaloye, R., Morard, S., Barboux, C., Abbet, D., Gruber, V., Riedo, M., Gachet, S. (2013). Rapidly moving rock glaciers in Mattertal. In: Mattertal - ein Tal in Bewegung. Graf, C. (eds). Publikation fur Jahrestagung der Schweizerischen Geomorphologischen Gesellschaft 29. Juni - 1. Juli 2011, St. Niklaus, Birmensdorf, Eidg. Forschungsanstalt WSL. 21–31.

Roer, I., Haeberli, W., Avian, M., Kaufmann, V., Delaloye, R., Lambiel, C., Kääb, A. (2008). Observations and considerations on destabilizing active rockglaciers in the European Alps. In : Kane, D.L. & K.M. Hinkel (eds): Proceedings of the 9th International Conference on Permafrost, June 29-July 3, 2008, Fairbanks, Alaska, 2, 1505-1510.

P 9.10

Along-strike changes in landscape architecture condition the mechanical coupling between hanging and subducting plates: An attempt to explain the absence of the Coastal Cordillera in the Andes of Northern Chile

Andrea Madella[1], Romain Delunel[1], Fritz Schlunegger[1], Sönke Szidat[2]

[1] *Institut für Geologie, Universität Bern, Baltzerstrasse 1+3, CH-3012 Bern (andrea.madella@geo.unibe.ch)*
[2] *Departement für Chemie und Biochemie, Universität Bern, Freiestrasse 3, CH-3012 Bern*

The western Andean margin of Peru and northern Chile comprises the Coastal Cordillera near the Pacific coast, the volcanic arc that delineates the western margin of the Altiplano Plateau, and the Western Escarpment that links the Altiplano with the Coastal Cordillera. This architecture is remarkably constant along the entire Andean margin. An exception, however, is present near Arica at 21°S where the Andes change their strike direction by c. 45° from NW-SE to N-S. There, a Coastal Cordillera is completely absent over a lateral width of circa 50 km, which has posed a substantial problem in the geodynamic interpretations of this mountain range. Here, we investigate the post-Oligocene landscape evolution in Northernmost Chile and Southernmost Peru. We particularly focus on the Coastal Cordillera and on the related unsolved and poorly documented problem of the missing range at the latitude near Arica, where the Andes form a c. 45°-large bend.

We discuss the implications of along-strike unhomogeneity in coastal uplift in terms of continental basin evolution and sediment discharge into the trench, analyzing the possible consequences at the subduction interplate boundary. In order to do this, we compile structural data from the literature and complement this dataset with new observations on orthophotos, which we relate to the erosional history of the Andean landscape within a detailed chronological and stratigraphic framework. We finally combine this information with data about the offshore and onshore pattern of seismicity, which ultimately allows us to determine along-strike changes in the coupling relationships between the hanging South American continental plate and the subducting Nazca oceanic plate.

The results show that a climate-driven sediment starvation in the trench West of the central Andes has most likely increased the friction at the interplate boundary, which in turn can be invoked to explain a renewed phase of uplift at least during the Quaternary, and even longer (Lamb & Davis 2003). Nevertheless, near Arica, the absence of a sediment barrier at the coast since 2.7 My and possibly earlier, combined with the amphitheater-shaped topography of the Western Andes at this latitude, has resulted in a three times higher sediment discharge in this area compared to the regions farther south and north. We interpret that the larger supply of sediment along this reach could have reduced the friction at the interface between the hanging and subducting plates, keeping the uplift push at lower levels and the Coastal Cordillera submerged below Arica. In addition we speculate that the postulated low-friction anomaly might explain the lower frequency of large subduction earthquakes in the area.

REFERENCES

Lamb, S., & Davis P. 2003: Cenozoic climate change as a possible cause for the rise of the Andes, Nature, 425, 792-797.

P 9.11

Spatio-temporal quantification of geomorphological processes in the recently deglaciated area surrounding the Findelengletscher

Alexander Ruff[1], Andreas Vieli[1], Isabelle Gärtner-Roer[1] & Philip C. Jörg[1]

[1] *Department of Geography, University of Zurich, Winterthurerstrasse 190, CH-8057 Zürich (alexander.ruff@uzh.ch)*

The ongoing melting of the Findelengletscher in the Valais exposes landscapes that are in an unstable or metastable state, and consequently accountable to modification, erosion and sediment release. The aim is to map the geomorphological processes and thereafter quantify the spatio-temporal dynamics and sediment transfer rates of these processes, similar to the paraglacial concept (Ballantyne 2002).

This is possible due to the unique dataset consisting of digital elevation models (DEMs) having a 1m resolution from 2005, 2009, 2010, and 2014. The first three measurements are from repeated airborne light detection ranging (LiDAR) campaigns (Joerg et al. 2012, and Joerg & Zemp 2014). This years data was collected by the mapping drone eBee which takes aerial images and produces a DEM at even higher resolution the the LiDAR data. A geomorphological map is designed and the appropriate processes are linked to them. The nine year timeserie reveals the temporal movements of the processes and allows a precise quantification thereof but leaves us with the problem of adressing the uncertainties of deadice melt and sediment loss through fluvial runoff. First results will be presented at the Swiss Geoscience Meeting.

REFERENCES

Ballantyne, C. K. (2002). Paraglacial geomorphology. Quaternary Science Reviews, 21(18-19), 1935–2017. doi:10.1016/S0277-3791(02)00005-7

Joerg, P. C., Morsdorf, F. & Zemp, M. (2012), `Uncertainty assessment of multi-temporal airborne laser scanning data : A case study on an Alpine glacier', Remote Sensing Environment 127, 118-129.

Joerg, P. C. & Zemp, M. (2014), `Evaluating Volumetric Glacier Change Methods Using Airborne Laser Scanning Data', Geografiska Annaler: Series A, Physical Geography, pp. n/a. URL: http://doi.wiley.com/10.1111/geoa.12036

P 9.12

"Via Soreda": a geotouristical trail in the hearth of the Parc Adula project

Cristian Scapozza[1] & Christian Ambrosi[1]

[1] *Istituto scienze della Terra (IST), Scuola Universitaria Professionale della Svizzera Italiana (SUPSI), Campus Trevano, CH-6952 Canobbio ([surname.name]@supsi.ch)*

In the framework of the Parc Adula project, the National Park candidate located between Canton Ticino and Graubünden, the geoheritage – defined as the natural, archaeological and historical heritage related to geology and geomorphology – constitutes one of the fundamental pillars of the natural heritage of the entire area of the park, and is recognized both at Swiss and international level. For this natural park, the geoheritage promotion will then be an essential part of the integrated promotion of the natural heritage of the entire region.

The geotrail "Via Soreda" makes it possible the geoheritage promotion in the hearth of the Parc Adula project, connecting not only two Cantons (Ticino and Graubünden) or two regions (Valle di Blenio and Valser Tal), but also two different language regions (italian and romansch/german) sorrounding the Adula/Rheinwaldhorn massif. The trail develops from the Lake Luzzone (Blenio Valley) to the Lake Zervreila (Vals Valley) and cross the Soreda Pass (2759 m asl).

From the historical point of view, this geotrail makes it also possible to revive an ancient trail used already in the Late Middle Ages, and which allowed farmers from the Blenio Valley to exploit the Alpe Soreda or Lampertschalp (litt.: "alps of the lombards"), located in the upper Vals Valley. From a symbolic point of view, therefore, the Via Soreda aims to exploit the ancient route which was used to connect the two communities living on both sides of the Soreda Pass.

The geotrail is supported by a geotouristical map where it is possible to find a simplified geological and geomorphological mapping and additional information as the topography, the conditions of the trail, the travel times and the position of nine geo-stop. The content of the nine geo-stop is illustrated on the backside of the map by a series of didactical cards, structured by a landscape history divided on four main chapters (Figure 1): the history of the rocks ("storia delle rocce"), the history of the deformations ("storia delle deformazioni"), the history of the landforms ("storia delle forme") and the Human history ("storia dell'Uomo"). These four histories of the landscape make it possible to put in perspective the Human history with the history of the Earth, and to show the stratification of geological, geomorphological and anthropogenic events which have modelled the current alpine landscapes.

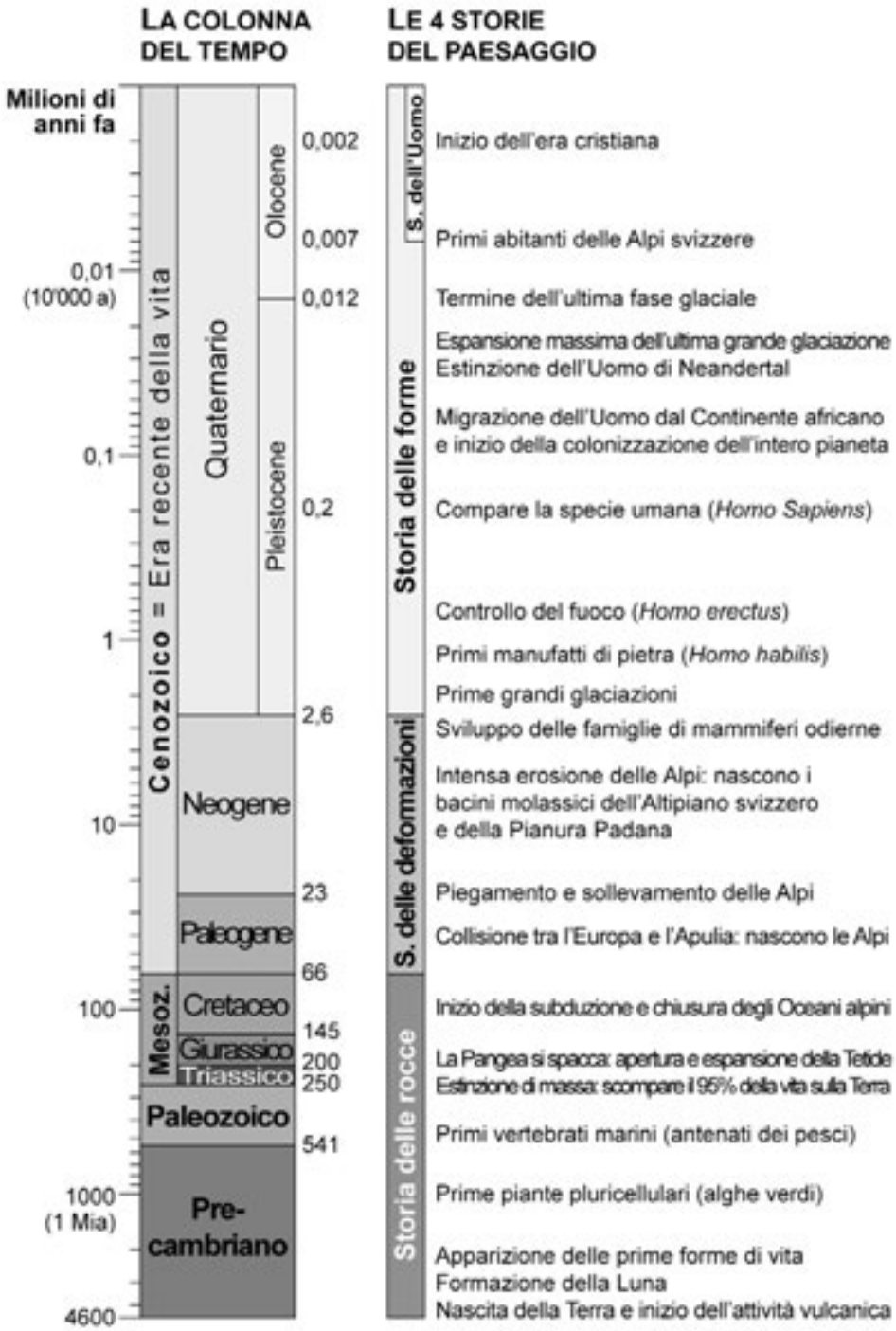

Figure 1. The four histories of the landscape used for support the geo(morpho)logical information of the geotouristical map of the Via Soreda geotrail.

P 9.13

A new high-resolution bathymetric map of Lake Zurich

Michael Strupler[1], Tobias Schwestermann[1], Michael Hilbe[2], Flavio S. Anselmetti[2], Michael Strasser[1]

[1] *Geological Institute, ETH Zurich, Sonneggstrasse 5, CH-8092 Zurich, Switzerland (michael.strupler@erdw.ethz.ch)*
[2] *Institute of Geological Sciences, University of Bern, Baltzerstrasse 1+3, CH-3012 Bern, Switzerland*

While subaerial geomorphic features can often be identified and described by eye, the subaquatic geomorphology is hidden below water bodies. Valuable tools for a broad range of audiences are bathymetric maps, which are created by different methods, from the interpolation of manually measured point-depths to remote sensing methods. For limnogeological applications, the subaquatic geomorphology derived from swath bathymetric measurements offers a great tool for the investigation of past and present sediment dynamic processes; especially if combined with sedimentological or reflection seismic data.

During the last few decades, a bathymetric map of Lake Zurich with isobath-intervals of 2.5 m (based on the interpolation of a dense-grid of single-beam echosounding measurements; Schlund, 1972) has successfully been used as base for various investigations on Lake Zurich's subbottom (e.g. the geological map of Schindler (1976) or the mass-movement catalogue of Strasser (2007)).

During a research expedition in spring 2014, Lake Zurich was surveyed with a Kongsberg EM2040 multibeam echosounder (300 kHz) in order to construct a high-resolution bathymetric dataset. The echosounder was mounted on ETH Zurichs research vessel "Arethuse". Data processing took place with CARIS HIPS and SIPS 8.1.

The new bathymetry with a grid resolution of 1 m displays a plenitude of geomorphic features in a yet unseen detail. Here, we present various examples of subaquatic landforms on the bottom and slopes of Lake Zurich, which were created by glacial, gravity-, earthquake- and current-driven processes or human impact. A morphologic step divides Lake Zurich's northern, up to 136 m deep, basin, which is rich on sedimentdynamic events from a flat, 20-25 m deep southern basin. The new bathymetry data provide new evidence of current-related bedform structures along this morphological step, while shallow- and deep-seated subaquatic landslides in the deep basin (originally described by Schindler (1976), Kelts (1978) and Strasser (2007)) are now imaged in great detail, which allows the discussion of headscarp erosion and frontal bulging.

We further compare the new 2014 bathymetry dataset with the 1972 dataset with respect to the different spatial resolutions but also towards identification of active sediment dynamic processes from differential bathymetric data.

As a long-term goal, the new bathymetric dataset and extracted parameters thereof will serve as basis to model the basin-wide subaquatic slope-failure susceptibility towards establishing a subaquatic geohazard map of Lake Zurich.

REFERENCES

Kelts, K. 1978: Geological and sedimentological evolution of lakes Zürich and Zug, Switzerland. Diss. ETH Zürich, Nr. 6164.

Schindler, C., 1976: Eine geologische Karte des Zuerichsees und ihre Deutung: Eclogae geol. Helv. 69, 125–138.

Schlund, R.A. 1972: Zürichsee: topogr. Plan 1:5 000. Ingenieurbüro Dr. R.A. Schlund, Zürich; Meliorations- und Vermessungsamt des Kt. Zürich.

Strasser, M. 2007: Quantifying Late Quaternary Natural Hazards in Swiss Lakes: Subaquatic Landslides, Slope Stability Assessments, Paleoseismic Reconstructions and Lake Outbursts. Diss. ETH Zürich, Nr. 17285.

P 9.14

Distribution of sinkholes And their sensitivity to Falling in praw-bistoon calcareous masses

Tahere Jalilian[1], Manizhe Gohroudi Tali [2], Javad Darvishi Khatooni[3]

[1] *Department of Geomorphology, University of shahid Beheshti, Iran*
[2] *Associate shahid Beheshti University, Department of Physical Geography*
[3] *Geological survey of Iran*

Fractures are one of the most important factors in capability of carbonate rocks permeability. System of fractures and joints bring about penetration and access of water into the deeper layers. Therefore, karstic processes can developed along them and result in variety of karst morphology. In mountainous massif of Parav - Bistoun, Various forms of the karst landscapes such as karrens, uvalas, dolines, caves and soon have emerged due to specific lithology and tectonic. The Depressions are interesting because of great influence of fractures on them and their dimensions. Thus, in this study, morphotectonic consideration of depressions an important part of karstic studies has been marked.

The area has various depressions with different dimentions. The biggest depression has depth of 115 m and diameter of 180 m. It shows azimuth angle of 30 degrees. Other karstic forms of area are caves, which recognized as the deepest cave in the whole Middle East and have depth and length of about 751 and 1361m, respectively(Jafarbeyglou etal, 2011).
According to the geomorphological evidence of the region (Parav cave with a depth of 751 m and local erosion levels such as great fields of karst in surfaces of low relief) the thickness of Bistoun limestone together with high purity that have potential for dissolution, Depressions of the area lie within dissolution - break down class from sextet categories that introduced by Ford &Williams (2007, p. 341).

Prav-Bisetoon massif composed of limestone and is located in over thrusted Zagros (high-broken), west of Iran at Kermanshah province. The main form is Karsts in sinkholes which the formation and development is affected by thrust, Faults and fractures in this region. The land form provides appropriate conditions for feeding and development of ground water resources and has influenced region hydrogeology. Topographic maps, Digital elevation model, ETM+ and LISS (III) images and field work were used. The sinkholes were identified accordingon field observations, algorithm of topographic maps, Radar images, thermal Indicatorsand reflection images. Sensitivity analyses of sinkholes have done based on field work, Standardization of variables, Preparation itstable locations Matching and statistical methods. The Results were shown, 183 sinkholes and their Regression models of Sensitivity to collapse(FIG 1). An assessment method was done on location analysis of sinkholes due to lineaments, faults, rivers channel and statistical tests(FIG 2).

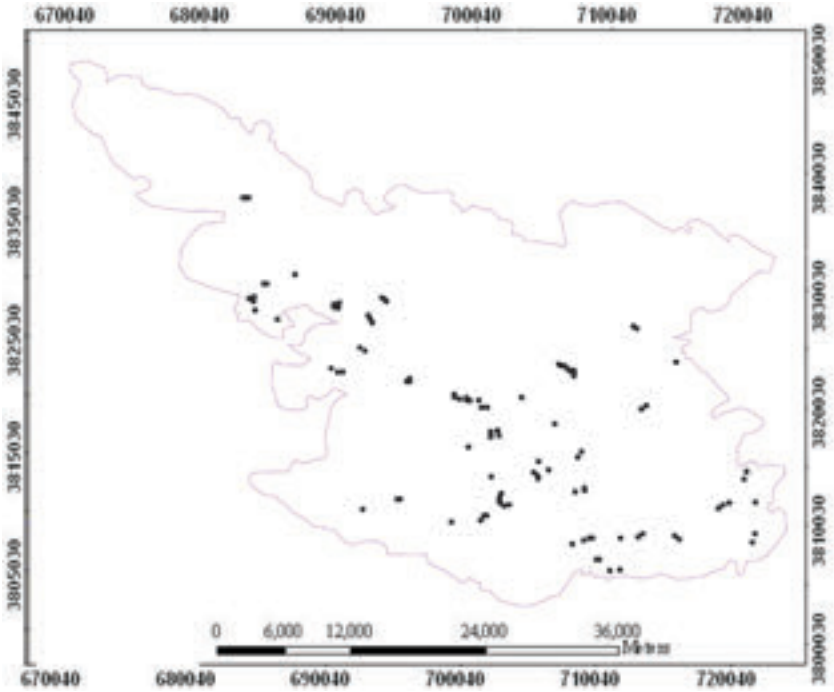

Figure 2. Location of Sinkholes in Prav-Bisetoon

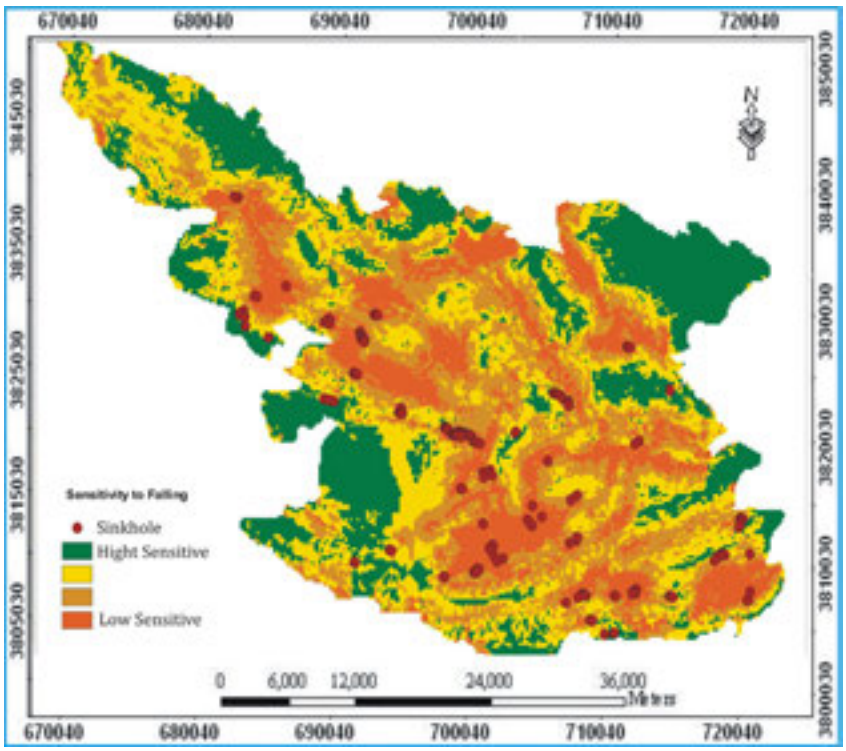

Figure 2. Sensitivity to Falling in Prav-Bisetoon

REFERENCES

Ford. D. and Williams. P, (2007), Karst Hydrogeology and Geomorphology, John Wiley & Sons Ltd1-562.

Jafarbeyglou, m., Moghimi. E. Safari F. 2011. Evaluating morphotectonic karst sinks in Parav - Bistoun mass using DEM, Geography and Environmental lanning Journal 22th. Year, vol. 44, No.4, Winter 2012

P 9.15

Potential fate of eroded SOC after erosion

Liangang Xiao[1], Wolfgang Fister[1], Philip Greenwood[1], Yaxian Hu[1], Nikolaus J. Kuhn[1]

[1] *Physical Geography and Environmental Change group, Department of Environmental Sciences, University of Basel, Klingelbergstrasse 27, CH-4056 Basel (liangang.xiao@unibas.ch)*

Globally, soils contain more than three times as much carbon as either atmosphere or terrestrial vegetation. Soil erosion moves soil organic carbon (SOC) from the site of soil and SOC formation and to depositional environments. There some SOC might be sequestered. Combined with dynamic replacement at the site of erosion, the effect can significantly influence the carbon cycle. However, the fate of SOC moved by erosion has been subject to an intense controversy. Two opposing views prevail: erosion may contribute to SOC mineralization during transport and thus act as a source for atmospheric CO_2; the burial of SOC, on the other hand, can be seen as a sink while dynamic replacement maintains SOC at the eroding site and thus increase the C-stocks in soils and sediments. The debate suffers from a lack of information on the distribution, movement and fate of SOC in terrestrial ecosystems. This study aims to improve our understanding of the transport and subsequent fate of the eroded soil and the associated SOC. The research presented here focused on the SOC content and potential transport distance of erode soil. During a series of simulated rainfall soil eroded on crusted loess soils near Basel, Switzerland, was collected. The sediment was fractionated according to its settling velocity, with classes set to correspond to either a transfer into rivers or a deposition on slopes. The soil mass, SOC concentration and cumulative CO_2 emission of each fraction were measured.

Our results show that about 50% of the eroded sediment and 60% of the eroded SOC are likely to be deposited on the slopes, even during a high rainfall intensity event. This is 3 times greater than the association of SOC with mineral particles suggests. The CO_2 emission of the eroded soil is increased by 40% compared to disturbed bulk soil. This confirms that aggregate breakdown reduces the protection of SOC in aggregates. Both results of this study show that taking (i) the effect of aggregation on SOC redistribution and (ii) the subsequent CO_2 emission during the transport have to be considered to achieve a reliable assessment of the effect of soil erosion on the global C-cycle. They also indicate that our current balances may underestimate the CO_2 emission caused by soil erosion.

10. Quaternary environments: landscapes, climate, ecosystems, human activity during the past 2.6 million years

Irka Hajdas, Susan Ivy Ochs

Swiss Society for Quaternary Research (CH-QUAT)

TALKS:

10.1 Boulicault L., Sartori M., Moreau J., Corboud P., Moscariello A.: Late Holocene lacustrine deposits newly discovered within the Losentse alluvial fan in the central Rhône Valley, SW Switzerland.

10.2 Camozzi, O., Stalder, C., Rüggeberg, A., Spezzaferri, S.: Response of Cold-Water Corals (CWC) to large-scale paleoceanographic changes in the Western Melilla Mound Field (WMMF) eastern Alboran Sea: evidence from micro- and macrofauna assemblages and stable isotopes

10.3 Claude A., Akçar N., Ivy-Ochs S., Schlunegger F., Kubik P., Rahn M., Dehnert A., Schlüchter C.: Timing of Early and Middle Pleistocene glaciations in the Alps

10.4 Donau F., Grischott R., Kober F., Hajdas, I., Hippe H., Lupker M., Ivy-Ochs S., Christl M., Strasser M.: Holocene sediment budget and sediment dynamics of Lake Sils in the Upper Engadin

10.5 Häuselmann A.D., Tabersky D., Günther D., Cheng H., Fleitmann D.: Glacier presence petrified in a Swiss high alpine stalagmite

10.6 Hippe K., Hajdas I., Ivy-Ochs S., Maisch M.: Chronology of Middle Würm climate changes in the Swiss Alpine foreland

10.7 King G., Herman F., Valla P. Guralnik B.: OSL-thermochronology of Na- and K-feldspar from Namche Barwa, Tibet

10.8 Litty C., Schunegger F: Using grain size downstream variation to reconstruct erosional and sedimentological dynamics in the Pisco valley, western Peru.

10.9 Trauerstein M., Preusser F., Lowick S.E., Veit H.: Challenges in using luminescence dating to provide age control on Late Quaternary soil development on the central Swiss Plateau

10.10 Wegmüller F., Koehler H., Pümpin C., Wuscher P., Sévêque N.: Excavations at the Middle Palaeolithic site of Mutzig-Rain (Alsace, France)

10.11 Wüthrich L., Lutz S., Zech R., Zech M., Sirocko F.: Late Glacial vegetation reconstruction based on leaf waxes from the Gemündener Maar, Germany

POSTERS:

P 10.1 Ambrosi C., Scapozza C., Castelletti C., Soma L., Dall'Agnolo S.: Stratigraphy of Quaternary Deposits of the Mendrisiotto (Southern Swiss Alps)

P 10.2 Dubois N., Frédyier L., Brunner I.: Heavy metal distribution in lake sediments from the Joux Valley

P 10.3 El Kateb A., Stalder C., Neururer C., Spezzaferri S.: Pollution by phosphogypsum discharge into the Gulf of Gabes (Tunisia): Preliminary results.

P 10.4 Javad Darvishi Khatooni., Raziyeh Lak: Khuzestan dust source identification with using Satellite images and Sedimentary Geochemistry

P 10.5 Javad Darvishi Khatooni., Raziyeh Lak., Ali Azhdari: Study Khuzestan dusts pollution with using Sedimentary Geochemistry

P 10.6 Javad Darvishi Khatooni., Raziyeh Lak., Majid Moeini., Ali Azhdari: Dust containment priority in Khozestan plain, Iran

P 10.7 Lanny V., Schäfer I. K., Eglinton T. I., Zech R.: Long chain n-alkanes and n-carboxylic acids as molecular proxies for paleovegetation

P 10.8 Lavrieux M., Dubois N., Schubert C., Hofstetter T., Eglinton T.: The age of terrestrial biomarkers in lacustrine sediments as an historical indicator for anthropogenic soil erosion

P 10.9 Meuriot L., Dubois N., Molnar P., Girardclos S., Wüest A., Raman L., Brunner I.: Recent mass transport deposits in Lake Biel: tracking their ages, causes and consequences

P 10.10 Rodrigues L., Lombardo U., Veit H.: Understanding Pre-Columbian environmental adaptations strategies in agriculture: A case study of raised fields in Exaltación, in the Bolivian lowlands

P 10.11 Roser K., Schoeni A., Foerster M., Röösli M.: Development of an RF-EMF exposure surrogate for epidemiologic research from modelling, personal measurements and operator data

P 10.12 Silva T.A., Bakker M., Costa A., Girardclos S., Lane S.N., Loizeau J.L., Molnar P., Schlunegger F., Stutenbecker L.: Quantifying the impact of anthropogenic activities on the erosional and sediment budget in the Rhône River basin– the SEDFATE project.

P 10.13 Sojc, U., Hajdas, I., Ivy-Ochs, S., Akçar, N., Deline, P.: Building high resolution radiocarbon dating chronologies for the reconstruction of late Holocene landslide events in the Mont Blanc area, Italy

P 10.14 Vocadlova K., Petr L., Zackova K., Krizek M.: A record of Late Glacial and Holocene environmental changes in the Bohemian Forest, Czech Republic: The history of a central European upland after LGM

P 10.15 Wirth S.B., Sessions A.L.: The D/H signal of Holocene and modern leaf waxes in the sediments and catchment of a south-Alpine lake

P 10.16 Zurfluh, R., Kober, F., Ivy-Ochs, S., Hajdas, I., Christl, M.: Post-glacial Landscape Evolution of the Upper Haslital Aare between Handegg and Guttannen (Bernese Alps)

10.1

Late Holocene Lacustrine Deposits newly discovered within the Losentse Alluvial Fan in the Central Rhône Valley, SW Switzerland.

Lise Boulicault[1], Mario Sartori[1], Julien Moreau[2], Pierre Corboud[3], Andrea Moscariello[1]

[1] *Department of Earth and Environmental Sciences, University of Geneva, Rue des Maraîchers 13, 1205 Genève, Suisse (lise.boulicault@etu.unige.ch, andrea.moscariello@unige.ch, mario.sartori@unige.ch)*
[2] *Department of Geosciences and Natural Resource Management, Section of Geology, University of Copenhagen, Øster Voldgade 10, 1350 København, Denmark (julien.moreau@ign.ku.dk)*
[3] *Laboratory of prehistoric archaeologiy and anthropology, Institute F-A Forel, University of Geneva, route des Acacias, 18, 1211 Genève, Suisse (Pierre.Corboud@unige.ch)*

In this study, we focus on the Losentse alluvial fan, one of the largest fans of the central Rhône Valley, SW of Switzerland. This work aims to understand the evolution of the fan through time and space, in particular with respect to the regional evolution of this portion of Rhône Valley.

The Losentse fan extends over c. 8 km^2, with a radius of 3 km and a slope of ~4° to the south. The Losentse channel incises the fan and shows natural cross-sections up to 10 m high and 500-m long where detailed sedimentary logs were measured. The fan mostly consists of a vertical stack of amalgamated gravels and sands interpreted as sedimentary gravity flows and sheet-flows deposits forming gently dipping tabular beds. The beds are occasionally interrupted by graded lenticular gravels and coarse-grained sand associated with bed load processes.

The detailed sedimentary analysis revealed, the presence of c. 2 m-thick clayey and silty deposits containing several wood fragments and well preserved paludal gastropods intercalated within the debris flow succession,. The deposits are draping the distal and mid parts of the fan up to the elevation of 520 m (asl). To explore the fine-grained lacustrine deposits continuity, two Ground Penetrating Radar (GPR) antennas have been used to produce images of the subsurface of the fan. The combination of 250 and 50 MHz antennas provide different resolutions and penetrations useful to better image bellow and above the shallow and slightly conductive layer represented by the lacustrine deposits. Seven kilometres of profiles oriented parallel to the fan slope and along the contour lines have been acquired. The GPR data show the wide 3D spatial extension the conductive layer. The correlation of those profiles with the sedimentary logs allows us to interpret this sharp reflector as being the fine-grained lacustrine layer within the fan. Four AMS Carbon-14 datings of gastropods and pieces of wood contained within the fine-grained deposit yield ages ranging between 2810 and 1970 +/- 30 yrs cal. BP. We interpret those deposits as the record of a major lacustrine event which occurred between the end of the Late Bronze Age and the end of the Iron Age.

The lacustrine deposits found in the Losentse fan are 45 m above the current local elevation of the Rhône Valley, which in this valley segment, measures 3.5 km in width. At present, no geomorphological evidences and no plausible mechanism for the deposit of such a dam have been found. On the other hand, other lacustrine deposits have been discovered at 1.5 km downstream and 15 km upstream of the Losentse fan. These fine-grained deposits are both located below 520 m. They are very similar to the Losentse lacustrine deposits in terms of grain-sizes, thicknesses, lateral extensions and ages.

As a result, we suggest that a common regional lacustrine event occurred in the Rhône Valley between the end of the Late Bronze Age and the Iron Age. The mechanism that should have dammed the Rhône Valley is not known at the moment. The sector of the valley more suitable to locate a natural dam is the Saint Maurice glacial sill, which shows two thresholds at c. 520 m (asl), is cut by two very narrow channels and is highly exposed to landslide and debris-flow events.

The comparison between our hypothesis of the existence of a temporary lake occupying the Rhône Valley seems consistent with the occurrence of several ancient settlements discovered below 520 m (asl) during the period of extension of the lacustrine event. However, the ranges of uncertainties associated with both geological and archeological datings are high and make these comparisons difficult at the moment.

Dating of other lake deposits found in the valley, searching of a potential dam and double-checking the chronological consistency of the archeological and geological data in more detail will have to be carried out in order to validate our hypothesis. The effects of a temporary lake in the Rhône Valley on the known fluctuations of the Geneva Lake's level during the Late Bronze age could also be also explored.

10.2

Response of Cold-Water Corals (CWC) to large-scale paleoceanographic changes in the Western Melilla Mound Field (WMMF) eastern Alboran Sea: evidence from micro- and macrofauna assemblages and stable isotopes

Osvaldo Camozzi a, Claudio Stalder a, Andres Rüggeberg a ,b ,c, Silvia Spezzaferri a

a Department of Geosciences, Earth Sciences, University of Fribourg, Chemin du Musée 6, 1700 Fribourg, Switzerland
b GEOMAR-Helmholtz Centre For Ocean Research, Kiel, Germany
c Renard Centre for Marine Geology, Dept. of Geology and Soil Sciences, Ghent University, Ghent, Belgium

Cold-Water Corals (CWC) are globally distributed in the oceans, living under limiting growth factors such as sea water temperature, salinity, dissolved oxygen, currents regime and food availability (Freiwald et al., 2004). Only few investigations on benthic foraminifera related to CWC habitat have been performed so far. The area of the Western Melilla Mound Field (WMMF), eastern Alboran Sea, has not been studied for micropaleontological research so far. This area was sampled in 2008 during the cruise TTR-17, retrieving several gravity cores and box-cores to study deep-sea corals. The following work concentrates on the 340 cm long sediment core 399G, recovered at a water depth of 258 m, which is mainly composed of a brown-greyish clay matrix containing fragments of CWC.

The scleractinian coral community is represented by the most common species Lophelia pertusa, abundant from the base of the core to 80 cm. *Madrepora oculata* is mostly present in the upper part from 0–80 cm. The coral *Dendrophyllia* is less abundant and also present in the top of the core together with *M. oculata*. The core was sampled for micropaleontological (benthic foraminifera) analyses at a 20 cm resolution. Additional measurements such as Rock-Eval and Total Organic Carbon (TOC), stable $\delta^{18}O$ and $\delta^{13}C$ isotopes on benthic and planktonic foraminifera, sedimentary Phosphorous (P) and radiocarbon dating were performed on the core. Statistical analyses of the benthic microfauna were carried out on the fractions 250, 125 and 63 µm. Raw data were treated using the Software PRIMER 6 for 165 benthic foraminifera species. The statistical treatment showed three different clusters in the core:

Cluster 1 (300–340 cm) is dominated by the infaunal-epifaunal *Cassidulina laevigata* and shallow infaunal species *Cibicides ungerianus*,
Cluster 2 (100–280 cm) is characterized by *C. laevigata* and infaunal *Bolivina dilatata*,
Cluster 3 (0–80 cm) is linked to infaunal species *Globocassidulina subglosa–Bulimina marginata*.

Radiocarbon dating on benthic foraminifera showed a sedimentary record spanning from 1,120 yr cal. BP until 33,355 yr cal. BP. Inferring that the CWC have approximately the same age of sediments, this result could likely correspond to the oldest CWC discovered in the Melilla mounds until today. The TOC analyses display two positive peaks at 100 and between 240-280 cm.

This could be linked with the deposition of Organic-Rich Layers (ORLs), corresponding to the eastern Mediterranean sapropels, which are linked to enhanced biological productivity, poor ventilated water masses and freshwater input (Cramp and O'Sullivan, 1999).
The organic P correlates with the two ORLs. The detrital P and the Rock-Eval data suggest that the organic matter deposited during the ORLs has a relatively high terrigenous composition, likely from fluvial supply.

REFERENCES

Cramp, A., and O'Sullivan, G. (1999): Neogene sapropels in the Mediterranean: a review. Marine Geology, 153, 11-28.
Freiwald, A., Fosså, J.H., Grehan, A., Koslow, T., Roberts, J.M. (2004): Cold-water coral reefs. UNEP-WCMC, Cambridge, UK, 86.

10.3

Timing of Early and Middle Pleistocene glaciations in the Alps

Anne Claude[1], Naki Akçar[1], Susan Ivy-Ochs[2], Fritz Schlunegger[1,1]Peter Kubik[2], Meinert Rahn[3], Andreas Dehnert[3] & Christian Schlüchter[1]

[1] *Institut für Geologie, Universität Bern, Baltzerstrasse 1-3, CH-3012 Bern (anne.claude@geo.unibe.ch)*
[2] *Labor für Ionenstrahlphysik (LIP), ETH Zürich, Schafmattstrasse 20, CH-8093 Zürich*
[3] *Eidgenössisches Nuklearsicherheitsinspektorat ENSI, Industriestrasse 19, CH-5200 Brugg*

The onset of glaciations in the northern hemisphere is attributed to approximately 2.7 Ma (Maslin and Ridgwell 2005). Since then, the extent of glaciations is marked by glacial-interglacial cycles on a hemispherical scale. Was the onset of glaciations in the Alps synchronous? It is still unrevealed. Building of ice sheets must have resulted in an environmental change, which is documented in the oldest Quaternary deposits in the Alps. The focus of this study is on this geoarchive, the Deckenschotter, which are glaciofluvial gravels covering Tertiary Molasse or Mesozoic bedrock. These gravels are topographically distinct and discontinuous archives, having a reverse stratigraphic relationship, i.e. older deposits are located at higher altitudes and vice versa. To track the pace of onset of Early and Middle Pleistocene glaciations in the Alps and thus contribute to the understanding of the large-scale evolution history of the Alpine Foreland, we first investigate the sedimentology of Swiss Deckenschotter at key sites in order to determine the depositional environment, transport pattern, provenance and catchment area of these deposits. Then, we reconstruct the chronostratigraphy by applying two different methods: depth-profile and isochron-burial datings. Depth-profile dating uses the fact that the build-up of cosmogenic nuclides decreases with depth following the known principles (Gosse and Philips 2001). The recently introduced isochron-burial dating is based on different pre-burial but same post-burial histories of quartz pebbles originating from the same timeline.

Here we present first results of two Höhere Deckenschtter sites at Stadlberg and Irchel, at an elevation of 600 m and 670 m a.s.l., respectively. At these sites, in an abandoned gravel pit, sediment samples were taken for depth-profile dating with ^{10}Be and additionally quartz pebbles were collected for isochron-burial dating with ^{10}Be and ^{26}Al. First results from Stadlerberg indicate that this sequence was accumulated during a cold period approximately 2 Ma ago. We thus assume that the Quaternary glaciations in the Alps should have begun prior to 2 Ma. Moreover, the petrography of the pebbles indicate that the Deckenschotter units at both sites show a provenance including the Swiss Midland Basin, the Hörnli- and Napf talus fan as well as some parts of the Alps, excluding the Valais and Grisons.

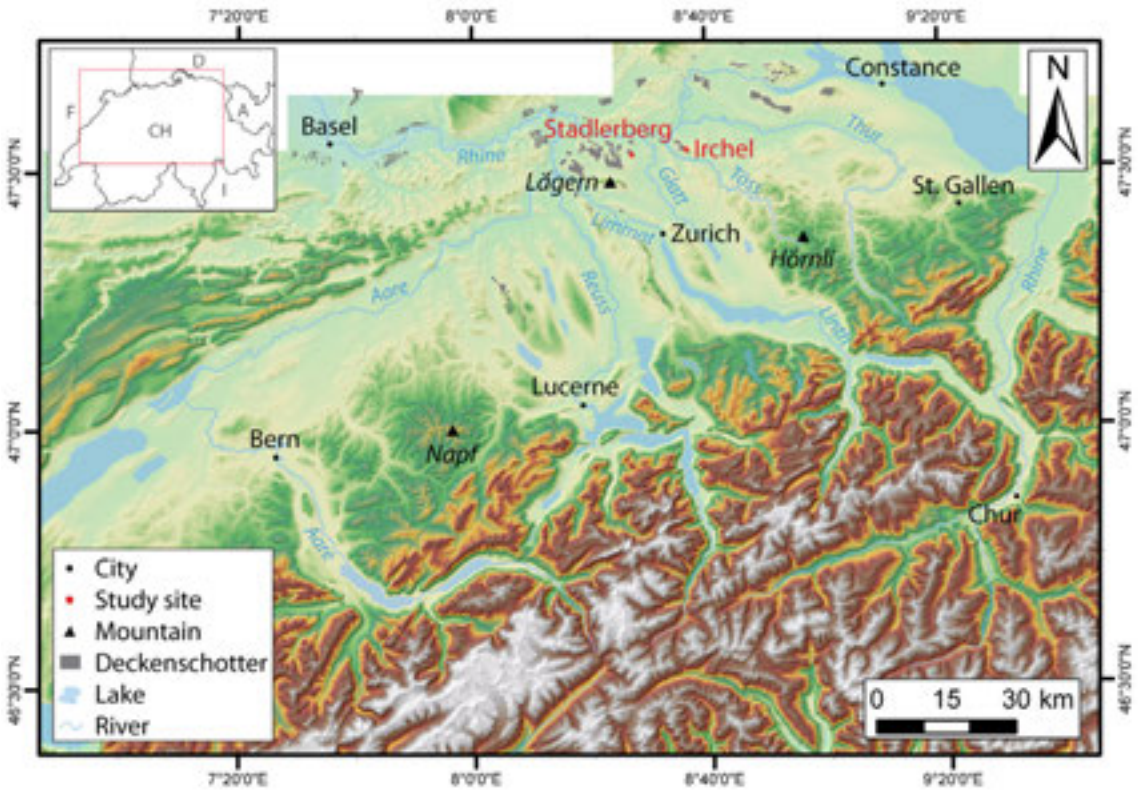

Figure 1. Location of the Stadlerberg and Irchel study sites and distribution of Swiss Deckenschotter.

REFERENCES
Gosse, J.C. & Philips, F.M. 2001. Terrestrial in situ cosmogenic nuclides: theory and application. Quateranry Science Reviews 20, 1475-1560.
Maslin, M.A. & Ridgwell, A.J. 2005: Mid-Pleistocene revolution and the 'eccentric myth'. Geological Society, London, Sepcial Publications 247, 19-34.

10.4

Holocene sediment budget and sediment dynamics of Lake Sils in the Upper Engadin

Florian Donau[1], Reto Grischott[1], Florian Kober[1/2], Irka Hajdas[3]; Kristina Hippe[3], Maarten Lupker[4], Susan Ivy-Ochs[3], Markus Christl[3] & Michael Strasser[1]

[1] *Geological Institut, ETH Zürich, Sonneggstr. 5, CH-8092 Zürich (f.donau@gmail.com)*
[1 /2] *now at Nagra, Hardstrasse 73, 5430 Wettingen*
[3] *Institut of Particle Physics, ETH Zürich, Otto-Stern-Weg 5 CH-8093 Zürich*
[4] Institut of Geochemistry and Petrology, ETH Zürich, Clausiusstrasse 25, CH-8092 Zürich

Postglacial sediment archives can be used to deduce past climate variations and to infer geomorphic catchment processes. It has been suggested, that tremendous changes in erosion rates and sediment fluxes are characteristic for this time period, commonly framed in the paraglacial cycle. Linking the geomorphic processes and sediment archives of such a sediment cascade from source to sink, however, remains hampered due to limited appropriate tracers and absolute dating techniques. In this study, we employ a multi-method-approach for Lake Sils, upper Engadin, where the majority of the sediment has been supplied from the catchment of the Val Fedoz and has been predominantly deposited in the Isola delta complex. On the one hand, catchment wide cosmogenic ^{10}Be denudation rates within the modern Val Fedoz and from Holocene delta sediments were obtained, suggesting rates of ~1 mm/yr for the late Holocene (Grischott et al, 2013). On the other hand, this presentation focuses on the evaluation of the sink system as a result of climate forced erosion in the Fedoz catchment. A high resolution seismic survey was combined together with two long piston cores from a distal and proximal position in relation to the Isola Delta. Geophysical and sedimentological data were obtained along with an AMS radiocarbon dating approach to reconstruct the Holocene sediment history of the lake. In combination with the seismic survey an isopach map and sedimentation rate time series were derived. The pattern of sediment distribution confirms the observation, that the Isola Delta is the major source of sediment in the lake basins during the Holocene. However, most likely a second tributary system existed during the Younger Dryas phase from the Maloja side. A comparison with regional and local climate records suggests that south Alpine climate trends control the geomorphic processes – and thus erosional an depositional regime - during the Holocene Thermal Maximum. Due to the complexity of deposition and a limited temporal overlap of source archives and sink records a clear linkage is difficult and under further investigation. A classical paraglacial cycle is not immediate obvious and the data imply that the regional climate has a larger influence on the sedimentation rate then the general proglacial sedimentary cycle.

REFERENCES
Grischott, R. et al., 2013: Paleo-denudation rates and possible links with climate variations in the Alps, Vol. 15, EGU2013-4843-1

10.5

Glacier presence petrified in a Swiss high alpine stalagmite

Anamaria Diana Häuselmann[1], Daniel Tabersky[2], Detlef Günther[2], Hai Cheng[3] & Dominik Fleitmann[1,4]

[1] *Institute of Geological Sciences, University of Bern and Oeschger Centre for Climate Change Research, Baltzerstrasse 1+3, CH-3012 Bern (ana@speleo.ch)*
[2] *Department of Chemistry and Applied Biosciences, Laboratory of Inorganic Chemistry, ETH Zürich, Wolfgang-Pauli-Strasse 10, CH-8093 Zürich*
[3] *Institute of Global Environmental Change, Xi`an Jiaotong University, Xi`an, Shaanxi 710049, China*
[4] *Department of Archaeology, School of Human and Environmental Sciences, University of Reading, Whiteknights, PO Box 227, Reading RG6 6AB, Great Britain*

Speleothems (stalactites, stalagmites, flowstones) are used as paleoclimatic and environmental archives. Minimum conditions for calcite to precipitate are a supply of drip water and a temperature in the cave above 0°C. In high alpine environments, speleothem growth was documented not only during climate optimum intervals, but equally during severe cold condition at the cave site (e.g. glacial intervals, Spötl and Mangini, 2007). This will indicate (1) the presence of a warm-based glacier above the cave (providing both thermal isolation and water supply), or (2) permafrost conditions above the cave were overcome during an interstadial (warm period during a glacial period stage).

We present our results from stalagmite MF3, collected in Schafsloch Cave (Alpstein Mts., Appenzell Alps, 1890 m asl). 23 ^{230}Th ages document eight individual growth phases in the 20 cm long sample. The growth phases cover the time interval between 230 and 130 ka BP, including the penultimate glaciation in the Alps. Stable isotopes and trace element analysis proved to be extremely valuable to investigate surface processes in this area, whereas all other surface evidences were eroded during the last glaciation. Based on a multi-analysis approach, we identified and dated for the first time the former presence of a valley glacier above the cave during the penultimate glaciation. Soil evolution in the area during glacial and interglacial transitions is documented based on the organic matter content and trace elements in the calcite.

REFERENCES

Spötl, Ch., & Mangini, A. 2007: Speleothems and Paleoglaciers, Earth and Planetary Science Letters, 245, 323-331.

10.6

Chronology of Middle Würm climate changes in the Swiss Alpine foreland

Kristina Hippe[1], Irka Hajdas[1], Susan Ivy-Ochs[1] & Max Maisch[2]

[1] *Laboratory of Ion Beam Physics, ETH Zürich, Schafmattstrasse 20, CH-8093 Zürich (hippe@phys.ethz.ch)*
[2] *Department of Geography, University of Zürich, Winterthurerstrasse 190, CH-8057 Zürich*

The northern Alpine foreland plays a key role in the investigation of Quaternary climate evolution and the reconstruction of the glacial history of the Alps. However, the extent and timing of the various phases of glacier advance and retreat (stadials and interstadials) is still debated, in particular for the time prior to the Last Glacial Maximum (LGM). To improve the understanding of the phase of ice build-up during the Middle Würm (~50 to 25 ka), we have performed radiocarbon dating of selected key sites in the Swiss Alpine foreland.

Deposits of compressed peat ("Schieferkohle") in the Swiss Alpine foreland are one important archive for late Pleistocene climate changes. These organic deposits of up to several meters thickness are truncated by LGM glaciofluvial and glacial sediments. The presence of peat is interpreted to correspond to phases of glacier-hostile, interstadial climate conditions. Although several peat sections have already been studied in the 1960s and 70s using pollen analysis, reliable age data are not widely available.

Here, we present radiocarbon ages from several peat deposits located at Dürnten, SE of Zürich. Based on detailed pollen analysis in three drill cores from Dürnten, Welten (1982) has reconstructed several stadial-interstadial cycles since the end of the Riss glaciation and especially throughout the Würm. On one of these well-preserved drill cores, we were able to obtain radiocarbon ages. These allow to place the palynological data into an absolute timeframe and to establish a detailed chronology of the Middle Würm climate variations. Additionally, we present ^{14}C ages from surface outcrops of compressed peat which have been discovered in river beds and due to current construction work in Dürnten.

REFERENCES

Welten, M. 1982: Pollenanalytische Untersuchungen im Jüngeren Quartär des nördlichen Alpenvorlandes der Schweiz. Beiträge zur Geologischen Karte der Schweiz, N.F. 156. Stämpfli & Co., Bern, 174 pp.

10.7

OSL-thermochronology of Na- and K-feldspar from Namche Barwa, Tibet

Georgina King[1], Frédéric Herman[1], Pierre Valla[1] & Benny Guralnik[1]

[1] *Institute of Earth Surface Dynamics, University of Lausanne (georgina.king@unil.ch)*
[2] *Department of Earth Sciences, ETH-Zurich*

In contrast to other thermochronometric methods, optically stimulated luminescence (OSL)-thermochronology has a relatively low closure temperature (~30-70 °C) which offers the potential to constrain near-surface changes in exhumation rates over Quaternary timescales. However, as OSL signals saturate, successful applications of OSL-thermochronology are limited to rapidly exhuming environments or elevated temperature settings (e.g. tunnels or bore holes).

The Namche Barwa massif (eastern Himalayan syntaxis) is thought to have experienced extremely rapid exhumation throughout the late-Cenozoic to Quaternary period (e.g. Seward and Burg, 2008). This setting is therefore challenging for the application of traditional low-temperature thermochronometers, but provides a useful test-site for the application of OSL-thermchronology in resolving late-stage cooling histories. Six bedrock samples were hand crushed before using conventional methods to extract Na- and K-feldspar fractions. A multiple elevated temperature (MET) protocol was used which comprises infra-red stimulated luminescence (IRSL) measurements at 50, 100, 150 and 225 °C to record multiple IRSL signals for each individual sample. The different MET signals may have different thermal stabilities (thus different closure temperatures), and could therefore provide better constraint on cooling and exhumation rates. In addition to thermal trapped-charge depletion, feldspars also exhibit athermal charge loss (fading) which was measured and corrected for.

Preliminary results show that all Na-feldspar IRSL signals are in field saturation, whereas the IRSL50, IRSL100 and IRSL150 signals of the K-feldspar extracts of some samples exhibit thermal signatures. Incorporating sample specific laboratory-constrained kinetic parameters for these signals into a charge-trapping model, results in a predicted cooling rate of ~150 °C Ma^{-1} for sample NB140, in close agreement with independent cooling rate control from apatite fission-track ages adjacent to the sampling site (Seward and Burg, 2008). These results suggest that OSL-thermochronology has the potential to constrain Quaternary cooling histories and exhumation rates in rapidly-exhuming settings.

REFERENCES

Seward, D., & Burg J-P. 2008: Growth of the Namche Barwa Syntaxis and associated evolution of the Tsangpo Gorge: Constraints from structural and thermochronological data, Tectonophysics, 451, 282-289.

10.8

Tectonic Control on Topographic and Exhumational Segmentation of the Himalaya

Camille Litty[1,2], Peter Van Der Beek[1], Mallory Baudin[1], Jonathan Mercier[1], Xavier Robert[1] and Elisabeth Hardwick[1]

(1) University of Grenoble, ISTerre, Grenoble, France, (2) Universität Bern, Institute of Geological Sciences, Berne, Switzerland

Although the Himalayan range is commonly presented as cylindrical along-strike, geological structures, topography, precipitation, and exhumation rates as recorded by low-temperature thermochronology data all vary significantly from west to east. In particular, segments of the belt that are characterized by a clear topographic step between the Lesser and Higher Himalaya, associated with a peak in precipitation and focused exhumation (e.g. central Nepal, Himachal Pradesh) alternate with segments where the topography increases more linearly to the north, precipitation peaks at lower elevations and exhumation rates appear to be lower (e.g. western Nepal, Bhutan). The potential climatic or tectonic controls on these spatially variable topographic, precipitation and exhumational patterns have been widely discussed in recent years but remain unclear.

Thermo-kinematic modelling predicts that the geometry of the main Himalayan detachment (in particular the presence or absence of a major mid-crustal ramp) strongly controls the kinematics, exhumation and topography of the orogen. Where a major crustal ramp is present, the topography shows a steep gradient that focuses exhumation and orographic precipitation whereas the topography is gentler and exhumation less focused in the absence of a ramp. We test this prediction by comparing the pattern of topography, river incision and long-term exhumation in central Nepal, where a major crustal ramp has been imaged by geophysical methods, with new results from the remote Karnali River transect in far western Nepal, where a ramp is predicted to be absent or minor. Our results therefore imply that along-strike climatic variations in the Himalaya respond to tectonics rather than driving it. The presence or absence of a mid-crustal ramp may be due to inherited structures on the underthrusting Indian Plate or, alternatively, may reflect transient behaviour of the accreting Lesser Himalayan thrust stack, which may oscillate between frontal accretion (without a ramp) or basal accretion in the presence of a ramp.

10.9

Challenges in using luminescence dating to provide age control on Late Quaternary soil development on the central Swiss Plateau

Mareike Trauerstein[1], Frank Preusser[2], Sally E. Lowick[3] & Heinz Veit[1]

[1] *Institute of Geography, University of Bern*
[2] *Department of Physical Geography and Quaternary Geology, Stockholm University*
[3] *Institute of Geological Sciences and the Oeschger Centre for Climate Research, University of Bern*

Well developed palaeosols (fBt-horizons) reaching a depth of more than 2 m are a widespread feature on glaciofluvial gravels in the central Swiss alpine foreland. These palaeosols are covered by loess-like sediments containing a weakly developed Holocene soil (Btv-horizon). Assuming full interglacial environmental conditions for the evolution of a Bt-horizon, the fossil Bt-horizons can be interpreted to represent the last interglacial (Eem), but so far there is no numerical age control.

Luminescence dating of the parent material of the palaeosols, i.e. the glaciofluvial sediments, and the overlying loess-like deposits could provide age contrains on the soil formation. Therefore, a case study was performed on 10 samples from the Aebisholz site, at which 5 samples were taken from the loess-like deposits and 5 samples from sand lenses in the glaciofluvial deposits parenting the fossil Bt horizon. Whereas the dating of the loess-like sediment appears straightforward, glaciofluvial sediments are known to be prone to incomplete bleaching during transport, which makes the dating more complex. For potentially partially-bleached sediments the application of a single grain method appears sensible, although the choice of mineral is not evident. Quartz single grain dating is considered a solid approach, but northern alpine quartz appears to exhibit dim signals and potentially unstable luminescence signal components. The use of feldspar for single grain methods is still at an experimental stage as it can be complicated by the presence of varying fading rates, although previous studies have shown that fading seems to be a minor problem for northern alpine feldspar. For the investigated glaciofluvial samples in this study, single grain measurements using feldspar show equivalent dose distributions that are significantly overdispersed pointing to partial bleaching and/or varying fading rates, and making it very difficult to extract the true depositional age. Single grain measurements using quartz lead to equivalent dose distributions showing slightly higher overdispersions than expected for well-bleached sediments, and also raising the question of whether the quartz signal also suffers partial bleaching in those samples. An alternative explanation could be a strongly inhomogenous radiation field. The methodological challenges of dating the glaciofluvial sediment samples, resulting luminescence ages and their implications for potential periods of Bt horizon formation on the central Swiss Plateau will be discussed.

10.10

Excavations at the Middle Palaeolithic site of Mutzig-Rain (Alsace, France)

Fabio Wegmüller[1], Héloïse Koehler[2], Christine Pümpin [1], Patrice Wuscher [2] & Noémie Sévêque[3]

[1] *Institut for Prehistory and Archaeological Science (IPAS) University of Basel Switzerland, (fabio.wegmueller@unibas.ch, christine.puempin@unibas.ch)*
[2] *Pôle d'Archéologie Interdépartemental Rhénan (PAIR) Sélestat (F) (heloise.koehler@pair-archeologie.fr, patrice.wuscher@pair-archeologie.fr)*
[3] *Laboratoire Préhistoire et Quaternaire, Université de Lille (noemie.seveque@etu.univ-lille3.fr)*

The site of Mutzig "Rain" was discovered by chance in 1992 during construction works. Subsequently several test trenches were made in the surounding area between 1992 and 1996. This test trenches brought to light a large Middle Paleolithic site. Since 2009, systematic excavations have been carried out by the Pôle d'Archéologie Interdépartemental Rhénan (PAIR), the Universities of Strasbourg, Basel, Cologne and Lille. During this excavation different layers with a rich archaeological and paleontological record were discovered documented. The abundant lithic and faunal assemblages are well preserved and date back to the Mousterian period ca. 90,000 years ago.

This presentation aims to present the site and its exceptional archaeological record as well as to discuss the first result from the archaeological, paleontological, geomorphological and micromorphological analyses.

10.11

Late Glacial Vegetation Reconstruction based on Leaf Waxes from the Gemündener Maar, Germany

Lorenz Wüthrich[1], Selina Lutz[1], Roland Zech[1], Michael Zech[2], Frank Sirocko[3]

[1] *Institute of Geography, University of Berne, Hallerstrasse 12, CH-3012 Bern (lorenz.wuethrich@giub.unibe.ch)*
[2] *Departement of Soil Physics and Chair of Geomorphology, University of Bayreuth, Universitätsstrasse 30, D-95440 Bayreuth*
[3] *Institute of Geosciences, Johannes Gutenberg University, J.-J. Becher Weg 21, D-55128 Mainz*

Lake sediments are valuable archives for the reconstruction of past changes in climate and vegetation. In the present study, we analyze samples from the Gemündener Maar, a lake situated in the western Eiffel, Germany, for their leaf wax composition: In the bottom part of the core, corresponding to the Oldest Dryas (i.e. older than ~15 ka), *n*- alkanes have a high average chain length (ACL), which points to a vegetation dominated by grass. During the Bölling/Alleröd, a decrease of the ACL can be interpreted as signal of more deciduous trees. During the Younger Dryas (~12.8 to 11.5 ka), the ACL increases again. The trees probably became again less abundant, before finally, the ACL records the return of deciduous trees during the early Holocene. In General, the total concentrations of *n*- alkanes are high enough to measure compound-specific isotopes. Fatty Acids are currently being measured to complement the alkane data.

P 10.1

Stratigraphy of Quaternary Deposits of the Mendrisiotto (Southern Swiss Alps)

Christian Ambrosi[1], Cristian Scapozza[1], Claudio Castelletti[1], Linda Soma[1] & Stephan Dall'Agnolo[2]

[1] *Istituto scienze della Terra (IST), Scuola Universitaria Professionale della Svizzera Italiana (SUPSI), Campus Trevano, CH-6952 Canobbio ([surname.name]@supsi.ch)*
[2] *Swiss Geological Survey, Federal Office for Topography swisstopo, Seftigenstrasse 264, CH-3084 Wabern (stephan.dall'agnolo@swisstopo.ch)*

In the framework of the geological mapping of sheet 1373 Mendrisio (Geological Atlas of Switzerland 1:25'000), the stratigraphy of Quaternary deposits of the southern alpine foreland was revised. The availability of numerical datings on different kind of deposits maked it possible to drawn a regional stratigraphy based on glacial events and on climate proxies at the continental and/or global scale, which allowed four main chronostratigraphical units to be differentiated.

In particular, were grouped Postglacial deposits ("Depositi del Postglaciale"; 0–0.0117 Ma), referred to the entire Holocene, deposits of the Last Glacial Maximum and the Lateglacial ("Depositi dell'Ultimo Massimo Glaciale e del Tardoglaciale"; 0.0117–0.029 Ma) and deposits preceding the Last Glacial Maximum ("Depositi precedenti all'Ultimo Massimo Glaciale; 0.029–0.781 Ma), both referred to the Middle and Late Pleistocene (Figure 1), and deposits of the Lower Pleistocene ("Depositi del Pleistocene inferiore"; 0.781–2.588 Ma), referred to the Early Pleistocene.

This approach was transferred to the legend of the geological map, making it possible an immediate representation of both facies and age of the Quaternary deposits. Besides allowing a definition of the chronostratigraphical units relevant for other geological maps in the same regional framework (harmonised cartography), this kind of representation makes it possible a quick visualisation of the spatial extent of the main morphoclimatic events, as, for example, the maximal glacial extent during the Last glaciation compared to the previous glaciations.

This kind of representation has also facilitated the knowledge about the dynamics and direction of the main glacial flows in the region of Mendrisio, confirming the important role played by the Larian lobe of the Adda glacier with respect to the glacial lobe of the Lake Lugano.

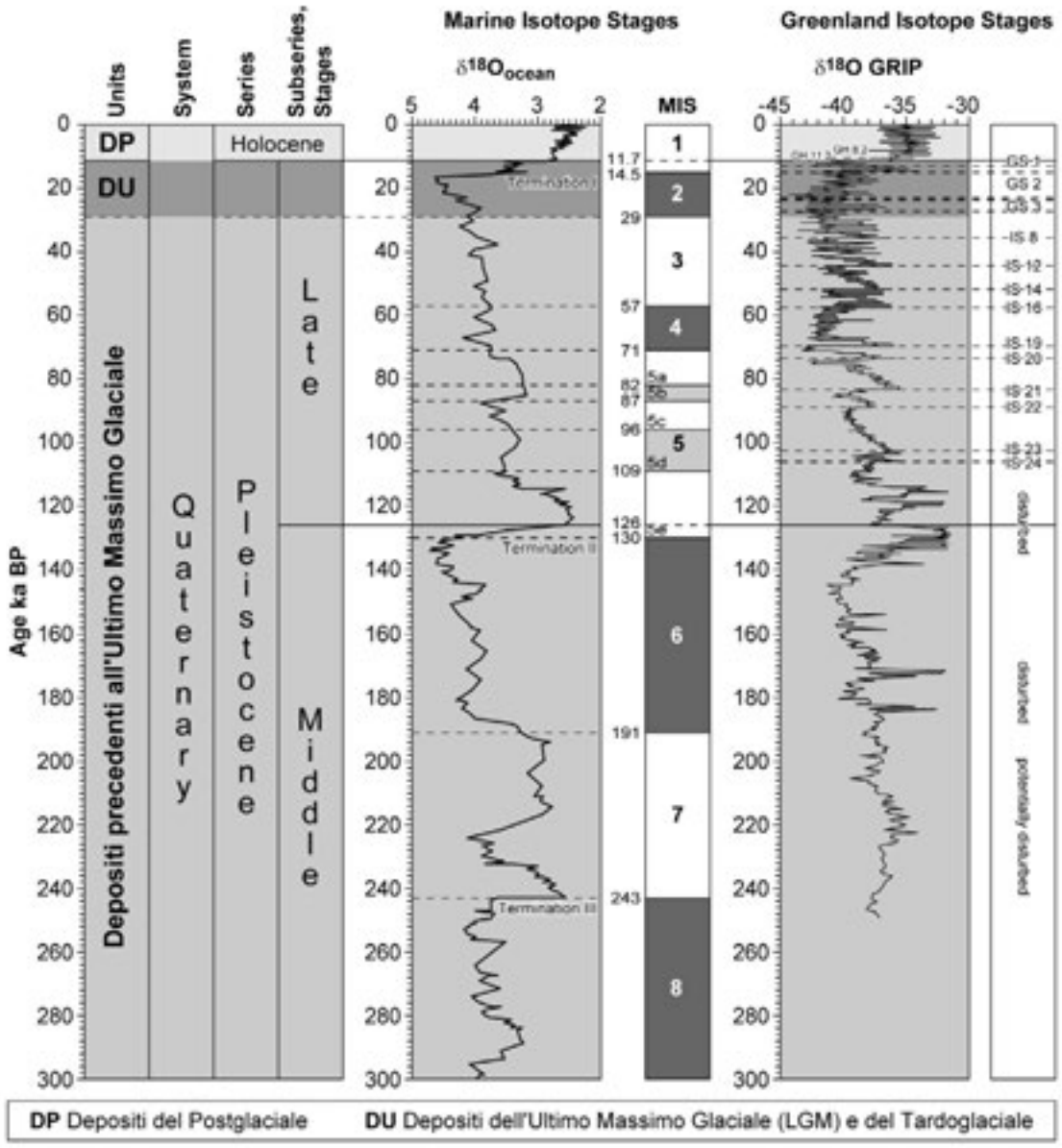

Figure 1. Chronostratigraphical units defined in the Mendrisiotto and correlation with the Marine Isotope Stages (MIS) and the Greenland Isotope Stages (GIS) for the last 300 ka. For GIS older than GS 3, only the main interstadials are reported.

P 10.2

Heavy metal distribution in lake sediments from the Joux Valley

Nathalie Dubois[1], Léa Frédyier[1,2] Irene Brunner[1]

[1] *Eawag (Swiss Federal Institute of Aquatic Science and Technology), Überlandstrasse 133, CH-8600 Dübendorf (nathalie.dubois@eawag.ch)*
[2] *EPFL, CH-1015 Lausanne, Switzerland*

Located on top of the Jura Mountain, the Joux Valley is quiet unique not only because of her harsh climate but also because of the odd mixture of agriculture and industries, which coexist there since centuries. Until the mid 16th century, forests were intensively cut for the production of wood charcoal, which was then used in forges and steelworks throughout the Valley (ref.). A few iron mines were also exploited (ref). Starting in the 18th century, the Joux Valley slowly became a center for the Swiss Watch Making Industry.

Here we will present preliminary investigations into the heavy metal content in sediments from the Lake Joux, Lake Brenet and Lake Rousses (France). Sediment cores retrieved in 2013 and 2014 were dated by ^{210}Pb and ^{137}Cs radioisotopes. Trace element were analyzed both with an XRF core scanner and sporadically by inductively coupled plasma mass spectrometry (ICP-MS). Anthropogenic metal pollution was traced by normalizing to conservative elements, which record significant changes in soil erosion.

P 10.3

Pollution by phosphogypsum discharge into the Gulf of Gabes (Tunisia): Preliminary results.

Akram El Kateb[1], Claudio Stalder[1], Christoph Neururer[1], Silvia Spezzaferri[1]

[1] *Department of Geosciences, University of Fribourg, Ch. Du Musée 6, CH-1700 Fribourg, (akram.elkateb@unifr.ch)*

Phosphorites are the main mineral resource of Tunisia. Important deposits are located in the western part especially in the Gafsa basin. Five mining centres are currently exploited and ore phosphate is treated in three main industries located along the eastern marine coast: Sfax, Skhira and Gabes.

Phosphate treatment consists of the transformation of phosphorite into phosphoric acid using sulfuric acid with consequent production of large amount of phosphogypsum waste.

Phosphogypsum as a waste product is stored in spoil tips along the coasts and near the industries of Sfax and Skhira causing contamination of the marine environment by leaching processes (Zairi and Rouis, 1999). At Gabes, the waste products are discharged directly into the sea, including waste waters, industrial sludges and phosphogypsum.

In July 2014, an expedition was organized in Tunisia to collect the necessary information and samples to estimate the environmental impact by the phosphate industry of Gabes. Two different transects were sampled: A) from the shore to around 18 km off-shore in the Gulf of Gabes, considered as a polluted site and B) from the north-western margin of Djerba Island to around 15 km off-shore, considered as a pristine site.

During this campaign, sediments and water from the sea floor were sampled, video survey was performed and multiparameter (pH, temperature and dissolved oxygen) of the water quality were measured with a landing system. Water sampler, video survey system and landing system were developed and built at the Department of Geoscience of University of Fribourg especially for this study. Additionally, different analyses are being performed on sediment samples at the University of Fribourg as: 1) Total organic carbon (TOC); 2) elemental CHN; 3) Mineral carbon (MINC); 4) Grain size; 5) X-Ray diffraction.

Preliminary data from the landing system show low pH value (<6) next to the pollutant discharge area of Gabes. The overall temperature is generally higher along the Gabes transect than the Djerba transect and the dissolved oxygen values follow the opposite trend. The absence of sea grass prairies and siltation in the Gulf of Gabes were observed by the video survey. These different parameters are possibly caused by an important anthropogenic impact with consequent eutrophication of the marine environment.

REFERENCES

Zairi, M. & Rouis, M.J. 1999: Impacts environnementaux du stockage du phosphogypse à Sfax (Tunisie). Bulletin des laboratoires des Ponts et Chaussées, 219, 29-44.

P 10.4

Khuzestan dust source identification with using Satellite images and Sedimentary Geochemistry

Javad Darvishi Khatooni[1], Raziyeh Lak[2]

[1] *Geological survey of Iran (javaddarvishi2007@yahoo.com)*
[2] *Research Institute for earth sciences, geological survey of Iran*

Dust storm is one of the most important environmental problems in the west of Iran. To indicate the environmental impact of these phenomena, the characterization of dust storm loads is vital(Najafi etal. 2013). Recently Khuzestan province in southwest of Iran is affected by dust storm phenomena. This feature makes some problem in agriculture, Transportation, Communication and human health side effect in this province. Due to no enough research and study on physical and chemical characteristics of this dust storm in Iran, providing a systematic investigation is necessary. In addition of Geochemistry of particles Geo-Environmental characteristics of Trace elements as a major pollution is very important (Darvishi khatooni, 2014).

To indicate the environmental impact of these phenomena, the characterization of dust storm loads is vital. The objective of this study is to identify the mineralogical and chemical composition, trace elements of dust particles deposited during two years dust storm event over the west of Iran to obtain total suspended particulate. For example in 2 June 2012 according to satellite images the dust have risen from deserts(dried wetlands and lakes) of South East Iraq such as Horolazim and Horohhemar. In Ahvaz and Abadan Were sampled from dust that Elemental and mineralogical analysis of sediments shows very different Compounds. Differences in the source of dust (Various dried wetlands) is a major factor in this subject (table 1 & fig 1-A).

mineralogical analysis show HALITE+ CALCITE+ DOLOMITE+ QUARTZ for Abadan and CALCITE+QUARTZ+ GYPSUM(minor) for Ahvaz.

According to analysis and source of dust that Introduced, Mineralogical composition of dust that rising from the East and North-West Jordan, Syria and Iraq (Regions 1 and 3), Often is contains calcite, quartz, clay minerals and traces of dolomite, gypsum and feldspar that supplied from the dried lakes and wetlands and ancient lake sediments. Mineralogical composition Region 2 (South East Iraq) include halite, dolomite, calcite, quartz, gypsum. that supplied from the dried lakes and wetlands South West of Iraq, such as Horolazim and Horohhemar. Calcite, quartz, and feldspar is dust mineralogical composition that are incoming of Saudi Arabia (fig 1-B).

EL	Ahvaz	Abadan	EL	Ahvaz	Abadan	EL	Ahvaz	Abadan
Ag	<0.1	0.1	Hf	3.66	10.7	Hg	<0.04	0.06
As	4.6	3.6	La	11.25	27.1	Ho	0.42	1.1
B	28.64	21	Li	13.41	25.1	Th	3.48	12.2
Ba	193	315.2	Lu	0.12	0.3	Ti	1912	3182.1
Be	0.32	1.4	Mn	402	523.7	Tl	<0.5	0.8
Bi	<0.5	<0.5	Mo	3.72	1.3	Tm	0.13	0.2
Cd	0.31	0.1	Nb	8.25	18	U	5.42	3.4
Ce	12.46	28	Nd	1.64	24.8	V	55.07	97
Co	29.38	20.4	Ni	130	115.8	Sn	1.42	4.4
Cr	46.84	147.9	P	755	852.6	Sr	373	565.9
Cs	4.94	3.8	Pb	24.89	6.6	Ta	0.91	0.7
Cu	12.46	30.9	Pr	3.09	3.8	Tb	0.27	1.2
Dy	3.55	3.5	Rb	27.87	153.3	Te	0.29	<0.03
Er	<0.5	1.5	S	23869	>10000	w	1.29	
Eu	0.23	0.8	Sb	0.48	0.3	Y	9.61	15.6
Ga	3.52	11.4	Sc	6.99	11.7	Yb	0.95	1.9
Gd	2.22	3.7	Se	0.09	0.1	Zn	91.83	80.5
Ge	1.26	1	Sm	2.4	4.3	Zr	94.51	138.1

Table 1. Elemental analysis of dust sediments (2012.06.02)

Figure 1. A: Dust storm, Imaging Date 2012.06.02 & B: Source of the dust in Khuzestan in order of preference

REFERENCES
Darvishi khatooni, J. 2014: Khuzestan dust source identification with using Satellite images and Sedimentary Geochemistry. Geological survey of Iran. Internal report.
Najafi, M.S., Khoshakhllagh, F., Zamanzadeh, S. M., Shirazi, M. H., Samadi, M., & Hajikhani, S. 2013: Characteristics of TSP Loads during the Middle East Springtime Dust Storm (MESDS) in Western Iran. Arab J Geosci, DOI 10.1007/s12517-013-1086-z.

P 10.5
Study Khuzestan dusts pollution with using Sedimentary Geochemistry

Javad Darvishi Khatooni[1], Raziyeh Lak[2], Ali Azhdari[1]

[1] *Geological survey of Iran (javaddarvishi2007@yahoo.com)*
[2] *Research Institute for earth sciences, geological survey of Iran*

Dust storm is one of the most important environmental problems in the west of Iran. To indicate the environmental impact of these phenomena, the characterization of dust storm loads is vital(Najafi etal. 2013). Recently Khuzestan province in southwest of Iran is affected by dust storm phenomena. This feature makes some problem in agriculture, Transportation, Communication and human health side effect in this province(FIG 1). Due to no enough research and study on physical and chemical characteristics of this dust storm in Iran, providing a systematic investigation is necessary. In addition of Geochemistry of particles Geo-Environmental characteristics of Trace elements as a major pollution is very important (Darvishi khatooni, 2014).

To indicate the environmental impact of these phenomena, the characterization of dust storm loads is vital. The objective of this study is to identify the mineralogical and chemical composition, trace elements of dust particles deposited during two years dust storm event over the west of Iran to obtain total suspended particulate.

Dust samples were collected from 3 cities in the south west of Iran. In addition to determining the sources of dust samples on the dates of sampling, synthetic approaches including remote sensing technique of dust detection and analysis of weather map were used. In this way, 27 samples from dust storms during 2 years in Khuzestan province were collected for XRD and ICP-MS analysis.

XRD result show that composition of these dust particles is similar to other dust particles in the world and Silty-Clay is dominant composition.

Enrichment factor values are classified as follows: EF <1, there is no enrichment (Ag, Mn, Sc, Ti, Tm, w),: EF <3 low enrichment (Ba, Be, Ce, Co, Cr , Dy, Er, Eu, Ga, Gd, Ge, Ho, Lu, Nd, Nb, P, Pr, Sb, Sm, Sr, Ta, Tl, V, Y),: EF: 3-5 enrichment medium (B, Bi, Cs, Cu, Hf, Hg, La, Li, Mo, Ni, Rb, Se, Sn, Tb, Th),: EF: 5-10 enrichment of moderate to severe (U), EF: 10- 25: severe enrichment (In, Pb), EF: 25-50: very severe enriched (As, Cd),: EF> 50 extremely severe enriched (S). In this study, the enrichment factor values for trace elements has been calculated. Enriched in some elements such as Hf and Ni are dangerous and Enriched heavy metals, especially Ni, V, Ba Hf, can be caused by hydrocarbon material pollution in Iraq and Khuzestan. Radioactive elements such as uranium enriched high concentrations show that it can be achieved remnants of war. Elements such as sulfur and arsenic, which are highly toxic and highly enriched indicate that anthropogenic sources are obtained (FIG 2).

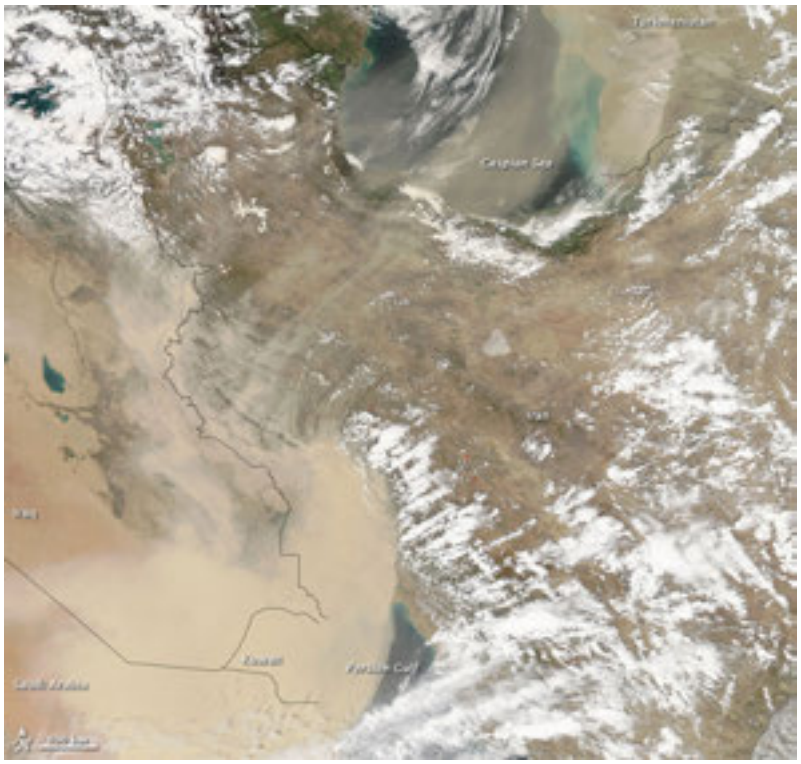

Figure 1. Dust storm, Imaging Date 2011.04.13

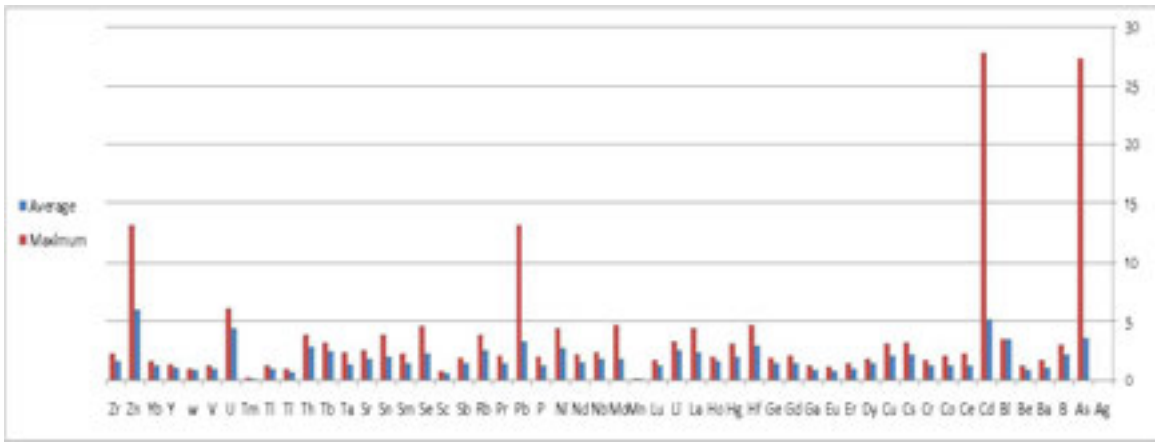

Figure 2. Enriched factor for different elements of dust particles in Khuzestan

REFERENCES

Darvishi khatooni, J. 2014: Khuzestan dust source identification with using Satellite images and Sedimentary Geochemistry. Geological survey of Iran. Internal report.

Najafi, M.S., Khoshakhllagh, F., Zamanzadeh, S. M., Shirazi, M. H., Samadi, M., & Hajikhani, S. 2013: Characteristics of TSP Loads during the Middle East Springtime Dust Storm (MESDS) in Western Iran. Arab J Geosci, DOI 10.1007/s12517-013-1086-z.

P 10.6

Dust containment priority in Khozestan plain, Iran

Javad Darvishi Khatooni[1], Raziyeh Lak[2], Majid Moeini[1], Ali Azhdari[1]

[1] *Geological survey of Iran (javaddarvishi2007@yahoo.com)*
[2] *Research Institute for earth sciences, geological survey of Iran*

Dust storm is one of the most important natural phenomena and a kind of severe natural disaster that begins and diffuses under the influence of atmospheric systems. It occurs frequently in desert lands and their surrounding areas in arid and semi-arid regions (Miri et al. 2009). The main factors influencing the amount of dust in the air include precipitation, vegetation cover, wind velocity, and soil particle size of dust-generating sources(Ta et al. 2004). Playa lakes are an important source for Aeolian and dusty storm sediments because of their location in the low land, arid and desert region with strong windy systems and exit fine and unconsolidated sediment. Iran is located in the west of Asia, and in the arid and semi-arid belts (Hojati et al. 2011). The annual rainfall ranges from 224 to 275 mm, and the central Iran has remarkable dust emission sources, which are one of the most prominent dust sources in the dust belt.

The northern parts of the region (northern Khuzestan), especially the mountainous areas, experience cold weather in winter and warm weather in summer. In mountainous areas, the annual mean of minimum temperature in the coldest month is less than –4 °C (in January). The southern parts of Khuzestan province, especially the low elevations and coastal areas, experience tropical weather. The annual mean of maximum temperature in the warm period is about 50 °C (in July) and the minimum winter temperature is 9 °C (in February).

In this research 71 surface sediment samples were taken for sedimentology and sedimentary geochemistry investigation. These samples were analyses in the geological survey of Iran laboratory. Sieve analyses, laser analyses, calcimetry, mineralogy (XRD), morphoscopy, morphometry and chemical analyses (ICP & AAS) have been done. The Results show that silt and clay size sediments are dominated that have suitable potential to wide distance and long time transportation. Sediments type in Khozestan plain is Slightly gravelly sandy mud, Slightly gravelly mud, Gravelly muddy sand, Slightly gravelly sand, Sandy mud.

With respect to particle, Most of the samples form very little silt and clay and gravel. Five area was found as dust containment priorities. Distribution of clay minerals (less than 2 microns) showed that Lands between the Abadan and Khorramshahr, Shadegan and Mahshahr cities in the South and in the North West Susangerd city is the main source that produced dust in the Khozestan province(Darvishi khatooni, 2014).

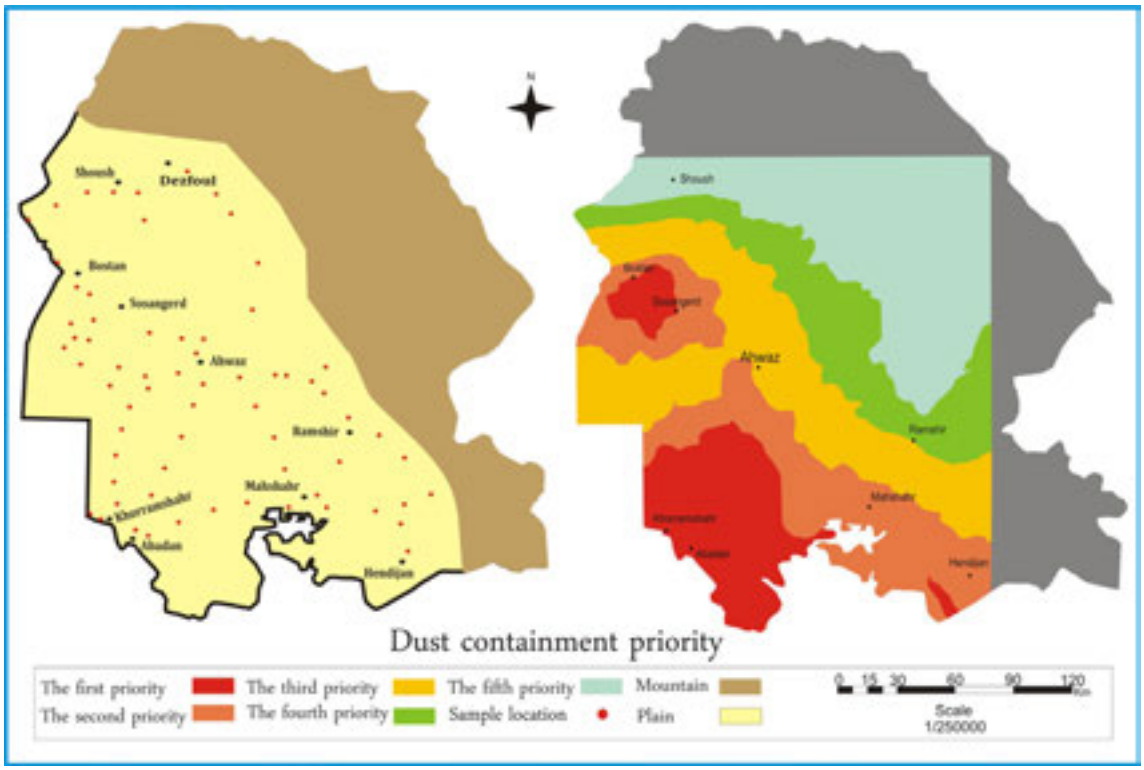

Figure 1. Dust containment priority and sample location in Khozestan plain

REFERENCES
Darvishi khatooni, J. 2014: Study wind sediments Khuzestan province. Geological survey of Iran. Internal report.
Miri A, Ahmdi H, Ekhtesasi MR, Panjehkeh N, Ghanbarie A (2009) Environmental and socio-economic impacts of dust storms in Sistan Region, Iran. J Environ Stud 66:343–355
Hojati S, Khademi H, Faz Cano A, Landi A (2011) Characteristics of dust deposited along a transect between central Iran and the Zagros Mountains. Catena J 88:27–36
Ta W, Xiao H, Qu J, Xiao Z, Yang G, Wang T, Zhang X (2004) Measurements of dust deposition in Gansu Province, China, 1986–2000. Geomorphology 57:41–51

P 10.7

Long chain n-alkanes and n-carboxylic acids as molecular proxies for paleovegetation

Verena Lanny[1], Imke Kathrin Schäfer[2], Timothy Ian Eglinton[3] & Roland Zech[2]

[1] *Institute of Geological Science, University of Bern, Baltzerstrasse 1+3, CH-3012 Bern (verena.lanny@geo.unibe.ch)*
[2] *Institute of Geography, University of Bern, Hallerstrasse 12, CH-3012 Bern*
[3] *Department of Earth Science, ETH Zürich, Sonneggstrasse 5, CH-8092 Zürich*

Leaf waxes, such as long chain *n*-alkanes and *n*-carboxylic acids, may have a great potential for the reconstruction of past environmental and climate conditions (e.g. (Zech et al. 2013). The *n*-C_{27} and *n*-C_{29} alkanes often predominantly occur in trees and shrubs, *n*-C_{31} and *n*-C_{33} are more abundant in grasses and herbs while *n*-C_{23} and *n*-C_{25} characterize the input of freshwater plants (Ficken et al. 2000) or Sphagnum moss (Pancost et al. 2002). A decrease in humidity can also affect the synthesis of the dominating *n*-alkane, because it leads to a synthesis of *n*-alkanes with higher carbon chain lengths (Smith et al. 2001). However, little is known about chain-length distributions of *n*-carboxylic acids, and very few studies have systematically investigated leaf waxes in topsoils.

The aim of our study is to examine the potential of *n*-alkanes and *n*-carboxylic acids as proxies for the reconstruction of past vegetation. First results come from a study of approximately 100 litter and topsoil samples that were taken during a sampling campaign in November 2012 on a transect from Southern Germany to Sweden. The data show that sites under deciduous trees often contain a lot of C_{27} *n*-alkanes and C_{28} *n*-carboxylic acids. Coniferous sites are characterized by dominance, yet relatively low concentrations in *n*-alkanes C_{29} and C_{31} and have relatively high concentrations of *n*-carboxylic acids C_{22} and C_{24}. Grass sites show a Cmax at C_{31} for *n*-alkanes and have more C_{32} and C_{34} *n*-carboxylic acids than tree sites. Differences in homologue patterns are most pronounced in the litter samples, but are well preserved also in the topsoils (0-3 cm depth, a little less in the lower topsoils from 3-10 cm). These results illustrate the potential of combining *n*-alkane and *n*-carboxylic acid analyses for paleo-vegetation reconstructions, yet indicate that the degree of degradation may have to be taken into consideration (Zech et al. 2013). To assess the full potential of the *n*-alkanes and *n*-carboxylic acids as proxies for past vegetation we are currently analyzing additional samples from Spain, southeastern Europe, Armenia and Siberia.

REFERENCES
Ficken, K.J., Li, B., Swain, D.L. & Eglinton G. 2000: An n-alkane proxy for the sedimentary input of submerged/floating freshwater aquatic macrophytes. Organic Geochemistry, 31, 745-749.
Pancost, R.D., Baas, M., van Geel, B. & Damsté J.S.S. 2002: Biomarkers as proxies for plant inputs to peats: an example from a sub-boreal ombrotrophic bog. Organic Geochemistry, 33, 675-690.
Smith, D.G., Mayes, R.W. & Raats J.G. 2001: Effect of species, plant parts, and season of harvest on n-alkane concentrations in the cuticular wax of common rangeland grasses from southern Africa. Australian Journal of Agriculture Research, 52, 875-882.
Zech M., Krause T., Meszner M. & Faust D. 2013: Incorrect when uncorrected: Reconstructing vegetation history using n-alkane biomarkers in loess-paleosol sequences: A case study from the Saxonian loess region, Germany. Quaternary International, 296, 108–116.
Zech, R., Zech, M., Marković, S., Hambach, U. & Huang Y. 2013: Humid glacials, arid interglacials? Critical thoughts on pedogenesis and paleoclimate based on multi-proxy analyses of the loess–paleosol sequence Crvenka, Northern Serbia. Palaeogeography, Palaeoclimatology, Palaeoecology, 387, 165-175.

P 10.8

The age of terrestrial biomarkers in lacustrine sediments as an historical indicator for anthropogenic soil erosion

Marlène Lavrieux[1], Nathalie Dubois[1], Carsten Schubert[2], Thomas Hofstetter[1], Timothy Eglinton[3]

[1] *Eawag (Swiss Federal Institute of Aquatic Science and Technology), Überlandstrasse 133, CH-8600 Dübendorf (marlene.lavrieux@eawag.ch)*
[2] *Eawag (Swiss Federal Institute of Aquatic Science and Technology), Seestrasse 79, CH-6047 Kastanienbaum*
[3] *ETH Zürich (Swiss Federal Institute of Technology in Zurich), Geologisches Institut, Sonneggstrasse 5, CH-8092 Zürich*

Soils are an invaluable resource, as they represent the base for food production, and play an essential role in nutrient and hydrological cycles, and atmospheric carbon dioxide levels. Human activities have accelerated their natural erosional processes to a critical point (e.g. Le Bissonnais et al., 2001; Gobet et al., 2003), so that the preservation of soils now becomes a major challenge. The knowledge of the extent and rate of soil degradation is though still very limited. To accurately assess the impacts of human activities on soil, information is needed on organic carbon dynamics before farming started, as well as how it changed with the evolution of agricultural practices.

Lake sediments are reliable continuous high-resolution archives recording natural and anthropogenic conditions that prevailed in their surroundings, integrating a catchment-wide signal (e.g. Dearing, 2006; Jacob et al., 2008; Ariztegui et al., 2010; Lavrieux et al., 2013). Paleolimnological records have already revealed the impacts of land use changes on lake sedimentation (e.g. higher detritism caused by deforestation) and how it affects lacustrine trophic levels. However, the impact on the soil itself remains poorly known.

This pilot study aims at evaluating the impact of human activities on the residence time of organic carbon in soil, *i.e.* to establish the links between development of agricultural practices and soil degradation. The rationale is that the emergence of modern agricultural practices, such as plowing, deeply affected the soil, entailing a rapid flushing of old soil and the release of a stock of fossil terrestrial molecules (*i.e.* biomarkers) towards the sedimentary archive. These biomarkers are radiocarbon (^{14}C) dated to assess their age. Then, their age difference with "fresh" (*i.e.* instantaneously deposited) terrestrial plant macrofossils found in the same sedimentary horizon, and therefore contemporaneous, is estimated. In our hypothesis, these terrestrial biomarkers are thus supposed to be older than the surrounding sediment. However, it may be possible that soil was significantly destabilized centuries before by early deforestation. This hypothesis will be validated or invalidated by ongoing measurements.

This presentation will show the preliminary results obtained on a sedimentary core recovered in Lake Joux (Jura Mountains, Switzerland). Information provided by the different proxies (magnetic susceptibility and X-ray fluorescence measurements, high-resolution pictures, radiocarbon dates) illustrate anthropogenic activities imprints on the sedimentary dynamics.

REFERENCES

Ariztegui, D., Gilli, A., Anselmetti, F. S., Goni, R. A., Belardi, J. B., & Espinosa, S. 2010: Lake-level changes in central Patagonia (Argentina): crossing environmental thresholds for Lateglacial and Holocene human occupation, Journal of Quaternary Science 25, 1092-1099.

Dearing, J.A. 2006: Climate-human-environment interactions: resolving our past, Climate of the Past 2, 187-203.

Gobet, E., Tinner, W., Hochuli, P.A., van Leeuwen, J.F.N., & Ammann, B. 2003: Middle to late Holocene vegetation history of the Upper Engadine (Swiss Alps): the role of man and fire, Vegetation History and Archaeobotany 12, 143-163.

Jacob, J., Disnar, J.R., Arnaud, F., Chapron, E., Debret, M., Lallier-Vergès, E., Desmet, M., Revel-Rolland, M., 2008: Millet cultivation history in the French Alps as evidenced by a sedimentary molecule, Journal of Archaeological Science 35, 814-820.

Lavrieux, M., Disnar, J.R., Chapron, E., Bréheret, J.G., Jacob, J., Miras, Y., Reyss, J.L., Andrieu- Ponel, V., & Arnaud, F., 2013: 6,700-year sedimentary record of climatic and anthropogenic signals in Lake Aydat (French Massif Central), The Holocene 23, 1317-1328.

Le Bissonnais, Y., Montier, C., Jamagne, M., Daroussin, J., & King, D., 2001: Mapping erosion risk for cultivated soil in France, Catena 46, 207-220.

P 10.9

Recent mass transport deposits in Lake Biel: tracking their ages, causes and consequences

Laetitia Meuriot[1,2], Nathalie Dubois[1], Peter Molnar[2], Stéphanie Girardclos[3], Alfred Wüest[4,5], Love Raman[5] & Irene Brunner[1]

[1] *Eawag (Swiss Federal Institute of Aquatic Science and Technology), Überlandstrasse 133, CH-8600 Dübendorf (nathalie.dubois@eawag.ch)*
[2] *ETH Zürich (Swiss Federal Institute of Technology in Zurich), Geologisches Institut, Sonneggstrasse 5, CH-8092 Zürich*
[3] *Section des sciences de la Terre, University of Geneva, Rue de Maraîchaire 13, CH-1205 Genève*
[4] *Eawag (Swiss Federal Institute of Aquatic Science and Technology), Seestrasse 79, CH-6047 Kastanienbaum*
[5] *EPFL, ENAC IIE APHYS, GR A2 424, CH-1015 Lausanne, Switzerland*

In 2010, a seismic reflection survey in Lake Biel's North Eastern basin revealed a recent mass transport deposit in the vicinity of the intake pipe of a drinking water treatment plant. During this work, sediment cores were retrieved in and around the identified zone in order to provide evidences of the timing, causes and consequences of the observed deposit. The spatial distribution of the identified lithologies, the correlation of the cores with the seismic lines and the chronologies indicate that not only one but several mass movements occurred repeatedly, initiated at the East bank of the lake. Results need to be confirmed by a multibeam survey, and will be of interest for the optimisation of the location of the treatment plant's intake.

P 10.10

Understanding Pre-Columbian environmental adaptations strategies in agriculture: A case study of raised fields in Exaltación, in the Bolivian lowlands

Rodrigues Leonor[1], Lombardo Umberto [1], Veit Heinz[1]

[1] *Geographisches Institut, University of Bern, Hallerstrasse 12, CH-3012 Bern (leonor.rodrigues@giub.unibe.ch)*

The floodplain of Llanos the Moxos (LM) situated in the Bolivian lowlands is subject to annual variability in flooding with extreme floods resulting in substantial impacts on people's livelihoods. This year's flooding was extremely severe and indigenous communities, who always live on the most elevated parts along river levees, were highly affected; their houses were heavily damaged and entire crops were lost (Ecologist 2014). Since the early Holocene the LM has been inhabited (Lombardo et al. 2013). Studies regarding South America, also including the LM, have shown that the Holocene time period experienced significant climate fluctuations to which people had to adapt (Carson et al. 2014, Plotzki et al. 2013; Mayewski et al., 2004). A variety of Pre-Columbian earthworks in the lowlands of Bolivia, belonging to different time periods, can be found in this region and are one important source to help understand past adaptation strategies to climate and landscape changes during the Holocene (Lombardo et al. 2013; Prümers et al., 2006; Michel, 1993; Walker, 2014). One of the most striking examples is the thousands of kilometres of raised fields built in the LM, in south-western Amazonia. Pre-Columbian Raised Fields are earth platforms of differing shape and dimension that are elevated above the landscapes natural surface. There is still little explanation concerning their construction, management or time frame during which they were in use. A detailed study in the proximity Exaltación has shown this site to be of considerable importance for the study of raised fields because fields here co-occur in two totally different settings. Some Fields were built in a depression consisting of silty clay and organic rich material while others were constructed on the upland on a palaeo-leeve comprising highly weathered loamy sediments (Fig 1). Nowadays during the rainy season the fields in the depression are inundated whereas the fields located on the elevated paleo-levee are not subjected to flooding. The coexistence of this two distinct settings raises some important questions regarding the time of construction and use or/and cultivation of different

kind of crops. In order to investigate this issues a topographic transect of 630m from the paleo levee through the depression was measured using a digital level Sokkia D50 (Fig.1). Three sites were chosen for excavation of pits comprising always the elevated bed of the Field and the adjunct canal. Description and standard soil horizon/layer identification procedures were carried out followed by sampling every 10 cm for standard soil lab analysis. The results show that the fields in the depression, in reference to the fields on the elevated part, were built on an area lying approximately 1m lower. This difference in elevation in combination with the fact that the sediments are silty clay suggest the existence of prolonged local wet conditions (until well into the dry season when water can be scarce). The results of the cation exchange capacity (CEC) indicate that the soil in the depression is much more fertile compared to the soil of the nearby elevated part. Nevertheless, also the soil in the depression has a very high amount of exchangeable aluminium; which is toxic to most plants in these quantities. For a better understanding of this subject further analysis are in progress. So far the most likely explanation is that the fields in the depression were very probably not used during the same season as the fields in the surrounding upland. This site seems to be a unique example were fields co-exist in different settings and is of considerable importance for further studies to understand why and how Pre-Columbian people were using and managing the raised fields in the LM.

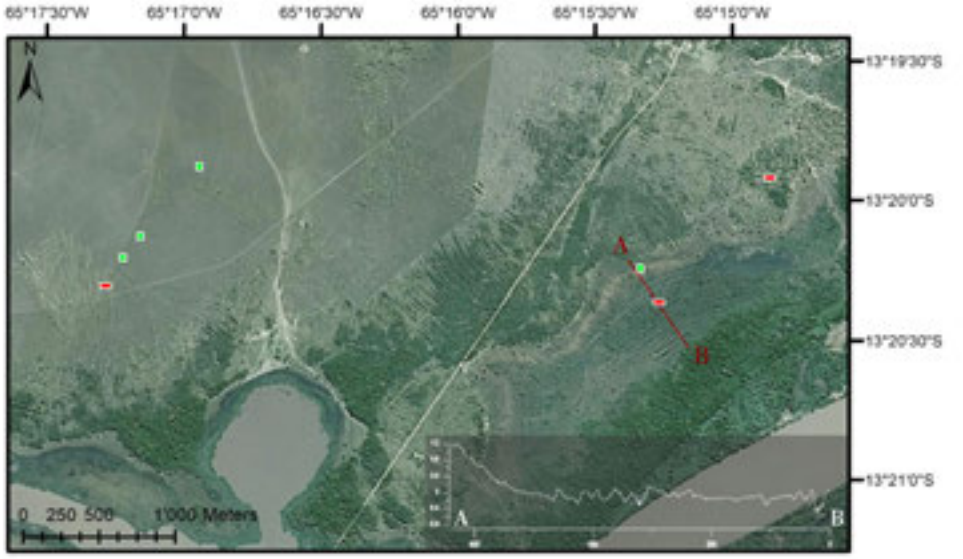

Figure 1: Study site close to Exaltación showing excavated pits of fields (red squares) and reference profiles (green squares). Transect trough the depression from A to B showing the elevation profile.

REFERENCES

Ecologist (2014, March 11) Bolivia and Britain—a tale of two floods.

Carson, J.F., Whitney, B.S., Mayle, F.E., Iriarte, J., Prümers, H., Soto, J.D., Watling, J., 2014. Environmental impact of geomoetric earthwork construction in pre-Columbian Amazonia. PNAS - Proceedings of the National Academy of Sciences. 111, 10497–10502.

Lombardo, U., Canal-Beeby, E., Fehr, S., Veit, H., 2011. Raised fields in the Bolivian Amazonia: a prehistoric green revolution or a flood risk mitigation strategy? Journal of Archaeological Science, 38, 502-512.

Lombardo, U., Szabo, K., Capriles, J. M., May, J.-H., Amelung, W., Hutterer, R., Lehndorff, E., Plotzki, A., Veit, H., 2013. Early and Middle Holocene Hunter-Gatherer Occupations in Western Amazonia: The Hidden Shell Middens. PLoS ONE, 8 (8), 1-14.

Mayewski, P.A. et al., 2004. Holocene climate variability. Quaternary Research, 62, 243-255.

Michel, M., 1993, Prospección arqueológica de San Ignacio de Moxos. Prov. Moxos, Departamento de Beni: La Paz,Universidad Mayor de San Andrés.

Plotzki, A., 2013: Late Pleistocene to Holocene fluvial dynamics and environmental conditions in the Llanos de Moxos, Bolivian Amazon, Ph.D., Philosophisch naturwissenschaftlichen Fakultät, Universität Bern, Bern, 2013.

Prümers, H., Jaimes-Betancourt, C., & Plaza-Martinez, R., 2006, Algunas tumbas prehispánica de Bella Vista, Prov. Iténez, Bolivia: Zeitschrift für Archäologie Außereuropäischer Kulturen, v. 1, p. 251-284.

Walker, J., 2004. Agricultural Change in the Bolivian Amazon. University of Pittsburgh Latin American Archaeology Publications and Fundación Kenneth Lee, Trinidad

P 10.11

Development of an RF-EMF exposure surrogate for epidemiologic research from modelling, personal measurements and operator data

Katharina Roser[1], Anna Schöni[1], Milena Foerster[1], Martin Röösli[1]

[1] *Swiss Tropical and Public Health Institute, Basel, CH*
[1] *University of Basel, Basel, CH*

Introduction
Nowadays exposure to radiofrequency electromagnetic fields (RF-EMF) is ubiquitous and their potential effect on health, behaviour and cognition are still unknown. For epidemiologic research on that topic accurate exposure assessment is a crucial part. The aim was to develop an integrative exposure surrogate measure to estimate both, whole-body and brain exposure which can be applied in epidemiological research on RF-EMF emitted from different sources.

Methods
The HERMES (Health Effects Related to Mobile PhonE use in adolescentS) study, an ongoing cohort study conducted in Central Switzerland, aims to prospectively investigate whether the exposure to RF-EMF emitted by mobile phones and other wireless communication devices affects cognitive functions or causes behavioural problems and non-specific health disturbances in adolescents. 439 adolescents with a mean age of 14 years participated in the baseline investigation of the HERMES study conducted in 2012 and 2013.
In a subgroup of the study participants personal measurements were conducted. The adolescents carried a portable measurement device, a so-called exposimeter, to measure individual near- and far-field exposure on 13 different frequency bands for three consecutive days.

Far-field exposure to fixed site transmitters was modelled using a geospatial propagation model(Bürgi et al. 2010). Contribution of far-field exposure from WLAN (Wireless Local Area Network) and DECT (Digital Enhanced Cordless Telecommunications) base stations have been identified by means of regression models from personal measurements. Predictors of the near-field exposure were identified from the literature (Lauer et al. 2013).

To evaluate the impact of differences in the power control of GSM (Global System for Mobile Communications) and UMTS (Universal Mobile Telecommunications System) mobile phones, personal measurement data was related to mobile phone operator data.

Results
Based on personal measurements from 71 adolescents carrying an exposimeter between 42 and 121 hours and filling out an activity diary, the following far-field WLAN and DECT exposure predictors have been identified: WLAN at school, WLAN at home and not switching off the base station during night and DECT phone base station placed in the bedroom, the living room or the kitchen. For the uplink far-field exposure the number of smartphones used by the family and the time spent in trains and buses were relevant predictors.

We found indication that type of network is relevant since duration of GSM calls was associated with personal uplink exposure levels whereas duration of UMTS calls was not (see table 1).

mean uplink [mW/m²]	coefficient	standard error	p value	95% confidence interval
duration calls GSM [min/day]	0.015	0.004	0.001	[0.007,0.023]
duration calls UMTS [min/day]	-0.023	0.015	0.134	[-0.053,0.007]
duration calls Unknown [min/day]	0.091	0.63	0.886	[-1.182,1.365]
constant term	0.032	0.017	0.072	[-0.003,0.066]

Table 1: Result of the multivariable regression predicting the mean uplink exposure by means of duration of calls with the mobile phone using different networks (number of observations = 44).

Conclusion
The preliminary results indicate only a few relevant exposure predictors.
Although the proposed approach is proven to be feasible to combine near- and far-field exposure sources to an integrative whole-body and brain exposure value, more data is needed to obtain more robust and significant estimates.

The HERMES-cohort study will use the developed exposure surrogate for epidemiological studies on mobile phone use in adolescents and its potential detrimental health, behavioural and cognitive outcomes. It will provide a more accurate assessment of this variable than subjective or modelled exposure assessment since it takes different sources of exposure in account and is based on personal measurements.

REFERENCES

Bürgi A et al. (2010) A model for radiofrequency electromagnetic field predictions at outdoor and indoor locations in the context of epidemiological research Bioelectromagnetics 31:226-236

Lauer O, Frei P, Gosselin MC, Joseph W, Röösli M, Fröhlich J (2013) Combining near-and far-field exposure for an organ-specific and whole-body RF-EMF proxy for epidemiological research: A reference case Bioelectromagnetics 34:366-374

P 10.12

Quantifying the impact of anthropogenic activities on the erosional and sediment budget in the Rhône River basin– the SEDFATE project.

Tiago Adrião Silva[1], Maarten Bakker[2], Anna Costa[3], Stéphanie Girardclos[1,4], Stuart Nicholas Lane[2], Jean-Luc Loizeau[1], Peter Molnar[3], Fritz Schlunegger [5], Laura Stutenbecker[5].

[1] *Section of Earth and Environmental Sciences, University of Geneva, 1205-Geneva, Switzerland (Tiago.Adriao@unige.ch)*
[2] *Institute of Earth Dynamics, University of Lausanne, 1015-Lausanne, Switzerland*
[3] *Institute of Environmental Engineering, ETHZ, 8093-Zurich, Switzerland*
[4] *Institute for Environmental sciences, University of Geneva, 1227-Carouge, Switzerland*
[5] *Institute of Geological Sciences, University of Berne, 3012-Bern, Switzerland*

In the most recent geological past, mountainous landscapes such as the European Alps have been shaped by erosional and sediment transport processes during multiple glacial and interglacial cycles. In addition to a climate driving force, seismic (short-term), tectonic and realted exhumation processes have a profound impact in shaping the sediment availability in these systems. The glacial inheritance of these landscapes has influenced the sediment availability through the conditioning of the hydrological and geomorphic responses of the system. During the past ca. 200 years, human activities have modified the processes operating in these environments, which has changed the sediment budget in the watersheds. Specific tasks like dam construction flow abstraction, sediment flushing, river channelization, gravel mining and changes in land use,have had measurable impacts on the hydrologic and geomorphologic conditions in these environments.

SEDFATE is a collaborative project, funded through the Swiss National Science Foundation (n. CRSII2_147689), which aims at disentangling the controls of human activities from those associated with climatic variations on the erosional and sediment transport mechanisms. It focuses on the Rhône River basin where the routing of the sediment will be traced from the source to its sink in Lake Geneva. We have framed these tasks in 4 sub-projects, where specific aspects relevant for the overall scope will be addressed..

Sub-project A (UniGe) focuses on the pattern of sediment flux to Lake Geneva. Sedimentation rates, detailed bathymetric and seismic data will be used to quantify the sediment flux. Sedimentological signature of the sediments will be characterized and traced upstream to the Rhône River basin.

Sub-project B (UniBe) analyzes the sediment assemblage of selected sub-basins of the Rhône River and will correlate them with sedimentation rate changes in the Lake Geneva sedimentary record. Sediment sources will be determined through XRF, REE and heavy mineral assemblage analyses. Erosional fluxes will be measured with in-situ ^{10}Be. Physical sediment fluxes will be determined through cosmogenic nuclide dating and geomorphological analysis..

Sub-project C (UniL) will focus on the Val d'Hérens basin, which hosts the Grande Dixence dam that retains 30% of the total water abstraction in the Rhône River. The impact of water abstraction, sluicing and flushing on the downstream sediment transport and redistribution will be assessed. This will be achieved by the analysis of representative water intakes, remote sensing, in-stream measurements and sediment transport modeling.

Sub-project D (ETHZ) upscales the findings of sub-project C in the Val d'Hérens and will implement a physically-based model to the Rhône River basin. Sediment production and transfer, and their uncertainties, is the main focus of this sub-project. Variations and trends in the in sediment transport will be assessed through hydroclimatic and streamflow analysis of data for the last ca. 100 years.

The interdisciplinary approach of the SEDFATE project is designed to successfully quantify the sediment transfer rate variation in the Rhône River as a result from anthropogenic activities against a background of climatic change.

P 10.13

Building high resolution radiocarbon dating chronologies for the reconstruction of late Holocene landslide events in the Mont Blanc area, Italy

Ursula Sojc[1], Irka Hajdas[1], Susan Ivy Ochs[1], Naki Akçar[2], Philip Deline[2]

[1] *Institute of Particle Physics, ETH Zurich, Otto-Stern-Weg 5, CH-8093 Zurich (sojcu@student.ethz.ch)*
[2] *Institute of Geological Sciences, University of Bern, Baltzerstraße 1–3, CH-3012 Bern*
[3] *EDYTEM Lab, Université de Savoie, CNRS, F-73376 Le Bourget-du-Lac*

The Ferret valley Arp Nouva peat bog located in the Mont Blanc massif was critically evaluated since previously published radiocarbon dates have led to controversial conclusions on the formation of the swamp. Radiocarbon dating of roots from three pits of up to 1 m depth was applied to discuss the question whether the historical documented rock avalanche occurring in AD 1717 overran the peat bog or formed it at a later stage. For the deepest root samples ages between 302-145 cal yr BP and 284-84 cal yr BP were obtained, which fit very well into the time frame of the historical documented AD 1717 rock avalanche event. It can therefore be concluded that the rock avalanche formed the Arp Nouva peat bog by downstream blockage of the Bellecombe torrent. Furthermore, careful sample preparation with consequent separation of roots from the bulk peat sample has shown that the problem of too old ^{14}C ages can be circumvented. This work demonstrates that a combined geomorphological and geochronological approach is the most reliable way to reconstruct landscape evolution, especially in light of apparent chronological problems. The key to successful ^{14}C dating is a careful sample selection and the identification of material that might be not ideal for chronological reconstructions.

P 10.14

A Record Of Late Glacial And Holocene Environmental Changes In The Bohemian Forest, Czech Republic: The History Of A Central European Upland After LGM

Klára Vočadlová[1], Libor Petr[1], Pavla Žáčková[3] & Marek Křížek[4]

[1] *University of West Bohemia in Pilsen, Centre of Biology, Geoscience and Environmental Education, Klatovská 51, 306 19 Plzeň, Czech Republic, (vocadlov@cbg.zcu.cz)*
[2] *Masaryk University, Faculty of Science, Department of Botany and Zoology, Kotlářská 2, 61137 Brno, Czech Republic*
[3] *Charles University in Prague, Faculty of Science, Department of Botany, Benátská 2, 12801 Prague, Czech Republic*
[4] *Charles University in Prague, Faculty of Science, Department of Physical Geography and Geoecology, Albertov 6, 12843 Prague, Czech Republic*

During cold periods of the Late Pleistocene, the Bohemian (Bavarian) Forest, a central European Hercynian mountain range, belonged to an area lying between the extensive Alpine and Scandinavian ice sheets. Only local mountain glaciation, mostly limited to cirques, developed in the Bohemian Forest during the Late Pleistocene. These small glaciers could more sensitively react to environmental changes and reflect regional climate changes. The objectives of the research were (i) to compare the sedimentary record and local glacial chronologies from the Bohemian Forest and (ii) to determine the impact of regional and supraregional (European) climate changes on the environment and the dynamics of natural processes in the central European medium-altitude mountain range.

A multi-proxy reconstruction of the mid-altitude environment of the Bohemian Forest in the Late Glacial and Holocene is established. A core in a peatbog in the Černé Lake cirque was analysed with respect to various lithological and geochemical parameters, pollen and macrofossil content, supplemented by 2 OSL and 10 AMS radiocarbon dates. The sediment sequence indicates not only high synchronisation of the local processes with environmental changes in the larger region of central Europe but also some local specific events. Unlike the central European mountain ranges the Younger Dryas in the Bohemian Forest was not connected with glacier readvances but it was a dry cold episode with low lake levels which prevails till the early Preboreal. Most of the environmental changes during the Late Glacial and Early Holocene were sudden compared to gradual changes in the Middle and Late Holocene. Consecutive changes in the sedimentation and vegetation succession (limnic environment – fen/peatbog – open raised bog) correspond to the Holocene Sub-series. Further, we discussed rubidium content in the sediment as a proxy of environmental changes (wind activity, soil erosion, and afforestation) during the Late Glacial and Early Holocene. Afforestation and soil development began in the region during Early Holocene. Treeline exceeded the altitude of ~1000 m a. s. l. before 9.7–9.3 cal. ka and coincided with rapid geochemical changes in the sediment. The beginning of the Middle Holocene was connected with peat aggradation and decline of shallow water reservoirs in the mountain range.

P 10.15

The D/H signal of Holocene and modern leaf waxes in the sediments and catchment of a south-Alpine lake

Stefanie B. Wirth[1,2] & Alex L. Sessions[1]

[1] *Division of Geological and Planetary Sciences, California Institute of Technology, Pasadena, CA, USA (swirth@gps.caltech.edu)*
[2] *Centre for Hydrogeology and Geothermics, University of Neuchâtel, Rue Emile-Argand 11, CH-2000 Neuchâtel*

The hydrogen isotopic composition (D/H) of leaf waxes is a high-potential tool for studying past and present hydro-climatic conditions (Sachse et al. 2012). Yet, for an improved understanding and thus interpretation of D/H paleo-records more research on the climatic and catchment-specific mechanisms governing the D/H composition of leaf waxes is required.

Here we present a Holocene D/H record of *n*-C_{28} fatty acids from the sediments of Lake Ghirla, located at the foot of the southern Alps (N-Italy). Complementing the paleo-record, we conducted a catchment study investigating the D/H composition of modern leaf waxes of the main tree species, river-bed sediment, and riverine water samples. This study on modern samples serves for assessing potential isotopic effects on the sedimentary leaf wax D/H signal due to the catchment's altitude profile (600 m) as well as tree vegetation changing over time.

The leaf wax paleo-record is characterized by an overall three-part division showing a δD enrichment trend (-155 to -140 vs SMOW ‰) from 11.5-6.6 cal kyr BP, followed by a period with more depleted values (~-160 ‰) from 6.5 cal kyr BP until 100 years ago, and an abrupt increase (plus 30 ‰) in the δD composition for the most recent 60 years. These main characteristics are interrupted by shorter excursions, of which the most conspicuous occur at 8.5-8.1 cal kyr BP (minus 15 ‰), at 2.7-2.2 cal kyr BP (minus 10 ‰), and at 400-150 cal yr BP (plus 15 ‰). Catchment samples collected during the dry and warm spring of 2014 indicate an inverse altitude effect for riverine water samples (+0.3‰/100m) and leaf waxes (+6.3‰/100m), which we interpret as increasing evapotranspiration with higher altitude. No altitude effect is observed for catchment samples collected during the wet spring of 2013. In regard to the leaf samples from different tree species, no systematic difference of the leaf wax δD values was recognized.

Interpreting the paleo-record, our results suggest isotopic enrichment during dry and warm climatic periods (early/mid-Holocene, recent decades), which may be primarily due to enhanced evapotranspiration. In fact, warm Alpine climate of the past has been attributed with rather dry summer conditions (Wirth et al. 2013a,b) favoring evapotranspiration during the vegetation period. In contrast, the more depleted D/H signal from 6.5 cal kyr BP until 100 years ago may reflect wetter and possibly also cooler climatic conditions. The isotopic enrichment at 400-150 cal yr BP (Little Ice Age, cool and wet), however, does not follow this pattern and thus requires further research. Two potential scenarios are an increased contribution of Mediterranean moisture, which is compared to North Atlantic moisture isotopically enriched (LeGrande & Schmidt 2006), or erosion of older soils due to enhanced precipitation and thus deposition of compounds out of chronological order with the lacustrine sediment sequence.

REFERENCES

LeGrande, A.N. & Schmidt, G.A. 2006: Global gridded data set of the oxygen isotopic composition in seawater, Geophys. Res. Lett. 33, L12604.

Sachse, D. et al. 2012: Molecular Paleohydrology: Interpreting the Hydrogen-Isotopic Composition of Lipid Biomarkers from Photosynthesizing Organisms, Annu. Rev. Earth Planet. Sci. 40, 221-249.

Wirth, S.B., Gilli, A., Simonneau, A., Ariztegui, D., Vannière, B., Glur, L., Chapron, E., Magny, M. & Anselmetti, F.S. 2013a: A 2000-year long seasonal record of floods in the southern European Alps, Geophys. Res. Lett. 40, 4025–4029.

Wirth, S.B., Glur, L., Gilli, A. & Anselmetti, F.S. 2013b: Holocene flood frequency across the Central Alps – solar forcing and evidence for variations in North Atlantic atmospheric circulation, Quat. Sci. Rev. 80, 112-128.

P 10.16

Post-glacial Landscape Evolution of the Upper Haslital Aare between Handegg and Guttannen (Bernese Alps)

Raphel Zurfluh[1], Florian Kober[1/2], Susan Ivy-Ochs[3], Irka Hajdas[3] & Markus Christl[3]

[1] *Geological Institut, ETH Zürich, Sonneggstr. 5, CH-8092 Zürich (zurfluhr@student.ethz.ch)*
[1 /2] *now at Nagra, Hardstrasse 73, 5430 Wettingen*
[3] *Institut of Particle Physics, ETH Zürich, Otto-Stern-Weg 5 CH-8093 Zürich*

Postglacial environments in alpine settings are affected by the adjustment to the prevailing interglacial climate conditions by various geomorphic processes. Quantitative information of valley reshaping processes, ages of landforms and specifically valley fillings, however, are scarce in the Central Alps. The upper Haslital (Bernese Oberland) between Handegg and Guttannen represents an ideal study area to investigate the post-glacial evolution of an alpine valley. The mapping of the inner valley revealed that mass-wasting processes with debris flow and rock fall deposits as well as talus cones dominate the valley floor. One of the largest fan-systems, beside the Rotlaui Fan, is the currently active Spreitlaui fan system which was investigated in detail in terms of geomorphic forms and processes, sedimentary units and dated for an absolute age chronology. Cosmogenic surface exposure dating of thirteen boulders on distinct geomorphic units yielded ages between 1.4 kyr and 7.7 kyr. Further absolute ages were obtained by the radiocarbon dating by sampling the modern Spreitgraben and investigating an available 90 m core. The measured ages show an oldest age around ~10 kyr cal. BP at a core depth of 85 m. Together with interpretations of available seismic profiles a qualitative reconstruction of the Holocene sedimentation pattern was possible. An early phase of the Spreitlaui formation, right after the retreat of the Aare glacier, was characterized by high sedimentation rates. Afterwards, at least one but possibly two landslide events (likely ~8 and ~3 kyr) occurred within the Spreitlaui system. Their timing correlates broadly with the landslide activity observed elsewhere in the Alps, specifically in the late Holocene. Additionally, dated debris flow events overlap with phases of high flood activity in the northern Alps. This suggests that the postglacial landscape evolution of the Haslital is largely controlled by climate forcing in combination with a glacially preconditioned landscape, characterized by threshold slopes and large amounts of freely available debris.

11. Cryospheric Sciences

J. Alean, A. Bauder, B. Krummenacher, J. Nötzli, C. Lambiel,
M. Lüthi, J. Schweizer, M. Schwikowski

Swiss Snow, Ice and Permafrost Society

TALKS:

11.1 Barandun M., Sold L., Huss M., Azisov E., Salzmann N., Usubaliev R., Hoelzle M.: Accumulation rates on Abramov Glacier, Kyrgyz Pamir between 2001 and 2013

11.2 Boffi G., Wieser A., Binder D., Schöner W.: GNSS-based monitoring of kinematic glacier surface deformation at the A.P. Olsen Ice Cap

11.3 Bosson JB., Lambiel C.: Current evolution of small glacier systems in alpine permafrost environments in relation with their internal structure

11.4 Braillard L., Delaloye R., Abbet D., Barboux C., Morard S., Staub B.: Onset and development of destabilization phases of rock glaciers in the Swiss Alps

11.5 Caduff R., Wiesmann A., Bühler Y.: Quantification and mapping of snow surface dynamics with terrestrial radar interferometry: From avalanche mapping to snow creep measurements

11.6 Capelli A., Kapil J. C., Reiweger I., van Herwijnen A., Schweizer J. , Or D.: Propagation characteristics of acoustic waves in snow under laboratory conditions

11.7 Comola F., Schaefli B., Rinaldo A., Lehning M.: Flow and Temperature Dynamics in the Hydrologic Response of Alpine Catchments: Travel Time Formulation and Geomorphologic Signatures

11.8 Gabbi J., Huss M., Bauder A., Schwikowski M.: The impact of Saharan dust events on long-term glacier mass balance in the Alps

11.9 Huss M., Dhulst L., Bauder A.: Ten new long-term glaciological mass balance series for Swiss glaciers

11.10 Langhammer L., Dunse T., Langley K., Isaksson E., Hagen J.O.: Deriving long-term firn stratigraphy from optical borehole camera measurements on Austfonna, Svalbard

11.11 Reiweger I., Gaume J., Schweizer J.: Failure Criterion for Weak Snow Layers

11.12 Sommer C., Mott R., Lehning M., Haussener S.: Variability of snow thickness changes in steep rock faces based on terrestrial laser scanning

11.13 Stawicki M., Magnusson J., Jonas T.: Sensitivity of operational snow melt predictions to different modelling setups

11.14 Werder M. A.: Fast ice flow, troughs, overdeepenings and subglacial hydrology

POSTERS:

P 11.1 Becker P.: Ice flow in the Alps during the last glacial maximum, a modeling approach

P 11.2 Capt, M., Bosson, J.-B., Micheletti, N., Lambiel, C.: Multitemporal scale surface changes of small glacier systems in permafrost environments

P 11.3 Fischer M., Huss M., Hoelzle M.: Use of a new long-range terrestrial LiDAR system to monitor the mass balance of very small glaciers

P 11.4 Molina E., Sikos F., Rados M., Chaparro N., Samata J., Montoya N., Jiménes L., Gonzales G., Torres L., Gómes J., Cruz R., Giraldez C., Drenkhan F., Haeberli W., Huggel C., Schauwecker S.: Initiation Of Mass Balance Monitoring At Glaciar Suyuparina, Cordillera Vilcanota, Peru

P 11.5 Colonia D., Haeberli W., Torres J., Schauwecke S., Cochachin A., Tacsi A., Santiago A.: An Inventory Of Possible Future Lakes In The Cordillera Blanca, Peru

P 11.6 Hoelzle, M., Hauck, C.: Long-term energy balance measurements at three different mountain permafrost sites in the Swiss Alps

P 11.7 Leinss S., Hajnsek I.: Swiss glaciers: TanDEM-X time series vs. SwissAlti3D

P 11.8 Naegeli K., Huss M., Hoelzle, M.: Evaluation of automatic weather station data to observe the characteristics and changes in glacier surface albedo

P 11.9 Salzmann N., Huss M., Machguth H., Sold L., Linsbauer A., Joerg P., Leysinger-Vieli G., Hoelzle M.: 10 years of MB measurements on Findelengletscher, VS, Switzerland

P 11.10 Crivelli Ph., Horender S., Paterna E., Lehning M.: Measuring snow surface topologies and its changes using Microsoft's Kinect

P 11.11 Haberkorn A., Phillips M., Kenner R., Rhyner H., Hoelzle M.: Ground thermal regime and its relation to snow cover in Alpine rock walls

P 11.12 Jörg-Hess S., Griessinger N., Zappa M.: Extended-range probabilistic forecasts of snow water equivalent and runoff in mountainous areas

P 11.13 Marmy A., Rajczak J., Kotlarski S., Salzmann N., Hauck C.: Projections of permafrost evolution in the Swiss Alps coupling climate and soil models

P 11.14 Nendaz T., Lambiel C.: Long term monitoring of the Mont Dolin rock glacier (Swiss Alps)

P 11.15 Staub B., Hasler A., Delaloye R.: Gap filling procedures for ground surface temperature time series of the PERMOS network

P 11.16 Wicki A., Hauck C., Pellet C., Hilbich C., Kemna A., Weigand M., Wege S.: Spatial and temporal variability of soil moisture in permanently frozen ground at Schilthorn (Swiss Alps)

P 11.17 Schneebeli M., Proksch M., Matzl M., Weissbach S.: Antarctic snow stratigraphy - new methods and insights

P 11.18 Proksch M., Gouttevin I., Langer M., Ebner P., Fierz C., Schneebeli M.: Snow microstructure and modelling in support of permafrost science

P 11.19 Wiese M., Schneebeli M.: Imaging of snow algae in natural snow using phase-contrast tomography

P 11.20 Helfricht K., Lehning, M., Sailer R., Kuhn M.: The contribution of locally extreme snow depths to the winter snow cover volume of Alpine glaciers in the Ötztal Alps, Austria

P 11.21 Sold L., Huss M., Hoelzle M.: Towards a better representation of snow accumulation distribution in glacier mass balance models

11.1

Accumulation rates on Abramov Glacier, Kyrgyz Pamir between 2001 and 2013

Martina Barandun[1], Leo Sold[1], Matthias Huss[1,2], Erlan Azisov[3], Nadine Salzmann[1], Ryskul Usubaliev[3], & Martin Hoelzle[1]

[1] *Department of Geoscience, University of Fribourg, Fribourg, Switzerland (martina.barandun@unifr.ch)*
[2] *Laboratory of Hydraulics, Hydrology and Glaciology (VAW), ETH Zurich, Zurich, Switzerland*
[3] *Central Asian Institute of Applied Geosciences (CAIAG), Bishkek, Kyrgyzstan*

Glacier mass balance is a good indicator for climate change. In Central Asia melting glacier ice presents a significant contribution to total runoff, and the water supply is highly critical for irrigation in the downstream areas of the major mountain ranges in this region. Data from long-term glacier monitoring programmes provide the scientific basis for climate change analysis and the development of sound models for future projection and impact assessments. Abramov Glacier, an important reference glacier located in the Kyrgyz Pamir, was continuously monitored from 1968 to 1998. With the breakdown of the USSR the scientific program at the majority of monitored glaciers in Central Asia stopped immediately. On Abramov Glacier, mass balance measurements have only been re-established in 2011. To guaranty continuous long-term monitoring, methods have to be developed to close the data gap between 1998 and 2011.

In summer 2013 we applied 800MHz Ground Penetrating Radar (GPR) in the accumulation area of Abramov Glacier to detect annual layers in the upper most firn. The GPR profile of almost 3 km length reaches a depth of almost 18m. A maximum of 13 pronounced internal reflection horizons was observed. The well visible horizons are interpreted as high-density or ice layers that formed at previous summer surfaces. The collected data presents a unique indication on the snow accumulation pattern during the past decade but is sensitive to a potential misinterpretation of reflection horizons in the radar profiles, leading to a shift of the layer chronology. We assume that all detected reflection horizons are previous summer surfaces, but take into account that thin or non-existing layers cannot be resolved by the GPR.

We used the GPR data to calculate annual accumulation rates (Sold et al, 2014) and derived possible maximal elevation changes at point locations on the profile using simple assumptions. The inferred elevation changes were then compared to the results of a distributed mass balance model (Huss et al, 2009) and to surface elevation changes based on digital terrain models from 2000 and 2011 (Gardelle et al. 2013). Whereas the model tends to underestimate the detected change in height based on the GPR data, the geodetic calculations indicate an overestimation.

Further, we calculated the centered mass balance at single point locations in the accumulation and the ablation area, for which GPR data and long-term glaciological measurements since 1968 were available. Trend analyses show an intensified ablation and a simultaneous increase in accumulation at the selected locations over the past 15 years. However, to make more sound statements, additional information such as the dating of an ice core is need.

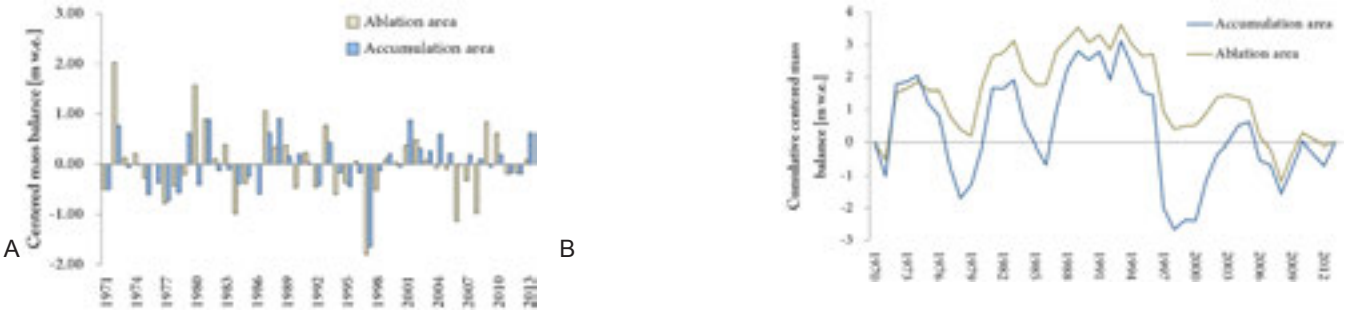

Figure 1. Centered (A) and cumulativ centered (B) mass balance for a point location in the accumulation area and for one in the ablation area. From 1971 to 1994 and from 2012 to 2013 glaciological measurements and from 2001 to 2011 GPR data was used. Note that measurement gaps are filled in with the modeled mass balance at the point location.

REFERENCES

Gardelle, J., Berthier, E., Arnaud, Y., & Kääb, A. 2013: Region-wide glacier mass balances over the Pamir-Karakoram-Himalaya during 1999-2011. The Cryosphere, 7, 1263-1286.

Huss, M., Bauder, A., & Funk, M. 2009: Homogenization of long-term mass-balance time series. Annals of Glaciology, 50(50), 198-206.

Sold, L., Huss, M., Eichler, A., Schwikowski, M., and Hoelzle, M. (Accepted). Recent accumulation rates of an alpine glacier derived from firn cores and repeated helicopter-borne GPR. The Cryosphere Discussions.

11.2

GNSS-based monitoring of kinematic glacier surface deformation at the A.P. Olsen Ice Cap

Geo Boffi[1], Andreas Wieser[1], Daniel Binder[2], Wolfgang Schöner[2]

[1] *Institute of Geodesy and Photogrammetry, ETH Zürich, Stefano-Franscini-Platz 5, 8093 Zürich (geo.boffi@geod.baug.ethz.ch)*
[2] *Climate Research Department, Central Institute for Meteorology and Geodynamics (ZAMG), 1190 Vienna, Austria*

Annual glacial lake outburst floods (GLOF) at the southeast outlet glacier of the A.P. Olsen Ice Cap (northern-east Greenland) represent a hydrological extreme event with major consequences on the glacier motion. The response of the cold glacier to these events is not fully explained by the current understanding of glacier mechanics (Sugiyama et al. 2007). For this reason Spatially and temporally well distributed measurements of surface dynamics and surface deformations are highly valuable source of information for the assessment of this kind of glacial processes because it allows investigating glacier dynamics under rapidly changing stress conditions. This should help to better understand the relation between glacier surface dynamics and glacial hydrology.

A geodetic and geophysical monitoring network has been installed in spring 2012 with the goal of delivering a continuous data set of GPS observations and passive seismic data during the fill- and drain cycle of the ice-dammed lake. The kinematic monitoring is established using a network of low-cost and low power single-frequency GPS stations. All of them are set up for continuous measurements with a sampling rate of 10 s in order to detect sub-daily changes in glacier dynamics as well as changes with longer time scales, e.g. seasonal ones. In order to provide a GPS reference solution for at least one station (i.e. to partially validate the results), an additional station is equipped (since spring 2014) with a double frequency receiver. For obtaining better time resolution of the surface dynamics and stress field changes than with static processing of time windows of a few hours, we process all GPS data kinematically at 0.1 Hz using a Kalman Filter. A coordinate random walk model is employed to represent site motions.

The results obtained so far indicate that a relative accuracy (between GPS stations) of a few centimeters is achievable for the kinematic solutions using differential processing of single-frequency data. The 2012 GPS data show changes of the horizontal flow velocity on the order of 4 mm/h and for a short time (approximately 8 hours) even a reversal of local flow direction at station 2 (fig. 1a) immediately before and during the GLOF. Sugiyama et al. (2007) reported similar dynamic consequences during the outburst of Gornerlake, Switzerland. Besides the observed dynamics during the outburst, the GPS data revealed also a highly dynamic GLOF initiation phase. About one week before the GLOF significant horizontal displacement and uplift of 5 to 10 cm occurred at stations 2-4 (fig. 1b) as compared to the trend of surface motion (accounting for ablation).

Figure 1 Horizontal displacement during the GLOF-period in 2012 (left). Horiziontal and vertical motion anomalies of stations 2, 3 and 4 during initiation phase and outburst of the GLOF.

The results of the GPS processing with their high temporal resolution and accuracy are useful for better understanding of sub- and englacial triggering mechanisms of outburst floods, but so far they required significant manual interaction during data processing to avoid divergence of the processed time series due to undetected errors in the raw data. The dynamic model used within the Kalman Filter needs to be optimized for the slow motion, and additional quality control mechanisms need to be developed in order to automatically detect and avoid divergence of the filter.

REFERENCES

Sugiyama S., A. Bauder, P. Weiss and M. Funk. 2007. Reversal of ice motion during the outburst of a glacier-dammed lake on Gornergletscher, Switzerland. J. Glaciol., 53(181), 172–180.

11.3

Current evolution of small glacier systems in alpine permafrost environments in relation with their internal structure

Jean-Baptiste Bosson & Christophe Lambiel

[1] *Institut des dynamiques de la surface terrestre (IDYST), Université de Lausanne, Bâtiment Géopolis UNIL Mouline, CH-1015 Lausanne (jean-baptiste.bosson@unil.ch)*

Numerous small glacier systems (<0.5 km^2) are present in alpine permafrost environments. In addition to their weak glacial dynamics and polythermal regime, they are commonly characterized in high relief environments by a huge amount of debris and glacier-permafrost interactions. These landforms, where massive glacier ice (covered or not by debris), ice-debris mixture and unconsolidated sediments coexist and sometimes interact, experience contrasted responses in the context of intensifying global change. Despite their important role of alpine water and sediment flux systems and because they are situated at the frontier between glacial and periglacial researches, the characterisation of these systems and of their current evolution in a rapidly changing cryosphere remains a challenging task.

This study explores the current differential evolution within three small glacier systems located in permafrost environments: Tsarmine (Arolla, VS), Entre la Reille (les Diablerets, VD) and les Rognes (St-Gervais, France). The spatial heterogeneity of surface dynamics (annual and seasonal velocities, surface lowering, summer vs. winter dominant dynamics, early summer vs. late summer dominant dynamics, downslope movement vs. surface lowering dominant dynamics) pointed out with 3 years dGPS monitoring correspond to changes in internal structure characteristics (distribution of ground ice, ice/sediment proportion, thickness of debris cover, probable nature and temperature of the ice), illustrated by electrical resistivity tomographies. Any direct measurements have been carried out in the spatially limited bare ice areas of these systems. In sedimentary surface areas, four main zones with specific behaviours can be outlined:

- *Debris covered glacier parts* have important surface dynamic. In addition to ice flowing and sliding, a rapid melt-out occurs. Summer dominant activity typically illustrates the hydrological forcing on glaciers where basal sliding and ice melt are intensified.
- *Low active heavily debris covered glacier parts* have a weaker surface dynamics, dominated by ice melt. Climate signal is attenuated and delayed in consequence of the weak thermal conductivity of the thick debris cover.
- *Marginal ice-debris mixture* (rock glacier, ice-cored moraine) present weak to moderate geomorphic activity. Changes seem to be linked with the downslope slow deformation of frozen sediment body. The several meters thick active layer noticeably attenuated and inverted (winter dominant activity) the climate signal.
- *Debris accumulations without ice* have a null to weak surface activity. The weak detected movements are mainly related to superficial postglacial rebalancing and localised summer mass wasting.

11.4

Onset and development of destabilization phases of rock glaciers in the Swiss Alps.

Luc Braillard[1], Reynald Delaloye[1], Damien Abbet[1], Chloé Barboux[1], Sébastien Morard[1], Benno Staub[1]

[1] *Department of Geosciences/Geography, University of Fribourg, Chemin du Musée 4, CH-1700 Fribourg (name.surname@unifr.ch)*

Destabilized rock glaciers are periglacial landforms moving faster than a few meters per year on mountain slopes, exposing sometimes scarps or crevasses features. The current (5-10 years) kinematical behaviour of 8 rock glaciers located in the Swiss Alps has been systematically investigated by performing regularly repeated DGPS surveys. Moreover, information concerning their internal structure has been gained by performing geophysical measurements.

We present here the results of a study that focuses on the onset and on the development of these destabilization phases. Based essentially on the analyse of former aerial and terrestrial photos going back to 1930, this contribution aims to provide results and discussion elements on the triggering and controlling factors of the destabilization phase(s).

Our study points out the large diversity of occurrence, development and kinematical behaviour of the destabilization phases on the investigated rock glaciers. One documented destabilization phase occurred for instance already around 1940 (Grabengufer), another one probably started already before (Dirru), another one in 1958 (Gugla/Laengenschnee), another one only during the last ten years (Gugla/Bielzug), etc. Destabilization phases can be short (a few years) and intense (velocity up to 100 m/year or even more), but also continuing for several tens of years. They can concern a part of or the entire rock glacier, reactivating former inactive – but still frozen – terminal sections.

The involved triggering mechanisms can be diverse. Beside the role played by the internal structure of the rock glacier, destabilization phases can be the result of the combined influence of several factors such as: thermal state of the permafrost, topography of the stable bedrock on top of which the rock glacier is moving, modification of the geometry of the rock glacier, or local overloading in debris (consecutive to the Little Ice Age advance of a glacier, to a landslide or to increased rock fall activity from headwalls). In the two latter situations a mechanical surge is triggered, which can take up to decades to reach the rock glacier front. The progression of the rock glacier front over a steep topography can in turn pull down a large part (if not the whole) of the rock glacier behind it.

11.5

Quantification and mapping of snow surface dynamics with terrestrial radar interferometry: From avalanche mapping to snow creep measurements

Rafael Caduff[1], Andreas Wiesmann[1], Yves Bühler[2]

[1] *GAMMA Remote Sensing AG, Worbstrasse 225, CH-3073 Gümligen, Switzerland (caduff@gamma-rs.ch)*
[2] *WSL Institute for Snow and Avalanche Research SLF, Flüelastrasse 11, CH-7260 Davos, Switzerland*

Information about snow dynamics is important for snow avalanche hazard assessment and mitigation measure planning in alpine areas. An important piece of information is the accurate mapping of avalanche extents and the identification of the release time regardless of weather conditions in particular for road and railway safety. Coherent observations with Ku-Band terrestrial radar interferometry at sampling intervals below the decorrelation time for snow surfaces (minutes to few hours) can be used to map disturbances of the snow surfaces. Changes in snow properties e.g. snow metamorphosis and melting as well as mechanical disturbances (e.g. freerider-tracks, wind drift, avalanches) change the scattering behavior (magnitude and phase of the backscattered echo) of the radar resolution cell from one radar image to another. Those changes can be expressed with the interferometric coherence. Coherence maps finally are used to locate changes induced by avalanche events in the spatial and the temporal domain. The resolution of the radar imagery allows even the detection of very small events (few tens of meters).

We present recent results from Winter 2013/2014. A first campaign includes the short term monitoring with the GAMMA Portable Radar Interferometer (GPRI, Figure 1) during two avalanche blasting experiments performed on 31 January 2014 at Flüelapass, Davos, GR. The results revealed the feasibility of accurate avalanche extent mapping even during strong changing weather conditions (Figure 1a). Additionally, high-frequency radar sampling at a fixed look angle during an avalanche release led to insights in the velocity profile of an avalanche. A preliminary assessment of the frontal velocity revealed maximum values of 71 km/h (Figure 1b). Independent validation of the measured values however is still ongoing. A second, continuous campaign started on 31 January 2014 and ended on 24 April 2014. The test site was the Dorfberg slope in Davos, GR. Results include the detection and mapping of a few smaller snow-glide events using interferometric coherence maps. The temporal resolution of the detection of such an event is given by the observation rate of the system and the on-site data processing time. A sampling rate of one scene per minute could be applied.

The experiment setup allowed as well temporal sampling faster than the decorrelation time of snow which led to the interpretation of the differential phase. Continued phase shifts in the area were detected resulting from snow surface deformation (snow creep/glide). Using the interferometric phase, maps of continuous mechanic snow surface deformation in line of sight can be created, showing the slope-wide snow creep activity. Such areas could be validated with webcam imagery showing extension ruptures and bulging of creeping snow (Figure 1c). A maximum line of sight surface displacement per day of 2.3 m was detected during the campaign. Additionally, a deformation history prior to a small snow glide event could be measured which showed an acceleration of the displacement velocity prior to the release of the snowpack (Figure 1d).

In our presentation we will give a short introduction into the measurement principle of terrestrial radar interferometry regarding snow observations and state necessary preconditions and limitations for the different modes presented followed by an introduction of the measurement setup at the different test-sites,. The main focus will be on the results and a critical discussion thereof. Finally, an outlook on future validation will be given and potential fields of application will be discussed.

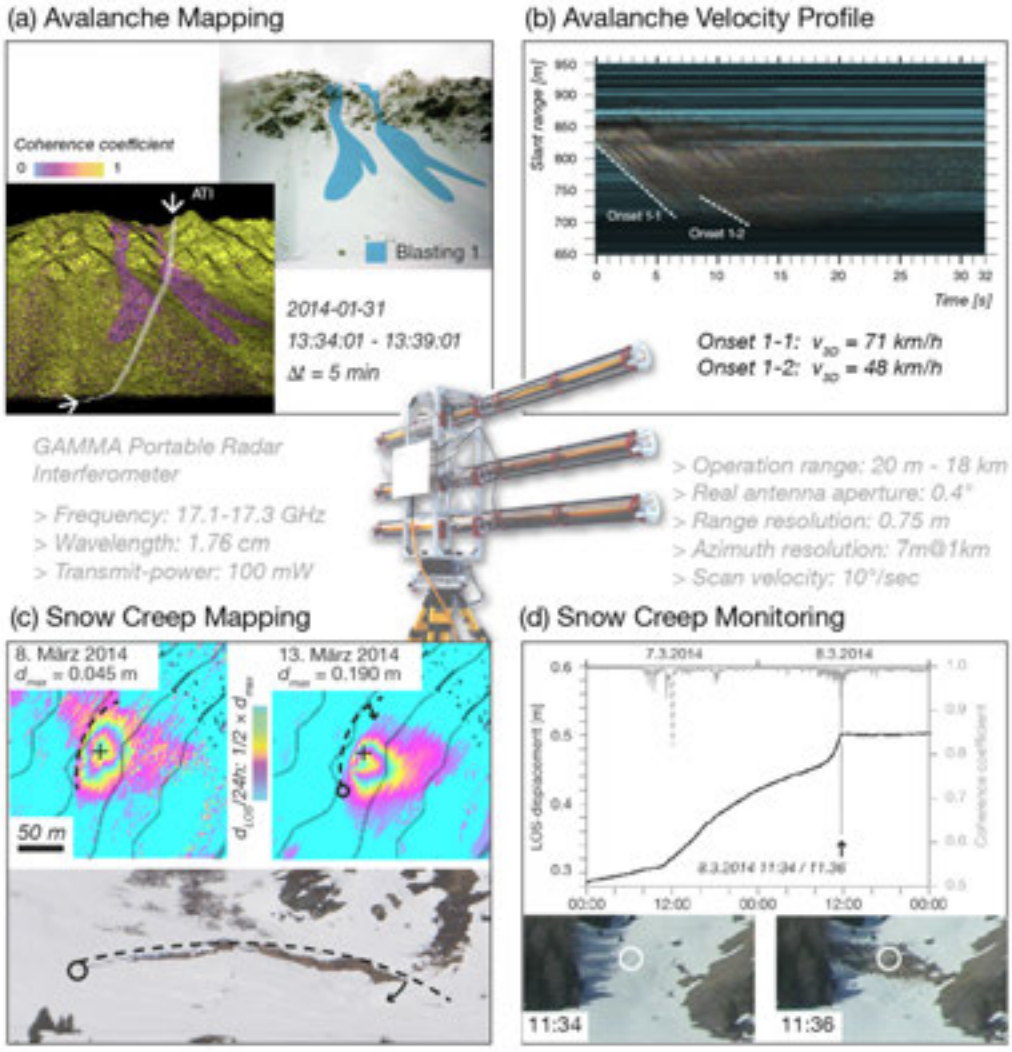

Figure 1. Results from the GPRI campaigns 2014. (a) Avalanche map after an artificial release at Flüelapass, Davos, GR, validated with photography. (b) Temporal profile of an avalanche and corresponding measured frontal velocities. Location of profile line indicated as ATI-Line in (a). (c) Details of an area with measured snow creep. Scale is normalized. The photo shows that the entire snow pack is affected by the deformation. (d) Detail of the temporal evolution of the surface displacement prior to a small snow slab breakoff.

11.6

Propagation characteristics of acoustic waves in snow under laboratory conditions

Achille Capelli[1], Jagdish Chandra Kapil[2], Ingrid Reiweger[1], Alec van Herwijnen[1], Jürg Schweizer [1] & Dani Or[3]

[1] *WSL Institute for Snow and Avalanche Research SLF, Flüelastrasse 11, CH-7260 Davos Dorf (achille.capelli@slf.ch)*
[2] *Snow and Avalanche Study Establishment SASE, Chandigarh (UT)-160036, India*
[3] *Department of Environmental Sciences, ETH Zurich, Universitätsstrasse 16, CH-8092 Zurich*

Acoustic emission (AE) analysis is a promising technique for monitoring snow slope stability with potential application in early warning systems for avalanches. Current research efforts focuses on identification and localization of acoustic emission features preceding snow failure and avalanches. However, our knowledge of sound propagation characteristics in snow, including velocity and attenuation, is still limited. While some characteristics have been determined for the frequency range below 10 kHz, recent snow failure experiments suggest that the peak frequency is in the ultrasound range between 30 kHz to 500 kHz.

We therefore studied the propagation of pencil lead fracture (PLF) signals through snow in the ultrasound frequency range by performing laboratory experiments with columns of artificially produced snow of varying density and temperature. The attenuation constant was obtained by varying the size of the columns to eliminate possible influences of the snow-sensor coupling. The attenuation constant was measured for the entire PLF burst signal and for single frequency components.

In addition, propagation velocities were calculated from the arrival times of the acoustic signals. While longitudinal wave velocities could be determined successfully, the results obtained from transversal waves were ambiguous and may need further investigation. Their successful detection would allow determining the elastic properties of snow (elastic moduli and Poisson's ratio) from the p- and s-wave velocity. This would be highly relevant, as the elastic properties of snow are not well known.

11.7

Flow and Temperature Dynamics in the Hydrologic Response of Alpine Catchments: Travel Time Formulation and Geomorphologic Signatures

Francesco Comola[1], Bettina Schaefli[2], Andrea Rinaldo[2, 3], Michael Lehning[1, 4]

[1] *Laboratory of Cryospheric Science, School of Architecture, Civil and Environmental Engineering , Ecole Polytechnique Fèdèrale de Lausanne, Route Cantonale, CH-1015 Lausanne (francesco.comola@epfl.ch)*
[2] *Laboratory of Ecohydrology, School of Architecture, Civil and Environmental Engineering , Ecole Polytechnique Fèdèrale de Lausanne, Route Cantonale, CH-1015 Lausanne*
[3] *Dipartimento di Ingegneria Civile, Edile e Ambientale Università di Padova, via Loredan 20, I-35131 Padovay*
[4] *WSL Institute for Snow and Avalanche Research SLF, Flüelastrasse 11, CH-7260, Davos Dorf*

We present a travel time formulation of water and energy transport at sub-catchment scale. The derived equations are implemented in Alpine3D, a physically-based model of snow processes, which provides the necessary boundary conditions to perform hydro-thermal response simulations of Alpine catchments. The model set-up accounts for advective and non-advective energy fluxes to perform spatially distributed simulations of streamflow and temperature in river networks having an arbitrary degree of geomorphological complexity. The model gives reliable predictions of streamflow and temperature, as shown by comparing modeled and measured hydrographs and thermographs at the outlet of the Dischma catchment (45 km^2) in the Swiss Alps. Our model setup is applied to investigate the role of hillslope aspects, representing the main control on radiation and snowmelt patterns, in the flow regime of the study catchment. The distributed simulation results show that snowmelt-induced discharge exhibits a visible geomorphologic signature of aspects at sub-catchment scale, but this progressively fades out going from headwater streams to the outlet. Accordingly, the geomorphologic signature is scale-dependent: it is significant at small scales where the high aspect correlation generates predominant orientations but is lost at larger scales where aspects are de-correlated and different orientations are averaged out. We further apply the model to investigate the geomorphologic signature of drainage density in the thermal regime of the study catchment. The results show that the contribution of the advective energy fluxes becomes progressively smaller when the drainage density increases, while the one of the non-advective energy fluxes becomes larger. Moreover, such variations balance out at the catchment outlet, where the temperature signal is not sensitive to the increasing drainage density. The relevance of the performed invetigations stems from the increasing scientific interest concerning the impacts of the warming climate on water resources management and temperature-influenced ecological processes.

11.8

The impact of Saharan dust events on long-term glacier mass balance in the Alps

Jeannette Gabbi[1], Matthias Huss[1], Andreas Bauder[1] & Margit Schwikowski[2]

[1] *Laboratory of Hydraulics, Hydrology and Glaciology (VAW), ETH Zurich, Wolfgang-Pauli-Strasse 27, CH-8093 Zurich (gabbij@vaw.baug.ethz.ch)*
[2] *Paul Scherrer Institute (PSI), CH-5232 Villigen PSI*

Saharan dust falls are frequently observed in the Alpine region and are easily recognized by the unique yellowish coloration of the snow surface. Such Saharan dust events contribute to a large part to the total mineral dust deposited in snow and impact the surface energy budget by reducing the snow and ice albedo. In this study we investigate the long-term effect of such Saharan dust events on the surface albedo and the glacier's mass balance.

The analysis is performed over the period 1914-2013 for two field sites on Claridenfirn, Swiss Alps, where an outstanding 100-year record of seasonal mass balance measurements is available. Based on the detailed knowledge about the mass balance, annual melt and accumulation rates are derived. A firn/ice core drilled at the glacier saddle of Colle Gnifetti (Swiss Alps) provides information on the impurity concentration in precipitation over the last century.

A mass balance model combined with a parameterization for snow and ice albedo based on the specific surface area of snow and the snow impurity concentration is employed to assess the dust-albedo feedback. In order to track the position and thickness of snow layers a snow density model is implemented. Atmospheric dust enters the system of snow layers by precipitation and remains in the corresponding layer as long as there is no melt. When melt occurs, the water-insoluble part of the dust of the melted snow is supposed to accumulate in the top surface layer.

The upper site has experienced only positive net mass balance and dust layers are continuously buried so that the impact of strong Saharan dust events is mainly restricted to the corresponding year. In the case of the lower site, the surface albedo is more strongly influenced by dust events of previous years due to periods with negative mass balances. Model results suggest that the enhanced melting in the 1940s yield even higher dust concentrations in 1947 compared to years with exceptional high Saharan dust deposition due to the accumulation of dust at the surface as the corresponding site migrates from accumulation to ablation area.

11.9

Ten new long-term glaciological mass balance series for Swiss glaciers

Matthias Huss[1,2], Laurie Dhulst[1] & Andreas Bauder[1]

[1] *Laboratory of Hydraulics, Hydrology and Glaciology (VAW), ETH Zurich, Wolfgang-Pauli-Strasse 27, CH-8093 Zurich, Switzerland*
[2] *Department of Geosciences, University of Fribourg, Chemin du Musée 4, CH-1700 Fribourg, Switzerland*

Mountain glaciers are highly sensitive to changes in climate forcing and their surface mass balance is a valuable indicator of climate change. Globally coordinated monitoring efforts have contributed to a comprehensive set of time series documenting variations in glacier-wide mass balance for about a hundred glaciers. However, only few time series are longer than twenty years and even less start before the 1980s (Zemp et al., 2009). Glaciers in the European Alps are most densely covered with mass balance records. However, given the strong differences in the response of individual glaciers as well as the partly poor representativeness of some series for their respective region, even in the Alps more direct information on mass balance variability is required. Furthermore, only a small fraction of the records yields seasonal mass budget components which are of eminent importance for understanding glacier response to shifts in climatic forcing throughout the 20th century.

In this study, we present ten new long-term series of glacier-wide seasonal mass balance for glaciers in the Swiss Alps mostly starting in the 1950s and continued until today. Additionally, our data set includes several shorter series partly reaching back to the 1920s. Previously unpublished or unevaluated measurements of winter and summer balance form the base of these records. Data was compiled from old archives and from various sources. Most of the in-situ measurements were not intended as full monitoring programs which might explain that these highly valuable data sets were not consistently evaluated so far and were thus unavailable to the scientific community.

Using a new technique employing modelling for spatial extrapolation and homogenization of the seasonal point measurements we infer continuous series of area-averaged mass balance (Huss et al., 2009). The results are validated against independent decadal ice volume changes from photogrammetric surveys (Bauder et al., 2007). Five of the new seasonal mass balance series cover more than 50 years and add a substantial amount of information on the dynamics of regional glacier mass change (Fig. 1). This will strengthen the worldwide data collection on glacier monitoring, especially during the data-sparse period before the 1980s. We compare our results to existing long-term series and present an updated assessment of mass balance variability and sensitivity throughout the European Alps in connection with external drivers.

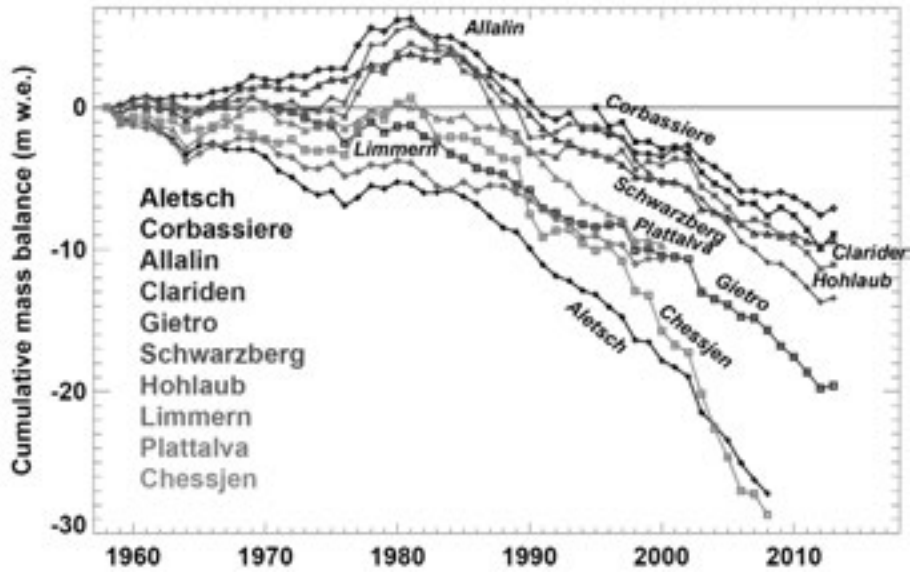

Figure 1. Cumulative glaciological mass balance series for ten Swiss glaciers since 1958.

REFERENCES

Bauder, A., Funk, M., & Huss, M. 2007: Ice-volume changes of selected glaciers in the Swiss Alps since the end of the 19th century, Annals of Glaciology, 46(1), 145-149.

Huss, M., Bauder, A., & Funk, M. 2009: Homogenization of long-term mass-balance time series, Annals of Glaciology, 50(50), 198-206.

Zemp, M., Hoelzle, M., & Haeberli, W. 2009: Six decades of glacier mass-balance observations: a review of the worldwide monitoring network, Annals of Glaciology, 50(50), 101-111.

11.10

Deriving long-term firn stratigraphy from optical borehole camera measurements on Austfonna, Svalbard

Lisbeth Langhammer[1,2] Thorben Dunse[1], Kirsty Langley[1], Elisabeth Isaksson[3] & Jon Ove Hagen[1]

[1] *Department of Geosciences, University of Oslo, Sem Sælands vei 1, NO-0371 Oslo*
[2] *Institute of Geophysics, ETH Zürich, Sonneggstrasse 5, CH - 8092 Zürich (lisbeth.langhammer@erdw.ethz.ch)*
[3] *Norwegian Polar Institue, Fram Cente, NO-9269 Tromsø*

The density of snow and firn is crucial for estimating the mass balance of ice masses by GPR, as well as airborne and spaceborne radar altimeter systems. To determine internal reflection horizons in the firn, independent ground-truth observations are required.

We present a borehole video camera system that provides a proxy of the firn structure in wet-snow zone conditions. A Junior Ultra Low Light borehole video camera and four shallow firn cores were used to investigate the firn stratigraphy close to the Summit camp on the Austfonna Ice Cap, Svalbard. Four videos from residual firn core boreholes and one ice auger borehole are analyzed to simulate an intensity-derived firn stratigraphy record.The firn cores themselves provided ground truth data. The camera lens measures the intensity of light, which is emitted from LEDs and reflected from the borehole wall. To extract a continuous intensity record from the video a Borehole camera video analysis tool was developed. Averaged grayscale values from a predefined section of the borehole wall or an attached mirror underneath the lens were correlated to the position of the camera in the borehole. Depending on a unique threshold value for each video log, the intensity signal was classified as firn or ice sections and compared to the firn cores from the same location. High to moderate agreement (91-63%) between the ground truth data and the intensity-derived stratigraphy is achieved. Two out of four intensity records show approximately the same amount of ice as was present in the corresponding firn core. In general, thin ice layers are underrepresented, whereas thicker ice agglomerations are more likely to be detected with the borehole camera. The quality of the intensity records is highly influenced by the technical set-up and operation of the camera system in cold climate environments. Further improvement of the set-up is recommended to achieve the same quality as ground truth firn core records.

The described borehole camera system is a logistically inexpensive tool to observe the stratigraphy of firn in regions with substantial refreezing of meltwater below the surface. Ice structure, firn stratigraphy and densification surveys as well as in situ or spaceborne remote sensing measurements of the mass balance benefit from the implementation of the borehole camera system in the field.

11.11

Mixed-mode shear-compression failure criterion for weak snowpack layers

Ingrid Reiweger, Johan Gaume, Jürg Schweizer

WSL Institute for Snow and Avalanche Research SLF, Flüelastrasse 11, CH-7260 Davos Dorf (reiweger@slf.ch)

Snow slab avalanches begin with a failure in a weak snow layer beneath a cohesive slab followed by crack propagation within the weak layer. The nature of the initial failure within the weak layer is unknown – but debated. Different avalanche release models assume contradictory failure criteria as input parameters. We analysed laboratory experiments on snow failure with samples containing a weak snow layer of either depth hoar or buried surface hoar. These layers are the most relevant ones for avalanche release. The failure behavior of these layers – the most relevant for avalanche release – can well be described with a modified Mohr-Coulomb model. Therefore, we propose a mixed-mode failure criterion to be used in avalanche release models.

11.12

Variability of snow thickness changes in steep rock faces based on terrestrial laser scanning

Christian Sommer[1,2], Rebecca Mott[1], Michael Lehning[1] & Sophia Haussener[2]

[1] *WSL-Institut für Schnee- und Lawinenforschung SLF, Flüelastrasse 11, CH-7260 Davos Dorf (sommer@slf.ch)*
[2] *Section de génie mécanique, EPFL, CH-1015 Lausane*

During this Master's thesis, Terrestrial Laser Scanning (TLS) was used to measure snow thickness changes (perpendicular to the surface) in rock faces. The goal was to identify which processes and parameters are important for the variability of snow accumulation and ablation. The knowledge of the spatial variability of the snow cover is important for hydrology, ecology, climatology and avalanche forecasting. Two different rock faces in the region of Davos in eastern Switzerland were scanned before and after snowfall events, each with a different laser scanner. An elaborate postprocessing procedure was necessary to produce useful results. The snow thickness changes were analysed qualitatively and quantitatively using simple statistics and linear correlation coefficients. Furthermore, the applicability and precision of TLS was studied.

It was concluded that given an appropriate postprocessing, TLS is a viable experimental method. Most important is a precise registration, which usually necessitates Multi Station Adjustment (MSA). The snow thickness changes could then be measured with a precision of several centimetres.

It could be shown that snow is mostly deposited in the flatter and smoother areas of a rock face. Very steep terrain (up to 70°) could however still accumulate and retain a considerable amount of snow. Extremely steep (up to 85°) and rough areas can only temporarily hold a small amount of snow. Wind and avalanches appear to be the dominant processes responsible for the snow distribution. For snowfall events with only weak wind, the snow thickness changes correlate with topographic parameters such as slope angle and roughness, but the correlation is always quite weak.

REFERENCES

Deems, J., Painter, T. & Finnegan, D. 2013: Lidar measurement of snow depth: a review. Journal of Glaciology 59.215, 467–479.

Wirz, V., Schirmer, M., Gruber, S. & Lehning, M. 2011: Spatio-temporal measurements and analysis of snow depth in a rock face. The Cryosphere 5.4, 893–905.

11.13

Sensitivity of operational snow melt predictions to different modelling setups

Mirjam Stawicki[1], Jan Magnusson [2] & Tobias Jonas [2]

[1] *Geographisches Institut, University of Bern, Hallerstrasse 12, CH-3012 Bern (mirjam.stawicki@unibe.ch)*
[2] *WSL-Institute for Snow and Avalanche Research SLF, Flüelastrasse 11, CH-7260 Davos Dorf*

In Switzerland, snow is an essential component of the hydrological cycle. About one third of the total annual precipitation falls as snow and it is estimated that as much as 42% of the total runoff origins from snowmelt.

The operational snow hydrological service (OSHD) run by the WSL-Institute for snow and avalanche research SLF monitors the spatio-temporal distribution of snow water resources in Switzerland. The OSHD provides periodic snowmelt forecasts which contribute to the Swiss federal warning framework for natural hazards. These forecasts are based on snow model simulations that incorporate observational data from several monitoring networks using advanced data assimilation techniques.

In this study the current OSHD snow model framework was evaluated for 132 strong snow melt events that occurred over the last 15 years. A special model testbed allowed assessing the impact of data assimilation and the sensitivity to different model input scenarios. We demonstrate that assimilation of snow monitoring data affects snowmelt predictions in two different ways. Moreover we highlight systematic discrepancies between model results when driven by observational data versus data from the numerical weather prediction system COSMO.

11.14

Fast ice flow, troughs, overdeepenings and subglacial hydrology

Mauro A Werder[1]

[1] *Geographisches Institute, Universität Zürich*

This presentation explores the role of subglacial hydrology in fast flowing topographically constrained outlet glaciers. Subglacial water flow is strongly influenced by the bed topography through the dependence of the melting point of ice on pressure. Thi means that water descending into a trough or an overdeepening has more energy available to melt channels and conversely water ascending out has less or even no energy available for melt. The latter process leads to a reduced drainage capacity and, consequently, to increased water pressures.

Therefore these processes lead to increased water pressures in subglacial troughs, in particular with overdeepened sections. I will discuss the implications for the formation of troughs and overdeepenings.

P 11.1

Ice flow in the Alps during the last glacial maximum, a modeling approach

Patrick Becker

Versuchsanstalt für Wasserbau, Hydrologie und Glaziologie, ETH Zürich, Wolfgang-Pauli-Str. 27, CH-8093 Zürich (becker@vaw.baug.ethz.ch)

About 30,000 years before present at the end of the Würm Ice Age, glaciers reached the maximum extent and most of the Alpine mountain environment and wide parts of the Alpine forelands were covered by ice. The impact of the last glacial maximum (LGM) to the surrounding environment offers a good opportunity to study the predominating extent of glaciation as well as the predominating climate in an indirectly manner.

Latest studies by the group of C. Schlüchter assembled evidences found in the field to reconstruct a map of the glacier extent at LGM. The map shows the situation at the Rhone valley: Ice was flowing from the main accumulation area, the Rhone ice dome, situated close to todays location of the Rhone glacier, through the Rhone valley towards the Lake Geneva. Behind the lake the ice diffluenced by the barrier of the Jura to northeast and southwest. Furthermore the study discussed erratic boulders that have been found in the Alpine foreland which origin was assigned to the Saas valley, Upper Valais. This long transport trajectory indicate the extent of the glacier. It is not completely clear if they were transported within one Ice Age (single glacier advance) all the long way down to the forelands or whether they were transported by multiple glacier advances.

Further uncertainties are caused by evidences found at the Simplonpass area. E. g. striations have been identified at the Staldhorn indicating an ice flow from north to south. This would indicate a transfluence of ice of the Rhone glacier out of the Rhone valley over the Simplonpass into the drainage system of the Po river.

The reason for this transfluence is still not well understood. At the time of LGM one can assume a feed of the glaciation in the Rhone valley by the inflow of glaciers originating at the Matter valley, Saas valley and the Aletsch region. One reason for the transfluence could be caused by the glacier outflow coming from the Visp valley (drained by ice masses from Matter and Saas valley):

One can hypothesize a barrier of the Rhone valley built by ice masses coming from the Visp valley. Hence, the ice of Rhone glacier could have been dammed and forced to south over the Simplonpass.

The problem will be studied with the aid of a numerical simulation. The flow of glaciers is governed by the Stokes Equations. Numerically solving them is computationally expensive for large glaciers. For this reason we use the Parallel Ice Sheet Model (PISM), a free software implementation of a hybrid scheme that combines the Shallow Ice Approximation (SIA) and the Shallow Shelf Approximation (SSA). PISM uses the SSA as a „sliding law“ for grounded ice which is already modeled everywhere by the non-sliding SIA.

In a first step the retreat of Grosser Aletschgletscher in the last 100 years will be studied. During this period the glacier surface topography as well as the climate forcing that is given by the mass balance is well-known. Results will be validated against observations from measurements.

Further large scale computations or the Upper Valais at the time of the LGM will be carried out to get insights into the glacier drainage system. Simulating the Upper Valais area should clarify the question of a possible North-South-Transfluence over the Simplonpass into the Piedmont region, Italy.

P 11.2

Multitemporal scale surface changes of small glacier systems in permafrost environments

Maxime Capt[1], Jean-Baptiste Bosson[1], Natan Micheletti[1] & Christophe Lambiel[1]

[1] *Institut des dynamiques de la surface terrestre (IDYST), Université de Lausanne, Bâtiment Géopolis UNIL Mouline, CH-1015 Lausanne (maxime.capt@unil.ch)*

Since the end of the Little Ice Age, glaciers have experienced intense mass loss in response to global change. In the Alps, this shrinking has not been uniform over the twenty-first century: some periods have been favorable to glaciers stabilization, or even their advance. Moreover, the burying of some glaciers under a several centimeters thick debris cover significantly reduces the ice melt and stabilize the glacier front. The research on debris-covered glaciers has increased in last decades but numerous questions remain open, especially in permafrost environments where clean ice, debris-covered ice, frozen and unfrozen sediments accumulations may complexly coexist.

This study examines the dynamics of two small glaciers in the permafrost environments of western Switzerland: Tsarmine (Arolla, Valais) and Entre la Reille (Diablerets, Vaud). These small glacier systems (<0.5 km^2) are characterized by extended debris-covered ice, huge moraine constructions and marginal rock glacier morphology. Through the manipulation of DTMs and orthophotos, this study highlights the spatial differences in the surface dynamics within these systems, at several time scales (decadal, annual and seasonal).

The displacement vectors as well as the loss/gain volumes maps show that there is a relationship with climate in these areas, and that the dynamics change significantly between the different zones in relation to their specificities (ice composition, nature of the ice, debris cover extension and thickness). At Tsarmine for example, the debris-covered glacier surface motion can exceed 3m/year while the values are lower than 60cm/year on the marginal rock glacier. At seasonnal scale, LiDAR (light detection and ranging) scans comparison point out the importance of hydrological forcing (especially related to snow and ice melt) on surface dynamics : the ice melt and the surface motion are accelerated.

REFERENCES

Goudie, A.S. (2004). Encyclopedia of geomorphology – Volume 2. Londres: Goudie, A.S.

Otto et al. (2009). Quantifying sediment storage in a high alpine valley (Turtmanntal, Switzerland). Earth surface processes and landforms, 34, 1726-1742.

Vaughan et al. (2013). 5th Assessment Report of the IPCC. Cambridge University Press: 317-382.

P 11.3

Use of a new long-range terrestrial LiDAR system to monitor the mass balance of very small glaciers

Fischer Mauro[1], Huss Matthias[1,2] & Martin Hoelzle[1]

[1] *Department of Geosciences, University of Fribourg, Chemin du Musée 4, CH-1700 Fribourg, Switzerland (mauro.fischer@unifr.ch)*
[2] *Laboratory of Hydraulics, Hydrology and Glaciology (VAW), ETH Zurich, CH-8093 Zurich, Switzerland*

More than 80% of all Swiss glaciers are smaller than 0.5 km^2 and hence belong to the size class of very small glaciers (Fischer et al. 2014a), occuring mostly in cirques, niches and below headwalls where topoclimatical factors and snow accumulation patterns are favourable for the persistence of snow and ice. Very small glaciers have, however, hardly been studied and empirical field measurements are sparse.

Since 2012, both seasonal and annual mass balance of seven very small glaciers in Switzerland is measured using the glaciological method (snow soundings and density measurements at the end of the accumulation season, measuring melt at ablation stakes at the end of the ablation period). Monitoring glacier mass balance is important as it directly reflects the climatic forcing on the glacier. Mass balance can also be reconstructed by means of the geodetic method, which is based on the comparison of two different Digital Elevation Models (DEMs) (e.g. Fischer et al. 2014b). So far, the accuracy of such DEMs mostly derived from airborne or terrestrial laserscanning, photogrammetry or topographic maps limited the time resolution of reliable mass balance measurements resulting from the geodetic method to a multi-annual or decadal scale (Cox and March 2004, Huss et al. 2009). Most recently, the creation of highly accurate DEMs of snowy and icy terrain using a new generation of long-range terrestrial LiDAR (Light Detection And Ranging) devices became possible. This is highly promising for future accurate determination of annual and even seasonal mass balance of small Alpine glaciers (e.g. Grünewald et al. 2010). It may have the potential to circumvent laborious and time consuming glaciological mass balance measurements. Furthermore and because ice flow is reduced for very small glaciers, it may help to improve our understanding of the spatial and temporal component of accumulation and melt processes on Alpine glaciers.

Here we present first results of the comparison of seasonal and annual ice volume changes determined with the new *Riegl* VZ®-6000 long-range LiDAR device with in-situ glaciological seasonal and annual mass balance surveys performed on five very small glaciers in Switzerland (Glacier de Prapio (VD), Glacier du Sex Rouge (VD), St. Anna- and Schwarzbachfirn (UR), and Pizolgletscher (SG)) over the hydrological year 2013/14.

REFERENCES

Cox, L. H., & March, R. S. 2004: Comparison of geodetic and glaciological mass-balance techniques, Gulkana Glacier, Alaska, U.S.A. Journal of Glaciology, 50, 363-370.

Fischer, M., Huss, M., Barboux, C., & Hoelzle, M. 2014a: The new Swiss Glacier Inventory SGI2010: Relevance of using high-resolution source data in areas dominated by very small glaciers. Arctic, Antarctic, and Alpine Research, in press.

Fischer, M., Huss, M., & Hoelzle, M. 2014b: Surface elevation and mass changes of all Swiss glaciers 1980-2010. The Cryosphere Discussions, 8, 4581–4617.

Grünewald, T., Schirmer, M., Mott, R., & Lehning, M. 2010: Spatial and temporal variability of snow depth and ablation rates in a small mountain catchment. The Cryosphere, 4, 215-225.

Huss, M., Bauder, A., & Funk, M. 2009. Homogenization of long-term mass-balance time series. Annals of Glaciology, 50, 198-206.

P 11.4

INITIATION OF MASS BALANCE MONITORING AT GLACIAR SUYUPARINA, CORDILLERA VILCANOTA, PERU

Edwin Molina[1], Felipe Sikos[1], Maxwell Rados[1], Nicacio Chaparro[1], Jaime Samata[1], Nilton Montoya[1], Luís Jiménes[1], Gilbert Gonzales[2], Lucas Torres[2], Jesús Gómes[2], Rolando Cruz[2], Claudia Giraldez[3], Fabian Drenkhan[3], Wilfried Haeberli[3], Christian Huggel[3], Simone Schauwecker[3]

[1] *Universidad Nacional de San Antonia Abad del Cusco, Vicerectorado de Investigción, Facultad de Ingeniería Geológica y Geografía, Departemento Académico de Geografía (emporcel@hotmail.com)*
[2] *Unidad de Glaciologia y Recursos Hidricos, Autoridad Nacional del Agua, Huaraz, Perú*
[3] *Geography Department, University of Zurich, Zurich, Switzerland*

The Cordillera Vilcanota is at the origin of the Rio Vilcanota-Urubamba, containing about 25% of all glaciers in Peru and constuting an important national and regional water resource. In recent decades, glacier shrinkage appears to have been accelerating. Between1988 and 2010, glacier area was reduced at an annual rate of about 4 km^2 from some 360 km^2 to some 270 km^2 (-25%; Hanshaw and Bookhagen 2014) and a total volume loss of 40-45% (from 17-20 km^3 to 9.2-12.4 km^3) can be estimated for the time period 1962-2006 (Salzmann et al. 2013); most of this volume loss seems to have opccurred since the 1980s. Glacier mass balance values had so far not been available but are now initiated at Glaciar Suyuparina with a 3-year program. On a long term, the observations should become part of the national and international glacier monitoring network (cf. WGMS 2013). The project is also part of a major effort – through a combination of projects – to develop hydrological models for the mountain chain in view of policy-oriented climate impact assessments at local to regional scales.

Glaciar Suyuparina is a rather steep south-west oriented mountain glacier (Figure 1) some 15 km north of the Quelccaya Ice Cap, with a surface area of a few km^2 and reaching from a maximum altitude of 5469 m asl down to about 5150 m asl. With an elevation range of some 300 m and a mid-range elevation at 5300 m, the equilibrium line altitude (ELA) with a characteristic accumulation area ratio for zero mass balance on tropical glaciers of about 80% is expected to be near 5200 m asl. Glacier-wide mass balance is determined using the direct glaciological method (stakes and pits) for process understanding and high resolution in time combined with DEM differencing for overall volume/mass changes and calibration of the mesurements. A first high-resolution DEM from airborne LIDAR measurements is available for May 2013. The first year of field observations indicates large local variability of ablation values due to a pronounced microtopography with near-vertical ice cliffs oriented towards the sun and probably having a predominant effect on total ablation (Figure 1). As expected, ablation gradients are extreme (1 – 2 m per year and 100m elevation).

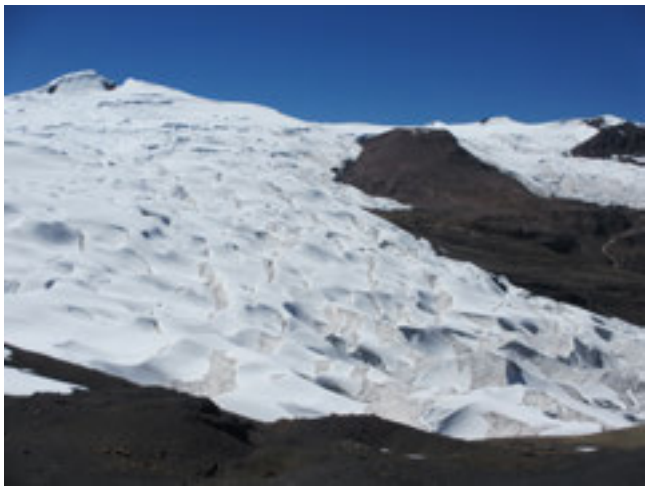

Figure 1. Glaciar Suyuparina in the Cordillera Vilcanota. Note the marked microtopography and its effects on ablation patterns. Photograph W. Haeberli July 2014.

REFERENCES

Hanshaw, M.N. & Bookhagen, B. 2014: Glacial areas, lake areas, and snow lines from 1975 to 2012: status of the Cordillera Vilcanota, including the Quelccaya Ice Cap, northern central Andes, Peru. The Cryosphere 8, 359-376.

Salzmann, N., Huggel, C., Rohrer, M., Silverio, W., Mark, B.G., Burns, P.& Portocarrero, C. 2013: Glacier changes and climate trends derived from multiple sources in the data scarce Cordillera Vilcanota region, southern Peruvian Andes. The Cryosphere 7, 102-118. The Cryosphere, 7, 103–118,

WGMS 2013: Glacier Mass Balance Bulletin No. 12 (2010-2011). Zemp, M., Nussbaumer, S.U., Naegeli, K., Gärtner-Roer, I., Paul, F., Hoelzle, M. and Haeberli, W. (eds.), ICSU (WDS) / IUGG (IACS) / UNEP / UNESCO / WMO, World Glacier Monitoring Service, Zurich, Switzerland: 106 pp., publication based on database version: doi: 10.5904/wgms-fog-2013-11.

P 11.5

AN INVENTORY OF POSSIBLE FUTURE LAKES IN THE CORDILLERA BLANCA, PERU

Daniel Colonia[1], Wilfried Haeberli[2], Judith Torres[1], Simone Schauwecker[2], Alejo Cochachin[1], Arnaldo Tacsi[1] & Alexzander Santiago[1]

[1] *Unidad de Glaciologia y Recursos Hidricos (UGRH), Autoridad Nacional del Agua (ANA), Huaraz, Perú (dcolonia@ana.gob.pe; dfco18@hotmail.com)*
[2] *Geography Department, University of Zurich, Zurich, Switzerland*

Climate change causes dramatic mass losses of glaciers in the Cordillera Blanca. Between the 1970 and 2003 inventories, 27% of the glacier area disappeared (UGRH 2010) and until 2003, a total of 830 new lakes had formed in deglaciating terrain. The identification of possible future lakes is important to understand changes in freshwater storage in the corresponding source areas and to plan for preventive measures concerning possible lake outbursts. A major number of catastrophic events had indeed happened in the Cordillera Blanca (cf. Carey et al. 2012) such as, for instance, the disastrous „aluvión" from the outburst of Laguna Palcacocha on 13 December 1941, destroying the centre of Huaraz and killing several thousand people. As most of the new lakes form in immediate neigbourhood of steep hanging glaciers and high-altitude permafrost rock walls, the probability of severe floods/debris flows from impact waves caused by large rock/ice-avalanches or large moraine landslides is increasing with continued atmospheric warming and ice vanishing (Haeberli et al. 2010). In the catchments of the Rios Santa, Marañón and Pativilca future new lakes constitute a potential hazard to humans and infrastructures.

Modeling of glacier-bed overdeepenings and possible future lakes forming in such topographic glacier-bed depressions when becoming ice-free was done using the SRTM DEM from the year 2000 with a 90 m resolution and the 2003 glacier outlines from the glacier inventory of the Cordillera Blanca (UGRH 2010). The GIS-based analysis followed three main steps: (1) identification of flat glacier areas with less than 10° surface slope as a first-order spatial approximation to possible occurrences of glacier-bed overdeepenings; (2) application using Google Earth of three morphological indications of glacier-bed overdeepenings following Frey et al. (2010): steepening surface slope, onset of crevasse formation, lateral flow-narrowing; and (3) verification of the results from steps (1) and (2) by comparison with GlabTop modeling of bed topographies (Linsbauer et al. 2012) using the SRTM DEM, contour lines and constructed branch lines for all glaciers of the Cordillear Blanca.

The results show that 31 major new lakes may form in the future with 23 being expected in the catchment of the Rio Santa, 7 in the one of Rio Marañón and 1 in the one of Rio Pativilca. Some of the lakes indeed already started to develop (Figure 1). The total volume of the major potential new lakes is estimated at some 60-65 million m^3. This corresponds to about half a percent of the total glacier volume remaining in the year 2003 and estimated at 15.69 km^3. This relatively small percentage is due to the fact that most flat glacier parts where bed-overdeepenings can be expected have already disappeared.

The procedure applied as a pilot study for the Cordillera Blanca will be used for the other Cordilleras of Peru in order to provide a knowledge and planning basis to the responsible governmental authorities in view of freshwater resources, hazard prevention, energy production and landscape diversity.

REFERENCES

Carey, M., Huggel, C., Bury, J., Portocarrero, C. & Haeberli, W. 2012: An integrated socio-environmental framework for glacier hazard management and climate change adaptation: lessons from Lake 513, Cordillera Blanca, Peru. Climatic Change112, 3, 733-767.

Frey, H., Haeberli, W., Linsbauer, A., Huggel, C. & Paul, F. 2010: A multi level strategy for anticipating future glacier lake formation and associated hazard potentials. Natural Hazards and Earth System Science 10, 339-352.

Haeberli, W., Clague, J.J., Huggel, C. & Kääb, A. 2010: Hazards from lakes in high-mountain glacier and permafrost regions: Climate change effects and process interactions. Avances de la Geomorphología en España, 2008-2010, XI Reunión Nacional de Geomorphología, Solsona, 439-446.

Linsbauer, A., Paul, F. & Haeberli, W. 2012: Modeling glacier thickness distribution and bed topography over entire mountain ranges with GlabTop: Application of a fast and robust approach. Journal of Geophysical Research 117, F03007, doi:10.1029/2011JF002313

UGRH 2010: Inventario de Glaciares Cordillera Blanca, Lima, Perú, Autoridad Nacional del Agua. 120 p.

Figure 1. The flat tongue of Glaciar Artesonraju in the Cordillera Blanca, where a new lake with a considerable volume is likely to form during the coming decades. First stages of lake formation can already be observed at the ice margin. Photograph: D. Colonia, July 2014

P 11.6

Long-term energy balance measurements at three different mountain permafrost sites in the Swiss Alps

Martin Hoelzle[1] & Christian Hauck

[1] *Department of Geosciences, University of Fribourg, Chemin du musée 4, CH-1700 Fribourg (martin.hoelzle@unifr.ch)*

In the framework of the PERMOS permafrost monitoring program, meteorological data is collected at several high altitude sites in the Swiss Alps since the late 1990s. From these stations, three were selected, which are equipped with standard meteorological sensors such as a four component radiation sensor, air temperature, humidity, wind speed and direction as well as ground temperatures and snow height (Hoelzle and Gruber 2008). The energy balance constitutes one of the most important input parameter for the ground heat flux regime, and it is therefore crucial to understand the influence of the individual fluxes. As the individual measurements and the different approaches to calculate the energy balance show large uncertainties, a special focus is laid on the quantification of the uncertainty range of each flux.

All three selected sites differ considerably by their ground material composition. The Murtèl-Corvatsch site (Engadine, Eastern Swiss Alps) is situated on a rock glacier consisting mainly on coarse blocky debris in the active layer followed by an ice supersaturated layer of around 25 m thickness. The Schilthorn site is located at the Northern slope of a mountain summit in the Bernese Alps and is composed by deeply weathered micaceous shales, which are covered by fine grained debris of sandy and silty material. Finally, the Stockhorn site (Southern Valais Alps close to Zermatt) is located on a small plateau slightly inclined to the south and the bedrock consists of Albit-Muskovit schists. It shows at some places the development of patterned ground, especially where the station is located. Based on geophysical soundings the ice content at the Schilthorn and at the Stockhorn plateau sites are estimated to be much less compared to the Murtèl-Corvatsch site.

First results show that the mean surface temperature at Murtèl-Corvatsch (1997-2013) and Schilthorn (1999-2013) are quite similar with -3.23°C and -3.56°C, respectively, whereas at Stockhorn (2002-2013) the surface temperatures are colder with a mean of -8.98°C. The corresponding mean ground temperatures for the same investigation period measured in the PERMOS boreholes are for Murtèl-Corvatsch (0.55 m depth) -0.24°C, Schilthorn (0.2 m depth) -0.07°C and Stockhorn (0.3 m depth) -0.42°C. The measured net radiation is the most important energy input for the surface at each site and shows for Murtèl-Corvatsch 27.31 W m^{-2}, Schilthorn 32.52 W m^{-2} and Stockhorn 22.91 W m^{-2}. The calculated turbulent fluxes based on measurements of wind speed, air temperature and relative humidity using two different approaches (bowen ratio and bulk methods) shows for all sites values of around 8 to 10 W m^{-2} for the Bowen ratio method and 4 to 15 W m^{-2} for the bulk method. Large differences are observed in the energy, which is used for melting the snow cover at the different sites. At Schilthorn a value of 22.86 W m^{-2}, at Murtèl-Corvatsch 11.26 W m^{-2} and at Stockhorn 6.06 W m^{-2} is measured reflecting the different amount of snow depth at these sites. The overall deviation of the energy balance amounts to 10.58 W m^{-2} at Murtèl-Corvatsch, 5.57 W m^{-2} at Schilthorn and 0.06 W m^{-2} at Stockhorn, reflecting also that especially at the Murtèl-Corvatsch site not all fluxes are detected, which confirms recent results by Scherler et al. (2014).

The high temporal variability of the individual fluxes and the additional large uncertainties in the determination of the turbulent heat fluxes (mainly caused by the lack of accurate input conditions of soil moisture contents at the surface as well as reasonable values for the surface roughness) does currently not allow a more precise determination of the whole energy balance in this high alpine terrain. However, the long-term measurement series of the individual fluxes at these sites are a unique prerequisite for detailed modelling studies using these data as validation or as calibration measures.

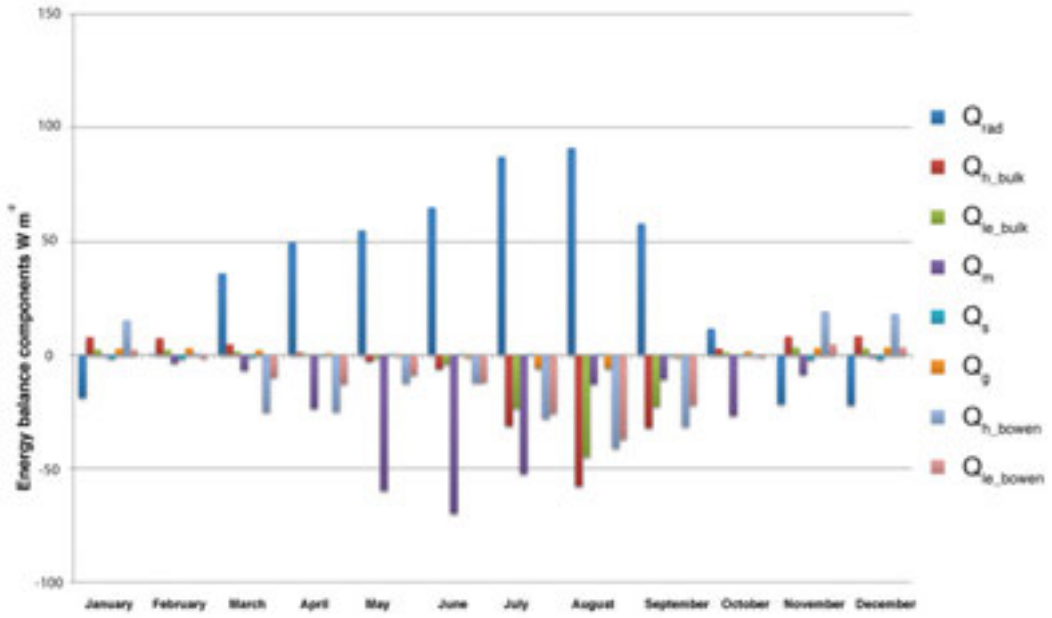

Figure 1. Mean of all energy balance components calculated for the Schilthorn site for the period 1999-2013.

REFERENCES

Scherler, M, Schneider, S., Hoelzle, M. and Hauck, C. 2013: A two-sided approach to estimate heat transfer processes within the active layer of rock glacier Murtèl-Corvatsch. Earth Surface Dynamics Discussion, 1, 141-175.

Hoelzle, M. and Gruber, S. 2008: Borehole and ground surface temperatures and their relationship to meteorological conditions in the Swiss Alps. Ninth International Conference on Permafrost, Fairbanks, Alaska, 1, 723-728.

P 11.7

Swiss glaciers: TanDEM-X time series vs. SwissAlti3D

Silvan Leinss[1], Irena Hajnsek[1,2]

[1] *Institut für Umweltingenieurwissenschaften (IfU), ETH Zürich, Stefano-Franscini-Platz 3, 8093 Zürich (leinss@ifu.baug.ethz.ch)*
[2] *Microwaves and Radar Institute, German Aerospace Center (DLR), Germany*

High precision digital elevation models (DEMs), derived from air- and space-borne sensors have reached a vertical accuracy on the meter scale. The precision is pushing towards the scale, on which glaciers and even the seasonal snow cover changes during one year. Therefore, a comparison of digital elevation models allows to monitor volume changes of glaciers and snow cover. Due to the vertical precision and the fast changes of snow and glaciers, knowledge of the exact date of the acquisitions as well as the penetration depth in case of radar based methods is of high importance.

The SwissAlti3D is up to now the best available DEM for Switzerland and is updated every six years with airborne stereographic and lidar data of the past few years, if necessary. However, it is composed of very different data sources where the exact date of acquisition is not necessarily available and complicates therefore short-term comparisons.

The TanDEM-X satellite mission [Krieger 2007, Krieger 2010], build create a high precision globe-spanning DEM (the so called WorldDEM™), acquired all data within three years to provide a globally consistent digital elevation model. The DEM is based on singlepass SAR-Interferometry, which uses a radar frequency of 9.65 GHz. This frequency has been chosen, to provide a spatial resolution of a few meter and to avoid too much penetration into the underlying ground. However, the penetration into snow is a crucial parameter and can reach a couple of meters for very dry and cold snow [Davis, 1993]. However, it quickly changes as soon as the moisture content within the snow volume increases above a fraction of a percent [Abe, 1990] where the penetration depth is not more than few cm.

I will present a comparison of the SwissAlti3D with TanDEM-X acquisition from various glaciers of Switzerland (Aletsch-, Findelen-, Gorner-, Rhonegletscher). Further, I will show results from TanDEM-X time series, with an acquisition every 11 days. TanDEM-X time series of Aletsch- and Rhonegletscher have been calibrated by a large number of reference points to get a vertical resolution on the sub-meter scale.

The time series show annual oscillations due to snow accumulation and snow and ice melt. The comparison of data from different years shows an average volume/height loss of 3 - 4 meter per year.

A comparison of autumn with spring acquisitions allows to derive snow accumulation maps. Fresh snow accumulation of 3 - 5 meter per year have been determined.

The penetration depth can be estimated from sudden changes in the height but also from changes in the backscatter signal which indicates the transition from dry to wet snow. Penetration depths for dry snow of up to 7 meter have been found.

REFERENCES

G. Krieger, I. Hajnsek, K. Papathanassiou, M. Younis, and A. Moreira, "Interferometric synthetic aperture radar (SAR) missions employing formation flying," Proceedings of the IEEE, vol. 98, no. 5, pp. 816–843, 2010.

G. Krieger, H. Fiedler, M. Zink, I. Hajnsek, M. Younis, S. Huber, M. Bachmann, J. Hueso Gonzalez, M.Werner, and A. Moreira, "TanDEM-X: A satellite formation for high-resolution SAR interferometry," IEEE transactions on geoscience and remote sensing, vol. 45, no. 11, pp. 3317–3341, November 2007.

C. Davis and V. Poznyak, "The depth of penetration in antarctic firn at 10 GHz," IEEE Transactions on Geoscience and Remote Sensing, vol. 31, no. 5, pp.
1107 –1111, 1993.

T. Abe, Y. Yamaguchi, and M. Sengoku, "Experimental study of microwave transmission in snowpack," IEEE Transactions on Geoscience and Remote
Sensing, vol. 28, no. 5, pp. 915 –921, 1990.

P 11.8

Evaluation of automatic weather station data to observe the characteristics and changes in glacier surface albedo

Kathrin Naegeli[1], Matthias Huss[1] & Martin Hoelzle[1]

[1] *Department of Geosciences, University of Fribourg, Switzerland (kathrin.naegeli@unifr.ch)*

The albedo has a major impact on the energy balance of a glacier surface. It mainly influences the amount of absorbed/reflected radiation and is therefore a major controlling factor of surface melt especially during the ablation period. The glacier surface in the ablation area itself is not only consisting on pure ice surface but depends in a complicated way on many factors, such as cryoconite concentration, impurities due to mineral dust, soot or organic matter, amount of liquid water, grain size or ice surface morphology. Several studies have focused on temporal and spatial variations of albedo and its importance in calculating the energy balance of a glacier surface [e.g. Oerlemans and Klok, 2002; Jonsell et al., 2003; Brock, 2004] and more recently on cryoconite composition [e.g. Casey et al., 2012] and glacier surface mapping [e.g. Chandler et al., 2014]. However, still fairly little is known about the state, changes and impact of glacier surface albedo in the Swiss Alps, which is particularly critical since there are obvious changes in surface characteristics on most alpine glaciers over the last years.

To study the characteristics and changes of glacier surface albedo various measurements were conducted throughout the ablation seasons on Glacier de la Plaine Morte in 2013 and 2014. Adjacent to repeated portable albedo measurements along profiles, ice melt was intensively monitored using over 20 ablation stakes distributed along these profiles but also randomly places in dark and bright ice areas of the glacier. Additionally, cryoconite samples were collected to obtain more information about the composition of the surface materials. Moreover, an automatic weather station measuring air and ice temperatures, relative humidity, wind speed and direction, precipitation as well as the four radiation components was installed on the winter snow surface in the beginning of July and dismantled in late fall, measuring the climate variables at a temporal resolution of 10 minutes.

In the context of this ongoing work, we present first evaluations of these climate variable data with a special focus on the temporal evolution of glacier surface albedo, most prominently the snow-ice transition in beginning of August, but also the impact of snowfall events throughout the ablation season. Furthermore, the spatial variations of glacier surface albedo are analysed combining the repeated albedo point measurements with the spatially distributed ablation measurements and collected cryoconite samples.

REFERENCES

Brock, B.W. 2004: An analysis of short-term albedo variations at Haut Glacier d'Arolla, Switzerland. Geografiska Annaler, 86(1), 53–65.

Casey, K., Kääb, A. & Benn, D.I. 2012: Geochemical characterization of supraglacial debris via in situ and optical remote sensing methods: a case study in Khumbu Himalaya, Nepal. The Cryosphere, 6(1), 85–100.

Chandler, D.M., Alcock, J.D., Wadham, J.L., Mackie, S.L. & Telling, J. 2014: Seasonal changes of ice surface characteristics and productivity in the ablation zone of the Greenland Ice Sheet. The Cryosphere Discussion, 8(1), 1337–1382.

Jonsell, U., Hock, R. & Holmgren, B. 2003: Spatial and temporal variations in albedo on Storglaciären, Sweden. Journal of Glaciology, 49(164), 59–68.

Oerlemans, J. & Klok, E.J.L. 2002: Energy balance of a glacier surface: analysis of autmatic weather station data from the Morteratschgletscher, Switzerland. Arctic, Antarctic, and Alpine Research, 34(4), 477–485.

P 11.9

10 years of MB measurements on Findelengletscher, VS, Switzerland

Nadine Salzmann[1], Matthias Huss[1], Horst Machguth[2], Leo Sold[1], Andreas Linsbauer[1], Philip Jörg[3], Gwendolyn Leysinger-Vieli[3], Martin Hoelzle[1]

[1] *Department of Geosciences, University of Fribourg, Chemin de Musée 4, CH-1700 Fribourg (nadine.salzmann@unifr.ch)*
[2] *Department of Civil Engineering, Technical University of Denmark, Brovej 18, DK-2800*
[3] *Department of Geography, University of Zurich, Winterthurerstrasse 190, CH-8057 Zurich*

Mass balance observations on Findelengletscher were started in 2004 (Machguth et al. 2006). At that time, the main objective for the measurements was the generation of reference data for the validation and calibration of a mass balance model, rather than for the purpose of a long-term mass balance programme. In 2009, the Universities of Fribourg and Zurich decided to jointly start a long-term mass balance monitoring programme on Findelengletscher (and the nearby Adlergletscher), because of its ideal setting. Findelengletscher is relatively large (about 13km^2), easily accessible and has an almost debris-free surface. Since 2009, summer and winter mass balance was measured each year using state-of-the-art in-situ methods. In addition, high-resolution digital elevation models are available for the years 2005, 2009, 2010 and 2012.

Moreover, a number of other studies are ongoing related to glacier monitoring, such as an improved representation of winter snow accumulation distribution by means of helicopter-borne ground-penetrating radar and the remote determination of firn layer thickness (Sold et al. 2013, 2014). Furthermore, several subsurface monitoring projects are located In the vicinity of Findelengletscher, at the PERMOS site (PERmafrost MOnitoring Switzerland) at Stockhorn. The combined permafrost and glacier monitoring activities provide a great basis for integrated cryospheric analyses.

Here, we present a complete and homogenous evaluation of the 10-year seasonal mass balance time series of Findelen and Adlergletscher. We apply and compare different approaches for the calculation of glacier-wide mass balance from point field measurements (contour line and profile method, modelling). Results are validated against independent ice volume changes for the period 2005-2010 (Joerg et al. 2012). By including all available information (winter accumulation distribution, annual mass balance, and meteorological data) into an integrated scheme for mass balance evaluation, good agreement with the geodetic method is found and allows us to present a re-analyzed series of the 10-year monitoring activities on Findelengletscher. In addition, we compare the results for Findelen and Adlergletscher with other long-term series included in the Swiss glacier monitoring network and discuss the differences with respect to recent climate change in the Alps.

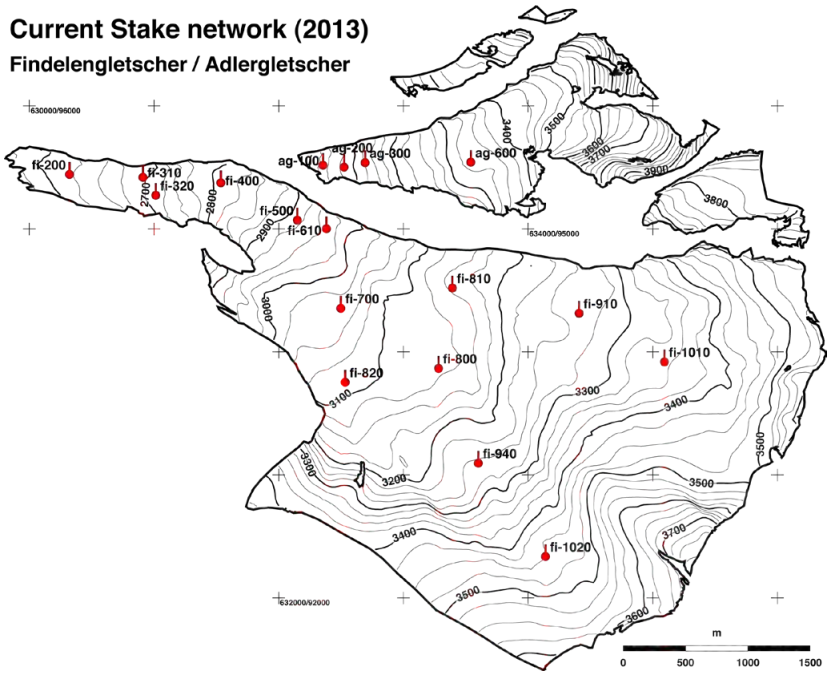

Figure 1. Current stake network and glacier outlines of Findelen and Adlergletscher.

REFERENCES

Joerg, P.C., Morsdorf, F. & Zemp, M. (2012): Uncertainty assessment of multi-temporal airborne laser scanning data: A case study on an Alpine glacier. Remote Sensing of Environment, 127, 118-129.

Machguth, H., Eisen, O., Paul, F. & Hoelzle, M. (2006): Strong spatial variability of snow accumulation observed with helicopter-borne GPR on two adjacent Alpine glaciers. Geophysical Research Letters 33, L13503.

Sold, L., Huss, M., Hoelzle, M., Andereggen, H. Joerg, P. C., & Zemp, M. 2013: Methodological approaches to infer end-of-winter snow distribution on alpine glaciers. Journal of Glaciology, 59(218), 1047–1059, doi:10.3189/2013JoG13J015.

Sold, L., Huss, M., Eichler, A., Schwikowski, M. & Hoelzle, M. 2014. Recent accumulation rates of an alpine glacier derived from firn cores and repeated helicopter-borne GPR. The Cryosphere Discuss., 8, 4431-4462, doi:10.5194/tcd-8-4431-2014.

P 11.10

Measuring snow surface topologies and its changes using Microsoft's Kinect

Philip Crivelli[1], Stefan Horender[1,2], Enrico Paterna[1], Michael Lehning[1,3]

[1] *WSL Institute for Snow and Avalanche Research, SLF Davos, Flüelastrasse 11, CH-7260 Davos, Switzerland (philip.crivelli@slf.ch)*
[2] *TROPOS, Leibniz-Institut für Troposphärenforschung, Permoserstrasse 15, 04318 Leipzig, Germany*
[3] *CRYOS, School of Architecture, Civil and Environmental Engineering, Ecole Polytechnique Federal de Lausanne, Lausanne*

The evolution of the snow surface during a snow drift event in a cold wind tunnel was recorded with Microsoft's Kinect device. Microsoft's Kinect device can be used as a low cost alternative to common three dimensional scanners. Since its introduction as a tool for video games, the scientific community gained more and more interest in its applications. To validate its performance, we first measured the topology of a small hill consisting of either sand or fresh snow and compared the Kinect 3D results with a profile through the hill obtained by shadow images. We found that this setup can record the snow surface with a satisfying precision in the range of millimeters.

Previously, experimentally recording snowdrift was done with different tools such as snow particle counters (SPC), shadow graphic imaginary, acoustic devices (FlowCapt), impact sensors, or particle traps. These tools can represent a flux profile or a point measurement. We propose to use Microsoft's Kinect device as a tool to analyze the surface change during snowdrift events. To the authors' knowledge, no studies have been performed that document quantitatively the processes on the snow surface during snow drift in such a large control volume in a wind tunnel.

We present the evolution of a snow surface during a drifting snow event and calculate a mass flux from the mass balance for a defined control volume.

Outlook: we also will try to measure surface ripples and "mini" zastrugi formed during drifting snow experiments, since the nearly instantaneous break down of these structures may lead to large fluctuations in the drifting mass flux, as has been observed earlier.

P 11.11

Ground thermal regime and its relation to snow cover in Alpine rock walls

Anna Haberkorn[1,2], Marcia Phillips[1], Robert Kenner[1], Hansueli Rhyner[1], Martin Hoelzle[2]

[1] *WSL Institute for Snow and Avalanche Research SLF, Flüelastrasse 11, CH-7260 Davos (haberkorn@slf.ch)*
[2] *Department of Geosciences, University of Fribourg, Chemin du Musée 4, CH-1700 Fribourg*

Changes in rock temperature and variability in the ice and water content of permafrost rock walls can lead to rock wall instability. Rising air temperatures and consequently rock temperatures are key control factors of permafrost degradation. Additionally the thickness and duration of the heterogeneously distributed and patchy snow cover in high alpine mountain regions alters the evolution of ground surface temperatures, since the snow influences the energy balance of the ground due to changes of both the radiation budget and turbulent fluxes of sensible and latent heat at the ground surface.

The majority of steep mountain rock slopes are usually non-vertical, fractured and variable inclined. Consequently a strong spatial and temporal variable snow cover is likely to exist and its depth depends on the slope angle, aspect, surface roughness and surface concavity. The snow cover either has an insulating or cooling effect on rock temperatures, depending on its thickness (Hoelzle et. al, 2003). The snow cover significantly affects the energy balance and water supply, thus altering the ice and water content of the rock wall discontinuities, which can lead to rock instabilities.

To assess the temporal and spatial evolution and distribution of the snowpack and the corresponding influence on the rock thermal regime several south and north facing permafrost rock walls in the Swiss Alps have been investigated since 2012. To obtain information on both rock temperatures and on snow cover duration, near-surface rock temperature (*NSRT*) measurements are carried out in 10 cm depth, using iButtons. Snow cover stratigraphy and temperatures are investigated in-situ with snow pits. Automatic cameras register snow distribution and weather conditions hourly. Terrestrial laser scans (*TLS*) are carried out to obtain the depth and the spatial distribution of the snow cover at regular intervals and borehole temperatures are measured to determine the influence of the snow cover at depth at one particular site. *NSRT* measurements in steep rock slopes provide valuable information on the thermal regime of the rock surface and on snow cover distribution, which are both highly dependent on aspect, slope, shading effects and surface roughness. The south facing slopes are subject to high daily temperature variations of up to 20 °C in summer and winter, if no snow can accumulate, whereas *NSRT* remains close to 0 °C under snowpack conditions without permafrost beneath (see Figure 1). On these rock slopes the snow cover typically consists of rounded grains, melt crusts and ice lenses at the snow-rock interface. *NSRT* on the north facing slopes are closely linked to air temperature under snow-free conditions, while the *NSRT* data indicate a delayed and damped atmospheric signal under a thick snowpack. On these slopes the winter snowpack typically consists of faceted crystals and depth hoar. No decrease of snow depth with slope angles up to 70° were observed by *TLS* in rough terrain due to micro-topographic structures. All aspects and angles can accumulate ephemeral rime during storms.

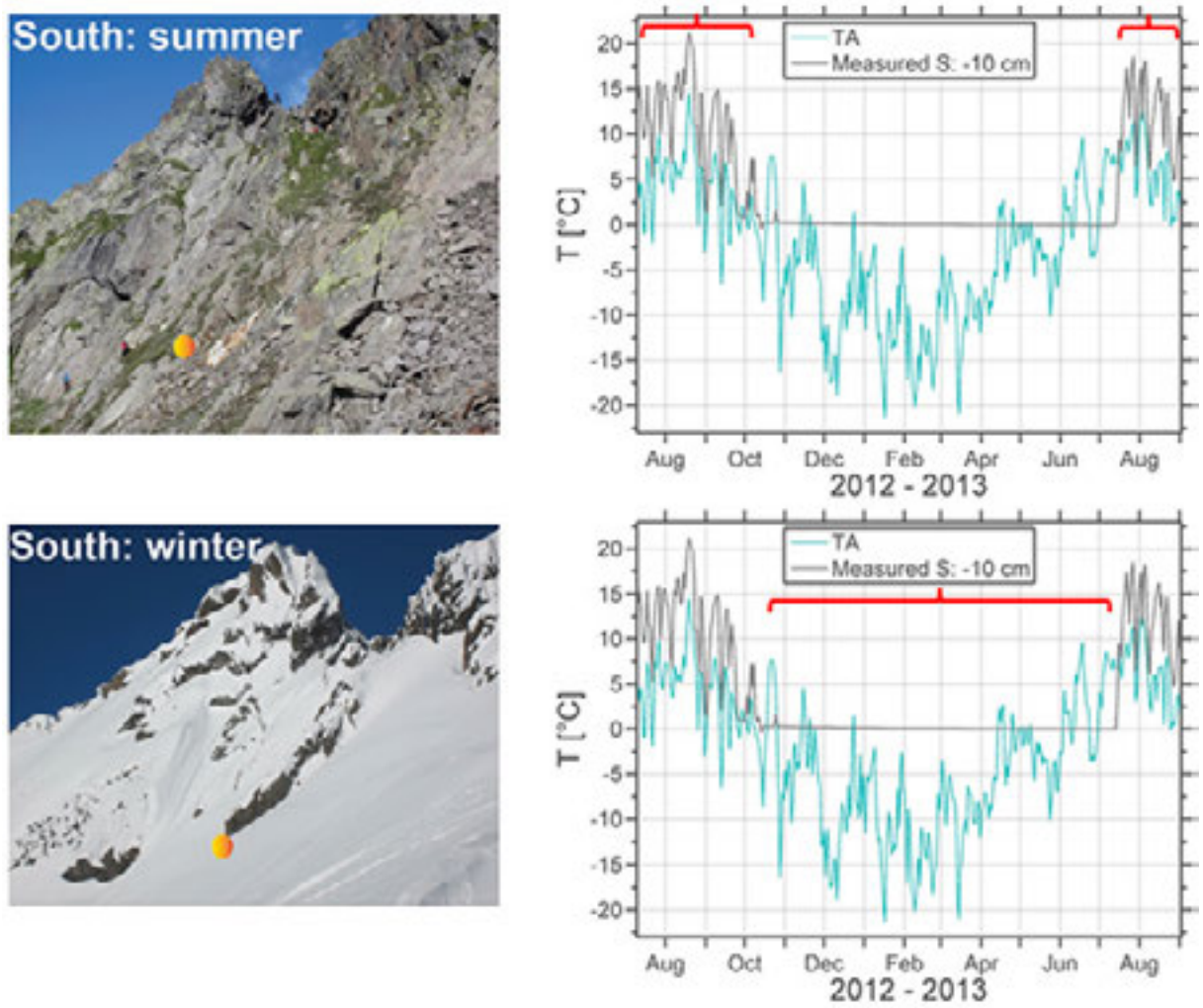

Figure 1. One year of data of *NSRT* measured at a south facing rock wall in summer (top) and winter (bottom) and air temperature (TA) measured at an adjacent automatic weather station. The orange circles indicate the measurment location, whereas the red brackets highlight the summer and winter season.

REFERENCES

Hoelzle, M., Haeberli, W. & Stocker-Mittaz, C. 2003: Miniature ground temperature data logger measurements 2000-2002 in the Murtèl-Corvatsch area, Eastern Swiss Alps. In: Phillips, M., Springman, S. and Arenson, L. (eds), Proceedings of the 8th International Conference on Permafrost, Swets & Zeitlinger, Lisse, 419-424.

P 11.12

Extended-range probabilistic forecasts of snow water equivalent and runoff in mountainous areas

Jörg-Hess Stefanie[1], Griessinger Nena[2], Zappa Massimiliano[1]

[1] *Swiss Federal Research Institute WSL, Zürcherstrasse 111, CH-8903 Birmensdorf (stefanie.joerg@wsl.ch)*
[2] *Swiss Federal Research Institute WSL/SLF, Flüelastrasse 11, CH-7260 Davos Dorf*

Good initial states can improve the skill of hydrological ensemble predictions. Better hydrological forecasts can be produced with better estimates of snow storage. In mountainous regions such as Switzerland, snow is an important component of the hydrological system. Including estimates of snow cover in hydrological models is of great significance for the prediction of both flood and stream flow drought events. In this study, gridded snow water equivalent maps (SWE maps), derived from daily snow depth measurements, are used within the gridded version of the conceptual hydrological model PREVAH to replace the model SWE at initialization (Figure 1). The ECMWF VarEPS reforecast is used as meteorological input for 32 day forecasts of stream flow and SWE. Experiments were performed in several parts of the Alpine Rhine and the Thur rivers. Predictions with the imported SWE maps could successfully enhance the predictability of SWE up to a lead time of 25 days, especially at the beginning and the end of the snow season. Additionally, the prediction of the runoff volume was improved, particularly in catchments where the snow accumulation, and thus the runoff volume had been greatly overestimated. These improvements in predictions have been made, without affecting the ability of the forecast system to discriminate between the different runoff volumes observed. Evaluations of spatial similarity were applied in this study for the first time in water resource forecasting.

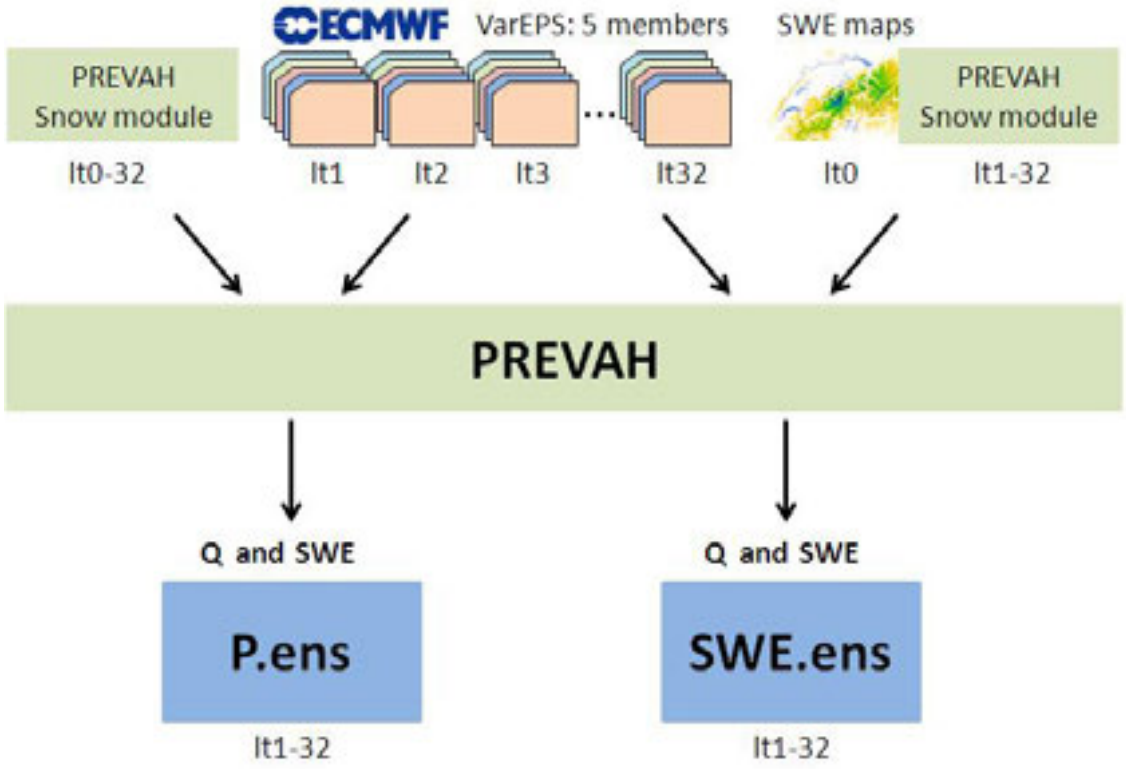

Figure 1: Setup for the simulations of runoff and SWE. Predictions with the hydrological model PREVAH are forced with the ensemble numerical weather prediction VarEPS. Predictions for the lead times 1-32 (lt 1-32) that use the simulated SWE from PREVAH are denoted P.ens, and those that imported SWE maps at initialization SWE.ens.

P 11.13

Projections of permafrost evolution in the Swiss Alps coupling climate and soil models

Antoine Marmy[1], Jan Rajczak[2], Sven Kotlarski[2], Nadine Salzmann[1], Christian Hauck[1]

[1] *Alpine Cryosphere and Geomorphology Group, Department of Geosciences, University of Fribourg, Switzerland*
[2] *Institute for Atmospheric and Climate Science, ETH Zurich, Switzerland*

In the context of a global climate warming, the long-term modelling of permafrost in the Swiss Alps is one of the most challenging but also one of the most interesting research topics. The challenge of long-term modelling of permafrost in mountain areas relates to the scarcity of reliable onsite meteorological data as well as subsurface ground temperature time series making the calibration procedure tricky. In this contribution, we present the results of the calibration and the long-term modelling of 5 permafrost sites in the Swiss Alps: Lapires, Schilthorn, Stockhorn, Ritigraben and Murtel, covering a broad range of morphological characteristics including rock slopes, talus slopes ans rock glaciers.

The calibration of the soil model COUP has been carried out for all sites using the General Likelihood Uncertainty Estimation (GLUE) method (Jansson 2012), an inverse modelling approach testing a multitude of parameter combinations to find the parameter set giving the best fit with the observations. The parameters used for calibration concern both the upper boundary conditions (snow and albedo) and subsurface parameters (such as porosity, thermal and hydraulic conductivities). Once the calibration is considered satisfactory, the model has been run for all sites until the end of the 21st century using downscaled climate model outputs driven by the A1B scenario for 14 different GCM/RCM chains. The statistical downscaling approach employed include a 2-step bias-correction procedure: first, downscaling of simulated RCM time series for several meteorological variables to high-quality MeteoSwiss stations using quantile mapping and, second, a further quantile mapping step between the MeteoSwiss stations and the corresponding on-site meteorological data of the permafrost stations.

The resulting projections of ground temperature change, active layer thickness and snow cover duration are compared among the different sites and among different GCM/RCM chains.

REFERENCES

Jansson, P.E. 2012: CoupModel: Model use, calibration and validation. Trans. ASABE 55 1335-1344.

P 11.14

Long term monitoring of the Mont Dolin rock glacier (Swiss Alps)

Nendaz Thierry[1], Lambiel Christophe[1]

[1] *Institut des dynamiques de la surface terrestre, Université de Lausanne, Mouline – Géopolis, 1015 Lausanne (thierry.nendaz@unil.ch)*

The current global climate change implies some perturbations in permafrost environments. The dynamics of landforms like rock glaciers can, therefore, be modified due to the climatic changes. However, the response to climate change is different from site to site because of the importance of both local (e.g. solar radiation) and regional (e.g. precipitations, annual temperature) factors.

The Mont Dolin talus rock glacier is located in a south-oriented glacial cirque in Arolla (VS). Using differential GPS surveys and photogrammetric data, this study provides a long term monitoring of this rock glacier. In addition, Electrical Resistivity Tomographies (ERT) have been carried out in summer 2013 to define its current internal structure and especially the distribution of permafrost. Results suggest a weak geomorphic activity, illustrated by decimetric topographical changes in the past fifty years, and by the very slow (up to 9 cm per year) permafrost creep during the last decade. The ERT results suggest the presence of massive ice at the limit between the rock glacier and the talus slope. Moreover, ice content tends to decrease from this spot up to the front of the rock glacier.

Located at the lower limit of the permafrost belt, the Mont Dolin rock glacier seems to be undergoing fossilisation. Furthermore, the link between ice content and geomorphic activity is not obvious. The sediment supply due to gravity seems to be the most important factor in areas where the thickness has increased.

P 11.15

Gap filling procedures for ground surface temperature time series of the PERMOS network

Staub Benno[1], Hasler Andreas[1], Delaloye Reynald[1]

[1] *Département Géosciences, Unité Géographie, Université de Fribourg, Chemin du Musée 4, CH-1700 Fribourg (benno.staub@unifr.ch)*

The acquisition of permafrost monitoring data in high mountain environments like the Swiss Alps is complicated by technical issues related to the rough terrain and climate as well as limited accessibility and budget. As a result, many of these time series are interrupted by gaps of different duration (hours-years) what complicates the calculation of aggregates and indices. In the frame of the SNSF Sinergia project «The Evolution of Mountain Permafrost in Switzerland» (TEMPS, 2011–2014), a variety of processing routines are developed for data homogenization and analysis that can – in a further step – be operationalized in the Swiss Permafrost Monitoring Network (PERMOS).

The major aim behind this initiative is to get continuous time series of daily mean ground surface temperatures (GST) to allow analyses on the basis of running annual means (rMAGST) and indices like thawing and freezing degree days (TDD, FDD). Using complete GST time series and a large number of randomly generated synthetic gaps, the performance of various interpolation, regression and bias-correction techniques as well as approaches to quantify the uncertainty resulting on aggregates and indices are assessed.

Linear regression and quantile mapping have shown to be the most reliable gap filling approaches for daily mean GST records, but up to gap durations of one week linear interpolation is not significantly worse. Gaps that are affected by snow melt in spring or longer than three months require individual treatment separately for each season (depending on the snow cover evolution). To fill entire years, increasing the temporal resolution to weekly means seems promising. Finding the best regressor loggers is crucial and also the main source of uncertainty. Because the similarity of GST time series depends rather on site-specific characteristics like the surface type or topoclimatic properties than spatial proximity, all kinds of surface temperature records from a variety of study sites should be included, also borehole temperatures measured close to the surface. The integration of the procedure into the PERMOS data base has a high potential, also because additional data measured in the future might improve the quality of several hundred temperature time series from the past.

P 11.16

Spatial and temporal variability of soil moisture in permanently frozen ground at Schilthorn (Swiss Alps)

Adrian Wicki[1], Christian Hauck[1], Cécile Pellet[1], Christin Hilbich[1], Andreas Kemna[2], Maximilian Weigand[2] & Sebastian Wege[2]

[1] *Department of Geosciences, University of Fribourg, Chemin de Musée 4, CH-1070 Fribourg (adrian.wicki@unifr.ch)*
[2] *Department of Geodynamics and Geophysics, University of Bonn, Meckenheimer Allee 176, D-53115 Bonn*

The thermal behaviour of permanently frozen ground is largely influenced by the presence of soil moisture. However, especially in high mountain environments, the subsurface and therefore the spatial distribution of soil moisture can be very heterogeneous. As a consequence, the thermal regime of permafrost soils can vary significantly within some meters. Such small scale temperature variations are identified at the PERMOS permafrost research station on the Schilthorn summit (Swiss Alps). At two borehole locations, situated in the northern slope of the summit, subsurface temperatures are measured down to 14m and 100m depth, respectively. Although the two boreholes are only 15m apart, the thermal behaviour in the uppermost meters shows significantly different characteristics. Several studies suggested different soil moisture regimes as the main explanatory factor (Völksch 2004, Hilbich et al. 2011).

In this study, the spatial and temporal variability of soil moisture and ground ice in the slope above and in the vicinity of the boreholes is studied during summer 2014. More precisely, it aims at detecting percolation depths, possible preferential flow paths and the influence of subsurface features such as the presence of bedrock outcrops on groundwater flow. Furthermore, the results are set into a meteorological context in order to account for the temporal variability.

For this purpose, Electrical Resistivity Tomography (ERT) profiles are measured at several locations upslope of the boreholes. The measurements are repeated at various times throughout the summer when the surface is partly snow covered as well as snow-free. The resulting 2-D tomograms of specific electrical resistivity can be related to the spatial variability of soil moisture and ground ice at depths to 7 meters. Additionally, the temporal changes of the soil moisture distribution are calculated using a time-lapse inversion scheme. Finally, using Archie's law (Archie 1942), the soil moisture is quantified from the ERT measurements, where in-situ soil moisture data are used for calibration. This approach can also be used for existing data of the permanent ERT profile line, along which electrical resistivity is measured at a coarser resolution since 1999 (Hilbich et al. 2011).

As validation for the soil moisture dynamics derived from ERT, continuous measurements provided by Time Domain and Frequency Domain Reflectometry (TDR, FDR) sensors installed in the vicinity of the boreholes are used. In addition, continuous Self-Potential (SP) measurements conducted within the study area are used for the identification of preferential flow paths and the characterization of subsurface flow dynamics, which in turn can be related to the spatio-temporal soil moisture variations. Finally, soil moisture measuements will be conducted on soil samples from several locations. The results of the spatio-temporal soil moisture analysis are compared to meteorological conditions during summer 2014 in order to assess the impact of snow melt and precipitation events on the hydrological regime. The work is used as a base for further studies on the influence of soil moisture on the thermal behaviour of permafrost.

REFERENCES

Archie, G. E. 1942: The electrical resitivity log as an aid in determining some reservoir characteristics, Petroleum Transactions of American Institute of Mining and Metallurgical Engineers (AIME),146, 54–62.

Hilbich, C., Fuss, C. & Hauck C. 2011: Automated Time-lapse ERT for Improved Process Analysis and Monitoring of Frozen Ground. Permafrost and Periglacial Processes 22, 306-319.

Völksch, I. 2004: Untersuchung und Modellierung kleinräumiger Unterschiede im Verhalten von Gebirgspermafrost. Diploma thesis ETH Zürich.

P 11.17

Antarctic snow stratigraphy - new methods and insights

Martin Schneebeli[1], Martin Proksch[1], Margret Matzl[1], Stefanie Weissbach[2]

[1] *WSL Institute for Snow and Avalanche Research SLF, Davos, Switzerland (schneebeli@slf.ch)*
[2] *Alfred-Wegener-Institute for Polar and Marine Research, Bremerhaven, Germany*

The stratigraphy in Antarctica is a complex product of depositional and metamorphic processes. The depositional process is dominated by frequent re-deposition and rare atmospheric precipitation. Metamorphism is a ubiquitous and significant process occurring at the near surface of snow and firn. Relatively little is known about how snow metamorphism affects the physical and mechanical properties of snow in Antarctica, and observations are difficult by traditional means. One reason for the lack of knowledge is that depositional and metamorphic processes occur concurrently. Near-infrared photography, quantitative translucent profiles, high-resolution penetrometry, optical Specific Surface Area measuring instruments and micro-tomography are modern methods suitable for use in Antarctic snowpacks. These instruments gather detailed stratigraphic information at multiple scales. We applied these methods at three different sites in Antarctica: Allan Hills, Pointe Barnola and Kohnen Station. The characteristic stratigraphy and microstructures found at these locations will be presented and interpreted. The new methods are very efficient to reveal the complex structures. Based on our observations, we show that alternating temperature gradient metamorphism, which is the dominant type of metamorphism at the surface, has a strong effect on the re-mobilization of the hard snow surface during austral summer, and temperature gradient metamorphism is important during winter. Large erosional events, removing multiple years of deposition, can occur, and have a marked impact on stratigraphy.

P 11.18

Snow microstructure and modelling in support of permafrost science

Martin Proksch[1,4], Isabelle Gouttevin[2], Moritz Langer[3], Pirmin Ebner[1], Charles Fierz[1], Martin Schneebeli[1]

[1] *WSL Institute for Snow and Avalanche Research SLF, Flüelastrasse 11, CH-7260 Davos Dorf (proksch@slf.ch)*
[2] *Laboratory of Cryospheric Sciences CRYOS, Ecole polytechnique fédérale de Lausanne EPFL, CH-1015 Lausanne*
[3] *Alfred Wegener Institute, Helmholtz Centre for Polar and Marine Research, Research Unit Potsdam, Telegrafenberg A 43, 14473 Potsdam, Germany*
[4] *Institute for Meteorology and Geophysics IMGI, University of Innsbruck, Innrain 52f, 6020 Innsbruck*

Permafrost underlies ~22% of the Northern Hemisphere ground surface and has been observed and projected to undergo severe degradation in the context of global warming. Yet, permafrost modelling is still a challenging task, even at monitoring stations where observations of ground properties exist. One of the main locks is the representation of the thermal properties of snow, which very much depend on snow microstructure and accumulation depth.

Here, we present the results of a spring campain lead on Samoylov Island, Lena Delta (72.4°N, 126.5°E), Siberia, where snow was investigated in terms of stratigraphy and microstructural parameters. Several snow profiles and transects were measured in order to characterise the snow over the polygonal tundra landscape. Cast snow samples were analysed by micro-computed tomography in the cold laboratory at SLF, Davos in order to calculate physical properties for relevant transport processes in the snowpack, such as thermal conductivity and permeability.

Additionally, the snow cover model SNOWPACK is applied at Samoylov, to assess its capability to represent a high-arctic snowpack. Overall, SNOWPACK predicts realistic profiles of physical and structural properties similar to the observed ones. This is an encouraging step for the application of snow modelling in support of the permafrost science community.

P 11.19

Imaging of snow algae in natural snow using phase-contrast tomography

Mareike Wiese[1] & Martin Schneebeli[1]

[1] *WSL-Institut für Schnee- und Lawinenforschung, Flüelastrasse 11, CH-7260 Davos Dorf (mareike.wiese@slf.ch)*

Snow algae influence the radiative properties of snow. Snow with algal blooms often appears red and hence darker than snow without algae. These algae commonly occur on melting snow, but little is known about the precise location of the algae within the snow and their life-cycle and micro-habitat.

We took snow samples with snow algae in the Swiss Alps. Using phase-contrast tomography, we investigate whether we can find snow algae inside the snow samples with this imaging technique to get more information about their micro-habitat.

In the resulting images we can identify small particles of the typical size of snow algae (about 20 micrometer in diameter) besides the larger ice structure of the snow. Interestingly, the snow algae are located on the surface of snow grains. This finding supports the suggestion that snow algae migrate from the ground into the snow towards the snow surface, moving on the liquid water film on the surface of snow grains.

P 11.20

The contribution of locally extreme snow depths to the winter snow cover volume of Alpine glaciers in the Ötztal Alps, Austria

Kay Helfricht[1,2] Michael Lehning[3,4] Rudolf Sailer[5] & Michael Kuhn[2]

[1] *IGF - Institute for Interdisciplinary Mountain Research, Austrian Academy of Sciences Technikerstr. 21a, A-6020 Innsbruck (kay.helfricht@oeaw.ac.at)*
[2] *Institute of Meteorology and Geophysics, University of Innsbruck, Innrain 52f, A-6020 Innsbruck*
[3] *WSL, Institute for Snow and Avalanche Research SLF, Flüelastrasse 11, CH-7260 Davos Dorf*
[4] *CRYOS, School of Architecture, Civil and Environmental Engineering, EPFL, GR A0 402 (Bâtiment GR), Station 2, CH-1015 Lausanne*
[5] *Institute of Geography, University of Innsbruck, Innrain 52f, A-6020 Innsbruck*

Snow deposition and redistribution are major drivers of snow cover dynamics in mountainous terrain and play a major role in the mass balance of Alpine glaciers. The quantitative understanding of inhomogeneous snow distribution in mountains has recently benefited from advances in measuring technologies, such as laser scanning (lidar, e.g. Deems et al. 2013), but also from increased understanding of the physical processes. This contribution further advances the quantitative understanding of uneven snow distribution on glaciers by analysing the areas of maximum snow depth in a mountain catchment with large and small glaciers.

We analysed multi-temporal airborne laser scanning (ALS) data with a high spatial resolution to investigate the contribution of locally extreme snow depths to seasonal snow volume on glaciers in a large part of the Ötztal Alps and for several glaciers in a partly glacierized subcatchment.

Using multi-annual ALS observations, we found that maximum snow depths occur on rather thin borders along the glacier margin in the glacier accumulation zone. While snow depth distribution patterns in less extreme terrain have presented high inter-annual persistence, there is little persistence between winters of those extreme glacier accumulations. We therefore interpret the lack of persistence as the result of a predominance of gravity-driven redistribution (avalanches and sloughs), which has an inherently higher random component because it does not occur with all conditions in all winters. We further suggest that these extreme accumulations play a significant role in the glacier mass balance and that they may be successfully parameterized by simple mass redistribution algorithms, which have been presented in the literature (e.g. Gruber, 2007; Bernhardt and Schulz, 2010)

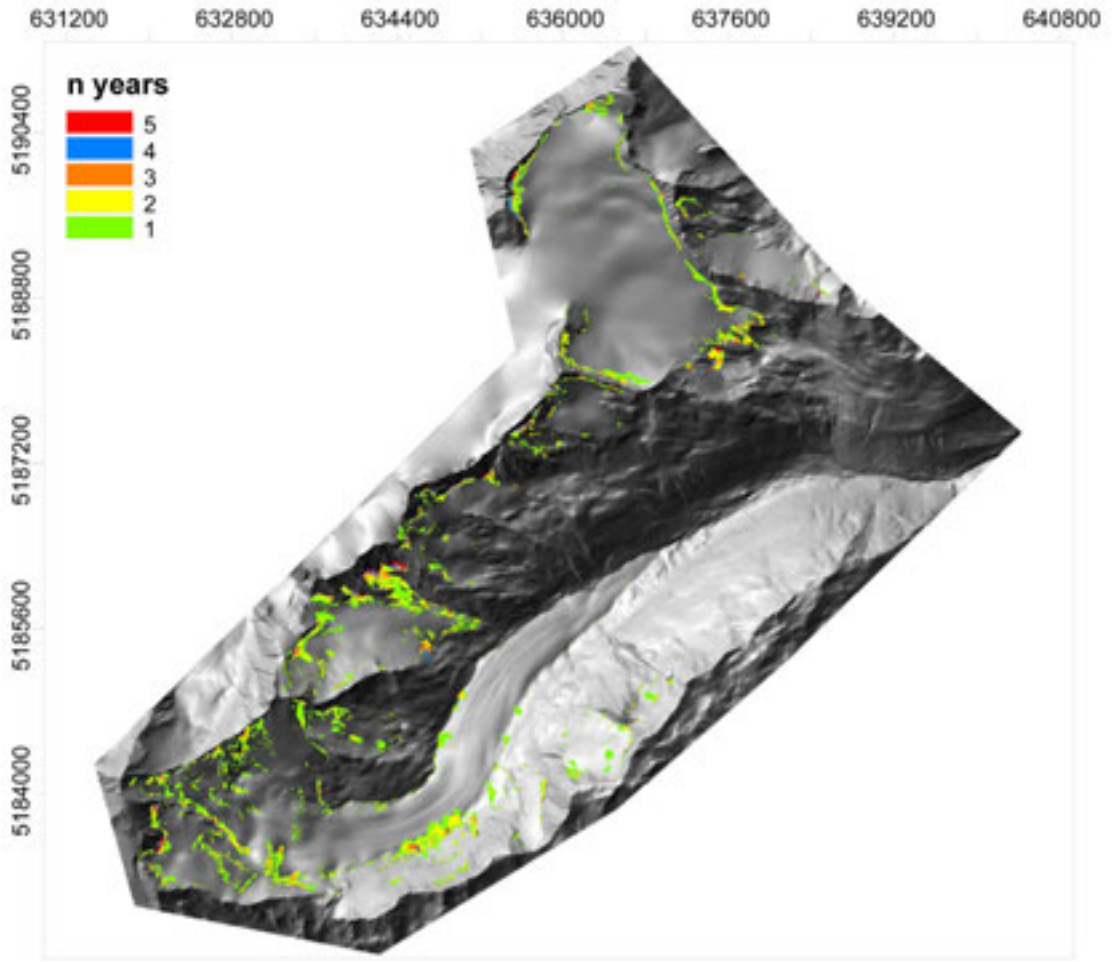

Figure 1. Distribution of areas affected by extreme snow depths on glacier surface by the number of years they occurred.

REFERENCES

Bernhardt, M. & Schulz, K., 2010. Snowslide: A simple routine for calculating gravitational snow transport. Geophysical Research Letters, 37(11), L11502.

Deems, J., Paintner, T., & Finnegan, D., 2013. Lidar measurement of snow depth: a review. Journal of Glaciology, 59(215), 467–479.

Gruber, S., 2007. A mass-conserving fast algorithm to parameterize gravitational transport and deposition using digital elevation models. Water Resources Research, 43(6).

P 11.21

Towards a better representation of snow accumulation distribution in glacier mass balance models

Leo Sold[1], Matthias Huss[1,2], Martin Hoelzle[1]

[1] *Department of Geosciences, University of Fribourg, Ch. du Musée 4, CH-1700 Fribourg (leo.sold@unifr.ch)*
[2] *Laboratory of Hydraulics, Hydrology and Glaciology, ETH Zurich, Wolfgang-Pauli-Strasse 27, CH-8093 Zürich*

Snow accumulation is a key variable in glacier mass balance modelling approaches. Its spatial distribution controls melt-out patterns and spatio-temporal surface albedo variations. If measurements of snow accumulation distribution exist they typically consist of probings and snow density pits. Because such surveys are time-consuming and laborious, measurements are sparse and can hardly be representative for large or medium-sized glaciers. If no observations are available, conventional models estimate the snow accumulation by applying a temperature threshold and elevation gradient to precipitation measurements. However, such a simplistic representation is a major drawback in current mass balance models and leads to major uncertainties in the results (Machguth et al., 2006, Huss et al. 2014).

We present multi-year measurements of snow accumulation on Findelengletscher (CH) using conventional snow probings and helicopter-borne ground-penetrating radar (GPR). The signal traveltime difference between the snow surface and the snow-ice or snow-firn boundary was converted to depth using a wave velocity estimate based on an empirical relation of the dielectric permittivity with snow density (Sold et al. 2013). For the direct integration in a mass balance model (Huss et al. 2009) the measurements were interpolated to a regular 25m x 25m grid. We applied different interpolation schemes covering the range from simple deterministic methods to geostatistical approaches such as kriging with external drift that incorporates information on the underlying terrain.

The availability of several years of snow accumulation distribution measurements further allows generating a normalised distribution grid that can be used as model input when no or only few direct observations are available. However, the underlying assumption of the involved processes being invariant in time limits the validity of this approach. In order to incorporate processes to a reasonable degree we set up a simple model that accounts for spatial variations in precipitation and wind-dependent redistribution of snow (Helfricht et al. *in press*).

We show that the use of extensive snow accumulation measurements such as by helicopter-borne GPR leads to a substantial improvement of the mass balance model results as indicated by independent validation data that cannot be achieved by sparse conventional measurements. Our data set can further be used to calibrate a simple model for the snow accumulation distribution that yields a considerable improvement compared to conventional accumulation modelling.

REFERENCES

Helfricht, K., Schöber, J., Schneider, K., Sailer, R. & Kuhn, M. in press: Interannual persistence of the seasonal snow cover in a glacierized catchment. Journal of Glaciology.

Huss, M., Bauder, A., & Funk, M. 2009: Homogenization of long-term mass-balance time series. Annals of Glaciology, 50(50), 198-206.

Huss, M., Zemp, M., Joerg, P. C., & Salzmann, N. 2014: High uncertainty in 21st century runoff projections from glacierized basins. Journal of Hydrology, 510, 35–48.

Machguth, H., Eisen, O., Paul, F., & Hoelzle, M. 2006: Strong spatial variability of snow accumulation observed with helicopter-borne GPR on two adjacent Alpine glaciers. Geophysical Research Letters, 33, L13503.

Sold, L., Huss, M., Hoelzle, M., Andereggen, H., Joerg, P. C., & Zemp, M. 2013: Methodological approaches to infer end-of-winter snow distribution on alpine glaciers. Journal of Glaciology, 59(218), 1047–1059.

13. Freshwater monitoring: from past to present and to future - Measurement and interpretation

B. Schädler, M. Doering, T. Jonas, A. Salvetti, M. Sinreich, P. Schmocker-Fackel

Swiss Society for Hydrology and Limnology SGHL,
Swiss Hydrological Commission CHy,
Swiss Hydrogeological Society SGH

TALKS:

13.1 Ammann L., Diem S., Poppei J.: Improving the understanding of river-groundwater interactions by analyzing time series of electrical conductivity

13.2 Etter S., Seibert, J., Vis M., Addor N., Huss M., Finger D.: Impacts of climate change on the water availability for the hydropower reservoir Gigerwaldsee using hydrological modeling

13.3 Gaudard A., Bouffard D., Wüest A.: Long-term monitoring and modelling of Lake Geneva, in the prospect of thermal energy usage

13.4 Mutzner R., Weijs S.V, Tarolli P., Calaf M., Oldroyd H.J., Parlange M.B.: Study of diurnal streamflow cycles in a high altitude catchment in the Swiss Alps

13.5 Reinhardt M., Kozel R.: Trenderhebung, Früherkennung und Erfolgskontrolle im Grundwassermonitoring - Konzepte der Nationalen Grundwasserbeobachtung NAQUA

13.6 Saadé-Sbeih M., Zwahlen F., Haj Asaad A., Gonzalez R., Jaubert R.: Assessing long term changes in the Orontes River basin (Lebanon and Syria): how to deal with variable, incomplete and heterogeneous datasets?

13.7 Surbeck H., Bossy F.: Supersaturation, a phenomenon ignored by most hydrogeologists

13.8 von Fumetti, S.: Long-term monitoring of natural springs in the Röseren valley near Liestal (BL)

13.9 Weijs S.V., Brauchli, T., Huwald, H.W.: Measuring surface flow velocity with smartphones: potential for citizen observatories

POSTERS:

P 13.1 Calianno M., Reynard E.: Quantifying Alpine water demands: setup for a micro-observatory of irrigation and drinking water supply in the Crans-Montana-Sierre region (Valais, Switzerland)

P 13.2 Gallice A., Schaefli B., Lehning M., Huwald H.: Modeling the monthly mean stream temperature dynamics

13.1

Improving the understanding of river-groundwater interactions by analyzing time series of electrical conductivity

Lorenz Ammann[1,2], Samuel Diem[2] & Joachim Poppei[2]

[1] *Institut für Umweltingenieurwissenschaften, ETH Zurich, Wolfgang-Pauli-Strasse 15, CH-8093 Zürich (loammann@ethz.ch)*
[2] *AF-Consult Switzerland Ltd, Groundwater Protection and Waste Disposal, Täfernstrasse 26, CH-5405 Baden (samuel.diem@afconsult.com)*

The residence time and the fraction of infiltrated river water are important parameters that determine the quality of drinking water derived by riverbank filtration. Hence, estimating these parameters is of high practical relevance and of particluar interest within the context of river restoration projects, which might affect the residence time in the aquifer and thus the quality of the produced drinking water.

Conventionally, the residence time between a river and a pumping well is estimated by injecting a tracer into the river and observing its break-through at the well. In large rivers, this method requires large amounts of tracer and the resulting flow parameters are only valid for the hydraulic conditions prevalent during the experiment. Alternatively, groundwater residence time distributions and the fraction of infiltrated river water may be estimated by analyzing time series of electrical conductivity (EC) measured in the river and in adjacent groundwater observation wells. Two suitable methods for time series analysis in this context are cross-correlation (Vogt et al. 2010) and non-parametric deconvolution (Cirpka et al. 2007). In contrast to the conventional approach, these methods integrate multiple hydraulic conditions and allow for assessing the uncertainty of the residence time distribution with the help of a probabilistic approach (non-parametric deconvolution). While they have been sucessfully applied to EC signals with mean residence times of max. 20 days (Vogt et al. 2009; Diem et al. 2014), their applicability to systems with larger residence times has not been tested yet. Another condition to keep in mind is that these methods are based on a steady-state assumption, i.e. the residence time distribution is assumed to be time-invariant.

The goals of the presented study were firstly to assess the applicability of the aforementioned methods to EC time series recorded in observation wells with groundwater residence times of more than one month. Secondly, we aimed at developing a transient formulation of deconvolution that accounts for a time-dependent residence time distribution.

For this purpose, we applied cross-correlation and non-parametric deconvolution to EC time series measured in the Aare River and in 5 groundwater observation wells between the cities of Olten and Aarau. The obtained fraction of river water varied between 20 and 90 % and the mean residence times ranged between 40 and 130 days. These residence times agreed well with those determined in an artificial tracer experiment previously performed at the study site, which validates the applicability of the used methods to systems characterized by residence times of more than one month.
The developed transient formulation of deconvolution allows quantifying the dependence of the residence time distribution and the recovery on external factors such as the river water level. The results revealed that elevated river water levels during a period of more than one month coincide with high fractions of river water at the observation wells, while the mean residence time was essentially unaffected. These results suggest that periods of elevated discharge increase the connectivity between the river and the aquifer, which leads to higher infiltration rates and higher fractions of river water at the boreholes, while the groundwater flow velocities and hence the travel times remain essentially unchanged.

In conclusion, cross-correlation and non-parametric deconvolution can be applied to EC time series measured at observation wells characterized by a wide range of groundwater residence times. EC may be measured cost-effectively and may provide the basis for an efficient estimation of the residence time distribution, its uncertainty and the fraction of infiltrated river water. The transient formulation of deconvolution helps improve our understanding of the dynamics of river-groundwater systems and might contribute to a sound safety assessment of drinking water wells e.g. within the context of river restoration.

REFERENCES

Cirpka, O.A., Fienen, M.N., Hofer, M., Hoehn, E., Tessarini, A., Kipfer, R. & Kitanidis, P.K. 2007: Analyzing bank filtration by deconvoluting time series of electric conductivity, Ground Water, 45, 318-328.

Diem, S., Renard, P. & Schirmer, M. 2014: Assessing the effect of different river water level interpolation schemes on modeled groundwater residence times, Journal of Hydrology, 510, 393-402.

Vogt, T., Hoehn, E., Schneider, P. & Cirpka, O.A. 2009: Untersuchung der Flusswasserinfiltration in voralpinen Schottern mittels Zeitreihenanalyse, Grundwasser, 14, 179-194.

Vogt, T., Hoehn, E., Schneider, P., Freund, A., Schirmer, M. & Cirpka, O.A. 2010: Fluctuations of electrical conductivity as a natural tracer for bank filtration in a losing stream, Advances in Water Resources, 33, 1296-1308.

13.2

Impacts of climate change on the water availability for the hydropower reservoir Gigerwaldsee using hydrological modeling

Simon Etter[1], Jan Seibert[1], Marc Vis[1], Nans Addor[1], Matthias Huss[2] David Finger[3]

[1] *Department of Geography, University of Zurich, Winterthurerstrasse 190, CH-8057 Zürich (simon.etter@outlook.com)*
[2] *Laboratory of Hydraulics, Hydrology and Glaciology (VAW), ETH Zürich, CH-9093 Zürich*
[3] *Icelandic Meteorological Office, Bústaðavegi 9, 150 Reykjavík, Iceland*

Increasing temperatures and changing precipitation patterns will diminish snow cover and force glaciers to shrink in mountain environments. The runoff in Alpine catchments such as the watershed of the Gigerwaldsee, providing water resources for hydro power production in the Swiss Alps, will be affected by those changes. Using an updated version of the conceptual hydrological model HBV-light (Seibert & Vis, 2012) future hydro-climatic changes in the catchment where simulated. The hydrological model was driven by seven GCM-RCM combinations from the ENSEMBLES project under the emission scenario A1B. The climate projections were bias-corrected using quantile mapping. Besides a baseline scenario (1992-2021), a mid-term future scenario (2036-2065) and a long term scenario (2069-2098) were calculated. For calibration, the model was driven with a gridded dataset from MeteoSwiss and glacier extents from 1990. The calibration was performed using three datasets: i) discharge data, derived from a volume-lake level relationship of the Gigerwaldsee, ii) the fraction of the snow covered area in the catchment, retrieved from MODIS snowcover images (Hall et al. 2002) and iii) extrapolated glacier mass balances (Huss, 2012). The parameters were determined using Pareto selection from 10'000 Monte Carlo simulation runs according to their performance over five objective functions as described in Finger et al. (2011). Two objective functions were used to evaluate the discharge simulation and two for snow cover, in each case one over the whole year and one only during summer. A fifth objective function was used for glacier mass balance simulations. An evaluation of different selections of parameter sets showed that relying on discharge, snowcover and glacier mass balance data led to a higher model consistency. The contribution of the climate scenarios, model parameters and glacier scenarios to the total uncertainty of the simulated future discharge was assessed using analysis of variance (ANOVA).

The results indicate a decrease in runoff during the high flow season due to shorter snowcover persistence and less precipitation and an increase in runoff in the low flow season due to higher temperatures and more precipitation (Figure 1). The runoff originating from snow melt is projected to decrease by 22% and 30%, respectively. The projected runoff from glaciers will diminish by 85% in the mid-term and disappear completely in the long-term. The results from discharge emerging from snow- and glacier melt are significant. The main cause for the spread in the results was found in the large differences between the climate scenarios. These results are in line with findings of a similar study about the Mattmark reservoir in the Vispa valley (Finger et al. 2012).

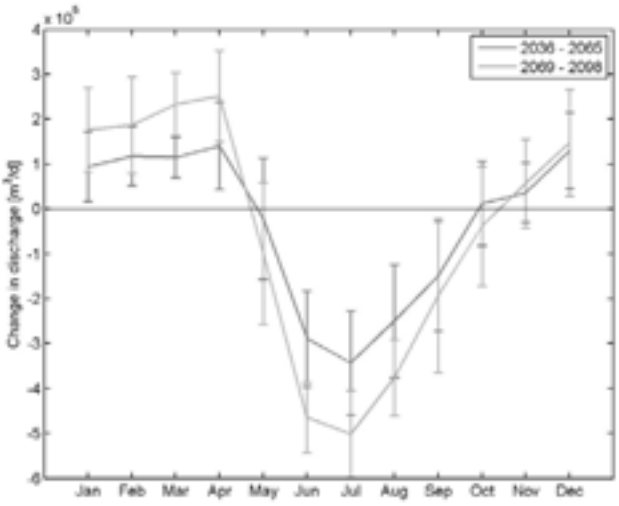

Figure 1. The climate change signal in the mid- and the long-term scenario compared to the baseline period (1992 - 2021). The whiskers indicate the standard deviation from the mean of all the simulation results.

REFERENCES

Finger, D., Heinrich, G., Gobiet, A., & Bauder, A. 2012: Projections of future water resources and their uncertainty in a glacierized catchment in the Swiss Alps and the subsequent effects on hydropower production during the 21st century. Water Resources Research, 48.

Finger, D., Pellicciotti, F., Konz, M., Rimkus S., & Burlando P. 2011: The value of glacier mass balance, satellite snow cover images, and hourly discharge for improving the performance of a physically based distributed hydrological model. Water Resources Researches, 47.

Hall, D. K., Riggs, G. a., Salomonson, V. V., DiGirolamo, N. E. and Bayr, K. J. 2002: MODIS snow-cover products. Remote Sensing of Environment, 83, 181-194.

Huss, M. 2012: Extrapolating glacier mass balance to the mountain-range scale: the European Alps 1900–2100. The Cryosphere, 6(4), 713–727.

Seibert, J., & Vis, M. J. P. 2012: Teaching hydrological modeling with a user-friendly catchment-runoff-model software package. Hydrology and Earth System Sciences, 16, 3315–3325.

13.3

Long-term monitoring and modelling of Lake Geneva, in the prospect of thermal energy usage

Adrien Gaudard[1], Damien Bouffard[1], Alfred Wüest[1,2]

[1] *Physics of Aquatic Systems Laboratory (APHYS) – Margaretha Kamprad Chair, EPFL, Lausanne, Switzerland (correspondence e-mail: adrien.gaudard@alumni.epfl.ch)*
[2] *Surface Waters – Research and Management, Eawag, Kastanienbaum, Switzerland*

Large water bodies are a sustainable and effective way to obtain and/or evacuate thermal energy, and are thus of great practical interest for surrounding towns and infrastructures. It is however essential to understand and manage this resource carefully so as not to disrupt the ecological and heat balances that permit its use in the long run, in the context of climatic change. In Switzerland, the water tower of Europe, lakes and reservoirs are at the forefront when looking for new sources of renewable energy. Although the capacity of running water (hydropower) is already extensively exploited, there is still potential for a wider use of the thermal energy of lakes.

Our study mainly rests on investigation of Lake Geneva, via thorough data analysis, physical interpretation and numerical modelling. The particular alpine topography of the reservoir allows an extremely long fetch for the wind to stimulate the whole basin. As a result, when compared to other European lakes, wind can have a much stronger influence and trigger powerful currents, mixing and internal waves (seiches). Concurrently, the regional climate and the large volume of Lake Geneva make it stable and maintain its deep water above 5 °C.

A remarkable dataset, consisting of nearly sixty years of conductivity-temperature-depth profiles, allowed examining and quantifying the long-term evolution of the lake. It is reliably shown that the lake warms up (at a rate of about +0.12 °C/decade in deep water). However, this trend is not homogeneous with respect to depth and season, due to the faster establishment of spring stratification.

A simple 1D model (SIMSTRAT) is used to prove overall lake warming under the influence of climate change, as well as seasonal patterns in shallow water (with a significantly stronger warming in spring and summer). The model provides statistical results in accordance with field data, and gives valuable insight on the lake response to external forcing. Simulations for the future are performed by applying predictive meteorological conditions to the model.

Additionally, a more comprehensive 3D model (Delft3D), which is forced using a realistic two-dimensional wind map at the lake surface, is utilized (Figure 1). This model demonstrates the extreme behaviour and the spatial structure of the thermocline: a dome-shaped profile is found over the lake, and internal waves are shown to reach 70 m depth in autumn. Additionally, the model allows assessing the quality of surface temperature measurements from satellite thermal images.

Shallower layers, which generally contain more energy, are more suitable for heat extraction. However, it is shown that surface water is naturally sensitive to short air-induced cooling events and that the whole epilimnion can host abundant biological life, as well as human-related activities. A trade-off is then found between energetic efficiency (shallow intake) and low risk (deep intake).

For cooling purposes, deeper layers, located further from atmospheric influence, are best adapted. Nevertheless, as working in these remote zones is more costly and difficult, water from intermediate depths is usually preferable. The decisive criterion is then the range of occurrence of internal waves, which must be avoided for optimal operation of a cooling system.

The particularities of Lake Geneva appear to make it more favourable for heat extraction than for cooling. In other lakes, depending mostly on the basin size, the topography and the climate, the situation may be different. Still, as supported by case analyses in Switzerland (in particular the shared EPFL/UNIL water intake), combined heating and cooling from mid-latitude lakes is shown to be highly interesting in both financial and energetic terms.

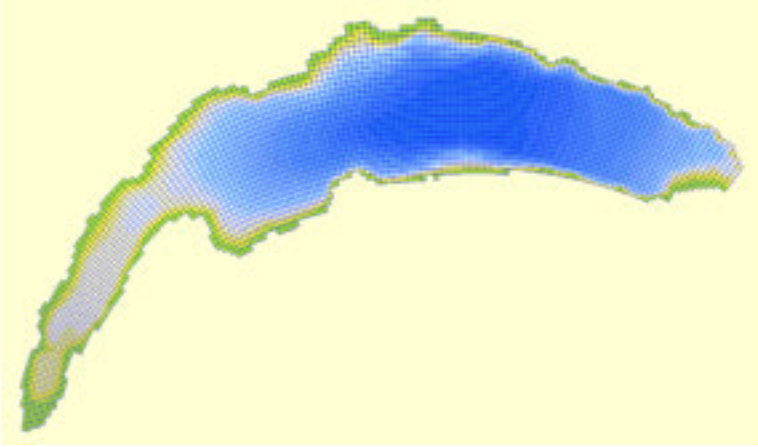

Figure 1. Computational grid for the 3D numerical model (depth is shown as a shading). Time- and space-varying wind is applied on each surface cell.

REFERENCES
Goudsmit, G.-H. et al. 2002: Application of k-ε turbulence models to enclosed basins: The role of internal seiches, Journal of Geophysical Research: Oceans (1978-2012), 107(C12), 23-1.
Lemmin, U. & Amouroux, A. 2012: The Influence of Climate Change on Lake Geneva, Climatic Change and Global Warming of Inland Waters: Impacts and Mitigation for Ecosystems and Societies, 201-217.
Peeters, F. et al. 2002: Modeling 50 years of historical temperature profiles in a large central European lake, Limnology and Oceanography, 47(1), 186-197.
Perroud, M. & Goyette, S. 2010: Impact of warmer climate on Lake Geneva water-temperature profiles, Boreal Environment research, 15(2).

13.4

Study of diurnal streamflow cycles in a high altitude catchment in the Swiss Alps

Raphaël Mutzner[1], Steven V. Weijs[1], Paolo Tarolli[2], Marc Calaf[3], Holly J. Oldroyd[1], Marc B. Parlange[1,4]

[1] *School of architecture, Civil and Environmental Engineering (ENAC), Laboratory of Environmental Fluid Mechanics and Hydrology, EPFL, Lausanne*
[2] *Department of Land, Environment, Agriculture and Forestry, University of Padova, Agripolis, viale dell'Universita 16, 35020 Legnaro (PD), ITALY.*
[3] *University of Utah, Department of Mechanical Engineering, Salt Lake City, UT, USA*
[4] *University of British Columbia, Department of Civil Engineering, Vancouver, BC, Canada*

The study of diurnal streamflow cycles is of critical importance for analysing freshwater quality and quantity, especially in headwater catchments. In glaciarized watersheds, diurnal streamflow cycles are typically dominated by snow or icemelt. During a field campaign in the summer 2012 in the Val Ferret watershed (draining area of 20.4 km^2, altitude ranging from 1773 m to 3206 m asl, see Figure 1), we deployed a wireless network of 24 meteorological stations, a fully equipped energy-balance station and cameras for time-lapse photography. Streamflow and water electrical conductivity were monitored at the outlet and two sub-basins of the watershed, where we observed diurnal streamflow cycles throughout the season.

In the first sub-basin, the diurnal streamflow cycle shifted from a snowmelt to an evapotranspiration dominated cycle whereas in the second sub-basin, the diurnal streamflow cycle was dominated by snowmelt/icemelt due to the presence of a small glacier. Comparisons between icemelt and evapotranspiration cycles showed that the two processes were happening at the same times of day but with a different sign. The amplitude of the snowmelt/icemelt cycle decreased expo-

nentially during the season and was larger than of the amplitude of the evapotranspiration cycle which was relatively constant during the season.

A conceptual model was applied to estimate the effect of evapotranspiration on the diurnal streamflow cycle in the icemelt dominated sub-basin. In the first sub-basin, active areas of evapotranspiration were computed dividing the daily volume of evapotranspirated water estimated with the diurnal streamflow cycle by the daily cumulated evapotranspiration measured at the energy balance station. Those areas were then attributed to the riparian area of the channel network which has been carefully monitored. The computation of the active evapotranspiration area was then applied to the second sub-basin for estimating daily evapotranspirated volume of water when the diurnal signal was icemelt dominated. Our study suggests that evapotranspiration damps the icemelt-diurnal streamflow cycle resulting in a possible underestimation of glacier mass balance.

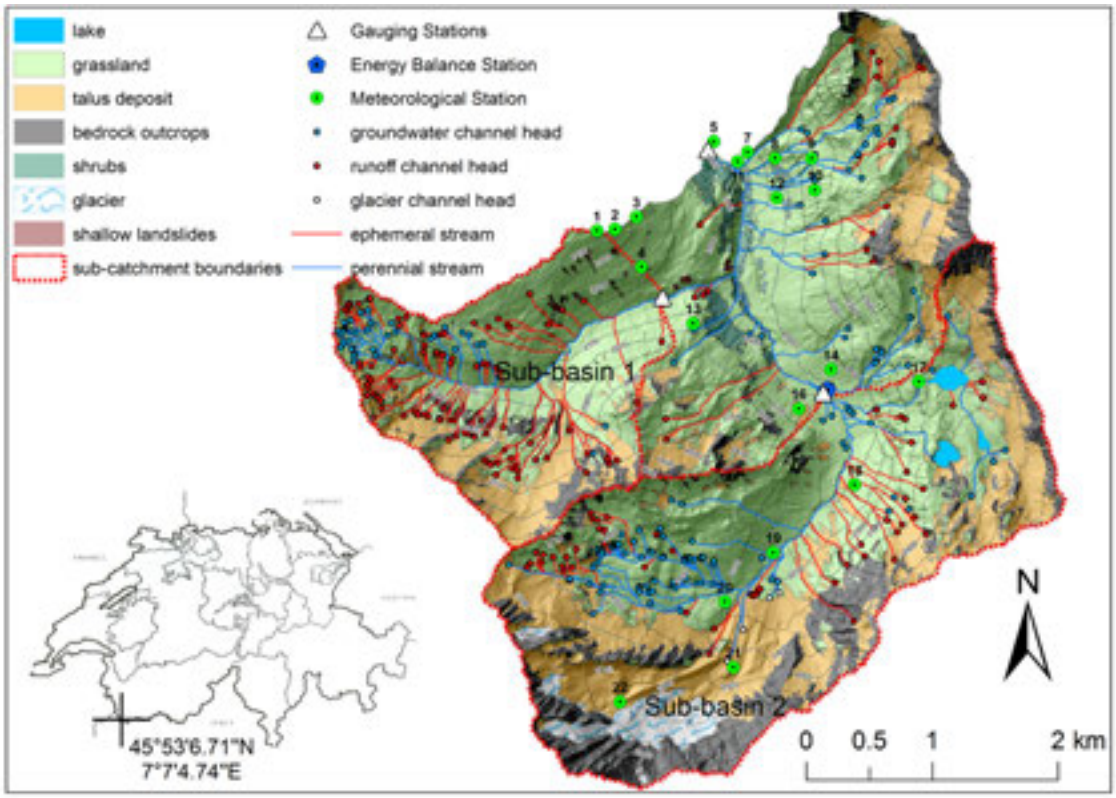

Figure 1 Map of the Val Ferret watershed showing the locations of the meteorological, Energy balance and gauging stations, the land cover, the locations of the monitored channel heads and the monitored network. The ephemeral and perennial parts of the channel network are represented by the solid red and blue lines, respectively.

13.5

Trenderhebung, Früherkennung und Erfolgskontrolle im Grundwassermonitoring - Konzepte der Nationalen Grundwasserbeobachtung NAQUA -

Miriam Reinhardt[1], Ronald Kozel[1]

[1] *Bundesamt für Umwelt BAFU, Abteilung Hydrologie, CH-3003 Bern (miriam.reinhardt@bafu.admin.ch)*

Grundwasser ist in allen Ländern Europas ein wichtiger einheimischer Rohstoff. So werden über 80% des Trinkwassers in der Schweiz aus Grundwasser gewonnen. Neben einer zunehmenden Versiegelung des Bodens durch das Siedlungswachstum wird das Grundwasser insbesondere durch Schadstoffe aus Landwirtschaft, Industrie, Gewerbe, Haushalten und Verkehr aber auch durch klimatische Veränderungen beeinflusst. Einmal ins Grundwasser gelangt, werden Schadstoffe dort kaum mehr abgebaut. Da sich Grundwasser zudem nur langsam erneuert, kommt vorausschauenden, präventiven Massnahmen zum Schutz des Grundwassers besondere Bedeutung zu. Um die Grundwasserressourcen zu erhalten und bestehende Beeinträchtigen zu beheben, ist eine nachhaltige Bewirtschaftung und ein integraler Schutz der Ressource Grundwasser unerlässlich. Um hierfür zielgerichtete Massnahmen entwickeln zu können, müssen die entscheidenden Zusammenhänge und Einflussgrössen verstanden und Defizite bzw. Handlungsfelder identifiziert werden. Diese Grundlagen kann ein landesweites Monitoring wie die Nationale Grundwasserbeobachtung NAQUA zur Verfügung stellen.

Entsprechend ihrem gesetzlichen Auftrag (Art. 50 und 57 GSchG) liefert die Nationale Grundwasserbeobachtung NAQUA ein landesweit repräsentatives Bild über Zustand und Entwicklung des Grundwassers in der Schweiz, sowohl in qualitativer als auch in quantitativer Hinsicht. Sie hat zum Ziel

- Zustand und Entwicklung der Grundwasser-Qualität und -Quantität auf Landesebene zu dokumentieren (Trenderhebung),
- das Auftreten problematischer Stoffe bzw. unerwünschter Entwicklungen frühzeitig zu erkennen und gezielt zu verfolgen (Früherkennung),
- die Wirksamkeit bereits ergriffener Schutzmassnahmen (z. B. ökologische Massnahmen in der Landwirtschaft) zu kontrollieren und die Notwendigkeit weitergehender Schutzmassnahmen aufzuzeigen (Erfolgskontrolle),
- die wichtigsten Grundwasservorkommen der Schweiz zu charakterisieren und zu klassifizieren.

Die Nationale Grundwasserbeobachtung bildet damit die Grundlage für einen gesamtschweizerisch koordinierten Schutz der natürlichen Ressource Grundwasser und dient somit letztlich dem Schutz des Menschen vor schädlichen Organismen und Stoffen.

Informationen über die Nationale Grundwasserbeobachtung und aktuelle Daten im Internet: http://www.bafu.admin.ch/naqua.

13.6

Assessing long term changes in the Orontes River basin (Lebanon and Syria): how to deal with variable, incomplete and heterogeneous datasets?

Myriam Saadé-Sbeih[1], François Zwahlen[2], Ahmed Haj Asaad[1], Raoul Gonzalez[1] & Ronald Jaubert[1]

[1] *Graduate Institute of International and Development Studies, Chemin Eugène-Rigot 2, CH-1202 Geneva (myriam.saade@graduateinstitute.ch)*
[2] *Centre for Hydrogeology and Geothermics (CHYN), University of Neuchâtel, Rue Emile-Argand 11, CH-2000 Neuchâtel*

The Orontes River basin is representative of the global changes in water use that occurred during the 20th and beginning of the 21st Centuries in the southern and eastern parts of the Mediterranean basin. In the Syrian part of the Orontes basin, since the 1950s large-scale surface water development has been a symbol of post-independancy and a major piece of the agricultural policy: the so-called "hydraulic mission" (Allan 2003; Molle 2009) was mostly translated into the state irrigation scheme of Al Ghab and the construction of several dams of different capacities and importance. Since the 1980s and especially in the 1990s, both Lebanese and Syria parts of the Orontes River basin witnessed a groudwater revolution (Giordano & Villholth 2007) with the development of individual pumping systems and a strong increase of groundwater extraction, mostly for agricultural purposes.

The available studies on the Orontes basin prior to the Syrian conflict (Comair et al 2013; Kloosterman & Vermooten 2008; Kibaroglu et al 2005) indicate that intensive surface and ground water development has led to a sharp decrease of the Orontes river discharge in its middle course; the drying up of several springs and overexploitation of groundwater in several areas. However, while the different studies agree on major trends, data are frequently contradictory. Furthermore, due to the transboundary nature of the Orontes River basin and thus the political sensitivity of related hydro(geo)logical data, available data are hardly accessible.

The purpose of this contribution is to confront the different datasets in order to understand the evolution of the recharge/discharge dynamics across the Lebanese and Syrian parts of the basin and the impact of water development on the fresh water system. The approach adopted consists of calculating water balance for 4 sub-catchments and for 3 years representative of the 1930s; 1970s; 2000s (respectively before the development of surface and ground water; after the development of surface water; after the development of groundwater).

The study first discusses the magnitude and spatialization of the anthropogenic disturbance and its consequences on the hydrosystem: for the overall basin, the water consumption increased from 265 MCM/y in the 1930s to 2230 MCM/y in the late 2000s, leading to spatially differentiated changes, critical mostly in the Al Ghab area. It secondly discusses the results sensitivity according to existing data availability and quality. The heterogeneity and incompletness of the dataset indeed reinforce the difficulty in distinguishing between "natural" variability (of rainfall, spring and river discharge…) and human-induced long term changes.

REFERENCES

Allan, J.A., 2003: IWRM/IWRAM: A new sanctioned discourse? Discussion Paper No.50. Water Issues Study Group, University of London.

Comair, G. F., McKinney D. C., Scoullos M. J., Espinoza G.E., Flinker R.E. 2013: Transboundary cooperation in internationanl basins : Clarification and experiences from the Orontes River Basin agreement, Part 1 et Part 2, Environmental Science and Policy, 31, 133-140.

Giordano M., & Villholth K. G. 2007: The Agricultural Groundwater Revolution Opportunities and Threats to Development, IWMI, Colombo.

Kibaroglu A., Klaphake A., Kramer A., Scheumann W. & Carius A. 2008: Cooperation on Turkey's transboundary waters, Adelphi research report.

Kloosterman, F.H., Vermooten J.S.A., 2008: Final Report, Development of a Numerical Groundwater Flow Model for the Larger Orontes Basin. Dutch-Syrian Water Cooperation, TNO report.

Molle, F., 2009: Hydraulic Bureaucracies and the Hydraulic Mission: Flows of Water, Flows of Power, Water Alternatives, 2(3), 328-349.

13.7

Supersaturation, a phenomenon ignored by most hydrogeologists

Heinz Surbeck[1], Frederic Bossy[2]

[1] *Nucfilm GmbH, Cordast; Switzerland, heinz.surbeck@sensemail.ch*
[2] *HydroSol Sarl, Bulle, Switzerland, frederic.bossy@hydrosol.ch*

Dissolved gases in groundwater are only rarely in equilibrium with the atmosphere. Hydrostatic pressure on soil gas bubbles dissolving in percolating water, compression of air pockets in karst systems, air leaks in pumps or pipes, releases of water from dams or drilling with compressed air all lead to supersaturation. Supersaturation means that the Total Dissolved Gas Pressure (TDGP), the sum of the partial pressures of the dissolved gases is higher than the atmospheric pressure. In the field of rare gas or isotope age determination this is frequently called “excess air”.

Supersaturation is stressing fish seriously at 5 % above atmospheric pressure. At 30 % it is deadly.

TDGP is easy to be measured. At thin walled silcone tube, closed on one side and connected on the other side to a pressure sensor is all you need.

Particularily high supersaturation has been found at a karst spring in Neirivue, canton of Fribourg, Switzerland. This water is used for a fish farm.

Details on the instrumentation and data are presented for this spring, including data on the efficiency of a degassing unit used to protect the fish from supersaturation.

In addition we will try to motivate hydrogeologist to have a closer look at supersaturation. Apart from the problem fishes get from it offers a wealth of still rarely used information.

13.8

Long-term monitoring of natural springs in the Röseren valley near Liestal (BL)

Stefanie von Fumetti

[1] *Forschungsgruppe Biogeographie, Departement for Environmental Sciences, University of Basel, St. Johanns-Vorstadt 10, CH-4056 Basel (stefanie.vonfumetti@unibas.ch)*

Natural springs are ecotones at the interface between the groundwater and the surface water. Ecologically they are of special importance as they provide a relatively stable habitat for species adapted to a constant aquatic environment. In Switzerland, natural springs are not strictly legally protected (Zollhöfer 2007). Their ecological relevance is however increasing their importance in research and nature conservation. The springs in the Swiss Tabular Jura reflect the limestone characteristics of the region: limesinter-rheocrenes and karstic springs occur relatively often. In the Röseren valley near Liestal (BL) many natural springs still exist. Since 2003 they are being investigated regularly. Thereby the focus is foremost on the macroinvertebrate assemblages and on the physico-chemical as well as structural parameters. In the 12 most frequently investigated springs the macrozoobenthic organisms were quantitatively sampled 2 to 10 times with a small surber-sampler in the past 11 years. The abiotic parameters were always monitored as well. Over time the physico-chemistry of the springs has stayed constant; some springs are slightly polluted with nitrate. Altogether over 70 species and higher taxa have been found in the springs; the number of taxa ranges between 22 and 38. The percentage of crenobiont taxa, spring specialists, is on average 30 %, which is high in comparison to other springs in the Swiss Jura Mountains (Küry 2013). The similarity of the species assemblages throughout the years within a spring was analysed with the SIMPER-method (PRIMER-E, Clarke & Gorley2006). Some springs showed a high similarity of nearly 70 % of their species assemblages, whereas in others the composition of the species assemblages varied considerably. A non-metric multidimensional scaling (nMDS) based on the faunistic data revealed a grouping of the springs according to the different spring types (R: 0.752, p: 0.001). The results illustrate that the springs in the Röseren valley are valuable spring habitats, which are inhabited by species assemblages that vary to a certain degree, but did not change totally, in the past 10 years. Ongoing research will focus on the question if environmental changes caused by Global Climate Change will intensify the variability of the species assemblages. In any case, the protection of these valuable habitats shall be enforced.

REFERENCES

Clarke, K.R. & Gorley, R.N. 2006: PRIMER v6: user manual. Plymouth, 1-190.

Küry, D. 2013: Charakterisierung und Schutz natürlicher und naturnaher Quellen im Kanton Basel-Landschaft. Gewässerschutzverband Nordwestschweiz, Basel, 1-55.

Zollhöfer, J.M. 1997: Quellen die unbekannten Biotope: erfassen, bewerten, schützen. Zürich, 1-153.

13.9

Measuring surface flow velocity with smartphones: potential for citizen observatories

Steven V. Weijs[1], Tristan Brauchli[1], Hendrik Huwald[1]

[1] *CRYOS, Ecole Polytechnique Fédérale de Lausanne (EPFL), Station 2, CH-1015 Lausanne (steven.weijs@epfl.ch)*

Stream flow velocity is an important variable for discharge estimation and research on sediment dynamics. Given the influence of the latter on rating curves (stage-discharge relations), and the relative scarcity of direct streamflow measurements, surface velocity measurements can offer important information for, e.g., flood warning, hydropower, and hydrological science and engineering in general.

With the growing amount of sensing and computing power in the hands of persons that frequently see daylight and go outside, and the advances in image processing techniques, there is now a tremendous potential to obtain hydrologically relevant data from motivated citizens. This is the main focus of the interdisciplinary WeSenseIt project.

In this subproject, we investigate the feasibility of stream flow surface velocity measurements from movie clips taken by (smartphone-) cameras. First results from movie-clip derived velocity information will be shown and compared to reference measurements.

P 13.1

Quantifying Alpine water demands: setup for a micro-observatory of irrigation and drinking water supply in the Crans-Montana-Sierre region (Valais, Switzerland)

Martin Calianno[1], Emmanuel Reynard[1]

[1] *Institute of Geography and Sustainability, University of Lausanne, Géopolis, CH-1015 Lausanne (martin.calianno@unil.ch)*

Several integrated studies on water management have recently been conducted in the Alps. They main aim is to confront water resources to water use in order to identify water scarcity issues that could possibly occur in mountainous regions (Bonriposi, 2013). Regarding the quantification of water resources availability, these works often rely on well-known hydro-climatic science and exhaustive datasets. However, regarding water use, direct measurements are rare and researchers either depend on rough estimations given by water managers or create indirect datasets using proxies. Therefore, there is a strong need to correctly quantify water uses and to define a monitoring methodology in Alpine regions (Reynard, 2000).

This poster puts forward the setup of a field campaign in Central Valais. It aims at quantifying water supplies for the two main water uses of the area: irrigation and drinking water. This campaign is divided into three steps:
1°) A clarification and definition of concepts related to water use. This preliminary step is essential to understand the meaning of the measurements that will be undertaken.
2°) A study on the spatial and temporal extent of water uses. This second part gives insights on the spatial and temporal patterns of Alpine water uses, thus allowing comparisons and production of consistent water balances.
3°) A case study, where the results of the two previous steps are applied. A micro-observatory of water supplies is currently being set up in the investigated area, with direct and continuous measurements.

This micro-observatory is located in the Crans-Montana-Sierre hillside and focuses on two water uses.
The first one is drinking water related to the Crans-Montana mountain resort. Based on currently existing equipment and new established monitors (installed on water meters), starting October 2014, water supplies will be continuously measured for three years at different time steps. Currently, water meters of the Montana municipality are already set up with radio transmitters, enabling monthly to daily measurements. In addition, smart metering will be set on a sample of users (2 hotels, 1 apartments block and 2 chalets), thus allowing hourly measurements. Additional radio transmitters will also be installed on a sample of existing water meters (for 2 hotels, 2 villas and 2 apartments blocks) in the municipality of Sierre, located in the Rhone River valley. This fully equipped setting will thus provide continuous monitoring of drinking water supply from high altitudes down to the Rhone River Valley.

Water supplies for irrigation will be also quantified. A water meter will be set up on an irrigated grasslands parcel and another one upstream of the vineyards irrigation network. These meters will be read manually during the irrigation season.

Finally, qualitative interviews will be undertaken among actors of these water uses in order to define users' characteristics, to better understand habits and practices and, subsequently, to explain the figures collected by the micro-observatory. This will then allow us to draw some indicators forecasting water uses in similar contexts.

REFERENCES

Bonriposi, M. 2013: Analyse systémique et prospective des usages de l'eau dans la région de Crans-Montana-Sierre (Suisse). Thèse de doctorat en géographie, Université de Lausanne.

Reynard, E. 2000: Gestion patrimoniale et intégrée des ressources en eau dans les stations touristiques de montagne. Les cas de Crans-Montana-Aminona et Nendaz (Valais). Thèse de doctorat en Lettres, Université de Lausanne.

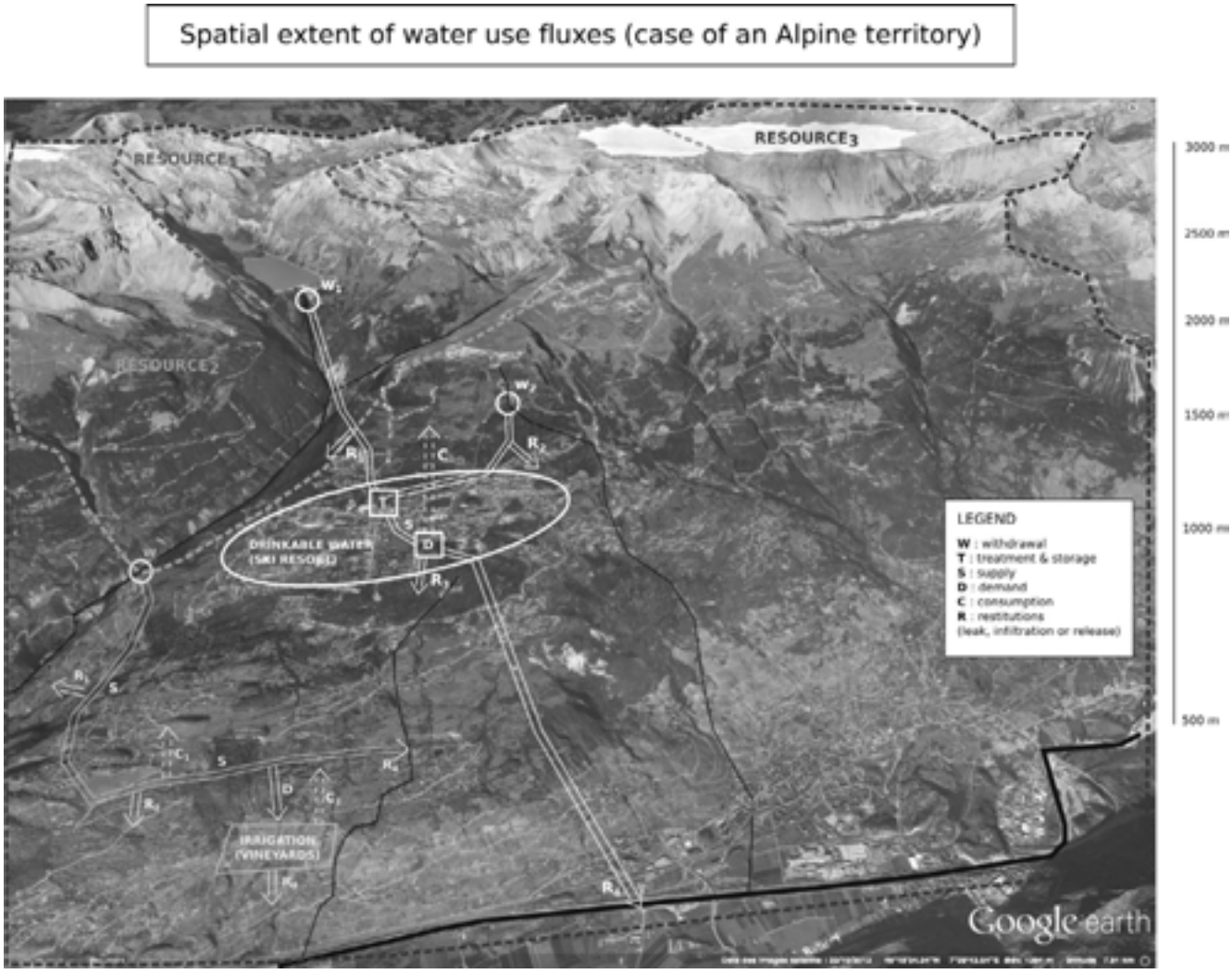

Figure 1. Spatial extent of water uses in the case of Crans-Montana hillslope.

P 13.2

Modeling the monthly mean stream temperature dynamics

Aurélien Gallice[1], Bettina Schaefli[1], Michael Lehning[1], Hendrik Huwald[1]

[1] *School of Architecture, Civil and Environmental Engineering, Ecole Polytechnique Fédérale de Lausanne (EPFL)*

Water temperature is a hydrological factor which affects the habitat suitability of many aquatic (fish) species, and is therefore of great concern in the actual context of climate change. Two types of models are currently used to simulate stream temperature: physically-based models, which are typically applied only over limited areas, and regression models, which usually lack the ability to make predictions in ungauged areas. As an attempt to bridge the gap between these two types, we propose a hybrid model based on the energy-balance equation, in which the terms are related to catchment physiographic variables via empirical relationships. The physiographic variables are chosen so as to be available over the entire country (Switzerland), enabling the model to be used in ungauged catchments. This approach is on the one hand more physically-based than the usual regression models – hereby limiting the degree of empiricism associated with its derivation – but on the other hand seeks simplicity and applicability over large areas – making it more practical than the usual physically-based models. In order to test this model, we use it to predict the monthly mean stream temperature over 23 selected medium-sized catchments (3–300 km^2) in Switzerland. While selecting the catchments, particular attention is given to cover a large range of different geomorphological conditions, especially regarding altitude, slope and aspect. It is shown that the model compares favorably with standard empirical models such as multi-linear regression.

14. National Research Programme NRP 68: Research for improving soil knowledge and for sustainable use of soils

A. Papritz, F. Hagedorn, J. Leifeld

National Research Programme «Sustainable Use of Soil as a Resource» (NRP 68)
Swiss Soil Science Society

TALKS:

14.1 Bader C., Leifeld J., Müller M., Schulin R.: Sustainable management of organic soils in Switzerland – CO_2 emissions from organic soils under agricultural use

14.2 Campos-Herrera R., Jaffuel G., Chiriboga X., Blanco-Perez R., Fesselet M., Mäder P., Mascher F., Turlings TCJ.: Assessment of the Natural Occurrence of Entomopathogenic Nematodes in Swiss Agricultural Soils

14.3 Colombi T., Kirchgessner N., Keller T., Walter A.: Above and below ground indicators for stress induced by compacted soils of small grain cereals and soybean

14.4 Della Peruta R., Gómez Giménez M., Keller A.: An integrated Modelling framework to monitor and predict trends of agricultural management (iMSoil). The Land Management Model (LMM).

14.5 Ferré M., Müller A., Engel S.: Sustainable management of organic soils in Switzerland – economic and policy analysis

14.6 Gómez-Sanz E., Jaenicke S., Goesmann A., Smits T.H.M., Duffy B.: Metagenomic analysis of long-term land-use effects on soil microbial communities in 600-year Alpine pasture system

14.7 Gosheva S., Gimmi U., Niklaus P., Walthert L., Hagedorn F.: Are Swiss forest soil carbon stocks resilient to historical land-use?

14.8 Krause H-M., Well R., Mäder P., Kappler A., Behrens S., Gattinger A.,: Influence of soil management on N_2O producing and reducing microbial communities

14.9 Manalili M., Keller T., Colombi T., Ruiz S., Schymanski S., Kirchgessner N., Reiser R., Oberholzer H., Rek J., Weisskopf P., Walter A., Or D.: A Soil Structure Observatory (SSO) to study structural recovery of compacted soil by natural processes

14.10 van der Heijden M.G.A., Schläppi K., Bender F., Verbruggen E., Rillig M., Wagg C., Oehl F.,: Restoration of soil functions and improving plant yield with the help of arbuscular mycorrhizal fungi

14.11 Van der Voort T.S., McIntyre C., Zell C., Feng X., Hagedorn F., Schleppi P., Eglinton T.I.: Scales of spatial & temporal variability in radiocarbon contents of organic carbon across different regions in Swiss soils

14.12 Yildiz A., Graf F., Rickli C., Springman S. M.: Quantification of Vegetation Effects on the Stress-Strain Behaviour of Soil

POSTERS:

P 14.1 Gomez Gimenez M., Della Peruta R., Schaepman ME., De Jong R.: Remote sensing sources for land cover differentiation of arable land and grassland to improve a Land Management Model

P 14.2 Papritz A., Baltensweiler A., Carizzoni M., de Jong R., Diek S., Fraefel M., Greiner L., Grêt-Regamey A., Grob U., Keller A., Nussbaum A., Schaepman M., Walthert L., Zimmermann S.: NRP68 project PMSoil: Spatial prediction of soil properties and soil function potentials from legacy soil data and environmental covariates

P 14.3 Diek S., De Jong R., Papritz A., Schaepman M.: Exploring the use of imaging spectroscopy in order to derive soil properties for agricultural areas in Zürich Oberland.

P 14.4 Fraefel M., Baltensweiler A.: Multi-Scale Terrain Modelling for Predictive Soil Mapping in Switzerland

P 14.5 Nussbaum M., Papritz A., Fraefel M., Baltensweiler A.: Predictive mapping of soil pH in forests of Zurich by component wise gradient boosting

P 14.6 Greiner L., Keller A., Zimmermann S., Papritz A.: Towards Soil Function Assessment for Switzerland

P 14.7 Ruiz S. A., Or D., Schymanski S. J. : Soil bioturbation by earthworms and plant roots- mechanical and energetic considerations for plastic deformation

P 14.8 González Domínguez B., Niklaus P., Abiven S.: Are Soils Systematically Influenced By Their Soil Ecosystem Properties?

P 14.9 Feng X., Pannatier E., van der Voort T., Montlucon D., Eglinton T.: Exploiting dissolved lignin as sentinels of soil organic matter vulnerability

P 14.10 Zell C., Van der Voort T., Feng X., Hagedorn F., Scheppi P., Eglinton T.: Molecular and radiocarbon sentinels of soil organic matter vulnerability: a project introduction

P 14.11 Hirte J., Leifeld J., Oberholzer H.R., Abiven S., Mayer J.: Long-term management effects on root biomass and carbon rhizodeposition of field grown maize

P 14.12 Friedli C., Abiven S., Walter A., Hund A.: Breeding and drought influence root biomass and rooting depth: lessons learned from the Swiss Era wheats.

14.1

Sustainable management of organic soils in Switzerland – CO_2 emissions from organic soils under agricultural use

Cédric Bader[1], Jens Leifeld[1], Moritz Müller[2], Rainer Schulin[3]

[1] *Agroscope Reckenholz Tänikon, Reckenholzstrasse 191, CH-8046 Zürich, (cedric.bader@agroscope.admin.ch)*
[2] *HAFL, Berner Fachhochschule, Länggasse 85, CH-3052 Zollikofen*
[3] *D-USYS, ETH Zürich, Universitätstrasse 16,CH 8092 Zürich*

The organic soils of peatlands represent a major global sink for terrestrial carbon. They cover approximately 4.16 x 106 km² of the earth's surface (Joosten et al. 2004) and store between 15-20% of organic soil carbon (Parish et al. 2008). Agricultural use of organic soils requires drainage, changing conditions in these soils from anoxic to oxic. As a consequence, the organic carbon that had been accumulated often over millennia is rapidly mineralized, so that these soils then are no longer a sink but become a source of CO_2. The emission rates of CO_2 from drained organic soils lie between 1 and 11 t C $ha^{-1}a^{-1}$ (Byrne et al. 2004, Couwenberg et al. 2011). In Switzerland, every year approximately 0.69 Mt CO_2 are emitted from 22'000 ha of drained organic soils (FOEN 2012). These rates correspond to 14% of agricultural CO_2 emissions.

The aim of our study is to analyse the amount and origin of CO_2 emitted from organic soils under three land-use types (forest, arable cropland and grassland). Our study area is located in Gals (BE) a community of the Bernese Lakeland. The peatlands of this region were drained in the 1870ies, and the site as well as the surrounding area is now managed by a state prison. Since decades our study sites are under the same land-use. In Mai 2014 we took three soil samples from each land-use site from a depth of 20-30cm. The samples were taken at different distances from a major drainage ditch (Fig.1).

Roots were removed manually, and the moisture content of the samples was equilibrated at a pF-value of 2.To determine the respiration rate 80 g of each sample were incubated for several weeks in a Respicond VII analyser at 20°C. Half of the sub-samples were spiked with 0.2-0.4 g of labelled corn stalk enriched in $\partial^{13}C$ ($\partial^{13}C$=2000‰) in order to mimic plant residue inputs in the field. The addition of fresh plant material resulted in a positive priming effect, and intensified respiration rates by 33, 82 and 88% in the forest, cropland and grassland samples, respectively. Comparing the stable isotopic signals of CO_2 emitted from spiked and control samples as well as the corn itself will reveal the contribution of corn and peat towards soil respiration. Using radiocarbon information from the peat samples, emitted CO_2 and corn, we also evaluate the contributions of old peat or young organic matter other than corn in the samples to the CO_2 emissions.

The samples are also analysed for their chemical composition, in particular the amounts of C, H, N and O. Infrared spectra will be recorded to determine the relative abundance of easily degradable polysaccharides.

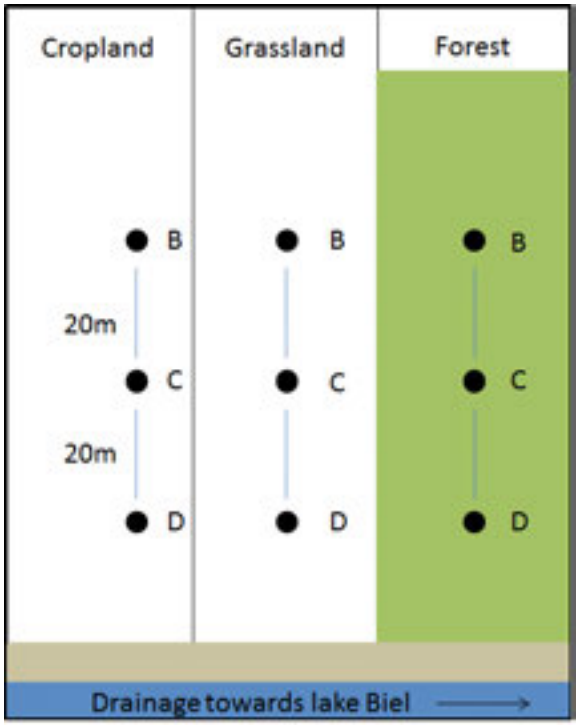

Figure 1: Study site in Gals (BE)

REFERENCES
Couwenberg, J., Thiele, A., Tanneberger, F., Augustin, J., Baerisch, S., Dubovik, D., Liashchynskaya, N., Michaelis, D., Minke, M., Skuratovich, A., Joosten, H., 2011. Assessing greenhouse gas emissions from peatlands using vegetation as a proxy. Hydrobiologia 674: 67-89.
FOEN, 2012. Swiss Agency for the Environment, Forests and Landscape FOEN. Switzerland's Greenhouse Gas Inventory 1990–2010. National Inventory Report
Höper, H., 2007. Freisetzung von Treibhausgasen aus deutschen Mooren. Telma 37, 85-116.
Joosten, H.: The IMCG Global Peatland Database, www.imcg.net/gpd/gpd.htm, 2004
Parish, F., Sirin, A., Charman, D., Joosten, H., Minayeva, T., Silvius, M. & Stringer, L. 2008. Assessment on peatlands, biodiversity and climate change: main report. Global Environment Centre, Kuala Lumpur and Wetlands International, Wageningen

14.2

Assessment of the Natural Occurrence of Entomopathogenic Nematodes in Swiss Agricultural Soils

Raquel Campos-Herrera[1], Geoffrey Jaffuel[1], Xavier Chiriboga[1], Rubén Blanco-Pérez[1], Marie Fesselet[2], Paul Mäder[3], Fabio Mascher[2] & Ted CJ Turlings[1]

[1] *FARCE Laboratory, University of Neuchâtel, Emile-Argand 11, Neuchâtel CH 2000 (raquel.campos@unine.ch)*
[2] *Département Fédéral de l'Économie, de la Formation et de la Recherche DEFR, Agroscope, Institut des Sciences en Production Végétale IPV, Route de Duillier 50, CP 1012, 1260 Nyon*
[3] *Forschungsinstitut für biologischen Landbau (FiBL), Research Institute of Organic Agriculture / Institut de Recherche de l'Agriculture Biologique Ackerstrasse 113, Postfach 219 CH 5070 Frick*

As part of a research consortium that explores how soil health can be improved by applying ecological and rational approaches (NRP68: Biology), we study how entomopathogenic nematodes (EPNs) can be better exploited for the biological control of soil-dwelling insect pests in annual crops. We hypothesized that the frequent disturbance of soils in annual crops will compromise the natural occurrence and activity of EPN due to frequent exposure to harsh abiotic conditions and limited availability of insect host. These factors are expected to also negatively affect other members of the soil food web, such as free-living nematodes (FLN) that compete for insect cadavers, ectoparasitic bacteria that limit the nematodes movement in the soil, and nematophagous fungi (NF), all of which have previously been shown to be spatially associated and distributed with EPN.

We combined traditional and new molecular methods to evaluate how below ground multitrophic interactions affect EPN activity and occurrence in three long term running Swiss field trials. Two of the experiments, both located in Nyon, focused on tillage soils: one experiment compared tillage *versus* light-tillage, as well as monoculture (continuous wheat) *versus* crop rotation (maize alternated with other crops) (P20), whereas the second experiment studied four levels of tillage in two soil types planted with wheat (P29). In the DOK trial based in Therwil we evaluated the impact of crop type (maize, wheat and grass) and fertilization program (conventional with manure, organic and biodynamic, each performed at two fertilizer levels, as well as a conventional system without manure and a unfertilized control).

We obtained composite soil samples (20 cores of 2.5 diam. X 20 cm depth per sample; Fig. 1A) from each plot during two sampling periods: April and in October 2013. To analyse the samples we employed previously published molecular probes for six EPN species (*Heterorhabditis bacteriophora, H. zealandica, Steinernema affine, S. carpocapsae, S. feltiae,* and *S. glaseri*) and designed and optimized the system for seven additional EPN species that might co-occur in Swiss soils (*H. megidis, S. bicornutum, S. intermedium, S. intermedium*-group, *S. kraussei-silvaticum, S. poinari* and *S. weiseri*). Other members of the EPN soil food web (six NF, one ectoparasitic bacterium, and the FLN *Acrobeloides*-group) were also quantified after sucrose centrifugation protocols (Fig. 1B) to assess how the soil food web is assembled under the mentioned practices.

In the tillage soils (P20 and P29), real time qPCR analysis detected only trace levels of six EPN species (*H. megidis, H. bacteriophora, S. affine, S. carpocapsae, S. kraussei-silvaticum* and *S. feltiae*), which was in agreement with the low mortalities observed

when we baited soil samples with larvae of *Galleria mellonella* (<5%). Overall, tillage did not affect the natural EPN occurrence in either experiments. Monoculture favored EPN activity as measured by bait larvae mortality, but it also favored their FLN competitors ($P < 0.01$), whereas it reduced NF richness ($P < 0.05$). Heavy soil harbored larger quantities of the natural enemies of EPN.

In the DOK trial, the same EPN species were detected, except *S. kraussei-silvaticum*. Soil management systems had no impact on the presence of these organisms ($P > 0.05$). However, crop type significantly shaped the activity ($P = 0.01$) and abundance ($P = 0.007$) of nematodes (EPN + FLN), which all were found to be more abundant and active in wheat plots ($P = 0.01$) (Fig. 1C and D). As in the tillage soils, the total numbers of EPN were very low, implying that their natural presence is not sufficient to have a suppressive effect on soil-dwelling insect pest.

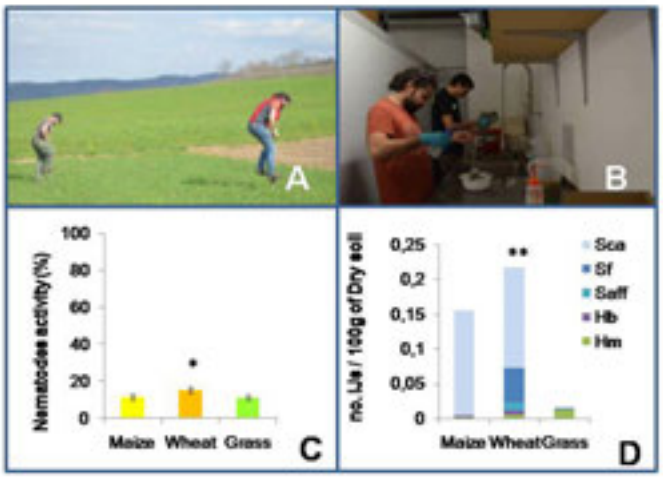

Figure 1. Nematode sampling (A), nematode soil food web extraction from soil samples by sucrose centrifugation (B) and effect of the crop type in the nematode activity (EPN + FLN) (C) and abundance (D). Entomopathogenic nematodes species: *Steinernema carpocapsae* (Sca), *S. feltiae* (Sf), *S. affine* (Saff), *Heterorhabditis bacteriophora* (Hb) and *H. megidis* (Hm); infective juveniles (IJs).

Our main conclusion is that under the ecological scenarios that we sampled, the most effective biological control strategy with EPN would be an augmentation rather than a conservation approach. Optimizing the timing and method of EPN application might provide effective alternatives to repeated convential applications. Ongoing collaborative experiments in Swiss annual crops will provide further insights into the natural occurrence, survival and persistence of EPN. This information will be used to develop new strategies for the general application of beneficial organisms to enhance soil health.

14.3

Above and below ground indicators for stress induced by compacted soils of small grain cereals and soybean

Tino Colombi1[1], Norbert Kirchgessner1, Thomas Keller2 and Achim Walter1

[1] *Swiss Federal Institute of Technology Zurich (ETHZ), Institute of Agricultural Sciences (IAS), Universitätsstrasse 2, 8092 Zurich (tino.colombi@usys.ethz.ch)*
[2] *Agroscope Zurich Reckenholz, Group for Soil Fertility and Soil Protection, Reckenholzstrasse 191, 8046 Zurich*

Soil compaction due to heavy agricultural machinery is a major environmental threat to arable soils, which is still difficult to detect and to quantify at the crop level. Increased mechanical impedance and disturbed water, solute and gas flows in compacted soils reduce root growth and crop productivity. A precise quantification of the above- and below-ground reaction of crops to this stress will help to identify indicators for compaction and suitable species, genotypes and management opportunities to mitigate compaction.

Soybean and small grain cereals were chosen to cover the variation between some of the globally most relevant crops in terms of plant development and root system architecture. To account for different plant developmental stages experiments were conducted under controlled conditions and in the field with the same soil.

In growth chamber experiments early responses of roots to two different soil bulk densities (1.34 and 1.60 g cm^{-3}) were evaluated using X-ray computed tomography periodically throughout 14 days. Five days after sowing soil compaction caused increased root diameters and decreased lateral root numbers in both species. Plant height and shoot dry weight decreased due to compaction in wheat, whereas no such responses occurred in soybean.

In the field the soil was compacted by multiple track-by-track passing with a heavy vehicle. In the case of triticale the topsoil was either ploughed or remained undisturbed, whereas for soybean the top five centimeters were tilled after compaction. Leaf growth rates and shoot biomass of both species decreased due to compaction. For triticale very similar root architectural responses to compaction were observed as under controlled conditions. Even if the topsoil was ploughed, numbers of nodal and lateral roots decreased, while their diameters increased under compaction. In soybean the lateral root number also decreased, while root diameters also decreased as a result of compaction.

These results showed that the reaction of root systems to soil compaction might differ substantially between different plant species and developmental stages. This points out the necessity to look at the entire growth cycle of crops, when identifying root traits that have the potential to mitigate soil compaction and maintain crop productivity under soil compaction.

14.4

An integrated Modelling framework to monitor and predict trends of agricultural management (iMSoil). The Land Management Model (LMM).

Raniero Della Peruta[1], Marta Gómez Giménez [2], Armin Keller[1]

[1] *Swiss Soil Monitoring Network, Agroscope, Reckenholzstrasse 191, CH-8046 Zurich (raniero.dellaperuta@agroscope.admin.ch)*
[2] *Remote Sensing Laboratories, University of Zurich, Winterthurerstrasse 190, CH-8057 Zurich*

Agricultural systems are subject to various pressures induced by a number of socio-economic drivers, leading to changes in farming practice. These changes can result in the intensification of agricultural land management, with implications on crop and livestock production, fertilization practices, pest management, tillage, and ultimately can adversely affect important soil functions. In order to steer the development into desired directions, tools are required by which the effects of these pressures on agricultural management and the resulting impacts on soil functions can be predicted or detected as early as possible. The use of integrated models, combining different scientific disciplines within a common framework,

can be very helpful in this context. Significant progress has been made in this field over the last decades. However, the development of such modeling frameworks has been hampered in the past by a lack of spatially explicit soil and land management information at regional scale. Moreover, the inherent characteristics and processes of the soil system have been often oversimplified.

The iMSoil project, funded by the Swiss National Science Foundation in the national research programme NRP68 "soil as a resource" (www.nrp68.ch) aims at developing and implementing an integrated modeling framework (IMF) which can overcome the limitations mentioned above, by combining socio-economic, agricultural land management, and biophysical models, in order to predict the long-term impacts of different socio-economic scenarios on the soil quality.

This presentation focus on the Land Management Model (LMM) that is one of the main component of the IMF. The LMM estimates fertiliser and pesticide application rates and calculates surface balances (input and output at the soil surface) of various elements such as N, P, Cu, Zn for each land management unit (i.e. a field or block of fields). These estimates are obtained through a downscaling approach which makes use of available geo-referenced farm census data, national fertilization guidelines and various concentration datasets combined with land use information derived from remote sensing data (the poster presented by Gómez Giménez et al. shows how remote sensing thecniques were used to distinguish the main land use types). Farm census data (essentially the area covered by each crop and the livestock number), together with compiled datasets and measurements of element concentrations in manure and element crop uptake, is used to estimate the crop spatial pattern and the element input to each land management unit. For this purpose an algorithm was developed that takes into account land use type, terrain attributes and the distance of the management units from the farm. Manure trading between farms is also simulated, based on a number of rules derived from Swiss legislation and interviews with agronomic consultants. Firstly, nutrient surplus or deficit at farm level is calculated. Then, the algorithm try to match manure offer and demand considering manure quantity, number of possible treatments and distance between farms. The LMM results are spatially explicit and can be displayed as maps representing, for example, annual phosphorus inputs (Figure 1).

The iMSoil project is currently testing the IMF on a case study region located in canton Zurich. Given the availability of Swiss farm census data, spatially explicit annual element balances can potentially be calculated since 1998 for the whole country. Thus, the changes occurred in the agricultural system over the last 16 years, as well as their impact on nutrient and trace element fluxes and on soil functions, can be quantified.

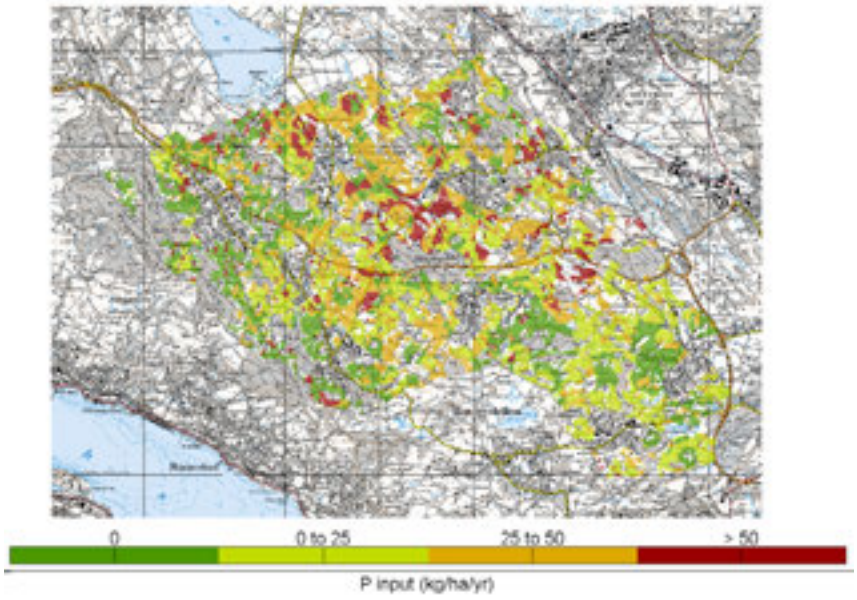

Figure 1. Phosphorus inputs for the year 2011 (kg P ha^{-1} yr^{-1}) over one of the iMSoil study areas (located in Canton Zurich), estimated using the land management downscaling approach (LMM).

REFERENCES

Della Peruta. R., Keller, A., Schulin, R. 2014: Sensitivity analysis, calibration and validation of EPIC for modelling soil phosphorus dynamics in Swiss agro-ecosystems. Environmental modelling and software (accepted).

Gärtner, D., Keller, A., Schulin, R. 2013: A simple regional downscaling approach for spatially distributing land use types for agricultural land. Agric. Syst. 120, 10-19.

14.5

Sustainable management of organic soils in Switzerland – economic and policy analysis

Marie Ferré[1], Adrian Müller[1] & Stefanie Engel[1]

[1] *Chair of Environmental Policy and Economic, Institute of Environmental Decisions, ETH – Zürich, Universitästrasse 22, 8092 Zürich, Switzerland*

SNF Project – NRP 68. Partners: PD. Dr. Jens Leifeld and Cédric Bader (Agroscope Reckenholz-Tänikon – ART - Switzerland), and Prof. Dr. Moritz Müller (Hochschule für Agrar-, Forst- und Lebensmittelwissenschaften – HAFL, Switzerland)

Agricultural production activities on peat soils lead to severe forms of degradation of this natural resource. This is mainly due to the intensive soil drainage, necessary to enable production. The current non-sustainable farming practices (from the perspective of the peat soil resource) combined with the effect of climate change increasingly contribute to the conversion of peat soils from carbon sinks to carbon sources with accompanying losses of soil fertility and of ecosystem values such as biodiversity (Xintu, 2009). These impacts are not restricted to the field but also concern the surrounding ecosystem. Besides, the continuing degradation of former peatland challenges the future of production activities at these places. This study aims at analyzing, from both production system and policy angles, the mechanisms which could prevent long-term disappearance of agriculturally utilized peat soils in Switzerland.

This study is composed of three interdependent parts. The first part consists of the selection of an indicator or a set of indicators able to capture the farming system performance on managed peat soils in an encompassing way, by accounting for "traditional" agricultural inputs (including factors of production characteristic to peatlands and differentiating pollution-causing inputs from non-pollution causing inputs) and outputs, as well as undesirable outputs (e.g. greenhouse gas emissions) and ecosystem services provision (e.g. soil water retention capacity). This indicator or set of indicators will be based on a productivity and efficiency analysis of farms operating on peat soils using a multiple-inputs multiple-outputs model and will enable assessment and comparison of land management options (e.g. intensive versus extensive land uses). Two complementary methods will be used for this analysis: data envelopment analysis (DEA) and stochastic frontier analysis (SFA). Economic data concerning the farming production system will be obtained from secondary data. Data relative to undesirable outputs, positive externalities provision, and some of the pollution-causing inputs will be obtained from the analysis of primary data collected in the companion NRP68's PhD project. At a broader level, the objective of this part is to build a conceptual framework in farm performance analysis applied to specific natural resource management (here peat soils) that considers the complete farming system, enables accounting for farm factors which are relevant at a landscape or regional level, are inter-dependent between farms, and allows the design of an indicator facilitating the comparison between different land uses.

The second part develops policy instruments orienting the farming system towards the adoption of more sustainable management practices, as identified in the NRP 68' companion research project. In the context of peat soil management, and considering the management of drainage systems, cooperation among farmers is hypothesized as a promising possibility to the adoption of alternative soil practices. Nevertheless, the study assumes that a wise combination of self-organization and external incentives is likely to perform optimally (Stallman, 2011). In this context, the field investigation will study the potential for market-incentive based policies and collective action around peat soil resource management. An experimental computerized game will be designed to study farmers' reactions and behaviors to different policy options and institutional features targeting the management of peat soil resource. The two main purposes of the game are 1) to study how farmers are willing to and interested in cooperating around the implementation of alternative peat soil management strategies and thus towards maintaining productivity on these soils on the long run, and 2) to study the types of incentives which could complement and strengthen such cooperation, through studying their effects on farmers' behaviors.

The last part focuses on analyzing and predicting the acceptance and effects of the implementation of the selected policy instruments. As compared to the previous part on design of policy options from the perspective of the conservation of peat soil's natural resource, this part will adopt the farmer's perspective, also using the results of the experimental game. It will be about studying the acceptance by farmers of the selected policy options as well as the potential effects and impacts of the associated measures on farmers' profession, farmers' territorial roles, positions and perceptions etc. After identifying eventual challenges and obstacles in the implementation of the selected policy instrument, the research will focus on ways to overcome them. Complementarily to the experimental game's results, the study may use assessment methods such as focus groups and interviews with different actors of the territory.

REFERENCES
Murty, M., Russell, R.R, & Levkoff, S. 2012: On modeling pollution-generating technologies, Journal of Environmental Economics and Management, 64, 117-135
Picazo-Tadeo, A.J., Beltrán-Esteve, M., & Gómez-Limón, J.A. 2012: Assessing eco-efficiency with directional distance functions, European Journal of Operational Research, 220, 798–809
Stallman, H. R. 2011: Ecosystem services in agriculture: Determining suitability for provision by collective management, Ecological Economics, 71, 131-139
Wiskerke, J.S.C., Bock, B.B., Stuiver, M., & Renting, H. 2003: Environmental co-operatives as a new mode of rural governance, pp. 9-25, Wageningen University, the Netherlands
Xintu, L. 2009: Conditions of peatlands formation, In Coil, oil shale, natural bitumen, heavy oil and peat, Vol. II, Changchun Institute of Geography, China

14.6

Metagenomic analysis of long-term land-use effects on soil microbial communities in 600-year Alpine pasture system

Gómez-Sanz E. 1, Jaenicke S. 2, Goesmann A. 2,3, Smits T.H.M. 1, Duffy B. 1

[1] *Environmental Genomics and Systems Biology Research Group, Institute of Natural Resource Sciences, ZHAW, Wädenswil, Switzerland;*
[2] *CeBiTec, Universität Bielefeld, Bielefeld, Germany;*
[3] *Bioinformatics and Systems Biology, Justus-Liebig-Universität, Giessen, Germany*

This study aimed to obtain a comprehensive profile of microbial communities and antimicrobial resistance (AMR) determinants in two proximal soil systems with a different treatment history, located at the alpine Glaspass (Switzerland). One of the sampling fields has been amended with manure for the past centuries (termed intensive), whereas the other corresponds to a free-range grazing area free of manure applications (extensive).

DNA was extracted from one pooled sample [10 equidistant pooled (5 replicates) samples] per soil system. Two metagenomic approaches were undertaken to estimate microbial diversity: (i) DNA was directly sequenced using a single run Illumina MiSeq (300 bp paired-end reads) per soil sample, yielding around 12 and 17 million reads, respectively; and (ii) 16S rRNA amplicon sequencing was performed yielding around 88,000 and 130,000 reads, respectively.

Both sequencing approaches showed similar trends in microbial communities. The five most abundant Bergey's classes detected were Betaproteobacteria, Actinobacteria, Alphaproteobacteria (all predominant in the dataset termed intensive), Acidobacteria Gp1 and Gammaproteobacteria (both predominant in extensive). Chitinophagaceae and Xanthomonadaceae were the predominant Bergey's families detected in the intensive and extensive dataset, respectively. Gp5 (Gp3 based on 16S rRNA profiling) and Gp6 were the most abundant Bergey's genera in intensive, while Gp1 and Gp2 were prominent in extensive.

The MvirDB database was used to search for AMR determinants. Entries retrieved from both soil systems included numerous (multi)drug efflux pumps (for tetracyclines, macrolides, phenicols); antibiotic target protection proteins (macrolides-lincosamides-streptogramins, tetracyclines, fluoroquinolones); antibiotic modifying (aminoglycosides, lincosamides, phenicols, tetracycline) or degradation enzymes (betalactams); and antimicrobial target replacement proteins (diaminopyrimidines, sulfonamides, glycopeptides, betalactams). A set of reads was also assigned to integrases (IntI3, IntI1) and transposases, which were also detected in the Enzyme Commision (EC) and COG number category annotations. An ongoing functional metagenomics approach of both soils systems is devoted to the characterization of novel AMR determinants.

Keywords: comparative metagenomics, 16S rRNA profiling, soil systems, manure, antimicrobial resistance

14.7

Are Swiss forest soil carbon stocks resilient to historical land-use?

Sia Gosheva[1], Urs Gimmi[1], Pascal Niklaus[2], Lorenz Walthert[1], Frank Hagedorn[1]

[1] *Forest Soils and Biogeochemistry, Swiss Federal Institute of Forest, Snow and Landscape Research (WSL), Zürcherstrasse 111, CH-8903 Birmensdorf (sia.gosheva@wsl.ch)*
[2] *Insitute of Evolutional Biology and Environmental Studies, University of Zurich, Winterthurerstrasse 190, CH-8057 Zurich*

Forest cover in Switzerland has increased by approximately 22% in the last century (Ginzler et al. 2011). Since soils store the highest amounts of carbon in the terrestrial ecosystems, it is important to understand if and how these forest cover changes have affected soil carbon stocks. However, our knowledge is currently still very limited due to the lack of historical soil samples and the lack of soil studies on historical land-use.

Our approach was to reconstruct past forest cover changes and to estimate how these changes have affected current soil C storage. Using the coordinates of 1000 soil profiles from the soil data base of the Swiss Federal Institute for Forest, Snow and Landscape Research (WSL), we reconstructed forest cover changes for the last 150 years. For that goal, we evaluated historical and modern topographic maps using ArcGIS, classifying forest cover into forest, no-forest, forest edge, and open forest. The oldest nationwide maps containing forest cover for the territory of Switzerland are the Dufour original surveys, dating back to 1850. For the period around 1900 and 1950, we used Siegfried maps, and between 1950 until 2011 – modern topographic maps. This allowed us to estimate the time since afforestation, the minimal forest age, and the forest cover continuity for all currently forested sites. Moreover, we examined the effect of tree species composition on soil carbon to further improve our knowledge of the interactions between above-ground vegetation and soil.

Our analysis shows that approx. 75% of the current forest soil profiles have been located in forest areas already in 1850, whereas 12% sites have been located outside a forest at the time. Further 12% have been located at a forest edge and 1% - in an open forest. Surprisingly, our results indicate slightly higher SOC stocks in younger forest sites compared to sites that have permanently been forested. This result could be seen in both the organic layer and the mineral soil (Figures 1 and 2, respectively). Moreover, we observed higher SOC stocks under coniferous than under decidous or mixed forests – however, this was only evident in the organic layer, but not in the mineral soil.

We tested a number of potential explanations for the higher C-stocks in new forests such as altitude, temperature, pH, soil structure. However, none of these drivers differed significantly between the permanent and the new forest sites. Probably, the younger forests have been growing on soils with inherently higher C-stocks, such as favorable land previously used for grassland. Thus, we come to the conclusion that forest cover has a neglible effect on carbon stocks in Swiss forest soils.

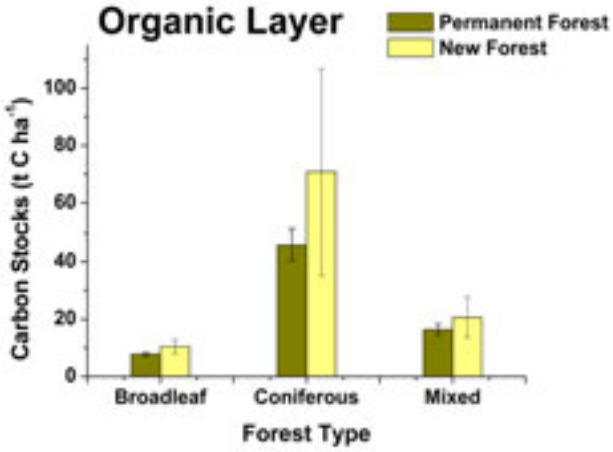

Figure 1. Forest type and cover effect on C-stocks in organic layer

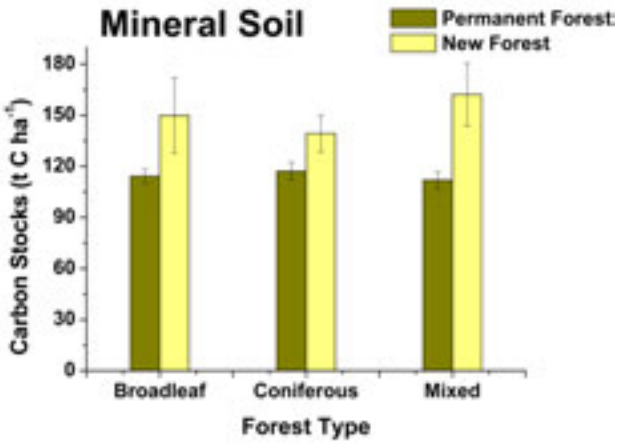

Figure 2. Forest type and cover effect on C-stocks in mineral soil.

REFERENCES

Ginzler, C., Brändli, U-B., Hägeli, M. 2011: Waldflächenentwicklung der letzten 120 Jahren in der Schweiz, Schweiz Z Forstwes 162 (2011) 9: 337-343.

14.8

Influence of soil management on N_2O producing and reducing microbial communities

Hans-Martin Krause[1], Reinhard Well[2], Andreas Kappler[3], Paul Mäder[1], Sebastian Behrens[3], Andreas Gattinger[1]

[1] *Soil Sciences, Research Institute of Organic Agriculture, Ackerstrasse 113, CH-5070 Frick (hans-martin.krause@fibl.ch)*
[2] *Institute of Climate-Smart Agriculture, Thünen Institute, Bundesallee 50, 38116 Braunschweig*
[3] *Geomicrobiology, Center for Applied Geosciences, University Tübingen, Hölderlinstrasse 12, 72074 Tübingen*

N_2O is a potent greenhouse gas, with an atmospheric half lifetime of 113 years, which also contributes to ozone layer destruction. Agriculturally managed soils hold for the gross of anthropogenic N_2O release. In order to develop effective mitigation strategies a detailed understanding of processes and mechanisms leading to N_2O formation and reduction in croplands is urgently needed. Although the influence of single parameters on N_2O emission is quite well understood, knowledge on the underlying mechanisms especially under complex farming systems is still sparse. Different farming strategies like reduced tillage, organic soil management and biochar addition have the potential to influence extend of N_2O emissions from croplands.

As cycling of fixed N in soils is almost entirely controlled by microbial activities it is crucial to understand the impact of soil management on N cycling microbial communities. Generally, N_2O is produced by nitrifying and denitrifying microbial communities. However, when assessing impact of microbial communities on N_2O emissions special emphasis must be put on N_2O reducing microbial communities. This functional guild can perform the last step of denitrification, the reduction from N_2O to N_2, and thus reduces N_2O emissions from soils.

In order to assess impact of reduced tillage, biochar addition and organic soil management on N_2O emissions individual field and incubation experiments under controlled conditions were conducted. Here we present the first results of an incubation study in which the impact of organic and mineral fertilization history on potential N_2O emissions was assessed. Therefore, soil was taken from the DOK trial in Therwil/BL and incubated for 17 days under controlled conditions optimal for denitrification processes.

Apart from monitoring N_2O emissions qPCR analysis of functional genes was employed to quantify archaeal and bacterial *amoA*, *nirK* and *nirS* as proxy for nitrifying and denitrifying communities. N_2O reducing bacteria were assessed by quantifying the functional gene *nosZ*. Additionally mRNA analysis was used to measure expression of these functional genes. In order to verify molecular biological data ^{15}N tracing technique was used to determine N_2O/N_2 product ratio and fertilizer derived sources of N_2O emissions.

First results show increased N_2O emission potential of organic fertilization history. Higher N_2O/N_2 product ratios indicate less complete denitrification in this treatment. Increased C_{org} contents seem to provide excess electrons for all denitrification processes, which leads to a decrease of the kinetically unfavorable process of N_2O reduction.

These results emphasize the need for appropriate soil management to minimize N_2O emissions especially for soils with organic fertilization history.

14.9

A Soil Structure Observatory (SSO) to study structural recovery of compacted soil by natural processes

Mervin Pogs Manalili[1], Thomas Keller[1], Tino Colombi[2], Siul Ruiz[3], Stan Schymanski[3], Norbert Kirchgessner[2], René Reiser[1], Hansrudolf Oberholzer[1], Jan Rek[1], Peter Weisskopf[1], Achim Walter[2], and Dani Or[3]

[1] *Department of Natural Resources and Agriculture, Agroscope, Reckenholzstrasse 191, CH-8046 Zürich (mervin.manalili@agroscope.admin.ch)*
[2] *Institute of Agricultural Sciences, ETH Zürich, Universitätstrasse 2, CH-8092 Zürich*
[3] *Institute of Terrestrial Ecosystems, ETH Zürich, Universitätstrasse 16, CH-8092 Zürich*

Agricultural soil compaction adversely impacts the soil's structure, productivity and ecological processes thereby affecting crop growth and other ecosystem services. Most soil compaction studies focus on quantifying compaction and immediate impacts on soil hydrology and productivity. Little is known about mechanisms and rates of natural soil structure recovery after compaction. However, knowledge of soil structural regeneration is required for quantification of the real costs of soil compaction. The primary objective of the newly-launched long-term soil structure observatory (SSO) is to quantify post-compaction structural restoration at years to decade time scales. The SSO was established on a loamy soil in Zurich, Switzerland, and monitors key biophysical properties affecting soil structure restoration such as root growth, shrink-swell of soils and earthworms bioturbation. We implemented three compaction treatments: uncompacted surface, full surface compaction and wheel-track compaction. On each of these treatments we apply four cropping systems (bare soil; permanent grass; crop rotation - no till; and crop rotation - conventional tillage) replicated in three blocks. The site was characterized pre- and post-compaction, and sensor banks were installed for continuous monitoring of soil water content and matric potential, temperature, CO_2 and O_2 concentrations, redox potential and oxygen diffusion rates. Soil sampling and measurements are done periodically, including soil surface elevation, soil physical properties, earthworm abundance and burrows, below and above ground crop measurements, as well as electrical resistivity tomography (ERT) and ground penetrating radar (GPR) imaging to observe structural changes over time at the plot scale. Comparison of soil properties before and after compaction show a significant decrease in soil porosity and infiltration rates (2 orders of magnitude), a decrease in O_2 and increase in CO_2 soil air concentrations in compacted plots. GPR and ERT images show differences in electrical permittivity and resistivity in compacted relative to uncompacted plots. This SSO study aims to monitor the evolution of soil structure and the soil functions associated with it, under different treatments during the next 10 years.

14.10

Restoration of soil functions and improving plant yield with the help of arbuscular mycorrhizal fungi

Marcel van der Heijden[1], Klaus Schläppi[1], Franz Bender[1], Erik Verbruggen[2], Matthias Rillig[2], Cameron Wagg[1], Fritz Oehl[1],

[1] *Plant Soil Interactions, Institute for Sustainability Sciences, Agroscope, Reckenholzstrasse 191, CH-8046 Zürich (marcel.vanderheijden@agroscope.admin.ch)*
[2] *Institut für Biologie, Freie, Universität Berlin, Berlin, Germany*

Soils are the basis for nutrient production and a main component for maintaining biological diversity. Arbuscular mycorrhiza fungi (AMF), a common group of soil fungi, play a crucial role for various important soil ecosystem services. They form symbiotic relationships with most terrestrial plants, including most crop plants. They can improve plant growth and promote plant diversity (van der Heijden et al. 2008). In this project we used molecular tools (single molecule real-time (SMRT) sequencing and 454 sequencing) to characterise fungal communities in a wide range of fields with different land use intensity. We present first insights into AMF communities in roots of wheat plants and we show that one particular group of soil fungi (Sebacinales) are characteristic for organically managed arable fields (Figure 1, Verbruggen et al. 2014). Using this information we aim to characterise fungi as bioindicator species for different land management practices (Oehl et al. 2011). Secondly, we have performed inoculation trials to test whether introduction of AMF in field soil can enhance plant yield, nutrient uptake and nutrient use efficiency (Bender & van der Heijden 2014). First results indicate that inoculation of AMF can enhance plant yield and nutrient use efficiency in some soils, but results are variable and dependent on soil type and crop species. Moreover, in ongoing work, the obtained AMF community profiles will be used as a basis for the targeted inoculation of AMF species in field soils. We examine if the taxonomy-based application of AMF inoculum enhances plant productivity.

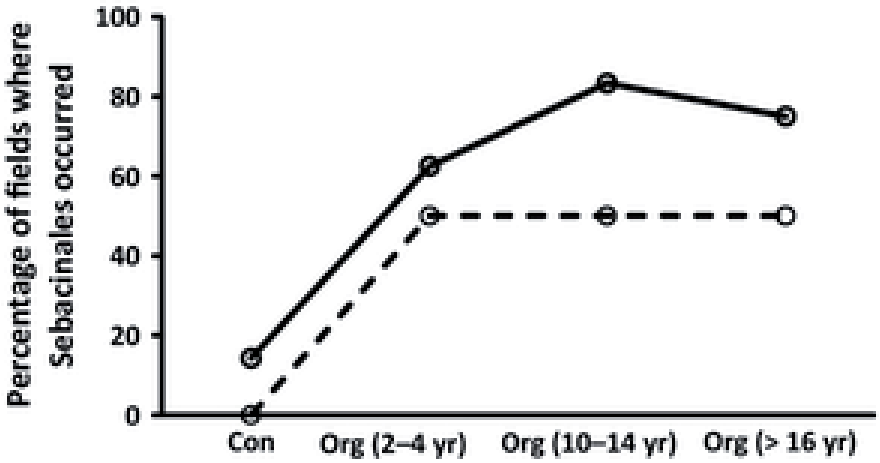

Figure 1. The percentage of fields within each management group (Con, conventional; Org, under organic management) in which members of Sebacinales were detected in wheat roots. NGS (open circles, dashed line), represents fields where Sebacinales were detected using Next Generation Sequencing; Total (open circles, solid line) represents the number of fields including both NGS and Sebacinales specific PCR (effect of management NGS: $\chi 2=5.64$, $P=0.027$; Total: $\chi 2=7.48$, $P< 0.01$) (see Verbruggen et al. 2014).

REFERENCES

Bender S.F, van der Heijden, M.G.A (2014) Soil biota enhance agricultural sustainability by improving crop yield, nutrient uptake and reducing nitrogen leaching losses. Journal of Applied Ecology (in press)

Oehl, F., Jansa, J., Ineichen, K., Mäder, P., van der Heijden, M.G.A. (2011) Arbuskuläre Mykorrhizapilze als Bioindikatoren in Schweizer Landwirtschaftsböden. Agrarforschung Schweiz 2: 304-311

van der Heijden, M.G.A., Bardgett, R.D., van Straalen, N.M (2008). The unseen majority: soil microbes as drivers of plant diversity and productivity in terrestrial ecosystems. Ecology Letters 11: 296-310

Verbruggen E, Rillig, M, Wehner J, Hegglin D, Wittwer R, van der Heijden, M.G.A., (2014) Sebacinales, but not total root associated fungal communities, are affected by land use intensity. New Phytologist (in press).

14.11

Scales of spatial & temporal variability in radiocarbon contents of organic carbon across different regions in Swiss soils

Tessa S. van der Voort1, Cameron McIntyre2, Claudia Zell1, Xiaojuan Feng1,3, Frank Hagedorn4, Patrick Schleppi4, Timothy Eglinton1

[1] *Institute of Geology, ETH Zürich, Sonneggstrasse 5, 8092 Zürich, Switzerland*
[2] *Department of Physics, Laboratory of Ion Beam Physics, ETH Zurich, Otto-Stern-Weg 5, 8093 Zurich*
[3] *Institute of Botany, Chinese Academy of Sciences, 20 Nanxincun Xiangshan, Tuzilou 218 Beijing 100093, China*
[4] *Swiss Federal Research Institute WSL, Forest soils and biogeochemistry, Zürcherstrasse 111, 8903 Birmensdorf, Switzerland*

Soil organic matter (SOM) forms the largest terrestrial pool of carbon outside of sedimentary rocks, and it provides the fundamental reservoir for nutrients that sustains vegetation and associated microbial communities. With ongoing changes in land-use and climate, SOM is subject to change, with potentially major consequences for soil as a resource and for global biogeochemical cycles. Radiocarbon is a powerful tool for assessing OM dynamics and is increasingly used in studies of carbon turnover in soils. However, due to the nature of the measurement, comprehensive ^{14}C studies of soils systems remain relatively rare. In particular, information on spatial variability in the radiocarbon contents of soils is limited, yet this information is crucial for establishing the range of baseline properties and for detecting potential modifications to the SOM pool.

The present study aims to develop and apply a comprehensive four-dimensional approach to explore heterogeneity in bulk SOM ^{14}C, with a broader goal of assessing controls on organic matter stability and vulnerability in soils across Switzerland. Focusing on range of Swiss soil types, we examine spatial variability in ^{14}C as well as ^{13}C and C:N ratios over plot (decimeter to meter) to regional scales, vertical variability from surface to deeper soil horizons, and temporal variability by comparing present-day with archived (legacy) samples.

Preliminary results show that differences in SOM ^{14}C age across small lateral and vertical distances within soil systems can be as large as those between regions, underlining the importance of considering compositional heterogeneity in assessing SOM dynamics. These studies of bulk variability are being followed up with analyses of SOM sub-fractions, including ^{14}C measurements at the molecular level in order to SOM components that are most sensitive to climate change and anthropogenic pressures. Such investigations of ^{14}C variability over various space and time domains will shed light on the scales of processes that drive the composition and vulnerability of SOM, and provide valuable constraints on models of SOM turnover.

14.12

Quantification of Vegetation Effects on the Stress-Strain Behaviour of Soil

Anil Yildiz[1], Frank Graf[1], Christian Rickli[2] & Sarah M. Springman[3]

[1] *WSL Institute for Snow and Avalanche Research SLF, Flüelastrasse 11, CH-7260 Davos Dorf (anil.yildiz@slf.ch)*
[2] *Swiss Federal Institute for Forest, Snow and Landscape Research WSL, Zürcherstrasse 111, CH-8903 Birmensdorf*
[3] *Institute for Geotechnical Engineering, ETH Zürich, Wolfgang-Pauli-Strasse 15, CH-8093 Zürich*

The effects of vegetation on the stability of soil has been widely investigated and well recognized in the last decades. Root reinforcement has been investigated based on different approaches including laboratory or in-situ shear tests of rooted soil, employing analytical models of soil-root interaction or by the use of relatively novel methods such as the Fibre Bundle Model (FBM). Traditional methods, generally, consider roots passing through the shear surface and full development of tensile strength of the roots (Wu *et al*. 1979). However it has been shown that lateral roots contribute to strength as well, and roots and soil do not necessarily fail simultaneously (Sakals & Sidle 2004; Potten *et al*. 2004). A robust inclinable large-scale direct shear apparatus was constructed in order to evaluate the effect of a soil-root system on the shear behaviour of soil. It is intended to present the design and mechanical aspects of the apparatus, as well as the results of the ongoing initial tests in this study.

Direct shear tests have been conducted on unplanted and planted soil samples at a constant rate of horizontal displacement of 1 mm/min to a maximum horizontal displacement of 200 mm. Three different normal stress levels, namely 6 kPa, 11 kPa and 18 kPa, are chosen to be comparable to the average depth of shallow landslides. Planted samples consisting of combinations of a tree (*Alnus incana*), legume (*Trifolium pratense*), and grass (*Poa pratensis*) have been prepared using moraine (SP-SM) from a recent landslide area in Central Switzerland. Planted samples are maintained in shear boxes (500x500x400 mm) inclined at 30° simulating a slope and corresponding natural growth of roots on it. Both unplanted and planted samples are saturated prior to testing by applying rainfall at a constant intensity (100 mm/h) in order to simulate the loss of strength after a heavy rainfall period. Analyses of the test data will not only be based on increased shear strength due to root reinforcement, but also the general stress-strain behaviour of root-permeated soil and the dilatancy.

REFERENCES

Pollen, N., Simon, A. & Collison A. 2004: Advances in Assessing the Mechanical and Hydrological Effects of Riperian Vegetation on Streambank Stability, Riparian Vegetation and Fluvial Geomorphology, 125-139.

Sakals, M. E., & Sidle, R. C. 2004: A spatial and temporal model of root cohesion in forest soils, Canadian Journal of Forest Research, 34, 950-958.

Wu, T. H., McKindell, W. P., III, & Swanston, D. N. 1979: Strength of tree roots and landslides on Prince of Wales Island, Alaska, Canadian Geotechnical Journal, 16, 19-33.

P 14.1

Remote sensing sources for land cover differentiation of arable land and grassland to improve a Land Management Model

Marta Gómez Giménez[1], Raniero Della Peruta[2], Armin Keller[2] , Michael E. Schaepman[1] & Rogier de Jong[1]

[1] *Remote Sensing Laboratories, Department of Geography, University of Zurich-Irchel Winterthurerstrasse 190, CH-8057 Zurich (marta.gomez@geo.uzh.ch)*
[2] *Agroscope Reckenholz-Tänikon (ART) Swiss Soil Monitoring Network (NABO), Reckenholzstrasse 191 CH-8046 Zurich*

INTRODUCTION:
Agriculture plays an important role as service provider to human activities. This sector is characterized by sustainability and market-oriented principles, which have been well established through different actions e.g. laws, constitution articles and subsidies (Conseil 1998); (OECD 1998); (Confédération 1999). About one third of Switzerland with an extention of 41,285 km^2 is occupied by Utilised Agricultural Area (UAA). The total UAA is classified by the Federal Statistics Office (FSO) in 7 classes: grassland (70.9%), cereals (maize, oats, barley, wheat and other cereals), potatoes, sugar and fodder beet, oilseeds, permanent crops, other arable land and other UAA (FSO 2011). Monitoring the state and the dynamics of the UAA and knowledge of the land managament of this area is essential for many environmental models that deal with agricultural systems. For instance, to foster sustainable land management and ensure fluxes of natural resources without jeopardising biodiversity and conservation goals stated in the Swiss Agricultural Policy.

OBJECTIVE:
The objective of this study is to improve a Land Management Model (LMM) within an Integrated Modelling framework to monitor and predict trends of agricultural management (NRP68 iMSoil project). Remote sensing (RS) sources are used to improve the differentiation between arable land and grassland in space and time compared to the often-used areal statistics. Based on the spatial units provided by RS and geo-referenced farm census data, the LMM estimates fertiliser and pesticide application rates and calculates surface balances (input and output at the soil surface) for various elements such as N, P, Cu, Zn for each land management unit. In order to link RS sources with the LMM we follow a tiered approach: I) Land cover classification, II) Land use classification and III) Land management classification. This study is focused on the first stage with a land cover differentiation of arable land and grassland in an agro-ecosystem located in the Canton Zurich.

DATA AND METHODS:
Two Landsat 8 images from summer and winter were used. Atmospheric corrections were applied and topographic corrections were avoided due to the smooth orography with most of the slopes around 3%. A pixel-based classification approach was carried out in the northern part of the study site leaving the southern part for validation. Maximum likelihood classification was chosen for its robustness and sufficient training areas were collected to meet statistical criteria. Ancillary data and one spectral index were used to mask out images, to avoid misclassification and to validate the results. The final product with 30m spatial resolution was aggregated into cells of 1 ha to assess the LMM's spatial resolution sensitivity.
RESULTS: The classification assessment reported an overall accuracy of 88.4% and 82.7% for the summer and winter images respectively. Combining both classifications improved the arable land and grassland estimation. Nevertheless, the comparison with a farm census showed that arable land was underestimated for 9%, as well as the total agricultural area, i.e. 285 ha less than the proportion reported by farmers. The use of ancillary data e.g. vector layers validated in the field and a spectral index are useful to avoid misclassifications and contribute to maintain a coherent amount of agricultural area between classifications. However, it might be generalizing some land covers classes (e.g. urban areas) and underestimating the total agricultural area, further analyses are needed to determine this issue. In addition, low spectral separability between classes such as crops and grassland and the impossibility of differentiating temporary grassland (as part of arable land) with only two images and without *a priori* land cover knowledge produce the overestimation of the grassland area. The first test run with the LMM showed that spatial resolution is a key point for land allocation to the farms. Increasing the spatial resolution (from 100m to 30 m) decreased the amount of non-allocated farmland by 860.5 ha.

CONCLUSIONS:
The combination of two Landsat 8 images from different seasons improves the discrimination of arable land and grassland. However, a longer multi-temporal analysis of images is required to estimate the agricultural extent more accurately and improve the differentiation between the land use types. Higher spatial resolution sources would be needed to improve the overall classification accuracy as well as a field campaign to train the classifier and validate the results. Thus, the use of a non-parametric classifer, for which less number of training samples do not lead to worse results (Pal and Mather 2003); will be more suitable for futher analysis. The LMM sensitity to spatial resolution makes appropriate change the methodology approach to a object oriented classification. These recommendations will be implemented in the next project stage.

REFERENCES
Confédération. 1999. Constitution fédérale de la Confédération suisse. Confédération suisse.
Conseil. 1998. Ordonnance sur les paiements directs versés dans l'agriculture (Ordonnance sur les paiments directs, OPD). Conseil fédéral suisse.
FSO. 2011. Agriculture and Forestry. Swiss Agriculture. Pocket Statistics. Federal Statistics Office. Federal Department of Home Affairs., 36. Neuchâtel.
OECD. 1998. The Environmental Effects of Reforming Agricultural Policies. Paris: OECD.
Pal, M. & P. M. Mather (2003) An assessment of the effectiveness of decision tree methods for land cover classification. Remote sensing of environment, 86, 554-565.

P 14.2

NRP68 project PMSoil: Spatial prediction of soil properties and soil function potentials from legacy soil data and environmental covariates

Andreas Papritz[1], Andri Baltensweiler[2], Marco Carizzoni[3], Rogier de Jong[4], Sanne Diek[4], Marielle Fraefel[2], Lucie Greiner[5], Adrienne Grêt-Regamey[6], Urs Grob[5], Armin Keller[5], Madlene Nussbaum[1], Michael Schaepman[4], Lorenz Walthert[2], Stephan Zimmermann[2]

[1] *Institute of Terrestrial Ecosystems (ITES), ETH Zurich, Universitätstrasse 16, 8092 Zürich (papritz@env.ethz.ch)*
[2] *Swiss Federal Institute for Forest, Snow and Landscape Research (WSL), Zürcherstrasse 111, 8903 Birmensdorf*
[3] *BABU GmbH, Büro für Altlasten, Boden und Umwelt, Rautistrasse 13, 8047 Zürich*
[4] *Remote Sensing Laboratories, University of Zurich, Winterthurerstrasse 190, 8057 Zürich*
[5] *Swiss Soil Monitoring Network (NABO), Institute for Sustainability Sciences ISS Agrosocpe, Reckenholzstrasse 191, 8046 Zürich*
[6] *Planning of Landscape and Urban Systems, ETH Zurich, HIL, CH-8092 Zürich*

Soils play an essential role in ecosystems and provide important services for humans. Soils are the dominant basis for food and fodder production and are also needed for housing and infrastructure. But soils provide many more functions, for example, by retaining water after heavy rainfall and supplying water to plants from this storage during drought periods, providing habitats to organisms, storing carbon, preventing nutrients and pollutants from leaking into ground- and freshwaters, etc. Soil functions are often not noticed, let alone valued, except when soils fail to provide them.

A sustainable use of the soil resources needs to balance human requirements with the capacity of the soils to provide the various services. Currently, land use decisions in spatial planning are largely taken without consideration of the potentials of the soils for the various functions. One important reason for this unfortunate situation in Switzerland is the widespread lack of accurate large-scale spatial information on soils. Spatial information on soil properties is available only for less than 30 % of the agricultural land in Switzerland. In addition, standardised evaluation methods for assessing soil functions in Switzerland are still lacking. Most soil functions cannot be measured directly but must be deduced from basic soil properties, site characteristics and pedotransfer functions by modelling.

The project PMSoil aims (i) to develop digital soil mapping procedures for generating spatial soil information from legacy soil data and comprehensive environmental covariate information on pedogenetic conditions and land management, (ii) to establish an inference system of pedotransfer functions to derive soil function potentials from basic soil properties and (iii) to map basic soil properties and the potentials for selected soil functions in three study regions in the Cantons of Zurich and Berne (Figure 1).

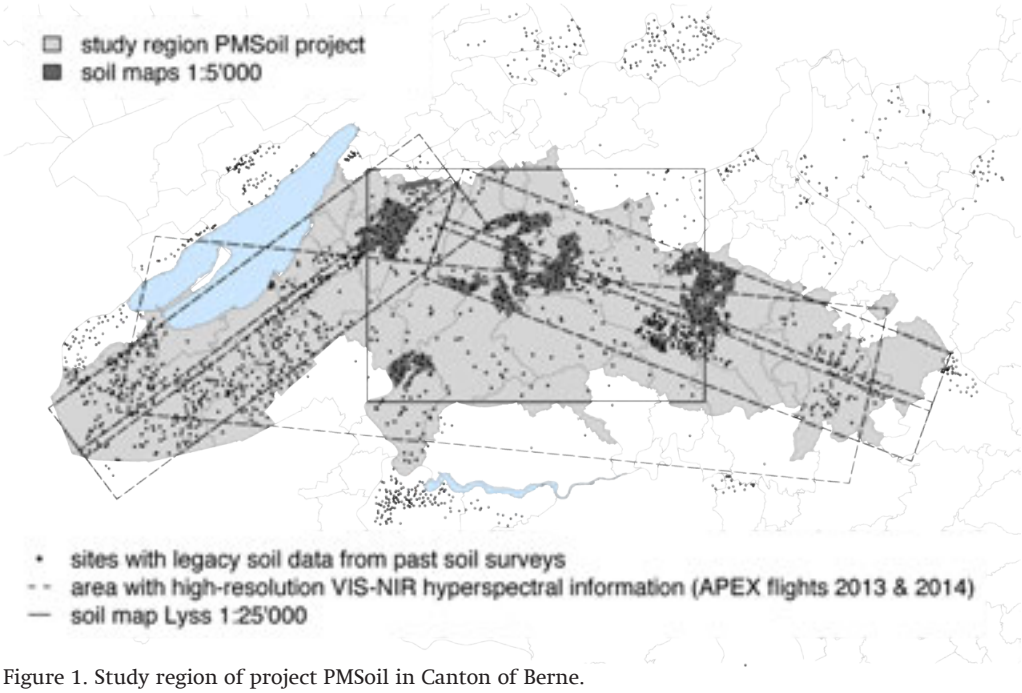

Figure 1. Study region of project PMSoil in Canton of Berne.

In more detail, the work of the PMSoil research team focuses on

- development of procedures for harmonizing legacy soil data stemming from various sources, which is a prerequisite for using such data for spatial analyses (workpackage WP A),
- modelling terrain attributes, which are important environmental covariates for spatial prediction of soil properties (WP B),
- optimized use of remotely sensed hyperspectral information on soils for predicting soil properties in a mosaic of partly vegetation-covered land (WP B),
- use of machine learning methods (boosted geo-additive models) for predicting soil properties parsimoniously from a possibly large set of environmental covariates (WP C),
- development and validation of soil function assessment methods for Swiss soils (WP D)
- and applying jointly the results of these research envdeavours in the study regions to create soil property maps and to map the potentials for particular soil functions which are of interest to the stakeholders.

The work of PMSoil is closely linked to the NRP68 projects OPSOL (A. Grêt-Regamey et al.) and iMSoil (A. Keller et al.) . The three projects jointly strive to provide answers to the pressing question how the scarce resource “soil”, which is currently still lost at a very fast pace in Switzerland (about 3’000 ha each year), can be better preserved and more sustainably managed in the future.

The presentation will introduce the objectives and the approach adopted in the project PMSoil with the aim to give some complementary to the more specific presentations about environmental covariate generation (WP B, presentations by S. Diek et al. and M. Fraefel et al.), statistical modelling (WP C, presentation by M. Nussbaum et al.) and soil function assessment (WP D, presentation by L. Greiner et al.).

P 14.3

Exploring the use of imaging spectroscopy in order to derive soil properties for agricultural areas in Zürich Oberland.

Sanne Diek[1], Rogier de Jong[1], Andreas Papritz[2] & Michael Schaepman[1]

[1] *Remote Sensing Laboratories, University of Zürich, Winterthurerstrasse 190, 8057 Zürich, Switzerland (sanne.diek@geo.uzh.ch)*
[2] *Soil and Terrestrial Environmental Physics, ETH Zürich, Universitätstrasse 16, 8092 Zürich, Switzerland*

Soil is a resource in Switzerland that is both essential and under pressure. An efficient system for soil management is therefore highly needed. In the framework of NRP68 the project PMSoil is aiming to provide contiguous spatial soil information and to establish an evaluation system for assessing soil functions for Swiss soils. Within this framework remote sensing serves as secondary information source for digital soil mapping. The use of remote sensing has the potential of providing quantitative spatial and temporal information of extended areas (Ben-Dor et al., 2009), while ist acquisition requires only a limited amount of fieldwork.

The use of soil spectroscopy is promising, however most research is based on laboratory-derived reflectance spectra and field studies were mainly executed in semi-arid areas (Mulder et al., 2011). Difficulties with vegetation cover, differences in soil moisture and management are eluded in this way. Therefore, we explored the use of soil spectroscopy for agricultural areas in Zurich Oberland. Fully processed airborne imaging spectrometer data from the Airborne Prism Experiment (APEX) sensor was available (September 2013 and May 2014) as well as harmonized soil data from the kanton of Zurich (canton ZH soil mapping 1:5.000, canton ZH soil monitoring, and canton ZH soil pollution surveys; data from 1960 to 2012). Field spectroscopy measurements and soil samples were taken at the same time APEX was flown. Based on existing algorithms (HYSOMA (Chabrillat et al., 2011)), soil properties, including soil organic matter, soil texture (clay and sand), and soil moisture were derived. The variables were retrieved using a combination of index-based and physically-based retrievals. The performance of the existing algorithms for deriving properties like clay, soil moisture and organic matter was tested with the harmonized soil data. Furhermore we explored the use of several interpolation methods in order to create full coverage soil property maps.

We discuss the challenges that need to be dealt with in order to use soil spectroscopy in an area like Switzerland. The neccessity of using in field measurements is discussed, as well as suggestions for improvement of existing algorithms.

REFERENCES

Ben-Dor, E., Chabrillat, S., Demattê, J.A.M., Taylor, G.R., Hill, J., Whiting, M.L., Sommer, S., 2009. Using Imaging Spectroscopy to study soil properties. Remote Sensing of Environment 113 (Supplement 1), S38-S55.

Mulder, V.L., de Bruin, S., Schaepman, M.E., Mayr, T.R., 2011. The use of remote sensing in soil and terrain mapping - A review. Geoderma 162(1-2), 1-19.

Chabrillat, S., Eisele, A., Guillaso, S., Rogaß, C., Ben-Dor, E., & Kaufmann, H. (2011, April). HYSOMA: An easy-to-use software interface for soil mapping applications of hyperspectral imagery. In Proceedings of the 7th EARSeL SIG Imaging Spectroscopy Workshop, Edinburgh (UK).

P 14.4

Multi-Scale Terrain Modelling for Predictive Soil Mapping in Switzerland

Marielle Fraefel[1], Andri Baltensweiler[1]

[1] *Swiss Federal Institute for Forest, Snow and Landscape Research WSL, Zürcherstrasse 111, 8903 Birmensdorf (marielle.fraefel@wsl.ch)*

Spatial information on soil properties in Switzerland is fragmentary and does not meet the increasing demand. In order to establish a validated and cost-effective procedure for creating soil property and soil function maps in Switzerland, the project PMSoil applies digital soil mapping (DSM) using geostatistical models based on a) harmonised legacy soil data, b) terrain characteristics, and c) remote-sensing data. Digital soil mapping has evolved considerably in recent years and has the potential to create soil maps at affordable cost, but has hardly been used in Switzerland so far.

Because topography is one of the main influencing factors on soil formation, and because high-resolution digital terrain models have become available in many regions, terrain attributes play a leading role as predictors in digital soil mapping (McBratney et al. 2003). However, the choice of relevant terrain attributes and, in particular, the spatial scale on which these should be computed has been a matter of debate in the past years (Behrens et al. 2010b, Lagacherie et al. 2006).

Within the framework of the PMSoil project, we compiled a large set of local and regional terrain attributes in three study regions in the cantons of Zurich and Berne. In the canton of Zurich, we relied on the swissALTI3D digital terrain model (2m resolution). For the study regions in the canton of Berne, cantonal LiDAR data was used (where available) and different filtering and interpolation methods and tools were compared to create a very precise, high-resolution DTM. To address the scale issue, various terrain attributes were calculated on different spatial scales by applying averaging windows of varying sizes. In addition, selected terrain attributes were calculated based on resampled versions of the DTM as well as using computation windows of different sizes.

In contrast to this set of terrain attributes, the contextual mapping approach (Behrens et al. 2010a) integrates a range of spatial scales and allows to consider directional components without referring to terrain attributes as calculated in "conventional" terrain analyses. This approach is implemented in the same study areas and will be compared to the terrain-attribute approach by studying the effect on the predictive soil maps, allowing us to define the best set of terrain characteristics and scales for the compilation of digital soil maps in each study region.

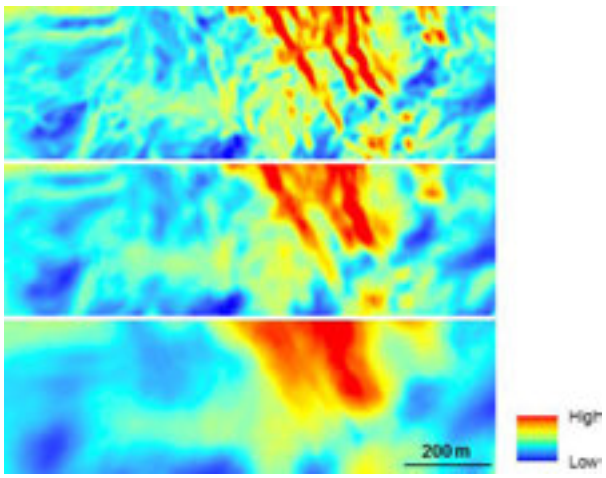

Figure 1. Slope raster smoothed with moving windows of different sizes (5x5, 10x10, and 25x25 cells).

REFERENCES

Behrens, T., Schmidt, K., Zhu, A. X. & Scholten, T. 2010a: The ConMap approach for terrain-based digital soil mapping. European Journal of Soil Science, 61, 133-143.

Behrens, T., Zhu, A. X., Schmidt, K. & Scholten, T. 2010b: Multi-scale digital terrain analysis and feature selection for digital soil mapping. Geoderma, 155, 175-185.

Lagacherie, P., McBratney, A. B. & Voltz, M. (Eds.) 2006: Digital Soil Mapping: An Introductory Perspective, Amsterdam, Elsevier.

McBratney, A. B., Mendonça Santos, M. L. & Minasny, B. 2003: On digital soil mapping. Geoderma, 117, 3-52.

P 14.5

Predictive mapping of soil pH in forests of Zurich by component wise gradient boosting

Madlene Nussbaum[1], Andreas Papritz[1], Mariell Fraefel[2], Andri Baltensweiler[2]

[1] *Institute of Terrestrial Ecosystems (ITES), ETH Zurich, Universitätstrasse 16, 8092 Zürich (madlene.nussbaum@env.ethz.ch)*
[2] *Swiss Federal Institute for Forest, Snow and Landscape Research (WSL), Zürcherstrasse 111, 8903 Birmensdorf*

Acidification of forested soils is, judged on the size of the affected area, one of the biggest problems that soil protection agencies are currently facing in Switzerland. Deposition of nitrogen, emitted into the atmosphere by agriculture and road traffic and subsequently deposited onto forests, is the main cause for accelerated acidification of forest soils. Delineation of strongly acidified soils on maps has become important for successful mitigation. For many regions precise maps are missing. Hence, digital maps of soil properties characterizing acidification are needed.

A wide range of statistical approaches has been used for soil property mapping. However, no method clearly outperforms the others. When many environmental covariates are available (e. g. with hyperspectral remote sensing data) the selection of the model with best predictive power becomes even more difficult. Besides the issue of covariate selection, methods such as regression or external-drift kriging models are limited to model linear relations between a response variable and environmental covariates. On the other hand, some machine learning tools as Random Forest that model non-linear relations result in black-box models. To overcome some of these drawbacks we used a gradient boosting approach that included as base learners linear and smooth non-linear terms. Non-stationary relationships were predicted by a smooth spatial surface.

To investigate the feasibility of the gradient boosting approach for digital soil mapping we mapped the topsoil pH for the forest area of the Canton of Zurich, Switzerland. The mapping included legacy data of 1'200 soil profiles. Model performance was evaluated by a data set of 170 soil profiles not used for model calibration.

P 14.6

Towards Soil Function Assessment for Switzerland

Lucie Greiner[1], Armin Keller[1], Stefan Zimmermann[2], Andreas Papritz[3]

[1] *Swiss Soil Monitoring Network (NABO), Institute for Sustainability Sciences ISS Agrosocpe, Reckenholzstrasse 191, CH-8046 Zürich (lucie.greiner@agroscope.admin.ch)*
[2] *Soil Functions and Soil Protection, Swiss Federal Research Institute WSL, Zürcherstrasse 111, CH-8903 Birmensdorf*
[3] *Institute of Terrestrial Ecosystems, ETHZ, Universitätstrasse 16, CH-8092 Zürich*

Soil fulfils important functions for humans and the environment. Rather visible for human society, soils function as the dominant basis for food and fodder production and with increasing demand as carrier for housing and infrastructure. In addition, soils provide many more functions, as retaining water after heavy rainfall or supplying plant available water during dry periods, providing habitats to organisms, storing carbon, preventing nutrients and pollutants from leaking into ground- and freshwaters. In principle, most soil functions are hardly noticed and at the same time taken for granted from human perspective.

As a consequence, a crucial aspect towards a sustainable use of soil resources is to foster the awareness about the soils importance, not only in fulfilling carrier and production function but also about its' regulation and habitat function. Likewise knowledge about the state of the soil is fundamental (Bouma et al. 2012). Hence, a tool is needed to increase the awareness about soils and to communicate relevant soil information to stakeholders and policy in spatial planning procedures. Based on the experience in some other European countries a transparent and soil-science based soil function assessment (SFA) providing spatial information with maps for soil function fulfillment is a promising tool to include soil in spatial planning processes.

However, soil functions are not directly measureable, but can be derived from soil properties such as texture, organic matter content, soil depth, bulk density, for instance. To assess soil functions for sustainable use of soils, one requires spatial information about soil properties and an inference system to derive soil functions from soil properties, i.e. scientific sound assessment methods to quantify soil functions.

Soil is important for several ecosystem services, but currently there are more general frameworks and related studies that provide hardly any concepts and detailed methods how soil functions can be assessed (Dominati et al. 2010). In contrast, geological survey institutions that are responsible for soil mapping in their countries, developed simplified assessment methods for various soil functions (see for a compilation of German methods Ad-ho-AG Boden 2007, and ÖNORM 2013 for Austrian methods).

In Switzerland - despite the efforts made by some Cantons such as Basel-Land, Solothurn or Zürich - a common Swiss national framework for soil function assessment and a method catalogue for potentially applicable SFA-methods is still missing yet.

In order to fill this gap the National Research Programme (NRP) 68 project PMSoil 'Predictive mapping of soil properties for the evaluation of soil functions at regional scale' aims to assess soil functions for two regional case studies in Switzerland. Applicable SFA-methods that were mainly developed in Germany will be compiled and tested for Swiss soil data classification and soil function maps generated. The SFA methods will be evaluated for two case study regions based on a large number of soil profiles originating from conventional soil mapping surveys and on soil property maps generated by the digital soil mapping approach in PMSoil. We focus mainly on the following three soil functions: regulation (water cycle, nutrient cycle, acidity buffering), agricultural production and habitat function. The generated soil function maps will serve then as the soil information layers for the land-use-decision model in the NRP 68 OPSOL project.

The poster shows how some soil sub-functions can be assessed for soil legacy data in Switzerland (soil profiles) and points out the differences in existing SFA methods from various countries and their potential to be adapted to Swiss conditions.

REFERENCES

Ad-hoc-AG Boden 2007: Methodenkatalog zur Bewertung natürlicher Bodenfunktionen, der Archivfunktion des Bodens, der Gefahr der Entstehung schädlicher Bodenveränderungen sowie der Nutzungsfunktion „Rohstofflagerstätte" nach BBodSchG. Ad-hoc AG Boden des Bund/Länder-Ausschusses Bodenforschung (BLAGEO) – Personenkreis „Grundlagen der Bodenfunktionsbewertung".

Bouma, J., Broll, G., Crane, T., Dewitte, O., Gardi, C., Schulte, R. & Towers, W. 2012: Soil information in support of policy making and awareness raising. Current Opinion in Environmental Sustainability, 4, 552-558.

Dominati, E., Patterson, M. & Mackay, A. 2010: A framework for classifying and quantifying the natural capital and ecosystem services of soils." Ecological Economics 69, 9, 1858-1868.

ÖNORM 2013: Bodenfunktionsbewertung: Methodische Umsetzung der ÖNORM L 1076. Bundesministerium für Land- und Forstwirtschaft, Umwelt und Wasserwirtschaft. 1010 Wien.

P 14.7

Soil bioturbation by earthworms and plant roots- mechanical and energetic considerations for plastic deformation

Ruiz S. A., Or D., Schymanski S. J.

Soil structure is a critical factor in agriculture for determining hydrological and ecological functions including water storage, deep recharge and plant growth. Compaction is known to adversely impact the resulting hydrology and crop productivity as well as other ecological functions of this habitat. An important class of soil structural restoration processes are related to biomechanical activity associated with borrowing of earthworms and root proliferation in impacted soil volumes. This study utilizes mechanical processes in order to simulate earthworm and plant root bioturbation in order to determine the mechanical energy investments into the system. As a model process, we consider steady state plastic cavity expansion to determine the burrowing pressures of earthworms and plant roots under various soil conditions. Cavity expansion models are then linked with cone penetration in order to quantify the burrowing process of plant root growth or earthworm locomotion related to different penetration angles. The associated cavity pressures and expanded radii determined the amount of mechanical energy invested for bioturbation under different hydration conditions and root/earthworm geometries. By considering earthworm physical and ecological parameter such as population density, burrowing rate, and burrowing behavior, we use the mechanical energy to infer estimations of necessary soil organic matter requirements for earthworm populations. Results illustrate a reduction in strain energy with increasing water content and trade-offs between pressure and energy investment for various root and earthworm geometries and soil hydrological statuses. This study also provides a quantitative framework for estimating the associated energy requirements (soil organic matter, plant assimilates) needed to sustain structure regeneration by earthworms and plant roots, and highlights the potential mechanical limits of such activities.

P 14.8

Are Soils Systematically Influenced By Their Soil Ecosystem Properties?

Beatriz González Domínguez[1], [2], Pascal Niklaus[2] & Samuel Abiven[1]

[1] *Department of Geography, University of Zurich, 8050 Zurich, Switzerland.*
[2] *Institute of Evolutionary Biology and Environmental Studies, University of Zurich, 8050 Zurich, Switzerland.*

Organic matter in forest soils is of increasing interest due to its connection to the atmosphere and potential role as a source and sink of CO_2.

When fresh organic matter is incorporated into the soil it becomes stabilized within the matrix through biologically mediated physico-chemical processes. It is well known that microbes are the main agents mineralising soil organic matter (SOM); however, the answer to what are the drivers with the greatest influence on SOM vulnerability is still unclear.

In Schmidt et al., 2011 soil ecosystem properties are described as the environment that has a direct influence of soil carbon dynamics. Based on this concept, it is hypothesised in this project that the main variables influencing soil ecosystem properties, and therefore the vulnerability of SOM, are, firstly, climate (i.e. temperature and soil moisture) and, secondly, soil (i.e. pH and clay content) and terrain properties (i.e. slope and aspect).

Based on these hypotheses, 54 study sites, all part of the Swiss Federal Institute for Forest, Snow and Landscape Research network, were selected to represent different combinations of the variables of interest for testing. The methodology followed was in line with the one applied in Barrufol et al., 2013.

Infrared spectroscopy has already been used as a quick method to gain information on the bulk soil (Haaland & Thomas, 1988; Zimmermann, Leifeld, & Fuhrer, 2007).

In the proposed poster, the results from relating soil ecosystems properties and middle infrared spectrometry data will be shown and explained in detail.

REFERENCES

Barrufol M, Schmid B, Bruelheide H, Chi X, Hector A, Ma K, Michalski S, Tang Z, Niklaus PA. 2013. Biodiversity promotes tree growth during succession in subtropical forest. PloS one 8: e81246.

Haaland DM, Thomas E V. 1988. Partial least-squares methods for spectral analyses. 1. Relation to other quantitative calibration methods and the extraction of qualitative information. Analytical Chemistry 60: 1193–1202.

Schmidt MWI, Torn MS, Abiven S, Dittmar T, Guggenberger G, Janssens IA, Kleber M, Kögel-Knabner I, Lehmann J, Manning DAC, et al. 2011. Persistence of soil organic matter as an ecosystem property. Nature 478: 49–56.

Zimmermann M, Leifeld J, Fuhrer J. 2007. Quantifying soil organic carbon fractions by infrared-spectroscopy. Soil Biology and Biochemistry 39: 224–231.

P 14.9

Exploiting dissolved lignin as sentinels of soil organic matter vulnerability

Xiaojuan Feng[1,2], Elisabeth Graf Pannatier[3], Tessa S. van der Voort[1], Daniel B. Montlucon[1], Timothy I. Eglinton[1]

[1] *Geological Institute, ETH Zürich, Sonneggstrasse 5, CH - 8092 Zürich (xfeng@erdw.ethz.ch)*
[2] *Institute of Botany, Chinese Academy of Science, 20 Nanxincun Xiangshan, Beijing 100093, China*
[3] *Swiss Federal Institute for Forest, Snow and Landscape Research (WSL), Zürcherstrasse 111, CH-8903 Birmensdorf*

Dissolved organic carbon (DOC) is the most biologically available and mobile fraction of soil organic matter (SOM). Its central role in nutrient cycling and sensitivity to environmental changes make it a promising candidate to monitor changes in SOM quality during land use and climatic changes. As the second most abundant biopolymer of terrestrial vascular plants, lignin-derived aromatic moieties are considered to be a main component of soil DOC and play a central role in regulating DOC production in forest litter layers (Kalbitz et al. 2006). Hence dissolved lignin is especially worthy of investigation in terms of its fate, stability and applicability as a sentinel of SOM vulnerability.

While the distribution and degradation of dissolved lignin have been extensively investigated, little is known about its radiocarbon age, which carries information on its source as well as residence time within the system. The recent development of high pressure liquid chromatography (HPLC)-based method has made it possible to isolate lignin-derived phenols from soil DOC for radiocarbon dating. The purpose of this study is to exploit the molecular composition and ^{14}C age of dissolved lignin as "early signs" of changes in soil carbon cycling (such as inputs of fresh litter and leaching of pre-aged soil components, etc.).

Towards this end, we utilize the Long-term Forest Ecosystem Research (LWF) station operated by WSL and employed compound-specific radiocarbon analysis to examine the ^{14}C age of lignin phenols in soil solutions as compared with that of bulk DOC and SOM. In a Norway spruce forest (Beatenberg), while SOM exhibited decreasing ^{14}C contents with depths, soil DOC and dissolved lignin showed predominantly modern ^{14}C ages down to 80 cm in the soil profile in May 2012, suggesting a dominant input of recent carbon probably due to the flush of surface DOC after snow melt. We further examine seasonal variations of ^{14}C ages in soil DOC and lignin across the LWF sites and estimate the contribution of fresh litter and pre-aged SOM to the soil DOC pool using two-end-member mixing model. This study provides the first set of ^{14}C data on dissolved lignin in soils and sheds new insights on soil carbon dynamics and fate of DOC in forest soils.

REFERENCES

Kalbitz, K., Kaiser, K., Bargholz, J. & Dardenne, P. 2006: Lignin degradation controls the production of dissolved organic matter in decomposing foliar litter. European Journal of Soil Science 57, 504-516.

P 14.10

Molecular and radiocarbon sentinels of soil organic matter vulnerability: a project introduction

Claudia Zell[1], Tessa van der Voort[1], Xiaojuan Feng[1,2], Frank Hagedorn[3], Patrick Schleppi[3],Timothy Eglinton[1]

[1] *ETH Zurich, Geological Institute, Sonneggstrasse 5, CH-8092 Zurich, Switzerland*
[2] *Institute of Botany, Chinese Academy of Sciences, 20 Nanxincun Xiangshan, Tuzilou 218 Beijing 100093, China*
[3] *Swiss Federal Research Institute WSL, Forest soils and biogeochemistry, Zürcherstrasse 111, 8903 Birmensdorf, Switzerland*

Investigation of soil organic matter (SOM) vulnerability constitutes an important and pressing challenge due to its value as a resource, its role in the carbon cycle and increasing pressures that soils are experiencing. Particular concerns exist regarding how the large pool of OM that is currently stabilized in soils will respond to the influence of climate change and increasing anthropogenic pressures. Causative factors and underlying processes that may change SOM stability are not yet well understood. In this project, we seek to utilize molecular and radiocarbon signatures as powerful and sensitive tools for assessing sources and dynamics of SOM pools. The overall goal of the project, which is part of the national research program NRP 68 "Soil as a Resource", is to provide more insights into the stability of SOM matter over different temporal and spatial scales. The project, which also forms part of the "SwissSOM" carbon cluster within the NRP68 program, encompasses a wide range of forest soils that are also part of the Long-Term Forest Ecosystem Monitoring program (LWF) of the Swiss Federal Institute for Forest, Snow and Landscape research (WSL). In addition, agricultural soils are investigated in collaboration with Agroscope. The comparison of contemporary and legacy (aged) samples enable insights into the changes that soils have undergone during recent years.

This research activities follow two main strategies: (1) Assessment of ^{14}C variations in bulk soils and soil fractions over a range of spatial scales (plot to regional scales), with a goal is to create a database that will serve as a benchmark against which to gauge future change; (2) Isotopic characterization of lignin and plant wax biomarkers as molecular proxies to trace organic matter dynamics within different soil fractions. We will show preliminary results, including plant wax concentrations in different soil types.

P 14.11

Long-term management effects on root biomass and carbon rhizodeposition of field grown maize

Juliane Hirte[1], Jens Leifeld[1], Hans-Rudolf Oberholzer[1], Samuel Abiven[2] & Jochen Mayer[1]

[1] *Agroscope ISS, Reckenholzstrasse 191, CH-8046 Zürich (juliane.hirte@agroscope.admin.ch)*
[2] *University of Zurich UZH, Winterthurerstrasse 190, CH-8057 Zürich*

Below ground carbon (BGC) inputs by agricultural plants into the soil are an important variable in soil carbon (C) modelling (Bolinder et al. 1997). The sources for BGC inputs are dead root biomass and C release by living roots, a process termed C rhizodeposition. Although drivers of BGC inputs have been studied in different contexts there is no consistent information about the effect of the agricultural management system on BGC inputs. Root biomass can increase or decrease with intensification depending on the nutritional state of the "reference system" (e.g. no or optimal fertilization; Costa et al. 2002) while C rhizodeposition may more strongly be affected by environmental factors than by management (Jones et al. 2009). In this research project, as part of the National Research Program 68 "Sustainable use of soil as a resource", we therefore address the following research questions:
(i) What are the proportions of root biomass and C rhizodeposition of the total BGC input in the surface- and subsoil under maize cultivation at different sites?
(ii) Does long-term fertilization practice affect total root biomass, root distribution, shoot/root ratios, and C rhizodeposition of maize?

In the growing season of 2013, we conducted field experiments with maize on two long-term experimental sites ("DOK", Therwil BL and "ZOFE", Zurich) including seven different managment system- and/or fertilization intensity treatments. Four plants per treatment (= 4 field replications) were grown in microplots and were multiple pulse-labelled with ^{13}C-CO_2 in weekly intervals until physiological maturity. The microplot soil was sampled in three layers to 0.75 m depth, coarse- and fine root biomasses were determined by picking and wet sieving, respectively, and the soil and all plant parts were analysed for their $\delta^{13}C$ values.

First results reveal no significant differences between total root biomasses of the 3 "DOK" treatments. Further results will be presented for
total root biomass, root distribution, shoot/root ratios, and C rhizodeposition of maize from both sites.

REFERENCES

Bolinder, M. A., Angers, D. A., & Dubuc, J. P. 1997: Estimating shoot to root ratios and annual carbon inputs in soils for cereal crops, Agriculture, ecosystems & environment, 63(1), 61-66.

Costa, C., Dwyer, L. M., Zhou, X., Dutilleul, P., Hamel, C., Reid, L. M., & Smith, D. L. 2002: Root Morphology of Contrasting Maize Genotypes, Agronomy Journal, 94, 96–101.

Jones, D. L., Nguyen C., & Finlay, R. D. 2009: Carbon flow in the rhizosphere: carbon trading at the soil–root interface, Plant Soil, 321, 5–33.

P 14.12

Breeding and drought influence root biomass and rooting depth: lessons learned from the Swiss Era wheats.

Cordula Friedli[1], Samuel Abiven[2] Achim Walter[1] & Andreas Hund[1]

[1] *Institute of Agricultural Science, ETHZ, Universitätstrasse 2, CH-8092 Zürich (cordula.friedli@usys.ethz.ch)*
[2] *Soil Science and Biogeochemistry, University of Zurich, Winterthurerstr. 190, CH-8057 Zurich*

Improving root architecture is an important aim to adapt plants to reduced water and nutrient availability as well as to enhance carbon sequestration. Specifically, deep rooting is discussed as a promising strategy to improve plant growth and to enhance soil organic matter in deep soil layers (e.g. Manschadi et al. 2008, Wasson et al. 2012). Soils are the largest repository of organic carbon in terrestrial ecosystems, but it stocks vary depending on year, crop rotation, management practice and, possibly, crop evolution due to breeding. SOC is primarily plant-derived and the sources can originate from (i) root and shoot remains or (ii) root exudates and other root-borne organic substances (Rasse et al. 2005). Therefore, breeding for deeper roots could be one way to mitigate plant limitations and climate change.

However, during the last century, wheat breeders have dramatically reduced plant height by introducing dwarfing genes into their material. This led to increased yield, as the crop could be managed with greater inputs without the risk of lodging. In addition, relatively more biomass was allocated to the harvested grains which increased the so-called harvest index. Thus, while grain yield rose with increasing inputs and harvest index, the increase in biomass was not in the focus of breeders. What about the roots? There is limited information about how rooting depth and root biomass was affected by breeders (e.g. Waines & Ehdaie 2007) and no studies which investigated root architecture of Swiss wheat. Yet, a deeper understanding of this process is urgently necessary to understand future trends and options for nutrient capture and carbon input to the soil. Most of the agricultural area of Switzerland was and still is planted with wheat varieties derived from the Swiss federal breeding programme, now operated by Agroscope (Fossati). Thus, knowing about the trends in root biomass and root distribution of these varieties may enhance our understanding of historic and future trends of carbon inputs of one of the most important Swiss crops covering an area of 83000 ha.

The objective of our study were to elucidate i) how root architecture of winter wheat changed over 90 years of breeding and ii) how root architecture of winter wheat is influenced by emerging drought during early vegetative and/or during late reproductive development. To achieve this, we identified the 14 most important Swiss bread wheat varieties, dominating the landscape during 90 years between 1920 and 2010. We call this selection “Swiss Era Wheats”.

All 14 era varieties were grown in our Deep Root Observation Platform (DROP) at Eschikon Field Station. The platform consist of 144 Plexiglas© columns (1.60 m length, 0.10 m in diameter), which can be weighed to determine water uptake by the plant. Two water stress treatments were established: early water stressed until flowering and water stressed from flowering until maturity. Both water stress treatments were established starting at complete field capacity. Thus, water stress in the root zones developed gradually starting from the upper part of the soil column with most intensive rooting. Plants were harvested at flowering and maturity, and root biomass distribution in the columns was determined in 250 mm intervals.

Our preliminary results indicate that reduction in plant height led to a severe reduction in rooting depth under well watered conditions. However, under early water stress, short, modern varieties could cope with their tall, old ancestors. The implication of the observed trend for carbon input will be discussed.

REFERENCES

Manschadi, A.M., Hammer, G.L., Christopher, J.T.& de Voil P. 2008: Genotypic variation in seedling root architectural traits and implications for drought adaptation in wheat (Triticum aestivum L.), Plant and Soil, 303, 115 – 129.

Rasse, D., Rumpel, C., & Dignac, M.-F. 2005: Is soil carbon mostly root carbon? Mechanisms for a specific stabilisation, Plant and Soil, 269, 341 – 256.

Waines, J., G. & Ehdaie, B. 2007 : Domestication of Crop Physiology : Roots of Green-Revolution Wheat, Annals of Botany, 100, 991 – 998.

Wasson, A., Richards, R., Charath, R., Misra, S., Prasad, S., Rebetzke, G. & Kirkegaard, J. 2012: Traits and selection strategies to improve root systems and water uptake in water-limited wheat crops, Journal of Experimental Botany, 63, 9, 3485 – 3498.

15. Biogeochemical cycles in a changing environment

16. Atmospheric Processes and Interactions with the Biosphere

Patrick Schleppi, Peter Waldner, Werner Eugster (session 15)

Christoph Ammann, Urs Neu, Werner Eugster (session 16)

ACP – Commission on Atmospheric Chemistry and Physics,
ProClim – Forum for Climate and Global Change,
IGBP- Swiss Committee,

TALKS SESSION 15:

15.1 Bassin S., Mayer J., Oberholzer H.R., Volk M., Fuhrer J.: N pools and fate of a stable isotope tracer in subalpine grassland exposed to combined elevated O_3 and N deposition

15.2 Blattmann T., Plötze M., Wessels M., McIntyre C., Eglinton T.: Mineral impacts on organic matter cycling

15.3 Camino-Serrano M., Janssens I., Luyssaert S., Ciais P., Gielen B., Guenet B., Vicca S., Waldner P., Graf Pannatier E. and others: Spatial and temporal trends of soil solution dissolved organic carbon (DOC) in European forests

15.4 Jeannin P.-Y., Hessenauer M., Meury P.-X: Climate change, soil CO_2 and groundwater mineralization in karst regions

15.5 Mestrot A., Boch S., Burn M., Wilcke W.: Arsenic biovolatilisation in lichens

15.6 Schleppi P., Curtaz F., Krause K.: Nitrate leaching from a sub-alpine coniferous forest subjected to experimentally increased N deposition for 20 years, and effects of tree girdling and felling

15.7 Schwarz S., Bigalke, M., Wilcke, W.: Structural controls of colloidal sulphide formation in flood plain soils

15.8 Zuijdgeest A.L., Baumgartner S., Wehrli B.: CO_2 evasion from tropical wetland higher than previously estimated

TALKS SESSION 16:

16.1 Arsenovic P., Stenke A., Rozanov E., Peter T.: Solar influence on the future climate

16.2 Harris I., Wunderlin P., Joss A., Emmenegger L., Kipf M., Wolf B., Siegrist H., Mohn J.: Online N_2O isotopic measurements for the identification of microbial N_2O production pathways

16.3 Henne S., Brunner D., Oney B., Leuenberger M., Bamberger I., Eugster W.: Validation of Swiss methane emissions by near surface observations and inverse modeling

16.4 Meyer A., Vernier J.-P., Luo B., Lohmann U., Peter T.: Did the 2011 Nabro eruption affect cirrus optical properties?

POSTERS SESSIONS 15 + 16:

P 15.1 Haghipour N., Eglinton T.I., Montluçon D., Tavagna M.L: How reliable are GDGTs for reconstruction of river basin properties? A preliminary investigation of the Cauvery River system (India)?

P 15.2 Hu Y., Schäfer G., Kuhn N.J.: Carbon quality and potential CO_2 emissions from Miscanthus fields: Is Miscanthus an ideal bioenergy crop?

P 15.3 Brauchli T., Bigler N., Bahr A., Weijs S. V.,Higgins C.,Huwald H.: A low-cost sensible heat flux sensor for potential use in wireless sensor networks and citizen observatories

P 15.4 Coulon A., Stenke A., Peter T.: What are the drivers of interannual fluctuations of atmospheric methane concentrations?

P 15.5 Perroud M., Goyette S.: Development and validation of a coupled single column lake - atmospheric model to simulate thermal profiles in Lake Geneva

15.1

N pools and fate of a stable isotope tracer in subalpine grassland exposed to combined elevated O_3 and N deposition

Seraina Bassin[1], Jochen Mayer[1], Hans Ruedi Oberholzer[1], Matthias Volk & Jürg Fuhrer[1]

[1] *Agroscope Research Station, Reckenholzstr. 191, CH-8046 Zürich*
(seraina.bassin@agroscope.admin.ch)

To investigate the effect air pollution on ecosystem processes in subalpine pastures, monoliths of a Geo-Montani-Nardetum grassland were exposed for seven years at 2000 m a.s.l. in a free air fumigation system to elevated ozone (O_3) concentrations (ambient, 1.7 x ambient concentration) and increased nitrogen (N) deposition (background, +50 kg N ha^{-1} yr^{-1}) in a cross-factorial design (Bassin et al. 2013, Volk et al. 2014). In the seventh growing season, after snow melt in May, a ^{15}N stable isotope tracer was applied to the vegetation. Two days later, in July, and end of August, two soil cores were taken each from the monoliths. N pools were determined for green phytomass, necromass, litter, roots, soluble soil N, extractable soil N, soil microbial biomass, and N stabilized in soil.

Of the added tracer, 65% was recovered two days after application, of which 30% was found in roots and only 7% in microbial biomass, indicating that in this ecosystem plants are superior competitors for mineral N. In line with this, after seven years of N addition, N pools of green phytomass, necromass and roots were increased by 30-40%, while most of the soil pools, including microbial biomass, remained unaffected, indicating that the added mineral N was primarily taken up and stored in plant biomass, preventing the ecosystem to acquire typical features of eutrophication such as accelerated N cycling, N leaching and acidification. In contrast, O_3 had only minor effects on plant pools, but significantly increased immobilization of N in microbial biomass and soil. This was likely the result of an O_3-induced increase of root turnover rates together with impaired root litter quality causing reduced mineralization rates. Moreover, as a consequence of the separate pollutant effects, considerable O_3 x N interactions were observed, indicating that N availability for plants decreased when O_3 was added alone, while it substantially increased under combined O_3 and N deposition. Conclusively, both O_3 and N deposition caused an accumulation of N, either in soil pools (O_3) or in plants (N). Although this N seems to be immobilized in a relatively stable form, it may be released to the environment once the climatic conditions are changing.

REFERENCES

Bassin S., Volk M., Fuhrer J. 2013: Species composition of subalpine grassland is sensitive to nitrogen deposition, but not to ozone, after seven years of treatment. Ecosystems, 16, 1105-1117.

Volk M., Wolff V., Bassin S., Ammann C., Fuhrer J. 2014: High tolerance of subalpine grassland to long-term ozone exposure is independent of N input and climatic drivers. Environmental Pollution, 189, 161-168.

15.2

Mineral impacts on organic matter cycling

Thomas Blattmann[1], Michael Plötze[2], Martin Wessels[3], Cameron McIntyre[1,4] & Timothy Eglinton[1]

[1] *Geological Institute, ETH Zurich, Sonneggstrasse 5, CH-8092 Zurich (thomas.blattmann@erdw.ethz.ch)*
[2] *Institute for Geotechnical Engineering, ETH Zurich, Stefano-Franscini-Platz 3, CH-8093 Zurich*
[3] *ISF Langenargen, Argenweg 50/1, D-88085 Langenargen*
[4] *Ion Beam Physics, ETH Zurich, Otto-Stern-Weg 5, CH-8093 Zurich*

Environmental matrices such as sediments and soils are composed of a large inorganic mineral component as well as a small portion of organic matter. Organic matter archives allow us to peer back in time and study life's activities in the geologic past. Manifold interactions between organic and mineral matter (Keil & Mayer, 2013) motivate research to help us understand the nature of these interactions that, in turn, allow us to better understand mineral controls on nature's organic matter signatures that propagate into the geologic record. This study focuses on understanding modern day organic matter-mineral interactions along a source-to-sink pathway of the Lake Constance (Bodensee) catchment and basin.

Traditionally, properties such as stable carbon isotopic compositions and organic carbon-to-nitrogen ratios have been utilized for assessing organic matter provenance. In addition to information derived from these parameters, this study exploited the additional resolution provided radiocarbon isotopic composition in order to improve interpretation and quantification of organic carbon type and processing. In addition to determining stable carbon isotopic composition and radiocarbon content of organic carbon, quantitative x-ray diffraction with Rietveld refinement was employed in order to identify and quantify mineralogical compositions. Bulk mineral surface areas were assessed with adsorption of nitrogen and water.

In lake sediments, we observed a positive relationship between mineral surface area and organic carbon content, suggesting that organic matter is closely associated with mineral surfaces. Based on a novel linear inversion approach using quantitative mineralogical information, we succeeded in extracting mineral-specific surface areas, which allow us to identify and assess the importance of different minerals in a given environmental matrix for stabilizing organic matter. The associations between different organic matter types and different minerals is subject to ongoing investigation.

REFERENCES

Keil, R.G., and Mayer, L.M., 2014, 12.12 - Mineral Matrices and Organic Matter, in Holland, H.D., and Turekian, K.K., eds., Treatise on Geochemistry (Second Edition): Oxford, Elsevier, p. 337-359.

15.3

Spatial and temporal trends of soil solution dissolved organic carbon (DOC) in European forests

Marta Camino-Serrano[1], Ivan Janssens[1], Sebastiaan Luyssaert[2], Philippe Ciais[2], Bert Gielen[1], Bertrand Guenet[2], Sara Vicca[1], Peter Waldner[3] & Elisabeth Graf Pannatier [3]

[1] *PLECO, University of Antwerp, Universiteitsplein 1, B-2610 Wilrijk, Belgium (marta.caminoserrano@uantwerpen.be)*
[2] *Laboratoire des Sciences du Climat et de l'Environnement, Centre d'Etudes Orme des Merisiers, 91191 Gif sur Yvette France*
[3] *Research Unit Forest soils and Biogeochemistry, Swiss Federal Institute for Forest, Snow and Landscape Research WSL, Zürcherstrasse 111, CH-8903 Birmensdorf*

The lateral transport of dissolved organic carbon (DOC) is an important and poorly understood process linking terrestrial and aquatic ecosystems. However, this lateral flux of carbon is usually neglected in Land Surface Models (LSMs) despite its crucial role in the global carbon cycle. More accurate information is needed in order to be able to predict DOC dynamics. DOC concentration in soil solution mainly varies by geographical location, soil and vegetation types, topography, season and climate (Bolan et al., 2011; Kalbitz et al., 2000), but it also varies in time: DOC concentrations in surface waters have been reported to increase over the past decades across Europe and North-eastern United States (Evans et al., 2012). Drivers like climate, CO_2 increase, acid deposition, land use change and management are the main hypothesis to explain this increase. On the contrary, there is less agreement in the global trends of DOC concentrations in soil solution. Decreases, increases and no trends of soil solution DOC from forested soils have been reported (Lofgren & Zetterberg, 2011; Verstraeten et al., 2014).

Within this framework, the ICP Forests (International Co-operative Programme on Assessment and Monitoring of Air Pollution Effects on Forests) dataset constitute a very valuable source of data to explore DOC soil solution temporal and spatial trends at European scale. DOC data and other soil solution chemistry are collected for the ICP Forests Level II plots at a regular basis.The ICP Forests database also includes other meta-data, such as vegetation type, soil properties, and climate. The analysis of the ICP Forests dataset focuses on: 1) the study of the environmental and physical factors controlling the site-to-site variability of DOC concentrations ([DOC]) in soil solution across European forests, and 2) the analysis of the global temporal trend in soil solution DOC from forests across Europe.

Site-to-site variability was assessed for broadleaved and coniferous forests separately in order to identify for each of both forest types the drivers of [DOC] variability. The results show that, in general, NH_4^+ in soil solution, C/N ratio and iron or aluminum in soil and soil solution are the most important variables explaining spatial variability of DOC. For broadleaved sites, variables related to biological processes (NDVI in summer or litter decomposability) are more important in explaining the spatial distribution of DOC concentration in soil solution, while water balance variables and texture are important as explanatory variables in coniferous sites. The obtained relationships are used for the design, parameterization and validation of the DOC module that is being implemented in the LSM ORCHIDEE.

For the second part of the study, trends at the ICP Forests sites will be assessed using the Seasonal Kendall Test (SKT). In total, 150 ICP plots with long-term [DOC] data (more than 10 years) are available for 18 countries to investigate whether, apart from the local drivers of [DOC] trend, there is an underlying driver of change operating in a uniform manner across European forest sites. The potential drivers of [DOC] trends will be investigated, paying special attention to those reported previously, such as the recovery from acidification and N enrichment. In this presentation, we will show the preliminary results on the temporal trends of DOC concentrations in European forests soil solution.

In conclusion, the findings from this study will provide us with novel information on the general spatial and temporal trends of DOC at continental scale. These results have two main implications: first, we will be able to better understand the factors controlling the DOC concentrations in European forests soils, and, second, we can test and validate DOC modules in land surface models, and thus we will be able to improve the predictions of DOC dynamics in the context of the changing climate.

REFERENCES

Bolan, N. S., D. C. Adriano, A. Kunhikrishnan, T. James, R. McDowell, & N. Senesi. 2011: Dissolved Organic Matter: Biogeochemistry, Dynamics, and Environmental Significance in Soils. Advances in Agronomy, 110, 1-75.

Evans, C. D., et al. 2012: Acidity controls on dissolved organic carbon mobility in organic soils. Global Change Biology, 18(11): 3317-3331

Kalbitz, K., S. Solinger, J. H. Park, B. Michalzik, & E. Matzner .2000): Controls on the dynamics of dissolved organic matter in soils: A review. Soil Science, 165(4): 277-304.

Lofgren, S., & T. Zetterberg. 2011: Decreased DOC concentrations in soil water in forested areas in southern Sweden during 1987-2008. Science of the Total Environment, 409(10): 1916-1926.

Verstraeten, A., B. De Vos, J. Neirynck, P. Roskams, & M. Hens. 2014: Impact of air-borne or canopy-derived dissolved organic carbon (DOC) on forest soil solution DOC in Flanders, Belgium, Atmospheric Environment, 83: 155-165.

15.4

Climate change, soil CO_2 and groundwater mineralization in karst regions

Pierre-Yves Jeannin[1], Marc Hessenauer[2], Pierre-Xavier Meury[3]

[1] *Institut Suisse de Spéléologie et de Karstologie, ISSKA, Case postale 818, CH-2301 La Chaux-de-Fonds (pierre-yves.jeannin@isska.ch)*
[2] *MFR Géologie – Géothechnique SA, Rue de Chaux 9, CH-2800 Delémont*
[3] *Géo & environnement Sàrl, Rue des Prés 9, CH-2800 Delémont*

Water mineralization monitored over the past 25 years in Ajoie (Northern Switzerland) evidenced a clear increasing trend (Figure 1). The same was observed in French Jura and in several springs in Switzerland, supporting the idea of a general phenomena.

Water mineralization in limestone regions is mainly related to the dissolution of calcium carbonate, which is controlled by the partial pressure of CO_2 existing in soils (Schoeller 1980). HCO_3 values measured in water correspond to CO_2 equilibrium values in the order of 30'000 to 60'000 ppm.

Soil pCO_2 was measured during the cycle 2013-2014 (Figure 2), showing values in agreement with the expected CO_2 equilibrium concentrations in the soil.

The analysis of water chemistry showed that the increase is related to an increase in Calcium and Carbonates. It can thus be expected that the average pCO_2 in soil increased by about 0.5 to 1% between 1989 and 2014.

It is well known that climate warming induced an increase in average temperature in summer and increased the duration of biological activity (earlier spring and later autumn). It is further well known that CO2 production in soils directly depends on temperature (Davidson & Janssens, 2006). Therefore the measured increased mineralization is expected to results from climate warming.

It is not clear at this stage if this phenomenon must be considered as a CO_2 sink or source.

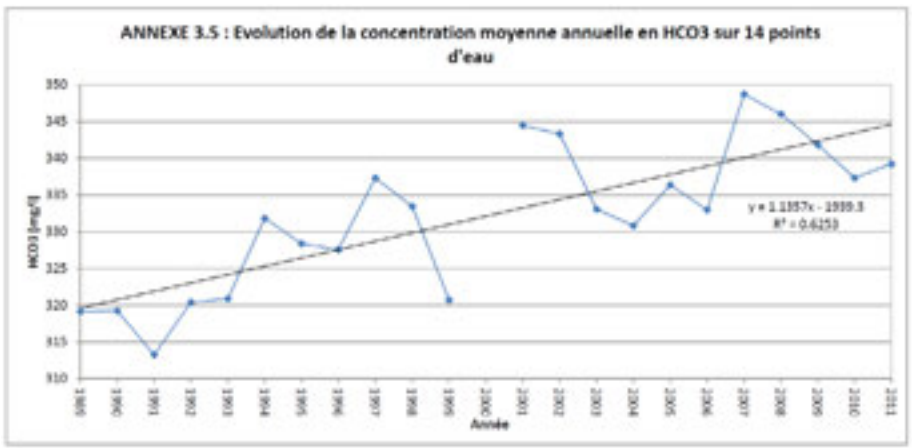

Figure 1. Evolution of the HCO_3 between 1989 and 2011. Measurements come from 14 different stations for which the trend is the most significant. HCO_3 increased by 25 mg/L over the observation period of time.

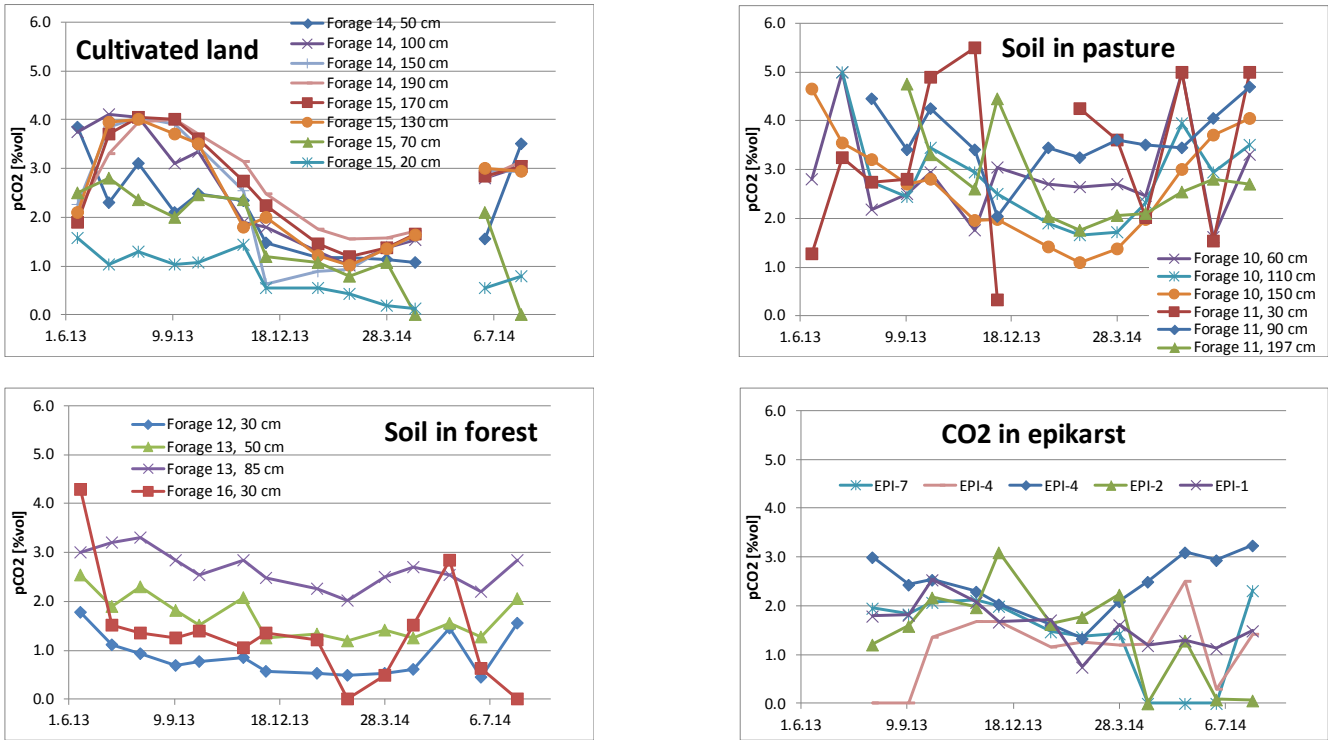

Figure 2. CO_2 partial pressure in soils in the Milandre test-site (Ajoie, Northern Switzerland). CO_2 is high in Summer and low in Winter. The highest concentrations are measured in soils of pastures.

REFERENCES

Davidson, E. A. & Janssens, I.A. 2006: Temperature sensitivity of soil carbon decomposition and feedbacks to climate change. Nature, 440, 165-173.

Schoeller, H. 1980: Influence du climat, de la température sur la teneur en HCO3– et H2CO3 des eaux souterraines. Journal of Hydrology, 46, 365-376.

15.5

Arsenic biovolatilisation in lichens

Adrien Mestrot[1], Steffen Boch[2], Marco Burn[2] & Wolfgang Wilcke[1]

[1] *Institute of Geography, University of Bern (adrien.mestrot@giub.unibe.ch))*
[2] *Institute of Plant Sciences, University of Bern.*
[3] *Institute of Geology, University of Bern*

Arsenic (As) is a ubiquitous, toxic element that is under considerable scrutiny. However, parts of its biogeochemical pathway have been less studied than others. This is the case of biomethylation and biovolatilisation; two intertwined natural mechanisms that lead to the formation of organic As species of varying properties and toxicities. Over the years, several microorganisms have been found to produce methylated and/or volatile As species such as methanoarchaea, cyanobacteria, sulfato-reductant bacteria and fungi. For this study, we investigated symbiotic organisms composed of algae or cyanobacteria and fungi: lichens. We discovered that rock lichens produce more volatile As than ever measured before in other microorganisms. This was also the very first time that volatile As production by lichens was measured. Our results show that these organisms, that cover 8% of the land surface area worldwide, are a significant source of As to the atmosphere and that As stored in rocks is potentially more mobile than previously thought. This study has huge implications towards As biogeochemical cycle.

Acknowlegments:

- Intra European Fellowship from the People Programme (Marie Curie Actions) of the European Union's Seventh Framework Programme *FP7/2007-2013/* under REA grant agreement n° [*326736*]
- UNIBERN Research Foundation

15.6

Nitrate leaching from a sub-alpine coniferous forest subjected to experimentally increased N deposition for 20 years, and effects of tree girdling and felling

Patrick Schleppi[1], Fabienne Curtaz[2], Kim Krause[3]

[1] *Swiss Fed. Inst. for Forest, Snow and Landscape Res. (WSL), CH-8903 Birmensdorf*
[2] *Department of Agricultural, Forest and Food Sciences, Univerity of Turin, IT-10095 Grugliasco, Torino*
[3] *Swiss Fed. Inst. for Forest, Snow and Landscape Res. (WSL), CH-8903 Birmensdorf (present address: Kaden & Partner AG, CH-8500 Frauenfeld)*

Atmospheric nitrogen (N) deposition can cause the eutrophication of otherwise N-limited ecosystems, including forests. Increased deposition rates were simulated in a small catchment within a spruce (*Picea abies*) forest at Alptal (central Switzerland, 1200 m a.s.l.). This treatment was applied by sprinkling rain water enriched with ammonium-nitrate (+25 kg/ha/year N) and compared with a control catchment receiving only rain water (12 kg/ha/year bulk N deposition) and where nitrate-N leaching amounts to approximately 3 kg/ha/year.

During rain events, nitrate concentration in runoff water was correlated with the water discharge, both showing simultaneous peaks. Labelling with ^{15}N showed that these peaks partly arise from nitrate deposited during the rain event itself. Preferential and lateral water flow promote very fast leaching in the upper layer of the gleyic soils. Nitrate losses doubled after only few weeks of the N addition experiment. This short-time effect was mainly driven by the hydrological characteristics of the site and could not be considered as a symptom of ecosystem N saturation. The ^{15}N signal disappeared from nitrate leaching within weeks as labelling stopped. Over the years, most of the added N was retained in the ecosystem, especially in the soil.

On each catchment, half of the large trees were girdled in the 15th year of the experiment and felled one year later. This resulted in a strong increase in nitrate leaching from the N-addition catchment, while only a small increase was measured in the control catchment. The abundance of ^{15}N during the leaching peak did not change compared to the preceding years. As a conclusion, the increased leaching appears to be induced by the reduced tree uptake and not so much by a remobilisation from the soil.

15.7

Structural controls of colloidal sulphide formation in flood plain soils

Susanne Schwarz[1], Moritz Bigalke[1], Wolfgang Wilcke[1]

[1] *Geographisches Institut, University of Berne, Hallerstrasse 12, CH-3012 Berne (susanne.schwarz@students.unibe.ch)*

Frequently, flood plain soils act as repositories of historical metal contamination (e.g. Cu, Pb, Cd) from numerous sources such as mining, industry, power generation, and sewage treatment works (Bigalke et al., 2010). Increases in flooding frequencies will induce more regular changes in soil redox conditions promoting changes in metal mobilisation, bioavailability and transport.The conversion of the ionic species into their colloidal sulphide will lead to a decrease in their geochemical reactivity, as they are transferred into the non-labile pool, however can trigger their transport into ground and surface waters. We observed distinct trace metal behaviour in a calcaerous riparian flood plain soil. Co, Cr, Fe, Ni were preferably encountered in the dissolved phase, whilst Ag, Cd, Cu, Pb sequestered as sulphide colloids (Abgottspon et al., submitted, Schwarz et al., in preparation).

We hypthesized the distinct trace metal behaviour to be associated to molecular structural controls that affect the formation of colloids under sulphate-reducing conditions in soil pore water.

To determine structural controls in colloidal metal sulphides, we incubated an alluvial, slighlty alkaline soil collected from the river Birs (Aesch, CH) under laboratory-controlled sulphate-reducing conditions over 28 days in artificial river water containing anions and cations similar to the Birs river water. Every second day we extracted soil pore water (< 10 µm) and filtered the solution through a 0.03 µm sulphur-free membrane. We quantified the incorporation of trace metals into colloidal metal sulphides by wet-chemical analyses of filtered and unfiltered solutions, and X-ray diffractrometry and X-ray near-edge structure spectroscopy at the S K-edge on the colloids collected on the filter.

We detected rapid colloidal CdS formation at day 2, followed by PbS at day 4 and finally CuS and Ag_2S at day 6. Further sulphide colloidal formation was inhibited by the complete consumption of dissolved sulphate at day 8 and structural controls (Schwarz et al., 2014).

Ag, Cd, Cu and Pb with completely filled d^{10} orbital electronic configuration are chemically inert and favour low solubility rates which leads to their fast sequestration as metal sulphide colloids. Complete sulphate consumption inhibited colloidal Zn (d^{10} electron configuration) sequestration. Co, Cr, Fe, Ni with partially filled (d^5-d^8) electron configuration can sequester metal sulphides with both S^{2-} and S_2^{2-} ions, the latter enhancing ligand field stabilisation and retarding interactions between these metals and dissolved sulphide leading to their dominance in the dissolved rather than colloidal phase. These metals are likely to co-precipitate with sequestered metals sulphides or carbonates.

REFERENCES

Bigalke, M., Weyer, S., Kobza, J., Wilcke, W. 2010.: Stable isotope Cu and Zn isotope ratios as tracers of sources and transport of Cu and Zn in contaminated soil. Geochimica et Cosmochimica Acta, 74, 6801-6813.

Abgottspon, F., Bigalke, M., & Wilcke, W. 2014.: Mobilization of trace elements in a carbonatic soil after experimental flooding. Environmental Pollution, submitted

Schwarz, S., Bigalke, M., Wilcke, W. 2014.: Structural controls of trace metal partitioning and sulphur dynamics in a calcaerous riparian flood plain soil. In preparation.

15.8

CO_2 evasion from tropical wetland higher than previously estimated

Alissa Zuijdgeest[1,2], Simon Baumgartner[1], Bernhard Wehrli[1,2]

[1] *Institute of Biogeochemistry and Pollutant Dynamics, ETH Zürich, Switzerland (alissa.zuijdgeest@usys.ethz.ch)*
[2] *Surface Waters – Research and Management, Eawag: Swiss Federal Institute of Aquatic Science and Technology, Switzerland*

Since the start of the industrial revolution, carbon dioxide (CO_2) concentrations in the atmosphere have steadily risen. In studying the carbon cycle and how rising atmospheric CO_2 concentrations would impact the cycle, inland waters have traditionally been treated as conduits transporting terrestrial carbon to the oceans. Recent work has shown that inland waters could potentially provide important pathways for transferring carbon to the atmosphere. A recent esimate (Raymond et al., 2013) resulted in CO_2 evasion rates of 1.8 petagrams of carbon (Pg C) per year from streams and rivers, and 0.32 Pg C yr^{-1} from lakes and reservoirs, totaling 2.1 Pg C yr^{-1}.

Inland waters in the tropics are potential hotspots for degassing of CO_2 (and methane) due to higher temperatures (lower saturation concentrations) and periodic flooding (low-oxygen conditions) (Belger et al., 2011; Melack et al., 2004; Richey et al., 2002). Tropical research has so far focussed on South America, and in particular the Amazon River, broader research efforts in Africa and Asia are needed to complete the global picture.

The Barotse Plains is an extensive, relatively pristine floodplain area bordering the Zambezi River in Western Zambia. In November 2013, we installed EXO 2 multiprobes upstream and downstream of this floodplain. At a 1-hour resolution, these sensors have provided a wealth of information over the last year. Combining direct pH measurements and a correlation between conductivity and total alkalinity, we are able to describe and quantify the total carbonate system in the floodplain systems.

Our study shows that, with conservative estimates for gas transfer velocities, this wetland is emitting more CO_2 than previously reported for tropical wetlands.

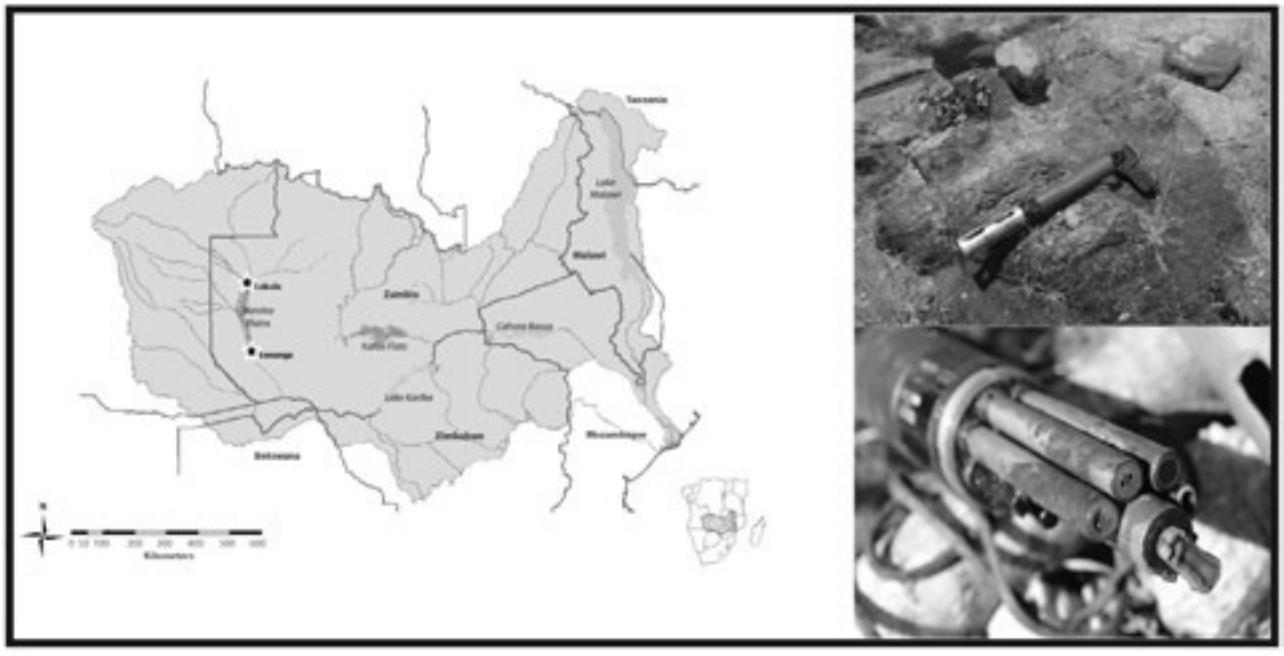

Figure 1. Map of the Zambezi catchment, with stars indicating sensor locations. Pictures show the deployed sensors.

REFERENCES

Belger, L., B. R. Forsberg, and J. M. Melack (2011), Carbon dioxide and methane emissions from interfluvial wetlands in the upper Negro River basin, Brazil, Biogeochemistry, 105(1-3), 171-183.

Melack, J. M., L. L. Hess, M. Gastil, B. R. Forsberg, S. K. Hamilton, I. B. T. Lima, and E. Novo (2004), Regionalization of methane emissions in the Amazon Basin with microwave remote sensing, Global Change Biology, 10(5), 530-544.

Raymond, P. A., et al. (2013), Global carbon dioxide emissions from inland waters, Nature, 503(7476), 355-359.

Richey, J. E., J. M. Melack, A. K. Aufdenkampe, V. M. Ballester, and L. L. Hess (2002), Outgassing from Amazonian rivers and wetlands as a large tropical source of atmospheric CO2, Nature, 416(6881), 617-620.

16.1

Solar influence on the future climate

Pavle Arsenovic[1], Andrea Stenke[1], Eugene Rozanov[1,2] & Thomas Peter[1]

[1] *Institute for atmospheric and climate science, ETH Zürich, Switzerland (pavle.arsenovic@env.ethz.ch)*
[2] *Physikalisch-Metorologisches Observatorium Davos - World Radiation Center, Davos, Switzerland*

Global warming became of the great interest to the mankind. There is growing evidence that anthropogenic greenhouse gases have become the dominant factor of climate change since 1970, although the natural factors such as solar activity and volcanic eruptions cannot be neglected. In the previous IPCC assessment (IPCC, 2007) the understanding level of the solar influence on climate was graded as very low. The results of the FUPSOL project (Future and Past Solar Influence on the Terrestrial Climate) aim to enrich this knowledge.

Model used for estimation of solar influence is SOCOLv3-MPIOM, which is a coupled atmosphere-ocean-chemistry model. The atmospheric component is ECHAM5, ocean component is MPIOM and chemistry module is MEZON. Greenhouse gases, tropospheric and stratospheric aerosols are included in the model.

Anet et al., 2013 ran three simulations for 2000-2100 period which only differ in solar forcing. The first simulation is called CONST and uses constant solar forcing with repeated 22 and 23 solar cycle to year 2100. Second simulation uses solar forcing with WEAK drop in irradiance (-4 W/m^2) and third uses STRONG drop (-6 W/m^2) compared to CONST.

The results of the simulations show that the predicted decline of solar activity may compensate up to 20% of warming caused by the greenhouse gases (Figure 1) and delay the recovery of ozone (Anet et al., 2013).

Further simulations (2100-2200) are done in order to examine to which degree the extended sun minimum can compensate warming caused by the greenhouse gases. These simulations use continued solar forcing to year 2200 but kept at minimum levels (-4 W/m^2 for WEAK and -6 W/m^2 for STRONG) for whole 2100-2200 period.

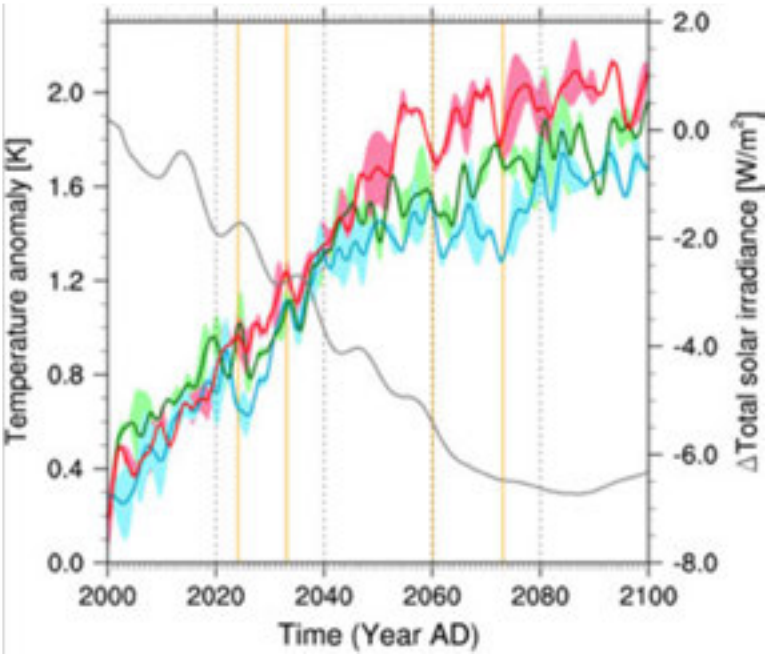

Figure 1. Globally averaged surface air temperature anomalies relative to 1986-2005 period. Red line – temperature anomaly when used constant solar forcing with 11-years cycles, green – when used weak drop in solar forcing (4 W/m2), blue – when used strong drop of 6 W/m2 (grey line) (Anet et al., 2013)

REFERENCES

Anet, J. G., et al. (2013), Impact of a potential 21st century "grand solar minimum" on surface temperatures and stratospheric ozone, Geophys. Res. Lett., 40, 4420–4425, doi:10.1002/grl.50806

Shapiro, A. I., W. Schmutz, E. Rozanov, M. Schoell, M. Haberreiter, A. V. Shapiro, and S. Nyeki (2011), A new approach to the long- term reconstruction of the solar irradiance leads to large historical solar forcing, Astron. Astrophys., 529, A67, 8 pp., doi:10.1051/0004-6361/ 20101 6173.

16.2

Online N_2O isotopic measurements for the identification of microbial N_2O production pathways

Harris, E.[1], Wunderlin, P.[2], Joss, A.[2], Emmenegger, L.[1], Kipf, M.[2], Wolf, B. [3], Siegrist, H.[2], Mohn, J.[1]

[1] *Empa, Laboratory for Air Pollution & Environmental Technology, Überlandstrasse 129, 8600 Dübendorf, Switzerland (eliza.harris@empa.ch)*
[2] *Eawag, Swiss Federal Institute of Aquatic Science and Technology, Überlandstrasse 133, P.O. Box 611, 8600 Dübendorf, Switzerland*
[3] *Institute of Meteorology and Climate Research (IMK-IFU), Kreuzeckbahnstrasse 19, 82467 Garmisch-Partenkirchen, Germany.*

Nitrous oxide is a strong greenhouse gas and the most important stratospheric ozone destructant released in the 21st century[1]. Enhanced microbial N_2O production is the primary source of anthropogenic N_2O, while industry and transport account for <20% of total anthropogenic emissions[2]. Microbial N_2O source processes are poorly defined and difficult to constrain, complicating efforts to reduce emissions. Isotopic studies of microbial N_2O production, both in the laboratory and in the ambient environment, can facilitate our understanding of source mechanisms and processes, and aid the development of targeted mitigation options.

This study presents the first online isotopic measurements of N_2O emitted from wastewater treatment. The processes observed will improve our understanding of direct N_2O production from wastewater treatment. In addition, the results will help to constrain the isotopic signatures of different microbial N_2O production pathways relevant to both natural and agricultural environments. Isotopic composition of offgas N_2O from a 400 L pilot scale, single-stage partial-nitritation anammox reactor was measured over a one-month period, and N_2O production pathways in the reactor were inferred based on the measured N_2O isotopic composition – in particular the N_2O isotopic site preference (SP = $\delta^{15}N^{\alpha} - \delta^{15}N^{\beta}$), which is characteristic for different N_2O production pathways[3-7].

N_2O emissions were investigated both under normal (optimal) operating conditions and during a number of experiments, designed to cover the range of conditions commonly encountered in a full-scale waste water treatment operation (Figure 1). When N_2O emissions peaked due to high dissolved O_2 ('high aeration' in Figure 1), low SP showed that N_2O was produced primarily via nitrifier denitrification by ammonia oxidizing bacteria (AOBs). N_2O production by AOBs via NH_2OH oxidation, in contrast, did not appear to be important under any conditions.

Over the majority of measurement period, the measured SP was much higher than expected, reaching 41‰ during normal operating conditions and achieving a maximum of 45‰ when nitrite was added under anoxic conditions (Figure 1). An unknown N_2O production pathway with SP >45‰ mediated by anammox bacteria was the explanation most consistent with the results, although the possibility of strong N_2O reduction by heterotrophic denitrifiers could not be entirely discounted.

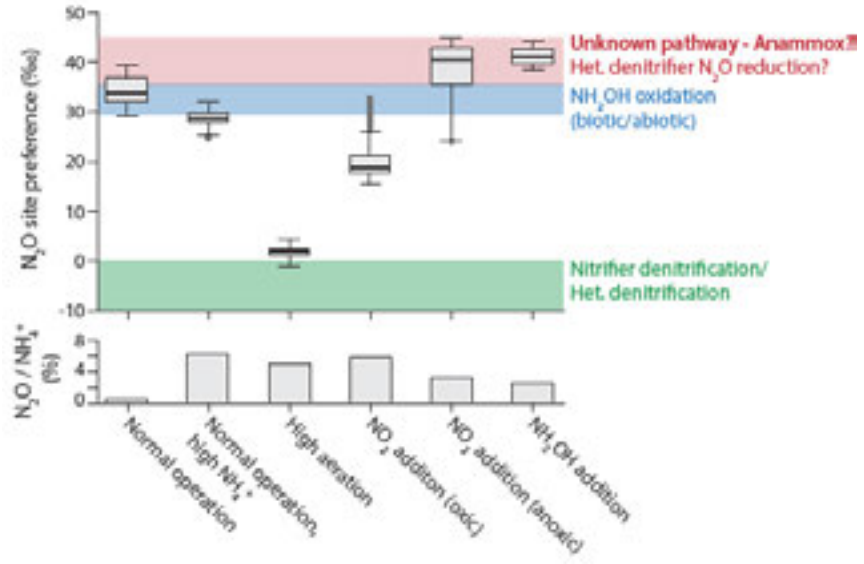

Figure 1. N_2O site preference and N_2O emissions per NH_4^+ consumed (N_2O/NH_4^+; %) over a range of experiments conducted with a single-stage partial nitritation-anammox reactor. Expected ranges for N_2O production via NH_2OH oxidation (biotic and abiotic) or denitrification are shown in blue and green respectively[2-5]; the red range indicates the measured SP values that cannot be explained by currently known N_2O production pathways.

REFERENCES
1. Ravishankara et al. (2009) Science, 326 (5949): 123-125
2. European Commission, Joint Research Centre / Netherlands Environmental Assessment Agency (2011) Emission Database for Global Atmospheric Research (EDGAR), release version 4.2, http://edgar.jrc.ec.europa.eu.
3. Wunderlin et al. (2013) Environmental Science and Technology, 47 (3): 1339-1348
4. Sutka et al. (2006) Applied and Environmental Microbiology, 72: 638-644
5. Toyoda et al. (2011) Global Biogeochemical Cycles, 25, doi:10.1029/2009GB003769
6. Heil et al. (2014) Geochimica et Cosmochimica Acta, 139: 72-82.
7. Ostrom et al. (2007) Journal of Geophysical Research – Biogeosciences, 112, doi: 10.1029/2006JG000287

16.3

Validation of Swiss methane emissions by near surface observations and inverse modeling

Stephan Henne[1], Dominik Brunner[1], Brian Oney[1], Markus Leuenberger[2], Ines Bamberger[3], Werner Eugster[3]

[1] *Laboratory for Air Pollution /Environmental Technology, Empa, Dübendorf, Switzerland (stephan.henne@empa.ch)*
[2] *Physics Institute, Climate and Environmental Physics and Oeschger Center for Climate Change Research, University of Bern, Switzerland*
[3] *Department of Environmental Systems Science, Institute of Agricultural Sciences, ETH Zurich, Switzerland*

On a global scale methane (CH_4) is the second most important long-lived greenhouse gas. It is released from both natural and anthropogenic processes and its atmospheric burden has almost doubled since preindustrial times. Current CH_4 emission estimates are associated with comparatively large uncertainties. The Swiss National Greenhouse Gas Inventory assigns an uncertainty of 18% to the country total CH_4 emissions as compared to only 3% for CO_2. In Switzerland, CH_4 is thought to be mainly released by agricultural activities (ruminants and manure management; >80%), while natural emissions from wetlands and wild animals represent a minor source (~3 %) (Hiller et al. 2014). The remaining emissions are mostly associated with losses from the natural gas distribution network. Several of the relevant CH_4 releases in Switzerland progress through microbial activities and, hence, are diffuse in nature and may be sensitive to environmental conditions at the source (temperature and percipitation), both posing a challenge to precise emission quantification. National emission estimates are currently based on "bottom-up" calculations which assign emission factors to certain emission processes and apply these to available activity data (for example emissions per cow multiplied by number of cows). If spatially explicit activity data are available, the spatial distribution of the emissions, as it is required for atmospheric models, can also be derived (Hiller et al. 2014). Spatial explicity inevitably leads to increased uncertainties for individual grid cells as compared to the national total emissions. Currently, the spatial attribution of CH_4 emission within Switzerland strongly differs between different European scale inventories and the national inventory (Hiller et al. 2014).

To validate the "bottom-up" Swiss CH_4 emission estimate and to reduce its uncertainty (total and spatial), "top-down" methods combining atmospheric CH_4 observations and regional scale transport simulations can be used. Here, we analyse continuous, near surface observations of CH_4 as collected within the newly established CarboCount CH measurement network (http://www.carbocount.ch). The network consists of 4 sites situated on the Swiss Plateau, comprising a tall tower site (212 m), two elevated (hilltop) sites and a small tower site (32 m). We analyse CH_4 and simultaneous carbon monoxide, and carbon dioxide observations with respect to local to regional scale CH_4 emissions. Furthermore, a Bayesian emission inversion framework is applied to the CH_4 observations in combination with source sensitivities (footprints) calculated with the regional scale version of the Lagrangian Particle Dispersion Model FLEXPART. The atmospheric model was driven by analysis fields from the non-hydrostatic numerical weather predication model COSMO at horizontal resolutions of up to 2 km x 2 km. Sensitivity inversions are applied to assess the overall uncertainty of the inversion system. The results of the emission inversion are compared to existing "bottom-up" estimates.

REFERENCES
Hiller, R. V., D. Bretscher, T. DelSontro, T. Diem, W. Eugster, R. Henneberger, S. Hobi, E. Hodson, D. Imer, M. Kreuzer, T. Künzle, L. Merbold, P. A. Niklaus, B. Rihm, A. Schellenberger, M. H. Schroth, C. J. Schubert, H. Siegrist, J. Stieger, N. Buchmann, and D. Brunner, 2014: Anthropogenic and natural methane fluxes in Switzerland synthesized within a spatially explicit inventory. Biogeosciences, 11, 1941-1959.

16.4

Did the 2011 Nabro eruption affect cirrus optical properties?

Angela Meyer[1], Jean-Paul Vernier[2], Beiping Luo[1], Ulrike Lohmann[1], Thomas Peter[1]

[1] *Institut für Atmosphäre und Klima, ETH Zürich, Universitätstrasse 16, CH-8092, Zürich (angela.meyer@env.ethz.ch)*
[2] *NASA Langley Research Center Hampton, Virginia, USA*

We have evaluated eight years of CALIPSO/CALIOP backscatter and depolarization data to address the question whether volcanic aerosols have an impact on the microphysical and optical properties of cirrus clouds. The CALIOP lidar instrument allows to discriminate cloud and aerosol particles based on their actively sensed backscatter and depolarization properties. We focus on the eruption of the Nabro volcano in June 2011, which added about 1 Tg of SO2 to the lower stratosphere (Theys et al. 2013) and was the strongest eruption since Pinatubo in this regard.

Previous observational studies have come to opposite conclusions regarding the impact of volcanic aerosols on cirrus properties (Sassen 1992, Luo et al 2002). Modelling studies of the Pinatubo eruption and of stratospheric sulfate geoengineering are also ambiguous in this regard (Lohmann et al. 2003, Kuebbeler et al. 2012, Cirisan et al. 2013).

We find that the year-to-year variability, which is likely caused by synoptic processes and climatic oscillations such as the North Atlantic Oscillation (NAO) and the El Niño-Southern Oscillation (ENSO), clearly outweighs any Nabro signal in the cirrus cloud backscatter and cirrus occurrence frequency at all latitudes both over land and ocean. We conclude that the cirrus-cloud radiative forcing caused by volcanically-induced changes in cirrus optical properties is negligible in the case of the Nabro eruption.

REFERENCES

Cirisan et al. 2013: Microphysical and radiative changes in cirrus clouds by geoengineering the stratosphere, JGR, doi:10.1002/jgrd.50388.

Kuebbeler et al. 2012: Effects of stratospheric sulfate aerosol geo-engineering on cirrus clouds, GRL, doi:10.1029/2012GL053797.

Lohmann et al. 2003: Impact of the Mount Pinatubo eruption on cirrus clouds formed by homogeneous freezing in the ECHAM4 GCM, JGR, doi: 10.1029/2002JD003185.

Luo et al. 2002: Did the Eruption of the Mt. Pinatubo Volcano Affect Cirrus Properties?, J. Clim., doi: 10.1175/1520-0442(2002)015<2806:DTEOTM>2.0.CO;2.

Sassen 1992: Evidence for Liquid-Phase Cirrus Cloud Formation from Volcanic Aerosols: Climatic Implications, Science, doi: 10.1126/science.257.5069.516.

Theys et al. 2013: Volcanic SO2 fluxes derived from satellite data: a survey using OMI, GOME-2, IASI and MODIS, ACP, doi:10.5194/acp-13-5945-2013.

P 15.1

How reliable are GDGTs for reconstruction of river basin properties? A preliminary investigation of the Cauvery River system (India)

Negar Haghipour[1], Timothy Eglinton [1], Daniel Montluçon[1], Maria Luisa Tavagna[1]

[1] *ETH Zurich, Geological Institute, Sonneggstrasse 5, CH-8092 Zurich, Switzerland*

The past few decades has seen the emergence and application of a wide array of lipid-based biomarker proxies for reconstructions of continental paleo-environment and paleo-elevation. Among these, the distribution of branched glycerol dialkyl glycerol teraethers (brGDGTs) has garnered broad interest and is becoming widely used as a proxy to reconstruct mean annual air temperatures (MAAT) and pH in soils and terrestrially-derived sediments, yet many questions remain regarding the robustness and calibration of proxy signals. We present results from an investigation of the Cauvery River basin in south India, to further examine the applicability of such proxies for paleo-elevation and paleoenvironmental studies in a low latitude fluvial system. River bank sediments were collected along the course of the river in order to study the evolution of proxy signals throughout the drainage basin. BrGDGT concentrations varied along the Cauvery River with values generally between 0.6 and 23 µg/g dry weight (gdw) but include some exceptionally high values (139 µg/gdw) in downstream regions. The brGDGTs show a weak, linear correlation between the MBT/CBT-derived temperatures and the altitude (R^2=0.63), suggesting that the MBT/CBT is influence by factors in addition to temperature in this part of India. Other characteristics such as seasonality, soil and sediment properties and in situ microbial production may contribute to the scatter in MBT/CBT values. These results call for further research before confidently applying brGDGTs as a proxy for paleo-topography and paleoclimate construction from fluvially-derived sediment sequences. On-going research involves investigation of other proxies that record landscape properties (e.g., higher plant waxes).

P 15.2

Carbon Quality and Potential CO_2 Emissions from Miscanthus Fields: Is Miscanthus An Ideal Bioenergy Crop?

Yaxian Hu[1], Gerhard Schäfer[2], Nikolaus J. Kuhn[1]

[1] *Physical Geography and Enviornmental Change, Department of Environmental Sciences, University of Basel, Klingelbergstrasse 27, CH-4056 Basel (yaxian.hu@unibas.ch)*
[2] *Laboratoire d'HYdrologie et de GEochimie de Strasbourg (LHyGes), Strasbourg University*

The use of biomass as a renewable energy source has become increasingly popular in Upper Rhine Region to confront the ever-worsen energy crisis. Miscanthus is one of the most favorite biofuel crops, due to its long standing, great yield, low energy and fertilizer input. However, current research on Miscanthus is mostly focused on the techniques to produce biofuel, economic benefits, or the impacts of side products such as ash and sulfur to human health. Research on the potential impacts of Miscanthus onto soil quality, especially after long-term adoption, is very limited. Some positive benefits, such as sequestrating organic carbon, have been repeatedly reported in previous research. Yet the quality of newly sequestrated organic carbon and its potential impacts onto global carbon cycling remain unclear. To fully account for the risks and benefits of Miscanthus, it is required to investigate the quality as well as the potential CO_2 emissions of soil organic carbon on Miscanthus fields.

As a part of the Interreg project[1] to assess the environmental impacts of biomass production, this study aims to evaluate the carbon quality and the potential CO2 emissions after long-term Miscanthus adoption. Soils were sampled at 0-10, 10-40, 40-70, and 70-100 cm depths in the two Miscanthus fields of 5 and 20 year old and a control site in Ammerzwiller, Alsance, France (47°41' N, 7°10' E). Soils from all depths were measured to determine soil texture, pH, organic carbon and nitrogen content. Topsoils of 0-10 cm and subsoils of 10-40 cm were also incubated for 40 days to determine their mineralization potentials. Our results show that: 1) only in top soils of 0-10 cm, the 20 year old Miscanthus field has significantly higher soil organic carbon concentrations (on average 4%), than the 5 years old Miscanthus field (on average 3%) and the control site (on average 2.8%). Similar tendency was also observed for organic nitrogen content as well C/N ratios. This indicates that the positive benefits of Miscanthus in sequestrating organic carbon and improving soil quality are probably only effective in top soils. 2) Soils from the 20 years old and 5 years old Miscanthus fields produced 71 and 15% more CO_2 than the control site, suggesting the great susceptibility of organic carbon on Miscanthus fields to mineralization. Our results detect a potentially extra contribution of Miscanthus fields to atmospheric CO_2, cautioning the widespread adoption of Miscanthus. Further studies with soils from other biofuel crops in other areas are required to assess the overall environmental impacts of biomass production in the Upper Rhine Region.

REFERENCES

[1] Project "Innovations for a sustainable biomass utilization in the Upper Rhine Region", funded by Europäischer Fonds für Regionale Entwicklung (EFRE) and Interreg. For more information on the project, please visit our project website: http://www.oui-biomasse.info/en/

P 15.3

A low-cost sensible heat flux sensor for potential use in wireless sensor networks and citizen observatories

Tristan Brauchli[1], Nicolas Bigler[1], Alexander Bahr[1], Steven Vincent Weijs[1], Chad Higgins[2], Hendrik Huwald[1]

[1] *School of Architecture, Civil and Environmental Engineering, Ecole Polytechnique Fédérale de Lausanne (EPFL), Switzerland*
[2] *Department of Biological and Ecological Engineering, Oregon State University, Corvallis*

The sensible heat flux is an important component of the land-atmosphere energy exchange but is relatively expensive to measure using standard techniques such as eddy covariance. Application of a flux variance method based on Monin-Obukhov similarity theory showed that under convective conditions, sensible heat flux can be computed reliably from high-frequency temperature fluctuations only. Recent efforts demonstrated the potential of this method, which may be of particular interest for use in autonomous wireless sensor networks. In the context of the "WeSenseIt" project, a citizen-based observatory of water, a low-cost sensible heat flux sensor is being developed, which could be used more widely. A commercial fast-response thermistor interfaced with a micro-controller can be connected to various data logging systems. First field tests (calibration and sensor inter-comparison) are currently in progress. These sensible heat flux sensors promise the capability of measuring spatially distributed sensible heat flux being currently very limited given the cost of standard systems. It is also planned to further explore the potential and suitability for application in less typical conditions, such as neutral or stable atmospheric conditions or use over inhomogeneous terrain.

P 15.4

What are the drivers of interannual fluctuations of atmospheric methane concentrations?

A.Coulon, A.Stenke and T.Peter

Institute for Atmospheric and Climate Science, ETH Zurich, Universitätstrasse 16, 8092 Zürich (ancelin.coulon@env.ethz.ch)

Atmospheric methane (CH_4) concentrations have more than doubled since pre-industrial times[1,2], making CH_4 the second most important greenhouse gas after CO_2 in terms of radiative forcing[3]. After a period of about 8 years with growth rates close to zero, methane concentrations are rising again since 2007[4]. With a 25-times larger global warming potential than CO_2, methane will play an even more important role in global climate change if it continues to rise. Changes in the strength of difference methane sources and/or in the main methane sink, the chemical oxidation by OH, are being discussed as potential reasons for the observed interannual variability in the methane growth rate.

Simulations have been performed using the SOCOL chemistry-climate model[5], for the time period 1980-2010, driven by observed meteorological fields in order to specify the modeled dynamics. To investigate the relative importance of different source categories such as natural wetlands, rice paddies, ruminants, industry, etc., and sink processes, a special tracer diagnostics has been implemented into SOCOL, which allows a tracking of methane emissions from different source categories and geographical regions. These new simulations are an innovative way to obtain a better understanding of the interannual variability of atmospheric methane.

Key factors of the interannual variability of atmospheric methane will be presented based on the implemented tracer diagnostic, showing the effects of both emissions and chemical loss, which is constrained by a methylchloroform tracer. Until the early 90's simulated global mean near-surface methane concentrations show a good agreement with observations. The tracer diagnostics indicate anthropogenic emissions over Europe as main contribution to the observed increase. After 2004 the model shows a pronounced methane increase not supported by observations. This result is mainly related to a strong - and very likely unrealistic[6] - increase of anthropogenic emissions over China in the applied emission data set. Furthermore, short term events are analyzed in detail, such as the strong impact of the biomass burning over Tropical Asia during the El-Nino period 1997/98.

REFERENCES

1-Etheridge D.M., L.P.Steele, R.J.Fancey, and R.L.Langenfelds 1998: Atmospheric methane between 1000 A.D. and present: Evidence of anthropogenic emissions and climate variability, J.Geophys.Res., 103(D13), 15, 979-15,993, doi:10.1029/98JD00923

2-Dlugokencky,E.J., et al. 2009 : Observational constraints on recent increases in the atmospheric CH4 burden, Geophys. Res.Lett., 36, L18803, doi:10.1029/2009GL039780

3-Myhre G., D.Shindell, F.-M.Bréon, W.Collins, J.Fuglestvedt, J.Huang, D.Koch, J.-F.Lamarque, D.Lee, B.Mendoza, T. Nakajima, A.Robock, G.Stephens, T.Takemura, and H.Zhang, 2013: Anthropogenic and Natural Radiative Forcing. In Climate Change 2013: The Physical Science Basis. Contribution of Working Group I to the Fifth Assessment Report of the Intergovernmental Panel on Climate Change [Stocker,T.F., D.Qin, G.-K.Plattner, M.Tignor, S.K.Allen, J.Boschung, A.Nauels, Y.Xia, V.Bex and P.M.Midgley (eds.)]. Cambridge Unervisity Press, Cambridge, United Kingdom and New York, NY, USA.

4-Rigby M. et al 2008: Renewed growth of atmospheric methane, Geophys.Res.Lett., 35, L22805

5-Stenke A., Schraner M., Rozanov E., Egorova T., Luo B.,and Peter T. 2013: The SOCOL version 3.0 Chemistry-Climate Model: Description, Evaluation and Implications from an Advanced Transport Algorithm ,Geosci.Model Dev., 6, 1407-1427.

6-Bergamaschi P., Houweling S., Sergers A., Krol M., Frankenberg C., Scheepmaker R.A., Dlugokencky E., Wosfy S.C., Kort E.A., Sweeney C., Schuck T., Brenninkmeijer C., Chen H., Beck V., Gerbig C, 2013: Atmospheric CH4 in the first decade of the 21st century: Inverse modeling analysis using SCIAMACHY satellite retrievals and NOAA surface measurements, Journal of Geophysical research, vol.118, 7350-7369, doi:10.1002/jgrd.50480

P 15.5

Development and validation of a coupled single column lake - atmospheric model to simulate thermal profiles in Lake Geneva

Marjorie Perroud[1], Stéphane Goyette[1]

[1] *Institute for Environmental Sciences, University of Geneva, 7 Rte de Drize, CH-1227 Carouge (marjorie.perroud@unige.ch)*

A single column atmospheric model coupled to a single column lake model with an application to Lake Geneva is presented. Results of multi-year climate simulation for the present day conditions as well as these for a future warmer climate scenario in the context of doubling the concentration of atmospheric CO_2 have already been published for the case of Lake Geneva, Switzerland (Goyette & Perroud 20110, Perroud & Goyette 2010). Here, the potential for shorter term realistic simulations is demonstrated. The atmospheric model, FIZC, is a column isolated from the Canadian Regional Climate Model (C-RCM, Caya & Laprise 1999). This atmospheric model is thus physically-based and it requires outputs from a previous C-RCM integration driven by NCEP-NCAR reanalyses. The issues of local lake weather conditions is addressed by combining precomputed atmospheric large-scale transports of momentum, heat, and moisture, called "the dynamics," and recomputed subgrid-scale parameterized effect (solar and infrared radiation fluxes, and latent and sensible heat fluxes), called "the physics," with the explicit numerical computations of the evolving lower boundary conditions provided by the lake model. The lake model, called k-epsilon (or k-ε), combines a buoyancy-extended k-ε model with a seiche excitation and damping model to predict the diffusivity below the surface mixed layer. In this model, the vertical turbulent diffusivities are determined from the turbulent kinetic energy and energy dissipation. In Figure 1, the evolution of the atmospheric and lake-water temperature profiles demonstrates the thermal responses of these two different fluid systems during 1990. The atmosphere is sensitive across a larger depth that the water, and short term variability is also higher due to its smaller heat capacity. Details of the atmospheric-lake interface module will be explained and sensitivity of the simulated thermal profiles to the coupler parameter values will be presented for a number of case studies.

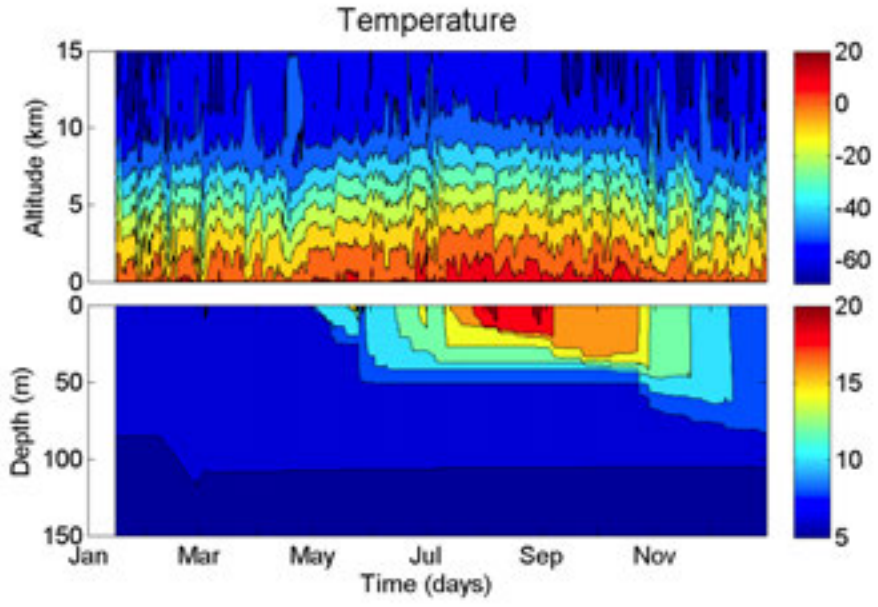

Figure 1. Evolution of the atmospheric (above) and lake-water temperatures (below) during 1990, units °C. Note the different scale on the vertical axis, depths are in meters below the surface and altitudes are in kilometers.

REFERENCES

Caya, D., & Laprise R. 1999,:A semi-implicit semi Lagrangian regional climate model: the Canadian RCM. Monthly Weather Review, 127 (3), 341-362.

Goyette, S., & Perroud,M. 2012: Interfacing a one-dimensional lake model with a single-column atmospheric model: Application to the deep Lake Geneva, Switzerland,.Water Resources Research, 48, W04507.

Perroud, M., & Goyette S. 2010: Impacts of warmer climate on Lake Geneva water temperature profiles. Boreal Environment Research, 15, 255-278.

18. Earth System Science related Earth Observation

Stefan Wunderle, Brigitte Buchmann, Alain Geiger
This Ruthishauser, Martine Rebetez, Christian Rixen

Swiss Commission for Remote Sensing,
Swiss Geodetic Commission
Swiss Commission for Phenology and Seasonality

TALKS:

18.1 Braun D.D.M., Damm A., de Jong R., Schaepman M.E.: Imaging spectroscopy based assessment of gross primary production in heterogeneous landscapes

18.2 Cossu F., Hocke K., Martynov A., Martius O., Mätzler C.: Atmospheric water parameters measured by a ground-based microwave radiometer and compared with the WRF model

18.3 Naegeli K., Huss M., Damm A., Schaepman M., Hoelzle, M.: Imaging spectroscopy to assess the composition of ice surface materials and their impact on glacier mass balance

18.4 Popp C., Andrews, B. J., Chance K., Cottroll, E.: Satellite detection of volcanic CO2 release of the Kasatochi eruption, 7 August 2008

18.5 Schweiger A.K., Risch A.C., Schütz M., Kneubühler M., Haller R., Schaepman M.E.: Quantitative and qualitative vegetation mapping in alpine grasslands using the imaging spectrometer APEX: A tool to explain animals' foraging sites?

18.6 Su Z.,Sun B., Geiger A., Rothacher M.: The potential benefits of Multi-constellation GNSS

18.7 Sütterlin M., Schaaf C. B., Stöckli R., Sun Q., Hüsler F., Wunderle S.: Towards a European surface albedo climatology

POSTERS:

P 18.1 de Jong R., Damm A., Garonna I., Schaepman M. E.: Changes in vegetation activity and land-surface phenology in Switzerland related to climatologies

P 18.2 Schneider F.D., Leiterer R., Morsdorf F., Schaepman M.E.: Remote sensing of forest ecosystems using airborne laser scanning and imaging spectroscopy

P 18.3 Lieberherr G., Riffler M., Wunderle S.: A European Lake Surface Water Temperature data set derived from NOAA/Metop-AVHRR (1983 – 2013)

P 18.4 Dionisio Calado A., Micheloud S., García Hernandez J., Foehn A., Ornstein P., Claude A.: Operational Snow Cover Mapping and Analysis in the Canton of Valais Based on MODIS Data

P 18.5 Hocke K., and Colleagues from NORS, MACC, NDACC: The Three Roles of the Rapid Data Delivery System of NORS/Copernicus

P 18.6 Wulf H., Joerg P.C., Leiterer R., Schaepman M.E.: New perspectives from Landsat 8 and Sentinel-2: Earth Observation Products

P 18.7 Honegger L., Castelltort S., Clark J., Adatte T., Puigdefàbregas C., Dykstra M., Fildani A.: Climatic signal propagation form source to sink in a Palaeogene sediment routing system, Pyrenean foreland basin, Spain

18.1

Imaging spectroscopy based assessment of gross primary production in heterogeneous landscapes

Daniela D.M. Braun[1 2], Alexander Damm[1], Rogier de Jong[1 2], Michael E. Schaepman[1 2]

[1] *Remote Sensing Laboratories, Universität Zürich, Winterthurerstrasse 190, CH-8057 Zürich (daniela.braun@geo.uzh.ch)*
[2] *University of Zurich Research Priority Programm (URPP) on Global Change and Biodiversity, Winterthurerstrasse 190, CH-8057 Zürich*

Gross primary production (GPP) is an important parameter in ecology for estimating ecosystem productivity. It is the rate of carbon dioxide (CO_2) uptake by terrestrial or aquatic vegetation through the process of photosynthesis, converting atmospheric CO_2 into organic compounds. It determines provisioning of ecosystem services on which humans indispensably rely, e.g., food, fiber, bioenergy, or fisheries. Profound modifications of biological or physical processes in ecosystems due to global change drivers influence biogeochemical cycles like the carbon cycle and, thus, affects the productivity of ecosystems, the related quantity and quality of ecosystem services (ES), and consequently the climate. Accurate spatial quantification of GPP is therefore important for monitoring carbon uptake and release in particular, and the overall C-budget of ecosystems and their productivity in general (Potter et al. 2009; Reeves et al. 2005). Further, assessments of GPP enable detecting potential carbon sinks and sources over time and how they are affected by direct and indirect drivers of change, e.g., human activities or climate change. This is important, as terrestrial and marine C sinks are one of the world's largest ecosystem services.

GPP is directly related to the light harvesting photosynthesis process. Remote sensing (RS) measuring reflected and emitted radiation from the Earth surface in various wavelengths is a useful tool to assess GPP of terrestrial and aquatic ecosystems at different scales. In particular, imaging spectroscopy (IS) allows retrieving various ecosystem parameter and processes involved in biogeochemical cycling, e.g., productivity of ecosystems and their changes. Several studies demonstrate the monitoring of the productivity of terrestrial and aquatic ecosystems at small- and large-scale (Gitelson et al. 2012; Matishov et al. 2010).

Although mapping GPP for certain land surface types was successfully demonstrated, the development of accurate approaches is still needed to integrate GPP estimates and ecosystem productivity across several Earth spheres to finally provide continuous spatial representations. We consequently aim with this study to investigate spatio-temporal changes of GPP in a heterogeneous landscape in Switzerland consisting of land use gradients. We propose a continuous field approach (CF) that allows integrating GPP estimations from the biosphere and the hydrosphere.

Airborne Prism Experiment (APEX) imaging spectroscopy data was used to assess GPP at landscape level continuously over different ecosystems and a land use gradient from semi-natural ecosystems to urban areas. The suggested approach relies on two information i) abundance maps of prevailing land cover classes (i.e., forest, grassland and lakes) and ii) GPP maps of respective land use types. We conducted spectral unmixing analyses to estimate abundance maps for forest, grassland and lakes. GPP is estimated following an approach of Gitelson et al. (2006) that utilizes a close relationship between GPP on the one hand and the total chlorophyll content of vegetation in combination with the incoming photosynthetic active radiation PAR_{in} on the other hand. Both parameters are obtained from APEX data and model simulation respectively.

Resulting continuous GPP maps display heterogeneity in productivity within the landscape and highlight areas of high and low ES supply. Combined analyses of development and natural conservation plans and GPP maps allow analyzing and predicting potential future changes in ecosystem productivity, their carbon budget and their contribution to climate change. Resulting GPP maps are considered helpful for decision-makers in land use planning to investigate different scenarios in order to maintain areas of high productivity and CO_2 sequestration.

REFERENCES

Gitelson, A.A., Peng, Y., Masek, J.G., Rundquist, D.C., Verma, S., Suyker, A., Baker, J.M., Hatfield, J.L., & Meyers, T. 2012: Remote estimation of crop gross primary production with Landsat data. Remote Sensing of Environment, 121, 404-414.

Gitelson, A.A., Viña, A., Verma, S.B., Rundquist, D.C., Arkebauer, T.J., Keydan, G., Leavitt, B., Ciganda, V., Burba, G.G., & Suyker, A.E. 2006: Relationship between gross primary production and chlorophyll content in crops: Implications for the synoptic monitoring of vegetation productivity. Journal of Geophysical Research D: Atmospheres, 111.

Matishov, G.G., Povazhnyi, V.V., Berdnikov, S.V., Moses, W.J., & Gitelson, A.A. 2010: Satellite estimation of chlorophyll-a concentration and phytoplankton primary production in the sea of Azov. Doklady Biological Sciences, 432, 216-219.

Powlson, D.S., Whitmore, A.P., & Goulding, K.W.T. 2011: Soil carbon sequestration to mitigate climate change: A critical re-examination to identify the true and the false. European Journal of Soil Science, 62, 42-55.

Reeves, M.C., Zhao, M., & Running, S.W. 2005: Usefulness and limits of MODIS GPP for estimating wheat yield. International Journal of Remote Sensing, 26, 1403-1421.

18.2

Atmospheric water parameters measured by a ground-based microwave radiometer and compared with the WRF model

Federico Cossu[1,3], Klemens Hocke[1,3], Andrey Martynov[2,3], Olivia Martius[2,3], Christian Mätzler[1,3]

[1] *Institute of Applied Physics, University of Bern, Sidlerstrasse 5, CH-3012 Bern (federico.cossu@iap.unibe.ch)*
[2] *Institute of Geography, University of Bern, Hallerstrasse 12, CH-3012 Bern*
[3] *Oeschger Centre for Climate Change Research, Falkenplatz 16, CH-3012 Bern*

The microwave radiometer TROWARA measures vertically integrated water vapour (IWV) and vertically integrated cloud liquid water (ILW) at Bern since 1994. The instrument has two microwave channels at 21.4 GHz (bandwidth 100 MHz) and at 31.5 GHz (bandwidth 200 MHz). In addition, a thermal infrared channel at λ=9.5–11.5 µm is used to estimate the cloud temperature. Thanks to the high temporal resolution (7 s) and to the almost continuous operation in any type of weather conditions (day/night, clear/overcast sky), TROWARA measurements are valuable for numerical weather prediction, nowcasting, climate research, satellite validation, and for long-term monitoring of atmospheric water (Mätzler & Morland 2009).

A new refined retrieval algorithm has been applied to TROWARA measurements for the year 2012 and the uncertainty in ILW has been significantly reduced. These high quality TROWARA data are compared with coincident data obtained from a regional climate model (RCM) simulation of summer 2012 in Switzerland performed with the Weather Research and Forecasting (WRF) model (Skamarock et al. 2008). The simulation was repeated with four different microphysical schemes. The time series of IWV and ILW (Fig. 1) and the characteristics of the statistical distributions of ILW are analysed for TROWARA and for the WRF model.

We found that the WRF model simulates very well the IWV time series measured by TROWARA with a mean bias of only 0.7 mm and with little differences between the microphysical schemes.
For what concerns ILW, the shape of the probability density function of TROWARA and of the WRF model is similar. The WRF model, however, overestimates the clear sky occurrence probability (83%) compared to TROWARA (60%). The microphysical schemes show a similar clear sky occurrence probability, while they differ more in the part of the distribution where ILW 0.01 mm.

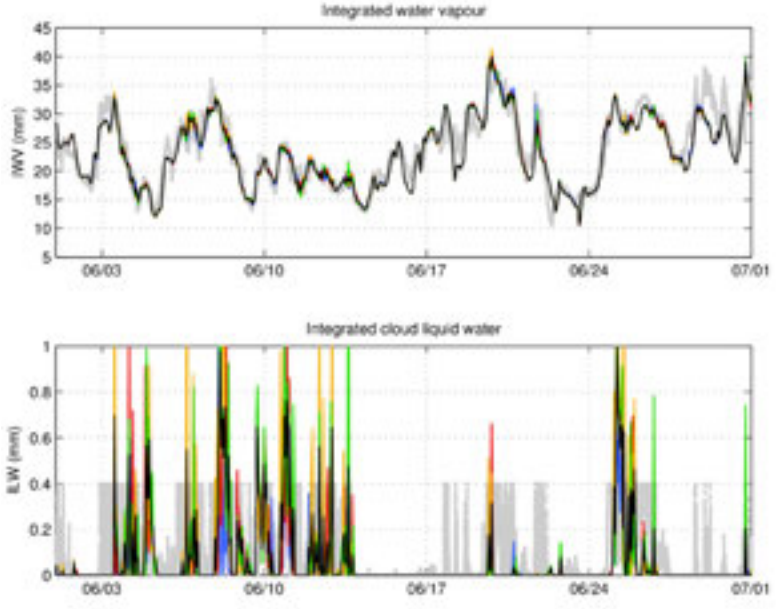

Figure 1. Integrated water vapour (IWV, top) and integrated cloud liquid water (ILW, bottom) measured by TROWARA in June 2012 (grey points) and simulated by the WRF model with four different microphysical schemes (blue, red, yellow and green lines with their mean in black).

REFERENCES

Mätzler, C. & Morland, J. 2009: Refined physical retrieval of integrated water vapor and cloud liquid for microwave radiometer data. IEEE Transactions on Geoscience and Remote Sensing 47, 1585-1594.

Skamarock, W. et al. 2008: A Description of the Advanced Research WRF Version 3. NCAR Technical Note.

18.3

Imaging spectroscopy to assess the composition of ice surface materials and their impact on glacier mass balance

Kathrin Naegeli[1], Matthias Huss[1], Alexander Damm[2], Michael Schaepman[2] & Martin Hoelzle[1]

[1] *Department of Geosciences, University of Fribourg, Switzerland (kathrin.naegeli@unifr.ch)*
[2] *Remote Sensing Laboratories, University of Zurich, Switzerland*

The ice-albedo feedback plays a crucial role in various glaciological processes but especially influences glacier ablation. Furthermore, glacier surface albedo is one of the most important variables in the energy balance of snow and ice and depends in a complicated way on many factors, such as cryoconite concentration, impurities due to mineral dust, soot or organic matter, grain size or ice surface morphology. Over the last two decades, several studies have focused on glacier surface albedo using automatic in-situ weather stations in combination with radiation measurement setups or satellite images [e.g. Klok et al., 2003; Paul et al., 2005; Oerlemans et al., 2009]. Due to limitations of both approaches in matching either the spatial or the temporal length scale of glacier albedo variations, strongly simplified assumptions on actual albedo values are still required. In the Swiss Alps, this is particularly critical since there are obvious changes in surface characteristics on most alpine glaciers over the last years.

In this study, we applied an approach combining observations and models to characterize glacier surfaces and focus in particular on the distribution of ice surface materials and their influence on glacier mass balance. The APEX (Airborne Prism EXperiment) image spectrometer was used to acquire spatial and spectral high resolution radiation measurements over the Glacier de la Plaine Morte, Switzerland, in summer 2013. Such high resolution data allow detailed and spatial explicit analyses of ice surfaces. For validation purposes, radiation measurements were acquired in-situ with an ASD field spectrometer in parallel to the airborne campaign. Further, data of a seasonal glacier mass balance monitoring program over the last five years, obtained using the direct glaciological method, was available. A distributed mass balance model forced by daily air temperature, precipitation and radiation, and calibrated to in-situ accumulation and ablation data, was used to calculate glacier-wide surface mass balance distribution.

We present first results obtained from APEX imaging spectroscopy data, including abundance maps of different glacier surface materials derived using the spectral angle mapper (SAM) and distributed albedo maps calculated from measured radiances. Furthermore, we present a set of experiments for analysing the suitability to implement such data products in a distributed mass balance model and for assessing the sensitivity of glacier wide mass balance computations on the assumption of bare-ice albedo. Our results will contribute to a better understanding of the spatial distribution of glacier melt, which is important to improve modelling attempts to study future glacier evolution.

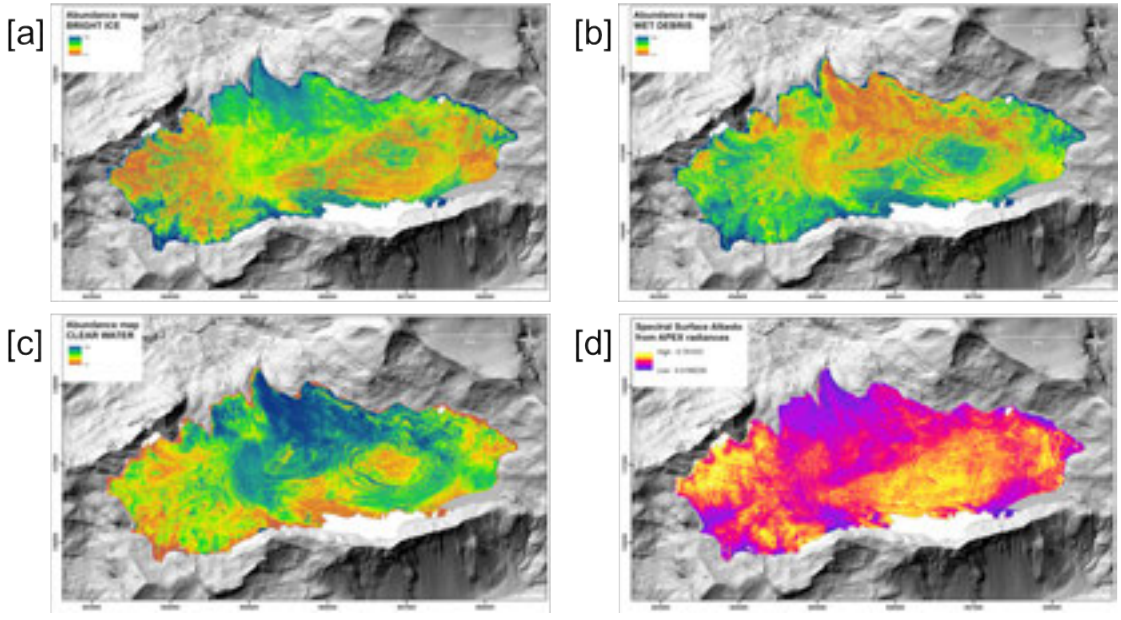

Figure 1. Abundance maps of three different materials present on the glacier surface calculated by means of a spectral angle mapper analysis of a hyperspectral scene covering Glacier de la Plaine Morte: (a) bright ice, (b) wet debris and (c) clear water. (d) Spectral surface albedo (λ=0.4-2.5 µm) calculated from APEX surface radiances.

REFERENCES
Klok, E.J.L., Greuell, W., & Oerlemans, J. 2003: Temporal and spatial variation of the surface albedo of Morteratschgletscher, Switzerland, as derived from 12 Landsat images. Journal of Glaciology, 49(167), 491–502.
Oerlemans, J., & Knap, W.H. 1998: A 1 year record of global radiation and albedo i n the ablation zone of Morteratschgletscher, Switzerland. Journal of Glaciology, 44(147), 231–238.
Oerlemans, J., Giesen, R.H. & Van Den Broeke, M.R. 2009: Retreating alpine glaciers: increased melt rates due to accumulation of dust (Vadret da Morteratsch, Switzerland). Journal of Glaciology, 55(192), 729–736.
Paul, F., Machguth, H. & Kääb, A. 2005: On the impact of glacier albedo under conditions of extreme glacier melt: the summer of 2003 in the Alps. EARSeL eProceedings, 4(2), 139–149.

18.4

Satellite detection of volcanic CO2 release of the Kasatochi eruption, 7 August 2008

Christoph Popp[1], Benjamin J. Andrews[1], Kelly Chance[2] & Elizabeth Cottrell[1]

[1] *National Museum of Natural History, Smithsonian Institution, Washington, DC, USA (poppc@si.edu)*
[2] *Harvard-Smithsonian Center for Astrophysics, Cambridge, MA, USA.*

Volcanoes are likely the largest source of carbon dioxide (CO_2) from the Earth's deep interior to the surface, but estimates of volcanic CO_2 emissions as well as the ratio of eruptive versus non-eruptive CO_2 releases are currently highly uncertain. Measurements from dedicated instruments aboard satellites may complement and enhance the spatially and temporally limited information from ground-based volcanic gas measurements. However, space-based detection and quantification of volcanic CO_2 is challenging because of the high atmospheric CO_2 background, and has to our knowledge not been reported yet. In this study, we present direct detection of CO_2 in the gas plume following the eruption of Kasatochi (Aleutian Islands, USA) on 7 August 2008 from satellite measurements from the SCIAMACHY and AIRS instruments. Our strategy is to apply a threshold on coincident spaceborne sulfur dioxide (SO_2) maps to distinguish between volcanic plume and background pixels. It is found that the CO_2 of the plume pixels statistically exceeds those of the background pixels for the SCIAMACHY and AIRS CO_2 products analyzed. In addition, significant correlations between SO_2 and CO_2 are found in the plume pixels as well as increasing CO_2:SO_2 ratios with time reflecting the relatively faster decay of SO_2 in the atmosphere. We extrapolate the decay of the CO_2:SO_2 ratio with time to estimate the CO_2:SO_2 ratio at the time of the eruption to estimate the total CO_2 release. We find CO_2 mass emission from Kasatochi in the order of 12 and 57 Tg, respectively, although the uncertainty range is very large. In conclusion, this study demonstrates that current space-borne remote sensing instruments can detect volcanic CO_2 from relatively large eruptions, that the magnitude 3-4 Kasatochi eruption in August 2008 likely released a large amount of CO_2, and that global CO_2 emissions from explosive volcanism are likely larger than previously thought.

18.5

Quantitative and qualitative vegetation mapping in alpine grasslands using the imaging spectrometer APEX: A tool to explain animals' foraging sites?

Anna-Katharina Schweiger[1,2,3]; Anita C. Risch[3], Martin Schütz[3], Mathias Kneubühler[2], Rudolf M. Haller[1] and Michael E. Schaepman[2]

[1] *Swiss National Park, Department of Research and Geoinformation, Chastè Planta-Wildenberg, CH-7530 Zernez (anna.schweiger@nationalpark.ch)*
[2] *Remote Sensing Laboratories, Department of Geography, University of Zurich – Irchel, Winterthurerstrasse 190, CH-8057 Zürich*
[3] *Research Unit Community Ecology, Swiss Federal Institute for Forest, Snow and Landscape Research WSL, Zürcherstrasse 111, CH-8903 Birmensdorf*

Alpine areas are characterized by their remoteness as well as their topographic variability and complexity. This variability creates large heterogeneity in soil and microclimatic conditions ultimately causing vegetation properties, such as community composition, biomass or nutrient content to vary at small spatial scales. Both the problem of accessibility of alpine areas, as well as the heterogeneity of vegetation patterns makes it unrealistic to assess vegetation properties over large areas with systematic in situ sampling. Ecologists, however, often need high resolution data to match the scale of the topic under study (Hebblewhite & Heydon 2010). Since entire food webs build upon soil and plant nutrient pools, spatially explicit information about these basic variables within a trophic system are needed to understand the organisation of communities. Remote sensing provides the only time and cost effective mean to acquire and map these environmental variables in high spatial and temporal resolution (Kerr & Ostrovsky 2003; Aplin 2005).

In our study area, the Val Trupchun in the Swiss National Park, three large ungulate species, ibex (*Capra ibex*), chamois (*Rupicapra rupicapra*) and red deer (*Cervus elaphus*), co-occur at high population densities. How ecologically similar species coexist in a shared environment is a classic question in resource ecology (see e.g. Hardin 1960). To investigate if and how food resources are shared among these three species we combined high resolution remote sensing with GPS data of radio-collared ungulates.

We used data from the airborne imaging spectrometer APEX (Jehle et al. 2010) and field plots to model and map grassland biomass, nitrogen and fibre content with 2 m x 2 m spatial resolution. Our 100 field reference plots covered the entire altitudinal gradient, and also all different levels of productivity and variations in plant species communities. The plant material was collected within a time window of 5 hours around the overflight. Despite the heterogeneity in our study area, our models predicted all three vegetation properties with high accuracies (biomass: $R^2 = 0.70$, RMSE = 156 $g.m^{-2}$ (fresh weight); nitrogen content: $R^2 = 0.53$, RMSE = 0.5 %; fibre content: $R^2 = 0.79$, RMSE = 2.5 %). We mapped grassland biomass, nitrogen and fibre content based on these models and analysed the foraging behaviour of the three ungulate species. To identify core foraging areas we split the animals' movement trajectories into behavioural phases by integrating the locations' autocorrelation structure in time and space. The comparison of resource availability in the core feeding areas revealed marked differences between the three species. While chamois foraged in areas with low biomass and intermediate levels of plant nitrogen, red deer chose areas with high biomass and low levels of plant nitrogen (Fig. 1) and ibex areas with both high biomass and high levels of plant nitrogen. These results point towards resource partitioning between the three species and confirm that high resolution remote sensing is a useful tool to gain a better understanding of fundamental ecological processes such as animal foraging behaviour.

REFERENCES

Aplin, P. 2005: Remote sensing: Ecology. Progress in Physical Geography 29, 104-11.

Hardin, G. 1960: The Competitive Exclusion Principle. Science 131, 1292-1297.

Hebblewhite, M. & Haydon, D.T. 2010: Distinguishing technology from biology: A critical review of the use of GPS telemetry data in ecology. Philosophical Transactions of the Royal Society B: Biological Sciences 365, 2303-2312.

Jehle, M., Hueni, A., Damm, A., D'Odorico, P., Weyermann, J., Kneubühler, M., Schläpfer, D., Schaepman, M.E. & Meuleman, K. 2010: APEX-Current status, performance and validation concept. Sensors, 2010 IEEE, 533-537.

Kerr, J.T. & Ostrovsky, M. 2003: From space to species: Ecological applications for remote sensing. Trends in Ecology and Evolution 18, 299-305.

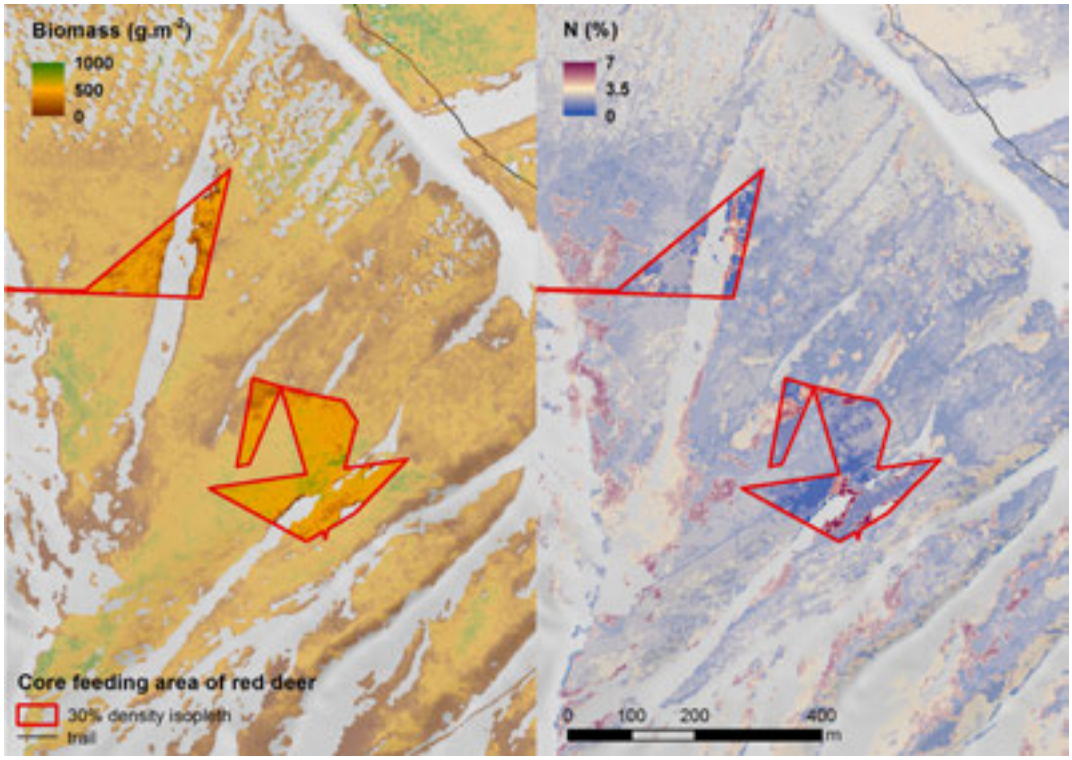

Figure 1. Core feeding area of an individual red deer.

18.6

The potential benefits of Multi-constellation GNSS

Zhenzhong Su*, Baoqi Sun*,** Alain Geiger*, Markus Rothacher*

*Institute of Geodesy and Photogrammetry, ETH Zurich, Robert-Gnehm-Weg 15, CH-8093 Zurich (zsu@ethz.ch)
** National Time Service Center, Chinese Academy of Sciences, 3 East Shuyuan Road, Lintong, Shaanxi, China, 710600

GNSS (Global Navigation Satellite System) has been used as an important earth observation tool, since the beginning of the US GPS (Global Positioning System). Its applications range from atmosphere, hydrosphere to lithosphere, such as ionospheric modeling, tropospheric water vapor estimation, tectonic deformation monitoring, sea level determination, GNSS seismology and so on. Besides the US GPS and Russian GLONASS (Globalnaya Navigatsionnaya Sputnikovaya Sistema), new GNSS systems like Chinese BeiDou Navigation Satellite System and Europe's Galileo are available now. The independent but compatible multi-constellation enhances the reliability, accuracy and availability of GNSS systems. Take ionospheric modeling as an example, denser ionospheric pierce points from more GNSS satellites means better input to the ionospheric modeling. For positioning and monitoring applications, the increased number of satellites from multiple constellations provide additional redundancy and better GDOP (Geometric Dilution of Precision), Users in Swiss alpine areas, where signals are prone to multipath interference and obstruction by mountains, will especially benefit because of an abundance of satellite signals.

In this contribution, we present the visibility of Chinese BeiDou system in Switzerland and the positioning solution computed from a GPS plus BeiDou constellation. We discuss the potential benefits as well as challenges of using such a multi-constellation GNSS.

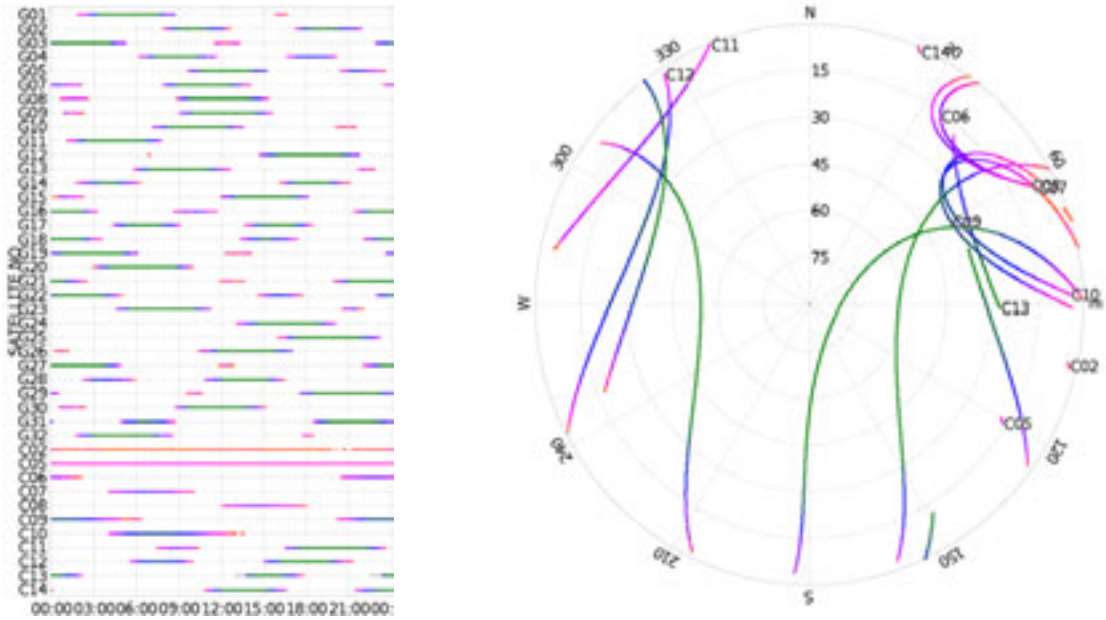

Figure 1. Left: Visible GPS and BeiDou satellites; Right: skyplot of BeiDou satellites (MGEX station: ZIM3)

REFERENCES

Geiger, A. & Cocard, M., 2003: Precise Determination of Offshore Sea Level. In: Swiss National Report on the Geodetic Activities in the years 1999-2003, presented to the IUGG General Assembly XXIII in Sapporo, Japan, ISSN 3-908440-06-8, Swiss Geodetic Commission

Höflinger, W., Cocard, M. & Geiger, A., 1992: IODEL: Ionosphärenmodellierung mit GPS. 2 Frequenzmessungen. Institut für Geodäsie und Photogrammetrie, ETH Zürich, Bericht Nr. 200. ISBN 3-906513-14-9, pp. 55.

Meindl, M., 2011: Combined Analysis of Observations from Different Global Navigation Satellite Systems, Vol. 83 of Geodätisch-geophysikalische Arbeiten in der Schweiz, Schweizerische Geodätische Kommission, Institut für Geodäsie und Photogrammetrie, Eidg. Technische Hochschule Zürich, Zürich, Switzerland, ISBN 978-3-908440-27-7

Perler, D., Geiger, A. & Hurter, F., 2011: 4D GPS water vapor tomography: New parameterized approaches, Journal of Geodesy, Springer, 85, 539-550

Psimoulis, P., Houlié, N., Meindl, M. & Rothacher, M., 2015: Consistency of GPS and strong-motion records: case study of Mw9.0 Tohoku-Oki 2011 earthquake, smart Structures and Systems, 26, 2 preprint

Villiger, A., Geiger, A., Wiget, A. & Marti, U., 2011: SWISS-4D II: Geodetic analysis of geodynamic deformations in Switzerland: XXV General Assembly of the International Union of Geodesy and Geophysics, 71-71

18.7

Towards a European surface albedo climatology

Melanie Sütterlin[1], Crystal Barker Schaaf[2,3], Reto Stöckli[4], Qingsong Sun[3], Fabia Hüsler[1], & Stefan Wunderle[1]

[1] *Institute of Geography, University of Bern, Hallerstrasse 12, CH-3012 Bern (melanie.suetterlin@giub.unibe.ch)*
[2] *Department of Earth and Environment, Boston University, 725 Commonwealth Avenue, Boston, MA 02215, USA*
[3] *School for the Environment, University of Massachusetts Boston, 100 Morrissey Blvd, Boston, MA 02125, USA*
[4] *Federal Office of Meteorology and Climatology, MeteoSwiss, Krähbühlstrasse 58, CH-8044 Zurich*

Regional and global climate models rely on precise information of surface albedo as it is a key parameter in the Earth's energy balance controlling the amount of reflected and absorbed radiation. Remote sensing products allow the global retrieval of surface albedo and its variability in space and time. To utilize reflectance as measured by space-borne instruments to derive surface albedo (and black-sky albedo) from satellite images, a BRDF (Bidirectional Reflectance Distribution Function) model is required. These models aim to reproduce the directional signature of the land surface reflectance by using surface reflectance values of multi-angular observations. In producing complete and physically consistent data records that are essential for studying ecosystem change, the quantification of uncertainties in satellite-derived land surface albedo products is a critical aspect. Therefore, it is mandatory, especially for the complex terrain of the European Alps, to further evaluate the potential of BRDF models in retrieving land surface properties and to generate consistent albedo datasets.

In this study, the RossThick-LiSparse-Reciprocal BRDF model is used to generate a BRDF/Albedo climate data record based on LAC data of the AVHRR. The algorithm follows the MODIS V005 standard BRDF methodology and relies on multi-day, cloud-free, atmospherically corrected surface reflectance values, and several quality flags (e.g., snow masks) to decide whether and in what manner the pixel values can be used for the retrieval process. Even though newer sensor technologies have become available, the AVHRR data record that reaches back to 1981 is of particular interest as it offers the longest and most complete record of visible satellite imagery on a daily basis. The algorithm has been adapted to AVHRR data and was successfully applied and tested using data of different NOAA and MetOp satellites for several years. Nadir BRDF-adjusted reflectance (NBAR), black-sky albedo and white-sky albedo was inter-compared to the MODIS BRDF/Albedo standard operational product MCD43A. The black-sky and white-sky albedos were combined as a function of solar geometry and atmospheric state in order to compute instantaneous actual albedo (blue-sky albedo) used for the comparison to in situ station measurements of albedo.

We thus are able to present the BRDF/Albedo data with a spatial resolution of 1.1km^2 based on AVHRR data over Europe. The products show a good correspondence with the MODIS BRDF products and the validation against field measurements indicates a promising sensitivity with regard to temporal changes. Based on these findings, the project aims to generate climatologically consistent albedo datasets, especially for the European Alpine region, and to show for the first time the spatial and temporal variability of albedo during the last 29 years. This dataset will serve to improve the understanding and representation of albedo in regional climate models.

P 18.1

Changes in vegetation activity and land-surface phenology in Switzerland related to climatologies

Rogier de Jong[1], Alexander Damm[1], Irene Garonna[1] & Michael Schaepman[1]

[1] *University of Zurich, Remote Sensing Laboratories, Winterthurerstrasse 190, 8057 Zürich, Switzerland*

Vegetation growth is driven and limited by a range of abiotic factors, notably by climatic controls like temperature, water availability and incident radiation (Field et al. 1986). Apart from these, anthropogenic factors and complex interactions with, for instance, the local soil or hydrology influence vegetation dynamics. The resulting changes are expressed in the intra-annual growth cycle of the vegetation, to which we refer as land-surface phenology (LSP). This pattern can be accuratly observed using time series of satellite-based measurements of vegetation activity but the challenge lies in attribution of drivers to the detected changes. Only with that information can we assess the effects of current climatic variations versus other, possibly anthropogenic, effects (de Jong et al. 2013). Our goal was, for Switzerland specifically, to quantify recent changes in vegetation activity and LSP and to reveal spatial relationships with changes in growth-limiting climatologies. This analysis supports the detection of 'hot-spots' of change for further studies of the interactions between vegetation and a-biotic factors within the Swiss Earth Observatory Network (SEON).

Various satellite sensors provide measurements of vegetation activity. Data of NOAA satellites give the longest run, 1982-2012, but with a coarse spatial resolution of ca. 9 km (Pinzon and Tucker, 2014). More recent sensors, like MODIS, provide a spatial resolution of 0.5 km although for a shorter time span (2000-2013). We analyzed both datasets: one for a longer-term general picture and the other for a more detailed spatial analysis. Gridded datasets of climatologies were provided by MeteoSwiss (2014) and the methodolgy was adopted from de Jong et. al. (2013) and Garonna et al. (2014).
Preliminary results of the longer-term observations indicate increases in vegetation activity, while observations since 2000 suggest a subsequent reduction. The comparison of coarse and fine spatial resolution data reveals a large spatial hetereogeneity of tend changes caused by complex topography and landscape fragmentation. Links with climatologies appeared to be not straightforward, due to the relatively short observational period of the high-resolution data and prevailing landscape herterogeneity. We present the methodological framework as it was developed for global studies, as well as the preliminary results for Switzerland, including maps of vegetation trend changes and links to climatologies.

REFERENCES

De Jong R, Schaepman ME, Furrer R, De Bruin S, Verburg PH (2013) Spatial relationship between climatologies and changes in global vegetation activity. Global Change Biology, 19, 1953-1964.

Field CB, Randerson JT, Malmström CM (1995) Global net primary production: Combining ecology and remote sensing. Remote Sensing of Environment, 51, 74-88.

Garonna I, De Jong R, De Wit A, Mücher S, Schmid B, Schaepman M (Early view) Strong contribution of autumn phenology to changes in satellite-derived growing season length estimates across Europe (1982–2011). Global Change Biology.

MeteoSwiss (2014). Gridded data of MeteoSwiss. Products: SRelM_ch02.lonlat, RhiresM_ch02.lonlat, TabsM_ch02.lonlat. Access date: Aug 15th 2014. URL: http://www.meteoswiss.admin.ch/web/en/services/data_portal/gridded_datasets.html

Pinzon J, Tucker C (2014) A Non-Stationary 1981-2012 AVHRR NDVI3g Time Series. Remote Sensing, 6, 6929-6960.

P 18.2

Remote sensing of forest ecosystems using airborne laser scanning and imaging spectroscopy

Fabian D Schneider[1], Reik Leiterer[1], Felix Morsdorf[1] & Michael E Schaepman[1]

[1] *Remote Sensing Laboratories, Department of Geography, University of Zurich, Winterthurerstr. 190, CH-8057 Zurich (fabian-daniel.schneider@geo.uzh.ch)*

Remote sensing offers the potential to provide spatially and temporally distributed information on key biophysical and biochemical variables of forest ecosystems. Airborne laser scanning (ALS) is especially well suited to characterize the forest structure. It allows to measure three-dimensional (3D) point clouds, which can be used for area-wide forest structural variable retrieval. Besides variables such as plant area index or canopy height, seasonal ALS data can be used to classify canopy background elements and canopy structure types (Leiterer et al. 2013, 2014).

Whereas laser scanning provides mainly geometrical information, passive optical imaging spectroscopy can be used to retrieve biochemical plant traits. However, this is challenging since atmospheric effects, canopy structure, illumination and viewing conditions have to be considered when airborne or spaceborne measurements are linked to leaf level traits. Therefore, the 3D radiative transfer model DART was parameterized using airborne, in situ and laboratory approaches to simulate imaging spectrometer data (Schneider et al. 2014). The model provides an advanced representation of the radiative regime, which is suitable to simulate most spatial and spectral features of imaging spectrometer data. The results show the potential to inversely derive biochemical plant traits from airborne and spaceborne earth observations.

REFERENCES

Leiterer, R., Furrer, R., Schaepman, M.E. & Morsdorf, F. 2014: Canopy structure types – forest characterization based on airborne laser scanning. Remote Sensing of Environment, submitted.

Leiterer, R., Mücke, W., Hollaus, M., Pfeifer, N. & Schaepman, M.E. 2013: Operational forest structure monitoring using airborne laser scanning. Photogrammetrie – Fernerkundung – Geoinformation, 173-184.

Schneider, F.D., Leiterer, R., Morsdorf, F., Gastellu-Etchegorry, J.-P., Lauret, N., Pfeifer, N. & Schaepman, M.E. 2014: Simulating imaging spectrometer data: 3D forest modeling based on LiDAR and in situ data. Remote Sensing of Environment 152, 235-250.

P 18.3

A European Lake Surface Water Temperature data set derived from NOAA/Metop-AVHRR (1983 – 2013)

Gian Lieberherr[1 2], Michael Riffler[1 2], Stefan Wunderle[1 2]

[1] *Institute of Geography, University of Bern, Switzerland*
[2] *Oeschger Centre for Climate Change Research, University of Bern, Switzerland*

Lake water temperature (LWT) is an important driver of lake ecosystems and it has been identified as an indicator of climate change. Not only far back-reaching retrievals of climate information from lake sediments are of interest, but also shorter and more accurate time-series of lake water temperature are great proxies for the recent climate.

By gathering water temperature data for European lakes, one can find a patchwork of datasets with varying temporal and spatial coverage, and retrieved with various methods. Hence the available data is spatially and temporally heterogeneous and therefore not well suited for the study of climate induced change.

This project aims to compile a robust dataset of European lake surface water temperature (LSWT) with a homogeneous spatial and temporal coverage. This will be done using a consistent satellite temperature retrieval method applied on the NOAA/Metop-AVHRR data archive of the Remote Sensing Group at the University of Bern. The archive is covering Europe with a time span of more than 30 years (1983 to today).

State-of-the-art procedures to retrieve surface temperature are all based on the split-window approach. Well-known procedures to retrieve sea surface temperature (SST) are the NOAA NESDIS non-linear SST (NLSST) and the Pathfinder-SST (PFSST) algorithms. Both methods are tailored for ocean monitoring on a global scale. But due to differences in emissivity and atmospheric conditions, the ocean-optimized methods lead to less accurate LSWT retrievals. In the work of Riffler et al. (2014) [1], a comparison of different methods with in situ measurements of Swiss lakes showed that using an optimized procedure (referred to Hulley et al. 2011 [2]) with local split-window coefficients performs better than using a approach which is globally valid.

To retrieve local split window coefficients, a method based on a fast radiative transfer (RT) model (RTTOV-11; Saunders et al. 2013) [3] is used. After simulating the AVHRR thermal infra-red channels 4 and 5 for each region, the local coefficients are derived by multi-linear regression.

To validate the retrieved LSWT dataset, in-situ measurement data for many European lakes are collected. The simulated LSWT are adapted for bulk measurements using the method of Minnett et al. (2011) [4] taking into account wind induced mixing of the uppermost water layer.

At the current state, the quality of night-time and day-time LSWT retrieval is evaluated. The accuracy of night-time-data is suspected to be lowered, due to cloud and land-contamination during retrieval. This is because geo-referencing and cloud-masking for night-time scenes are more likely to be inaccurate, as there is no information available for the visible spectrum. On the other hand night-time-data is supposed to be more robust, because of less fluctuation of the surface temperature induced by external influences, esp. solar radiation.

As a first result, the importance of these aspects are evaluated and discussed through a combined daytime/nighttime dataset. This first dataset consists in the temperature retrievals from two European lakes, one representing the mid-latitudes, and one representing the northern latitudes. This lays the foundation of further improvements for the processing of the whole available satellite data archive.

REFERENCES

[1] Riffler, M. and Wunderle, S., 2014, Lake surface water temperatures of European Alpine lakes (1989–2013) based on the Advanced Very High Resolution Radiometer (AVHRR) 1 km data set, Earth Syst. Sci. Data Discuss., 7, 305-334, doi:10.5194/essdd-7-305-2014

[2] Hulley, G.C., S. J. Hook, P. Schneider, 2011, Optimized split-window coefficients for deriving surface temperatures from inland water bodies, Remote Sensing of Environment 115 (2011) 3758–3769

[3] Saunders, R., Hocking, J., Rundle, D., Rayer, P., Matricardi, M., Geer, A., Lupu, C., Brunel, P. and Vidot, J. (2013): RTTOV-11 Science and Validation Report, available at http://research.metoffice.gov.uk/research/interproj/nwpsaf/rtm/docs_rttov11/rttov11_svr.pdf

[4] Minnett, P. J., M. Smith, and B. Ward, 2011: Measurements of the oceanic thermal skin effect. Deep Sea Research Part II: Topical Studies in Oceanography, 58,861-868.

P 18.4

Operational Snow Cover Mapping and Analysis in the Canton of Valais Based on MODIS Data

Alex Dionisio Calado[1], Stéphane Micheloud[1], Javier García Hernandez[1], Alain Foehn[1], Pascal Ornstein[1] & Aurélien Claude[1].

[1] *Centre de recherche sur l'environnement alpin, CREALP, Rue de l'Industrie 45, 1951 Sion, Suisse (javier.garcia@crealp.vs.ch)*

In alpine catchments, snowmelt is a factor that can significantly accentuate flow rates during flood periods. Indeed, during a heat wave and heavy rain periods, water accumulated as snow is released and contributes directly to the increase of river flow rates. Therefore, the monitoring of snow cover over a study basin is essential to understand and prevent potential risk situations.

The methods presented in this paper are based on data from the Moderate Resolution Imaging Spectroradiometer (MODIS) carried by the Aqua and Terra satellites, from the Earth Observing System (EOS) program of the NASA. The data is automatically acquired and processed on a daily basis over a 5520 km^2 area representing the Upper Rhone River basin, mainly located in the Canton of Valais (Switzerland). The processing chain is operational and produces daily snow maps and related statistics. The results are available to hydro-meteorological experts and are used for decision support.

One of the main limitations of MODIS technology is the presence of clouds in the data, which cover on average 56% of the images in the Rhône basin. Indeed, MODIS detects wavelengths ranging between 0.4 and 14 µm, which cannot penetrate clouds. In order to enable a complete statistical analysis of the data, a methodology has been set up to reduce cloud obscuration in MODIS data. First, the data collected from the Aqua and Terra satellites, which pass daily at an interval of 3 hours, is combined to reduce the total number of clouded pixels by around 10%. Then, the remaining cloud areas are filled in using a time interpolation-based method (López-Burgos et al., 2013). If a pixel is obscured by clouds, the most recent value from up to 7 previous days is used instead. The remaining obscured surface is thus reduced by a further 93%. On average, the final cloud obscuration rate thus obtained is less than 1%.

After cloud obscuration processing, a daily map of snow cover and relevant statistics are calculated for the whole Rhône basin and for twenty two hydrological sub-basins. For each daily map of snow cover, statistics of replaced clouds based on previous days are presented as a pie chart (Figure 1). Statistics on snow cover are generated for both daily and monthly time steps. The snow cover is then calculated and compared to the quantiles calculated over the available 12 past years data (figure 2).

A preliminary comparison of MODIS processed data and the snow cover data (interpolated from meteorological stations) from the Institute for Snow and Avalanche Research (SLF) has been realized for the periods of Dec. 2013 to May 2014. The MODIS data usually estimates sensibly less snow cover than SLF data. During winter and depending on the region, 0 to 5% less snow cover can be observed on average. During spring time, the variation can be greater, from 0 to 10% less than SLF. Further analysis is planned for future work.

The MODIS data processing could greatly enhance our knowledge about spatial snow cover distribution and its temporal evolution throughout the year. It offers a way to assess the inter-annual variability in space and time of snow covered areas that could be linked to climate change. It provides additional information that reduces the uncertainty on the hydrological state of the basin. In addition, the snow cover data is used to validate the snow cover simulated by the hydrological model of the MINERVE system (García Hernández et al., 2013), which generates real-time hydrological forecasts for the Upper Rhone River basin. MODIS data is also useful for water resources management within the project STRADA (CREALP, Projet INTERREG III_A – STRADA, 2013-2014).

REFERENCES

García Hernández, J., Boillat, J.-L., Feller, I. & Schleiss, A. J. 2013. Présent et futur des prévisions hydrologiques pour la gestion des crues. Le cas du Rhône alpin. Mémoire de la Société Vaudoise des Sciences Naturelles 25, 55-70.

López-Burgos, V., Gupta, H.V., & Clark, M. 2013: Reducing cloud obscuration of MODIS snow cover area products by combining spatio-temporal techniques with a probability of snow approach. Hydrology and Earth System Sciences, 17, 1809-1823.

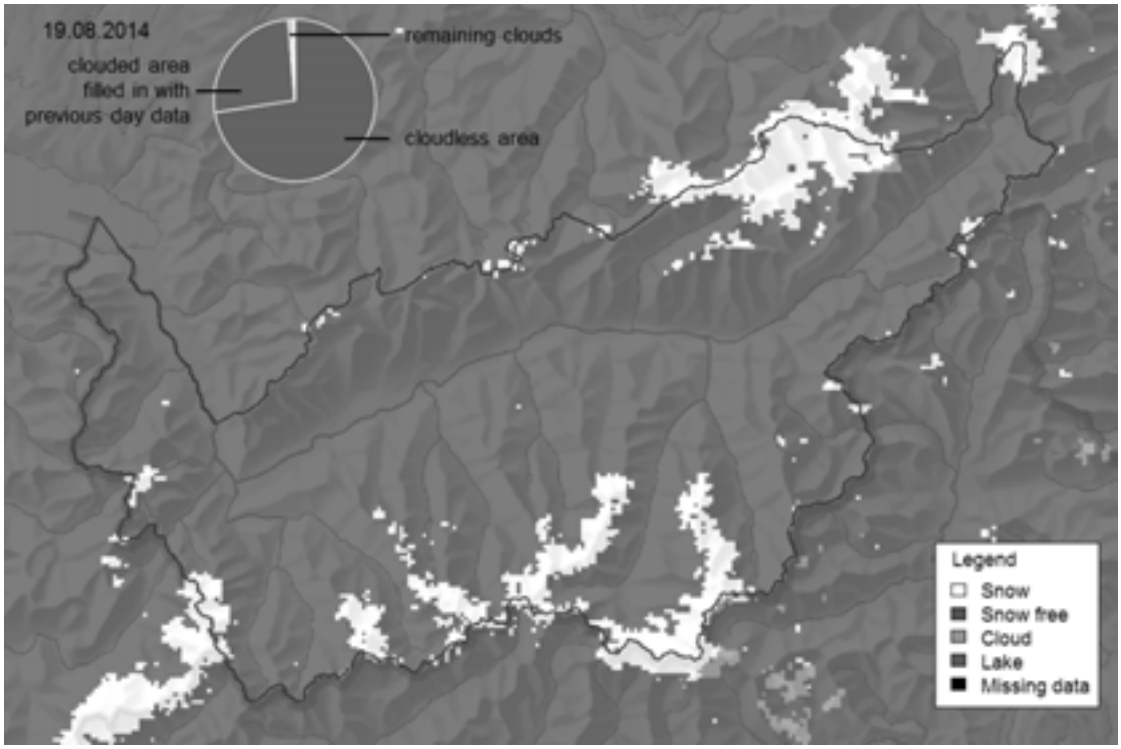

Figure 1. Valais snow cover and pie chart with cloud replacement information

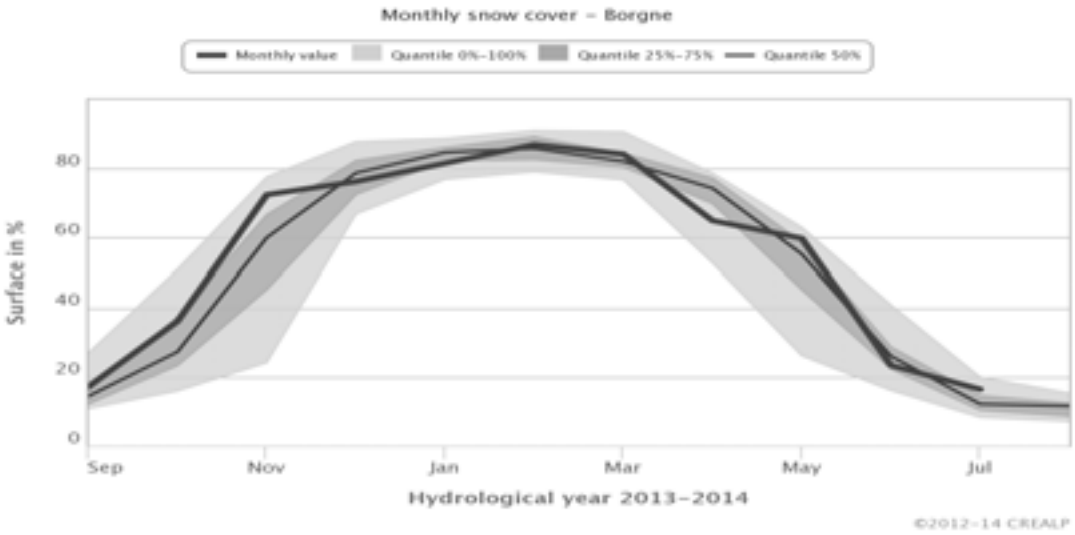

Figure 2. Monthly snow cover area for the Borgne basin in Valais.

P 18.5

The Three Roles of the Rapid Data Delivery System of NORS/Copernicus

K. Hocke (University of Bern) + Colleagues from NORS, NDACC, MACC

The Rapid Data Delivery System (RDDS) has been realized within the EU project NORS and NDACC. RDDS takes advantage on the infra-structure of the NDACC data center which is dedicated to the archiving of ground-based remote sensing data for the detection of long-term trends in the atmospheric composition. Complementary to NDACC, the ground-based remote sensing data of RDDS are suited for the rapid validation of satellites such as the Sentinel satellites of the Copernicus Earth Observation programme. Further, RDDS data are already taken for validation and tuning of the chemical weather forecast system MACC (EU project Monitoring of Atmospheric Composition and Climate). So, the first role of RDDS is the rapid validation of satellite data and MACC analyses. The second role of RDDS is capacity building since RDDS can serve as a testbed for new stations which may later fullfill the strict rules of NDACC data quality. In addition, the new data format GEOMS-HDF and the NORS validation server were firstly tested by RDDS, NORS and MACC, - of course with strong support from NDACC. The advantage is again that RDDS is more flexible in view of data quality, and it consists of less members and stations compared to NDACC so that new ideas can be easier discussed and tested within RDDS. The third role of RDDS could be the rapid and operational data assimilation of ground-based remote sensing data into chemical weather forecast systems. Unfortunately, the third role of RDDS is in conflict with its first role: to be an independent data source for validation of satellite data and MACC analyses.

P 18.6

New perspectives from Landsat 8 and Sentinel-2: Earth Observation Products

Hendrik Wulf[1], Philip C. Joerg[1], Reik Leiterer[1] & Michael E. Schaepman[1]

[1] *Remote Sensing Laboratories, University of Zurich, Winterthurerstr. 190, CH-8057 Zurich (hendrik.wulf@geo.uzh.ch)*

Earth observation facilitates a comprehensive monitoring and assessment of the status and changes in our environment. In recent years, the underlying remote sensing technologies have become more sophisticated while most data are easily accessible and freely available. This ongoing development underlines the growing importance of satellite imagery, which offers multiple opportunities to measure land-use changes (e.g. deforestation), manage natural resources (e.g. freshwater, agriculture), monitor and respond to natural disasters (e.g. fires, floods), or to predict, adapt to and mitigate climate change.

The Swiss National Point of Contact (NPOC) for satellite images aims to foster and promote the use of Earth Observation data to support Swiss authorities, research agencies, commercial providers, and end-users. It is a joint venture of the Remote Sensing Laboratories at the University of Zurich and the Federal Office of Topography (swisstopo). As part of our activities, the NPOC aims to support the use of state-of-the-art Earth Observation products by strengthening expertise and building up competences in the exploitation of satellite data. In this study, we demonstrate the use of Landsat and simulated Sentinel-2 (launch 2015) data to infer selected Essential Climate Variables (ECV) and associate remote sensing products, which provide information on the status and evolution of various terrestrial and aquatic ecosystems. The Landsat series offers a consistent data source dating back to 1972, which is suited for operational monitoring, assessing, and predicting land surface change over time. Complementary, the Sentinel-2 sensor and mission specifications hold further potential to continuously extract new surface parameters at an unprecedented spatio-temporal scale.
Spectral indices products are derived from Landsat surface reflectance data, which are generated by specialized software like LEDASP (Masek 2006) and fmask (Zhu & Woodcock 2012). This pre-processing, which generates Top of Atmosphere (TOA) Reflectance, Surface Reflectance, and Brightness Temperature data also accounts for data gaps by clouds and cloud shadows. Simulated Sentinel-2 surface reflectance data is based on airborne imaging spectroscopy acquisitions of the APEX (Airborne Prism Experiment) sensor and generated by the Sentinel-2 end-to-end simulator (Segl et al. 2012).

We illustrate the applicability of both sensors to:

i) characterize the hydrosphere by extracting surface reflectance derived spectral indices to derive chlorophyll-a concentration, total suspended solids, and secci depth transparency of Lake Geneva (Fig 1).

ii) quantify cryospheric changes by inferring information on snow cover extent, light-absorbing impurities in snow, and glacial albedo in the alpine terrain of the Findelen- and Plaine Morte Glacier (Fig 1), and

iii) to examine the biosphere and extract indices for chlorophyll absorption (MCARI2), leaf chlorophyll content (Chl), leaf carotenoid content (Car) and plant anthocyanin content (Anth) for the mixed deciduous Lägeren forest (Fig 1).

In response to natural disasters remote sensing also offers valuable information needed to manage the crises. In this context, we illustrate the use of satellite imagery to derive water extend of flooded areas and to detect active fires and burnt areas.

The selected examples of derived ECVs and associated remote sensing products across different spheres underline the unique potential of existing and upcoming satellite imagery to provide up-to-date and reliable information on the status of, and changes in, our environment. This freely available information will benefit services in land management, agriculture, forestry and hydrology as well as disaster control and humanitarian relief operations. Based on these selected examples of remote sensing products the NPOC aims to highlight the value of satellite imagery, in order to foster its use along with further scientific advice to potential earth observation data users.

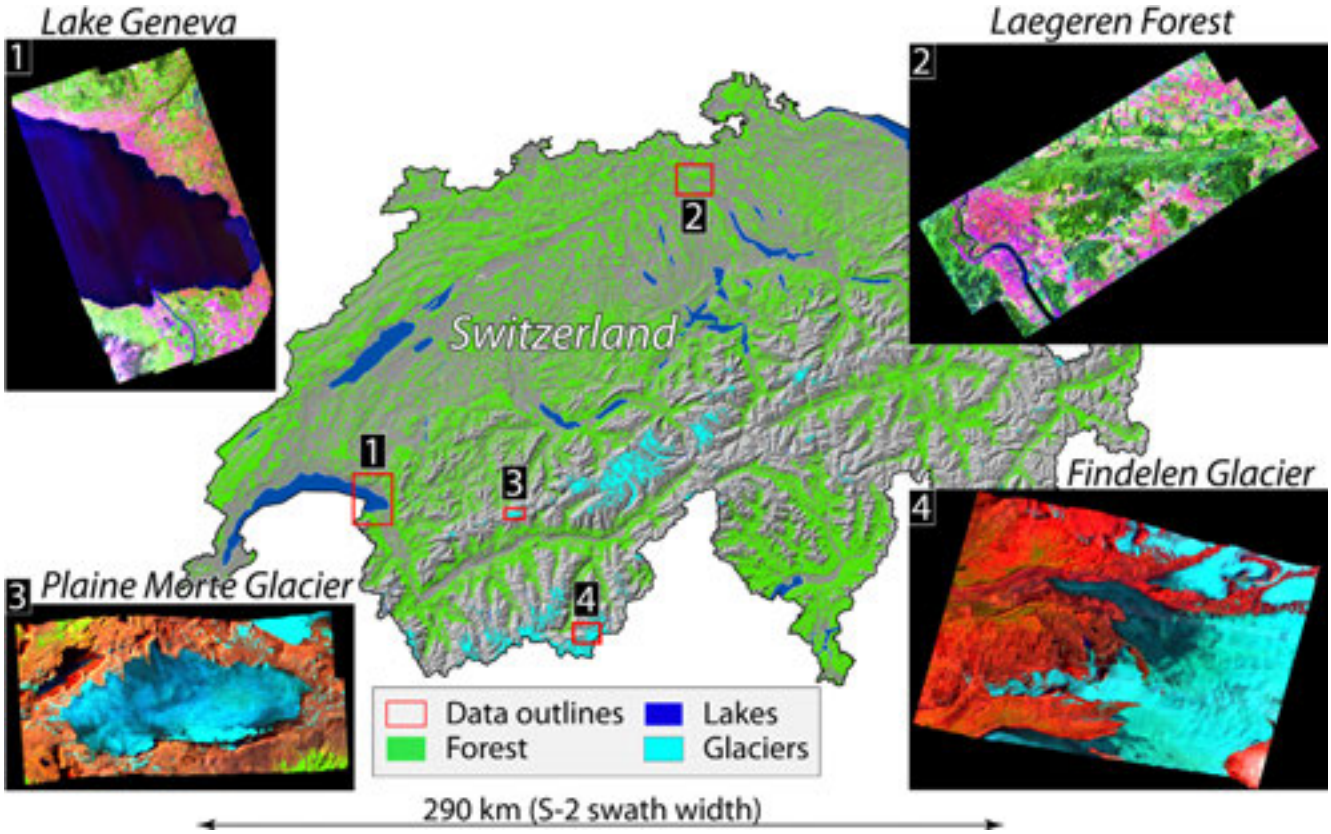

Figure 1. Forests, lakes and glaciers in Switzerland draped over a hillshade image. Red rectangles indicate the location of selected study areas covering different Earth spheres and ecosystems.

REFERENCES

Masek, J.G., Vermote, E.F., Saleous N.E., Wolfe, R., Hall, F.G., Huemmrich, K.F., Gao, F., Kutler, J., & Lim, T-K. 2006: A Landsat surface reflectance dataset for North America, 1990–2000. IEEE Geoscience and Remote Sensing Letters 3(1): 68-72.

Segl, K., Richter, R., Küster, T., Kaufmann, H. 2012: End-to-end sensor simulation for spectral band selection and optimization with application to the Sentinel-2 mission. Applied Optics, 51 (4), pp. 439-449.

Zhu, Z. & Woodcock, C. E. 2012: Object-based cloud and cloud shadow detection in Landsat imagery, Remote Sensing of Environment, 118, 83-94.

P 18.7

Climatic signal propagation form source to sink in a Palaeogene sediment routing system, Pyrenean foreland basin, Spain

Louis Honegger[1], Sébastien Castelltort[1], Julian Clark[2], Thierry Adatte[3], Cai Puigdefàbregas[4], Mason Dykstra[2], Andrea Fildani[2]

[1] *Département des Sciences de la Terre, Université de Genève, Rue des Maraîchers 13, CH-1205 Genève (louis.honegger@etu.unige.ch, sebastien.castelltort@unige.ch)*
[2] *Statoil, 6300 Bridge Point Parkway, Austin, TX, USA*
[3] *Institut des Sciences de la Terre, Université de Lausanne, CH-1015 Lausanne*
[4] *Institut de Ciències de la Terra (CSIC), Carrer Lluis Solé Sabaris, 08028 Barcelona, Spain*

Cyclicities of different types in the sedimentary record have long been documented. The ongoing debate is about the various origins that have been put forward to explain them: eustastic sea level changes, sediment supply variations or subsidence pulses. In the deep water system of the lower-middle Eocene Ainsa basin, in the southern Pyreneans (Spain), as well as in its fluvial counterparts in the Tremp-Graus basin, stratigraphic cyclicity in the form of repetitive alternations of sand and shale packages of intermediate timescales (10e4 to 10e6 years) has long been recognized and has typically been imputed to eustatic changes, with a modulation by active tectonics. Most of the studies have focused so far either on the deep water system or on their fluvial counterparts without a detailed effort at the correlation between both.

While eustatic variations are well known to have taken place at these periods and are thus plausible causes of the observed cyclicities, our objective is to evaluate the possible role of sediment supply variations in generating or modifying such cyclicities. This is particularly important in order to understand how sediment supply variations are tied to climate and tectonics in the source area over multi-millennial timescales and how the deep-sea sedimentary record can be used to reconstruct the Earth's history of surface response to climate change. To address these issues a mapping and multi-proxy approach was undertaken in the Tremp-Graus and Ainsa basins. We focus on the middle Eocene Castissent formation, a major fluvial excursion and its deep marine time-equivalent; the Arro-Gerbe section. XRF geochemistry, stable isotopes and clay analyses were made on four increasingly distal cross-sections to attempt to trace environmental signals across the whole source-to-sink system. These analyses coupled with thorough physical mapping on the field and a comprehension of the volumetrical partitioning of the sediments allow us to discuss hypotheses of climatic and eustatic controls of cyclicity.

REFERENCES

Cantalejo, B., & Pickering, K. T. (2014). Climate forcing of fine-grained deep-marine systems in an active tectonic setting: Middle Eocene, Ainsa Basin, Spanish Pyrenees. Palaeogeography, Palaeoclimatology, Palaeoecology, 410, 351–371. doi:10.1016/j.palaeo.2014.06.005

Marzo, M. (1988). Architecture of the Castissent fluvial sheet sandstones , Eocene , South Pyrenees , Spain, 719–738.

Nijman, W., & Nio, S.-D. (1975). The Eocene Montañana Delta.

19. Geoscience and Geoinformation - From data acquisition to modelling and visualisation

Nils Oesterling, Adrian Wiget, Massimiliano Cannata

Swiss Geological Survey – swisstopo,
Swiss Geodetic Commission,
Swiss Geotechnical Commission,
Swiss Geophysical Commission,
Swiss Hydrogeological Society

TALKS:

POSTERS:

P 19.1 Avelar S., Hanselmann K., Vasconcelos C.: Data Analysis for Modeling Dissolution of Carbonate Minerals in Hypersaline Lagoon Water

P 19.2 Calpini C., Simpson G., Frischknecht C., Girardclos S.: From data treatment to tsunami hazard assessment in lakes: the challenging case of Lake Geneva

P 19.3 Negro F., Kerrou J.: Regional hydrogeological modelling of the central Jura in the area of Neuchâtel. Part 1 : 3D geological modelling

P 19.4 Kerrou J., Negro F.: Regional hydrogeological modelling of the central Jura in the area of Neuchâtel. Part 2 : 3D groundwater flow and mass transport modelling

P 19.5 Mock S., Allenbach R., Reynolds L., Baumberger R., Herwegh M.: 3D structural modelling of the Swiss Molasse Basin in the Canton of Bern

P 19.6 Le Cotonnec A., Ventra D., Moscariello A.: Architecture and property distribution of coal-bearing successions in Late Carboniferous fluvio-deltaic deposits (SE Kentucky, USA)

P 19.7 Yuzugullu O., Erten E., Hajnsek I.: Growth Stage Determination of Rice Fields: EMS Model Search Space Solution

19.1

Making information available to stakeholders for improved management of groundwater resources in arid Chad

Maëlle Aubert[1], Yves Haeberlin[1], Ismael Musa Mohamed[2], Pascal Marguerat[3], François Zwahlen[4], Marc-André Bünzli[5], Marie-Louise Vogt[1/2], Jennifer Tschopp[1], Amira Kraiem[1], Tiffany Tchang[1], Adam Ali[1], Olivier Sénégas[1], Janvier Bazoun[1/2]

[1] *UNOSAT, United Nations Institute for Training and Research (UNITAR), Palais des Nations, CH-1211 Genève (maelle.aubert@unitar.org)*
[2] *Ministère de l'Elevage et de l'Hydraulique (MEH), N'Djaména, Tchad*
[3]swisstopo, Seftigenstrasse 264, CH-3084 Wabern
[4] *Centre d'Hydrogéologie et de Géothermie (CHYN), Rue Emile-Argand 11, CH-2000 Neuchâtel*
[5] *Humanitarian Aid and SHA, Swiss Agency for Development and Cooperation (SDC), Sägestrasse 77, Köniz, CH-3003 Bern*

Water resources are substantial in the Republic of Chad, but are unevenly distributed, locally difficult to access and above all poorly identified. The establishment of an active, sustainable and sovereign management of surface and ground waters, essential for achieving the development goals of Chad, necessitates improved knowledge of the resources and national capacity in the sector. Considering the situation, in 2009 the Chadian government asked the Swiss Agency for Development and Cooperation (SDC) to prepare a detailed concept paper addressing how to map Chad´s water resources. In 2012, an agreement was signed between the Water Ministry (currently Ministère de l'Elevage et de l'Hydraulique) and the SDC to support this initiative. This agreement gave birth to ResEau, a project implemented and managed by the Ministry and the United Nations Operational Satellite Applications Programme (UNITAR-UNOSAT), with the support of esteemed partners, including the Federal Office of Topography (swisstopo) and the Centre d'Hydrogéologie et de Géothermie (CHYN). The project is designed for a nine-year period lasting until 2020, at which point the entire country´s water potential will have been mapped.

The first phase of the ResEau project focuses on developing a knowledge base for the northern and eastern regions of Chad. To achieve this, the ResEau team has created a GIS and water library database, including geological, hydrological and well/borehole information for Chad. From this database two hydrogeological atlases are being prepared by UNOSAT and graphically edited by swisstopo, with the release of state of the art paper maps: a survey map series at a 1:500,000 scale and a facility and resource map series at a 1:200,000 scale. The survey maps illustrate the nature, location and productivity of regional and other minor aquifers. A detailed note at the back of the map provides a description of the hydrogeological units and rainfall, water quality, and socio-economic information to better understand the regional context. The facility and resource maps, prepared for urban areas or near remarkable hydrological sites, provide detailed information on water resources in these zones. In June 2014, three of the nine planned maps at 1:500,000 scale (Ennedi, Wadi Fira Est and Ouadi Kadja), and the first of the fifteen planned maps at 1:200,000 scale (Am Zoer) have been published in paper print and numerical formats (Figure 1). These maps, resulting from a combination of satellite and well/borehole data, offer a new synthesis of the region´s hydrogeology at an unprecedented level of detail; they will also buttress future Chadian hydrogeological expertise on a large scale. Validation via targeted field missions reinforces the scientific quality of these products. A final control occurs when the pre-print maps are submitted to the Chadian Ministry´s expertise.Indeed, besides backstopping validation by taking advantage of their knowledge of the territory, this process ensures that the maps being produced correspond to the needs of the Chadian government.

The publication of the 1:500,000 Ennedi hydrogeological sheet (Fig. 1) has already contributed to improving the knowledge and understanding of regional and local aquifers and thereby the water resources in the towns of Fada and Amdjarass. Key information learnt from the mapping and hydrogeological syntheses of the region covered by this map (16-18°N, 21-24°E) includes:

- Cambrian sandstones are a good regional aquifer, with water circulation over the basement contact, and perennial resurgences expressed by sources and gueltas (Archéï, Bachikélé).
- Fada sits on a multilayer Silurian sandstone aquifer, with the upper layer feeding the palm trees.
- Alluvial zones hold locally shallow, non-perennial water bodies, whose behavior and production are related to wadi hydrogeological regime and sand/clay composition of the sediments.
- Mortcha plain is very unfavorable for groundwater; only low-productive saprolite aquifers have been found at the foot of the sandstone massif.
- There is no evidence for fossil groundwater in this region; chemical and isotopic analyses indicate modern recharge from meteoric water.

The above facts do not point to a water shortage in the region, but draw attention to the need to take measures to better preserve and manage the fragile resource.

The water-related knowledge acquired by the ResEau team, as illustrated by the Ennedi example, is duly documented

through the publication of scientific reports and transferred to professionals in Chad. The goal is that by the end of the project, the Chadian government will possess a comprehensive water database to conduct its own studies and better manage the country´s water resources. Furthermore, the ResEau project is implementing complementary activities (GIS and hydrological formations, media,..) that aim to bring together the actors that have a stake in managing Chad´s water resources.

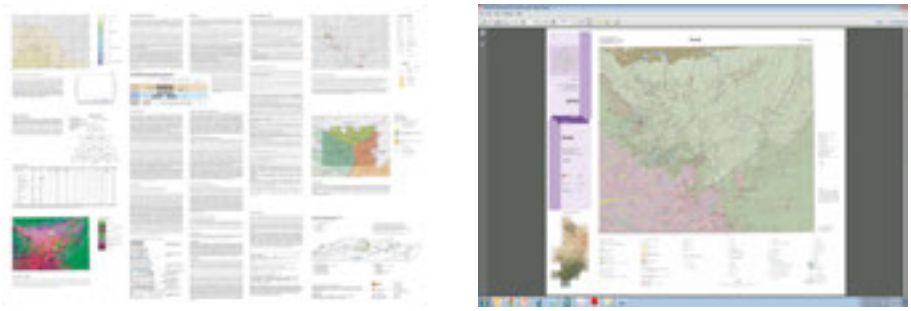

Figure 1. Hydrogeological survey map of the Republic of Chad at 1:500,000 scale, Ennedi sheet. (left) front side of map; (right) explanatory note and synoptic maps on the back side.

19.2

The Data Model Borehole Data – A structure for digital one-dimensional subsurface data

Sabine Brodhag[1], Nils Oesterling[1]

[1] *Federal Office of Topography swisstopo, Swiss Geological Survey, Seftigenstrasse 264, CH-3084 Wabern (sabine.brodhag@swisstopo.ch)*

Every year more and more boreholes are drilled in Switzerland. These boreholes provide important and unique information about the geological underground, for example its composition, structure etc. This information is key for understanding the subsurface and therefore, an essential basis for tackling various challenges of our society. Examples are: construction of housing and traffic infrastructure, supply of energy, water and other natural resources, protection for natural hazards etc.

The drilling of a borehole requires, in general, a permission of a cantonal or federal authority. This permission typically includes the condition to deliver the generated borehole data (e.g. well profile) to the respective authority. Several norms (e.g. SN 640 034; SN 670 004), guidelines and recommendations (e.g. by cantonal granting authorities) exist for analogue recordings of this data (e.g. description of the cuttings, illustration of well profile). This is different for digital data. Up to now, no common definition and structure of such data and no recommendation for its acquisition, storage and exchange exists neither on cantonal nor on a federal level. For this reason, many borehole data are delivered in an incomplete and incompatible state to the authorities. An efficient exchange of digital borehole data is therefore not possible. This problem applies not only to administration but also to scientific or economic drilling projects, where efficient data exchange is needed.

In order to tackle this problem, swisstopo established together with cantonal and federal offices and the private sector a working group which developed a common minimal data model for borehole data. This model describes various borehole types, soundings and artificial outcrops as a one-dimensional (linear) geometry and which can be represented as a single point at the earth's surface.

Since the access to borehole data is frequently restricted, the data model is separated into an inner core (where information is always freely available) and an extended core (information may be access-restricted) (Fig. 1). Apart from this two-part core, the data model may be extended by various thematic modules, some of which are currently in development.

The Data Model Borehole Data is a supplement to the Data Model Geology (Swisstopo) and specifies borehole data in greater detail. In addition to these two data models, swisstopo is working on a data model for metadata associated with geological documents (e.g. geological reports).

Figure 1. UML class diagram of the inner and extended core, as well different envisioned thematic modules. The Inner Core of the data model contains information which is always available without restriction. The Extended Core may contain information which is restricted.

REFERENCES

SN / VSS 2011: Darstellung der Projekte – Signaturen für die Geotechnik und die Geologie. SN 640 034.

SN / VSS 2005: Geotechnische Erkundung und Untersuchung – Benennung, Beschreibung und Klassifizierung von Boden – Teil 1 und 2. SN 670 004.

Bundesamt für Landestopografie swisstopo, Landesgeologie 2012: Datenmodell Geologie – Beschreibung im UML-Format und Objektkatalog, Version 2.1.

19.3

SITGAP 2.0 – Comprehensive system for risk management

Massimiliano Cannata[1], Milan Anotnovic[1]

[1] *Institute of Earth Sciences, SUPSI, Campus Trevano, 6952 Canobbio, Switzerland (massimiliano.cannata@supsi.ch)*

Several studies on climate changes have predicted an increase in high-intensity precipitations in Europe, which is likely increase the frequency and magnitude of natural hazards. Wherever is possible the more appropriate and auspicated risk management approach is a wise land use planning regulation in order to reduce as much as possible people and valuable objects exposition. Unfortunately, in most of the cases, people and developed areas are located in areas alredy threaten by different types of risks like, for example, floodings of nearby rivers, inundations from surronding lakes or landslides from the nearby mountain slopes. In all these cases, where the delocation of people and economic activities is not applicable, an early warning system may support the risk reduction by means of timely intervention actions and emergency plan actuation.

Thanks to impressive technological advances the visionary concept of the Digital Earth (Gore 1992, 1998) is being realizing: geospatial coverages and monitoring systems data are increasingly available on the Web, and more importantly, in a standard format. As a result, today is possible to develop innovative decision support systems (Molinari et al. 2013) which mesh-up several information sources and offers special features for risk scenarios evaluation. In agreement with the exposed view, the authors have recently developed a new Web system whose design is based on the Service Oriented Architecture pattern. Open source software (e.g.: Geoserver, PostGIS, OpenLayers) has been used throughout the whole system and geospatial Open Standards (e.g.: SOS, WMS, WFS) are the pillars it rely on.

SITGAP 2.0, implemented in collaboration with the Civil protection of Locarno e Vallemaggia, combines a number of data sources such as the Federal Register of Buildings and Dwellings, the Cantonal Register of residents, the Cadastral Surveying, the Cantonal Hydro-meteorological monitoring observations, the Meteoswiss weather forecasts, and others. As a result of this orchestration of data, SITGAP 2.0 serves features that allows, for example, to be informed on active alarms, to visualize lake level forecasts and associated flooding areas, to evaluate and map exposed elements and people, to plan and manage evacuation by searching for people living in particular areas or buildings, by registering evacuation actions and by searching for evacuated people.

System architecture and functionalities, and consideration on the integration and accessibility of the beneath information provides interesting discussion points for the identification of current and future needs.

Figure 1. SITGAP 2.0 Web interface illustrating a simulated active alarm with lake level forecasts, inundation area and exposed elements.

REFERENCES

Gore, A. 1992: Earth in the Balance. Boston, MA, Houghton Mifflin

Gore, A. 1998: The Digital Earth: Understanding our Planet in the 21st Century. WWW document, http://www.isde5.org/al_gore_speech.htm

Molinari, M.E., Cannata, M. & Meisina, C. 2013: r.massmov: an open-source landslide model for dynamic early warning systems. Natural Hazards. Advance online publication. doi: 10.1007/s11069-013-0867-8

19.4

Novel architecture for a borehole management system

Marcus Hoffmann[1], Massimiliano Cannata[1], Milan Antonovic[1]

[1] *Institute of Earth Science, University of Applied Sciences and Arts of Southern Switzerland, Campus Trevano 32, CH-6952 Canobbio (marcus.hoffmann @supsi.ch)*

Information and management of surveys, wells and springs in Ticino is based on a database born in the 1960s and currently managed by the Institute of Earth Sciences. In addition to basic information, such as coordinates, depth, location, register number and owner also information related to environmental measurements like water temperature, groundwater levels and results of diverse analyses, such as geological and chemical properties are stored in a relational database. Due to new technological and user requested needs, the current database is supposed to be migrated, developing a completely new structure using state-of-the-art technologies and architectures also compliant with the Swisstopo data model for boreholes. The proposed migration splits the dataset in two separate units:

- The administrative part will be migrated in JSON objects stored in a non-relational document database.
- One part of measurements related to the specific object will be handled by a standard SOS (istSOS) system, which describes the characteristics of a sample connected to the results of the analysis.

Figure 1 shows the current structure of the objects (wells, surveys and springs) with metadata and diverse types of measurements. A measurement based on a sample (orange) will be controlled by istSOS. Figure 2 shows a representation of elements of the SOS architecture which are mapped on standard key elements. This allows obtaining metadata of the procedures (such as modalities and adopted measuring instruments) and to search through these observations selecting parameters like name of the procedures, observed properties, spatial filters, temporal filters, group of procedures (offering) and others.

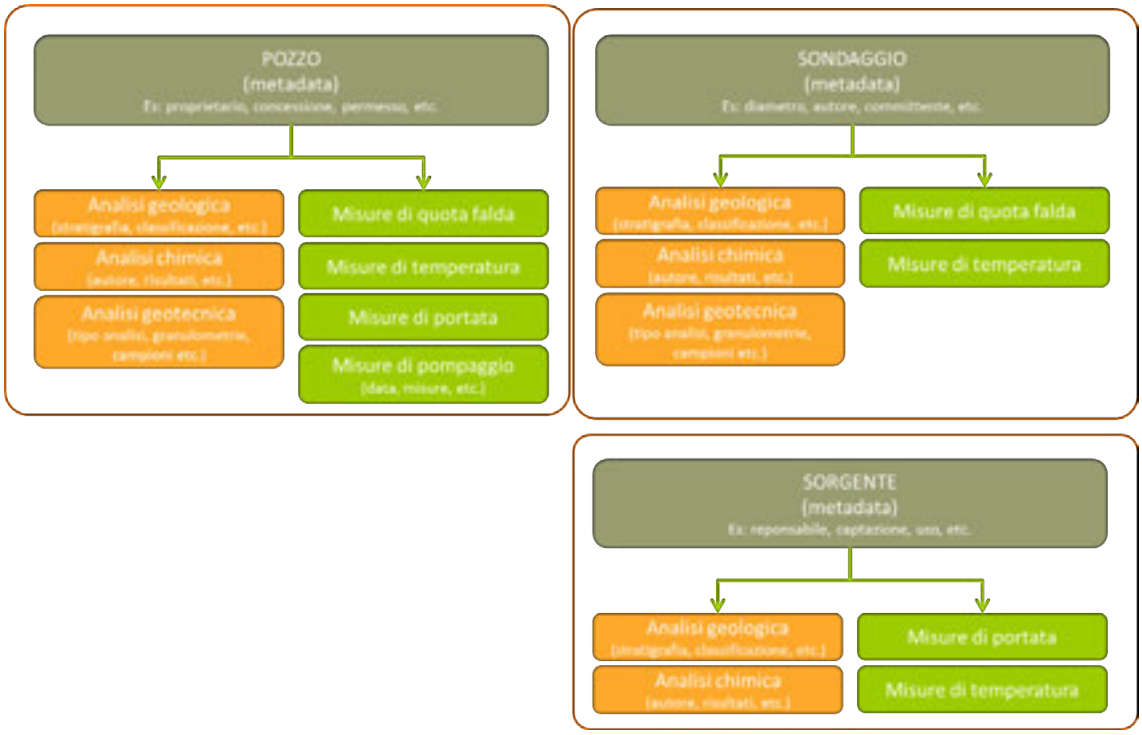

Figure 1. Schematization of the simplified structure of the current database

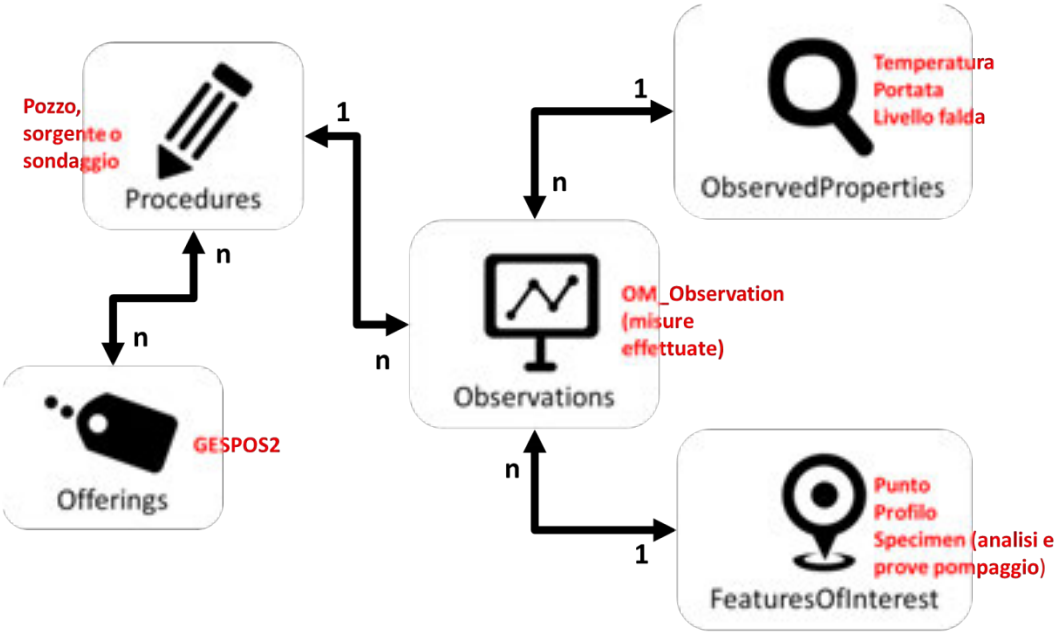

Figure 2. Mapping of the elements SOS with those of the new structure.

REFERENCES

Cannata M.& Antonovic M.: ISTSOS in Support of Enorasis for Optimizing Irrigation, Foss4G Europe 2014
Brodhag S., M., Salomè C. & Oesterling N.: Datenmodell Bohrdaten, Swisstopo 2013

19.5

KARSYS: a GIS- and 3D-based approach for the characterization of karst aquifers

Arnauld Malard, Pierre-Yves Jeannin, Eric Weber, Jonathan Vouillamoz[1]

[1] *Swiss Institute for Speleology and Karst Studies, La Chaux-de-Fonds, info@isska.ch, www.swisskarst.ch*

Only few methods do exist for the characterization of karst aquifers and rare are those which explicitly integrate 3D geological / hydrological data and hydraulic principles in a systematic way. The KARSYS approach (Jeannin et al. 2013) – already presented during the previous SGM's meetings – has been applied over a large part of the Swiss karst territory and abroad (Swisskarst project, Malard 2013) and it now entails a concrete and continuous workflow which basically combines: Database, GIS procedures and 3D Geological and hydrological modeling in order to address a large spectrum of pragmatic karst-related questions (mostly spatial issues as resources mapping, hazards in construction, geothermal probes regulations, etc.). Recent improvements and extensions have been implemented to the basic approach with the aim to address questions related to hydrological simulations (temporal issues: resources assessment, flood hazards, hazards in construction, etc.) whose results could be coupled with the physical karst model to provide a concrete image of the aquifer / system's functioning. The approach requires the use of common GIS, 3D modelling and hydrologic software programs as well as various dedicated home-made scripts and plugins to ensure the programs interoperability and the data integrity all along the workflow. The approach also includes a GIS dedicated data model which has been developed for (i) applying KARSYS and (ii) documenting karst aquifers properties.

The talk will present the workflow of a KARSYS application in the frame of flood hazards assessment from data acquisition to the implementation of a hydraulic pipe-flow model, passing through (i) the establishment of a conceptual karst aquifer model, (ii) the generation of a realistic (hydraulically-designed) conduits network, (iii) the simulation of the karst system's discharge rate and (iv) the evaluation of the related impact on the ground.

Advantages of this GIS- and 3-based approach are:

- KARSYS could be applied even with limited data and the model may be continuously refined by the implementation of additional data
- KARSYS could be applied at different scales by selecting appropriate data, providing results on the whole aquifer or solely on a selected karst system
- KARSYS provides spatial information which could be stored and surveyed through a dedicated GIS-database (Malard et al. in press) or transferred semi-automatically into hydrologic and hydraulic programs to provide temporal results. Finally spatial and temporal results could be combined to provide realistic image of the aquifer / system functioning.

REFERENCES

Jeannin, P.-Y., Eichenberger, U., Sinreich, M., Vouillamoz, J., Malard, A., & Weber, E. 2013: KARSYS: a pragmatic approach to karst hydrogeological system conceptualisation. Assessment of groundwater reserves and resources in Switzerland. Environmental Earth Sciences 69(3), 999-1013.

Malard, A. 2013: SWISSKARST: comprendre et documenter les systèmes karstiques de Suisse. Geosciences Actuel 1: 15-18.

Malard, A., Jeannin, P., Sinreich, M., Weber, E., Vouillamoz, J., & Eichenberger, U. in press: Praxisorientierter Ansatz zur Kartographischen Darstellung von Karst-Grundwasserressourcen - Erfahrungen aus dem SWISSKARST-Projekt. Grundwasser - Zeitschrift der Fachsektion Hydrogeologie.

19.6

Permanent rock glacier monitoring with a stereo pair of optical cameras

Fabian Neyer[1], Philippe Limpach[1], Tonio Gsell[2], Alain Geiger[1], and Jan Beutel[2]

[1] *Institute for Geodesy and Photogrammetry, ETH Zürich, Robert-Gnehm-Weg 15, CH-8093 Zürich (fabian.neyer@geod.baug.ethz.ch)*
[2] *Computer Engineering and Networks Laboratory, ETH Zürich, Gloriastrasse 35, CH-8092 Zürich*

Rock glaciers are of great interest to permafrost and natural hazard researchers because global warming is predicted to have a particular impact on the overall kinematic state of these perennially frozen ice/rock mixtures, thus changing their surface flow velocity and risk for slope failures. In recent years, remote sensing has become a very popular and powerful tool to study surface changes like the motion of rock glaciers. While radar interferometry (especially InSAR) is suitable for covering large areas, other methods prevail by an increased local accuracy in space and time (e.g. GPS, laser scanning, optical imaging).

With the fast development of high quality consumer cameras, optical image data acquisition in remote areas has become easier and significantly cheaper over the past few years. Due to the demand of surface displacement measurements for monitoring purposes, optical cameras are getting more and more popular also for continuous quantitative analyses. While normalized cross-correlation is the most popular algorithm in this research field, we use a highly adaptive robust least-squares matching strategy for tracking image features with sub-pixel accuracy.

Within the X-sense project (Nano-Tera, SNF), optical cameras, weather stations, and a number of low-cost GPS devices were installed in the project area (Mattertal Valley, Switzerland). Because the camera positioning locations were not assumed to be stable over long time periods (lack of stable bedrock), GPS devices are integrated in the camera installation.

This work presents some results of monitoring the upper part of the Grabengufer rock glacier with optical cameras applying least-squares feature matching and image rectification procedures. Using a stereo pair of permanently installed optical cameras, we reliably detect small 3-dimensional displacements corresponding to a sub-pixel level in various regions of the rock glacier. Modeling and compensating various environmental and hardware related effects (e.g., camera motion, image distortion variations) significantly improve the reliability of the results. For an independent validation of our estimates, we use two GPS stations that are permanently installed in different areas of the rock glacier and in the field of view of both cameras.

Our results show, that reliable cm to dm displacement estimates over relatively large areas can be obtained with high quality off-the-shelf cameras. Accounting for camera motion and distortion compensation by self-calibration significantly improves the accuracy. The combination of our proposed processing strategy, including optical cameras and low-cost GPS devices, and the permanently installed optical cameras delivering images in almost real-time, are valuable results for further studies.

19.7

Groundwater vulnerability mapping in forested catchments

Lorienne Thueler[1], Philip Brunner[1] & François Zwahlen[1]

[1] *Center for Hydrogeology and Geothermics (CHYN), University of Neuchâtel, Emile-Argand 11, CH-2000 Neuchâtel (lorienne.thueler@unine.ch)*

Groundwater vulnerability mapping provides the basis for the delimitation of groundwater protection zones. In Switzerland, three methods have been defined to establish groundwater protection zones. These methods depend of the type of aquifer: karstic (EPIK: (Doerfliger and Zwahlen 1998)), fractured (DISCO: (Pochon and Zwahlen 2003)) and unconsolidated aquifers (Biaggi, Schwienbacher et al. 2012). These methods, in particular EPIK, tend to overestimate the vulnerability of groundwater originated from forested catchment and therefore overestimate the protection zones in such kind of ecosystems. This effect is particularly important in Switzerland, where 42% of groundwater protection zones are located in forests (Meylan 2003). Until now, none of the existing methods has taken into account the specific characteristics of forest hydrology.

This study presents a new methodology named ForSIG (Thueler 2014), developed for groundwater vulnerability mapping in forested catchments. This method is semi-quantitative, based on a Parametric System Model. Sensitivity criteria controlling the functions of transfer/retention of pollutants are parameterized, rated and weighted. Vulnerability maps are created using GIS tools by superposing layers that contain sensitivity criteria. The particularity of the ForSIG method is that it takes into account the hydrological characteristics of forested catchments. Sensitivity criteria that were not previously considered were added to ForSIG: forest composition (softwood vs. hardwood ratio) and forest structure (repartition of the tree ages within the stands).

We will first discuss how and why the new considered criteria are crucial for groundwater vulnerability assessment in forested catchments. Then we will present the ForSIG method and the sensitivity criteria that are used to assess groundwater vulnerability. Finally, we will present a case study for a karstic aquifer: the Eperon spring catchment in the canton of Neuchâtel. The maps obtained with ForSIG are compared with the ones obtained with the EPIK method (Figure 1). The results show that the EPIK method generates maps with extended highly vulnerable areas that are unrealistic for groundwater protection zone limits in this forested context. In comparison, the ForSIG method offers vulnerability maps that are more consistent with forested environments and in good agreement with the known vulnerability of the Eperon spring catchment.

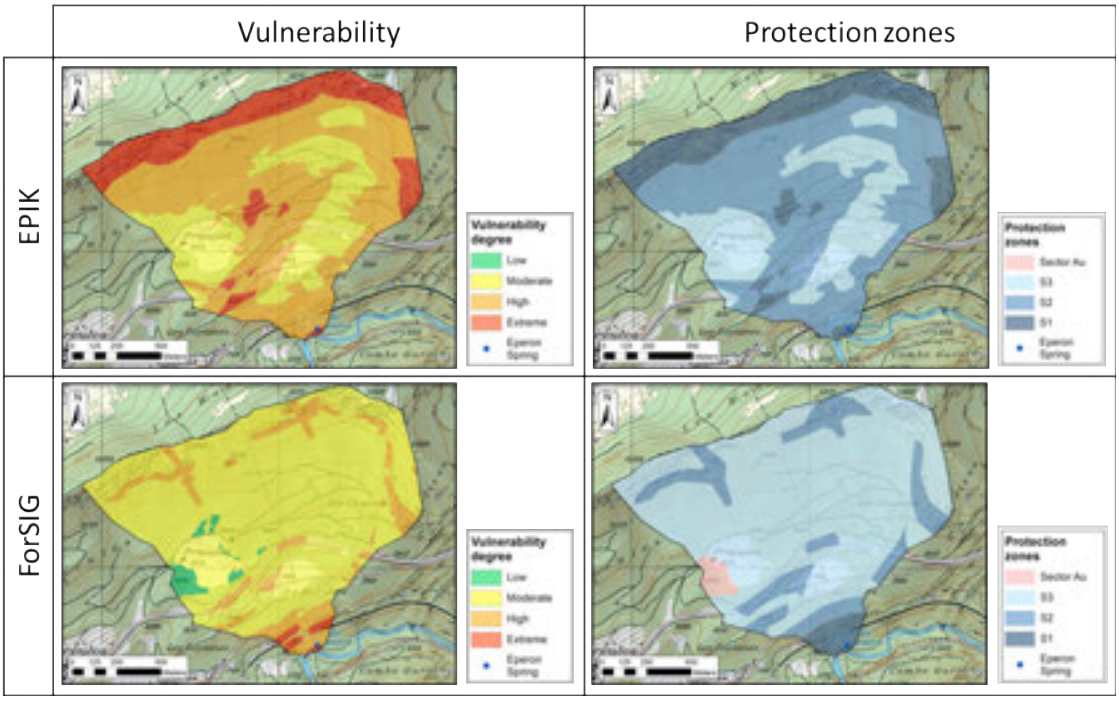

Figure 1: Vulnerability maps and groundwater protection zones maps for the Eperon spring in the canton of Neuchâtel. Comparison between EPIK and ForSIG.

REFERENCES
Biaggi, D., Schwienbacher, S. & Guldenfels, L. 2012: Zones de protection des eaux souterraines en roches meubles. Guide Pratique. L'environnement pratique, Office Fédéral de l'Environnement (OFEV), Berne, Suisse, 58.
Doerfliger, N. & Zwahlen, F. 1998: Groundwater vulnerability mapping in karstic regions (EPIK). Application to groundwater protection zone: practical guide, Office Fédéral de l'Environnement, des Forêts et du Paysage (OFEFP), Berne, Suisse, 56.
Meylan, B. 2003: Der Wald sorgt für sauberes Trinkwasser, Fachzeitschrift gwa - Gas Wasser Abwasser, 3, 191 - 199.
Pochon, A. & Zwahlen, F. 2003: Délimitation des zones de protection des eaux souterraines en milieu fissuré. Guide pratique. L'environnement pratique, Office Fédéralde l'Environnement, des Forêts et du Paysage (OFEFP), Office Fédéral des Eaux et de la Géologie (OFEG), Berne, Suisse, 83.
Thueler, L. 2014: Estimation et cartographie des aquifères en milieu forestier, PhD thesis, University of Neuchâtel, Neuchâtel, Suisse, 165.

19.8

Mobile Phone Apps for Rock Mass Rating in Engineering Geology

Manfred Thüring

Lombardi SA, Via R. Simen 19, CH-6648 Minusio (manfred.thuering@lombardi.ch)

One of the main tasks in engineering geology is to deliver a characterization of the rock mass and the derived geotechnical parameters to be used in the engineering design and construction process.

The most commonly used assessment schemes, Bieniawski's rock mass rating (RMR) and Barton's rock mass quality (Q) are based on the sum or the product of the main aspects of rock masses, such as it's intact properties and the condition of discontinuities as the main weakening element.

The assessment of RMR and Q are usually done in the field using tabulated forms on paper sheets and evaluated later on in the office. Smartphones are omnipresent and can be used for this kind of data recording, using electronic forms. Additionally, they can be used to record structural data, the current location, and for photographic documentation. Furthermore, the data can be stored on the device and sent by e-mail in order to reduce the risk of data loss. The data can be processesed for reporting.This technology promises thus a big potential to simplify the working life of an engineering geologist.

The assessment methods of RMR and Q have been programmed for personal usage using the user-friendly and freely available programming environment Android Studio (site: developer.android.com). The environment offers the possibility to develop apps for mobile phones and tablets running Android OS in the programming language Java with relatively little effort. Only basic programming knowledge is required.

REFERENCES
Bieniawski, Z.T: Engineering Rock Mass Classifications, John Wiley and Sons, New York, 1989.
Barton, N.R. (2002): Some new Q-value correlations to assist in site characterization and tunnel design. International Journal of Rock Mechanics and Mining Sciences 39 (2): 185-216.

19.9

UAV-based mapping of surface imperviousness for water runoff modelling

Piotr Tokarczyk[1], Jörg Rieckermann[2], Frank Blumensaat[2/3], Joao Paulo Leitao[2] & Konrad Schindler[1]

[1] *Institute of Geodesy and Photogrammetry , ETH Zurich, Stefano-Franscini-Platz 5, 8093 Zürich*
[2] *Swiss Federal Institute of Aquatic Science and Technology, Eawag, Überlandstrasse 133, 8600 Dübendorf*
[3] *Institute of Environmental Engineering, Chairs of Urban Water Management, ETH Zurich, Stefano-Franscini-Platz 5, 8093 Zürich*

Modelling rainfall-runoff processes in urban catchments has become an increasingly relevant issue, for instance to estimate the risk associated with urban flooding in densely populated areas. This needs hydrological models which, besides rainfall information, require good input data of detailed surface characteristics, such as imperviousness to accurately predict rainfall-runoff. One way to obtain such surface characteristics over large areas is airborne remote sensing. In this study, we assess for the first time the possibility to automatically generate high-resolution imperviousness maps for urban areas from imagery acquired with unmanned aerial vehicles (UAVs). Potential advantages of UAVs in comparison to satellite imagery or airborne remote sensing include better data quality, greater flexibility and, potentially, reduced cost. In the course of the study, the potential of UAVs for high-resolution hydrological applications was investigated, and an automatic processing pipeline with high-performance classification algorithms was proposed to extract accurate perviousness maps from high-resolution aerial images.

In a case study in the area of Lucerne, Switzerland, we generated imperviousness maps from two data sources, namely images acquired with a consumer camera on a standard micro-UAV platform and large-format aerial images acquired by swisstopo with a professional photogrammetric camera on a normal aircraft. We compare the two datasets at two levels: first we assess the quality of the automatically extracted perviousness maps; second we show an end-to-end comparison, in which the maps from different sources were used as input for a hydraulic sewer model (describing 1D surface runoff and hydrodynamic channel flow), previously calibrated with in-situ flow measurements.

The results from the image classification demonstrated that we are able to obtain imperviousness maps with an overall accuracy above 93% (Fig. 1).
While the results for the second level are still being processed, we anticipate that using UAV images together with an automated processing pipeline, it is possible to obtain rainfall-runoff predictions at least as accurate as when using standard methods and images.

a)

b)

c)

Figure 1:
a) an orthophoto generated from UAV imagery over a case study area;
b) manually labeled ground truth with three (im)perviousness classes: buildings (black), streets and sidewalks (grey) and vegetation (white);
c) classification result

19.10

Extraction of road networks from aerial photos with minimum cost paths and P^N-Potts potentials

Jan Dirk Wegner, Javier A. Montoya-Zegarra, and Konrad Schindler

Photogrammetry and Remote Sensing, ETH Zürich, Stefano-Frascini-Platz 5, CH-8093 Zürich (jan.wegner@geod.baug.ethz.ch)

We present a probabilistic representation of network structures in images. Our target application is the extraction of urban roads from aerial images. Roads appear as thin, elongated, partially curved structures forming a loopy graph, and this complex layout requires a prior that goes beyond standard smoothness and co-occurrence assumptions. In the proposed model the network is represented as a union of 1D paths connecting distant (super-)pixels. A large set of putative candidate paths is constructed in such a way that they include the true network as much as possible, by searching for minimum cost paths in the foreground (*road*) likelihood. Selecting the optimal subset of candidate paths is posed as MAP inference in a higher-order conditional random field. Each path forms a higher-order clique with a type of clique potential, which attracts the member nodes of cliques with high cumulative road evidence to the foreground label. That formulation induces a robust P^N-Potts model (Kohli et al., 2009), for which a global MAP solution can be found efficiently with graph cuts. Experiments with two road data sets show that the proposed model significantly improves per-pixel accuracies as well as the overall topological network quality with respect to several baselines.

In our approach the road network is thought of as the union of many elongated *paths*. In this way, network extraction can be cast as the search for a set of paths that together cover the entire network. The proposed method follows the recover-and-select strategy:

> In the *recover* step a large, over-complete set of potential *candidate paths* is generated, by finding the most road-like connections between many different pairs of seed points. The aim of candidate generation is high recall, ideally the candidate set covers the entire road network, at the cost of also containing many false positives that do not lie (completely) on roads.
>
> In the *select* step undesired false positives are pruned from the candidate set to yield a reduced set still covering as much as possible of the network, but with few false positives. This second step is formulated as the minimization of a global higher-order CRF energy, and can be solved to global optimality.

In more detail, our system consists of the following steps: First, an image is segmented into superpixels, which are from then on treated as the smallest entities (nodes) to be labeled. Per superpixel a feature vector is extracted and fed to a binary Random Forest classifier, which assigns each superpixel a unary road likelihood. Next, promising candidate paths are generated. To that end, superpixels with high road likelihoods are sampled randomly as seed nodes and linked with minimum cost paths. The hope is that *road* superpixels that have high *background* probability, e.g. due to a cast shadow, will be covered by a minimum cost path and thus become member of a clique where the majority of superpixels votes for *road*. The superpixels of each candidate path form a higher-order clique in a CRF. The potentials of these higher-order cliques are based on the P^N-Potts model of Kohli et al. (2009) that enforces *label consistency* within large cliques, meaning that superpixels within the clique are penalized for deviating from the majority label. In that sense, our method could be seen as an anisotropic "smoothing along the paths". The resulting CRF energy can be minimized with a graph cut, leading to a global optimum of the binary labeling task. Note that working with the actual long-range paths (cliques) is conceptually different from methods that divide long paths into short segments and classify each segment separately (Türetken et al., 2012). Like (Wang et al., 2011; Türetken et al., 2011) we prefer to work with complete paths, so as not to lose any connectivity information.

REFERENCES

Kohli, P., Ladicky, L., Torr, P.H.S., 2008. Robust higher order potentials for enforcing label consistency, in: IEEE Conference on Computer Vision and Pattern Recognition.

Türetken, E., González, G., Blum, C., Fua, P., 2011. Automated Reconstruction of Dendritic and Axonal Trees by Global Optimization with Geometric Priors. Neuroinformatics 9, 279 – 302.

Türetken, E., Benmansour, F., Fua, P., 2012. Automated Reconstruction of Tree Structures using Path Classifiers and Mixed Integer Programming, in: IEEE Conference on Computer Vision and Pattern Recognition.

Wang, Y., Narayanaswamy, A., Roysam, B., 2011. Novel 4-D open-curve active contour and curve completion approach for automated tree structure extraction, in: IEEE Conference on Computer Vision and Pattern Recognition.

19.11

Work for geologists – use for engineers: An example of handling extensive amount of geological information within a big construction project

Florian Zurfluh[1], Claude Girardin[1], Christoph Strasser[1], Sara Montani[1] & Daniele Biaggi[1]

[1] *Geotechnisches Institut AG, Bümplizstrasse 15, CH-3027 Bern (florian.zurfluh@geo-online.com)*

During big construction projects usually an immense amount of data is accumulated and it's the task of consulting geologists to deliver engineers well-structured and concisely presented information out of the "data chaos". In each step of a project ("Vorprojekt", "Generelles Projekt" and "Ausführungsprojekt") new data can be generated, often by different companies with various labelling systems. In addition, the dimensions or localisation of the planned construction can be adjusted. Therefore flexible instruments to handle and visualize geological data are needed. We will present two such suitable tools applied in a current project:

a) Project-related Geo Portal
b) Geological 3D-model

As example we selected the planed highway bypass construction at Biel/Bienne. We will focus on the content, the utility and also the limits of the tools.

a) Project-related Geo Portal

The main goal of the project-related Geo Portal is to make available all relevant data in a clearly arranged, centrally stored and easily manageable way. Particularly regular measurements (i.e. groundwater level) should be directly evaluable. In the current example, the solution for this task is a GIS based database, which is available via internet. This geo-referenced map includes all important measurement stations. Each station has a link to:

- borehole data (PDF)
- groundwater level (updated periodically, a recent diagram is drawn automatically and download of data is possible)
- chemical analyses
- properties such as for example hydraulic conductivity

If the raw data is processed properly, the Geo Portal is a very efficient tool to get an overview of all available and immediately usable data. The access is only protected by password, which makes it easily accessible by every involved person.

b) Geological 3D-model

The geology at the planned construction area in the central part of Biel/Bienne is relatively complicated. Several lithologies with different geotechnical and hydrogeological properties occur within a small area. Most of them have complex geometrical limits and if the planned locality of the construction is modified, relevant changes in the geological underground are expected. To have a flexible tool for planning and visualisation, a geological 3D-model was built.

Inputdata of the geological 3D-model:

- Borehole data (own drillcores and from archives),
- Geological surface map of the Geological Atlas of Switzerland 1:25'000,
- Digital Elevation Model (DEM).

After data collection, the borehole information had to be synchronized. We simplified the multifaceted geological situation at Biel/Bienne into 15 lithological units. The model was built using *leapfrog mining* software. A sedimentological approach was chosen (i.e. each unit has either "depositional" or "erosional" properties -> important for interpolation). The modelled area has the dimensions of 7.2 km (E-W) x 5.5 km (N-S) and includes the information of 178 boreholes. The deepest borehole has a length of 250 m and the average length is 25 m (Median 20 m). To construct the dipping of the geological units the model parameter was extended, although finally just the area around the planed highway path is needed.

The outlines of the modelled geological units are exported to CAD-formats, which then are used by engineers to construct transects at the desired localities. It is possible to inspect the model via free available visualisation software, where a fast overview can be gathered.

In summary, the most important gains of the model are:

- Fast and flexible construction of transects (in CAD-formats),
- Visualisation of complex geological units or structures, e.g. surface of solid rock (Molasse),
- Calculation of volumes of intended amount of excavated material (supply management).

Nevertheless, the model has its limits:

- Uncertainty is 2 m at areas with high density of information and about 5 m where a medium density of boreholedata is present,
- Optimal balance between smoothing factors (influences uncertainty) and file size has to be found,
- Certain CAD software cannot deal with the exported volumes -> 3D-layers had to be generated separately,
- The large extent of the model (which is needed for accurate modelling) produces large file sizes,
- Initially, the model was calculated using LV03 reference system. Nowadays the products have to be in LV95 coordinates -> each export has to be transformed.

The two presented tools permit the handling of large amount of data and are useful tools in the interacting work of geologists and engineers.

P 19.1

Data Analysis for Modeling Dissolution of Carbonate Minerals in Hypersaline Lagoon Water

Silvania Avelar, Kurt Hanselmann & Crisógono Vasconcelos

Geological Institute, ETH Zurich, Sonnegstrasse 5, CH-8092 Zürich (silvania.avelar@erdw.ethz.ch)

The characterization of the mineral dissolution/precipitation process involves a large number of parameters, which in turn results in large databases that must be interpreted with the aid of non-trivial statistical methods. In order to test and find an appropriate model to predict dissolution and precipitation of three carbonate minerals - calcite, aragonite and dolomite - in high salinity medium, we need precise and complete physico-chemical data of water drawn from different modern environments and conditions around the world. The model should make it possible to evaluate the influence of several parameters, for example, temperature, pH, anions, cations, total alkalinity and others, on mineral phase formation, as well as the likelihood of carbonate precipitation to occur in modern dolomite-forming environments. For that, it is essential to verify the existing data before using it for the intended predictions, as incomplete and imprecise data can only give a limited view with great uncertainty of the studied area. Unfortunately, there is at present not a single set of physico-chemical data publically available that is suitable enough to make assumptions about the conditions the data reflect.

The goal of this study is to establish a database of carbonate mineral formation in hypersaline lagoons that enables subsequent modeling and visualization of the data and better monitoring programs in such environments. An inventory was prepared with physico-chemical data collected over recent years by a number of different authors, who addressed water chemistry in brackish to hypersaline lagoons in Região dos Lagos of Rio de Janeiro, Brazil, where active precipitation of dolomite occurs (Höhn 1987, Vasconcelos and McKenzie 1997, Moreira et al 2004, Voegeli 2012, Bahniuk 2013). A complete physico-geochemical dataset of a hypersaline coastal lagoon, Lagoa Vermelha, was compiled in order to be included into the predictive carbonate precipitation model. This database requires precise data and reliable procedures for the verification of assumptions of the model. Missing data was either calculated according to the data assessment criteria or supplemented with data from a similar site, which was the nearby Brejo dos Espinhos lagoon.

The analysis of the physico-chemical data of Lagoa Vermelha used traditional chemical formulations (Stumm and Morgan 1996). We analysed the values of all existing data, evaluated their precision, corrected where necessary according to physico-chemical laws, and compiled a reliable set of data for the intended prediction model. Various relations between the physico-chemical data of Lagoa Vermelha were examined. The data analysis gives insights into the behavior of parameters of a modern dolomite-forming system.

This work can help to design proper data collection protocols for future studies on the formation of carbonate mineral phases in hypersaline lagoons and on the dissolution/ precipitation of calcite, aragonite and dolomite. Our study is still in its early stages; however, our observations already suggest that besides physico-chemical factors, external factors, for example microbes, might be involved in the dolomite precipitation process.

Further work includes specific comparison studies of physico-chemical data of Lagoa Vermelha, Rio de Janeiro, with data from another classic site of modern dolomite formation, the Coorong lakes, South of Australia. We also plan to propose a model to predict dissolution and precipitation of minerals, which will be based on machine learning techniques (Hastie et al 2001, Bishop 2006).

REFERENCES

Bahniuk, A. 2013: Coupling Organic and Inorganic Methods of Study Growth and Diagenis of Modern Microbial Carbonates, Rio de Janeiro State, Brazil: Implications for Interpreting Ancient Microbialite Facies Development. PhD Thesis, ETH Zurich, Switzerland.

Bishop, C. 2006: Pattern Recognition and Machine Learning. Berlin: Springer-Verlag.

Hastie, T., Tibshirani, R. & Friedman J. 2001: The Elements of Statistical Learning, Springer-Verlag.

Höhn, A. 1987: Geochemie einer Östlich von Rio de Janeiro gelegenen Hypersalinen Lagune. PhD Thesis, Johannes Gutenberg-Universität in Mainz, Germany.

Moreira, N.F., Walter, L.M., Vasconcelos, C., McKenzie, J.A. & McCall, P.J., 2004: Role of sulfide oxidation in dolomitization: Sediment and pore-water geochemistry of a modern hypersaline lagoon system, Geology, 32, 701-704.

Vasconcelos, C. & McKenzie, J.A. 1997: Microbial mediation of modern dolomite precipitation and diagenesis under anoxic conditions (Lagoa Vermelha, Rio de Janeiro, Brazil). Journal of Sedimentary Research, 67, 378-390.

Voegeli, N. 2012: Implications of Elevated Strontium Values in Microbial Mediated Dolomites: Brejo do Espinho and Lagoa Vermelha, Brazil. Master's Thesis, Department of Earth Sciences, Geological Institute, ETH Zurich. August 2012.

Stumm, W. & Morgan, J. J. 1996: Aquatic Chemistry, John Wiley & Sons.

P 19.2

From data treatment to tsunami hazard assessment in lakes: the challenging case of Lake Geneva

Caroline Calpini[1], Guy Simpson[1], Corine Frischknecht[1], Stéphanie Girardclos[1,2]

[1] *Section of Earth and environmental sciences, University of Geneva, rue des Maraîchers13, 1205 Geneva (Swizerland) (caroline.calpini@etu.unige.ch)*
[2] *Institute for environmental sciences, Route de Drize 7, 1227 Carouge, (Switzerland)*

Up to now catastrophic events linked to tsunami waves, such as the Indian Ocean Tsunami (2004) and the Tohoku-Oki Tsunami (2011), have raised strong societal interest in understanding and assessing risk associated with these disasters. However, killer waves are not only restricted to oceanic water bodies but can also occur in lakes.

This research focuses on the tsunami hazard within the Lake Geneva basin. Lake Geneva results from the Quaternary glaciations in Europe, and with an area of around 580 km^2 and a volume of 89 km^3, is considered the largest lake in Western Europe. It is formed by two sub-basins named "Grand Lac" and "Petit Lac".

Previous seismic, sedimentological and modelling studies in Lake Geneva have shown that at least five large sublacustrine mass failures triggered meter-amplitude tsunami waves along the shores during the last 4000 years (Kremer, 2014; Kremer et al., 2012), representing an annual average frequency of 0.0013 yr^{-1}. The oldest event (between 1872 and 1608 B.C.) is interpreted to have been caused by a cascading earthquake-mass movement-tsunami chain of events, whereas the youngest tsunami event (563 A.D.) is interpreted as being triggered by a rockfall causing a collapse of the Rhone Delta (Kremer et al., 2012).

Key parameters characterizing a tsunami are wave heights, speed and propagation path, wavelength (distance between two waves propagating) and inundation zone in meters (run-up). These are obtained using a new physical tsunami wave model based on a Non-Oscillatory central differencing scheme (Nessyahu & Tadmor, 1990) developed using *Matlab*. In order to be capable of obtaining maximum run-up distance on the lake shore, and all the other associated parameters, the model requires initial data describing the lake and its surroundings, meaning a combination of information related to topography and bathymetry. To obtain this data, a specific geoprocessing tool has been developed under *ArcGIS* for data treatment and for data exportation in the format required by the tsunami model under *Matlab*. At the moment, the tsunami hazard assessment is deterministic, allowing consideration of several possible source locations around the lake.

Since the last tsunami event (563 A.D.), the Lake Geneva region has evolved into a major economic and urban area; the Swiss part of Lake Geneva region makes 15% of the Swiss PIB (Grob, 2008). Most of the lake shores are inhabited and/or occupied by human infrastructure (e.g. factories, roads, cities). It is therefore important to understand and to model tsunami wave propagation in order to assess potential consequences that could occur whatever the trigger event would be.

REFERENCES

Fritsche, S., & Fäh, D. 2009: The 1946 magnitude 6.1 earthquake in the Valais: site-effects as contributor to the damage, Swiss Journal of Geosciences, 102(3), 423–439.

Grob, U. 2008: Le Bassin lémanique: centre financier, fief horloger, eldorado pour les sièges d'entreprises, La Vie Économique (Die Volkswirtschaft), 37–41.

Kremer, K. 2014: Reconstructing 4000 years of event history in deep Lake Geneva (Switzerland – France): Insights from the sedimentary record, PhD thesis University of Geneva, 221 pp.

Kremer, K., Simpson, G. & Girardclos, S. 2012: Giant Lake Geneva tsunami in ad 563, Nature Geoscience, 5, 756–757.

Nessyahu, H. & Tadmor, E. 1990: Non-oscillatory central differencing for hyperbolic conservation laws, Journal of Computational Physics, 87(2), 408–446.

P 19.3

Regional hydrogeological modelling of the central Jura in the area of Neuchâtel. Part 1 : 3D geological modelling

François Negro[1] & Jaouher Kerrou[1]

[1] *The Centre for Hydrogeology and Geothermics (CHYN), University of Neuchâtel, Emile-Argand 11, CH-2000 Neuchâtel (francois.negro@unine.ch)*

The canton of Neuchâtel is located in the central part of the Jura fold and thrust belt at the northwestern limit of the Molasse basin. The structure of this part of the Jura is a succession of thrust-related folds, composed of Mesozoic to Cenozoic cover rocks detached from their pre-Triassic basement, and limited by several major tear faults. Three main aquifers are recognised within the cover series in this area. These are from top to bottom: the upper Malm, the Dogger and the upper Muschelkalk. The main goal of this study is to understand the behaviour of groundwater flow in this multi-layered aquifer system and especially in the two main regional reservoirs, namely the upper Malm and the Dogger. This study is divided in two parts: part 1 presents the construction of the 3D geological model (this abstract) and part 2 (see companion abstract) the results of 3D groundwater flow and mass transport modelling.

3D geological modelling has been performed using 3D Geomodeller software (BRGM, Intrepid Geophysics). The model (80x80x5 km box) extends from the Pontarlier fault to the west, to city of Biel to the east. It is bounded to the north by the Doubs river and to the south by the lake of Neuchâtel. The 3D model has been built with a compilation of the available geological data in the area (geological maps, cross-sections, boreholes). Geological formations have been grouped according to their hydrogeological properties (i.e. aquifer or aquiclude). Around 90 geological cross-sections have been used to constrain the model at depth. Available interpretations of seismic lines have been used to constrain the deep structure of the model. Furthermore, only major tectonic structures relevant for groundwater flow have been included.

We present and discuss the structure of the 3D geological model and the way the model has been discretized into an unstructured 3D finite element mesh for groundwater flow and mass transport modelling (see companion abstract).

P 19.4

Regional hydrogeological modelling of the central Jura in the area of Neuchâtel. Part 2 : 3D groundwater flow and mass transport modelling

Jaouher Kerrou[1] & François Negro[1]

[1] *The Centre for Hydrogeology and Geothermics (CHYN), University of Neuchâtel, Rue Emile-Argand 11, CH-2000 Neuchâtel – Suisse (jaouher.kerrou@unine.ch)*

A large number of studies have been conducted on the geology and the groundwater resources in the region of Neuchâtel (e.g. Kiraly, 1973; Pasquier et al., 1999, 2006). This study aims to synthesize the available data in order to setup a regional hydrogeological numerical model that can be used : to understand the behaviour of groundwater flow and mass transfer in the multilayered aquifer system and especially in the two main regional reservoirs, namely the upper Malm and the Dogger; to evaluate groundwater resources and their vulnerability; and further to evaluate the regional geothermal potential. This study is presented in two parts: part 1 presents the building of the 3D geological model (see companion abstract) and part 2 (this abstract) the results of 3D groundwater flow and mass transport modelling.

In a first step, a hydrogeological conceptual model was setup. The model of 2200 Km^2 area extends from the Pontarlier fault to the west, to city of Biel to the east. It is bounded to the north by the Doubs river and to the south by the lake of Neuchâtel. The conceptual model is based on 3D geological modelling (c.f Part 1) of the folded Jura in the area of Neuchâtel accounting for geological cross-sections, deep borehole data and seismic lines. Geological formations have been grouped according to their hydrogeological properties (i.e. aquifer or aquiclude). The resulting model is a multilayered system of 10 hydrogeological units from Trias to Tertiary age.

Then, the regional geological model has been discretized into an unstructured 3D finite element mesh. The latter was constructed by integrating different structures such as the rivers network, the extension of major faults, the surface geology, the location of the main karstic springs. This mesh was then refined near rivers and faults. In total, the 3D mesh contains more than 7 million elements and 4 million nodes. The flow boundary conditions are mainly specified hydraulic heads (Dirichlet type) along the major rivers. Inflow fluxes (Neumann type) derived from hydrological balance were attributed elsewhere on the top surface to represent direct recharge by rain water. Moreover, specified hydraulic heads were attributed on the lake floor and the lateral boundaries. No flow conditions were assumed at the bottom.

The groundwater flow and mass transport equations, in an equivalent porous medium approach were solved using a standard finite element method. First, the recharge spreading layer was calibrated by adjusting the inflow fluxes and the hydraulic conductivities of the outcropping formations against hundreds of hydraulic heads and springs flow rates measurements. Then, the depth-dependent hydraulic parameters of the main aquifers were calibrated by inverse modelling. After, a sensitivity analysis has been performed to point out the hydraulic role of major faults. The results so far are presented and discussed.

REFERENCES

Kiraly, L., 1973 : Notice et carte hydrogéologique du canton de Neuchâtel. Bulletin de la Société Neuchateloise de Sciences Naturelles, 96.

Pasquier, F., Bouzelboudjen, M. & Zwahlen, F., 1999 : Carte Hydrogéologique de la Suisse, Sarine, feuille n° 6. Commission Géotechnique Suisse et Service Hydrologique et Géologique National.

Pasquier, F., Zwahlen, F. & Bichet, V., 2006 : Carte hydrogéologique de la Suisse, Vallorbe-Léman nord, feuille n° 8. Commission géotechnique suisse.

P 19.5

3D structural modelling of the Swiss Molasse Basin in the Canton of Bern

Samuel Mock[1], Robin Allenbach[2], Lance Reynolds[2], Roland Baumberger[2] & Marco Herwegh[1]

[1] *Institute of Geological Sciences, University of Bern, Baltzerstrasse 1+3, CH-3012 Bern (samuel.mock@geo.unibe.ch)*
[2] *Federal Office of Topography swisstopo, Swiss Geological Survey, Seftigenstrasse 264, CH-3084 Wabern*

In recent years the Swiss Molasse Basin has come under closer scrutiny for exploring geothermal energy, CO_2 sequestration and nuclear waste disposal potentials but also infrastructure and the planning of land use. 3D geological models have become an important instrument for addressing these issues. Their relevance expected to increase in the future. The "GeoMol CH" project, under the coordination of the Swiss Geological Survey(swisstopo), will produce a 3D model of the Swiss Molasse Basin. This model will serve as a valuable tool for the aforementioned topics. Our model of the Molasse Basin in the Canton of Bern forms part of the "GeoMol CH" project and will be built at a scale of 1:50'000. It is based on the Seismic Atlas of the Swiss Molasse Basin (Sommaruga et al., 2012) and studies done by Nagra (e.g. Meier, 2010; Roth et al., 2010). The final model will contain 12 geological horizons, from the top of the bedrock down to the base of the Mesozoic, thus including the major Cenozoic and Mesozoic strata. Furthermore, tectonic structures visible at the modeled scale will be incorporated into the model.

The 3D model covers an area of approximately 1'700 km^2 and reaches depths of about 5 km. This model is based mainly on interpretations of 2D reflection seismic and well data. It is necessary to include geological surface data in the modelling process, as the Cenozoic horizons are poorly discernable in the seismics. For fault interpretation, we will be applying an integrative approach using seismic data, as well as digital elevation models and orthophotos for verifying the lateral and vertical continuity of the structures. This poster, presents our modelling methodology and initial results.

REFERENCES

Meier, B. P. 2010: Ergänzende Interpretation reflexionsseismischer Linien zwischen dem östlichen und westlichen Molassebecken. Arbeitsbericht NAB 10-40, unpublished, Nagra, Wettingen.

Roth, P., Naef, H., and Schnellmann, M. 2010: Kompilation und Interpretation der Reflexionsseismik im Tafeljura und Molassebecken der Zentral- und Nordostschweiz, Arbeitsbericht NAB 10-39, unpublished, Nagra, Wettingen.

Sommaruga, A., Eichenberger, U., and Marillier, F. 2012: Seismic Atlas of the Swiss Molasse Basin. Beitr. Geol. Schweiz, Geophysik, 44..

P 19.6

Architecture and property distribution of coal-bearing successions in Late Carboniferous fluvio-deltaic deposits (SE Kentucky, USA)

Le Cotonnec, A., Ventra, D., Moscariello, A.

Section des Sciences de la Terre et de l'Environnement, Université de Genève, Rue des Maraîchers 13, CH-1205 Genève

The exploration of coal-bearing reservoirs for hydrocarbon resources, both conventional and unconventional worldwide, has increased the interest in similar fluvial/estuarine successions. In this context, East Kentucky offers excellent outcrop analogues for Carboniferous fluvial-dominated deltaic where facies associations, depositional environments and sequence-stratigraphic patterns can be observed in detail. Extensive roadcuts and a vast database of well/core data (coal and gas exploration), available at the KGS (Kentucky Geological Survey) make of East Kentucky an excellent field laboratory for studying clastic sedimentology and stratigraphy in coal-bearing successions.

The middle Pennsylvanian Pikeville and Hyden Formations are very well exposed along the US highways 23 and 119 in Pike County (SE Kentucky). The local stratigraphy is well known thanks to numerous studies focused on very extensive Pennsylvanian coal beds, used as stratigraphic markers for outcrop correlation. Both formations were deposited in a foreland basin adjacent to the then-active Appalachian orogeny. Fluvio-deltaic systems fed by the orogen prograded toward west and northwest across the basin, subject to periodic transgressions driven by high-amplitude glacio-eustatic base-level changes during the Late Palaeozoic Gondwanan glaciation.

Here we show preliminary results from two outcrops (Burning Fork and John's Creek) along the US119, allowing 3D interpretations and modelling, and covering respectively an area of 0.5km^2 and 0.15 km^2. They were studied through detailed logging at facies scale and high-resolution rock sampling for characterization of porosity and permeability and for QEMScan rock-typing analyses. The dominant facies associations allow us to distinguish deposits from three main depositional environments: low- to high-sinuosity rivers in coastal plains; paralic (estuarine or deltaic) settings; shallow-marine settings. Successions are formed by vertically stacked, erosively based depositional sequences with thickness from a few meters to a few tens of meters, with general architecture comprising three main elements: river-dominated valley fills; transitional sediments of coastal to marginal-marine environments, including coalbeds; and extensive marine shales locally intercalated with prograding mouth-bar deposits.

Integrated with available subsurface datasets, logs will be used to derive 3D facies and architectural models (Petrel) of sandstone bodies, with an aim to link their properties to sequence-stratigraphic phase.

P 19.7

Growth Stage Determination of Rice Fields: EMS Model Search Space Solution

Onur Yüzügüllü[1], Esra Erten[2], Irena Hajnsek[1]

[1] *Earth Observation and Remote Sensing, Institute of Environmental Engineering, ETH Zürich (yuzugullu@ifu.baug.ethz.ch)*
[2] *Department of Geomatics Engineering, Istanbul Technical University*

Rice crop based products have always been one of the most important crops in history of economy and mankind. In the last years, rice field monitoring have gained importance under the topic of precise agriculture of large areas. In this context, remote sensing techniques have been utilized for several applications including growth monitoring, product estimation and illness detection.

The objective of this study is to provide an algorithm to determine the growth stage of rice fields using polarimetric SAR (PolSAR) data. The proposed strategy to determine the growth stage of rice fields is outlined in Figure 1. Here, the electromagnetic scattering model, which consists of stalks (Karam & Fung, 1988) and deciduous leaves (Karam & Fung, 1989) is first considered. This forward scattering model, based on the radiative transfer approach, considers four different scatte-

ring mechanisms: volume, 2 different double-bounce (scattering from a scatterer followed by reflection off the boundary and surface scattering followed by a scattering from a scatterer) and reflection by the boundary followed by scattering from a scatterer and further followed by reflection from the boundary. For the retrieval of growth stage, firstly the solution space of the morphological growth cycle is simulated for all polarizations using the electromagnetic scattering model. Later, for each polarization channel, the search algorithm reduces the size of the sample space by comparing the intensity value obtained from the SAR data. For this stage, a three dimensional feature space (HH-intensity, VV-intensity and polarimetric phase difference between HH and VV) is clustered by the K-means algorithm to obtain the dominant cluster (at least 50% of the samples). Intensities representing the fields are calculated from the samples that are included in the dominant cluster. Following this step, the accepted range of intensity values are chosen based on the variance of the backscattering intensity within the dominant cluster. Even though there are different solution spaces for different polarizations, each plant has a definite structure in the physical world. Therefore, the solution sets for each polarization should match. This step provides the match to assure physical consistency. The selected morphologies for each pixel are saved for the next step of the analysis. This procedure is repeated until all the pixels within the field are analyzed. Following this step of the procedure, stored structures are compared based on their similarities inside the dominant cluster. To overcome the chance of ending with more than one possible structure, occurrence of different structures are observed and the structure with highest probability is selected. Finally, the growth stages are assigned to the fields according to the guidelines stated by BBCH-scale.

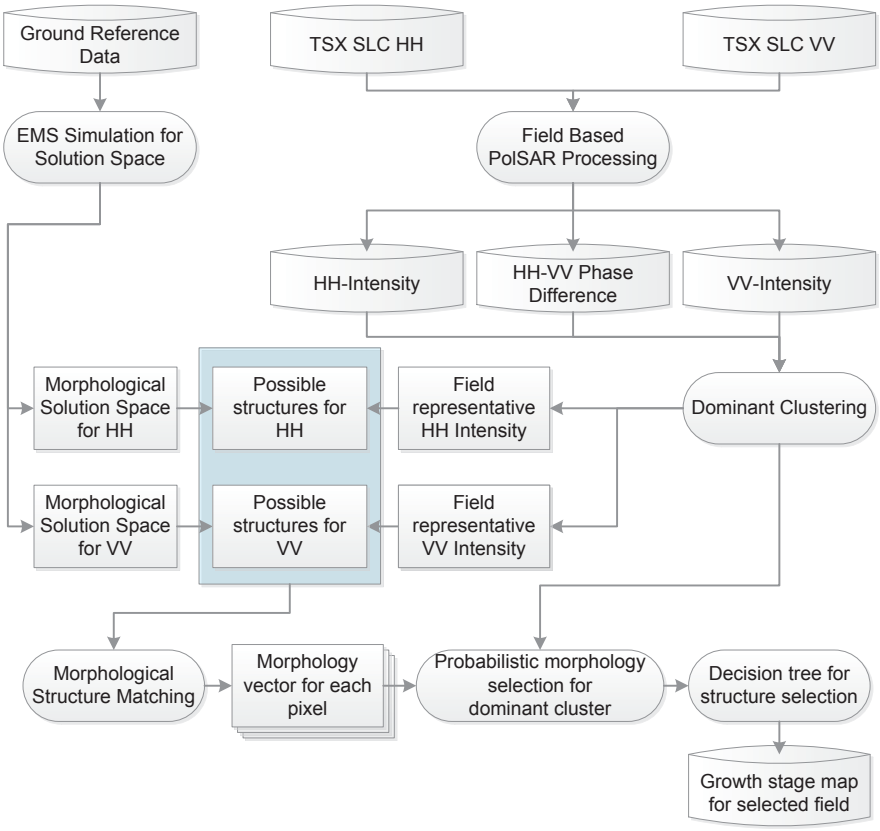

Figure 1. Flowchart employed for the growth stage determination analysis

The proposed algorithm is applied on a co-polar TerraSAR-X (TSX) dataset acquired over one rice cultivation site (Ipsala/Turkey) during May-September 2013. Moreover, a complete set of ground measurements comprising morphology (canopy height, stalk diameter, leaf size) and density (leaf, tiller and stalk number) parameters are collected during the same period. This ground reference data is used to train the forward model.

Currently, the proposed algorithm has been implemented only for the dataset of 2013 with promising results for the vegetative and reproductive stages. However, further research is needed to assess the full growth cycle.

REFERENCES

Karam, M. A., & Fung, A. K. 1988: Electromagnetic scattering from a layer of finite length, randomly oriented, dielectric, circular cylinders over a rough interface with application to vegetation. Remote Sensing, 9(6), 1109-1134.

Karam, M. A., & Fung, A. K. 1989: Leaf-shape effects in electromagnetic wave scattering from vegetation. IEEE transactions on geoscience and remote sensing, 27(6), 687-697.

20. Symposium in Human Geography

Olivier Graefe, Heike Mayer, Martin Müller

Swiss Geography Association (ASG)

TALKS:

20.1 Backhaus N.: Malaysian street food: production, contestation, and negotiation of public space

20.2 Charrière E., Girardclos S., Fekkak H., Baudouï R.: The role of public and private actors in dumped munitions in Lake Geneva. A history of waste management and policy.

20.3 Cima O.: Memory in the everyday: explorations from post-Soviet land management in Kyrgyzstan

20.4 Danielli G., Lüthi S.: Geotourism: How to govern fundamental Sustainability Transition processes

20.5 Meyer U.: Trees, periurban land and local politics in Niger›s capital Niamey

20.6 Militz, E.: The constitutive lack of discourse: national belonging and the desire for Turkey in Azerbaijan

20.7 Rao Dhananka S.: Planning their own homes. The capacities of the urban poor as planners and the constraints of public policy.

20.8 Weidmann L.: Communal land Reform in Namibia: Traditional authorities renegotiate their positions in land governance

POSTERS:

P 20.1 Miranda G.M.: Integrated management of water resources in a federal country: the case of Brazil.

P 20.2 Rattu P.: Sexuality, reproduction and biopower : a research on LGBTQ procreation and parenting

20.1

Malaysian street food: production, contestation, and negotiation of public space

Norman Backhaus

Geographisches Institut der Universität Zürich, Winterthurerstr. 190, 8057 Zürich; norman.backhaus@geo.uzh.ch

Street food provided by so called hawkers is an integral part of Asian urban spaces. Juggling formal requirements and informal rules they structure and produce public spaces by their trade (Etzold 2013). By occupying niches that both are close to their customers and located in "free" public space, they eke out a living and provide customers and neighbors not only with food but also with meeting places, a traditional pastime, and security (Backhaus & Keller 2001). Even though they mostly appropriate their economic and spatial niches without official permission (but with more or less tolerance) and operate independently, they have to follow to formal and informal rules. The practices that emerge from the entanglement of rules, space, and materiality create a hawker site that is constantly re-negotiated and often contested. Here Schatzki's (2002) concept of the site of the social will be used as theoretical background. With the example of two small Malaysian towns – the border town Changlun in the state of Kedah and Teluk Bahang on the island of Penang – and the results of recent surveys and qualitative interviews the workings of these sites will be explained. Moreover, a possible governance policy for the hawker sites will be formulated since they increasingly come under pressure of the authorities and are removed from many streets for various reasons (i.e. traffic congestion, alleged bad hygiene, noise, competition with shop keepers, political conflicts etc.).

REFERENCES

Backhaus, N., & Keller, S. A. 2001: Streetfood und Stadtkultur – Hawker in Telok Bahang/Malaysia. Asiatische Studien/ Etudes Asiatiques, 55(3), 577–610

Etzold, B. 2013: The politics of street food: Contested governance and vulnerabilities in Dhaka's field of street vending. Stuttgart: Franz Steiner Verlag.

Schatzki, T. R. 2002: The site of the social: A philosophical account of the constitution of social life and change. Library (p. xxii, 295 p.). University Park: Pennsylvania State University Press.

20.2

The role of public and private actors in dumped munitions in Lake Geneva. A history of waste management and policy.

Elodie Charrière[1], Stéphanie Girardclos[1,2], Hatem Fekkak[1] & Rémi Baudouï[1,3]

[1] *Institute for Environmental Sciences, University of Geneva, Route de Drize 7, CH-1227 Carouge (elodie.charriere@unige.ch)*
[2] *Section of Earth and Environmental Sciences, University of Geneva, Rue des Maraîchers 13, CH-1205 Geneva*
[3] *Département de Science politique et Relations Internationales, Faculté des Sciences de la Société, Université of Geneva, Boulevard du Pont d'Arve 40, CH-1211 Geneva 4*

Immediately after World War II, many governments around the world needed to get rid as fast as possible of huge stockpiles of conventional and chemical munitions to avoid possible security concerns. Several waste management approaches have been used, including open-pit burning, firing, exploding, dumping and land burial. For a number of reasons, mainly related to cost-efficiency, safety and fastness, the globally most common adopted solution was to dump munitions. A variety of geographic underwater munitions sites have been used, including *lakes,* ponds, marshes, streams, rivers, estuaries, harbours, canals, seas and oceans (Greene et al., 2009). Over time, the emergence of environmental conscience has brought this issue back on the political agenda with a particular attention on environmental risks. This legacy of munitions in varied underwater environments presents risks: exposure and contamination of underwater organisms and ecosystems as well as direct human health impact.

With this study, using personal interviews, reports and archival research methods, we intend to raise awareness about the specific political and geographical situation of Switzerland on this subject and to provide an overview of new research results and research gaps about munitions dumped in Lake Geneva. Moreover, our study aspires to highlight the culture of secrecy's capability to interfere with ecological policy, and to become an obstacle to implement proper risk management measures.

Swiss authorities found similar solutions to cope with unused munitions. Indeed, the Swiss army dumped munitions in various lakes - mainly in Lake Thun (4,600 tons), Lake of Uri (2,800 tons) and Lake Brienz (280 tons) - from the 1940s to the 1960s (DDPS, 2004b). However, the topic of Swiss dumped munitions is more complicated than it seems at first sight. In Switzerland, two specific situations have to be distinguished. The first one, as mentioned above, concerns the munitions that came from Federal factories in Thun and Altdorf, whereas the second one, comparatively less studied, involves munitions that originated from private factories. This involvement of private actors is particularly exemplified in our Lake Geneva case study. Contrary to the sites under the responsibility of the Defence Ministry, the investigation and the monitoring related to the munitions dumped in Lake Geneva is under the responsibility of the cantonal service for the protection of the environment, as in this case, the Department for Environment, Transport and Agriculture (DETA) for the Republic and Canton of Geneva (DDPS, 2004a).

With regard to the recommendations made by Matthias Paetzel, who suggests that munitions dump site investigations should include four steps of assessment (Paetzel, 2002), the investigation of Lake Geneva does not follow his recommendations. Our study demonstrates that a number of shortcomings exist. Firstly, the *Total inventory step* and the *Risk assessment step* have not been fully completed, and secondly, the *Monitoring step* is non-existent and the *Public availability step* has been biased. For all these reasons, one recommendation in our study is to fully investigate possible dumping sites in Lake Geneva, in order to reduce the numerous risk associated to underwater munitions. In conclusion, genuine ecological time bombs are sleeping at the bottom of Lake Geneva and other Swiss lakes.

REFERENCES

Département fédéral de la défense, de la protection de la population et des sports (DDPS). 2004a: *Historische Abklärungen zu Ablagerungen und Munitionsversenkungen in Schweizer Seen*, in particular „Investigations historiques relatives aux dépôts et aux immersions de munitions dans les lacs suisses. Lot 1 : Suisse Romande". Bern (Switzerland).

Département fédéral de la défense, de la protection de la population et des sports (DDPS). 2004b: *Résumé Etude historique concernant le dépôt et l'immersion de munitions dans les lacs suisses*. Bern (Switzerland).

Greene, P., Follett, G., and Henker, C. 2009: Munitions and dredging experience on the United States Coast. *Marine Technology Society Journal*, 43 (4), 127-131.

Paetzel, M. 2001: "Deep marine munition dump sites : example from Arendal, Norway". In *Chemical munition dump sites in coastal environments*, Edited by Missiaen, T., & Henriet, J.-P. Renard Centre of Marine Geology, University of Gent (Belgium). 133-144.

20.3

Memory in the everyday: explorations from post-Soviet land management in Kyrgyzstan

Ottavia Cima[1]

[1] *Geography Unit, Department of Geosciences, University of Fribourg, Chemin du Musée 4, CH-1700 Fribourg (ottavia.cima@unifr.ch)*

Central Asian countries have undergone complex social and economic transformations in the last decades. My research aims at illuminating a specific aspect of this process by looking at the role played by the memory of the past in today's everyday practices linked to land management in Kyrgyzstan. References back to the past have a dominant position in public space and official rituals in Kyrgyzstan, and they characterise everyday discourses, either nostalgically or disdainfully. They also shape institutional approaches to development and policy-making, which often emphasise the need to eradicate persisting "Soviet practices" that hamper the possibility of development.

The concept of memory has captured the interest of several disciplines, in particular sociology, history, and geography (see Legg 2007), which have investigated the relationship between memory and the physical space in which it is embedded (e.g. Nora 2003). However, accounts on memory have mostly focused on specific, extra-ordinary events as the objects of remembering and on specific, extra-ordinary places as the spatial dimension of remembering. Existing studies, thus, have neglected the process of remembering in ordinary contexts: little research exists on the working and the role of memory *of* the everyday *in* the everyday, as well as on the links between memory and a broader concept of *space* beyond specific *places*.

In Central Asia, the topic of land has been at the centre of social and economic transformation since the beginnings of the Soviet Union and it is thus particularly suited for the investigation of everyday memory. Kyrgyzstan is the Central Asian country that has shifted most quickly to a system of private owned land; however, until today the implementation of reforms presents some shortcomings (Bichsel et al. 2010). The access to land often still depends on traditional social structures and on hierarchies inherited form the past, as it is the case for instance for pasture land (see Kerven et al. 2011). Today, pasture land is owned by the state and since 2009 its access and use are managed by "grazing committees" composed of representatives of local herders. In fact, however, long-lasting established power relations are playing a role in the effective possibility of pasture access (id.). Thus, linking the concept of memory with the topic of land, my research asks how past land management practices, specifically the *memory* of such past practices, influence today's land management practices. Further, I ask how references to past practices are mobilised today to legitimise some practices and delegitimise other ones.

The research will mainly draw on oral history methods (see Obertreis 2011) but it also aims at developing a specific and innovative theoretical and methodological framework for the investigation of memory in the everyday. Especially, I would like to enrich traditional oral history methods by integrating ethnographic methods as participant observation and participatory methods. Though being aware that memory of the Soviet time will be often at the centre of the stage, I will conceptualise the notion of "past" in a way that allows to include in my observations memories of both the pre- and post-Soviet past.

Data collection and analysis will take place in the next years; for this reason, my contribution to the Swiss Geosciences Meeting 2014 will mainly refer to the definition of the theoretical and methodological framework, drawing on the insights of the first field visit.

REFERENCES

Bichsel, C., Fokou, G., Ibraimova, A., Kasymov, U., Steimann, B. & Thieme, S. 2010: Natural resource institutions in transformation: the tragedy and glory of the private. In: Hurni, H. & Wiesmann, U.: Global change and sustainable development: a synthesis of regional experiences from research partnerships, Geographica Bernensia, University of Bern, 255-269.

Kerven, C., Steimann, B., Ashley, L., Chad, D. & Rahim, I. 2011: Pastoralism and farming in Central Asia's mountains: a research review, Background paper 1, Mountain Societies Research Centre, University of Central Asia.

Legg, S. 2007: Reviewing geographies of memory/forgetting, Environment and Planning A, 39, 356-466.

Nora, P. 2003: Les lieux de mémoire, Gallimar, Paris.

Obertreis, J. 2011: Oral history, Steiner Verlag, Stuttgart.

20.4

Geotourism: How to govern fundamental Sustainability Transition processes in the Valley of Zermatt (Mattertal)

Giovanni Danielli, Stefan Lüthi

Lucerne University of Applied Sciences and Arts, Institute of Tourism, Rösslimatte 48, 6002 Luzern (giovanni.danielli@hslu.ch)
BHP – Brugger and Partners Ltd., Lagerstrasse 33, 8021 Zürich (stefan.luethi@bruggerconsulting.ch)

Sustainable Geotourism Region Mattertal (Switzerland): Valorisation of natural and cultural landscapes through new products and services

The Valley of Zermatt (Mattertal) in the canton of Valais (Switzerland) is characterized by a unique natural and cultural landscape with imposing glaciers, vast permafrost regions and a high biodiversity. With the municipality of Zermatt, the Mattertal has an internationally known holyday destination. Despite its unique landscape, the Mattertal is faced with various challenges: Many municipalities are struggling with out- migration and a decline in jobs. The regional value added is declining. The occupancy of hotels and second homes is subject to high seasonal fluctuations. The operational capability of many municipalities is at risk. At the same time, the natural resources and traditional cultural landscapes are increasingly under pressure. Thus, not only a valuable natural and cultural heritage, but also an important touristic potential gets more and more lost. Furthermore, the municipalities in the front part of the valley hardly benefit from Zermatt as internationally known holyday destination. There is no regional strategy to face these current challenges.

In this project, we address these challenges as part of a pilot program of the Swiss confederation entitled "using and valorising natural resources". The focus lies in the development of a sustainable Geotourism Region Mattertal. The following stakeholders are part of the project: The municipalities of the Mattertal (St. Niklaus, Grächen, Embd, Randa, Täsch and Zermatt), various departments of the canton of Valais (forest and landscape; economic development; spatial development) and several NGOs. The conceptual framework is defined by the international Geotourism-Charter, which is based on the three sustainability dimensions: economy, ecology, social. The Centre for Sustainable Destinations of the National Geographical Society defines Geotourism as „tourism that sustains or enhances the geographical character of a place – its environment, culture, aesthetics, heritage, and the well-being of its residents". The sustainability principles are at the core of this project.

The project pursues the following objectives:

- Development of a Geotourism sustainability strategy
- Gentle development of typical natural landscapes and upgrading of traditional cultural landscapes
- Development of a product portfolio for the monetary valorisation of natural and cultural landscapes
- Improvement of regional and sectoral cooperation
- Raising awareness of stakeholders in tourism and municipalities for regional approaches in the field of sustainable tourism
- Improving the exchange of experience among sustainability-oriented tourism destinations

With these performance goals, out-migration in the Mattertal should be reduced, the regional value added increased, the occupancy of hotels and second homes improved, the operational capacity of the municipalities strengthened and the natural and cultural landscape upgraded. Furthermore, the project addresses a central question in the context of sustainable tourism: How can we create demand-driven products and services out of public goods (where the exclusion principle does not work) meeting the sustainability principles. A part of the corresponding value added is intended to be re-invested in the upgrading of the natural and cultural landscape.

The strategy and the corresponding measures are developed in a multi-stage, participatory process. The cooperation takes place on three levels: horizontal (municipalities of the Mattertal), vertical (municipalities, canton of Valais, Swiss confederation) and across sectors (agriculture, forestry, tourism, nature and landscape protection etc.). The cooperation between Zermatt (as an internationally known tourism destination) and the surrounding municipalities is intended to create synergies and new experiences for a successful interaction between intensively and extensively used tourist destinations.

REFERENCES

Modellvorhaben Bundesamt für Raumentwicklung
http://www.are.admin.ch/dokumentation/00121/00224/index.html?lang=de&msg-id=53140
Center for sustainable destinations
http://travel.nationalgeographic.com/travel/sustainable/about_geotourism.html

20.5

Trees, periurban land and local politics in Niger's capital Niamey

Ursula Meyer

[1] *Institut de géographie et durabilité, Faculté des géosciences et environnement, Université de Lausanne, Mouline - Géopolis, 1015 Lausanne (ursula.meyer@unil.ch)*

This talk presents empirical results from recent field research conducted on the governance of land in the peripheral zone of the rapidly expanding capital of the Niger Republic. Niamey, like other capitals in the region, witnesses a frantic rush for land that is bought and resold largely by private investors who control land markets and manipulate access though speculation and monopoly. However, the number of formalized land plots though zoning exceeds the real demand of land for construction and reaches prices per m² that are well beyond the financial capacities of most of Niamey's population.

In this context, the presentation aims to shed light on the role and strategies of two of the major actors in the panoply that compete around periurban land and for control over it: first, customary urban land holders and second, private zoning entrepreneurs. Both act and position themselves vis-à-vis the State and gain strategic benefit from its democratising and liberalising nature. The former voice a discourse about autochthony and citizenship and constantly remind State authorities about the promises of democratisation and the recognition of their claims on urban property, especially in regard to their customary land in the Green Belt of Niamey. The latter started as mere middlemen when privatization of land zoning was implemented in the early 2000s. Since then, they have become a real counterweight to the State thought their hinge position and exclusive knowledge of land regulation and act, in some cases, as king makers during local and national elections. The Nigeren State, in turn, is forced to respond to citizen's claims as a negotiating partner on the one hand, and finds itself bound to clientelistic relationships with actors stronger that itself, on the other hand. It is argued that the local, as well as the central Nigeren State is constantly attempting to anchor its authority and legitimacy, but is compelled to build a fragile statehood though hybrid arrangements with diverse societal actors.

20.6

The constitutive lack of discourse: national belonging and the desire for Turkey in Azerbaijan

Elisabeth Militz[1]

[1] *Department of Geography, University of Zurich, Winterthurerstrasse 190, CH-8057 Zurich (elisabeth.militz@geo.uzh.ch)*

In Azerbaijan, discourses on Azerbaijaniness and Turkishness have been competing to define what it means to be Azerbaijani (Diuk, 2012). Either has failed to fully constitute Azerbaijani subjects, who are often suspended in between discursive positionings and experience a constitutive lack leaving them incomplete. This paper conceptualises this lack as what Lacan (2001 [1966]) calls the ‹Real› - a constitutive order of the social which remains outside symbolisation as impossibility and out of reach. Analysing this missing ‹Real› beyond the level of symbolisation allows explaining the discursive contradictions and desires for Turkey and being Turkish. It unmasks those cravings for closure in national discourses as driving forces of routine nationalisms.

On the basis of ethnographic interviews conducted between 2012 and 2014 in Azerbaijan, the paper traces both the discursive attempts at positioning subjects and their continuos, inevitable failure. The paper thus contributes to a better understanding of what lies beyond the limits of discourses.

REFERENCES

Diuk, N., 2012: The next generation in Russia, Ukraine, and Azerbaijan. Youth, politics, identity, and change. Latham: Rowman & Littlefield.

Lacan, J. 2001 [1966]: Ecrits. A selection. London, New York: Routledge.

20.7

Planning their own homes. The capacities of the urban poor as planners and the constraints of public policy

Swetha Rao Dhananka

Faculté des géoscience et environnement. Université de Lausanne, Quartier Mouilne, Bâtiment Géopolis 5548, 1015 Lausanne

This paper will compare two urban poor communities in the metropolitan city of Bangalore (India) in their quest for adequate housing. Both communities were assisted by NGOs through different interventions. While one community got housing allotted through a public scheme, the other purely made its way through Indian bureaucracy by means of mobilization and negotiation to assure land tenure to plan their own built environment. The outcome of the different housing intervention was that the former community was delivered housing that was now in concrete blocks, but the housing process did not unite the community and did not correspond to their needs. While the housing process took much longer for the latter community, they built the houses on their terms. The results of the study of the two communities will be put in relation to social movement theory to address the question of how the encounter between claim-making communities and political opportunities (Kriesi et al, 1995) presented by bureaucracy and public policy (Gupta, 2012) can be explored by the mobilization of urban poor communities in cities of the global South. I will argue that within such contexts, it is not only important to consider existing formal political opportunities, but also to foresee informal interferences (Helmke & Levitsky, 2004). It will be shown that social skill (Fligstein & McAdam, 2012) of the community and the brokering NGOs and the capacities to build strategic alliances are paramount to assert adequate housing on their own terms and to make shelter sustainable.

REFERENCES

Fligstein, N., & McAdam, D. (2012). *A theory of fields*. Oxford: Oxford University Press.

Gupta, A. (2012). *Red Tape. Bureaucracy, Structural Violence, and Poverty in India*. Durham: Duke University Press.

Helmke, G., & Levitsky, S. (2004). Informal Institutions and Comparative Politics: A Research Agenda. *Perspectives on Politics*, *2*(04), 725.

Kriesi, H., Koopmans, R., Wilhelm Duyvendak, J., & Giugni, M. G. (1995). *New Social Movements in Western Europe. A comparative Analysis*. *Comparative and General Pharmacology*. London: University of Minnesota Press.

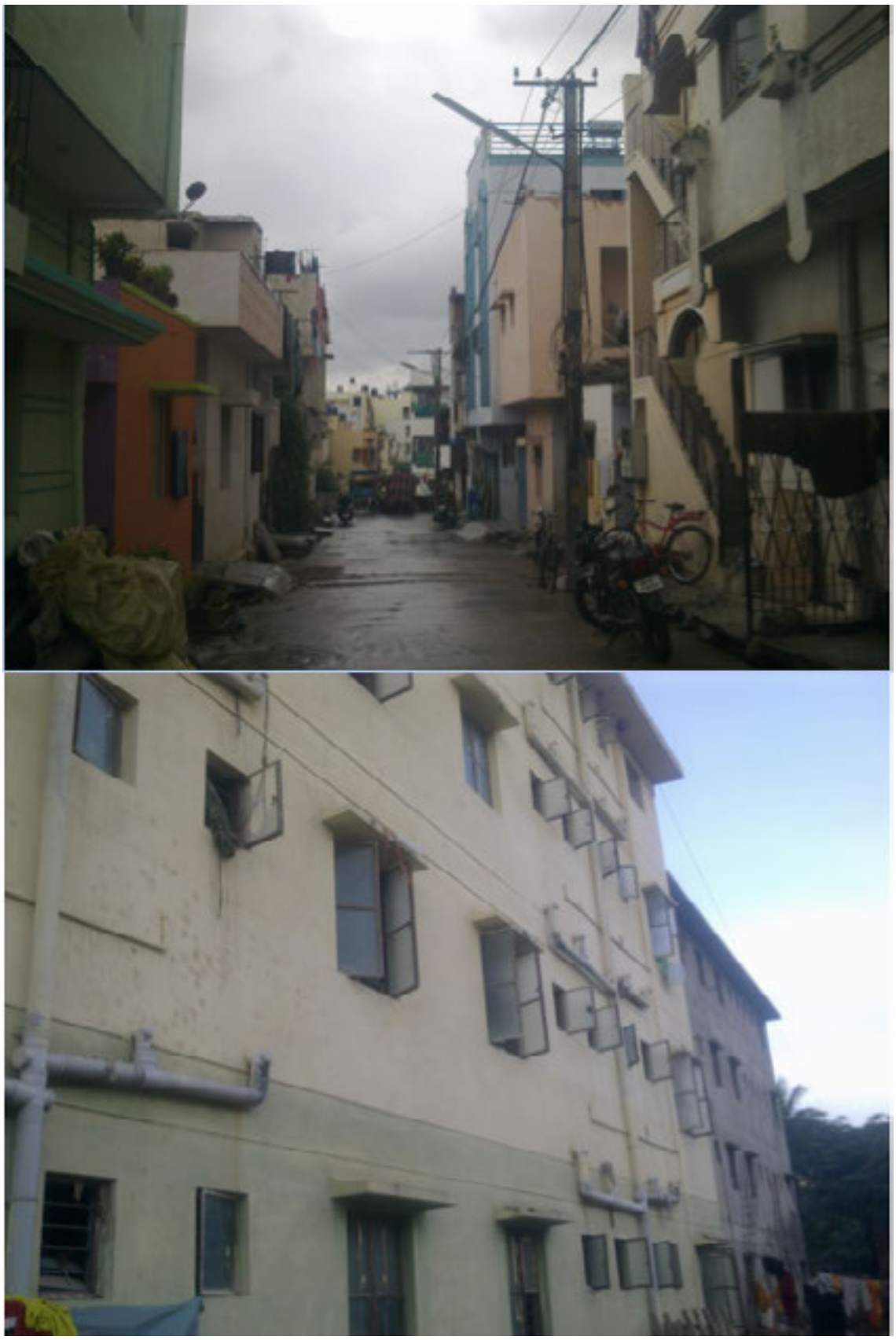

Figure 1. Housing outcomes. The photo above shows the layout of the community planning their own homes. The one beneath shows the houses delivered by public policy

20.8

Communal land Reform in Namibia: Traditional authorities renegotiate their positions in land governance

Laura Weidmann[1]

[1] *Unit of Geography, University of Fribourg, Chemin de Musée 4, 1700 Fribourg*

Namibia's multiple land rights system (dividing the country into state land, communal and commercial areas) is legally instituted since independence, but still the implementation process is very slow: This paper aims at pointing out two path dependencies which contribute to some of the difficulties faced by the communal land reform. The legal framework around communal land and the involvement of the traditional authority into its governance system, are based on several assumptions, two of which ought to be challenged in order to get a better understanding of the impacts of post-apartheid land governance on local socio-political realities: the first assumption holds that the concept and practice of traditional authorities stay unaltered by the registration; that they continue to ensure community cohesion through their work and presence. The second expectation is that commonage (or grazing areas, water points and other communal resources) continues to be accessible by all members of the community, while traditional authorities can ensure their fair and sustainable use.

However, empirical data offers arguments that "traditional" authorities, their tasks and strategies are much less static and homogeneous than foreseen in legal texts. The same holds true for other members of the community: individuals are unevenly integrated in political, economic and social networks – both in the commercial zone (through labour migration of various levels) and the communal zone. The constant decrease of communal rangeland serves on the one hand as an undisputable mirror to the ever-increasing population pressure on the resource of space and fertile land. On the other hand it reflects the spectrum of strategies of village members as well as different authorities widens when it comes to land governance, tenure security, and sustainable land use and community involvement. The communal land reform act and more specifically the registration of Communal land rights is on a continuous path of refinement, of establishing a practicable version of the legal framework. This transition process leads to unforeseen social dynamics, within which the traditional authorities are important players; they are forced to redefine or renegotiate their role and acceptance within and beyond their community.

P 20.1

Integrated management of water resources in a federal country: the case of Brazil

Graziele Muniz Miranda[1]

[1] *Institute of Geography and Sustainability, University of Lausanne, Quartier Mouline, Bâtiment Géopolis 1015 Lausanne (Graziele.MunizMiranda@unil.ch)*

The integrated water resources management (IWRM) can be defined as a process which promotes the coordinated development and management of water, land and related resources, in order to maximize fair, economic and social well-being without compromising the sustainability of vital ecosystems (GWP, 2000). It is a normative concept and there is much controversy among authors regarding its existence and viability.

The main criticisms of the IWRM according to many authors (Biswas, 2004 ;Molle, 2008 ; Graefe, 2011 ; Hering et Ingold, 2012) are :

- No consensus on the meaning of the concept;
- Increased bureaucracy, fight for power and slow decision-making with the expansion of the number of new institutions;
- Lack of commitment and knowledge of the players in relation to IWRM;
- Difficulty in reaching consensus on which uses and stakeholders have to be integrated; difficulty in creating a cooperative structure that considers those directly affected to deficits and potential winners or losers in the process;
- Few cases exist in practice that have incorporated IWRM in the legislation completely;
- It is difficult to measure its level of integration, because it is a normative and general concept;
- Many governments continue to manage as before and use the means of IWRM only for their own benefits;
- Several countries, especially in Latin America, Asia and Africa, have copied the model/laws made by rich countries without considering the reality of the country or consulting the people before the implementation of IWRM.

In many documents and legislation of several countries, the catchment is considered the unit of management and planning for IWRM. Multiple authors disagree with this for the following reasons: the border of the catchments are not always the same as the political boundaries, which can cause conflicts between states and boundaries; the border of the catchments for surface waters are not the same as underground waters; and the transfers of waters between catchments are not considered during the clipping of hydrographical basins (Graefe, 2011).

Some countries have adopted integrated management of water resources through catchment in their legislation. Brazil is an example of this; according to the law 9433/1997, water management should be decentralized and integrated with the creation of river basin committees and water agency according to the French model of water management.

Prior to the federal law, the state of São Paulo edited the 7663/1991 law that divides the state into 22 units of water resources management to operate the respective river basin committees. The UGRHI-5 contains the catchments Piracicaba, Capivari and Jundiaí and was the first committee to be implemented. As the catchment is contained in two states (São Paulo and Minas Gerais), it has a federal committee and a state committee.
Currently the major concerns about UGRHI-5 are the conflicts related to usages between catchments that do not belong to the territory of committees, such as the diversion of 31 m3/s of water from basins Piracica, Capivari and Jundiaí for the metropolitan region of São Paulo (located in another catchment).

In this poster we discuss the issue of implementing IWRM in countries with a federal structure. In fact, in these contexts, there is a risk of structure overlapping (regional institutions versus catchment organisms). On the other way, in federal countries the participation of local population in political decision processes is higher than in centralized countries, a situation that could facilitate the participation of public in the water management. The discussion will be illustrated by the case of Brazil (national level), with a focus on the São Paulo state (regional level) and Piracicaba, Capivari and Jundiaí catchments (local level).

REFERENCES

Biswas, A. 2004: Integrated water resources management: a reassessment. A water forum contribution, International Water Resources Association, 29, 2, 248-256.

Graefe, O. 2011: River basins as new environmental regions? The depolitization of water management. Procedia Social and Behavioral Sciences, 14, 24-27.

GWP (2000). La gestion intégrée des ressources en eau. Stockholm (Suède): Global Water Partnership.

Hering, J. G., and Ingold, K. M. 201: Water Resources Management: What should be Iitegrated?, Science, 336, 6086, 1234-1235.

Molle, F. 2008: Nirvana Concepts, Narratives and Policy Models: Insights from the Water Sector, Water Alternatives, 1, 1, 131-156.

P 20.2

Sexuality, reproduction and biopower : a research on LGBTQ procreation and parenting

Paola Rattu[1]

[1] *Institut of Geography and Sustainability, University of Lausanne, Bâtiment Gépolis, CH-1015 Lausanne (paola.rattu@unil.ch)*

In the Western societies, procreation has often been considered as inseparable from the sexual intercourses of heterosexual couples, and sexuality has often been controlled through biopower in order to control indivudals and populations. Nevertheless, gay, lebsian, bisexual, transexual and queer (LGBTQ) individuals and couples have often desired and/or welcomed children, for instance in stepfamilies or through adoption.

Assisted reproductive technologies (ART) allowed for the disjunction of sexual intercourses and procreation, and created new possibilities for singles and for LGBTQ couples. In parallel, LGBTQ couples also started experimenting new forms of parenting, such as coparenting (Garnier, 2012).

Even though both coparenting and ART require a proactive commitment of parents in the decision of procreating, this commitment can be either facilitated or hampered when external actors intervene in the procreating process, such as in the case of ART. In fact, medical, bureaucratic and legislative devices are often established in order to control ART and to prevent people with "anomal" (i.e. non-heterosexual) sexualities from accessing them. Thus, the biophysical realities of individual bodies become places of power struggles at the macro (for instance the countries, where the legislations are adopted) and at the micro levels (for intance, the hospitals where those legislations are enforced, in parallel with medical, bureaucratical and other sorts of control).

ART are part of "*sophisticated complex goods and processes developed through costly investment in basic research and development, and then distributed, unequally, around the world*" (Manderson, 2012, p.4)… often, "*to be purchased by those with the ability and the resources to travel*" (Witthaker, 2012, p. 160). The lack of access to ART generates reproductive exile, as well for heterosexual as for LGBTQ prospective parents (Bergmann, 2011). The inequalities of this exile have been widely documented for heterosexual couples. Nevertheless, few studies concern the stratification of LGBTQ reproduction. More generally, research on homoparenting has often highlighted the discrimination faced by the LGBTQ couples vis-à-vis heterosexual ones. Even though recent works have stessed the need of deconstructing generalizations and wide categories such as "lesbian mother", reproductive inequalities inside the LGBTQ communitiy are not well studied, and the majority of research has been carried on in anglo-saxon countries.

Combining insights from queer theory, cultural studies and, marginally, political ecology, this research aims to fill this knowledge gap, and to investigate its existence, its causes and its consequences in some European countries where the law prevents LGBTQ individuals and couples from accessing ART (examples of those countries are Italy, France and Switzerland).

Reproductive exile is expensive, and the quality of ART might influence prices. The hypothesis of a stratification of reproductive exile among LGBTQ couples and individuals seems thus reasonable. A reduced mobility of LGBTQ couples and individuals might force them to abandon their parental project or to develop new creative forms of parenting, such as coparenting; on the other side, wealthy couples might have a bigger range of choices, for instance regarding medical assistance or legal support.

In addition to a better understanding of the socio-spatial dynamics of LGBTQ procreation, this research aims to plea for an increased consideration of the bio-physical component of human life and of its co-construction with respect to socio-political and economical constraints and opportunities in the social sciences.

This research is ethically rooted on the cultural studies engagement consisting in « *faire de la politique par d'autres moyens, c'est-à-dire d'arriver à des niveaux de compréhension du social qui permettent de le modifier ; d'identifier des relations qui peuvent être de domination en essayant de voir comment elles peuvent ne pas être nécessaires ou contrariées ; de dire qu'il faut politiser la théorie et théoriser les politiques* » (Bourcier, 2005, pp. 26-27).

The results should allow nuancing homoparenting and casting light on the inequalities inside the LGBTQ community, as well as on alternative and resisting modes of parenting vis-à-vis the dominant hetero-sexualized model, in order to promote more fairness in access to procreation for LGBTQ individuals and couples.

REFERENCES

Bergmann, S. (2011). Fertility Tourism: Circumventive Routes That Enable Access to Reproductive Technologies and Substances, Signs, 36(2), 280-289.

Bourcier, M.H. 2005. Sexpolitiques : Queer Zones 2. Paris : La Fabrique éditions.

Garnier, É. 2012. L'Homoparentalité en France. Vincennes : Editions Thierry Marchaisse.

Manderson, L. 2012. Material words, sexy lives. Technologies of sexuality, identity and sexual health. In Manderson, L. (ed). Technologies of sexuality, identity and sexual health, 1-15. Oxon: Routledge.

Whittaker, A. 2012. Gender disappointment and cross-border high-tech selection. A new global sex trade. In Manderson, L. (ed). Technologies of sexualiy, identity and sexual health, 143-164. Oxon: Routledge.